

Applications of Iodonium Ylides for Donor-Acceptor Cyclopropane Synthesis

by

Tristan Chidley

A thesis
presented to the University of Waterloo
in fulfillment of the
thesis requirement for the degree of
Doctor of Philosophy
in
Chemistry

Waterloo, Ontario, Canada, 2021

© Tristan Chidley 2021

Examining Committee Membership

The following served on the Examining Committee for this thesis. The decision of the Examining Committee is by majority vote.

External Examiner	Sylvain Canesi Professor, Université du Québec à Montréal
Supervisor	Graham K. Murphy Associate Professor, University of Waterloo
Internal Member	Michael J. Chong Professor, University of Waterloo
Internal Member	Eric Fillion Professor, University of Waterloo
Internal Member	Scott Taylor Professor, University of Waterloo
Internal-external Member	Todd Holyoak Associate Professor, University of Waterloo

Author's Declaration

This thesis consists of material all of which I authored or co-authored: see Statement of Contributions included in the thesis. This is a true copy of the thesis, including any required final revisions, as accepted by my examiners.

I understand that my thesis may be made electronically available to the public.

Statement of Contributions

Tristan Chidley was the sole author for Chapters 1, 2, 3, 4 which were written under the supervision of Professor Graham Murphy and were not written for publication. I would like to acknowledge the work of Islam Jameel who helped me with synthesizing some of the iodonium ylides used in Chapter 3. I would also like to acknowledge the work of Shafa Rizwan who helped me with synthesizing some of the cyclopropanes used in Chapter 3. Professor Scott Hopkins contributed to computational studies in Chapter 3 which were used to predict how a series of iodonium ylides can be excited using visible light irradiation, including the HOMO and LUMO predictions.

Abstract

The application of hypervalent iodine (HVI) reagents in the field of organic chemistry has emerged as a viable option for many different useful organic transformations. There have been many considerable contributions made to organic synthesis from HVI reagents, and recently there has been a surge in new and innovative methods of incorporating these reagents into everyday use in the laboratory.

The ability to generate donor-acceptor (DA) cyclopropanes in an efficient manner has many benefits for the field of organic synthesis and discovering new efficient methods of synthesizing these compounds using alternative strategies is always useful. In this study, we have found that relatively cheap Wittig reagents can serve as a starting material, which upon reaction with iodobenzene, approximately 2 equiv can generate monocarbonyl iodonium ylides (MCIYs) *in situ* which can then go on to perform various reactions, analogous to carbene chemistry. This type of methodology can bypass the more common ways of accessing carbene chemistry which rely on diazo compounds, which do have some disadvantages as some are known to have toxic or explosive properties.

Chapter 2 builds on previous research in the Murphy lab that described a new method for accessing unstable MCIYs using a Wittig-type reaction. Wittig reagents (phosphonium ylides) were reacted with iodobenzene to form the MCIY, which was intercepted by a copper catalyst to form a metallocarbene, which in the presence of an alkene, forms cyclopropanes. This new reaction was published three years before I joined the group, and was able to generate cyclopropanes, but the reaction was not optimized and only gave yields of up to 29%. Unwanted dimerization of the Wittig reagent was occurring as a side reaction, accounting for an additional 27% of wasted material. These problems were addressed by synthesizing iodobenzene derivatives that contain different steric and electronic properties and using them in the Wittig-type reaction to maximize cyclopropanation efficiency.

Chapter 3 discusses the application of visible light for activating dicarbonyl iodonium ylides which are then capable of undergoing cyclopropanation with alkenes. Different photoreactors were built from scratch using LED light strips to customize a specific photoreactor setup ideal for this cyclopropanation reaction. UV-Vis emission data of the light source was collected and compared to the absorbances of the iodonium ylides, providing supporting

evidence to confirm the reaction was dependant on specific wavelengths of visible light. Subjecting the reaction of iodonium ylides and alkenes to different colours of visible light was also investigated to determine exactly what wavelength of light was required for inducing the cyclopropanation event. It was found that blue light supplied the right amount of energy to activate the iodonium ylide to an excited state, which in the presence of an alkene, formed donor-acceptor cyclopropane system. Red and green light, which are both slightly lower in energy than blue light, were not capable of activating the iodonium ylide, and no observable cyclopropanes were formed under these conditions. The HOMO and LUMO energies of six iodonium ylides were computationally generated, which also confirmed that the energy supplied by blue light should allow for the excitation event to occur.

Chapter 4 uses the newly discovered light-mediated cyclopropanation reaction to test the feasibility of establishing an asymmetric variant of the reaction. Chiral hypervalent iodine diacetates were synthesized from asymmetric aryl iodides for use in the synthesis of asymmetric iodonium ylides. Several different types of chiral systems were tested to determine if there was any possibility of using the light-mediated reactions for generating enantiomerically enriched cyclopropanes. The testing of structurally different chiral iodonium ylides was also investigated to determine what structural types would be tolerated in the cyclopropanation reaction, and what their effects on isolated yields would be.

Acknowledgements

I am very thankful to Dr. Graham Murphy for giving me a chance and accepting me into his research group. I really appreciate the trust that was given to me to explore new types of reactions and push the boundaries of science to make discoveries that ended up being successful and contributed to our field of organic chemistry. I am thankful to all the students who have worked and are still working in the Murphy group. I would like to thank Dr. Michael Chong for attending some of our earlier group meetings and engaging in interesting research discussions. I would also like to include an acknowledgement to the University of Waterloo for financial support as a graduate student in the Chemistry Department.

During my time at the University of Waterloo I had an enjoyable experience taking graduate level classes, which were extremely helpful in advancing my theoretical knowledge in the field of organic chemistry. I was grateful to have enthusiastic professors such as Dr. William Tam and Dr. Michael Chong who taught me a deeper understanding of organometallics and organic spectroscopy.

Instrument access was critical for me to obtain results and would not have been possible without the help and guidance from many professors, researchers, and technicians within the department of chemistry at the University of Waterloo. A thank you is extended to Jan Venne for help with NMR spectroscopy, and guidance on issues that were extremely important to me. I am grateful for Dr. Richard Smith who was able to help me with understanding mass spectrometry. I would like to thank Dr. Mónica Barra and Dr. Sonny Lee for access to UV-Vis spectrometers. Julie Goll provided access to IR and Polarimeter instruments, as well as being a helpful mentor when it came to TA duties. I am also thankful for being able to be a TA for Dr. Leanne Racicot. Also, Catherine Van Esch and Kim Rawson were very helpful with administrative assistance and for general help within the department of chemistry.

I would like to say thank you to the help I received from graduate students and researchers within the department of chemistry at the University of Waterloo. Students from the Fillion and Taylor group assisted me by making it easier to access departmental instruments and research chemicals. Scott Hopkins was also helpful with discussions and assistance of computational modeling of our cyclopropanation reaction.

I would like to acknowledge the help of undergraduate students within the Murphy group that I had the pleasure of mentoring, and who assisted me with laboratory activities. I would like to again thank the current and former graduate students from the Murphy group. I would like to extend a special thank you to Islam Jameel who helped me with discussions of chemical theory which resulted in the discovery of new reactions and a deeper understanding of my own research. Islam was extremely helpful in terms of motivating me to work harder and to always try to do my best.

I would like to thank my family for their unconditional love and support throughout my life and throughout my time at the University of Waterloo. They have contributed so much to my life, and I am happy to give back by dedicating this thesis to them.

I would also like to include an acknowledgment to the rock-n-roll band Tool for providing me with an unlimited amount of inspirational music that was a constructive backdrop while performing research in the laboratory.

Dedication

*For my parents, Ray and Dianne, and Islam
my niece Mileydi,
and Tool*

Table of Contents

Examining Committee Membership	ii
Author's Declaration	iii
Statement of Contributions	iv
Abstract	v
Acknowledgements	vii
Dedication	ix
List of Figures	xiv
List of Schemes	xix
List of Tables	xxv
List of Abbreviations	xxvi
List of Symbols	xxx
Chapter 1: Introduction	1
1.1 Iodine	1
1.2 Hypervalent Iodine (HVI).....	3
1.2.1 Synthesis of HVI Compounds	7
1.2.2 Structure and Bonding of HVI Compounds.....	10
1.2.2.1 Secondary Bonding of HVI Compounds.....	12
1.2.3 Reactivity of HVI Compounds	15
1.3 Ylides	19
1.3.1 Diazonium Ylides	21
1.3.2 Iodonium Ylides.....	24
1.3.2.1 Synthesis of Iodonium Ylides.....	25
1.3.2.2 Structure and Bonding of Iodonium Ylides.....	28
1.3.2.3 Reactivity of Iodonium Ylides	31
1.4 Carbenes.....	45
1.4.1 Carbenoids	49
1.4.2 Metal-Carbenes	50
1.4.3 Fischer Carbenes.....	50
1.4.4 Schrock Carbenes.....	51

1.4.5	N-Heterocyclic Carbenes (NHCs)	52
1.5	Cyclopropanes.....	54
1.5.1	Donor-Acceptor (DA) Cyclopropanes	56
1.5.2	Synthesis of Cyclopropanes.....	58
1.5.3	Structure and Bonding of Cyclopropanes	64
1.5.4	Reactivity of Cyclopropanes.....	66
1.6	Scope of Thesis.....	67
Chapter 2: Cyclopropanation of Monocarbonyl Iodonium Ylides		69
2.1	Background.....	69
2.2	Monocarbonyl Iodonium Ylides (MCIYs)	72
2.2.1	Synthesis of MCIYs.....	72
2.2.2	Structure and Bonding of MCIYs.....	77
2.2.3	Reactivity of MCIYs.....	81
2.2.4	Reactions of MCIYs	82
2.3	Wittig Reaction	90
2.3.1	Reaction of Wittig Reagents with HVI Compounds.....	92
2.4	Mixed Phosphonium-Iodonium Ylides.....	93
2.5	Iodosoarenes	94
2.5.1	Synthesis of Iodosoarenes.....	96
2.6	Cyclopropanation of MCIYs.....	98
2.7	Optimization of Cyclopropanation Reaction of MCIYs with Alkenes.....	101
2.7.1	Proposed Reaction Mechanism.....	112
2.8	Scope of The Reaction	114
2.8.1	Intramolecular Cyclopropanation of MCIYs	117
2.9	Insertion Reactions of MCIYs	120
2.10	Experimental.....	123
2.10.1	General Procedure 1 (GP1) - Synthesis of Cyclopropanes.....	123
2.11	NMR Spectra for Chapter 2	135
Chapter 3: Cyclopropanation of Iodonium Ylides & Alkenes Using Blue Light.....		145
3.1	Introduction.....	145
3.2	Photochemical Activation of Ylides	151

3.2.1	Activation of Diazonium Ylides with Light	151
3.2.2	Activation of Phosponium Ylides with Light	154
3.2.3	Activation of Sulfonium Ylides with Light	155
3.2.4	Activation of Iodonium Ylides with Light.....	157
3.2.4.1	Photochemical Transylidation Reactions	161
3.2.4.2	Photochemical Cycloaddition Reactions	162
3.3	Proposed Photochemical Activation of Iodonium Ylides with Blue Light	165
3.4	Computational Modeling of Iodonium Ylides Under Blue Light Irradiation.....	168
3.5	UV-Vis Absorbance of Iodonium Ylides	171
3.6	Photoreactor Design.....	174
3.6.1	Photoreactor #1 Round-bottom Flask Design.....	174
3.6.2	Photoreactor #2 Displacement Tube Design.....	175
3.6.3	Photoreactor #3 Bowl Design	176
3.6.4	Photoreactor #4 Design.....	180
3.7	Optimization of Photo-Induced Reaction of Iodonium Ylides with Alkenes.....	182
3.8	Cyclopropanation Reaction Scope	195
3.9	Mechanistic Analysis	200
3.9.1	Control Reactions for Photo-Isomerization of β -Methylstyrenes.....	204
3.10	One-Pot Cyclopropanation Reaction	209
3.11	Applications of Blue Light Induced Reactivity of Iodonium Ylides	211
3.11.1	Blue Light Induced Rearrangements	212
3.11.2	Blue Light-Induced Oxidation of Allylic Alcohols	214
3.11.3	Blue Light Induced O-H Insertion of Iodonium Ylides.....	219
3.11.4	Blue Light Induced Aziridination Reaction	219
3.11.5	Blue Light Induced Transylidation Reaction	221
3.12	Experimental	225
3.12.1	General Procedure 1 (GP1) - Synthesis of Iodonium Ylides	225
3.12.2	General Procedure 2 (GP2) - Synthesis of Cyclopropanes	235
3.13	NMR Spectra for Chapter 3	250
Chapter 4: Synthesis of Asymmetric Iodonium Ylides and Their Use in Blue Light-Induced Asymmetric Cyclopropanation with Alkenes		283

4.1	Background of Asymmetric HVI Compounds	283
4.1.1	Strategies for Controlling Stereoselectivity	285
4.1.2	Asymmetric Cyclopropanation of Iodonium Ylides and Alkenes	289
4.2	Preliminary Results	294
4.3	Synthesis of Chiral Aryl Iodides	298
4.3.1	Synthesis of L-Proline Derived Aryl Iodides	302
4.4	Synthesis of Chiral Diacetates	304
4.5	Synthesis of Chiral Iodonium Ylides	307
4.6	Synthesis of Chiral Cyclopropanes	312
4.7	Conclusions and Final Discussions	318
4.8	Experimental	319
4.8.1	General Procedure 1 (GP1) - Synthesis of Chiral Aryl Iodides	319
4.8.2	General Procedure 2 (GP2) - Synthesis of Chiral Diacetates	323
4.8.3	General Procedure 3 (GP3) - Synthesis of Chiral Iodonium Ylides	325
4.8.4	General Procedure 4 (GP4) - Synthesis of a Standard Racemic Cyclopropane ...	327
4.8.5	Synthesis of Chiral Cyclopropanes	329
4.9	NMR Spectra for Chapter 4	333
	References	349
	Appendix I: Crystal Structure Data of Cyclopropane	359
	Appendix II: Permission for Figure 1.18 and Figure 1.19	360

List of Figures

Figure 1.1 Oxidation states and examples of iodine in molecules.....	4
Figure 1.2 Martin-Arduengo N-X-L designation.....	5
Figure 1.3 Examples of HVI compounds with different oxidation states of iodine	6
Figure 1.4 Types of HVI compounds containing iodine (III).....	7
Figure 1.5 Qualitative bonding model in organoiodine (III) compounds	10
Figure 1.6 Hypervalent bonding model for aryl- λ^3 -iodanes	11
Figure 1.7 Molecular orbitals of the [3c-4e] hypervalent bonding model.....	11
Figure 1.8 Orientation of ligands in space in aryl- λ^3 -iodanes.....	12
Figure 1.9 Secondary bonding in $\text{PhI}(\text{OAc})_2$	13
Figure 1.10 Secondary bonding responsible for stability in cyclic iodonium ylides.....	13
Figure 1.11 X-Ray crystal structure of iodonium ylide 1.6	14
Figure 1.12 Secondary bonding interactions in acyclic iodonium ylides 1.6 and 1.7	15
Figure 1.13 General ylides stabilized by an α -keto group	20
Figure 1.14 Structural representation of general ylides as a carbene complex.....	21
Figure 1.15 Diazo compounds categorized by stability.....	22
Figure 1.16 Types of iodonium ylides	25
Figure 1.17 Dative σ bonding description in iodonium ylides	29
Figure 1.18 Computational bonding models of iodonium ylides.....	30
Figure 1.19 Computational bonding models of iodonium ylides.....	30
Figure 1.20 Average bond angle in iodonium ylides	31
Figure 1.21 Structure of phenyliodonium bis(trifluoromethanesulfonyl)methide.....	31
Figure 1.22 Intermediates of activation modes of iodonium ylides.....	32
Figure 1.23 Structures and hybridization of methane analogues and carbenes	46
Figure 1.24 General carbenoid structure.....	50
Figure 1.25 First metal-carbene complex (Fischer carbene).....	51
Figure 1.26 Examples of common NHC types and their nomenclature	52
Figure 1.27 Ring strain energies of small carbocycles	54
Figure 1.28 Cyclopropane structural properties.....	64
Figure 1.29 Coulson-Moffit model bond angles.....	65
Figure 1.30 Reactivity of cyclopropanes	66
Figure 2.1 Iodonium ylide types	69
Figure 2.2 Examples of phenol-stabilized iodonium ylides.....	71
Figure 2.3 Structures of dicarbonyl and monocarbonyl iodonium ylides.....	77
Figure 2.4 Conformation stabilities in cyclic, acyclic, and monocarbonyl iodonium ylides.....	78
Figure 2.5 Metal-coordinated to ylides in a chiral reaction pathway.....	89
Figure 2.6 Resonance structures and zigzag polymeric network of iodosobenzene.....	96
Figure 2.7 Synthesis of iodosoarenes from (diacetoxyiodo)arenes	96
Figure 2.8 Intramolecular secondary bonding in soluble iodosoarene	102
Figure 2.9 Structure of iodosylbenzene	110
Figure 2.10 Examples of a triaryl and trialkyl phosphoranes (Wittig reagents).....	112

Figure 2.11 Cyclopropanation of MCIYs reaction scope	117
Figure 2.12 ¹ H NMR (300 MHz, CDCl ₃) spectrum of ethyl 2-methoxy-3-(4-methoxyphenyl)cyclopropanecarboxylate	135
Figure 2.13 ¹³ C NMR (75 MHz, CDCl ₃) spectrum of ethyl 2-methoxy-3-(4-methoxyphenyl)cyclopropanecarboxylate	136
Figure 2.14 ¹ H NMR (300 MHz, CDCl ₃) spectrum of ethyl 2-methoxy-3-(4-methoxyphenyl)cyclopropanecarboxylate	137
Figure 2.15 ¹³ C NMR (75 MHz, CDCl ₃) spectrum of ethyl 2-methoxy-3-(4-methoxyphenyl)cyclopropanecarboxylate	138
Figure 2.16 ¹ H NMR (300 MHz, CDCl ₃) spectrum of ethyl 2-methoxy-3-(3,4,5-trimethoxyphenyl)cyclopropanecarboxylate.....	139
Figure 2.17 ¹³ C NMR (75 MHz, CDCl ₃) spectrum of ethyl 2-methoxy-3-(3,4,5-trimethoxyphenyl)cyclopropanecarboxylate.....	140
Figure 2.18 ¹ H NMR (300 MHz, CDCl ₃) spectrum of 2-methoxy-3-(4-methoxyphenyl)cyclopropyl)(phenyl)methanone.....	141
Figure 2.19 ¹³ C NMR (75 MHz, CDCl ₃) spectrum of 2-methoxy-3-(4-methoxyphenyl)cyclopropyl)(phenyl)methanone.....	142
Figure 2.20 ¹ H NMR (300 MHz, CDCl ₃) spectrum of 2-methoxy-3-(3,4,5-trimethoxyphenyl)cyclopropyl)(phenyl)methanone	143
Figure 2.21 ¹³ C NMR (75 MHz, CDCl ₃) spectrum of 2-methoxy-3-(3,4,5-trimethoxyphenyl)cyclopropyl)(phenyl)methanone	144
Figure 3.1 Electron energy levels in a molecule undergoing photochemical excitation	146
Figure 3.2 Interaction modes of photoexcited species.....	147
Figure 3.3 Comparison of incandescent, CFL, and LED light bulbs.....	148
Figure 3.4 Examples of components of a photoredox system	150
Figure 3.5 Diazo compounds tested for visible light activation	152
Figure 3.6 UV-Vis absorbances of diazos 3.1a , 3.1b , 3.2a , 3.2b (0.05 mM in CH ₂ Cl ₂).....	152
Figure 3.7 Structures of Hantzsch ester and [MesAcrMe]BF ₄ organophotocatalyst.....	155
Figure 3.8 Geometry of orbital systems in iodonium ylides.....	166
Figure 3.9 Representation of dimedone iodonium ylide as a MO diagram with 5 atoms	167
Figure 3.10 Electronic excitation levels of a 1,3-dicarbonyl anion system by light.....	167
Figure 3.11 Cyclic iodonium ylides used in computational studies	168
Figure 3.12 Calculated spectra, B3LYP/6-311++G(d,p) level of theoretical iodine	171
Figure 3.13 UV-Vis absorbance of ylide 3.16a overlaid on RGB LED colours.....	172
Figure 3.14 UV-Vis absorbance of styrene.....	173
Figure 3.15 Photoreactor #1 round-bottom flask design.....	174
Figure 3.16 Photoreactor #2 displacement tube design	176
Figure 3.17 Photoreactor #3 bowl design	177
Figure 3.18 Photoreactor#3 light intensity readings	178
Figure 3.19 Photoreactor #3 cyclopropane yield at different distances from LED	179
Figure 3.20 Photoreactor #4 design	181
Figure 3.21 Overlay of violet and blue LED with iodonium ylide 3.16j	185
Figure 3.22 Overlap of UV-Vis absorbance of 3.16a , 3.16b , 3.16g , 3.16h with blue LED.....	188

Figure 3.23 Overlap of UV-Vis absorbance of 3.16a , 3.16i , 3.16j with blue LED.....	189
Figure 3.24 Alkenes that did not react with iodonium yides	199
Figure 3.25 X-Ray crystal structure image & molecule of <i>trans</i> -cyclopropane 3.30l	203
Figure 3.26 Crystal structure of <i>trans</i> -cyclopropane 3.30l at 50% probability	204
Figure 3.27 Photo-induced isomerization check of <i>cis</i> - β -methylstyrene.....	206
Figure 3.28 Photo-induced isomerization check of <i>trans</i> - β -methylstyrene.....	206
Figure 3.29. ¹ H NMR (300 MHz, CDCl ₃) spectrum of (4-methylphenyl)(4,4-dimethyl-2,6-dioxocyclohexyl)iodonium	250
Figure 3.30 ¹³ C NMR (75 MHz, CDCl ₃) spectrum of (4-methylphenyl)(4,4-dimethyl-2,6-dioxocyclohexyl)iodonium	251
Figure 3.31 ¹ H NMR (300 MHz, CDCl ₃) spectrum of (4-cyanophenyl)(4,4-dimethyl-2,6-dioxocyclohexyl)iodonium	252
Figure 3.32 ¹³ C NMR (75 MHz, CDCl ₃) spectrum of (4-cyanophenyl)(4,4-dimethyl-2,6-dioxocyclohexyl)iodonium	253
Figure 3.33 ¹ H NMR (300 MHz, CDCl ₃) spectrum of (4-trifluoromethylphenyl)(4,4-dimethyl-2,6-dioxocyclohexyl)iodonium.....	254
Figure 3.34 ¹³ C NMR (75 MHz, CDCl ₃) spectrum of (4-trifluoromethylphenyl)(4,4-dimethyl-2,6-dioxocyclohexyl)iodonium.....	255
Figure 3.35 ¹⁹ F NMR (282 MHz, CDCl ₃) spectrum of (4-trifluoromethylphenyl)(4,4-dimethyl-2,6-dioxocyclohexyl)iodonium.....	256
Figure 3.36 ¹ H NMR (300 MHz, CDCl ₃) spectrum of (2,6-dimethoxy-4-methylphenyl)(4,4-dimethyl-2,6-dioxocyclohexyl)iodonium	257
Figure 3.37 ¹³ C NMR (75 MHz, CDCl ₃) spectrum of (2,6-dimethoxy-4-methylphenyl)(4,4-dimethyl-2,6-dioxocyclohexyl)iodonium	258
Figure 3.38 ¹ H NMR (300 MHz, CDCl ₃) spectrum of (4,4-dimethyl-2,6-dioxocyclohexyl)(naphthalen-1-yl)iodonium	259
Figure 3.39 ¹³ C NMR (75 MHz, CDCl ₃) spectrum of (4,4-dimethyl-2,6-dioxocyclohexyl)(naphthalen-1-yl)iodonium	260
Figure 3.40 ¹ H NMR (300 MHz, CDCl ₃) spectrum of (4-nitrophenyl)(4,4-dimethyl-2,6-dioxocyclohexyl)iodonium	261
Figure 3.41 ¹³ C NMR (75 MHz, CDCl ₃) spectrum of (4-nitrophenyl)(4,4-dimethyl-2,6-dioxocyclohexyl)iodonium	262
Figure 3.42 ¹ H NMR (300 MHz, CDCl ₃) spectrum of 1-(4-(tert-butyl)phenyl)-6,6-dimethyl-5,7-dioxaspiro[2.5]octane-4,8-dione	263
Figure 3.43 ¹³ C NMR (75 MHz, CDCl ₃) spectrum of 1-(4-(tert-butyl)phenyl)-6,6-dimethyl-5,7-dioxaspiro[2.5]octane-4,8-dione	264
Figure 3.44 ¹ H NMR (300 MHz, CDCl ₃) spectrum of 1-([1,1'-biphenyl]-4-yl)-6,6-dimethyl-5,7-dioxaspiro[2.5]octane-4,8-dione	265
Figure 3.45 ¹³ C NMR (75 MHz, CDCl ₃) spectrum of 1-([1,1'-biphenyl]-4-yl)-6,6-dimethyl-5,7-dioxaspiro[2.5]octane-4,8-dione	266
Figure 3.46 ¹ H NMR (300 MHz, CDCl ₃) spectrum of 1-(3,4,5-trimethoxyphenyl)-6,6-dimethyl-5,7-dioxaspiro[2.5]octane-4,8-dione.....	267

Figure 3.47 ^{13}C NMR (75 MHz, CDCl_3) spectrum of 1-(3,4,5-trimethoxyphenyl)-6,6-dimethyl-5,7-dioxaspiro[2.5]octane-4,8-dione.....	268
Figure 3.48 ^1H NMR (300 MHz, CDCl_3) spectrum of 6,6-dimethyl-1-(3'-nitro-[1,1'-biphenyl]-2-yl)-5,7-dioxaspiro[2.5]octane-4,8-dione.....	269
Figure 3.49 ^{13}C NMR (75 MHz, CDCl_3) spectrum of 6,6-dimethyl-1-(3'-nitro-[1,1'-biphenyl]-2-yl)-5,7-dioxaspiro[2.5]octane-4,8-dione.....	270
Figure 3.50 ^1H NMR (300 MHz, CDCl_3) spectrum of 1-(4-(benzyloxy)-[1,1'-biphenyl]-2-yl)-6,6-dimethyl-5,7-dioxaspiro[2.5]octane-4,8-dione.....	271
Figure 3.51 ^{13}C NMR (75 MHz, CDCl_3) spectrum of 1-(4-(benzyloxy)-[1,1'-biphenyl]-2-yl)-6,6-dimethyl-5,7-dioxaspiro[2.5]octane-4,8-dione.....	272
Figure 3.52 ^1H NMR (300 MHz, CDCl_3) spectrum of 2',2'-dimethylspiro[bicyclo[3.1.0]hexane-6,5'-[1,3]dioxane]-4',6'-dione.....	273
Figure 3.53 ^{13}C NMR (75 MHz, CDCl_3) spectrum of 2',2'-dimethylspiro[bicyclo[3.1.0]hexane-6,5'-[1,3]dioxane]-4',6'-dione.....	274
Figure 3.54 ^1H NMR (300 MHz, CDCl_3) spectrum of 1-benzyl-6,6-dimethyl-5,7-dioxaspiro[2.5]octane-4,8-dione.....	275
Figure 3.55 ^{13}C NMR (75 MHz, CDCl_3) spectrum of 1-benzyl-6,6-dimethyl-5,7-dioxaspiro[2.5]octane-4,8-dione.....	276
Figure 3.56 ^1H NMR (300 MHz, CDCl_3) spectrum of 1-decyl-6,6-dimethyl-5,7-dioxaspiro[2.5]octane-4,8-dione.....	277
Figure 3.57 ^{13}C NMR (75 MHz, CDCl_3) spectrum of 1-decyl-6,6-dimethyl-5,7-dioxaspiro[2.5]octane-4,8-dione.....	278
Figure 3.58 ^1H NMR (300 MHz, CDCl_3) spectrum of 1-([1,1'-biphenyl]-4-yl)-5,7-dimethyl-5,7-diazaspiro[2.5]octane-4,6,8-trione.....	279
Figure 3.59 ^{13}C NMR (75 MHz, CDCl_3) spectrum of 1-([1,1'-biphenyl]-4-yl)-5,7-dimethyl-5,7-diazaspiro[2.5]octane-4,6,8-trione.....	280
Figure 3.60 ^1H NMR (300 MHz, CDCl_3) spectrum of 1-(4-(tert-butyl)phenyl)-5,7-dimethyl-5,7-diazaspiro[2.5]octane-4,6,8-trione.....	281
Figure 3.61 ^{13}C NMR (75 MHz, CDCl_3) spectrum of 1-(4-(tert-butyl)phenyl)-5,7-dimethyl-5,7-diazaspiro[2.5]octane-4,6,8-trione.....	282
Figure 4.1 First reports of chiral HVI compounds.....	283
Figure 4.2 First examples of chiral HVI compounds derived from amino acids.....	284
Figure 4.3 Pioneers in the asymmetric hypervalent iodine field.....	284
Figure 4.4 Asymmetric catalytic α -sulfonylation reaction.....	285
Figure 4.5 Asymmetric fluorination of β -ketoesters.....	285
Figure 4.6 Examples of different strategies used to control stereochemistry.....	286
Figure 4.7 Structures representing helical chirality.....	287
Figure 4.8 Chiral supramolecular scaffold environmental control for <i>re</i> -face attack.....	289
Figure 4.9 Rhodium-based metal catalyst system.....	291
Figure 4.10 X-ray structure of $[\text{Cu}(\text{Ligand})(\text{MeCN})]^+$	292
Figure 4.11 Structures of D-(-)-lactate and L-(+)-lactate.....	299
Figure 4.12 Lactic acid-based C_2 -symmetric aryl iodide systems.....	299
Figure 4.13 L-Proline derived chiral aryl iodides developed by Zhdankin.....	302

Figure 4.14 L-Proline derived chiral iodonium ylide environment	303
Figure 4.15 Problems with <i>ortho</i> -ester oxidation	306
Figure 4.16 HFIP interaction with PIDA	310
Figure 4.17 ¹ H NMR (300 MHz, CDCl ₃) spectrum of (2R,2'R)-dibenzyl 2,2'-((2-iodo-5-(methoxycarbonyl)-1,3-phenylene)bis(oxy))dipropionate	333
Figure 4.18 ¹³ C NMR (75 MHz, CDCl ₃) spectrum of (2R,2'R)-dibenzyl 2,2'-((2-iodo-5-(methoxycarbonyl)-1,3-phenylene)bis(oxy))dipropionate	334
Figure 4.19 ¹ H NMR (300 MHz, CDCl ₃) spectrum of (S)-2-iodobenzyl 1-benzoylpyrrolidine-2-carboxylate	335
Figure 4.20 ¹³ C NMR (75 MHz, CDCl ₃) spectrum of (S)-2-iodobenzyl 1-benzoylpyrrolidine-2-carboxylate	336
Figure 4.21 ¹ H NMR (300 MHz, CDCl ₃) spectrum of dibenzyl 2,2'-((2-(diacetoxy-13-iodaneyl)-5-(methoxycarbonyl)-1,3-phenylene)bis(oxy)) (2R,2'R)-dipropionate	337
Figure 4.22 ¹³ C NMR (75 MHz, CDCl ₃) spectrum of dibenzyl 2,2'-((2-(diacetoxy-13-iodaneyl)-5-(methoxycarbonyl)-1,3-phenylene)bis(oxy)) (2R,2'R)-dipropionate	338
Figure 4.23 ¹ H NMR (300 MHz, CDCl ₃) spectrum of (2-(((benzoyl-L-prolyl)oxy)methyl)phenyl)-λ ³ -iodanediyl diacetate	339
Figure 4.24 ¹³ C NMR (75 MHz, CDCl ₃) spectrum of (2-(((benzoyl-L-prolyl)oxy)methyl)phenyl)-λ ³ -iodanediyl diacetate	340
Figure 4.25 ¹ H NMR (300 MHz, CDCl ₃) spectrum of ethyl (R)-2-(2-((2,2-dimethyl-4,6-dioxo-1,3-dioxan-5-ylidene)-λ ³ -iodaneyl)phenoxy)propanoate	341
Figure 4.26 ¹³ C NMR (75 MHz, CDCl ₃) spectrum of ethyl (R)-2-(2-((2,2-dimethyl-4,6-dioxo-1,3-dioxan-5-ylidene)-λ ³ -iodaneyl)phenoxy)propanoate	342
Figure 4.27 ¹ H NMR (300 MHz, CDCl ₃) spectrum of (2-(((benzoyl-L-prolyl)oxy)methyl)phenyl)-λ ³ -iodonium ylide	343
Figure 4.28 ¹³ C NMR (75 MHz, CDCl ₃) spectrum of (2-(((benzoyl-L-prolyl)oxy)methyl)phenyl)-λ ³ -iodonium ylide	344
Figure 4.29 ¹ H NMR (300 MHz, CDCl ₃) spectrum of diethyl 2,2'-((2-((2,2-dimethyl-4,6-dioxo-1,3-dioxan-5-ylidene)-λ ³ -iodaneyl)-1,3-phenylene)bis(oxy))(2R,2'R)-dipropionate	345
Figure 4.30 ¹³ C NMR (75 MHz, CDCl ₃) spectrum of diethyl 2,2'-((2-((2,2-dimethyl-4,6-dioxo-1,3-dioxan-5-ylidene)-λ ³ -iodaneyl)-1,3-phenylene)bis(oxy))(2R,2'R)-dipropionate	346
Figure 4.31 ¹ H NMR (300 MHz, CDCl ₃) spectrum of dibenzyl 2,2'-((2-((2,2-dimethyl-4,6-dioxo-1,3-dioxan-5-ylidene)-λ ³ -iodaneyl)-5-(methoxycarbonyl)-1,3-phenylene)bis(oxy))(2R,2'R)-dipropionate	347
Figure 4.32 ¹³ C NMR (75 MHz, CDCl ₃) spectrum of dibenzyl 2,2'-((2-((2,2-dimethyl-4,6-dioxo-1,3-dioxan-5-ylidene)-λ ³ -iodaneyl)-5-(methoxycarbonyl)-1,3-phenylene)bis(oxy))(2R,2'R)-dipropionate	348

List of Schemes

Scheme 1.1 Oxidation of iodobenzene to aryl- λ^3 -iodanes and aryl- λ^5 -iodanes	6
Scheme 1.2 Synthesis of (dichloriodo)benzene.....	7
Scheme 1.3 Synthesis of HVI compounds from iodobenzene	8
Scheme 1.4 Synthesis of (diacetoxy)arenes from iodoarenes	9
Scheme 1.5 Synthesis of (diacetoxy)iodoarenes using potassium peroxodisulfate	9
Scheme 1.6 Synthesis of (diacetoxy)iodoarenes using Selectfluor TM	9
Scheme 1.7 General coupling reactions for carbon-carbon bond formation.....	15
Scheme 1.8 Fundamental reactions of aryl- λ^3 -iodanes	16
Scheme 1.9 Reactions of aryl- λ^3 -iodanes with nucleophiles.....	17
Scheme 1.10 Dissociative and associative pathways for ligand exchange reactions.....	17
Scheme 1.11 Preparation of benzyltrimethylammonium tetrachloriodate 1.9	18
Scheme 1.12 Homolytic cleavage of aryl- λ^3 -iodanes.....	18
Scheme 1.13 Nucleophilic aromatic substitution by a SET process	19
Scheme 1.14 Resonance structures of general ylides.....	20
Scheme 1.15 Resonance structures of diazonium ylides.....	22
Scheme 1.16 Generation of metallocarbenes and free carbenes from diazo compounds	23
Scheme 1.17 General synthesis of iodonium ylides.....	26
Scheme 1.18 Synthesis of acyclic iodonium ylides.....	26
Scheme 1.19 Synthesis of dimedone iodonium ylide.....	27
Scheme 1.20 One-pot synthesis of Meldrum's acid iodonium ylide	27
Scheme 1.21 Synthesis of iodonium ylides using arylmetal compounds.....	28
Scheme 1.22 Resonance structures of iodonium ylides	29
Scheme 1.23 Metallocarbene reactions of iodonium ylides.....	33
Scheme 1.24 Metal-catalyzed asymmetric intramolecular C-H insertion reaction	34
Scheme 1.25 Thermal activation of acyclic vs cyclic iodonium ylides	35
Scheme 1.26 Thermally activated C-H insertion of acyclic iodonium ylides.....	35
Scheme 1.27 Thermally activated cyclopropanation of acyclic iodonium ylides with alkenes...	36
Scheme 1.28 Thermally activated aryl group migration in cyclic iodonium ylides.....	37
Scheme 1.29 Thermally activated ring contraction of iodonium ylides.....	38
Scheme 1.30 General scheme for halogen bonding activation of iodonium ylides with amines.	39
Scheme 1.31 Lewis acid activated reaction of acyclic iodonium ylides with aromatics	39
Scheme 1.32 Lewis acid-activated reaction mechanism of iodonium ylides with aromatics	40
Scheme 1.33 General ionic mode of activation of iodonium ylides with Brønsted acids.....	41
Scheme 1.34 Ionic mode of activation of iodonium ylides with Brønsted acids	41
Scheme 1.35 Ionic activation of iodonium ylides with Brønsted acids	42
Scheme 1.36 Ionic activation of cyclic iodonium ylides with acids	43
Scheme 1.37 Activation of iodonium ylides by SET	43
Scheme 1.38 Activation of acyclic iodonium ylides by SET.....	44
Scheme 1.39 Photochemical activation of acyclic iodonium ylides	45
Scheme 1.40 Formation of methylene carbene from diazomethane	46

Scheme 1.41 Irreversible and reversible carbene formation	47
Scheme 1.42 Capture of metallocarbenes by aryl iodides for iodonium ylide synthesis	47
Scheme 1.43 Stereochemical outcome of a singlet carbene reaction with a <i>cis</i> -alkene	48
Scheme 1.44 Stereochemical outcome of a triplet carbene reaction with a <i>cis</i> -alkene	49
Scheme 1.45 Metal-catalyzed metallocarbene formation from diazo compounds.....	50
Scheme 1.46 First alkylidene-metal complex (Schrock carbene)	51
Scheme 1.47 NHC generation from imidazolium salts	53
Scheme 1.48 Metallocarbene reactions of diazonium and iodonium ylides	53
Scheme 1.49 First cyclopropane synthesis by intramolecular Wurtz reaction.....	54
Scheme 1.50 Stereoselective preparation of acyclic hydrocarbon motifs	56
Scheme 1.51 General reactions of DA cyclopropanes	57
Scheme 1.52 Mechanism of Lewis acid-catalyzed 1,3-dipole formation in DA cyclopropanes .	58
Scheme 1.53 Historically important cyclopropanation reactions.....	61
Scheme 1.54 General [2+1] cycloaddition used in DA cyclopropane synthesis.....	62
Scheme 1.55 Cyclopropanation of diazonium ylides with alkenes	62
Scheme 1.56 Cyclopropanation of iodonium ylides with alkenes	63
Scheme 1.57 Metal-catalyzed cyclopropanation reaction of sulfonium ylides with alkenes.....	63
Scheme 1.58 Cycloadditions of nitrones with alkenes or cyclopropanes	67
Scheme 2.1 Phenol-stabilized iodonium ylide synthesis.....	70
Scheme 2.2 Phenol-stabilized iodonium ylide resonance structures.....	71
Scheme 2.3 Thermally induced 1,4-aryl migration of phenol-stabilized iodonium ylides	71
Scheme 2.4 Resonance structures of nitro-stabilized iodonium ylide.....	72
Scheme 2.5 Problems associated with MCIY synthesis.....	73
Scheme 2.6 Reactivity of $\text{PhI}(\text{OAc})_2$ with general methyl ketones	73
Scheme 2.7 Problem with undesired substitution instead of deprotonation.....	74
Scheme 2.8 Ochiai's acyl transfer method for MCIY synthesis	74
Scheme 2.9 Mechanism of MCIY formation by Ochiai's acyl transfer method.....	75
Scheme 2.10 Synthesis of ester precursor for Ochiai's MCIY synthesis.....	75
Scheme 2.11 Murphy group method for MCIY synthesis	76
Scheme 2.12 Possible mechanism of the Wittig-type reaction for MCIY synthesis.....	76
Scheme 2.13 Resonance structures of general MCIYs	77
Scheme 2.14 Conformational geometries of α -diazocarbonyl compounds.....	78
Scheme 2.15 Conformational geometries of MCIYs	79
Scheme 2.16 MCIY synthesis for NMR structural analysis.....	79
Scheme 2.17 Iodonium ylide trapping with DMSO for crystal structure analysis.....	80
Scheme 2.18 Iodonium ylide trapping with DMSO induced by UV light	80
Scheme 2.19 MCIY trapping with DMSO for potential crystal structural analysis.....	81
Scheme 2.20 Reaction of MCIY with aldehydes	81
Scheme 2.21 Umpolung reactivity of MCIYs in the presence of metals	82
Scheme 2.22 Cyclopropanation of nitro-stabilized iodonium ylides	83
Scheme 2.23 Reaction of nitro-stabilized iodonium ylides.....	83
Scheme 2.24 Mechanism of reaction of nitro-stabilized iodonium ylides	84
Scheme 2.25 Cyclopropanation of nitro-stabilized iodonium ylides	84

Scheme 2.26	Epoxidation reaction of MCIY with aldehydes	85
Scheme 2.27	Epoxidation reaction of MCIY with aldehydes	86
Scheme 2.28	Aziridination reaction of MCIYs with imines	87
Scheme 2.29	α -Alkylation reaction of MCIY with trialkylboranes	87
Scheme 2.30	Enantioselective [2,3]-rearrangement of iodonium ylides.....	88
Scheme 2.31	Metal-coordinated iodonium ylide intermediate.....	88
Scheme 2.32	Enantioselective [2,3]-sigmatropic rearrangement reaction	90
Scheme 2.33	General Wittig reaction of stabilized ylides with aldehydes	90
Scheme 2.34	Transition state (TS) for Wittig reactions with non-stabilized ylides.....	91
Scheme 2.35	Newman projection (NP) for Wittig reactions with non-stabilized ylides	91
Scheme 2.36	Mechanism of the Wittig reaction for non-stabilized ylides.....	92
Scheme 2.37	Reaction of phosphonium ylides with aryl- λ^3 -iodanes	92
Scheme 2.38	Reaction of phosphonium ylides with aryl- λ^3 -iodanes	93
Scheme 2.39	Mixed phosphonium-iodonium ylide resonance structures	93
Scheme 2.40	Mixed phosphonium-iodonium ylide synthesis from phosphonium ylides.....	94
Scheme 2.41	Synthesis of mixed phosphonium-iodonium ylide	94
Scheme 2.42	Synthesis of mixed phosphonium-iodonium ylide	94
Scheme 2.43	Synthesis of iodosoarenes from (dichloriodo)arenes.....	97
Scheme 2.44	Synthesis of iodosoarenes from (diacetoxyiodo)arenes.....	98
Scheme 2.45	Murphy group cyclopropanation reaction of MCIY.....	98
Scheme 2.46	Cyclopropanation of ethyl diazoacetate (EDA) with styrene	99
Scheme 2.47	Cross-coupling reactions between Wittig reagents and diazoesters	99
Scheme 2.48	Cyclopropanation of Wittig reagent with iodosobenzene and various alkenes	101
Scheme 2.49	Reaction of ortho-substituted iodosoarene with Wittig reagent	105
Scheme 2.50	Reaction of para-substituted iodosoarene with Wittig reagent.....	106
Scheme 2.51	Depolymerization of iodosobenzene (PhIO) _n with the use of salt additives.....	107
Scheme 2.52	Reactivity of Koser's reagent	109
Scheme 2.53	Reaction of Wittig reagent with iodine (V) iodoxybenzene	110
Scheme 2.54	Synthesis of soluble iodine (V) iodoxyarene.....	111
Scheme 2.55	Reaction of Wittig reagent with soluble iodine (V) iodoxyarene.....	111
Scheme 2.56	Cyclopropane synthesis attempt using trialkyl phosphoranes	112
Scheme 2.57	Mechanism of metalcarbene formation using Wittig reagents	113
Scheme 2.58	Pathways for cyclopropanation and dimerization products.....	113
Scheme 2.59	Alternative mechanism for Wittig-type reaction	114
Scheme 2.60	Optimal conditions for cyclopropanation reaction of MCIYs	115
Scheme 2.61	Intramolecular cyclopropanation of diazo	118
Scheme 2.62	Synthesis of Wittig reagent for intramolecular cyclopropanation	119
Scheme 2.63	Intramolecular cyclopropanation of in situ generated MCIY	119
Scheme 2.64	O-H Insertion reactions of diazos with alcohols.....	120
Scheme 2.65	Metalcarbene generation from diazos or Wittig reagents.....	121
Scheme 2.66	Reversible interaction of aryl iodide with metalcarbene	121
Scheme 2.67	Alcohols tested in O-H insertion reactions	122
Scheme 2.68	Reaction of Wittig reagent with iodosoarene and alcohols	122

Scheme 3.1 Photochemical activation of diazos with LED	153
Scheme 3.2 Photochemical cyclopropanation of aryldiazoacetate with styrene	153
Scheme 3.3 Photochemically-induced reactions of diazos using LED	154
Scheme 3.4 Visible light photoredox reaction of phosphonium ylides with alkenes.....	155
Scheme 3.5 Photocatalytic insertion of sulfonium ylides into C-H bonds.....	156
Scheme 3.6 Photoredox multicomponent cyclization reaction of sulfonium ylides	156
Scheme 3.7 Photochemical activation of acyclic iodonium ylides	158
Scheme 3.8 Photochemical cyclopropanation of acyclic iodonium ylides with alkenes	159
Scheme 3.9 Photo-dimerization intermediates of acyclic iodonium ylides	160
Scheme 3.10 Activation of iodonium ylides with blue light from LED	160
Scheme 3.11 First photochemical transylidation reaction of iodonium ylides	161
Scheme 3.12 Transylidation reactions under photochemical activation	162
Scheme 3.13 Photochemical [3+2] cycloaddition of an iodonium ylide with styrene.....	163
Scheme 3.14 Photochemical [3+2] cycloaddition of iodonium ylides with alkenes.....	163
Scheme 3.15 Photochemical induced cycloaddition reactivity of iodonium ylides.....	164
Scheme 3.16 Photochemical [2+1] cycloaddition of an iodonium ylide with cyclohexene	164
Scheme 3.17 Photochemical [2+2] cycloaddition	165
Scheme 3.18 Proposed photochemical [2+2] cycloaddition of iodonium ylides	166
Scheme 3.19 HOMO to LUMO photoexcitation of iodonium ylide 3.16a	170
Scheme 3.20 Reaction using photoreactor #1	175
Scheme 3.21 Cyclopropanation reaction using photoreactor #2	176
Scheme 3.22 Cyclopropanation reaction using photoreactor #4	182
Scheme 3.23 Synthesis of soluble Meldrum's acid iodonium ylide derivative	192
Scheme 3.24 Synthesis of soluble iodonium ylide derivative.....	192
Scheme 3.25 Photochemical reaction of trifluoromethyl ketone-stabilized iodonium ylide	193
Scheme 3.26 Failed cyclopropanation reaction with SO ₂ CF ₃ -stabilized iodonium ylide	194
Scheme 3.27 Possible photo-induced dimerization pathway of acyclic iodonium ylides.....	195
Scheme 3.28 Light-induced cyclopropanation reaction of iodonium ylides with alkenes.....	196
Scheme 3.29 Chemoselective cyclopropanation of 3.16j with O-H containing alkene.....	198
Scheme 3.30 Failed cyclopropanation of 3.16j with α -methyl styrene	198
Scheme 3.31 Failed reactions of iodonium ylides with carbonyl-containing alkenes	199
Scheme 3.32 Failed reactions of iodonium ylides with carbonyl-containing alkenes	199
Scheme 3.33 Regio-selective pathways for dihydrofuran formation	201
Scheme 3.34 Cyclopropanation of iodonium ylide with <i>trans</i> - β -methylstyrene	202
Scheme 3.35 Cyclopropanation of iodonium ylide with <i>cis</i> - β -methylstyrene	203
Scheme 3.36 Photocatalytic (<i>E</i>) to (<i>Z</i>) isomerization of alkenes by visible light	205
Scheme 3.37 Light-induced [2+2] cycloaddition between ketones and alkenes.....	207
Scheme 3.38 Photo-induced formal [2+2] asynchronous cycloaddition reaction mechanism...	208
Scheme 3.39 Free carbene generation from iodonium ylides	209
Scheme 3.40 One-pot cyclopropanation or dihydrofuran reaction	211
Scheme 3.41 Rearrangement reaction of iodonium ylides generated <i>in situ</i>	212
Scheme 3.42 Rearrangement reaction of iodonium ylide with allylic sulfide	213
Scheme 3.43 Cyclopropanation vs. rearrangement reaction of iodonium ylides	213

Scheme 3.44 Cyclopropanation vs. rearrangement reaction of iodonium ylides	214
Scheme 3.45 Light-activated oxidation of allylic alcohols with iodonium ylides	215
Scheme 3.46 Mechanism for oxidation of allylic alcohols with iodonium ylides	216
Scheme 3.47 Alternative mechanism for oxidation of allylic alcohols with iodonium ylides...	217
Scheme 3.48 Mechanism for oxidation of allylic alcohols with iodonium ylides	217
Scheme 3.49 Control reaction of Meldrum's acid iodonium ylide with cinnamyl alcohol	218
Scheme 3.50 Non-oxidative reaction of iodonium ylides with primary alcohols	218
Scheme 3.51 Failure of O-H insertion of iodonium ylides under blue light	219
Scheme 3.52 Failure of O-H insertion of iodonium ylides at 365 nm	219
Scheme 3.53 Synthesis of PhI=NTs	220
Scheme 3.54 Light-mediated aziridination reaction of iminoiodanes and styrene	220
Scheme 3.55 One-pot light-mediated aziridination reaction	220
Scheme 3.56 Synthesis of iodonium ylide for transylidation reaction	221
Scheme 3.57 Blue light-mediated transylidation reaction	222
Scheme 3.58 Failure of metal-mediated transylidation reaction using iodonium ylide	222
Scheme 3.59 Failure of metal-mediated transylidation reaction using diazo	223
Scheme 3.60 Mechanism of visible light-mediated transylidation reaction	223
Scheme 3.61 Conversion of excited state diradical species to ground state iodonium ylide	224
Scheme 4.1 Ishihara's 1st and 2nd generation precatalytic systems	288
Scheme 4.2 Ciufolini's precatalytic system	289
Scheme 4.3 Metal-catalyzed asymmetric cyclopropanation of iodonium ylides with alkenes ..	290
Scheme 4.4 Metal-catalyzed asymmetric cyclopropanation of iodonium ylides with alkenes ..	292
Scheme 4.5 Stereochemical model for Cu-catalyzed cyclopropanation of substituted alkenes.	293
Scheme 4.6 Metal-catalyzed asymmetric cyclopropanation of iodonium ylides with alkenes ..	294
Scheme 4.7 Racemic metal-free cyclopropanation reaction	295
Scheme 4.8 Asymmetric cyclopropanation of acyclic iodonium ylides with alkenes	296
Scheme 4.9 Synthesis of chiral cyclic iodonium ylide	296
Scheme 4.10 Asymmetric cyclopropanation of cyclic iodonium ylides with alkenes	296
Scheme 4.11 Synthesis of chiral iodosoarene	297
Scheme 4.12 N-Methylation of chiral system	297
Scheme 4.13 Synthesis of chiral tetracetate	298
Scheme 4.14 Synthesis of chiral aryl iodide	300
Scheme 4.15 Synthesis of 2-iodobenzene-1,3-diol from resorcinol	301
Scheme 4.16 Synthesis of methyl 3,5-dihydroxy-4-iodobenzoate	301
Scheme 4.17 Synthesis of chiral aryl iodides	302
Scheme 4.18 Synthesis of L-proline derived aryl iodide	304
Scheme 4.19 Synthesis of general chiral aryl iodide diacetates	304
Scheme 4.20 Synthesis of chiral aryl iodide diacetate	305
Scheme 4.21 Synthesis of chiral aryl iodide diacetate	305
Scheme 4.22 Synthesis of chiral aryl iodide diacetate	305
Scheme 4.23 Synthesis of chiral aryl iodide diacetate	306
Scheme 4.24 Synthesis of L-proline derived chiral aryl iodide diacetate	306
Scheme 4.25 Problems with <i>ortho</i> -ester oxidation	307

Scheme 4.26 General synthesis of chiral cyclic iodonium ylides	307
Scheme 4.27 Synthesis of chiral cyclic iodonium ylide.....	308
Scheme 4.28 Synthesis of chiral cyclic iodonium ylide.....	309
Scheme 4.29 Synthesis of chiral iodonium ylide	311
Scheme 4.30 Synthesis of chiral iodonium ylide	312
Scheme 4.31 Synthesis of racemic cyclopropane standards	312
Scheme 4.32 Cyclopropanation of chiral iodonium ylide using blue LEDs	315
Scheme 4.33 Cyclopropanation of chiral iodonium ylide using blue LEDs	315
Scheme 4.34 Efficient cyclopropanation of chiral iodonium ylide using blue LEDs	316
Scheme 4.35 One-pot procedure for chiral cyclopropane synthesis	317

List of Tables

Table 1.1 Electronegativity values and properties of the halogens.....	2
Table 1.2 Fischer and Schrock carbene properties.....	52
Table 2.1 Catalyst screening in cyclopropanation reaction of MCIY.....	100
Table 2.2 Screening of conditions for cyclopropanation reaction.....	103
Table 2.3 Screening of catalysts for cyclopropanation reaction.....	104
Table 2.4 Disproportionation rate of soluble iodosoarene.....	104
Table 2.5 Optimization of the cyclopropanation reaction.....	106
Table 2.6 Effects of additives on the cyclopropanation reaction.....	108
Table 2.7 The use of PIDA for the generation for cyclopropanation reaction.....	109
Table 3.1 Optimization studies of metal-free photocyclopropanation reaction.....	145
Table 3.2 Frequency, wavelength, and energy units of common light sources.....	146
Table 3.3 Wavelengths and calculated energies of colours used in a RGB LED strip.....	150
Table 3.4 Partial charges determined through computational analysis.....	169
Table 3.5 Light-intensity data for photoreactor #3.....	178
Table 3.6 Photoreactor #3 cyclopropanation using different colours.....	180
Table 3.7 Cyclopropanation control reactions.....	183
Table 3.8 Optimization of the cyclopropanation reaction using photoreactor #4.....	184
Table 3.9 Cyclopropanation of 3.16j with styrene using violet and blue LED.....	186
Table 3.10 Cyclopropanation of iodonium ylides containing different aryl groups.....	187
Table 3.11 Cyclopropanation reaction with different carbonyl-based iodonium ylides.....	189
Table 3.12 Cyclopropanation of acyclic iodonium ylides.....	193
Table 3.13 One-pot cyclopropanation reaction with dimedone.....	209
Table 3.14 One-pot cyclopropanation reaction with Meldrum's acid.....	210
Table 3.15 One-pot cyclopropanation reaction of α -aryl ester with styrene.....	211
Table 3.16 Light-activated oxidation of allylic alcohols with iodonium ylide.....	215
Table 4.1 Oxidation of chiral aryl iodide.....	295
Table 4.2 Synthesis of C_2 -symmetric chiral iodonium ylides.....	311
Table 4.3 Chiral HPLC data from racemic standards.....	313
Table 4.4 Cyclopropanation of chiral iodonium ylide using blue LEDs.....	313
Table 4.5 Chiral HPLC data from cyclopropanation reaction.....	314
Table 4.6 Chiral HPLC data from cyclopropanation reaction.....	316
Table 4.7 Chiral HPLC data from cyclopropanation reaction.....	317

List of Abbreviations

3c-4e	Three centre-four electron
acac	Acetylacetonate
Ac	Acetyl
Ar	Aryl Ring
ATR FTIR	Attenuated Total Reflection Fourier Transform Infrared
Bn	Benzyl
Boc	<i>tert</i> -Butyloxycarbonyl
Bu	Butyl
^t Bu	<i>tert</i> -Butyl
C	Celsius
calcd	Calculated
d	Doublet
DA	Donor-Acceptor
DCE	1,2-Dichloroethane
DCM	Dichloromethane
dd	Doublet of Doublets
DIAD	Diisopropyl Azodicarboxylate
DMF	Dimethylformamide
DMSO	Dimethyl Sulfoxide
E	Electrophile
EDG	Electron Donating Group
<i>ee</i>	Enantiomeric Excess
equiv	Molar Equivalent
ESI	Electrospray Ionization
Et	Ethyl
Et ₂ O	Diethyl Ether
EtOAc	Ethyl Acetate
EWG	Electron Withdrawing Group
g	Gram

GC-MS	Gas Chromatography-Mass Spectrometry
h	Hour
Hex	Hexane
hfacac	Hexafluoroacetylacetonate
HFIP	Hexafluoroisopropanol
HMDSO	Hexamethyldisiloxane
HOMO	Highest Occupied Molecular Orbital
HPLC	High-Performance Liquid Chromatography
HRMS	High-Resolution Mass Spectra
HTIB	Hydroxy(phenyl)iodo Tosylate (Koser's Reagent)
HVI	Hypervalent Iodine
Hz	Hertz
<i>in situ</i>	In Reaction Mixture
IR	Infrared Spectroscopy
ISC	Intersystem Crossing
IUPAC	International Union of Pure and Applied Chemistry
<i>J</i>	Coupling Constant
L	Ligand
LED	Light-Emitting Diode
LUMO	Lowest Unoccupied Molecular Orbital
m	Multiplet
<i>m</i>	Meta
MCIY	Monocarbonyl Iodonium Ylide
<i>m</i> CPBA	meta-Chloroperoxybenzoic Acid
Me	Methyl
mg	Milligram
MHz	Megahertz
min	Minute
mL	Millilitre
mmol	Millimole
MO	Molecular Orbital

mp	Melting Point
MS	Mass Spectrometry
m/z	Mass to Charge Ratio
nb	Nonbonding
NMR	Nuclear Magnetic Resonance
Nu	Nucleophile
<i>o</i>	Ortho
OTf	Trifluoromethanesulfonate
<i>p</i>	Para
Ph	Phenyl
PIDA	Phenyliodine Diacetate
PIFA	Phenyliodine bis(Trifluoroacetate)
ppm	Parts per Million
Pr	Propyl
^{<i>i</i>} Pr	<i>iso</i> -Propyl
q	Quartet
R	Any Alkyl Group
R _f	Retention Factor
RGB	Red Green Blue
rt	Room Temperature
s	Singlet
SET	Single-Electron-Transfer
SOMO	Singly Occupied Molecular Orbital
t	Triplet
T	Temperature
td	Triplet of Doublets
TDDFT	Time-Dependent Density Functional Theory
temp	Temperature
tfacac	Trifluoroacetylacetonate
TFE	Trifluoroethanol
THF	Tetrahydrofuran

TLC	Thin Layer Chromatography
Ts	Tosyl
UV	Ultraviolet

List of Symbols

\AA	Angstrom
\sim	Approximately
δ	Chemical Shift
$^{\circ}$	Degrees
$=$	Equal to
ν	Frequency
ρ	Hammett Reaction Constant
Δ	Heat
μ	Micro
π	Pi Bond
π^*	Pi Anti-bond
h	Planck's Constant
Ψ	Pseudorotation
σ	Sigma Bond
σ^*	Sigma Anti-bond
λ	Wavelength

Quote

*“And you will come to find
that we are all one mind
capable of all that’s imagined
and all conceivable”*

Maynard James Keenan

Chapter 1: Introduction

The use of hypervalent iodine (HVI) reagents in synthetic organic chemistry was introduced over 100 years ago, experiencing a steady climb in the amount of reactions and applications discovered over these years. HVI reagents are now routinely relied upon for organic transformations due to their beneficial chemical properties, reacting in a similar way to metals such as chromium, lead, mercury, and osmium, but without the environmental and toxic consequences. This chapter serves as an introduction to the chemistry of HVI reagents, including applications in the synthesis of cyclopropane ring systems.

The chemistry learned throughout the chapters in this thesis have resulted in new procedures to construct compounds such as cyclopropanes and answer mechanistically related questions into how these compounds form. Experimental observations have shown repeating patterns of reactivity that potentially could be adjusted to include the incorporation of new reaction types, which will hopefully benefit the synthetic community, and play an important role in the discovery of new reactions to come.

1.1 Iodine

Iodine was discovered in France in 1811 by Bernard Courtois (1777-1838) and was named by Joseph Louis Gay-Lussac (1778-1850) in 1813.¹ Despite some debate, Courtois is acknowledged as the true discoverer of iodine, and established a career in the manufacturing of iodine and iodine-based salts starting in 1822. The story of how iodine was discovered came from a shortage of gun powder during the Napoleonic wars in France, in the early 1800's.² The long 15-year war (1800-1815) caused strict government regulations, resulting in a shortage of gun powder which was obtained by harvesting the potassium nitrate from wood ash.³ A cheap alternative source for potassium salts was discovered to come from the ash of seaweed. While harvesting large amounts of seaweed, it was discovered that iodine was present in the raw material of the processed seaweed.

Iodine is an essential component of thyroid hormones which are known to regulate many important biochemical reactions within the human body and therefore 0.150 μg of iodine is required daily for a typical adult.⁴ Even though iodine is naturally abundant and primarily

located in the oceans, not all of Earth's population live close to shorelines or have access to food originating from the oceans.⁵ Approximately 40% of the Earth's population is at risk for iodine deficiency, which has been linked to goiter, hypothyroidism, intellectual disabilities, and in some cases, cancer.⁶ Some thyroid diseases are often attributed to iodine deficiencies in the diet.⁷ The involvement of iodine within biological systems illustrates the element's important properties, which can be further examined by understanding its unique structural features.

Iodine belongs to group VII elements on the periodic table known as halogens, which contain seven valence electrons, requiring one more electron to form a full octet, consisting of five chemically related elements shown in **Table 1.1**.

Table 1.1 Electronegativity values and properties of the halogens

Halogen	Molecular Formula	Electronegativity (Pauling)	Electronegativity (Allen)	Covalent Radius (pm)
Fluorine	F ₂	3.98	4.193	71
Chlorine	Cl ₂	3.16	2.869	99
Bromine	Br ₂	2.96	2.685	114
Iodine	I ₂	2.66	2.359	133
Astatine	At	2.2	2.39	-

Due to their relatively weak intermolecular forces fluorine and chlorine form “elemental gases” while bromine is a reddish-brown liquid, and iodine is a dark purple solid at room temperature. Astatine is extremely rare as it is radioactive and degrades spontaneously and is different from the rest of the halogens in that it has never been proven to exist in a diatomic state, while the other halogens can form homonuclear diatomic molecules.

Iodine is the largest, most electropositive, and most polarizable of the stable halogens.⁸ The highly polarizable nature of iodine makes it unique from the other halogens, and this difference is exploited in organic synthesis, where iodine is incorporated into many kinds of organic molecules and reagents.

A very common occurrence of iodine in organic chemistry is alkyl halides and aryl halides. The popular Grignard reaction makes use of alkyl and aryl halides and has been a popular tool for creating carbon-carbon bonds for the past 100 years. Alkyl and aryl halides are examples of organic molecules containing iodine, which are generally referred to as organoiodine compounds.

The link between iodine and its oxidation states is of great importance to being able to fully understand its properties and reactivity. Iodine is known to form chemical compounds in which the iodine has an oxidation state of -1, 0, +1, +3, +5, and +7. Assigning the oxidation states of iodine correctly is a matter of tremendous importance and has sometimes been the victim of inconsistencies, causing confusion, and making the entire situation hard to understand. This is the result of two different sets of electronegativity values, one is the Pauling scale, and the other is the Allen scale. Carbon is described as having an oxidation state of 2.55 (Pauling) or 2.544 (Allen) depending on what scaling system is used, while iodine has values of 2.66 (Pauling) or 2.359 (Allen) and therefore if electronegativity value scales are not used consistently, then errors in assigning oxidation states can occur due to the values being extremely close to one another. To stay consistent in this thesis and follow oxidation states described by the IUPAC system, oxidation states will be based on the Allen electronegativity scale. Using the Allen scale, iodine will have an oxidation state of +1 in monovalent iodine compounds such as iodobenzene.

1.2 Hypervalent Iodine (HVI)

To discuss the topic of hypervalent iodine, the concept of hypervalency must first be introduced, defined, and explained. Jeremy Musher introduced the term hypervalency in 1969 which was originally defined as elements in Group V-VIII of the periodic table that have the ability to exist in a higher energy valency form, even though they have a lower energy valency form and are not found in this lower energy level.⁹ This implies that the higher energy valency state which the element currently occupies is not the element's most stable chemical valence form when compared to their lower energy ground state, which is more stable. The International Union of Pure and Applied Chemistry (IUPAC) defined hypervalency as the ability of an atom in a molecular entity to expand its valence shell beyond the limits of the Lewis octet rule.¹⁰ The difference between Musher's definition of hypervalency and IUPAC's is that Musher's classification is based on oxidation state, while the IUPAC's definition is based on the number of valence electrons. Therefore, to understand and explain situations involving compounds containing hypervalent iodine atoms, one must analyze the oxidation state and number of valence electrons in the iodine atom within a given molecule.

An explanation as to why iodine can form stable hypervalent bonds stems from it being the most polarizable of the halogens. This highly polarizability feature of iodine is critical for enabling hypervalent bonding according to the most widely accepted model known as the Rundle-Pimentel model, and will be discussed in greater detail in a following section.¹¹ Other properties that make iodine capable of forming hypervalent bonds is its ability to exist in a range of oxidation states as shown in **Figure 1.1**.

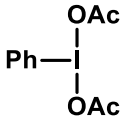
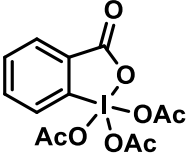
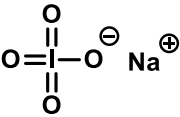
Non-Hypervalent Iodine			Hypervalent Iodine		
-1	0	+1	+3	+5	+7
K—I	I—I	Ph—I			
Potassium iodide	Iodine	Iodobenzene	(Diacetoxyiodo)benzene	Dess-Martin periodinane	Sodium periodate

Figure 1.1 Oxidation states and examples of iodine in molecules

Another property of iodine that enables the formation of hypervalent compounds is the ability to form stable products in which the iodine atom has an expanded octet, containing up to 14 valence electrons. Naming systems have been developed to categorize the different states of hypervalency in iodine, including the Martin-Arduengo designation and the lambda-convention.

The Martin-Arduengo *N-X-L* designation is a classification system used for polyvalent iodine species, and assignments are made using the *N-X-L* letters.¹² *N* is the number of valence electrons formally assignable to the valence shell of the central atom, *X*, either as unshared pairs of electrons or as pairs of electrons in the sigma bonds joining a number, *L*, of ligands to the atom *X*. For example, 10-I-3 describes a molecule with 10 valence electrons around an iodine atom, and this iodine atom has 3 ligands attached to it. The Martin-Arduengo *N-X-L* designation is used in **Figure 1.2** to classify four different general structural types of HVI compounds.

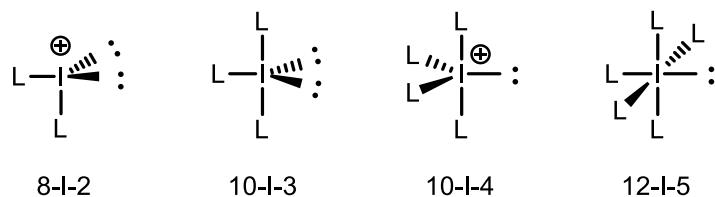


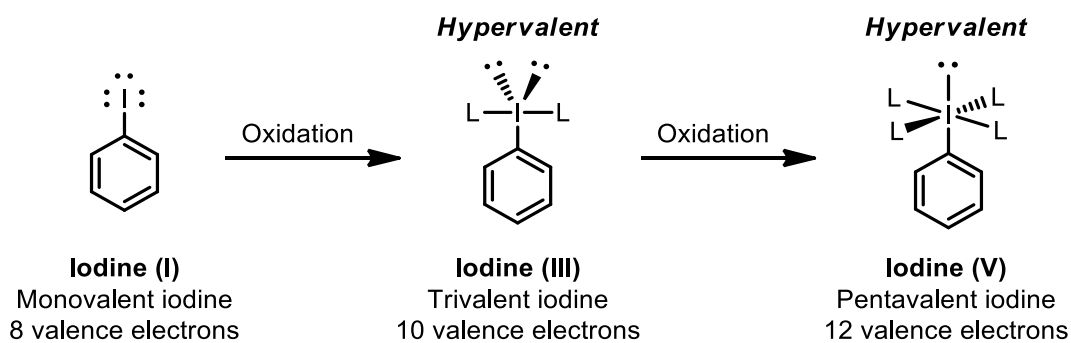
Figure 1.2 Martin-Arduengo N-X-L designation

The lambda convention is a nomenclature system used to describe HVI compounds using a λ^n notation. This style of naming uses n to represent the oxidation state of the iodine atom within the molecule, which also states the nonstandard bond number. The most common example of this is aryl- λ^3 -iodanes, which refer to the class of HVI compounds in which iodine has an oxidation state of +3. Popular named reagents that are examples of aryl- λ^3 -iodanes include Koser and Togni reagents. In these compounds, the iodine can also be called trivalent or iodine (III), and the whole molecule can be referred to as an iodane or iodinane.

When an iodine atom exists in an oxidation state of +5, it can be referred to as pentavalent or iodine (V). When a molecule contains iodine in an oxidation state of +5, it is known as a λ^5 -iodane using the lambda convention, and can also be called a periodane or periodinane. A popular named reagent that is an example of a λ^5 -iodane is Dess-Martin periodinane, which is used frequently in oxidation reactions. Examples of λ^5 -iodanes are relatively rare in the literature when compared to the vast amounts of λ^3 -iodanes.

Iodine in an oxidation state of +7 is very rare and only exists in inorganic molecules, for example, iodine heptafluoride (IF_7) and sodium periodate (NaIO_4). The synthesis of organic derivatives of iodine (VII) have been attempted, but to date no successful λ^7 -iodanes have ever been created.¹³

The oxidative transformation of iodine (I) to iodine (III), followed by another oxidation to iodine (V) is shown in **Scheme 1.1** illustrating a general approach of how iodoarenes are typically converted into hypervalent aryl- λ^3 -iodanes and hypervalent aryl- λ^5 -iodanes.



Scheme 1.1 Oxidation of iodobenzene to aryl- λ^3 -iodanes and aryl- λ^5 -iodanes

Examples of HVI compounds that encompass the three oxidation states (+3, +5, +7) that classify iodine as a hypervalent atom are shown in **Figure 1.3**. In addition to the oxidation states, the number of valence electrons in iodine are also stated for each of the three sections and lone pairs of electrons are drawn in the structures to emphasize an expanded octet.

Iodine (III) 10 Valence electrons	Iodine (V) 12 Valence electrons	Iodine (VII) 14 Valence electrons
 Iodobenzene dichloride	 Iodosobenzene	 Iodoxybenzene
 Diphenyliodonium chloride	 Togni's Reagent	 Dess-Martin periodinane
		 Sodium periodate
		<p style="text-align: center;">IF₇ Iodine heptafluoride</p> <p style="text-align: center;">Only Inorganic Examples</p>

Figure 1.3 Examples of HVI compounds with different oxidation states of iodine

As stated earlier, there is a vast amount of λ^3 -iodanes in the literature and they are used frequently in modern day organic synthesis for various oxidative transformations. Because there

are a significant range of different structural types of λ^3 -iodanes, generic structures of these different compounds are shown in **Figure 1.4**.

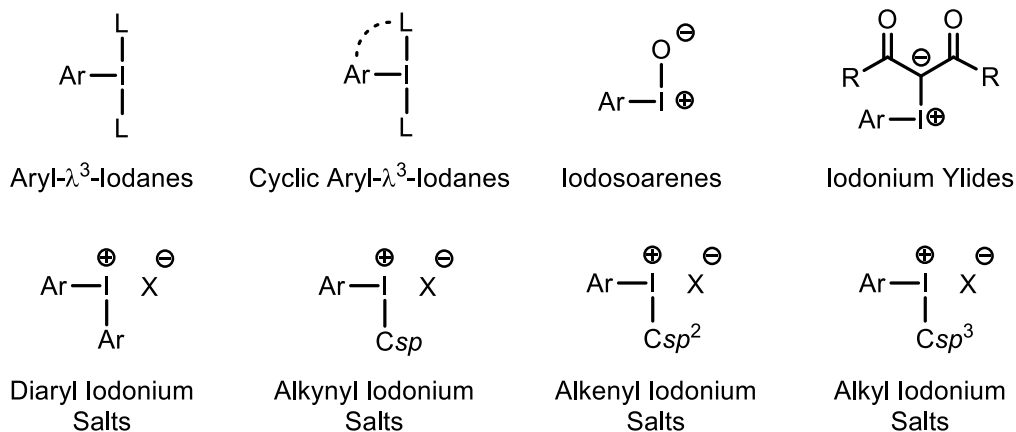
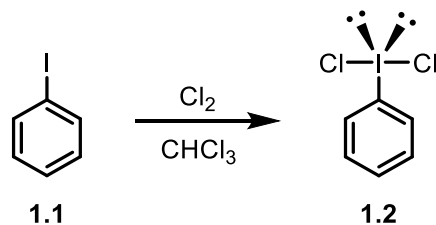


Figure 1.4 Types of HVI compounds containing iodine (III)

1.2.1 Synthesis of HVI Compounds

The very first synthesis of a HVI compound was reported by German chemist Willgerodt in 1886.¹⁴ Willgerodt discovered a process that turns monovalent iodobenzene (**1.1**) into hypervalent (dichloriodo)benzene (**1.2**) by bubbling Cl_2 into the solution, as shown in **Scheme 1.2**. This inexpensive, simple process is still used to this day, over 100 years since its discovery, for the synthesis of (dichloriodo)arenes.

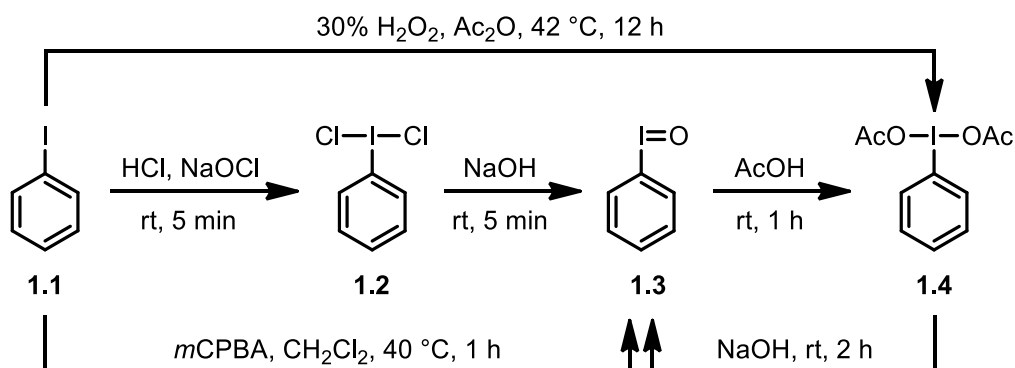


Scheme 1.2 Synthesis of (dichloriodo)benzene

Oxidation of aryl iodides with an appropriate oxidant is one of the most common and straightforward approaches for the synthesis of aryl- λ^3 -iodanes. Both EDGs and EWGs on the

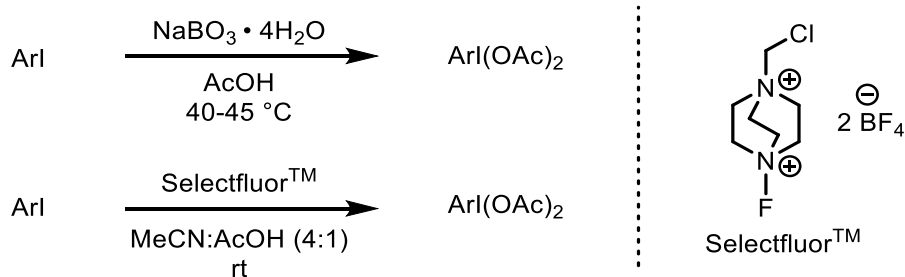
aryl iodide can be tolerated under the appropriate oxidation conditions, which makes it the method of choice for many chemists and was used primarily in this thesis to obtain the required aryl- λ^3 -iodanes.

Common methods used routinely by chemists to synthesize HVI compounds starting from monovalent iodobenzene (**1.1**) are shown in **Scheme 1.3**. The synthesis of (dichloroiodo)benzene (**1.2**) from iodobenzene (**1.1**) was reported by Zhang and Zhao¹⁵ by mixing hydrochloric acid with household bleach at room temperature but can also be achieved using Willgerodt's method with Cl_2 . Conversion of (dichloroiodo)benzene (**1.2**) into iodosobenzene (**1.3**) can easily be performed by simply adding a solution of NaOH and stirring at room temperature. Iodosobenzene (**1.3**) can then be converted into (diacetoxyiodo)benzene (**1.4**) with the straightforward addition of acetic acid.



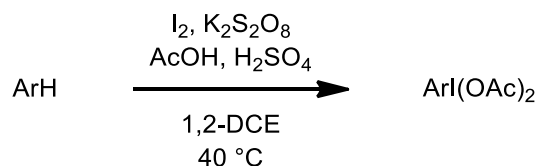
Scheme 1.3 Synthesis of HVI compounds from iodobenzene

The synthesis of (diacetoxyiodo)benzene (**1.4**) from iodobenzene (**1.1**) can be accomplished by multiple methods other than the acetic anhydride, hydrogen peroxide method shown above. Additional methods to perform this equivalent step include using sodium perborate¹⁶ or SelectfluorTM reagents as shown in the following **Scheme 1.4**.¹⁷ There are still other known procedures to accomplish the same oxidation reactions for the formation of (diacetoxyiodo)arenes, but the methods listed here are the more common ones, and were used to create the majority of (diacetoxyiodo)arenes in this thesis.



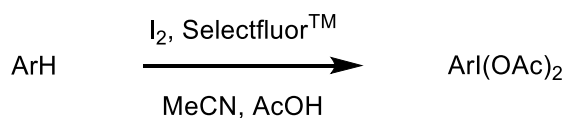
Scheme 1.4 Synthesis of (diacetoxy)arenes from iodoarenes

Alternative methods for synthesizing (diacetoxy)iodoarenes exist and include the direct introduction of the iodanyl group onto the arene. The main difference in this methodology is the iodine is installed onto the arene ring presumably through an oxidative iodination, which is then followed by an oxidative diacetoxylation, which occurs *in situ*, to yield the (diacetoxy)iodoarene. This methodology was found to be effective when using potassium peroxodisulfate as an oxidant as shown in **Scheme 1.5**.¹⁸



Scheme 1.5 Synthesis of (diacetoxy)iodoarenes using potassium peroxodisulfate

The use of iodine and SelectfluorTM is also effective in this type of oxidative chemistry as shown in **Scheme 1.6**.¹⁹ This chemistry is beneficial because in a single step an unfunctionalized arene can be converted into a (diacetoxy)iodoarene, instead of performing the aromatic iodination followed by diacetate formation as two separate steps. Although this methodology does have benefits, this direct installment of an iodanyl group onto an arene was not used in this thesis because it is not a regioselective reaction, giving unwanted mixtures of (diacetoxy)iodoarene isomers.



Scheme 1.6 Synthesis of (diacetoxy)iodoarenes using SelectfluorTM

1.2.2 Structure and Bonding of HVI Compounds

There have been different attempts to explain the structure and bonding in hypervalent iodine systems. Two models that have been proposed are described below and are differentiated by their descriptions as being qualitative or quantitative-based models.

A qualitative model for the bonding in organoiodine (III) compounds was proposed by utilizing a set of $5sp^2$ - $5pd$ hybrid orbitals for the iodine atom. In the equatorial plane there are a total of three sp^2 orbitals. One of the sp^2 orbitals would be singly occupied and bind to an equatorial ligand, the other two sp^2 hybrid orbitals would be doubly occupied and non-bonded. The two axial ligands are covalently bound to a pair of singly occupied pd hybrids, existing perpendicular to the equatorial plane and creating the T shape. The geometry of this qualitative model is trigonal bipyramidal and is shown in **Figure 1.5**.



Figure 1.5 Qualitative bonding model in organoiodine (III) compounds

An alternative quantitative model that involves the use of hypervalent bonds in which the iodine is bound to one equatorial carbon ligand and two axial ligands. The iodine is described as not being hybridized at all. The carbon ligand is bound by a normal two-electron covalent bond to the singly occupied $5p$ orbital in iodine. The other two ligands are attached to the double occupied $5p$ orbital of the iodine which results in a linear three-centred four-electron bond [3c-4e] as seen in **Figure 1.6**. The unshared electron pairs are described as not residing in $5s$ and $5p$ orbitals on iodine. This model is also in agreement with Moriarty, who described the bonding in a HVI molecule such as $C_6H_5ICl_2$ to use essentially pure p orbitals in the linear Cl-I-Cl system.²⁰ This bonding description was referred to as a [3c-4e] bond with two electrons from the doubly occupied $5p$ orbital on iodine and one electron from each of the $3p$ orbitals on the chlorine atoms.

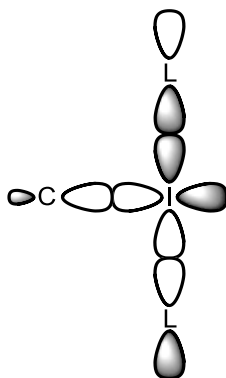


Figure 1.6 Hypervalent bonding model for aryl- λ^3 -iodanes

The idea behind the [3c-4e] bonding model was proposed independently by both Pimentel²¹ and Rundle^{11(a)} in 1951 and is based on molecular orbital (MO) theory. Orbital overlap occurs between a 5p orbital on iodine with the σ orbitals of the two ligands, creating a set of three σ molecular orbitals. The three molecular orbitals generated are one bonding (σ), one nonbonding (nb), and one antibonding (σ^*) orbital, and a total of four electrons occupy these. Filling in electrons from the lowest energy level and upwards, two electrons occupy the lower level (bonding orbital), and two electrons occupy the middle level (nonbonding orbital), leaving the top level (antibonding) void of electrons.

Each iodine-ligand bond has a bond order of 0.5 which makes these bonds elongated and weaker than a regular covalent bond. The whole ligand-iodine-ligand triad system is neutral overall but is highly polarized with greater electron density occurring on the ligands, creating an electrophilic iodine at the centre. The node in the nonbonding energy level is located directly in the centre, where iodine is, with zero electron density being contributed from the two electrons in this middle energy level. The [3c-4e] bonding model is currently the most popular representation of hypervalent bonding displayed in HVI reagents and is shown in **Figure 1.7**.

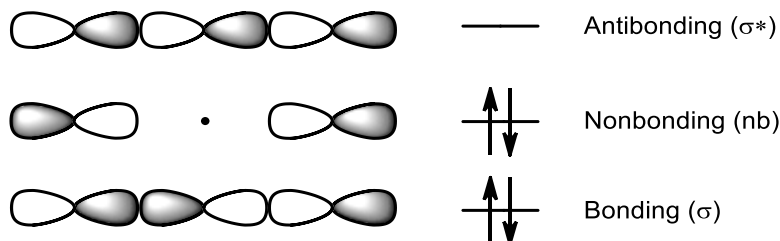


Figure 1.7 Molecular orbitals of the [3c-4e] hypervalent bonding model

With regards to the structure of aryl- λ^3 -iodane systems, in terms of the orientation around the HVI centre, there exist a counter-intuitive alignment of orbitals. Spatial orientation of the ligands in acyclic aryl- λ^3 -iodanes with respect to the aromatic ring are not in an energetically favourable orientation in the solid state, as shown in **Figure 1.8**.

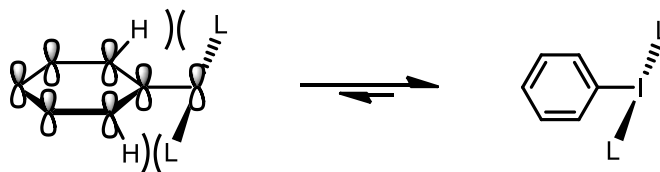


Figure 1.8 Orientation of ligands in space in aryl- λ^3 -iodanes

In acyclic aryl- λ^3 -iodanes, steric interactions between the ligands on iodine and the *ortho* carbon-hydrogen bonds of the aryl ring are apparently large enough to favour a conformation in which the aromatic nucleus is nearly orthogonal to the orientation of the linear L-I-L triad.²² Conjugative overlap between the *p*-orbitals of the benzene ring and the *5p* orbital on the iodine atom are almost eliminated in this conformation. The conformation preference is only known in the solid state and it is not known if there would still be this same preference in solution.

1.2.2.1 Secondary Bonding of HVI Compounds

Most HVI compounds are crystalline or white solids when in a pure form, and secondary bonding has been shown to be responsible for crystal packing in the solid state.²³ Secondary bonding results from intramolecular contacts and intermolecular interactions based on the various forms of crystal packing. Self-assembly of individual HVI molecules into complex supramolecular structures in the solid state and in solution has also been shown to originate from secondary bonding interactions.²⁴

Examination of the crystal structure of **1.4** reveals interactions between iodine and the four oxygen atoms, creating a coplanar arrangement due to the presence of secondary bonding, shown as dotted lines in **Figure 1.9**.²⁵ The coplanar arrangement has a dihedral angle of 75° with respect to the plane of the aromatic ring, creating four almost identical distances between the iodine and oxygen atoms.

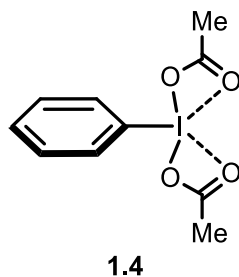


Figure 1.9 Secondary bonding in $\text{PhI}(\text{OAc})_2$

The X-ray crystal structure of (diacetoxyiodo)benzene complexed with BF_3 has been solved, and it can clearly be seen that the oxygen-iodine bonds are not exactly perpendicular to the carbon-iodine bond.²⁶ This bending allows for the other oxygens in the carbonyl group to approach closer to the electrophilic hypervalent iodine atom. This shorter distance allows for a stronger secondary bonding interaction to occur, and also level out the two different relative distances of the oxygen-iodine bonds, creating altogether four oxygen-iodine bonding interactions, including both primary (σ -bonds) and secondary bonds, to be closer in terms of energy.

It is well known that cyclic iodonium ylides are more stable than acyclic iodonium ylides. The increased stability can be explained by examining the rigidity of cyclic iodonium ylide **1.5** in which both carbonyl oxygens are locked in an orientation that positions the lone pairs to be close in proximity to the positively charged iodine atom.²⁷ The concept of secondary bonding can be used here to describe the favourable electrostatic interactions between the partial negatively charged oxygens with the positively charged iodine, as shown as dotted lines in **Figure 1.10**. These secondary bonding interactions can be used to explain the increased stability of cyclic iodonium ylides compared to their acyclic analogues.

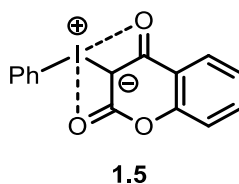


Figure 1.10 Secondary bonding responsible for stability in cyclic iodonium ylides

These relatively weak secondary bonding interactions can have a substantial effect on the overall properties of the compounds containing them. Single crystal X-ray diffraction analysis was performed on a series of iodonium ylides to identify where secondary bonding sites might be present. 2-Methoxyphenyliodonium bis(methoxycarbonyl)methanide (**1.6**) was analyzed in the solid state to reveal an intramolecular interaction between iodine and the oxygen atom of the *ortho* methoxy substituent at a 2.928 Å distance.²⁸ Another intramolecular interaction was observed between iodine and the carbonyl oxygen of the methoxycarbonyl group, at a 3.087 Å distance. The X-ray crystal structure of **1.6** is shown in **Figure 1.11**.

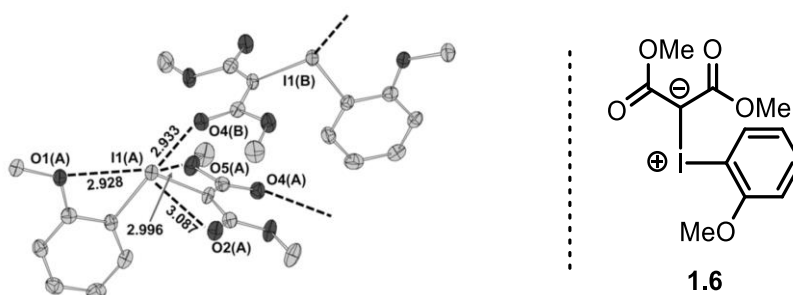


Figure 1.11 X-Ray crystal structure of iodonium ylide **1.6**

A key difference between this iodonium ylide (**1.6**) and an analogous iodonium ylide (**1.7**) that has the same structure except it does not contain the *ortho* methoxy substituent, is a difference in solubility and stability properties. Iodonium ylide **1.6** is known to be stable at room temperature, which in comparison to iodonium ylide **1.7** is not stable at room temperature and must be stored at -20 °C. Iodonium ylide **1.6** is also known to be insoluble in most organic solvents (except DMSO) while iodonium ylide **1.7** forms a homogeneous solution in dichloromethane when made at a concentration of 0.3 M. The only difference between iodonium ylide **1.6** and **1.7** is a single *ortho* methoxy group, which brings with it a single additional secondary bonding interaction, as shown in **Figure 1.12**. This additional secondary bonding interaction is responsible for a clear difference in overall properties, illustrating the impact that secondary bonding can have in HVI compounds.

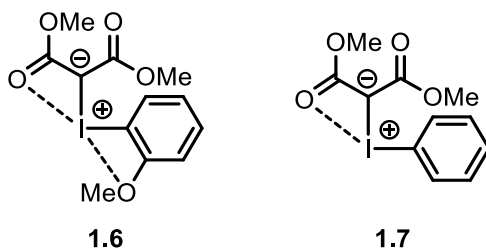
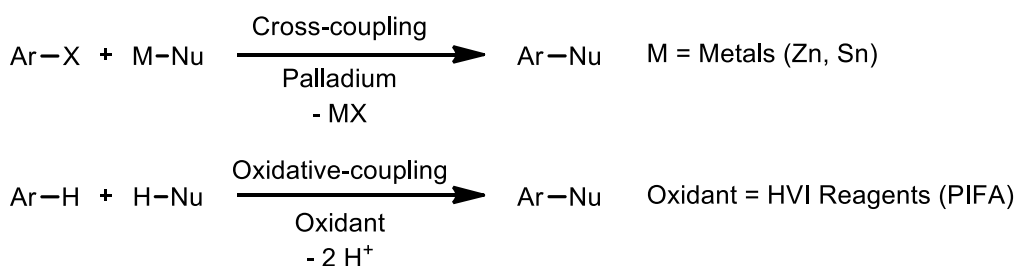


Figure 1.12 Secondary bonding interactions in acyclic iodonium ylides **1.6** and **1.7**

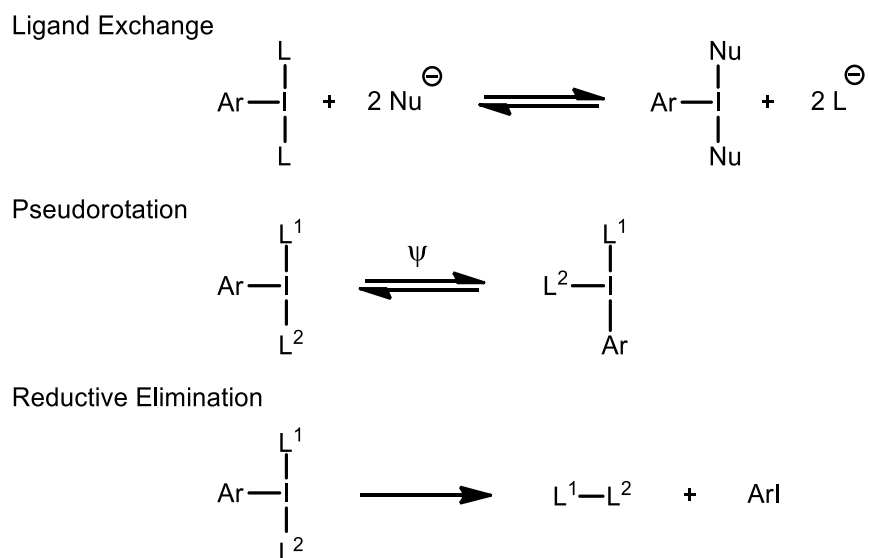
1.2.3 Reactivity of HVI Compounds

The unique properties of HVI compounds allow them to engage in reactivity that is comparable to the reactivity displayed by transition metals. Some terms used to describe fundamental processes for HVI compounds and transition metals are also similar including ligand exchange, pseudorotation, and reductive elimination. Some reviews have commented on the reactivity of HVI compounds as being comparable to transition metals such as mercury (II), thallium (III), or lead (IV).²⁹ HVI compounds are uniquely suited to not only mimic the reactivity of some transition metals, but even offer advantages that these metals can not do on their own. One example of this is the ability to replace metals in some cross-coupling reactions for the formation of carbon-carbon bonds. Traditional cross-coupling reactions rely on stoichiometric organometallic reagents & organic halides and produce metallic salts as waste and by-products from the coupling reaction.³⁰ HVI reagents such as bis(trifluoroacetoxy)iodobenzene (PIFA) for example, can perform the same reaction, in an oxidative-coupling process using unactivated coupling substrates as shown in **Scheme 1.7**.³¹ This strategy has many advantages as less waste material is generated, is more atom economical, and fewer synthetic steps are required for the overall transformation.



Scheme 1.7 General coupling reactions for carbon-carbon bond formation

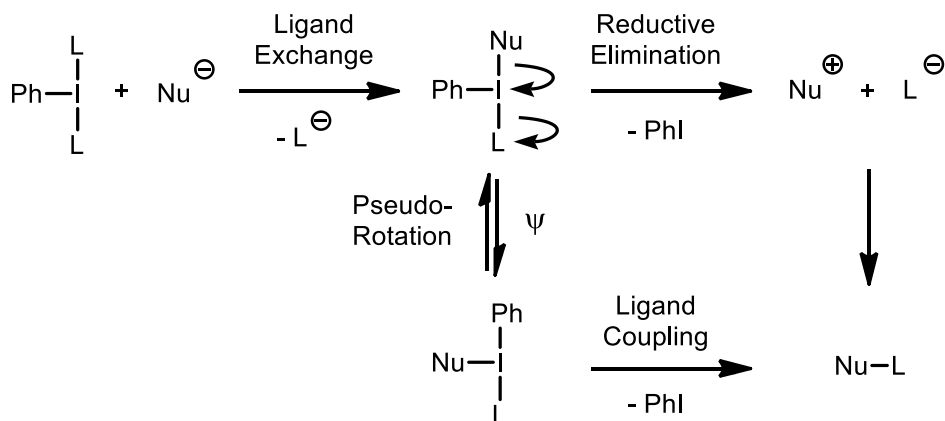
The fundamental reactions of HVI compounds are classified and named based on the type of transformation that occurs. The following terms are defined with respect to their function in HVI compounds. Ligand exchange describes a process by which different ligands can exchange with ligands originally bound to the hypervalent iodine, interconverting between different iodanes. Pseudorotation (Ψ) is a process that describes the rotation of ligands bound to the hypervalent iodine, giving different geometries of aryl- λ^3 -iodanes, and occurs in solution. The term reductive elimination describes a process by which ligands are coupled together, which in turn eliminates the aryl iodide and simultaneously lowers the oxidation state of iodine from +3 to +1. The reductive elimination process of HVI compounds has been studied by Ochiai and others, and have found the transformation to be thermodynamically favourable to such an extent that the leaving group ability of PhI is approximately 10^{12} times higher than that of I^- and 10^6 times higher than triflate (TfO^-).³² The term hypernucleofuge was introduced by Ochiai to describe the extremely high leaving group capabilities displayed in hypervalent compounds.³³ A hypernucleofuge is a leaving group that has a higher ability to leave than that of a superleaving group such as TfO^- . The three fundamental types of transformations that aryl- λ^3 -iodanes can encounter are shown in **Scheme 1.8**.



Scheme 1.8 Fundamental reactions of aryl- λ^3 -iodanes

A common reactivity mode in λ^3 -iodanes with a generic formula PhIL_2 involves an initial exchange of ligands on the iodine atom with external nucleophiles, which is then followed by

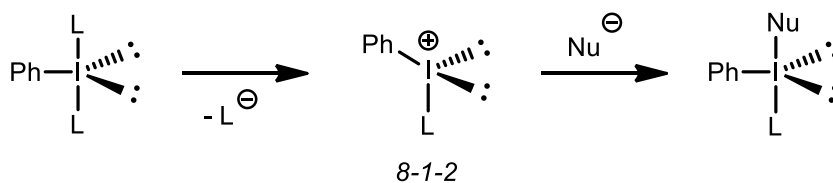
reductive elimination of iodobenzene. In this overall process as shown in **Scheme 1.9**, nucleophiles can be covalently bonded to ligands, in a manner that parallels transition metal-based reactions.



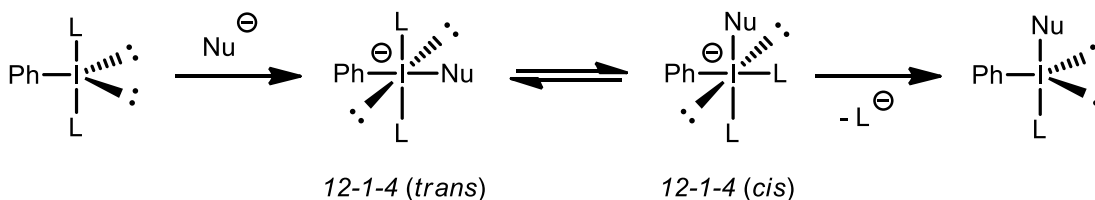
Scheme 1.9 Reactions of aryl- λ^3 -iodanes with nucleophiles

In the ligand exchange step above, there are two different general mechanistic pathways that are proposed to account for how nucleophiles can attach to the iodine in the λ^3 -iodanes. The two pathways are dissociative and associative, which are shown in **Scheme 1.10**.

Dissociative pathway

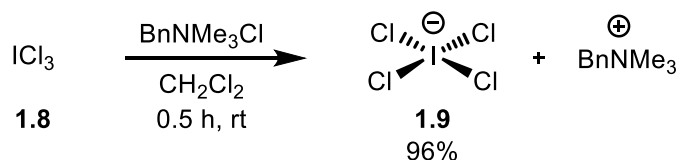


Associative pathway



Scheme 1.10 Dissociative and associative pathways for ligand exchange reactions

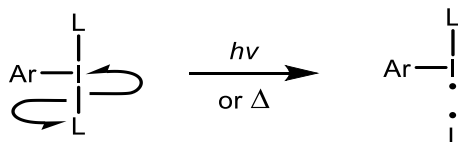
Even though it is hard to mechanistically distinguish between associative or dissociative pathways, there have been some studies that provide supporting evidence for an association pathway by isolating tetracoordinated iodine compounds. In a report by Kajigaeshi in 1988 the tetrachloroiodate species (**1.9**) was isolated as stable yellow crystals, by the reaction of iodine trichloride (**1.8**) with benzyltrimethylammonium chloride in dichloromethane as shown in **Scheme 1.11**.³⁴



Scheme 1.11 Preparation of benzyltrimethylammonium tetrachloroiodate **1.9**

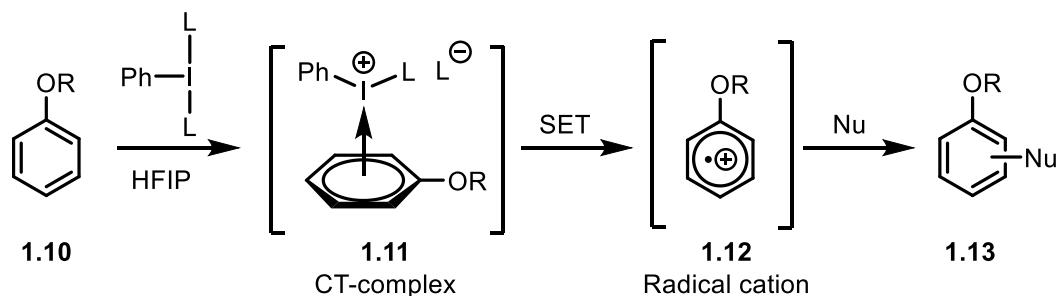
Other reports mention the ability of aryl- λ^3 -iodanes to interact with various additives (Bu_4NF , Bu_4NCl , Bu_4NBr , Bu_4NI , and HCl) in which the anionic counterion can form two isomeric tetracoordinated [12-I-4] iodate species (*cis* and *trans*) that exist as isomers equilibrating in solution.³⁵

The weakened hypervalent bonds have been targeted by synthetic chemists for use in many different reactions, including being used to generate radicals through homolysis.³⁶ Upon irradiation from a light source with sufficient energy, such as UV light, the iodine-ligand hypervalent bond will be the first bond to undergo homolysis due to the fact that it is the weakest bond in the molecule.³⁷ This same type of radical generation through homolytic cleavage can also be accessed through thermal heating conditions, as shown in **Scheme 1.12**. The photolysis of aryl- λ^3 -iodanes for the generation of carbon-based radicals such as trifluoromethyl and difluoromethyl radicals has also been reported to work with visible light ($\lambda = 400 \text{ nm}$) without requiring any additional reagents or catalysts.³⁸



Scheme 1.12 Homolytic cleavage of aryl- λ^3 -iodanes

The reactivity of HVI compounds can vary depending on reaction conditions. There are examples of HVI reagents acting as efficient and selective single-electron-transfer (SET) oxidizing agents.³⁹ These reactions involve electron-rich aromatic compounds (**1.10**), which are oxidized by aryl- λ^3 -iodane reagents when performed in specific solvents that are highly polar, but non-nucleophilic, such as Hexafluoroisopropanol (HFIP) or trifluoroethanol (TFE).⁴⁰ The following scheme shows a general oxidative nucleophilic aromatic substitution reaction, which is proposed to occur by a single-electron-transfer (SET) process. In these types of oxidative substitution reactions, a typical commonly used aryl- λ^3 -iodane reagent is PIFA and HFIP which is also commonly used as the solvent, which in combination between (PIFA and HFIP), creates specific reaction conditions allowing the SET process to occur. The combination of these two compounds enable a charge transfer complex (CT-complex, **1.11**) to form presumably *in situ* by the solvating effects of HFIP which will enhance the formation of the cationic iodine intermediate (**1.12**). This facilitates the SET event, forming a radical cation that is highly reactive, and will engage with the nucleophile to form the substituted product (**1.13**) shown in **Scheme 1.13**.



Scheme 1.13 Nucleophilic aromatic substitution by a SET process

1.3 Ylides

Ylides belong to a subclass of zwitterionic compounds that contain an anionic carbon covalently bonded to a cationic heteroatom.⁴¹ The charged atoms are positioned in a *vicinal* relationship, making ylides 1,2-dipolar compounds, and common positively charged heteroatoms include nitrogen, iodine, oxygen, phosphorus, and sulfur for example. Not all examples of ylides are stable, but the more commonly used ylides that appear in synthetic literature are stabilized by

one or more functional groups. A common type of ylide are ones that contain a carbonyl group which stabilizes the negatively charged α -carbon atom. Examples of α -keto stabilized ylides which are depicted as 1,2-dipoles, are shown in **Figure 1.13**. It is worth mentioning that although ylides are classified as 1,2-dipolar compounds, resonance structures that place the negative charge on the carbonyl oxygen are also acceptable forms and are more accurately represented that way due to oxygen being more electronegative than carbon.

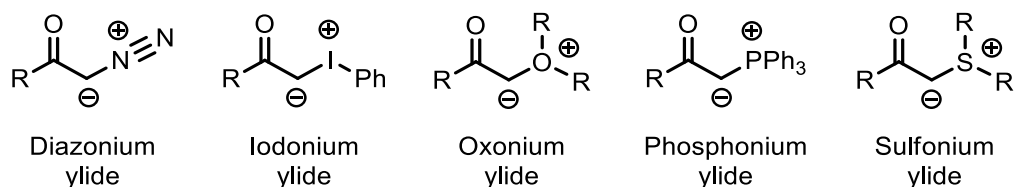
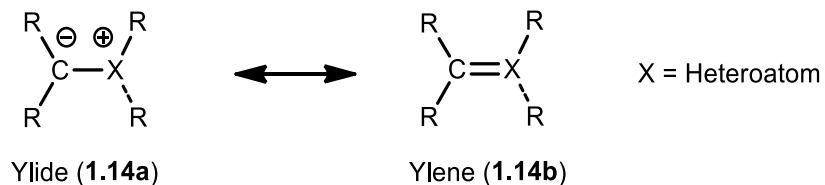


Figure 1.13 General ylides stabilized by an α -keto group

The first reports of ylides appeared in literature around the beginning of the twentieth century. Michaelis and Staudinger were the first researchers to report the isolation and reactions of ylides in chemistry.⁴² But Wittig is well known as the chemist who made significant advances in the area of ylide chemistry in the 1950s, including discovery of the famous Wittig reaction. This reaction was discovered by Georg Wittig in 1954 and for this, he was awarded the Nobel prize in chemistry in 1979.⁴³ Georg Wittig is also known for establishing the word “ylide” which comes from the combination of the two suffixes “yl” and “ide” that are used in chemical nomenclature.

The continuous developments in ylide chemistry has provided chemists with a deeper understanding of the bonding and electronic properties displayed by these unique systems. Ylides can be represented as an ylide (**1.14a**) or ylene (**1.14b**) resonance structure, as shown in **Scheme 1.14**.



Scheme 1.14 Resonance structures of general ylides

The question of which resonance structure best describes the overall ylide has evolved over the years to support the strictly zwitterionic ylide form **1.14a**, as opposed to the ylene form **1.14b**. It should be noted that this general statement is in most cases true but can vary depending on the heteroatom involved. In the zwitterionic ylide form **1.14a**, a strong Coulombic attraction is present, which accounts for the reduced carbon-heteroatom bond length commonly observed in ylide-based compounds.⁴⁴ Another piece of evidence in favour of the ylide form **1.14a**, is the unfavorable energy of the *d*-orbitals of main group elements.⁴⁵ More recent publications dealing with computational studies have suggested a substantial contribution to the electronic properties of the ylide comes from dative bonding.⁴⁶

Computational studies have advanced the understanding of how ylides react, showing closely related similarities to ligand-metal interactions displayed by transition metal chemistry.⁴⁷ These studies have shown that in some cases the ylidic carbon can be thought of as a “central atom” comparable to a metal centre in a complex.⁴⁸ This new dative description of ylides can be depicted as a carbene complex (**1.15**) as shown in **Figure 1.14**. This newly described dative bonding in ylides has resulted in some controversial discussions about the differences between dative and polar covalent bonding in ylide systems.⁴⁹

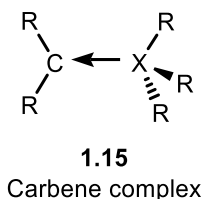


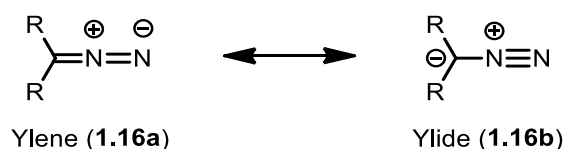
Figure 1.14 Structural representation of general ylides as a carbene complex

The quest to discover the true nature of bonding in ylides has refined our understanding of how they react and reflects upon the unique properties that makes these molecules synthetically valuable.

1.3.1 Diazonium Ylides

Diazonium ylides are popular reagents used in organic chemistry due to their ability to generate free carbenes or carbenoid intermediates (metallocarbenes).⁵⁰ Their initial discovery

started with the simplest diazo compound, diazomethane, which is a yellow gas, and was discovered by von Pechmann in 1894.⁵¹ Since then, a tremendous growth in their utilization in organic chemistry has taken place. Diazonium ylides, which are also referred to as diazo compounds, consist of an azo group (-N=N-) bound to an α -carbon atom. The standard resonance structures for representing general ylides applies to diazonium ylides and is shown in **Scheme 1.15**. In diazonium ylides, the more dominant resonance structure is believed to be the ylene form **1.16a**.



Scheme 1.15 Resonance structures of diazonium ylides

When drawn in the ylide form **1.16b**, the α -carbon atom bears a negative charge and the azo group bears a positive charge on nitrogen, resulting in a molecule with an overall neutral charge. Using this form, diazos can be categorized into three main groups depending on their ability to stabilize the negative charge on carbon. Groups that can withdrawal electron density away from the α -carbon, such as carbonyl groups, create a more stabilized diazo which are more commonly used in literature and are easier to isolate. Aryl or alkenyl groups are partially able to stabilize a negative charge on the α -carbon and are therefore referred to as semi-stabilized diazos. Alkyl groups or hydrogens are not able to provide any type of stability towards a negative charge, resulting in diazo compounds that are non-stabilized and are the most reactive types of diazos. The three different groups of diazo compounds organized by their trend in increasing reactivity is shown in **Figure 1.15**.

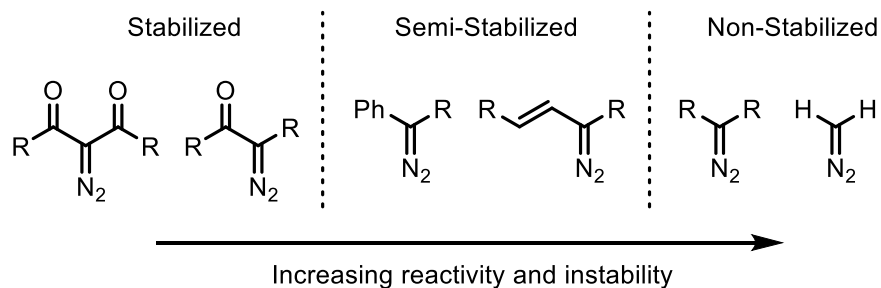
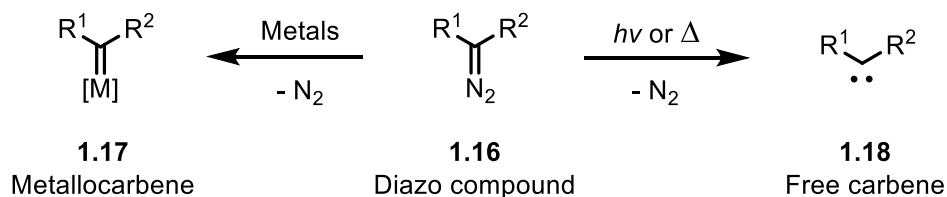


Figure 1.15 Diazo compounds categorized by stability

To make use of diazo compounds in organic chemistry they must be activated before they are able to react with various reaction partners. The activation of diazonium ylides is achieved by three main methods, which are using metals, light, or heat, as shown in **Scheme 1.16**. When using metals for the formation of metallocarbenes (**1.17**), the most common elements used are the transition metals copper and rhodium. When using electromagnetic radiation ($h\nu$) as a method of diazo activation, the most common light sources are UV-based such as mercury lamps, and more recently blue light from LEDs. These lights sources, in addition to heating, can be used to convert diazo compounds **1.16** into more reactive free carbenes **1.18**.



Scheme 1.16 Generation of metallocarbenes and free carbenes from diazo compounds

The reactivity of diazo compounds is based on the excellent leaving group ability of the N_2 . Once carbenes or carbenoids are generated from the desired activation method, they can engage with various reaction partners and participate in reactions such as cyclopropanation, ylide formation, insertions (C-H, N-H, O-H, etc), and rearrangements. The diversity of reaction types that can be accessed from diazo compounds has been a reason why they have established popularity in the organic chemistry community. Another benefit of using diazo compounds is that they are relatively easy to synthesize.

A negative aspect of diazonium ylides is based on reports that suggest some diazo compounds are toxic⁵² and even carcinogenic.⁵³ Another harmful property that make diazo compounds unsafe to work with is their explosive nature.⁵⁴ Many diazonium salts are explosive when dry, and some are even explosive when moist, and explosion can be initiated by heat, friction, or impact.

The unsafe, negative aspects of using diazo compounds have made them less desirable, and alternatives have been pursued. An example of a safer alternative to diazo compounds, is iodonium ylides. Iodonium ylides have been shown to participate in the same style of organic

reactions that diazonium ylides participate in and come with the added benefit of not being associated with unsafe chemical properties. It has been determined that diazonium ylides are relatively more reactive than the analogous iodonium ylide, but this subtle difference can be exploited to a strategic advantage.⁵⁵ The fine tuning of reaction conditions can be used to allow iodonium ylides to couple with specific reaction partners for desired outcomes, which would otherwise require harsher conditions such as heating if performing the same reaction with diazonium ylides. These advantages have been a driving force to establish iodonium ylides as a safer alternative to diazos, and their chemistry has been developed to determine the extent to which diazos can be replaced by these iodine-based counterparts.

1.3.2 Iodonium Ylides

The first stable iodonium ylide was discovered and synthesized by Neiland and co-workers in 1957.¹³⁷ After their discovery, many stable iodonium ylides have been synthesized, characterized, and utilized as reagents in organic synthesis. There are many different types of iodonium ylides which can be divided into two main categories, cyclic and acyclic types. Cyclic iodonium ylides are known to be more stable than acyclic ones, with acyclic bis-sulfonyl-derived iodonium ylides being an exception, which are generally stable at room temperature. The stability of acyclic iodonium ylides at room temperature is questionable and many researchers have found that they will decompose above -20 °C, so storage must be under cold conditions. Some examples from the main types of iodonium ylides are shown in **Figure 1.16** with cyclic iodonium ylides on the top row and acyclic iodonium ylides on the bottom row.

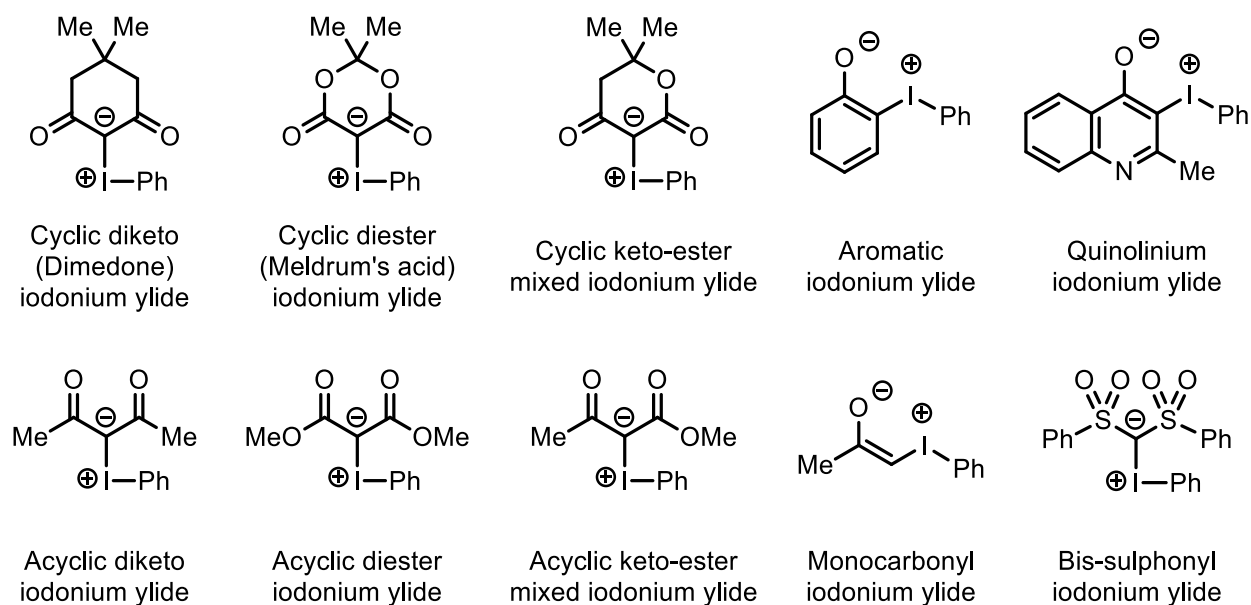


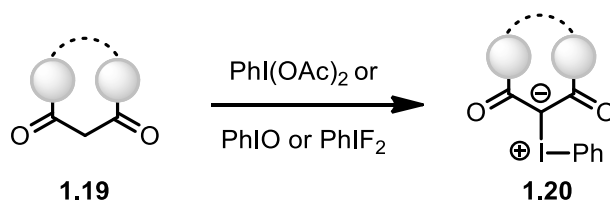
Figure 1.16 Types of iodonium ylides

All the examples shown above have a phenyl group bonded to the HVI atom, representing the most overwhelmingly common type of aryliodonium ylides encountered. Most of the aryliodonium ylides that show up in literature contain a phenyl group, and this lack of diversity opens up a window for exploration, which was taken advantage of in this thesis, specifically in chapters 3 and 4. In addition to this commonality in aryliodonium ylides, it is important to note the differences in iodonium ylides that do not contain an aromatic group attached to the HVI atom. There are examples of iodonium ylides that do not contain an aromatic group bonded to the HVI atom, but these are extremely rare due to the instability experienced when the group is not aromatic.

1.3.2.1 Synthesis of Iodonium Ylides

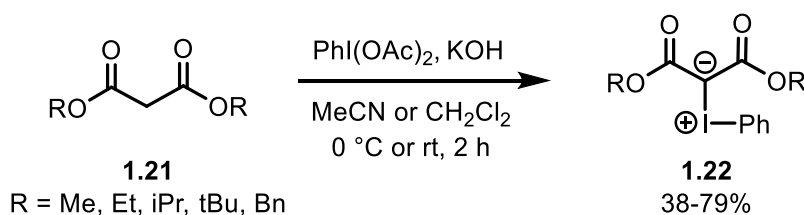
β -dicarbonyl-based iodonium ylides (**1.20**) can be synthesized from β -dicarbonyl systems with a free methylene group (**1.19**) in conjunction with HVI reagents such as (diacetoxyiodo)arenes, iodosoarenes, or (difluoro)arenes as shown in **Scheme 1.17**. This chemistry works on both acyclic and cyclic β -dicarbonyl systems. The carbonyls are often derived from ketones or esters, but amides are also compatible, and in addition to these

functional groups, cyano, nitro, and sulfonyl groups have also shown to be compatible in the formation of iodonium ylides. If the pKa of the α -proton in the β -dicarbonyl system is relatively high (10 or higher) then a base is required to induce deprotonation. When dealing with β -dicarbonyl systems such as Meldrum's acid or dimedone, for example, which both have a pKa of less than 8, then no base is required for iodonium ylide formation.



Scheme 1.17 General synthesis of iodonium ylides

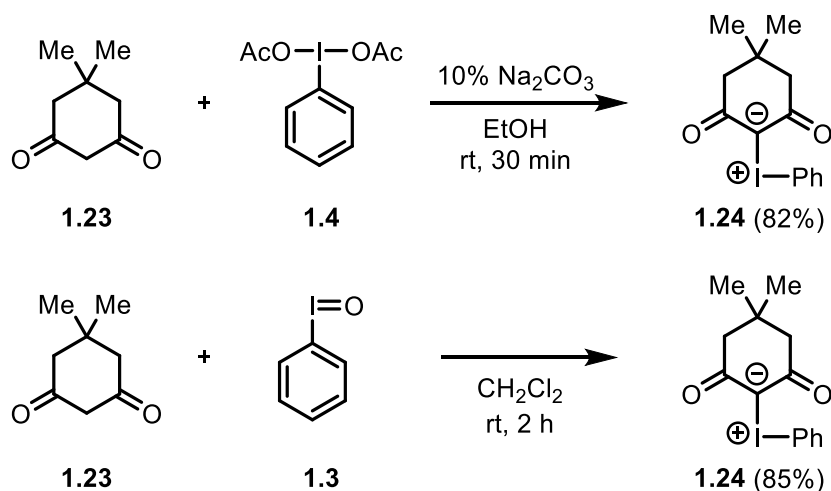
A general procedure for the synthesis of acyclic iodonium ylides derived from diesters was reported by Charette in 2009.⁵⁶ When malonate esters (**1.21**) were treated with (diacetoxyiodo)benzene in dichloromethane in the presence of potassium hydroxide, phenyliodonium ylides (**1.22**) are produced as shown in **Scheme 1.18**. The conditions were optimized for bis(methoxycarbonyl)(phenyliodonium)methanide in a similar reaction using acetonitrile and colder conditions (0 °C) and was published in Organic Syntheses.⁵⁷ The majority of examples of acyclic iodonium ylides decompose at room temperature, therefore their synthesis should ideally be performed at 0 °C. The workup and purification of acyclic iodonium ylides should be performed as quickly as possible, followed by storage in a freezer at -20 °C or colder.⁵⁸



Scheme 1.18 Synthesis of acyclic iodonium ylides

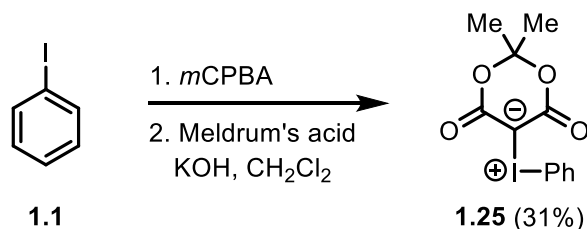
A general synthetic method for the synthesis of cyclic β -dicarbonyl iodonium ylides was first developed by Neilands⁵⁹ and later modified by Koser⁶⁰ and Schank.⁶¹ The methodologies were based on the condensation of iodosobenzene (**1.3**) or (diacetoxyiodo)benzene (**1.4**) with an

active β -dicarbonyl methylene compound. Since dimedone-derived iodonium ylide **1.24** is a commonly used starting material in many ylide-based reactions, the synthesis starting from dimedone (**1.23**) using either hypervalent iodine reagent **1.4** or **1.3** is shown in **Scheme 1.19**.



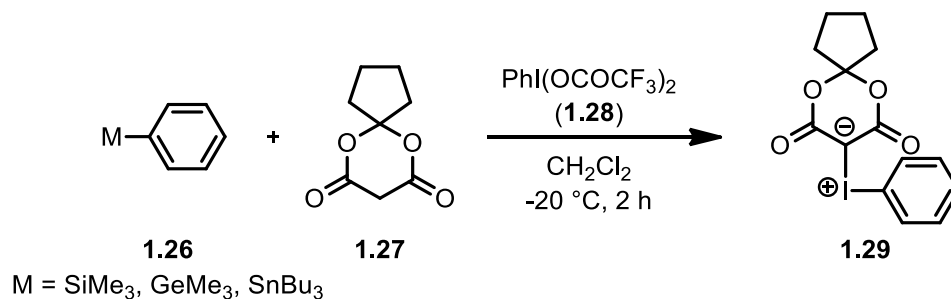
Scheme 1.19 Synthesis of dimedone iodonium ylide

A simplified method for synthesizing iodonium ylides by using a one-pot procedure starting from an iodoarene was reported by Ermert in 2013.⁶² The one-pot reaction uses *m*CPBA to oxidize iodobenzene (**1.1**) to the hypervalent iodine reagent iodosobenzene (**1.3**), which is then able to react with Meldrum's acid under basic conditions to form Meldrum's acid-derived iodonium ylide **1.25** (**Scheme 1.20**). The low yields obtained from this one-pot procedure could be raised significantly by using the original Koser and Schank procedure, which utilizes iodosobenzene (**1.3**) or (diacetoxyiodo)arene (**1.4**) in conjunction with an active β -dicarbonyl methylene compound.



Scheme 1.20 One-pot synthesis of Meldrum's acid iodonium ylide

Another type of iodonium ylide synthesis was accomplished using aromatic *ipso* substitution in a 2019 report by the Matsunaga group.⁶³ The authors describe this reaction as a direct synthesis of monoaryl- λ^3 -iodanes by chemo- and site-selective *ipso*-substitution reactions of stable arylmetal species (**1.26**, Ar-M, M = Si, Ge, Sn) with methylene compound **1.27** and (bis(trifluoroacetoxy)iodo)benzene **1.28** resulting in the formation of iodonium ylide **1.29** as shown in **Scheme 1.21**. This strategy has a specific advantage which is the installment of an iodonium ylide onto a metal-containing aryl system with the ability to control the placement in a regio-selective process. This advantage can outweigh the use of expensive metal-based starting materials (**1.26**) under circumstances when the installment of the iodonium ylide is needed in a specific site within a given molecule. The iodonium ylide formation occurs through the reaction of **1.26** with **1.28** which converts the metal-containing aryl system into a diacetate through an *ipso* substitution. The newly formed diacetate can then react with **1.27** to form **1.29**, therefore the aryl group within the iodonium ylide comes originally from the metal-containing starting material **1.26**.

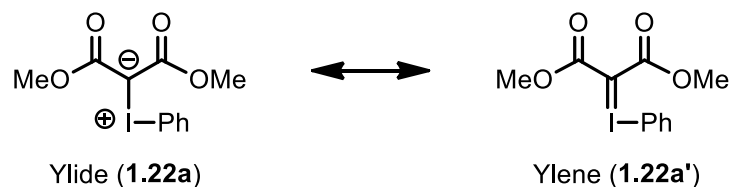


Scheme 1.21 Synthesis of iodonium ylides using arylmetal compounds

1.3.2.2 Structure and Bonding of Iodonium Ylides

The bonding in iodonium ylides has been investigated to determine the properties, with the carbon(ylide)-iodine bond being of specific interest. ¹²⁷I Mössbauer spectroscopy was applied to a series of iodonium ylides and from the results, it was concluded that the carbon(ylide)-iodine bond has a very weak double bond character with less than 0.1 electron contributing to the double bond.⁶⁴ From this study it was concluded that the carbon(ylide)-iodine bond is mostly zwitterionic in nature, represented by **1.22a**, and computational studies performed years later

were also in agreement with this conclusion. The two resonance structures that can be used to describe the bonding in iodonium ylides is shown in **Scheme 1.22**.



Scheme 1.22 Resonance structures of iodonium ylides

According to computational studies performed by Zhdankin in 2014, the double bond between iodine and other elements (such as oxygen, nitrogen, carbon) should not exist, and the actual carbon(ylide)-iodine bond in iodonium ylides is a dative 2c-2e (2-centre-2-electron) bond.⁶⁵ The bonding for acyclic iodonium ylide **1.22a** was described using an adaptive natural density partitioning (AdNDP) approach. These studies provided answers why iodonium ylides are much more stable as the β -dicarbonyl type, as the single dative $I \rightarrow C$ σ bond can only be formed if electron-withdrawing groups like CO_2Me take some electron density from the α -carbon atom. The α -carbon in iodonium ylide **1.22a** is calculated to have a charge of not -1.0 but -0.58 and the two electron withdrawing carbonyl groups are necessary to withdraw enough electron density away to allow the α -carbon atom to acquire two electrons from the iodine atom in the formation of a dative $I \rightarrow C$ σ bond. These computational studies suggested that the description of bonding in iodonium ylides could be presented as a donor-acceptor complex between a Lewis acid and a Lewis base. The PhI donor group can be thought of as a Lewis base, and the $\text{C}(\text{CO}_2\text{Me})_2$ acceptor group can be thought of as a Lewis acid as shown in **Figure 1.17**. Computational calculations were even able to propose a bond strength between the PhI and $\text{C}(\text{CO}_2\text{Me})_2$ groups, which was found to be $163.6 \text{ kcal mol}^{-1}$.

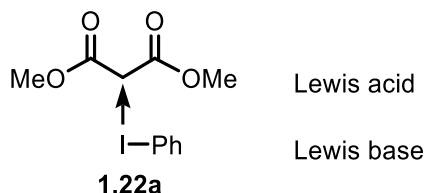


Figure 1.17 Dative σ bonding description in iodonium ylides

The carbon(ylide)-iodine bond is therefore described as being a 2c-2e dative $I \rightarrow C$ σ bond and the carbon(aryl)-iodine bond is described as a 2c-2e σ bond. The bonding images developed for iodonium ylide **1.22a** described by Zhdankin through AdNDP analysis is shown in **Figure 1.18**.⁶⁵

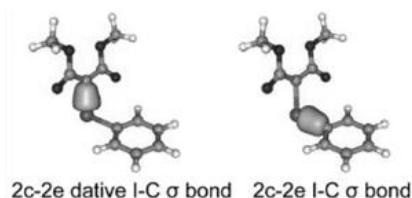


Figure 1.18 Computational bonding models of iodonium ylides

The bonding in the β -dicarbonyl section of an iodonium ylide was described by Zhdankin as being composed of two carbon-carbon 2c-2e σ bonds and one carbon-carbon 3c-2e π bond as well as two carbon-oxygen 2c-2e π bonds as shown in **Figure 1.19**, and this figure also shows the two lone pairs present on the iodine atom.⁶⁵

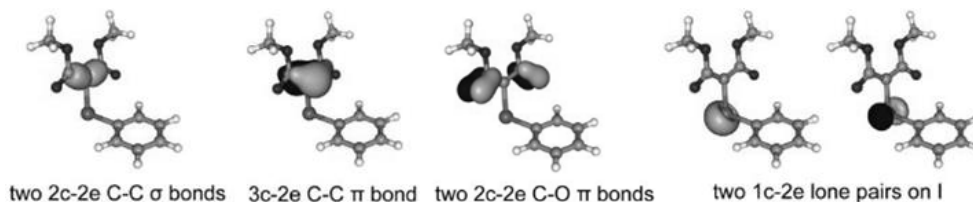


Figure 1.19 Computational bonding models of iodonium ylides

The bonding geometry in iodonium ylides is a rather unique bonding angle, as most organic-based molecules display standard bonding angles of 109° , 120° , or 180° . Single-crystal X-ray structures have been reported for approximately 15 iodonium ylides in the literature. According to the data gathered from a combination of all these crystal structures, the averaged bonding geometry of iodonium ylides have a carbon-iodine-carbon (C-I-C) bond angle close to 90° as shown in **Figure 1.20** using dimedone iodonium ylide (**1.24**) as an example. Some report that this 90° bonding angle implies a zwitterionic nature to the carbon-iodine ylide bond.

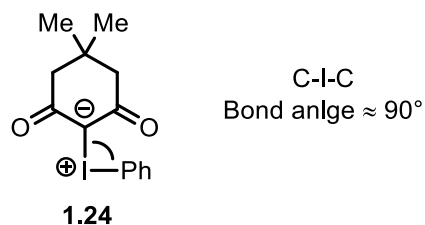


Figure 1.20 Average bond angle in iodonium ylides

Acyclic phenyliodonium ylides, such as **1.30** shown in **Figure 1.21**, have a geometry typical for an iodonium ylide with a C–I–C bond angle of 98° and a carbon(ylide)-iodine bond length of approximately 1.9 Å which was determined by single-crystal X-ray analysis.⁶⁶

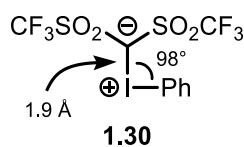


Figure 1.21 Structure of phenyliodonium bis(trifluoromethanesulfonyl)methide

1.3.2.3 Reactivity of Iodonium Ylides

Activation of iodonium ylides has been accomplished primarily by metals, and less frequently by thermal, photochemical, or metal-free conditions, but with the use of additives. With the use of transition metals such as copper or rhodium, metallocarbene intermediates resembling as **1.31** can form *in situ*. Recently, there has been an interest in establishing milder conditions for iodonium ylide activation, accomplished through halogen bonding, or less-intense light sources such as LEDs.⁶⁷ A list of all the known successful modes of iodonium ylide activation that has appeared in the literature include the following methods: metals, thermal, photochemical, halogen-bonding, ionic, single-electron transfer (SET), and Lewis acids. There are slight differences in reactivity when comparing acyclic to cyclic iodonium ylides, but generally they react in a similar manner, except for small differences observed upon photochemical activation, and larger differences observed upon thermal-induced activation. The application of heat towards cyclic iodonium ylides most often will result in rearrangement products resembling **1.32**, while acyclic iodonium ylides do not undergo rearrangements, but can form carbene intermediates resembling **1.33**. The major activation modes observed in iodonium

ylide reactions including the intermediates believed to be involved with each different type of reactivity are summarized in **Figure 1.22**. The application of UV light on iodonium ylides may form free carbenes such as **1.34** for example, but the existence of this carbene intermediate is still under debate. The application of light containing less energy than UV, such as visible light from LEDs, on iodonium ylides is the topic of chapter 3 in this thesis, and it is proposed that diradical intermediate **1.35** may form. The use of metals such as copper (I) or tertiary aryl amines that can function as halogen bond activators have been proposed to generate intermediates resembling **1.36** via SET events.

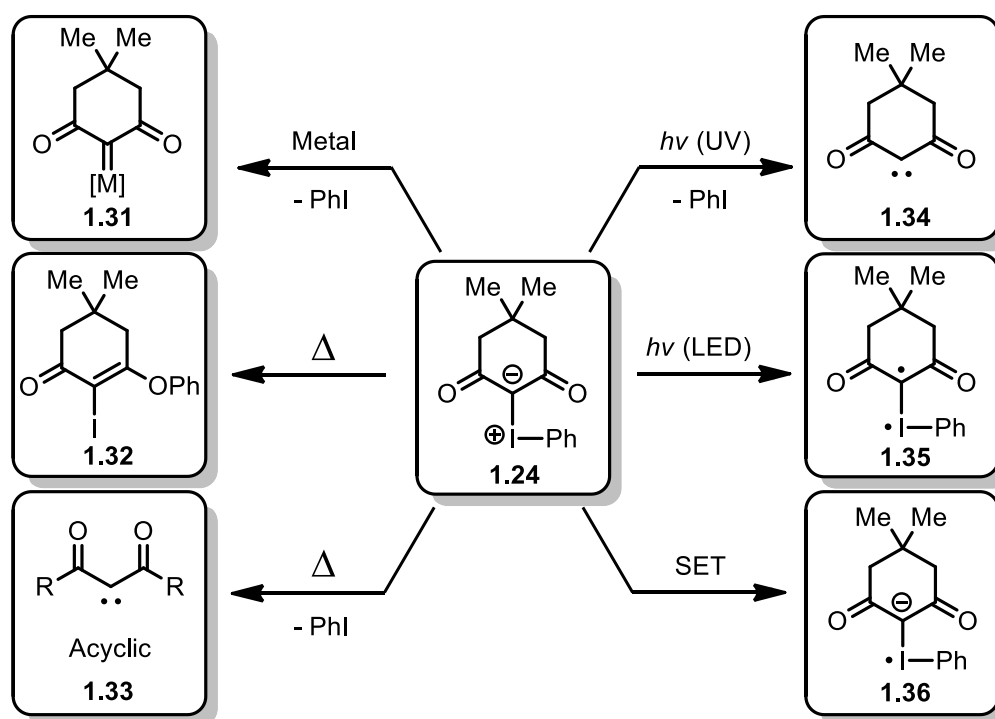
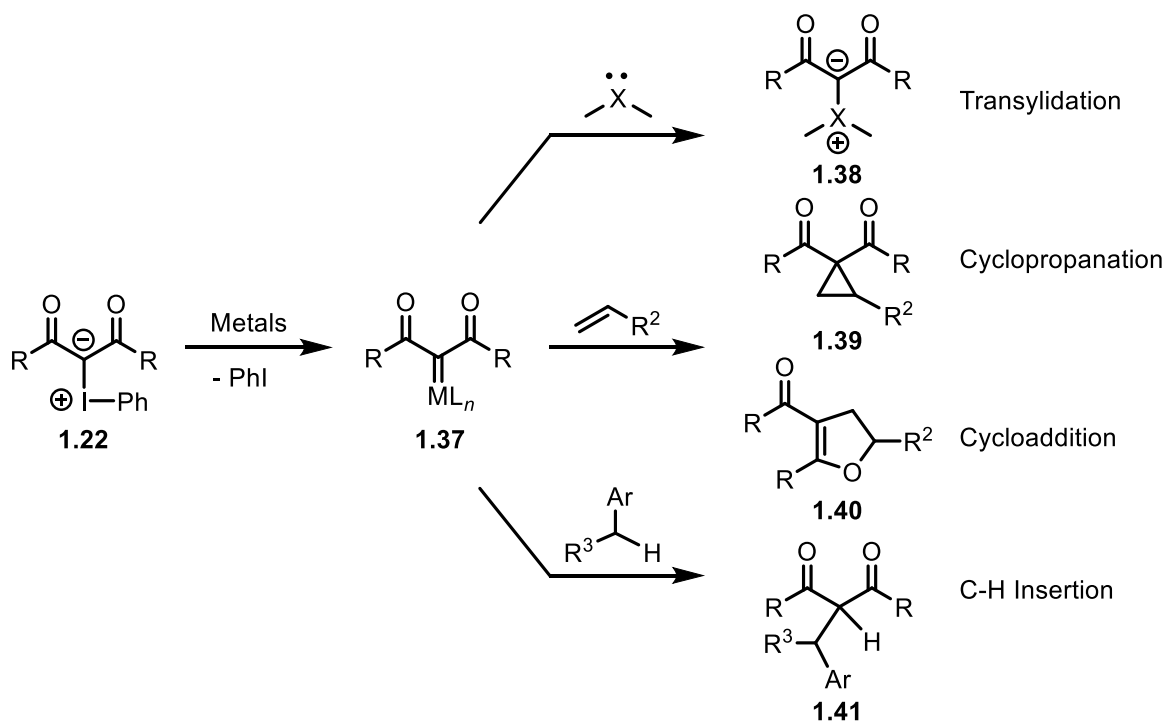


Figure 1.22 Intermediates of activation modes of iodonium ylides

1.3.2.3.1 Metal-Based Activation of Iodonium Ylides

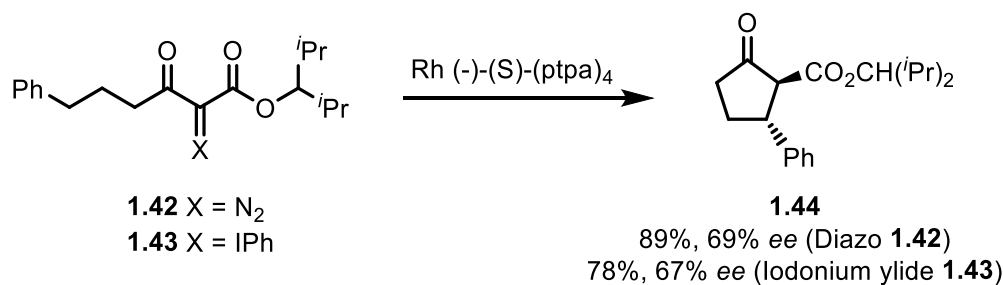
The use of transition metals for the activation of iodonium ylides has proven to be a successful way of accessing many different types of reactions such as cycloaddition, cyclopropanation, C-H insertion, and transylidation. The use of copper(II) or rhodium(II) for the cyclopropanation of iodonium ylides with alkenes is one of the most well-known applications of

iodonium ylides in organic synthesis. Under metal-catalyzed conditions, iodonium ylides have the theoretical ability to form metallocarbenes in a similar way to that of diazo compounds. The metallocarbenes are commonly used for cyclopropane synthesis when reacted with an alkene, or alternatively, reaction with an alkyne can deliver a cyclopropene. Analysis of the reaction mixtures from typical metal-catalyzed cyclopropanation reactions using iodonium ylides has been compared to the equivalent diazo-based reaction to reveal a commonality in the product compositional mixtures. Products formed from the rhodium(II)-catalyzed reactions of iodonium ylides with alkenes was found to be identical to that of the equivalent diazo-based reaction, indicating that the mechanism of these two processes is similar, and most likely involves metallocarbenes as the key intermediates.⁶⁸ These results have been observed by other groups, and using this understanding, many new reactions have been discovered, reinforcing the fact that iodonium ylides can be used as an alternative to diazo compounds for reactions that require metal-activation.⁶⁹ Iodonium ylides can be activated by metals to form metallocarbenes, which can then go on to react with various reaction partners forming the different products shown in **Scheme 1.23**.



Scheme 1.23 Metallo-carbene reactions of iodonium ylides

To see if iodonium ylides can act as diazo equivalents in an asymmetric reaction, an intramolecular C-H insertion reaction was performed, paying careful attention to see if chirality would be lost or translated when using iodonium ylides as the starting material. The asymmetric intramolecular C-H insertion reaction of an iodonium ylide (**1.43**), and the equivalent diazo compound (**1.42**), was conducted using the chiral rhodium (II) catalyst [Rh (-)-(S)-(ptpa)₄] = [dirhodium tetrakis(N-phthaloyl)-L-phenylalaninate] forming cyclic product **1.44** as shown in **Scheme 1.24**.



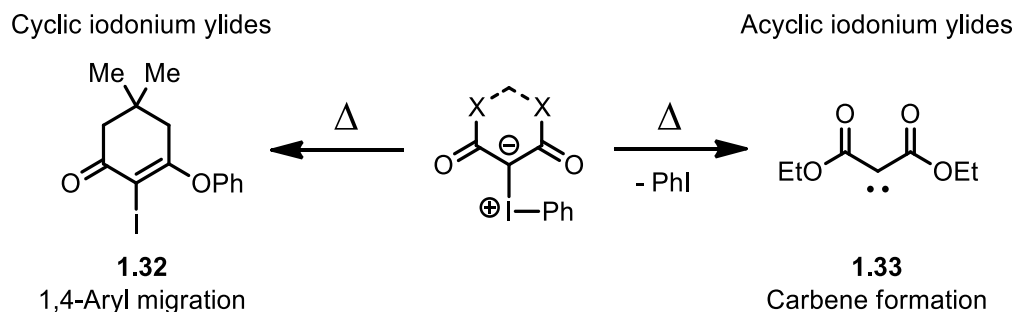
Scheme 1.24 Metal-catalyzed asymmetric intramolecular C-H insertion reaction

Performing the reaction above (**Scheme 1.24**) using diazo starting material **1.42**, the yield of the dicarbonyl C-H insertion product (**1.44**) was 89% having an *ee* of 69% (*R*) at C(3). The iodonium ylide starting material **1.43**, run under identical reaction conditions, afforded the same dicarbonyl C-H insertion product (**1.44**) with a yield of 78% and an *ee* of 67% (*R*) at C(3). This interesting reaction sheds light onto the nature of the chirality transfer going on between the ylide-based starting materials and the chiral metallocarbene intermediate formation, which is then obviously followed by the formation of the product as the catalytic rhodium is turned over. Providing proof that iodonium ylides can replicate the same asymmetric inducing abilities that diazos possess is important when considering the overall value that iodonium ylides truly have as diazo replacements under metal-activated conditions, as there are many other different reaction types that diazos can engage in with effective chirality transfer.

1.3.2.3.2 Thermal Activation of Iodonium Ylides

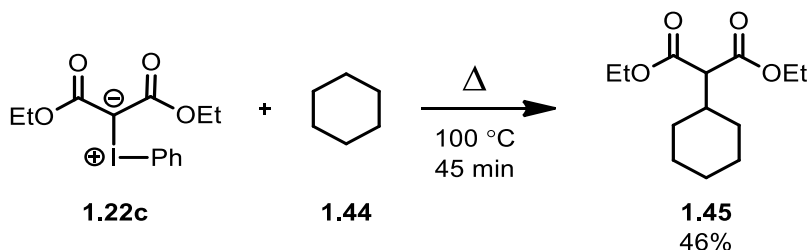
The thermal-induced intramolecular 1,4-aryl migration in cyclic iodonium ylides appears to be a phenomenon that only occurs with cyclic iodonium ylide systems. This rearrangement is

not witnessed in acyclic iodonium ylides, and the possibility of a free carbene, generated from acyclic systems, might be responsible for what accounts for their observed reactivity, as shown in **Scheme 1.25**.



Scheme 1.25 Thermal activation of acyclic vs cyclic iodonium ylides

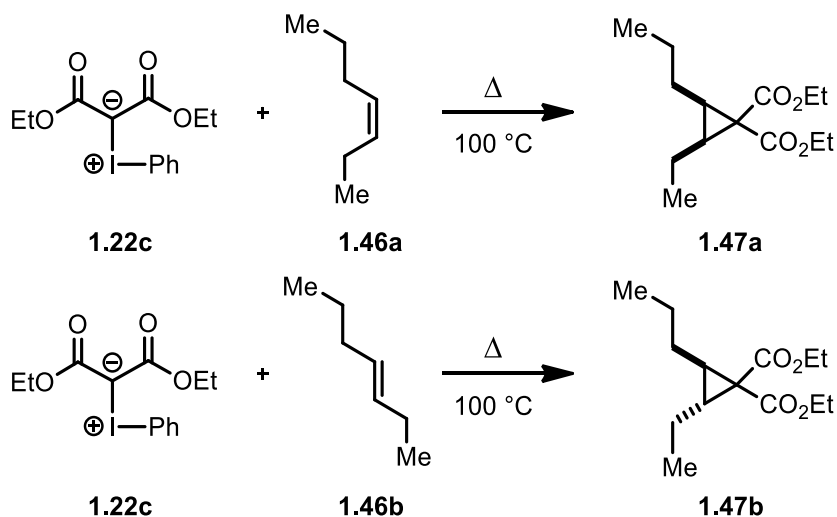
Examples of the observed, free carbene-like reactivity, can be seen in the following C-H insertion reaction, induced by heating acyclic iodonium ylide **1.22c** with cyclohexane (**1.44**) to 100 °C as shown in **Scheme 1.26**.⁵⁵ The yield of the C-H insertion product **1.45** was 46% which was determined from a ¹H NMR spectrum of the crude reaction mixture.



Scheme 1.26 Thermally activated C-H insertion of acyclic iodonium ylides

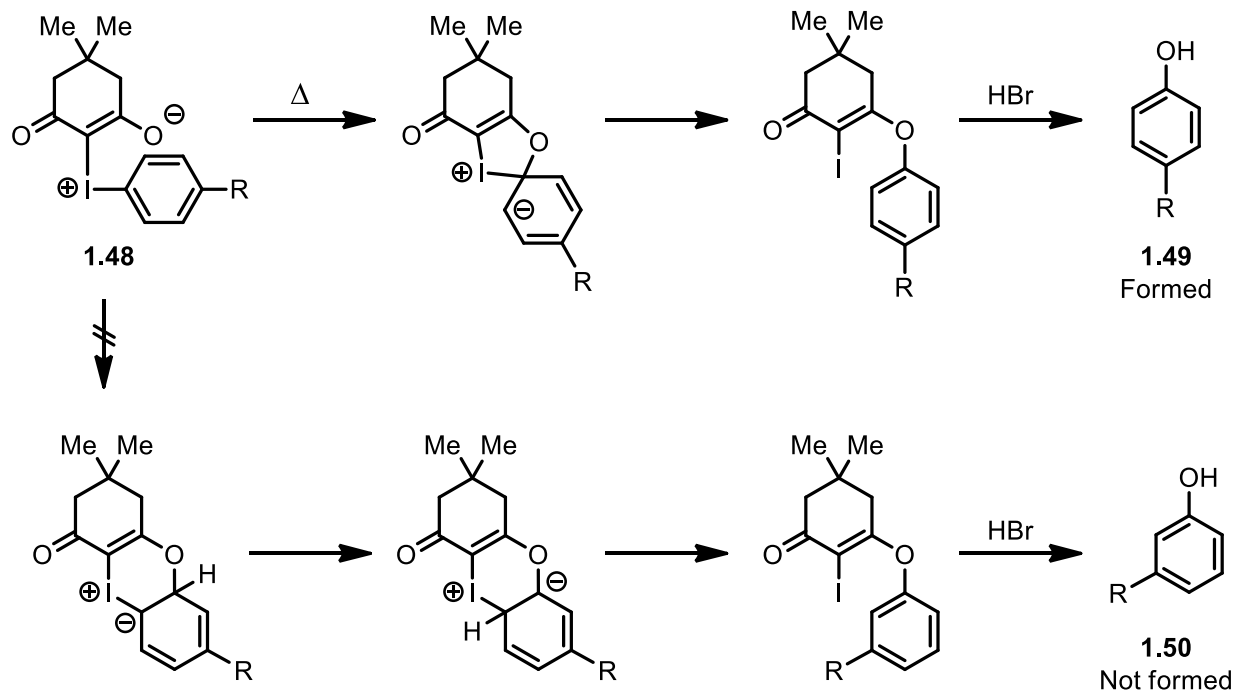
Further examples for the possibility of the involvement of free carbenes in the thermal-induced reactions of acyclic iodonium ylides can be witnessed in the cyclopropanation reactions shown in **Scheme 1.27**. The cyclopropanation reaction using 3-heptene was performed to examine the spin states of the intermediates generated from the thermal decomposition of acyclic iodonium ylides. Heating a mixture of iodonium ylide **1.22c** and *cis*-3-heptene **1.46a** led to formation of iodobenzene and *cis*-cyclopropane **1.47a** as well as several other minor products. The yields were not reported but GC analysis was performed, and it was observed that *trans*-

cyclopropane **1.47b** was present, but only accounted for 2% of the overall cyclopropanation yield. Alternatively, heating a mixture of **1.22c** and *trans*-3-heptene **1.46b** led to formation of iodobenzene, *trans*-cyclopropane **1.47b**, and several other minor products. The *cis*-cyclopropane **1.47a** was shown to account for less than 1% of the cyclopropanation products. These results indicate that the thermal decomposition of iodonium ylides is a source of singlet carbene intermediates, and the reaction of this singlet carbene with the alkene is faster than intersystem crossing (ISC).



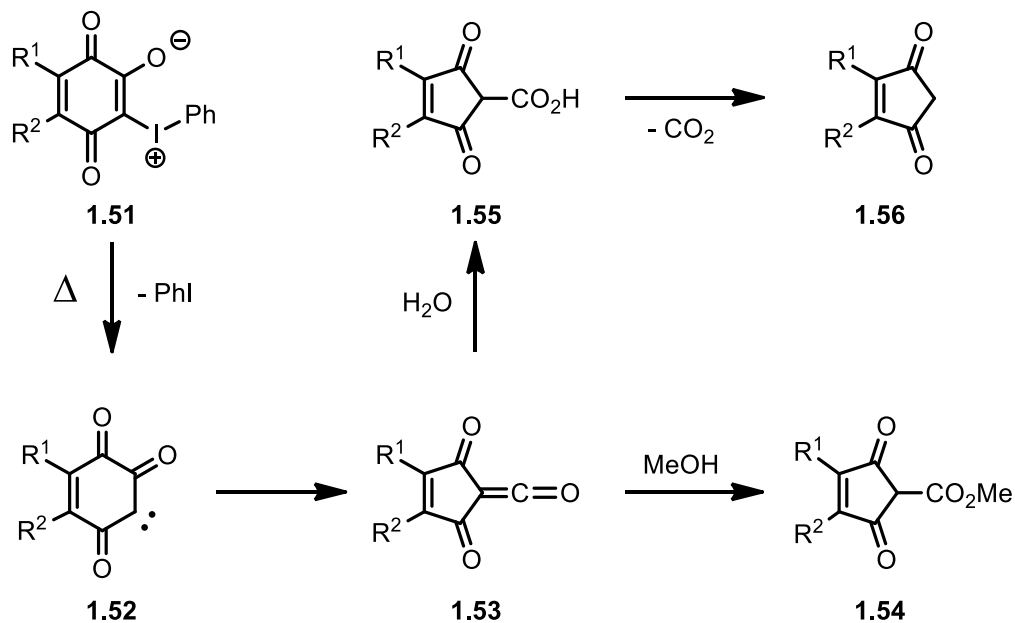
Scheme 1.27 Thermally activated cyclopropanation of acyclic iodonium ylides with alkenes

Aryl group migration is a common occurrence in cyclic iodonium ylides when subjected to elevated temperatures. The intramolecular thermal 1,4-phenyl migration has been witnessed by many research groups, and mechanistic studies have been performed to deduce the reaction mechanism. The current understanding is that the process occurs in a concerted mechanism when substitution occurring at the *ipso* carbon of the migrating aryl ring. Studies performed by the Nozaki group back in 1970 showed proof for the *ipso* substitution reaction to occur as shown in **Scheme 1.28**.¹⁴³ Iodonium ylide **1.48** was subjected to heated conditions, and after cleavage of the substituted phenol group using HBr, the products were analyzed to reveal a single regio-isomer had formed (**1.49**) with no traces of the other regio-isomer (**1.50**) being present. These results are indicative of an *ipso* substitution mechanism.



Scheme 1.28 Thermally activated aryl group migration in cyclic iodonium ylides

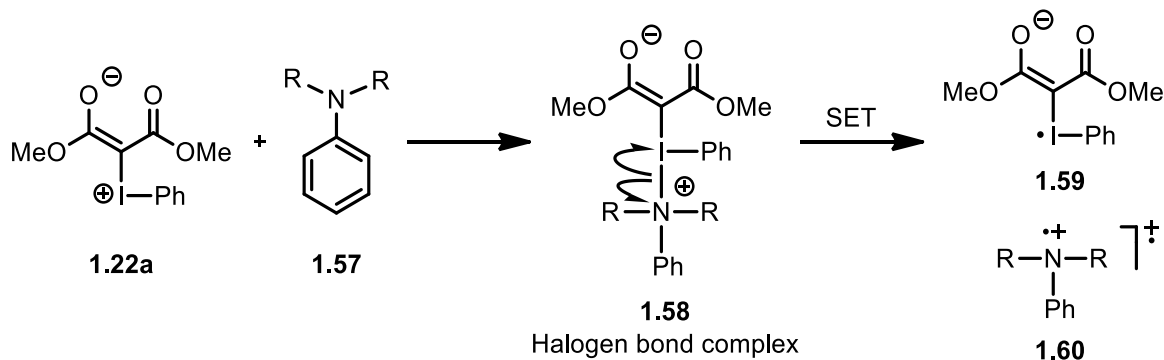
Another type of thermal-induced rearrangement reaction for iodonium ylides, was observed by Spyroudis in 2005.⁷⁰ Iodonium ylides derived from hydroxyquinones are the only type of cyclic iodonium ylide in which a thermal-induced ring contraction reaction occurs instead of the normal aryl group migration.⁷¹ This type of transformation generates a carbene, which then undergoes a Wolff rearrangement to give a ring contracted α,α -dioxoketene intermediate which can then either be trapped with methanol or interact with water to lose a molecule of carbon dioxide, as shown in **Scheme 1.29**.



Scheme 1.29 Thermally activated ring contraction of iodonium ylides

1.3.2.3.3 Halogen Bonding Activation of Iodonium Ylides

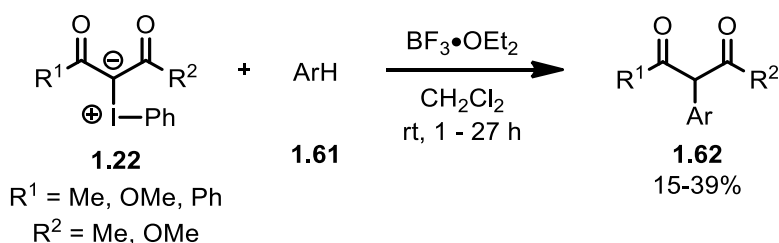
Recent work done by the Wang group at Shandong University in China have shown iodonium ylides to function as electrophiles and participate in cyclization⁶⁷ and multi-component coupling reactions⁷² through halogen bonding modes of activation. The reactions were explained by the formation of a halogen bond complex (**1.58**) containing the combination of an iodonium ylide (**1.22a**) with a tertiary aryl amine (**1.57**). The amine functions as a Lewis base, and in the halogen bond complex, a SET event can occur to generate a reactive cationic radical intermediate (**1.60**) as well as an anionic radical intermediate (**1.59**), as shown in **Scheme 1.30**. This new mode of activating iodonium ylides is exciting as this was a recent discovery, and many more innovative ways of activating iodonium ylides may remain unexplored.



Scheme 1.30 General scheme for halogen bonding activation of iodonium ylides with amines

1.3.2.3.4 Lewis Acid Activation of Iodonium Ylides

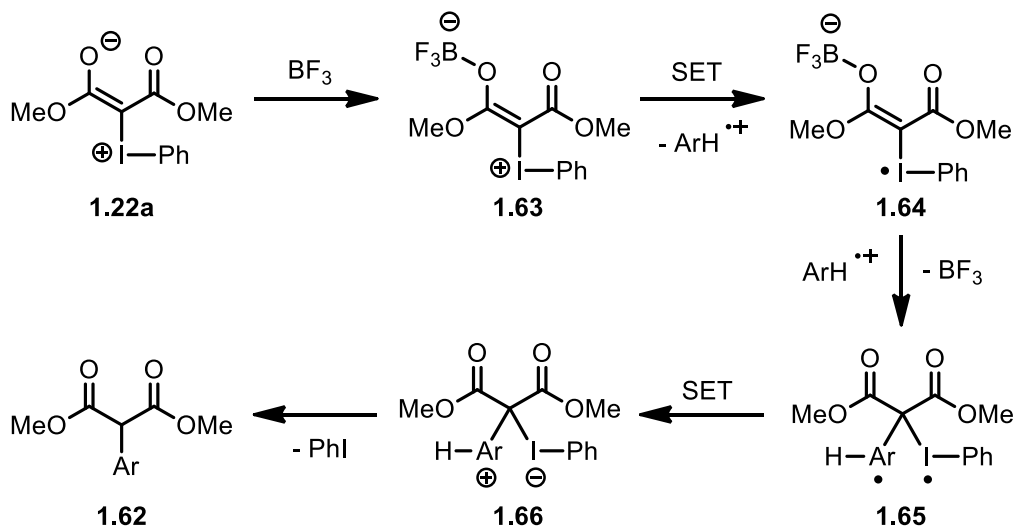
An oxidative-substitution reaction of electron-rich aromatic compounds (**1.61**) with BF_3 -activated iodonium ylides to give α -arylated compounds (**1.62**) was reported by Koser in 2007 and is shown in **Scheme 1.31**.⁷³ This chemistry relied on activating the iodonium ylides with a Lewis acid. The mechanism proposed is based on the BF_3 -complexed iodonium ylide as being a stronger oxidant than the free iodonium ylide. It was suggested that the $\text{BF}_3 \cdot \text{Et}_2\text{O}$ -promoted reactions of iodonium ylides with electron-rich aromatics involves an arene cation-radical mechanism, and therefore carbene or carbenoid intermediates are proposed not to occur under the Lewis acid-catalyzed conditions.



Scheme 1.31 Lewis acid activated reaction of acyclic iodonium ylides with aromatics

Iodonium ylides were shown to functionalize polycyclic aromatic hydrocarbons through the installation of β -dicarbonyl groups onto the aromatic substrates, with the assistance of a Lewis acid. A mechanism that accounts for this activation of iodonium ylides is shown in **Scheme 1.32**. The overall transformation required two separate SET events which are critical for

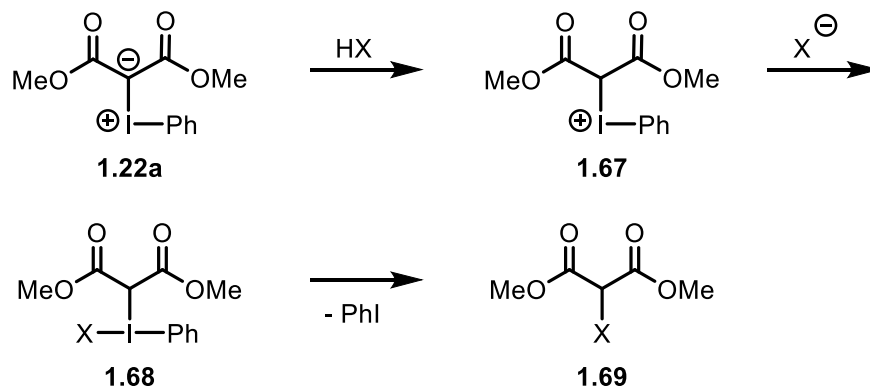
allowing this reaction to take place and occur because of the activating effects that the Lewis acid has on the iodonium ylide making it more susceptible at receiving an electron from the electron-rich aromatic system. Mechanistically, this Lewis acid-activated reaction relies upon SET events, which arguably, classifies this reaction under the mode of SET activation.



Scheme 1.32 Lewis acid-activated reaction mechanism of iodonium ylides with aromatics

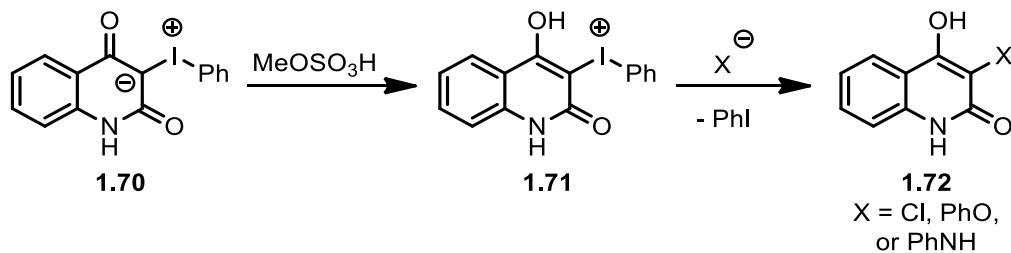
1.3.2.3.5 Ionic Activation of Iodonium Ylides

The reaction between iodonium ylide **1.22a** and Brønsted acids (HX) can initially yield an iodonium salt (**1.67**) which are usually unstable and can decompose through the displacement of the aryliodide by the counter-ion (X^-), possibly through intermediate **1.68** to form product **1.69**. This mode of reactivity is shown in **Scheme 1.33** and represents one way of using ionic activation to access reactivity from iodonium ylides, but a different type of reactivity can be accessed depending on the nature of the counter-ion (X^-) used, and the resulting stability of the iodonium salt.



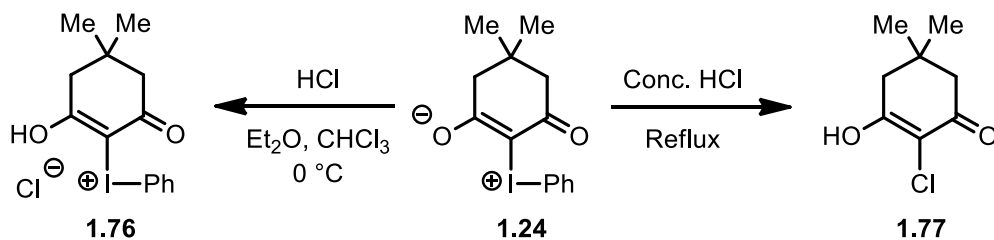
Scheme 1.33 General ionic mode of activation of iodonium ylides with Brønsted acids

In some cases, if the counter-ion is relatively non-nucleophilic, the iodonium salt can be isolated and then subjected to reactions with a variety of nucleophiles.⁷⁴ The reaction of iodonium ylide **1.70** with methyl hydrogen sulfate results in the formation of iodonium salt **1.71** which is stable enough to be isolated from the reaction mixture. This salt can then react with various nucleophilic compounds to give products with the structure of **1.72** as shown in **Scheme 1.34**. Overall, this type of reactivity in which iodonium ylides are activated by Brønsted acids, can be classified as an ionic mode of activation.



Scheme 1.34 Ionic mode of activation of iodonium ylides with Brønsted acids

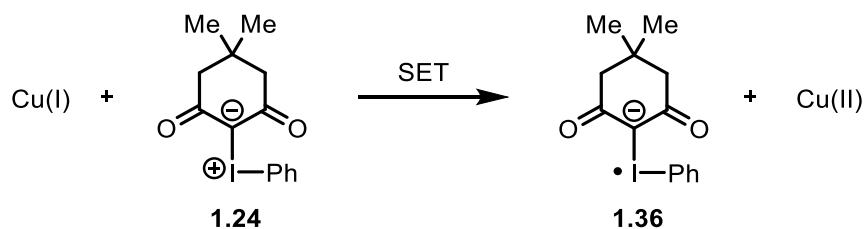
The use of ionic activation of iodonium ylides has been used in the synthesis of 2(5*H*)-furanones (butenolides) which are an important class of oxygen-containing heterocyclic compounds and are found in natural products, drugs, materials, and important intermediates in organic synthesis.⁷⁵ 2(5*H*)-Furanone derivatives have been considered as potential insecticides, fungicides, antibiotics, bactericides, anticancer agents, allergy inhibitors, and cyclooxygenase inhibitors.



Scheme 1.36 Ionic activation of cyclic iodonium ylides with acids

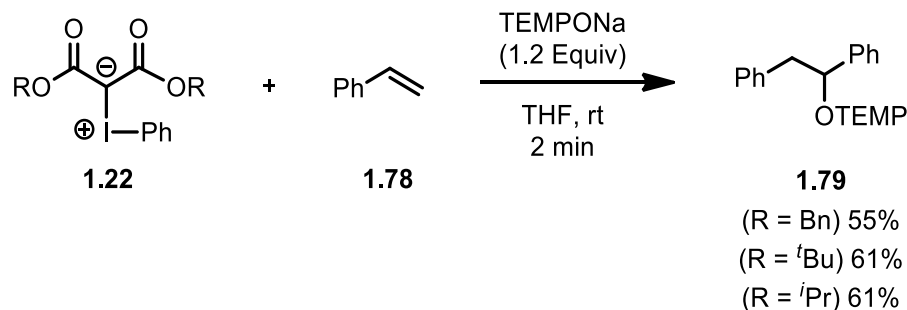
1.3.2.3.6 Single Electron Transfer (SET) Activation of Iodonium Ylides

In general, SET reactions of iodonium ylides show the transfer of one electron from an appropriate reagent to the hypervalent iodine atom. Dimedone iodonium ylide for example, can receive a single electron from reagents such as copper (I), where it can be illustrated that an electron goes towards the positively charged iodine atom to generate intermediate **1.36** as shown in **Scheme 1.37**.⁷⁹ The one electron reduction of the iodine atom is a common theme observed in multiple activation modes listed in this section, including halogen bonding and Lewis acid activation.



Scheme 1.37 Activation of iodonium ylides by SET

Hypervalent iodine reagents in general have been shown to participate in multiple types of SET reactions, but examples of SET reactions involving iodonium ylides has been only recently reported, one example of this is by Studer in 2016.⁸⁰ As shown in **Scheme 1.38**, acyclic iodonium ylides (**1.22**) were shown to react with TEMPO⁻Na and styrene (**1.78**) to form combined adduct **1.79**.

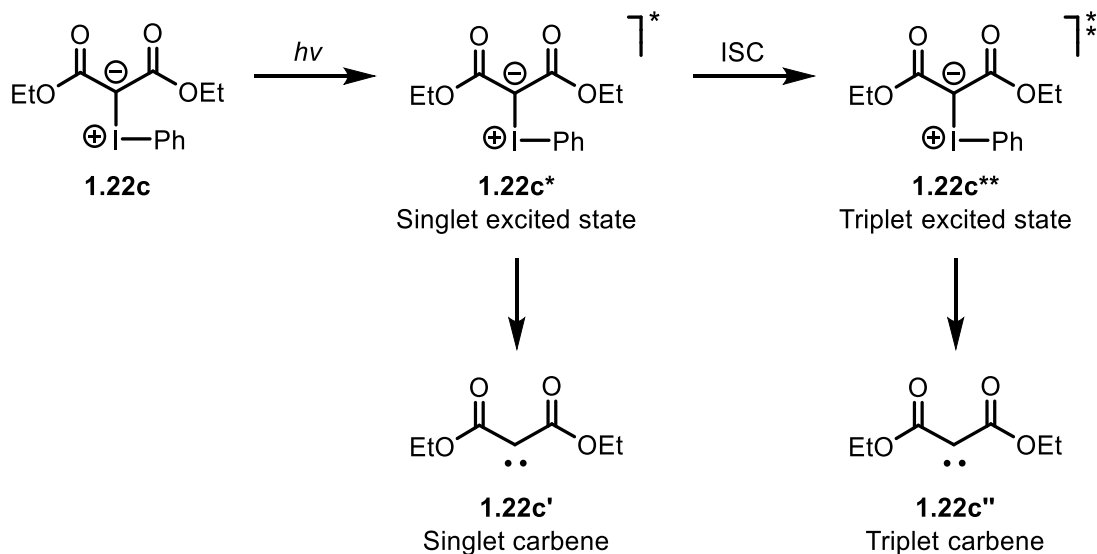


Scheme 1.38 Activation of acyclic iodonium ylides by SET

1.3.2.3.7 Photochemical Activation of Iodonium Ylides

The application of photochemistry towards iodonium ylides occurred in the mid 1980s by researchers such as Hadjirapoglou, Spyroudis and Varvoglis. In 1985 Spyroudis showed how UV light can be used to photochemically activate iodonium ylides, and in this photochemically activated state, the ylides are then able to undergo cycloadditions or transylidation reactions.⁸¹

The formation of free carbenes in these photochemically-activated reactions is still questionable, and the mechanisms are not fully understood. **Scheme 1.39** shows how the light-induced photochemical activation of iodonium ylide **1.22c** may occur, including the incorporation of singlet (**1.22c***) and triplet (**1.22c****) excited states, as well as singlet (**1.22c'**) and triplet (**1.22c''**) carbenes. The conversion of singlet to triplet excited states by ISC and more advanced mechanistic information will be explained in greater detail in Chapter 3.



Scheme 1.39 Photochemical activation of acyclic iodonium ylides

1.4 Carbenes

Historically, carbenes were first introduced by Eduard Buchner in 1903 in a cyclopropanation reaction using ethyl diazoacetate.⁸² Generally, most carbenes are considered short lived (free carbenes) and are usually prepared *in situ* from compounds such as diazonium ylides. There are examples of longer lived carbenes, so called persistent carbenes, which can be stabilized by a variety of ways, including aromatic rings or transition metals. A carbene is a neutral electron deficient species that defies the octet rule, having only 6 valence electrons, 2 of which are non-bonding.⁸³ These electrons can either be paired, and occupy the same sp^2 hybridized orbital to form a singlet carbene, or can exist as unpaired electrons, with two different sp^2 orbitals to form a triplet carbene, as shown in **Figure 1.23**. Singlet carbenes usually retain stereochemistry when engaging in reactions such as cycloadditions, while triplet carbenes do not retain stereochemistry. Carbynes are included in the figure and are defined as a compound whose structure consists of an electrically neutral carbon atom that has three non-bonded electrons. The central carbon atom in carbyne is sp hybridized, and has either one or three unpaired electrons, depending on its excitation state, and is known to have radical-like properties.

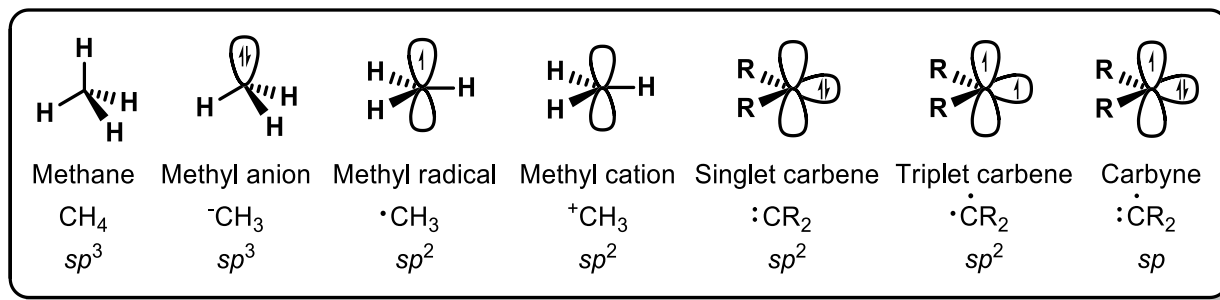
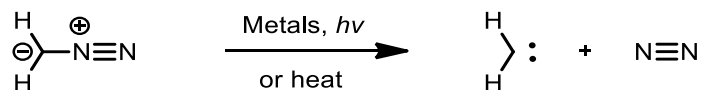


Figure 1.23 Structures and hybridization of methane analogues and carbenes

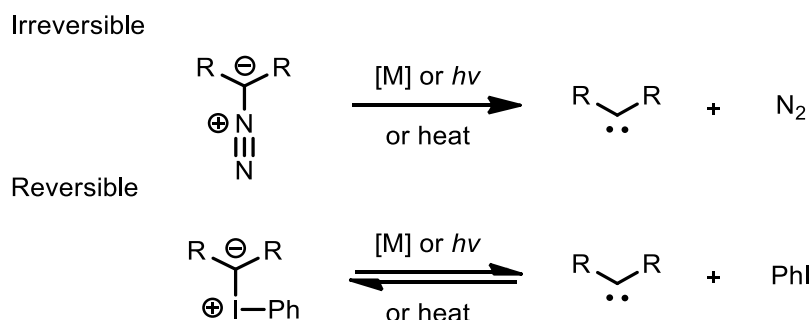
The simplest example of a carbene was prepared by Hermann Staudinger in 1912 when methylene carbene was generated by exposing a sample of diazomethane to the appropriate conditions which facilitate the loss of nitrogen gas and formation of the carbene.⁸⁴ Carbenes can be generated primarily by three main methods: metals, light, or heat, but no matter how they are formed, carbenes always display typical modes of reactivity. The main types of reactions that carbenes can participate in are cyclopropanation, insertions (C-H, N-H, O-H, S-H), nucleophilic addition, rearrangements, and ylide formation. It should be noted that if certain metals are used in the following carbene-forming reaction, the metal and the *in situ* generated carbene will interact and form a complex, known as a metalcarbene, and will have slightly different properties compared to the free carbene. A free carbene is commonly depicted as a singlet carbene with a lone pair of electrons assigned to the central carbon atom, leaving out the orbitals and charges for simplicity, as seen in **Scheme 1.40**.



Scheme 1.40 Formation of methylene carbene from diazomethane

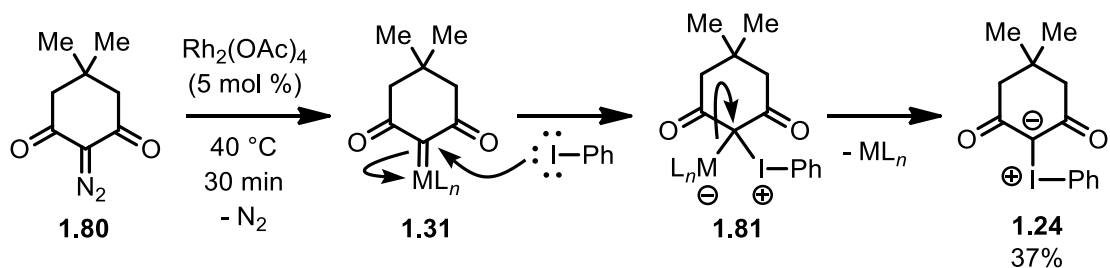
The ability of both diazonium and iodonium ylides to generate carbenes has raised the question of whether the properties of the carbene would be identical or different in reactivity. In the case of diazonium ylides, upon exposure to metals, light, or heat, the formation of a carbene is accompanied by the release of nitrogen gas which would provide additional entropic energy unless performed in a sealed environment. In the case of iodonium ylides, upon exposure to metals, light, or heat, the formation of a carbene is accompanied by the release of iodobenzene

which is not volatile and therefore will stay solvated in solution. In entropic terms, the release of a gas (nitrogen) is energetically more favourable than the release of a liquid (iodobenzene). The iodine in iodobenzene is also known to be highly polarizable, making it a relatively good nucleophile with lone pairs of electrons that can interact with the carbene possibly in a reversible manner. These two different potential scenarios are shown in **Scheme 1.41**.



Scheme 1.41 Irreversible and reversible carbene formation

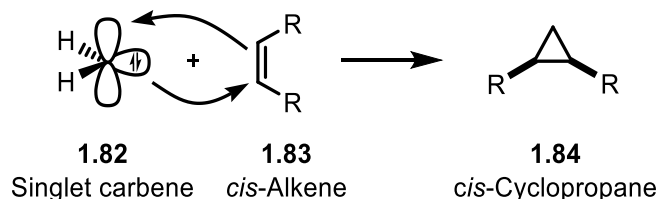
Iodobenzene was reported by Moriarty in 1985 to react with metallocarbenes generated from diazo compounds which supports the idea that iodonium ylides can react in a reversible manner in the presence of metals.¹⁴⁶ In this transylidation reaction, metallocarbene **1.31** generated from the metal-catalyzed decomposition of diazo **1.80** is attacked by the nucleophilic iodobenzene forming intermediate **1.81** which then forms iodonium ylide **1.24** as shown in **Scheme 1.42**.



Scheme 1.42 Capture of metallocarbenes by aryl iodides for iodonium ylide synthesis

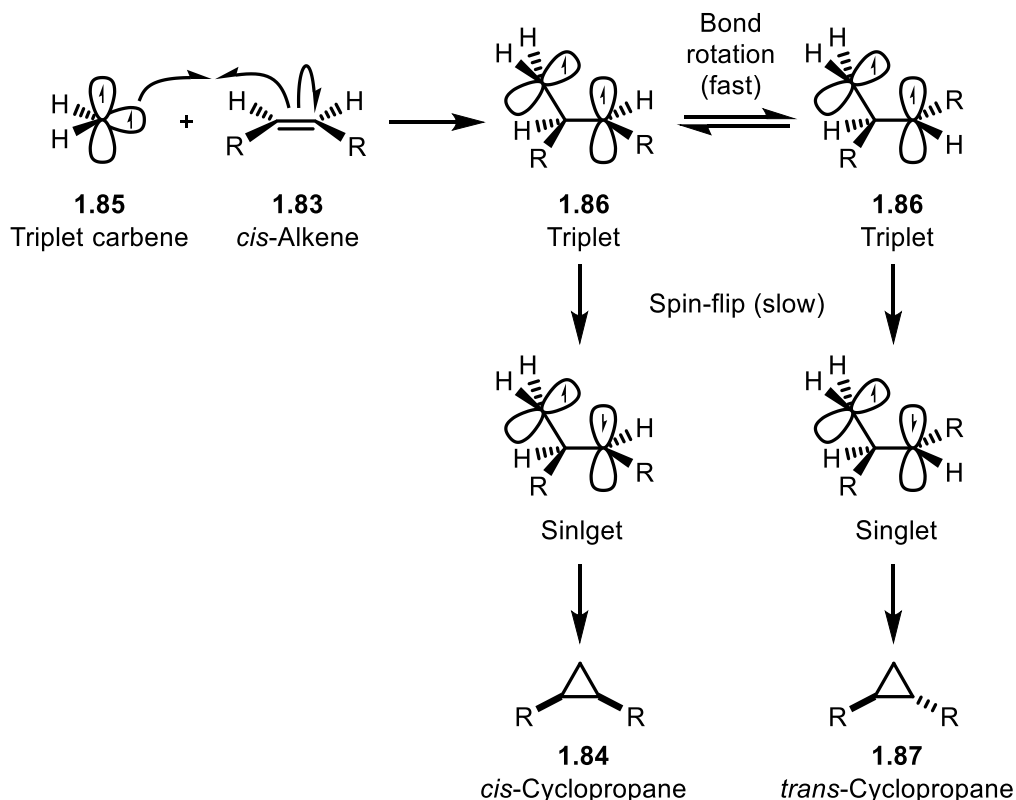
One of the most popular applications of carbenes is their use in cyclopropane synthesis. The stereochemistry in the cyclopropanation reaction of carbenes with alkenes can be predicted

based on what type of carbene is used. The stereospecific reaction of a singlet carbene (**1.82**) is shown in **Scheme 1.43**. This cyclopropanation reaction occurs in a concerted manner, not step-wise, with simultaneous bond breaking and bond making. Therefore, if the alkene starting material is *cis* (**1.83**), then the cyclopropane product (**1.84**) will also be *cis*.



Scheme 1.43 Stereochemical outcome of a singlet carbene reaction with a *cis*-alkene

The reaction of triplet carbene **1.85** with *cis*-alkene **1.83** will produce both the *cis* (**1.84**) and *trans* (**1.87**) cyclopropanes to form because of the biradical reactivity of the triplet carbene. The reaction occurs in a step-wise manner with intermediates (**1.86**) that form which are capable of undergoing bond rotation, before ring closure, to form the cyclopropane. A carbon-carbon bond rotation at room temperature is a relatively fast process in comparison to the spin-flipping process that occurs in the intermediates, as shown in **Scheme 1.44**. The spin-flipping event can only occur when there is a collision with another molecule or solvent, which converts the triplet intermediate into a singlet intermediate, which is then able to undergo ring closure to form a cyclopropane.⁸⁵ This implies that the reaction of triplet carbenes with alkenes is not a stereospecific reaction, for example, a *cis*-alkene will give a mixture of *cis* and *trans* cyclopropanes.



Scheme 1.44 Stereochemical outcome of a triplet carbene reaction with a *cis*-alkene

1.4.1 Carbenoids

The term carbenoid was first introduced by Closs and Moss in 1964 which described compounds that exhibit reactions qualitatively similar to those of carbenes, but without necessarily being free divalent carbon species.⁸⁶ Carbenoids (**1.88**) are characterized by a system that contains a metalated carbon, with metals such as lithium, magnesium, or zinc for example, which additionally bears a leaving group.⁸⁷ This arrangement, as seen in **Figure 1.24**, gives the central carbon an ambiphilic character. Despite having a carbanionic nature, they overall exhibit an electrophilic character, which has intrigued chemists over the years to use carbenoids for different applications in organic synthesis.⁸⁸ Historically, one of the first applications was in cyclopropanation chemistry, discovered by Simmons and Smith in 1958, which became known as the famous Simmons-Smith cyclopropanation reaction.

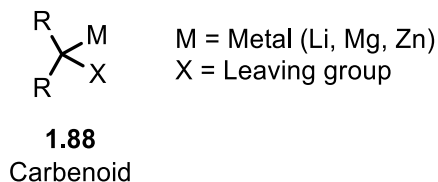
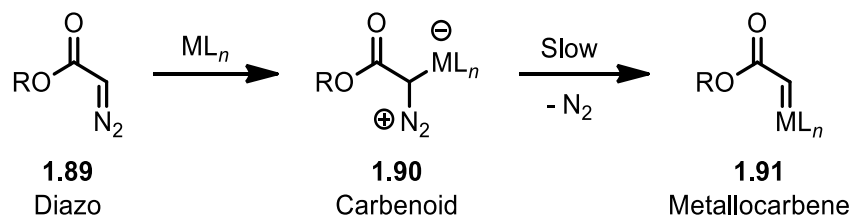


Figure 1.24 General carbenoid structure

1.4.2 Metal-Carbenes

Ylides are the most common precursors to metal carbene complexes, with diazo compounds specifically receiving considerable attention. Transition metals (M) such as copper or rhodium with a number (n) of ligands (L) bound to them can be used to activate diazo compounds (**1.89**), forming a carbenoid intermediate (**1.90**), which will then expel nitrogen gas, forming a metallocarbene (**1.91**) as shown in **Scheme 1.45**. Metallocarbenes are known to be electrophilic at the α -carbon, based on reactivity observations such as experiencing higher yields of product when reacting with more nucleophilic components.



Scheme 1.45 Metal-catalyzed metallocarbene formation from diazo compounds

Studies based off the kinetic isotope effect have shown the loss of nitrogen gas to be the slower step in the overall metallocarbene formation sequence, which implies that cleavage of the carbon-nitrogen bond is the rate-limiting step.⁸⁹

1.4.3 Fischer Carbenes

Fischer carbenes were discovered in 1964 by Ernst Otto Fischer and are characterized as a carbene with enhanced thermodynamic and kinetic stability, when compared to a non-stabilized free carbene.⁹⁰ The properties of Fischer carbenes allow for their application into more

diverse reactions with greater control over product formation. Also, limiting the amount of wasteful decomposition or dimerization that often occurs when working with free carbenes can be avoided. The first Fischer metal-carbene complex is shown in **Figure 1.25** with the characteristic heteroatom group (OMe) bonded directly to the carbene carbon.

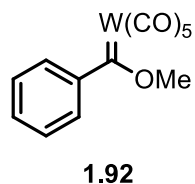
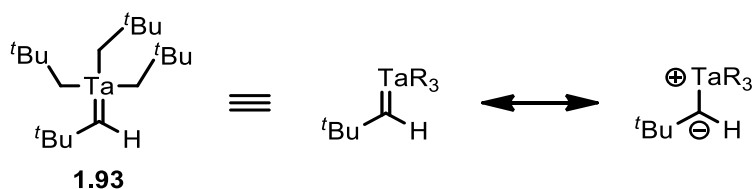


Figure 1.25 First metal-carbene complex (Fischer carbene)

1.4.4 Schrock Carbenes

Most examples of transition metal carbene complexes contain a carbon bonded to a heteroatom substituent, and only extremely rare examples have a carbon with a hydrogen attached to it. Schrock was the first to isolate a thermally stable neopentylidene complex of tantalum (**1.93**) in 1974, which is shown in **Scheme 1.46**, and has a hydrogen atom bonded directly to the carbene carbon.⁹¹

Schrock's alkylidene-metal complex initially had slight problems with stability due to overcrowding of the metal centre, and some of the compounds were decomposing after a short amount of time. Schrock noted that if coordination around the metal is too crowded, intramolecular α -hydrogen abstraction can occur leading to decomposition of the complex.⁹² After some improvements were made, Schrock created better alkylidene-metal complexes that were more stable and were easier to isolate.⁹³



Scheme 1.46 First alkylidene-metal complex (Schrock carbene)

The following **Table 1.2** lists some of the descriptions and properties of Fischer and Schrock carbenes for comparison.

Table 1.2 Fischer and Schrock carbene properties

Fischer carbenes	Schrock carbenes
<ul style="list-style-type: none"> • Discovered by Ernst Otto Fischer in 1964 • Low oxidation state metals • π-Acceptor metal ligands • Strong π-acceptors at the metal centre • Electrophilic at the carbon centre • Poor back-bonding metal • π-Donor substituents on methylene 	<ul style="list-style-type: none"> • Discovered by Richard Schrock in 1974 • High oxidation state metals • Non π-acceptor ligands • Non π-acceptors at the metal centre • Nucleophilic at the carbon centre • Strong back-bonding metal • Behave as strong bases

1.4.5 N-Heterocyclic Carbenes (NHCs)

Prior to 1960 carbenes were thought to be too reactive and short lived to be isolated, but progress in this area was made by researchers like Wanzlick who started investigating a new class of carbenes known as N-heterocyclic carbenes (NHCs). Wanzlick investigated the reactivity and stability of NHCs in 1962 and found these to be more stable than traditional free carbenes, offering the ability to perform more detailed studies.⁹⁴ A few years later Wanzlick reported the first applications of NHCs to function as ligands for metal complexes, and later on the use of NHCs was applied to organo-catalysis.⁹⁵ Advancements made in this field of chemistry eventually led to the first crystal structure of an NHC in 1991, providing researchers with concrete evidence of their formation.⁹⁶ Examples of commonly used NHCs in literature are shown in **Figure 1.26**.

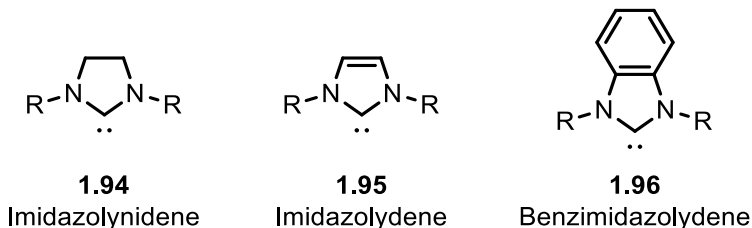
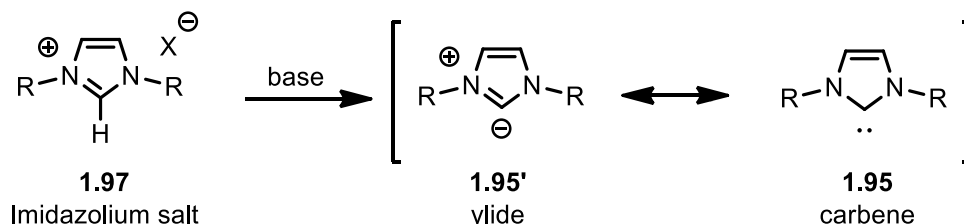


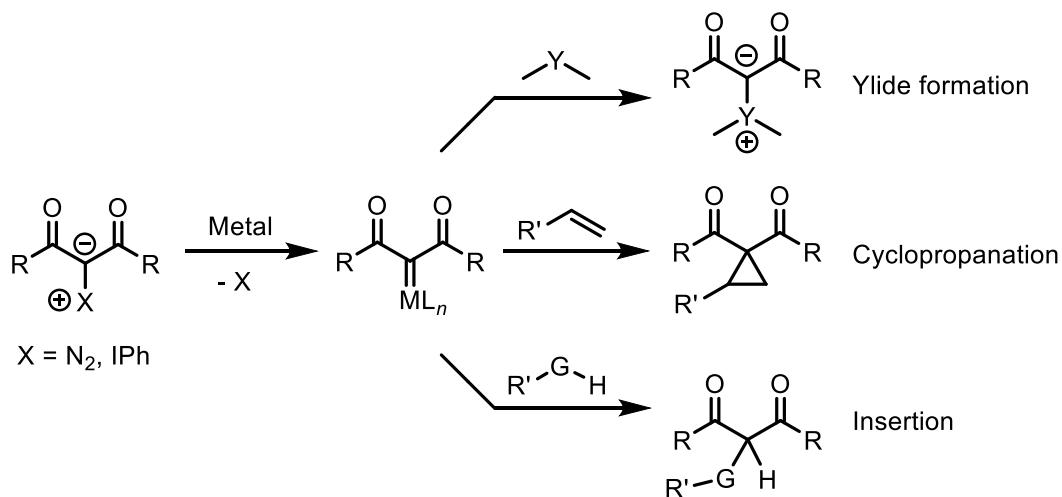
Figure 1.26 Examples of common NHC types and their nomenclature

Imidazolium salts are often used to generate NHCs as shown in **Scheme 1.47**. The acidic proton in imidazolium salts (**1.97**) has a pKa that ranges from 16-23 (in DMSO) which requires using a base such as NaH or *t*BuOK. Common counterions (X^-) include BF_4^- , Br^- , Cl^- , or ClO_4^- .



Scheme 1.47 NHC generation from imidazolium salts

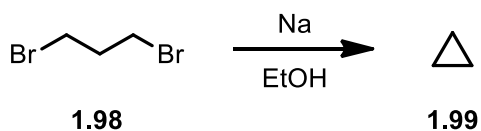
The main reaction types that metallocarbenes are used for, include ylide formation (transylidation), cyclopropanation, and insertion reactions (C-H, N-H, O-H, etc.). The metallocarbene can be efficiently accessed using diazonium and iodonium ylides in the presence of transition metals such as copper or rhodium. The metallocarbene formation from iodonium ylides is routinely performed at room temperature, while the formation from diazonium ylides often requires the use of heated conditions. Metallocarbene formation from ylides and reaction possibilities are shown in **Scheme 1.48**.



Scheme 1.48 Metallocarbene reactions of diazonium and iodonium ylides

1.5 Cyclopropanes

Cyclopropanes were discovered by the Austrian chemist August Freund (1835-1892) who was the first to propose the correct structure of cyclopropane in 1881.⁹⁷ This was quickly followed by the first synthesis of cyclopropane by Freund in 1882 which was achieved using an intramolecular Wurtz reaction.⁹⁸ Freund treated 1,3-dibromopropane (**1.98**) with sodium producing cyclopropane **1.99** as shown in **Scheme 1.49**.



Scheme 1.49 First cyclopropane synthesis by intramolecular Wurtz reaction

In 1887 Gustavson was able to improve upon the intramolecular Wurtz reaction by using zinc as the metal instead of sodium, which increased the yield to 75%.⁹⁹ The immense amount of applications of cyclopropanes were not fully recognized until years later, and in 1929 the anaesthetic properties of cyclopropane were discovered by Henderson and Lucas which eventually led to its industrial production in the years that followed.¹⁰⁰

Comparing the properties of cyclopropanes to larger cyclic hydrocarbon systems like cyclopentane or cyclohexane, we find the carbon-carbon bond angles in three-membered rings to distort from the ideal 109° angle for a typical tetrahedral system, raising ring strain energy as shown in **Figure 1.27**. This unique feature of cyclopropanes has allowed them to be used by the synthetic community for an array of various reactions with a wide range of reaction partners.¹⁰¹





			
Cyclopropane	Cyclobutane	Cyclopentane	Cyclohexane
27.6 kcal/mol	26.3 kcal/mol	6.2 kcal/mol	0.1 kcal/mol

Figure 1.27 Ring strain energies of small carbocycles

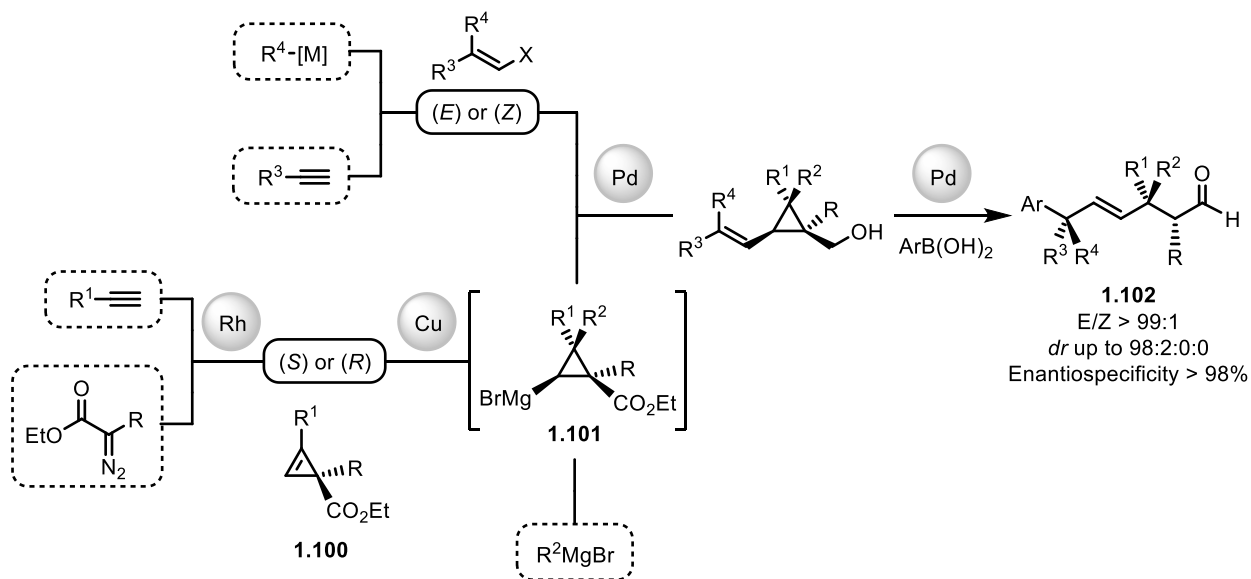
The benefits of using cyclopropanes in chemical reactions has also shown significance in natural settings, even mother nature has utilized the beneficial properties of cyclopropanes in biological systems when needed. There are numerous examples of cyclopropanes being found in biological settings as they are present in animals, plants, and microorganisms. They have a vast occurrence in biological molecules, including lipids, pheromones, and steroids for example, as well as showing up transiently in primary and secondary metabolites.¹⁰² The three membered ring of cyclopropanes has showed up in the core of antibiotics, antiviral, antitumor, neurochemical compounds, and enzyme inhibitors, illustrating their significance in natural biological systems.¹⁰³

Organic chemists have realized the advantages of incorporating cyclopropane ring systems into synthesis and have built many effective drugs with three membered rings in the core of the molecules, providing many medicinal applications.¹⁰⁴ The cyclopropane motif is highly significant in drug discovery and was acknowledged as the 10th most frequently found ring system in small molecule drugs.¹⁰⁵ The pursuit of complex molecules by means of total synthesis has also relied on strategies that take advantage of using cyclopropane as a source of carbon functionality.¹⁰⁶

It is evident in chemical literature, that cyclopropanes have found a wide range of uses in modern day organic synthesis, including cycloaddition reactions. When cyclopropanes are reacted with the appropriate reaction partner, carbon-heteroatom, and carbon-carbon bond forming reactions have been shown to be highly effective in the synthesis of many different types of cyclic molecular motifs. In addition to the applications of cyclopropanes in cycloaddition chemistry for the synthesis of cyclic motifs, there have been many clever applications of cyclopropanes for use in the construction of challenging acyclic carbon-based systems.

Synthetic methods of creating carbon-carbon bonds are of great interest and value to the synthetic community. The complexity of creating acyclic hydrocarbon-based systems is enhanced when stereocenters are present and control over setting these stereocenters is needed. A recent impressive study by Marek in 2018 was conducted that entails a succession of highly stereoselective carbon-carbon bond-forming reactions catalysed by transition metal complexes.¹⁰⁷ This work highlights an extremely useful strategy for constructing a diverse range of linear, carbon-carbon bonded systems (**1.102**) containing multiple contiguous stereocenters,

all with high levels of stereo-control, and is entirely based on the utilization of cyclopropanes (**1.101**) derived from cyclopropenes (**1.100**) as the key building blocks. The strategy used in this study is shown in **Scheme 1.50** and is a great example of how cyclopropanes can have extremely useful applications in organic synthesis.



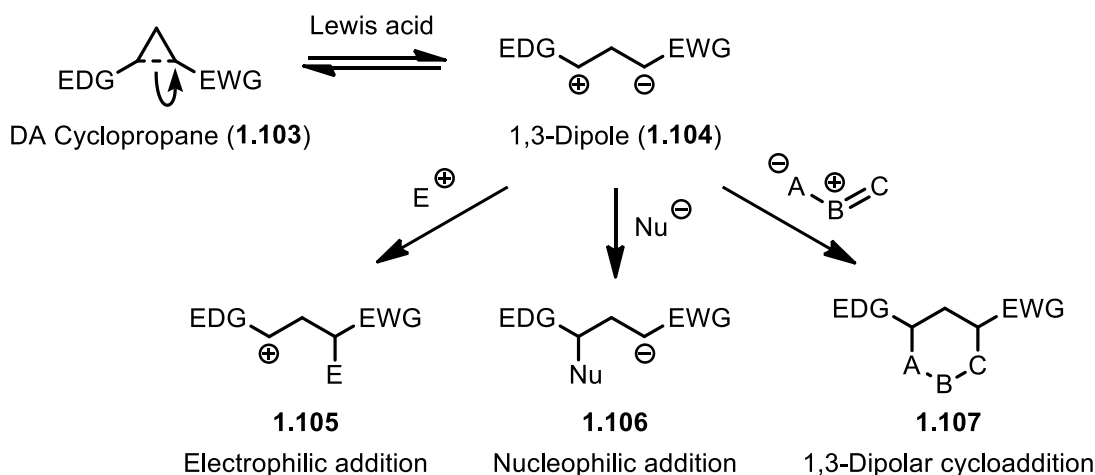
Scheme 1.50 Stereoselective preparation of acyclic hydrocarbon motifs

1.5.1 Donor-Acceptor (DA) Cyclopropanes

DA cyclopropanes give a chemist complete control over which σ -bond will break in a cyclopropane ring when appropriate conditions are applied. This regio-selective opening of the cyclopropane can be achieved by arranging an EDG (donor) *vicinal* to an EWG (acceptor) on the ring. The σ -bond located between the donor and acceptor groups is highly polarized and can be opened using Brønsted acids, Lewis acids, or other electrophilic reagents to allow for many different types of reactions to be accessed with the appropriate reaction partners.¹⁰⁸ Commonly used donor groups include alkoxy, amino, aryl, vinyl, and other groups that can stabilize carbocations. Examples of commonly used acceptor groups include esters, ketones, and other groups that can stabilize carbanions.¹⁰⁹

Activation of DA cyclopropanes (**1.103**) with Lewis acids allow for the formation of a zwitterionic 1,3-dipole intermediate (**1.104**). This 1,3-dipolar intermediate can engage with

electrophiles (E^+) and undergo electrophilic addition to form product **1.105** or engage with nucleophiles (Nu^-) and undergo nucleophilic addition to form **1.106**. The 1,3-dipolar intermediate is also able to engage with dipolarophiles and undergo cycloaddition reactions that can form carbocyclic or heterocyclic compounds (**1.107**). These different reaction pathways that DA cyclopropanes can access are summarized in **Scheme 1.51**.

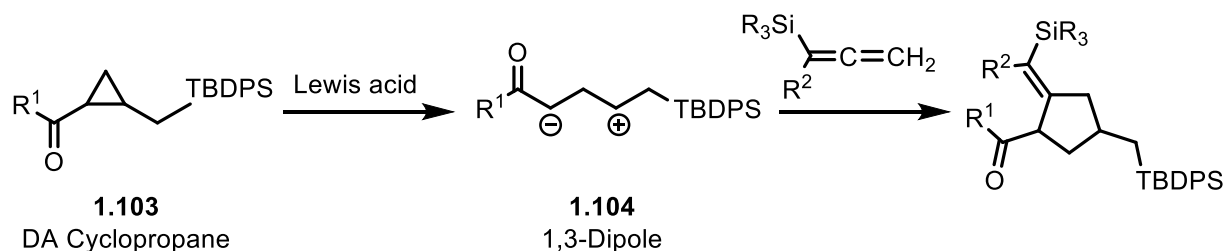


Scheme 1.51 General reactions of DA cyclopropanes

Activation of DA cyclopropanes has relied on electrophilic reagents to interact with the EWG and assist in ring opening by stabilizing the 1,3-dipole intermediate that forms *in situ*. Lewis acids are the most well-known reagent to accomplish this reactivity, and there are numerous reports published in the literature. Commonly used Lewis acids for the activation of DA cyclopropanes are often multidentate species such as $FeCl_3$, $GaCl_3$, $InBr_3$, $Sc(OTf)_3$, $Sn(OTf)_2$, and $Yb(OTf)_3$ for example. Reagents other than Lewis acids have also been shown to open DA cyclopropanes, including the use of HVI reagent $PhICl_2$ which results in a 1,3-dichlorination reaction of the opened cyclopropane.¹¹⁰ This reaction is based on the Lewis-acidic character of $PhICl_2$ and also the ability to generate Cl^- and Cl^+ *in situ*. In addition to these examples, Brønsted acid catalysts such as TfOH have also been shown to be a viable reagent for opening of DA cyclopropane systems and generating 1,3-dipolar intermediates that are able to react with electron-rich aromatics.¹¹¹

A mechanism on how the formation of a 1,3-dipole (**1.104**) is created from a DA cyclopropane (**1.103**) by Lewis acid catalysis is shown in **Scheme 1.52**. The activation of

cyclopropanes by a Lewis acid has been shown to form a ring opened intermediate proposed as containing a formal positive charge and negative charge to give a 1,3-dipole which can then be used to create products. In the example below a Lewis acid catalyst such as TiCl_4 was used in an intermolecular allene annulation with allenylsilanes to furnish [3+2] adducts which was mechanistically proposed to occur through a formal 1,3-dipole intermediate.¹¹²



Scheme 1.52 Mechanism of Lewis acid-catalyzed 1,3-dipole formation in DA cyclopropanes

1.5.2 Synthesis of Cyclopropanes

There is a rich history in the synthesis of cyclopropanes which dates back well over 100 years ago, to the 1880s. Three researchers (Conrad, Perkin, and Michael) from the years 1884 to 1887 all report new cyclopropanation reactions, even though the structure and properties of cyclopropane were still in their infancy and were just starting to be understood and investigated. Because of this, some of the earlier yields for cyclopropanation reactions were not reported, or are prone to errors, because of the lack of precision in interpreting data due to this uncertainty.

In 1884 Conrad reported a cyclopropanation reaction from the starting materials diethyl 2,3-dibromopropionate and diethyl sodiomalonate.¹¹³ This was quickly followed by a straightforward approach of synthesizing cyclopropanes using nucleophilic displacement ($\text{S}_{\text{N}}2$) chemistry, discovered by William Henry Perkin in 1884. Perkin's cyclopropanation reaction of diethyl malonate was accomplished using 1,2-dibromoethylene in the presence of the base sodium ethoxide.¹¹⁴ The American chemist Arthur Michael, famously known for discovering the Michael addition reaction, also discovered a cyclopropanation reaction in 1887 by reacting ethyl 2-bromoacrylate and (1,3-diethoxy-1,3-dioxopropan-2-yl)sodium to generate triethyl cyclopropane-1,1,2-tricarboxylate.¹¹⁵

After this initial burst in cyclopropane synthesis discoveries, this area of chemistry went relatively quiet for about 70 years. Doering and Hoffmann then performed the cyclopropanation reaction of cyclohexene by treating chloroform with $t\text{BuOK}$ in a base mediated α -elimination reaction, which was known to produce the free carbene equivalent, dichlorocarbene in 1954.¹¹⁶

Some of the more well known cyclopropanation reactions, considered “classics” were discovered in the 1950’s and 1960’s. These include reactions such as the Simmons-Smith cyclopropanation, discovered in 1958 by American chemists Howard E. Simmons and Ronald D. Smith.¹¹⁷ And the extremely useful Corey-Chaykovsky reactions of sulfur ylides with electron deficient alkenes was discovered by the American chemists Elias James Corey and Michael Chaykovsky. The Corey-Chaykovsky epoxidation reaction was discovered in 1962¹¹⁸ and the Corey-Chaykovsky cyclopropanation reaction was discovered in 1965.¹¹⁹

In 1989 the Kulinkovich reaction was discovered, which was a significant advancement in organotitanium chemistry, by treating aliphatic esters with ethyl magnesium bromide in the presence of $\text{Ti}(\text{O}^i\text{Pr})_4$ the formation of cyclopropanols could be achieved.¹²⁰

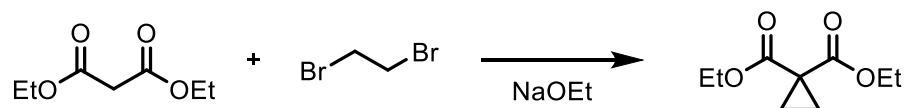
Transition metal-catalyzed carbene insertion cyclopropanation reactions of diazonium ylides into alkenes has been utilized by numerous organic chemists over the years and has been the focus of many reviews and publications.¹²¹ After the discovery that ylides are capable of forming cyclopropanes when reacted with alkenes, there has been a huge leap forward in utilizing this chemistry for all sorts of interesting applications. After diazonium ylide-based cyclopropanation was discovered, many other types of ylides were found to eventually be compatible with similar conditions.

More recent applications of cyclopropane synthesis have appeared in the literature, offering many new beneficial advantages and interesting ways of incorporating cyclopropane methodologies into all sorts of different reactions. A new copper-catalyzed [1+1+1] cyclotrimerization method for the synthesis of cyclopropanes was reported by Antonchick in 2016.¹²² This unprecedented cyclotrimerization reaction of simple ketones offers high stereoselectivity, and the unique ability for a cascade of regioselective functionalization reactions involving unreactive $\text{C}(\text{sp}^3)\text{-H}$ bonds. A recent olefin cyclopropanation reaction via photo-initiated diiodomethane (CH_2I_2) activation was reported by Suero in 2017, offering a new way to use diiodomethane (Simmons-Smith) for a cyclopropanation reaction.¹²³ Surely the area of

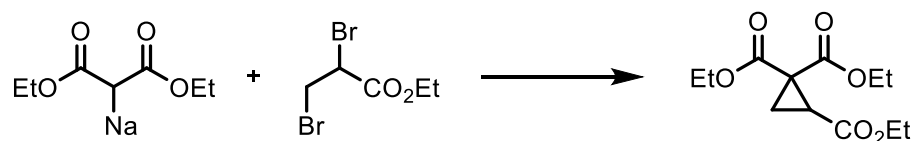
cyclopropanation chemistry is a field that will see many more discoveries in the future and will continue to grow as new reaction types are realized and reported.

Due to the incredible usefulness of constructing carbon-carbon bonds, newer methods of performing this chemistry is of interest, especially when the methods can perform the equivalent reaction but substituting metals with cheaper alternatives, such as light. This advancement of chemistry can be considered “green chemistry” and is a trending topic in modern day synthesis due to the multiple number of advantages, specially the beneficial effects or consequences it has on the environment, and in turn, the planet. Selected examples of cyclopropane synthesis that were either historically important, or useful as reliable synthetic methods are shown in **Scheme 1.53**.

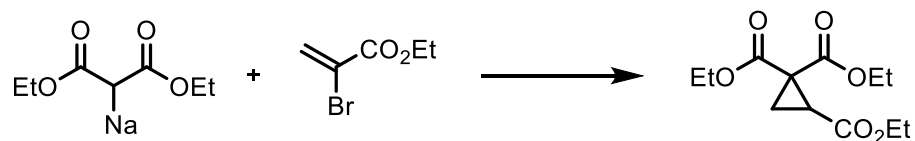
Perkin (1884)



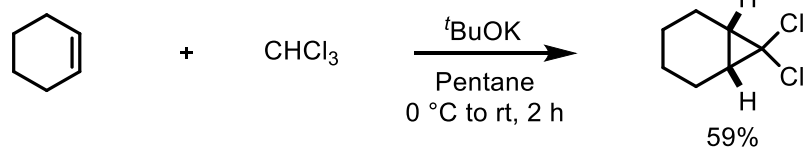
Conrad & Guthzeit (1884)



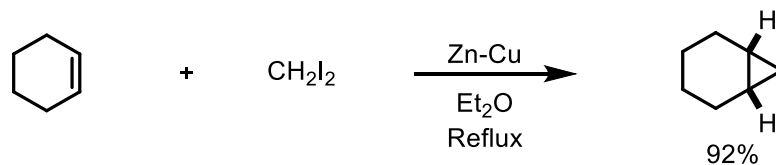
Michael (1887)



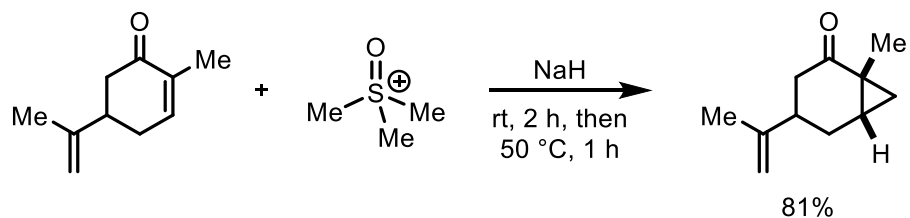
Doering (1954)



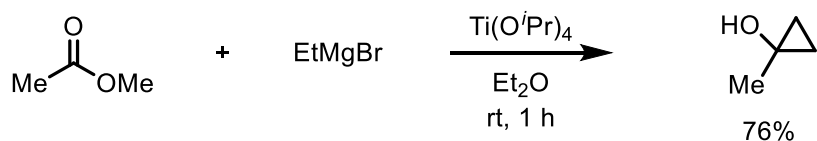
Simmons & Smith (1958)



Corey & Chaykovsky (1965)

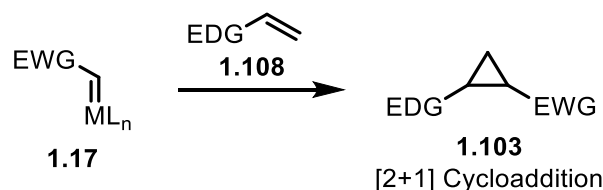


Kulinkovic (1989)



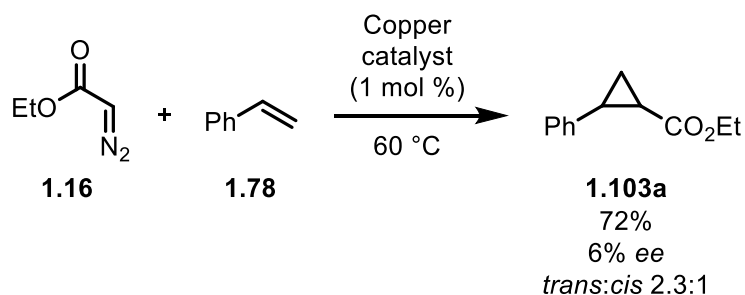
Scheme 1.53 Historically important cyclopropanation reactions

The use of cycloadditions for the synthesis of DA cyclopropanes has been shown to be a valuable and reliable strategy. As seen in **Scheme 1.54** [2+1] cycloadditions between metallocarbenes (**1.17**) and alkenes, are reliable methods for synthesizing cyclopropanes, especially DA cyclopropanes (**1.103**) when using alkenes bearing an EDG group (**1.108**). The source of the metallocarbene commonly comes from diazonium, iodonium, or sulfonium ylides for example.



Scheme 1.54 General [2+1] cycloaddition used in DA cyclopropane synthesis

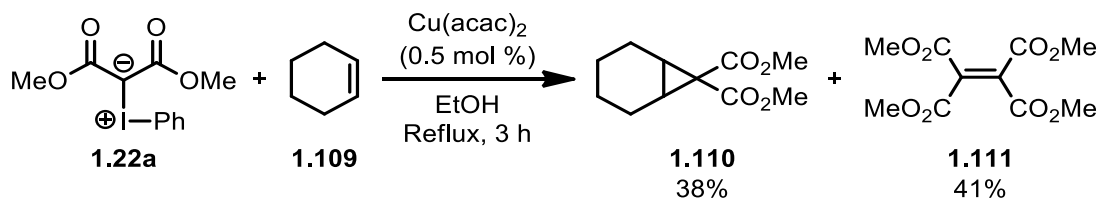
Some of the first reports of the use of these different types of ylides in cyclopropane synthesis is described below. One of the first examples of the use of diazonium ylides (**1.16**) in enantioselective synthesis of cyclopropane **1.103a** as shown in **Scheme 1.55**. This example of an enantioselective copper-based intermolecular cyclopropanation reaction was reported by Nozaki in 1966.¹²⁴



Scheme 1.55 Cyclopropanation of diazonium ylides with alkenes

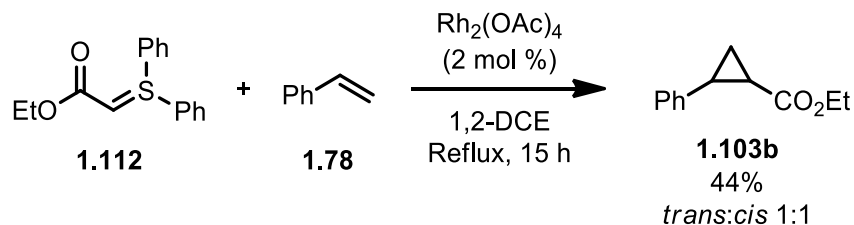
The cyclopropanation of alkenes with iodonium ylides was first discovered in 1982 when an example of this type of reaction was introduced to the literature.¹²⁵ Acyclic iodonium ylide **1.22a** was found to undergo a cyclopropanation reaction with cyclohexene (**1.109**) in the presence of a copper catalyst to form cyclopropane **1.110** and dimer **1.111**, as shown in **Scheme 1.56**. As this was the first cyclopropanation reaction from iodonium ylides, the authors were not expecting the product and therefore did not mention a mechanism or try to reason how the

transformation happened. They did however mention that this outcome is indicative of the intermediate formation of carbene or carbenoid species.



Scheme 1.56 Cyclopropanation of iodonium ylides with alkenes

A rhodium-catalyzed cyclopropanation reaction of ethyl diphenylsulfonium acetate with styrene was reported by Müller in 1999, and represents one of the first examples for the use of sulfonium ylides in cyclopropane synthesis.¹²⁶ The cyclopropanation reaction between sulfonium ylides (**1.112**) and olefins in the presence of rhodium and copper catalysts was first shown possible to give a racemic mixture of cyclopropanes (**1.103b**) as shown in **Scheme 1.57**, and was then followed up with an enantioselective variant. This reaction was tried with chiral ligands and the *ee* was shown to approach 48% at the highest, which was achieved using a rhodium-based catalyst. The use of a copper catalyst and chiral ligands derived from Pfaltz Cu–semicorrin complex furnished cyclopropanes with enantioselectivities of up to 80% *ee*.



Scheme 1.57 Metal-catalyzed cyclopropanation reaction of sulfonium ylides with alkenes

The Corey-Chaykovsky reaction, discovered by E. J. Corey and Chaykovsky, was an incredible achievement in the field of organic synthesis, and is routinely used by many chemists for the construction of cyclopropane rings. The reaction is based on the use of sulfonium and sulfoxonium ylides, demonstrating again, the usefulness of ylides in cyclopropane synthesis.

1.5.3 Structure and Bonding of Cyclopropanes

Structural properties of the cyclopropane ring system have been thoroughly investigated over the years since its discovery and has resulted in its utilization for many different synthetic applications. Cyclopropanes constitute the simplest cyclic hydrocarbon system possible, as three atoms is the smallest number of elements needed to construct a cyclic system. The small cyclopropane ring presents a defined 3-dimensional shape, conformational rigidity, and unique electronic properties making them suitable candidates for the potential of building many different interesting molecules with the option of built-in chirality if needed.

Physical descriptions of cyclopropanes have evolved over time to stay up to date with current observations of reactivity as new reactions and reaction types are continually discovered. In 1931 Linus Pauling described the bonding in cyclopropane rings as "banana bonds" due to the incredible amount of bending displayed by the carbon-carbon-carbon bond angles in a three-membered ring, when compared to the ideal 109° angle for a typical three-dimensional tetrahedral shape.¹²⁷ The banana bonding term can be thought of as a general representation of altered electron density to resemble a bent structure within small ring molecules as shown below in **Figure 1.28**. They are a special type of chemical bonding in which the ordinary hybridization state of two atoms making up the bond are modified with increased or decreased *s*-orbital character in order to accommodate a particular molecular geometry.¹²⁸ The banana bonding model (**1.99''**) of cyclopropanes (**1.99**) suggests that sp^3 hybridized carbons give rise to a stable, trigonal planar arrangement, even though instability is inferred as all hydrogens are eclipsed (**1.99'**).

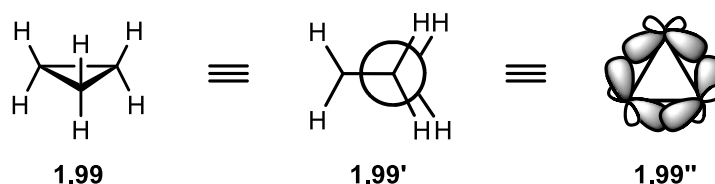


Figure 1.28 Cyclopropane structural properties

The concept of banana bonds was also described in the Coulson and Moffit model, which was presented to describe cyclopropanes as having sp^3 hybridized carbons, but with a greater

amount of *p*-character. The banana bonds were proposed to have greater electron density lying outside of the carbon-carbon bond axis. This phenomenon was eventually supported by evidence obtained by X-ray diffraction to provide accurate measurements of these bond angles, as shown below in **Figure 1.29**.¹²⁹

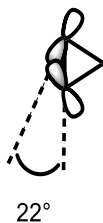


Figure 1.29 Coulson-Moffitt model bond angles

In 1947 the physical description of cyclopropanes was modified by Walsh who suggested that cyclopropanes could be considered as an insertion of methylene into ethylene, giving rise to a D_{3h} symmetric compound.¹³⁰ This alternative model became known as the Walsh model, and relied on semi-localized, so-called Walsh orbitals, in which the cyclopropane is described as a carbon with sp^2 σ -bonding and an in-plane π -bonding system overall.¹³¹ The unique sp^2 -like reactivity of cyclopropanes in this model is attributed to the poor overlap of the CH_2 orbitals, and this is described as the origin of the angular strain.¹³²

A further advancement in the understanding of the structure and bonding in cyclopropanes was described in the Dewar model. The Dewar model has implications that the three carbon-carbon bonds in the cyclopropane ring, which would equal six σ electrons, can fit the description of being aromatic, based on the Hückel $4n + 2$ rule.¹³³ This model is supported by the upfield shifts observed in the protons of cyclopropanes seen in NMR spectra. This upfield shift has been attributed to the anisotropy effect, which is also referred to as ring current, which is a property of cyclopropanes.¹³⁴

Despite each bonding model having strengths and weaknesses, there has been an effort to unify these models to come up with an accurate representation of the electronic structure of the cyclopropane ring.¹³⁵ This high level of understanding is critical for helping organic chemists to aid in the discovery of new reactions and to use cyclopropanes to their highest potential.

1.5.4 Reactivity of Cyclopropanes

Cyclopropane reactivity has been compared to alkenes, but with the addition of an extra methylene unit. Cyclopropanes containing an electron donating substituent, such as an alkoxy group, have the reactivity properties of a homo-enolate. In enolate system **1.113**, the α carbon would have a partial positive charge and the β carbon would have a partial negative charge. In the analogous cyclopropane with an alkoxy group attached (**1.114**), the α carbon would have a partial positive charge and the β carbon would have a partial negative charge. After opening of the cyclopropane into an acyclic structure, the β carbon would place the partial negatively charged carbon an extra carbon away from the α carbon, thereby creating an umpolung system. This same reasoning can be applied to Michael acceptor **1.115** and cyclopropanes containing an electron withdrawing substituent, such as an ester group (**1.116**), which have the reactivity properties of a homo-Michael acceptor. These reactivity differences between alkenes and cyclopropanes are shown below in **Figure 1.30**.

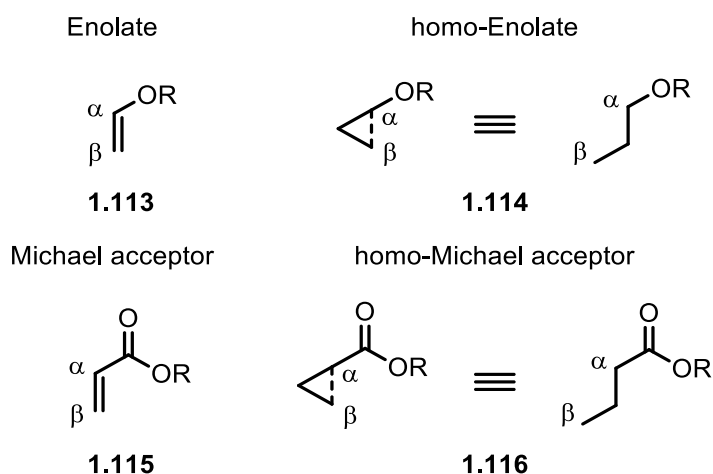
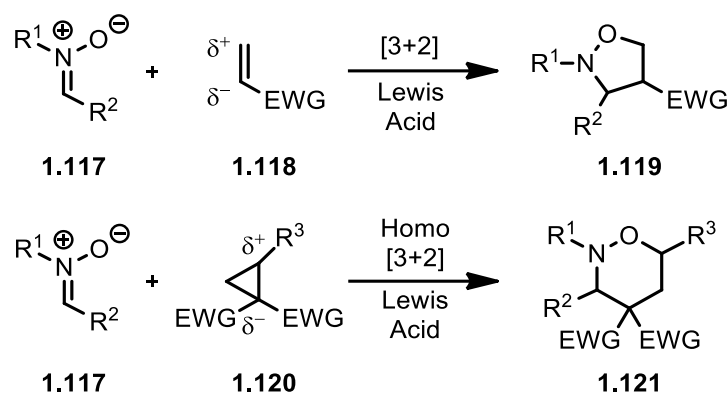


Figure 1.30 Reactivity of cyclopropanes

This one carbon homologation principle is also seen in cycloaddition reactions of cyclopropanes. The reaction of nitrones (**1.117**) with alkenes (**1.118**) undergoes a [3+2] cycloaddition which produces a five-membered ring (**1.119**), while the reaction of nitrones with cyclopropanes (**1.120**) undergoes a homo [3+2] cycloaddition to give a six-membered ring (**1.121**), as shown below in **Scheme 1.58**.



Scheme 1.58 Cycloadditions of nitrones with alkenes or cyclopropanes

This one carbon homologation extension principle has resulted in cyclopropanes to be regarded as umpolung synthons in organic synthesis.¹³⁶ This principle has been associated with the opening of larger cycloalkanes containing an odd number of carbon atoms, as the opening of these rings gives a linear carbon chain with alternating partial positive and negative charges that would otherwise not be directly accessible by other means.

1.6 Scope of Thesis

The purpose of this thesis was to investigate the ability of iodonium ylides to function in an analogous manner and sometime even superior to that of diazonium ylides for cyclopropanation reactions. Because iodonium ylides are known throughout the literature to react in a similar manner to diazo compounds but encompass safer properties such as not being toxic or carcinogenic, then it is beneficial to investigate their potential as diazo surrogates in an attempt to create more environmentally friendly synthetic alternatives.

Chapter 2 studies the use of ylides that contain a mono carbonyl stabilizing groups which has been thoroughly explored in diazo chemistry but has only begun to just scratch the surface in iodonium ylide chemistry. There is tremendous potential in this area for iodonium ylides to replace virtually all mono carbonyl diazonium ylide-based reactions in the future. While most of these reactions require transition metals, that was the focus of this chapter and progress was made in advancing the understanding of how MCIY react in a metallocarbene reaction which is beneficial to start replacing diazo reactions with the safer alternative iodonium ylides. The chemistry in the Murphy group back in 2013 was built upon and advanced with satisfaction

as optimal conditions were discovered and implemented for the cyclopropanation of Wittig reagents with alkenes, made possible by the activation of HVI-based iodosoarenes.

Chapter 3 describes the use of photochemistry for the cyclopropanation of dicarbonyl-based iodonium ylides with alkenes without the need for metal catalyst or additives. This novel methodology was a benefit to the synthetic community as it now offers an efficient and environmentally friendly approach for creating useful donor-acceptor cyclopropanes with nearly quantitative yields in some examples. The fundamentals of photo-activation of iodonium ylides was explored from the use of visible light generated from LEDs. Custom built photoreactors were designed and upgraded until an optimal system was developed for this new cyclopropanation reaction. The theoretical science behind this reaction was backup up by measuring the UV-Vis absorbances of the iodonium ylides by spectroscopy methods, and matched up with the LED emissions, also collected with spectroscopic instruments.

Chapter 4 goes into the details of enantioselective reactions using chiral iodonium ylides for chiral cyclopropane synthesis. Building on the visible light-mediated cyclopropanation reaction from Chapter 3, the possibilities were explored to see if this chemistry could be adapted for enantio-selective applications. This methodology would be of great importance to the synthetic community as most modern-day synthetic projects rely on creating molecules in enantiopure form for use in medicinal applications and for use in biological settings. Having access to reliable methods that can be used to synthesize chiral iodonium ylides may prove to one day have a use for reactions other than the ones described about in this thesis, so it would be useful to the synthetic community to have experience with and procedures on how to effectively synthesize chiral iodonium ylides using different sources of chirality, and understanding their respective properties to exploit their use in the near future.

Chapter 2: Cyclopropanation of Monocarbonyl Iodonium Ylides

2.1 Background

Iodonium ylides are an important class of HVI compounds; they were first synthesised in 1957 with Neiland's seminal work.¹³⁷ Since their initial discovery, iodonium ylides have found applications in synthetic chemistry by serving as efficient carbene precursors.⁵⁸ The most common type of iodonium ylides are derived from 1,3-dicarbonyl systems (**2.1**), with both carbonyls acting as EWGs to stabilize the zwitterionic negative charge. These ylides are easier to generate and are much more stable when compared to iodonium ylides that are stabilized by a single EWG making these species short-lived. Different types of iodonium ylides can be divided into sub-categories for organizational and comparative analysis. One sub-category is monocarbonyl iodonium ylides (MCIYs) which are known to be short-lived species and are derived from an iodonium ylide containing a single stabilizing carbonyl group (**2.2**). Another sub-category is iodonium ylides derived from phenolic substrates (**2.3**) that are relatively stable and contain an aromatic ring, often substituted with one or more EWGs, with nitro groups being more commonly used. The last sub-category of mono-stabilized iodonium ylides are ones containing a nitro functional group as the source of stability (**2.4**) and are also short-lived species. The sub-categories of mono-stabilized iodonium ylides compared to the more stable and common dicarbonyl iodonium ylides are shown below in **Figure 2.1**.

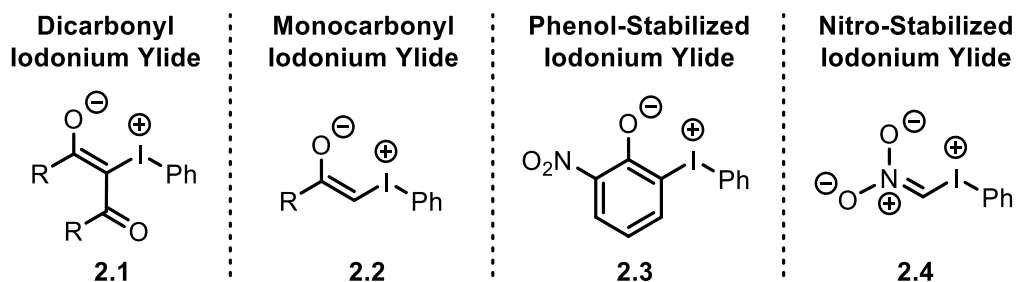
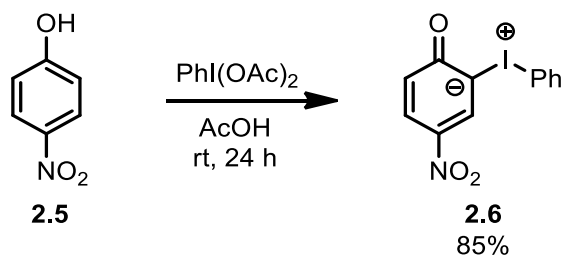


Figure 2.1 Iodonium ylide types

The first mention of mono-stabilized iodonium ylides in the literature was in a report by Pausacker in 1957.¹³⁸ Treatment of 4-nitrophenol (**2.5**) with $\text{PhI}(\text{OAc})_2$ in benzene generated a

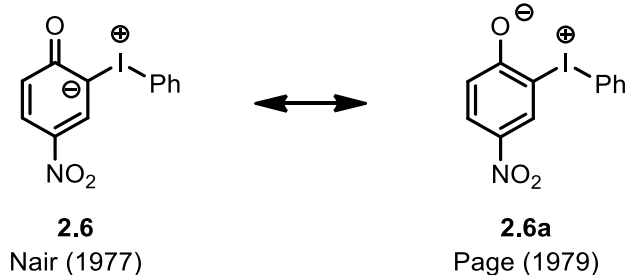
mixture of compounds, but in low yields, and iodonium ylide (**2.6**) was proposed as a possible product. The authors stated they were not confident in establishing the correct structure formed from the reaction, because in 1957 iodonium ylides had just been discovered so there was a lack of information and understanding.

The next publication of a mono-stabilized iodonium ylide was reported by Nair in 1977.¹³⁹ When equimolecular amounts of **2.5** and $\text{PhI}(\text{OAc})_2$ were dissolved in glacial acetic acid and left at rt for 24 h, a yellow amorphous precipitate was obtained, proposed to be structure **2.6** as the product (**Scheme 2.1**). This reaction was very similar to the one discovered by Pausacker 20 years ago, however, NMR studies were performed and confirmed the product to be **2.6**.



Scheme 2.1 Phenol-stabilized iodonium ylide synthesis

The phenol-stabilized iodonium ylide **2.6** that Nair and Pausacker had reported was again brought up in the literature in a publication by Page in 1979 who used X-ray crystallographic analysis to confirm what was already known.¹⁴⁰ The only difference is that the study revealed a more accurate representation of **2.6** which is supposedly represented better by drawing the aromatic system as fully aromatized (**2.6a**) as shown below in **Scheme 2.2**. This puts the primary charge locations on the iodine and oxygen atoms, with an iodine-oxygen ionic bond. The use of X-ray crystallographic analysis was critical for providing an exact distance of 2.768 Å between the iodine and oxygen atoms, which indicates that there is an intramolecular ionic attraction present.



Scheme 2.2 Phenol-stabilized iodonium ylide resonance structures

Some examples of phenol-stabilized iodonium ylides are shown below in **Figure 2.2** illustrating that most examples from this class contain at least one nitro functional group on the aromatic ring and the nitro group is always either *ortho* or *para* to the phenolate group.¹⁴¹

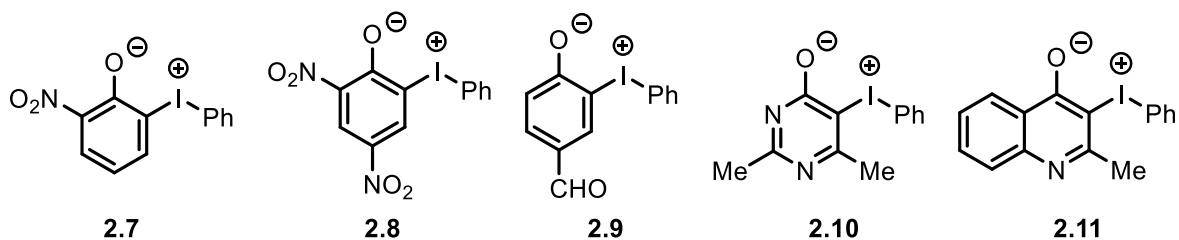
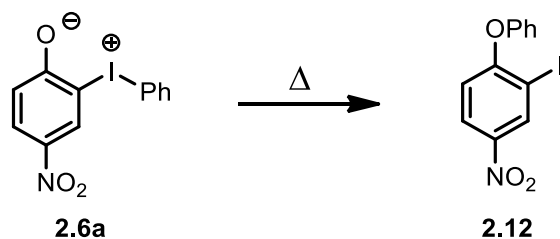


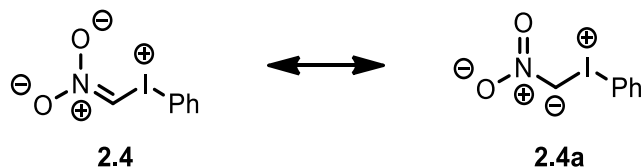
Figure 2.2 Examples of phenol-stabilized iodonium ylides

Monosubstituted phenol-stabilized iodonium ylides are thermally unstable and undergo a [1,4] sigmatropic rearrangement, also called a 1,4-aryl migration, if heated. The rearrangement is a well-known phenomenon that also occurs in cyclic iodonium ylides when heated.¹⁴² According to mechanistic and computational studies, the intramolecular 1,4-aryl migration is known to proceed through a concerted nucleophilic aromatic substitution reaction to give iodoether **2.12** as shown below in **Scheme 2.3**.¹⁴³



Scheme 2.3 Thermally induced 1,4-aryl migration of phenol-stabilized iodonium ylides

In addition to phenol-stabilized iodonium ylides, nitro-stabilized iodonium ylides are a rare class of compounds discovered by the Hansen¹⁴⁴ and Charette¹⁴⁵ groups and have limited applications in organic chemistry. An example of a nitro-stabilized iodonium ylide derived from nitromethane (**2.4**) and the resonance structure for this ylide is shown below in **Scheme 2.4**.



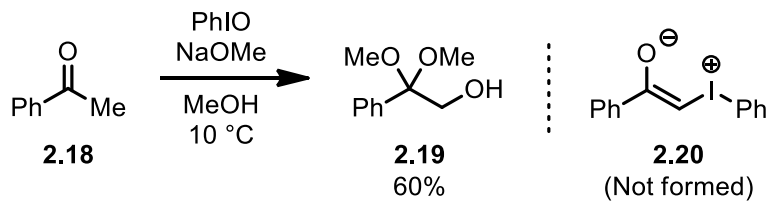
Scheme 2.4 Resonance structures of nitro-stabilized iodonium ylide

2.2 Monocarbonyl Iodonium Ylides (MCIYs)

Moriarty was one of the first researchers to introduce iodonium ylides stabilized by a single, or mono, carbonyl group in the 1980s. Moriarty was also first to acknowledge that working with MCIYs would be challenging in a 1985 report.¹⁴⁶ He was aware of low stability problems with the generation and characterization of MCIYs due to, which represented a long-standing problem in the field of HVI chemistry.

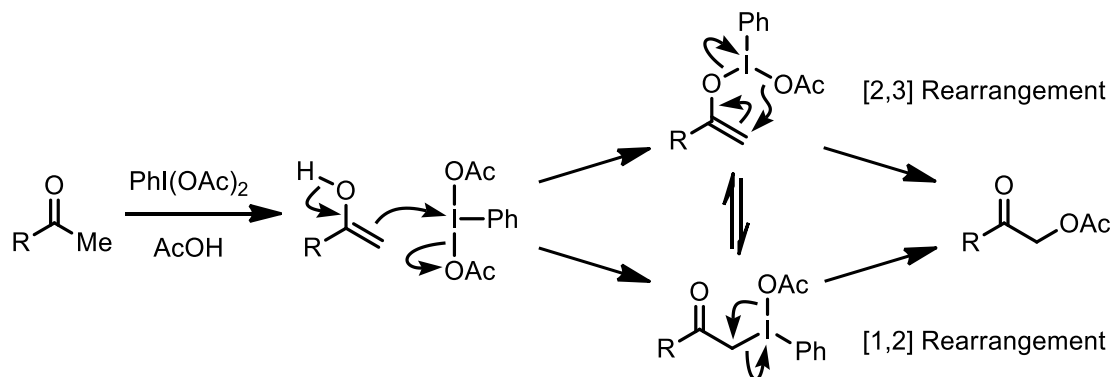
2.2.1 Synthesis of MCIYs

Following standard procedures to generate iodonium ylides that work well with β -dicarbonyl systems, Moriarty noted that these conditions failed when applied to monocarbonyl systems. The synthesis of β -dicarbonyl iodonium ylides can be accomplished by reacting a dicarbonyl methylene compound with PhIO or PhI(OAc)₂ in a straightforward approach. When PhIO was added to a mixture of acetophenone (**2.18**) and NaOMe, the monocarbonyl-derived iodonium ylide (**2.20**) did not form and the only product obtained was **2.19** as shown below in **Scheme 2.5**.



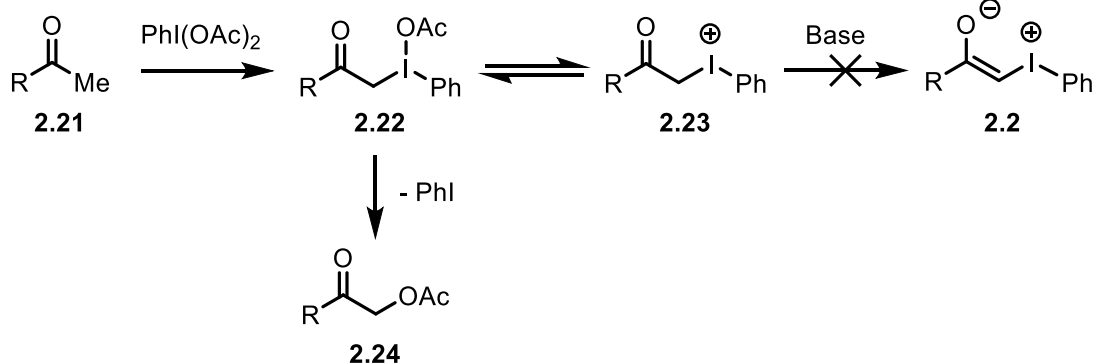
Scheme 2.5 Problems associated with MCIY synthesis

A mechanistic analysis of how single carbonyl-based systems react with HVI reagents such as $\text{PhI}(\text{OAc})_2$ is shown below in **Scheme 2.6** illustrating the difficulty in MCIY synthesis.



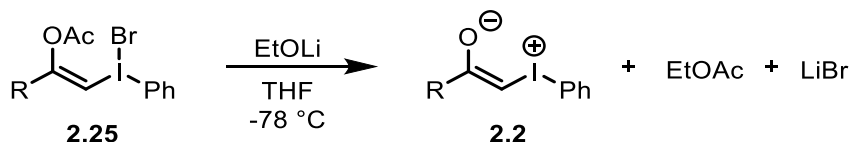
Scheme 2.6 Reactivity of $\text{PhI}(\text{OAc})_2$ with general methyl ketones

The α -functionalization of methyl ketones, as shown above, implies that the synthesis of MCIYs is not as straightforward as predicted and there are hurdles in the ability of a direct synthesis. The deprotonation of intermediate **2.23** does not occur, instead an unwanted substitution event takes place giving **2.24** with any ligand present in the hypervalent iodine reagent (AcO^- in this example) due to the hyper-leaving group capability (nucleofugality) of the PhI^+ ion to form neutral iodobenzene. Every base that has been attempted to deprotonate intermediate **2.23** has failed, and instead an uncontrollable substitution reaction occurs at the α -carbon as shown below in **Scheme 2.7**.



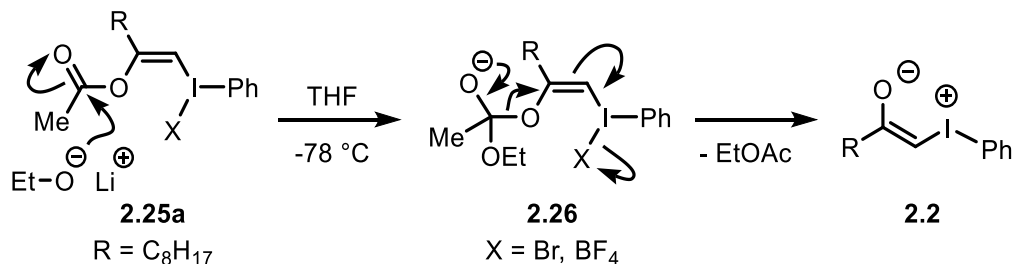
Scheme 2.7 Problem with undesired substitution instead of deprotonation

The inability to synthesize MCIYs remained unsolved until Ochiai reported a new method to overcome this issue in 1997.¹⁴⁷ Ochiai was able to advance the understanding and applications of MCIY chemistry with the introduction of an acyl transfer method, which for the first time, allowed for the generation of MCIYs, if performed between $-30\text{ }^\circ\text{C}$ and $-78\text{ }^\circ\text{C}$. Ochiai's MCIY synthesis method proceeds through an ester exchange reaction starting from **2.25** and lithium ethoxide to give **2.2** produced along with EtOAc and LiBr as shown below in **Scheme 2.8**.



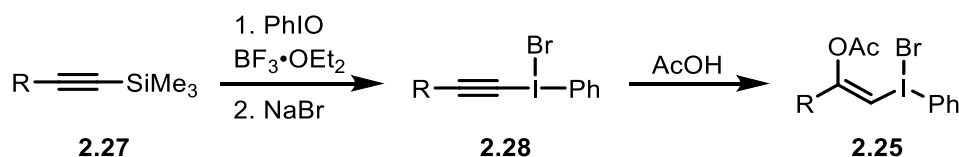
Scheme 2.8 Ochiai's acyl transfer method for MCIY synthesis

A mechanism of how this ester exchange transformation works is proposed to proceed through the formation of tetrahedral intermediate **2.26** followed by extrusion of **2.2** as shown below in **Scheme 2.9**.



Scheme 2.9 Mechanism of MCIY formation by Ochiai's acyl transfer method

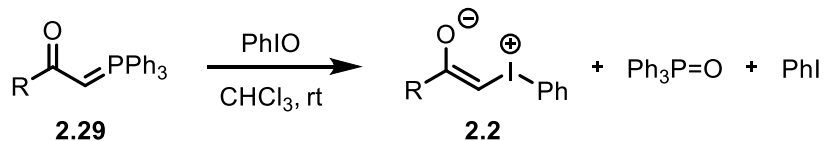
One of the drawbacks for using this method include synthesis of the required starting materials. The synthesis requires multiple steps, which is not always ideal since MCIYs are often just simple carbonyl-based compounds. The overall synthetic steps, starting from the initial alkyne **2.27**, are shown below in **Scheme 2.10** as reported by Ochiai.¹⁴⁸



Scheme 2.10 Synthesis of ester precursor for Ochiai's MCIY synthesis

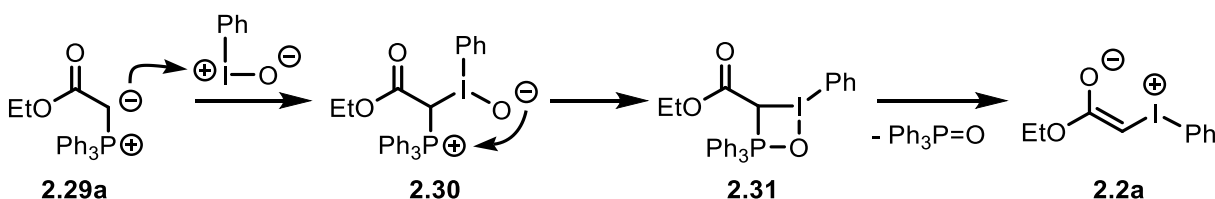
After Ochiai reported the acyl transfer method, MCIYs could then be generated in a consistent manner, which allowed for new reaction types to be discovered, these reactions will be discussed in this chapter. As there was only a single method to generate MCIYs, there has been little progress in this area of chemistry. This changed in 2013 when the Murphy group discovered a second way of generating MCIYs.

The Murphy group introduced a proof-of-concept report in 2013 that showed MCIYs (**2.2**) can be generated using Wittig reagents (**2.29**) in conjunction with iodosoarenes, producing triphenylphosphine oxide and iodobenzene as by-products, and is shown below in **Scheme 2.11**.¹⁴⁹ This simple methodology is beneficial in that it can be performed at room temperature, which opens up avenues for new types of reactivities. The optimization and utilization of this methodology is the concept behind this chapter.



Scheme 2.11 Murphy group method for MCIY synthesis

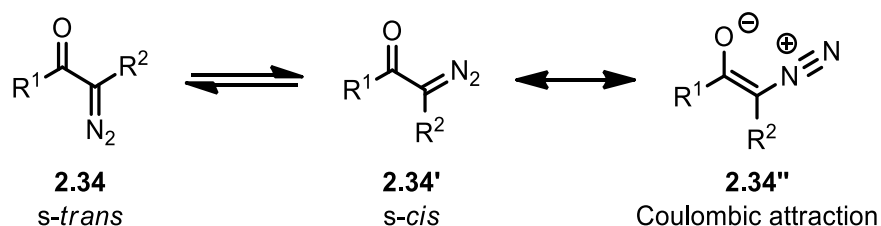
The driving force in the Wittig-type reaction above is reliant on the phosphorus-oxygen double bond, which is well known as the energetically favourable process that drives the classic Wittig reaction to completion. The ability of Wittig reagents to engage with HVI compounds is well documented, but iodosoarenes have not been applied to this style of reactivity. This Wittig-type reaction utilizes iodosobenzene for the first time, as a source of oxygen than can combine with triphenylphosphine and form triphenylphosphine oxide as a by-product, driving the transformation forward, forming the MCIY. To fully understand this reaction better, mechanistic studies should be performed, but even without a full mechanistic study, the transformation most likely would proceed as shown in the following **Scheme 2.12**.



Scheme 2.12 Possible mechanism of the Wittig-type reaction for MCIY synthesis

Benefits of this methodology include a new method for the facile generation of MCIYs and the ability to perform the reaction at room temp provided benefits which will be discussed later in this chapter. One of the problems with this synthetic method is the limitation of working with iodosoarenes which are not soluble in organic solvents, except for DMSO. Another problem is atom economy, as triphenylphosphine oxide ($\text{Ph}_3\text{P}=\text{O}$) is a by-product and must be removed from the crude reaction mixture.

This conformational bias can be disrupted though, if R² contains a large group, then the *s-trans* conformer will be sterically favoured. Understanding the structural properties of α -diazocarbonyl compounds is important as the properties of diazo compounds often show some resemblance to the structural properties observed in iodonium ylides. The preference of an *s-cis* or *cisoid* conformational geometry is consistent with observations made in other monocarbonylonyl (As, P, S) ylides.¹⁵¹



Scheme 2.14 Conformational geometries of α -diazocarbonyl compounds

The conformational properties and other structural properties in general of MCIYs are often difficult to obtain as they are not stable at room temperature. The conformational preference of MCIYs (**2.2**) to be *s-cis* or *cisoid* is predictable though, as this would be the same reason why cyclic iodonium ylides (**2.18**) are more stable than their acyclic (**2.1**) counterparts. As shown below in **Figure 2.4** cyclic iodonium ylides have both carbonyl oxygens pointed towards the positively charged hypervalent iodine atom. This provides an electrostatic attraction which is stabilizing in nature, similar to the Coulombic attraction observed in diazonium ylides.

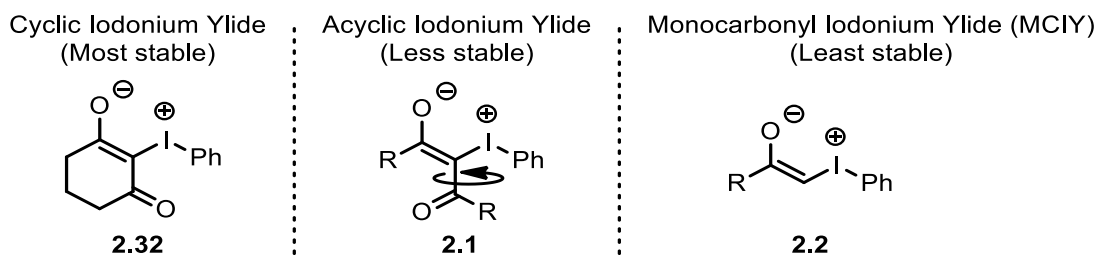
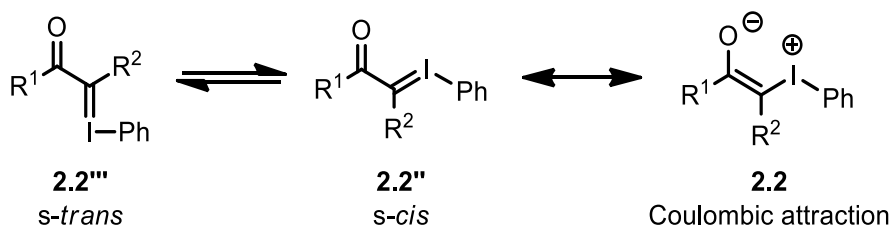


Figure 2.4 Conformation stabilities in cyclic, acyclic, and monocarbonyl iodonium ylides

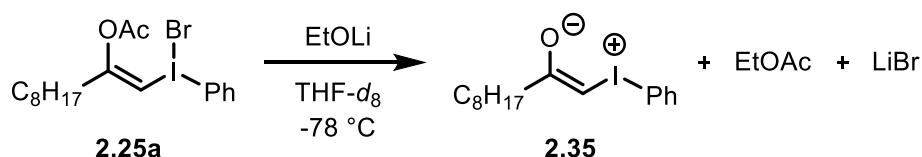
The fixed orientation of cyclic iodonium ylides has a maximizing ability to benefit from the Coulombic attractions. In acyclic iodonium ylides, the carbonyls are not locked and are free

to rotate along the carbon-carbon bond axis which would decrease the amount of favourable electrostatic interactions between the negative and positive charged atoms. The same concept can be said true about MCIY systems as these would also have rotational isomerism properties that are like acyclic iodonium ylides and based off the known properties of α -diazocarbonyl compounds, there should be a bias to favor the *s-cis* conformer as well. The *s-cis* (**2.2''**) and *s-trans* (**2.2'''**) conformers of MCIYs are shown below in **Scheme 2.15**. with the favoured zwitterionic *s-cis* (**2.2**) orientation benefiting from Coulombic attractions.



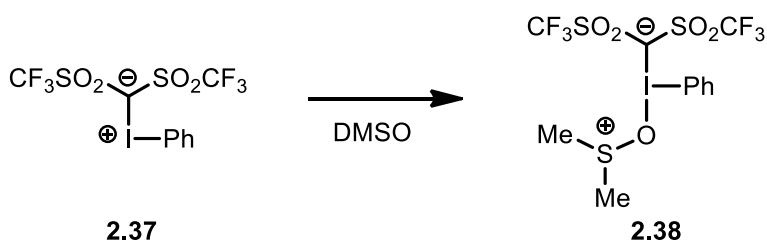
Scheme 2.15 Conformational geometries of MCIYs

Direct observation of MCIYs has remained a challenge due to their instability at room temperature and difficulty in synthesis, making direct structural analysis an issue. As a result of these undesirable properties, a crystal structure of a MCIY has never been obtained before, and there has been limited experimental evidence for their formation. ^1H NMR experiments were performed by Ochiai in 1997 at $-78\text{ }^\circ\text{C}$ in $\text{THF-}d_8$ to try and get proof that a MCIY was forming as anticipated.¹⁴⁷ The conversion of **2.25a** to *in situ* formed MCIY **2.35** used in Ochiai's NMR analysis is shown below in **Scheme 2.16**. These transient compounds were only observable at temperatures cooler than $-40\text{ }^\circ\text{C}$ and allowing the temperature to rise above $-40\text{ }^\circ\text{C}$ resulted in thermal degradation and loss of the ylide NMR signals.



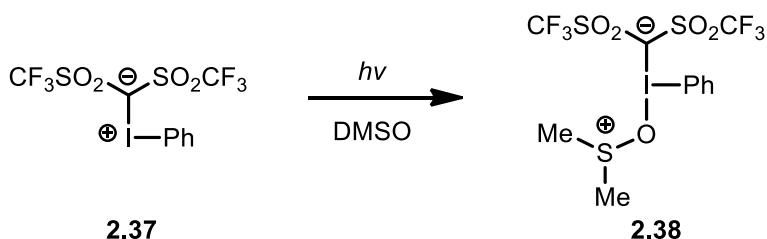
Scheme 2.16 MCIY synthesis for NMR structural analysis

Although a crystal structure of a MCIY has never been generated as of the present time being, alternative methods to observe an actual MCIY might be possible. The ability of trapping a MCIY might be a possible option, which is based on work done by Ochiai in 1999 in which an iodonium ylide was complexed with DMSO to form a crystal that was stable at room temp, and was then subjected to X-ray diffraction analysis.¹⁵² The complexation of phenyliodonium bis(triflyl)methide (**2.37**) with DMSO is shown below in the following **Scheme 2.17** and produced a complex (**2.38**) that was stable enough for the entire structure to be solved with X-ray diffraction.



Scheme 2.17 Iodonium ylide trapping with DMSO for crystal structure analysis

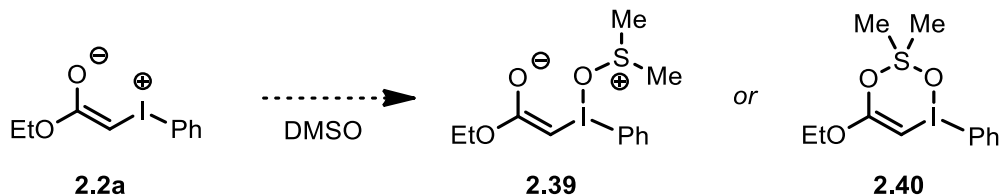
A similar experiment was performed by Zhu in 1993 in which phenyliodonium bis(triflyl)methide formed a complex with DMSO upon photo irradiation using UV light.¹⁵³ The complex (**2.38**) formed as a crystal, which could then be subjected to X-ray diffraction for structural analysis, confirming the correct structure.



Scheme 2.18 Iodonium ylide trapping with DMSO induced by UV light

The same concept could potentially be applied to a MCIY system, perhaps at -78 °C, in which DMSO might interact with *in situ* generated ylide **2.2a** forming a complex (**2.39** or **2.40**), which could then be analyzed by X-ray diffraction. As Zhu discovered, the application of photo

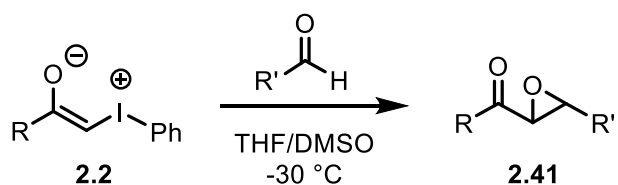
irradiation may also help with allowing a complex to form, which might provide a new method for trapping a MCIY for structural observation.



Scheme 2.19 MCIY trapping with DMSO for potential crystal structural analysis

2.2.3 Reactivity of MCIYs

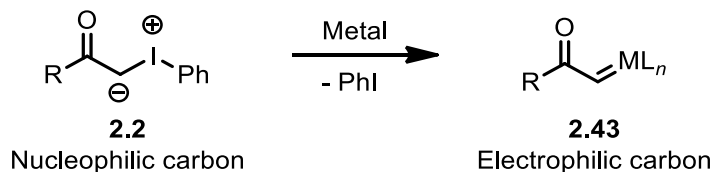
Monocarbonyl iodonium ylides are considered more nucleophilic when compared to dicarbonyl iodonium ylides since there are two EWGs attached to the nucleophilic carbon in dicarbonyl systems. With two EWGs, the nucleophilic negative charge is spread out over more atoms and therefore is less localized and available to act as a nucleophile. The increased nucleophilicity displayed in MCIY systems allows the nucleophilic α -carbon to react with aldehydes. A Hammett reaction constant ($\rho = 2.95$) for the α,β -epoxy ketone (**2.41**) synthesis reaction shown below in **Scheme 2.20** indicates that MCIYs are moderately nucleophilic in nature.¹⁴⁷ On the other hand, dicarbonyl iodonium ylides do not react with aldehydes reinforcing the fact that MCIYs are relatively more nucleophilic.



Scheme 2.20 Reaction of MCIY with aldehydes

Based on the reactivity of MCIYs documented in the literature, all previous reports show the ylide acting as a nucleophile and reacting with electrophilic reaction partners. The Murphy group was able to recognize the ability of intercepting a MCIY with a metal to form a metalcarbene in an *in situ* manner, which could then go onto react with reaction partners such as alkenes which was developed into a new cyclopropanation reaction. **Scheme 2.21** below

shows that when *in situ* generated MCIYs (**2.2**) are intercepted with a transition metal (M), a metallocarbene (**2.43**) is formed, which overall, turned a nucleophilic carbon centre into an electrophilic site. This enables reactions with nucleophilic-based reaction partners, which would be classified as a umpolung-based switch in reactivity.



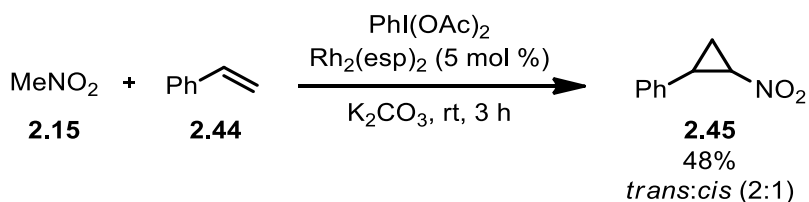
Scheme 2.21 Umpolung reactivity of MCIYs in the presence of metals

This new type of reactivity that MCIYs can now access is the subject of this chapter, and investigation into optimizing this process for peak performance is the objective. The metallocarbenes generated through this type of metal-based activation have been successfully coupled with alkenes to form cyclopropanes, and their ability to engage with other functional groups allows for the possibility of new reactions to potentially be discovered.

2.2.4 Reactions of MCIYs

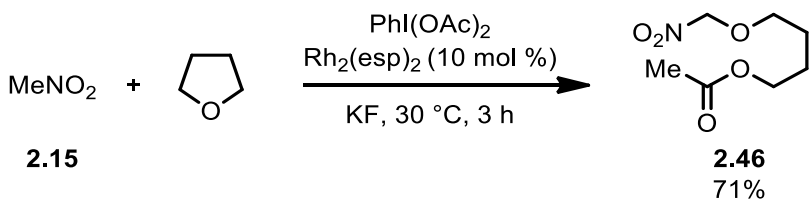
Since there are limited methods of synthesizing MCIYs and because of their unstable nature, very few research groups have established reliable synthetic applications. Examples in literature are rare, and research is only performed by a limited number of groups such as Hansen, Moriarty, Murphy, and Ochiai.

The focus of MCIY reactions performed in the Hansen group is based around using a nitro functional group as the stabilizing source of the ylide. This iodonium ylide is not a true monocarbonyl system because a nitro group does not contain a carbonyl group, but this example could be considered as a mono-stabilized iodonium ylide. The use of nitro-stabilized iodonium ylides was shown to be able to engage with transition metals and form metal-activated species capable of metallocarbene-like reactivity. Hansen showed an application of this reactivity by reacting nitromethane (**2.15**) with styrene (**2.44**) in the presence of a rhodium catalyst to form nitro-substituted cyclopropane (**2.45**) in a 2007 report.¹⁴⁴



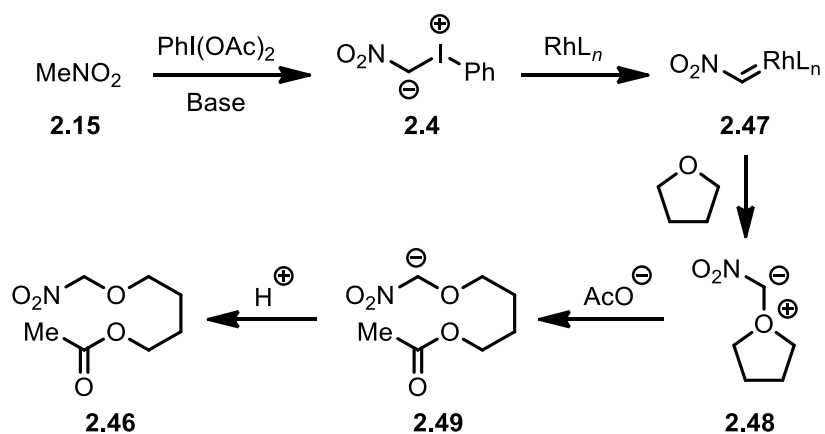
Scheme 2.22 Cyclopropanation of nitro-stabilized iodonium ylides

After the cyclopropanation reaction above was reported, the Hansen group again utilized a nitro-stabilized iodonium ylide for a novel reaction with cyclic ethers in 2008.¹⁵⁴ It was discovered that treatment of tetrahydrofuran (THF) with nitromethane, (diacetoxyiodo)benzene, a base, and a rhodium catalyst, afforded 4-(nitromethoxy)butyl acetate (**2.46**) as shown below in **Scheme 2.23**.



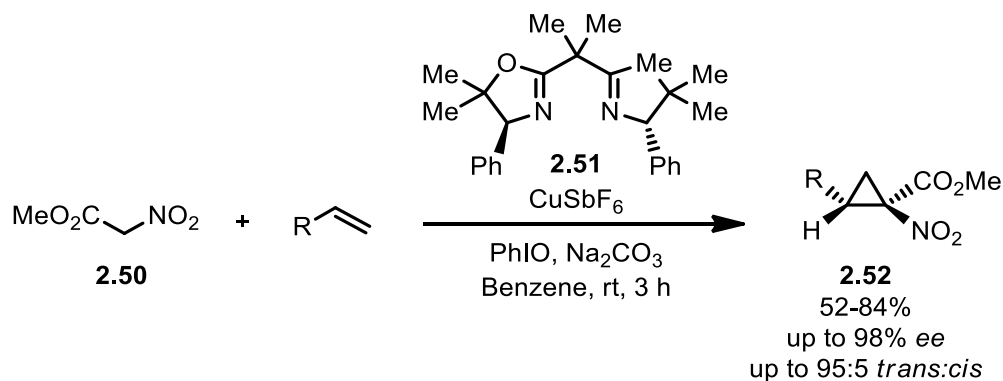
Scheme 2.23 Reaction of nitro-stabilized iodonium ylides

This reaction of nitromethane with cyclic ethers is classified as a three-component coupling reaction due to the carboxylate group, which originates from the HVI reagent, and is eventually incorporated into the product. The mechanism of this three-component coupling reaction is shown below in **Scheme 2.24** illustrating the carbenoid reactivity. After formation of the electrophilic carbenoid species (**2.47**), the oxygens in THF can engage this intermediate forming an ethereal oxonium ylide (**2.48**). Attack on the oxonium ylide by an acetate group will result in ring opening to form intermediate **2.49**, and after protonation, the final product (**2.46**) is produced.



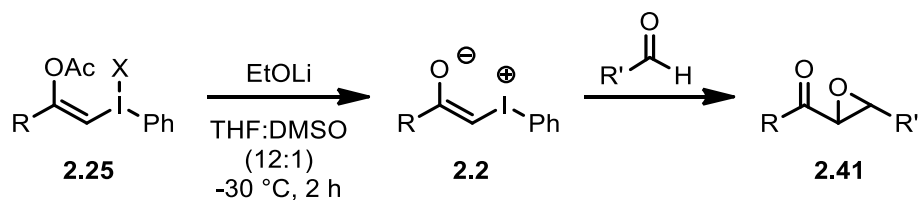
Scheme 2.24 Mechanism of reaction of nitro-stabilized iodonium ylides

A copper-catalyzed asymmetric cyclopropanation of alkenes with nitro-stabilized iodonium ylides generated *in situ* from iodosobenzene and methyl nitroacetate was reported by Charette in 2012.¹⁵⁵ High enantioselectivities (up to 98% *ee*) and diastereoselectivities (95:5 *dr trans:cis*) were achieved for a wide range of alkyl and aryl substituted alkenes, with the use of 2 mol % chiral bis(oxazoline) ligands (**2.51**) and a copper catalyst (2 mol %). This synthetically useful reaction allows for preparation of various nitrocyclopropyl carboxylates (**2.52**) as shown below in **Scheme 2.25**. The transformation proceeds in a similar way to Hansen's methodology with the proposition that the iodosobenzene and methyl nitroacetate (**2.50**) forms an iodonium ylide *in situ* which can then engage with the copper catalyst to form a metal carbene intermediate. This carbene intermediate can then undergo cyclopropanation with an alkene giving the desired nitrocyclopropane carboxylate.



Scheme 2.25 Cyclopropanation of nitro-stabilized iodonium ylides

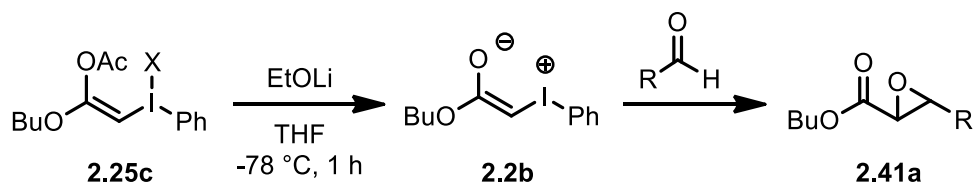
The use of MCIYs as alkylidene transfer reagents to aldehydes yielding α,β -epoxy ketones was reported by Ochiai in 1997.¹⁴⁷ The synthesis of α,β -epoxy ketones **2.41** from (β -acetoxyvinyl)iodonium salt **2.25** was performed using Ochiai's ester exchange reaction for MCIY *in situ* generation as shown below in **Scheme 2.26**. In this publication, the R groups on MCIY precursor **3** were limited to alkyl-based groups. The counterions (X) tested in λ^3 -iodanes **2.25** was either BF₄ or Br. Most of the reactions were carried out using 1 equiv of EtOLi and 1.5 equiv of an aldehyde in THF:DMSO (12:1) at -30 °C for 2 h under argon.



Scheme 2.26 Epoxidation reaction of MCIY with aldehydes

The *in situ* generated MCIYs (**2.2**) were attempted to be monitored using two-dimensional (2D) NMR techniques (¹H-¹H-COSY and ¹³C-¹H COSY), nuclear Overhauser enhancement spectroscopy (NOESY), and fast atom bombardment (FAB) mass spectrometry. This publication provided evidence for the generation of MCIYs which Ochiai then began to characterize and offer proof of the concept that this ester exchange methodology was generally applicable for the generation of these unstable MCIYs.

Ochiai's original epoxidation reaction of MCIYs with aldehydes that was discovered in 1997 was limited to ketone-based MCIYs, and in 2013, Miyamoto and Ochiai reported the inclusion of ester-based MCIYs for use in the epoxidation reaction, which showed how the ylide can serve as a Darzens reagent equivalent when reacted with aldehydes.¹⁵⁶ Substituted aldehydes were reacted with monoester iodonium ylide **2.2b** which was generated *in situ* from β -butoxy- β -acyloxyvinyl- λ^3 -iodane (**2.25c**) to give α,β -epoxy ester **2.41a** as shown below in **Scheme 2.27**. It was discovered that electron withdrawing *para* substituents on the aldehyde increased the rate of the epoxidation reaction. This data was used to generate a Hammett plot which showed an excellent correlation of the logarithm of the relative rates, $\log(k_X/k_H)$, with substituent constants, σ_p , and gave a reaction constant $\rho = 2.68$ ($r = 1.0$). These experiments reinforce what is known about the nucleophilic properties displayed by MCIYs.

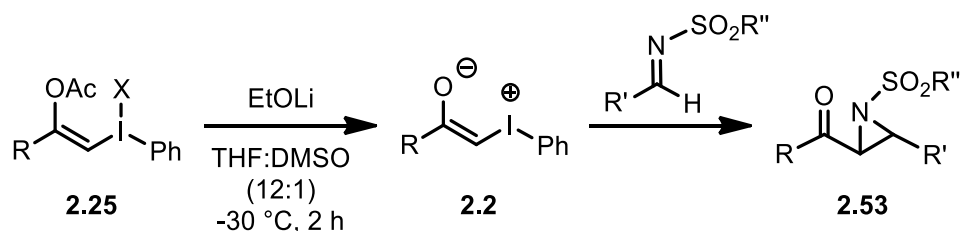


Scheme 2.27 Epoxidation reaction of MCIY with aldehydes

The counterions (X) tested in λ^3 -iodanes **2.25c** were BF_4 , Br, or I. λ^3 -iodanes with Br and I as a counterion were more stable than λ^3 -iodanes with the counterion BF_4 . Reduced decomposition was also observed at room temperature in regard to the counterion used. This was proposed to be due to the stronger coordination ability of the halide ions, which decreases the positive charge on the iodine(III) center, leading to greater overall stability of **2.25c**.

Evidence for the formation of MCIY **2.2b** was obtained when λ^3 -iodane **2.25c** (X = Br) was treated with $n\text{BuLi}$ (1.0 Equiv) in $[\text{D}_2]$ dichloromethane at $-78\text{ }^\circ\text{C}$ under an atmosphere of argon. ^1H NMR spectroscopy was then used to analyze the formation of the MCIY which showed formation of the ylide at $-70\text{ }^\circ\text{C}$ and disappearance of the ylide when the temperature was raised above $-50\text{ }^\circ\text{C}$. The formation of MCIY **2.2b** was monitored by examining the proton on the α -ylidic carbon atom which appeared at $\delta = 4.83$ ppm as a broad singlet. The formation of MCIY **2.2b** was further supported by low temperature ($-78\text{ }^\circ\text{C}$) ESI-MS measurements.

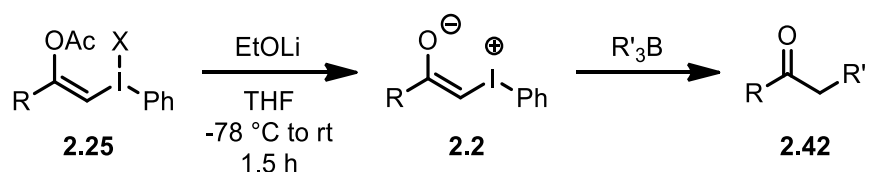
The successful use of MCIYs to act as alkylidene transfer reagents was demonstrated in an aziridination reaction with imines by Ochiai in 1998.¹⁵⁷ MCIYs were generated *in situ* and then reacted with *N*-(benzenesulfonyl)imines to give α,β -aziridino ketones (**2.53**). The aziridination of *N*-(2,4,6-trimethylbenzenesulfonyl)imines in THF afforded *cis*-aziridines as the major product, while that of *N*-benzoylimines in THF:DMSO gave the *trans*-isomer stereoselectively. The MCIYs were generated from Ochiai's ester exchange reaction as shown below in **Scheme 2.28**.



Scheme 2.28 Aziridination reaction of MCIYs with imines

The mechanism and nature of the stereoselective transformation of the aziridination reaction of MCIYs with imines was investigated by Ochiai in 1999.¹⁵² The stereochemical outcome of this aziridination was shown to be dependent on both the activating groups of the imines and the reaction solvents. The aziridination of *N*-(2,4,6-trimethylbenzenesulfonyl)imines in THF affords *cis*-aziridines as a major product while that of *N*-benzoylimines in THF-DMSO or THF gives the *trans* isomer stereoselectively. Data was collected so that the aziridination reaction could be represented in a Hammett plot, which showed a good linear relationship. The linear correlation of relative rate factors with the σ constants of substituents in the aromatic ring and afforded the reaction constant $\rho = 0.96$ ($r = 0.98$).

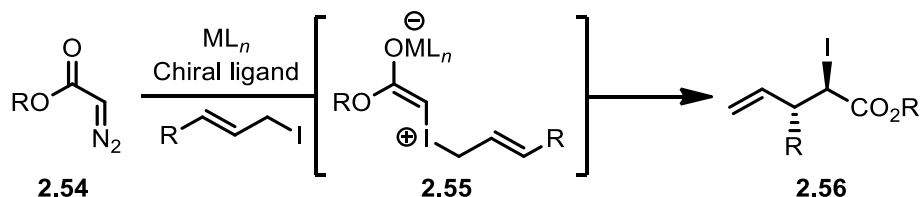
Another useful application of MCIYs is the α -alkylation of esters and ketones with trialkylboranes.¹⁵⁸ This process occurs through an initial Lewis acid-base interaction between the ylide and organoborane, followed by a 1,2-shift of the carbon ligand to give product **2.42** as shown below in **Scheme 2.29**.



Scheme 2.29 α -Alkylation reaction of MCIY with trialkylboranes

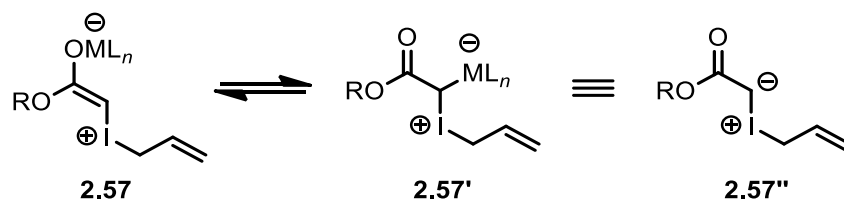
An enantioselective, diastereoselective, and regioselective copper-catalyzed [1,2] and [2,3]-rearrangement of iodonium ylides was developed by Tambar in 2016.¹⁵⁹ It was reported that in the presence of a copper catalyst, substituted allylic iodides couple with α -diazoesters to generate metal-coordinated iodonium ylides, which undergo [1,2] or [2,3]-rearrangements with high selectivities (up to 95:5 dr, and up to 97% *ee*).

The reaction relied on the use of chiral phosphine ligands derived from BINAP which interestingly favoured the formation of the [1,2]-rearrangement product. Alternatively, bisoxazoline derived ligands preferentially yielded the [2,3]-rearrangement product. A general reaction scheme of the [2,3]-rearrangement is shown below.



Scheme 2.30 Enantioselective [2,3]-rearrangement of iodonium ylides

It was not fully understood or explained mechanistically if the metal-bound intermediate was formed before a purely iodonium ylide intermediate was formed, or if the metal-bound intermediate was formed as a result of an iodonium ylide decomposing. Either way, this transformation presents the idea of an unstable iodonium ylide giving rise to a metal-bound intermediate which may also be thought of as a metallocarbene. Despite the authors showing the metal-coordinated iodonium ylide intermediate generated under the reaction conditions as presented as an equilibrium between the two structures as shown below in **Scheme 2.31**, the iodonium ylide intermediate would be unstable as it is a MCIY. The fact that this reaction works by operating through an unstable iodonium ylide that has only a single carbonyl electron withdrawing group to stabilize the negative charge on the α -carbon, provides supporting evidence than our cyclopropanation reaction of MCIYs might work as well.



Scheme 2.31 Metal-coordinated iodonium ylide intermediate

Tambar's work was based off an earlier report by Doyle in 1998 who showed an enantioselective [2,3]-sigmatropic rearrangement was possible using achiral starting materials,

but in the presence of a chiral catalyst.¹⁶⁰ Doyle's chemistry was based on the principle of diazo compounds decomposing into metallocarbenes which could then be in an equilibrium with a Lewis base (B:) which is able to coordinate to the metallocarbene and form chiral products, or form racemic products if the chiral ligand-metal complex was decomposed prior to reaction.

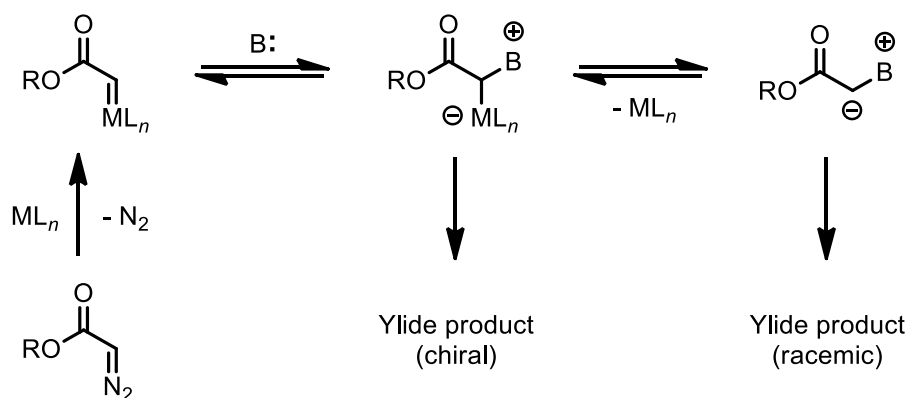
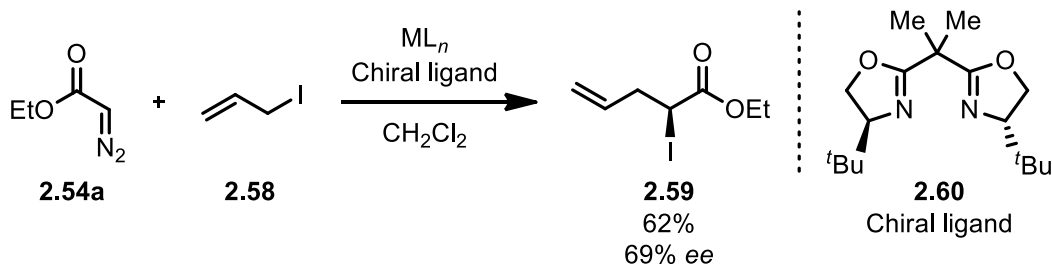


Figure 2.5 Metal-coordinated to ylides in a chiral reaction pathway

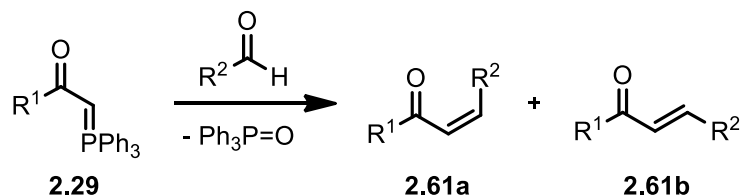
When ethyl diazoacetate (**2.54a**) and allyl iodide (**2.58**) were reacted in the presence of CuPF_6 using a chiral ligand (**2.60**) derived from bis-oxazoline, the following enantioselective [2,3]-sigmatropic rearrangement occurred giving product **2.59**, as shown below in **Scheme 2.32**. The origin of the enantioselectivity is explained by examining Doyle's figure above which states that an equilibrium can exist between the metallocarbene and the Lewis base, in this case being iodine. If this is true, then the intermediate would have to be an unstable MCIY, which could potentially form, even at room temperature, and lead to the final product. This provides encouraging insight into the chemistry presented in this chapter, which is proposed to occur in a similar manner, involving the generation of unstable MCIYs at room temperature, which can eventually lead to the desired product.



Scheme 2.32 Enantioselective [2,3]-sigmatropic rearrangement reaction

2.3 Wittig Reaction

The Wittig reaction was discovered by Georg Wittig in 1954 and is a well-known synthetic method that is used to couple aldehydes or ketones with triphenyl phosphonium ylides, also called Wittig reagents, to give a desired alkene with triphenylphosphine oxide being generated as a by-product. When stabilized ylides are used, such as **2.29**, there is a stereochemical preference to favor formation of the *trans*-alkene **2.61b** as opposed to the *cis*-alkene **2.61a** as shown below in **Scheme 2.33**.

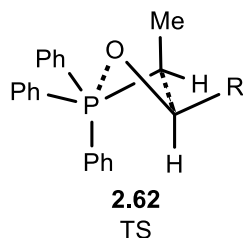


Scheme 2.33 General Wittig reaction of stabilized ylides with aldehydes

Studies performed on the Wittig reaction indicates that structural features of the carbonyl component (aldehyde or ketone) or ylide component can drastically influence the stereochemical outcome in the alkene.¹⁶¹ Interestingly, there is a counter intuitive preference for the formation of (*Z*)-alkenes in reactions between non-stabilized phosphonium ylides and aldehydes. This phenomenon has resulted in numerous mechanistic studies attempting to understand these observations. A transition state model proposed by Vedejs made considerable advancement to strengthen the stereochemical understandings of this reaction.¹⁶²

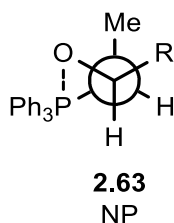
The conclusion of the paper by Vedejs in 1988 found that for typical non-stabilized ylides, they will react via an early transition state and under kinetic control. The *cis*-selective

transition state **TS** is drawn with a puckered 4-membered ring having the aldehyde substituent in a pseudoequatorial orientation, as far as possible from phosphorus ligands. The developing nonplanar oxaphosphetane transition state (TS, **2.62**) allows maximum separation between aldehyde, phosphorus substituents, and ylide α -carbon substituent as shown below in **Scheme 2.34**.



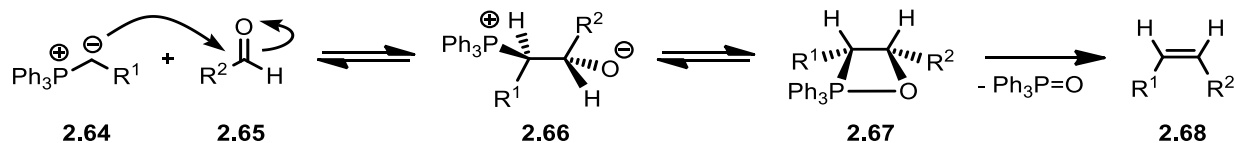
Scheme 2.34 Transition state (TS) for Wittig reactions with non-stabilized ylides

Vedejs proposed that for non-stabilized ylides reacting in a salt-free environment, the *cis*-selective transition state (TS) can be approximated by the Newman projection (NP, **2.63**) which neglects phosphorus bond angles and is shown below in **Scheme 2.35**.



Scheme 2.35 Newman projection (NP) for Wittig reactions with non-stabilized ylides

The mechanism of the Wittig reaction for non-stabilized ylides reacting with aldehydes to selectively form *cis*-alkenes is shown below in **Scheme 2.36**. A key feature of the Wittig reaction is the formation of a phosphorus-oxygen double bond which is one of the strongest double bonds in chemistry, having a bond energy of 575 kJ/mol.¹⁶³ This step in the mechanism is the driving force for the overall process, bringing the reaction to completion, making the Wittig reaction irreversible.

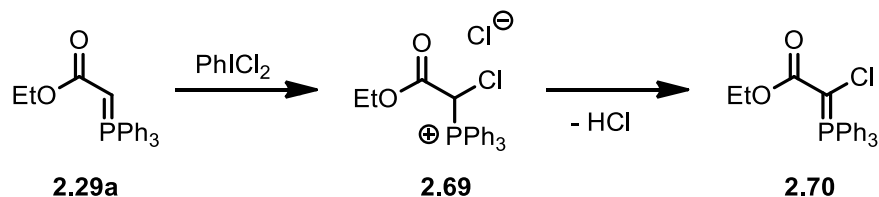


Scheme 2.36 Mechanism of the Wittig reaction for non-stabilized ylides

2.3.1 Reaction of Wittig Reagents with HVI Compounds

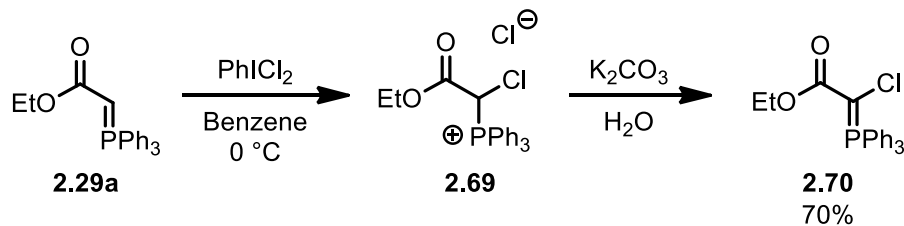
Chemical reactions are based on the ability of reagents or starting materials to react with each other if the properties between them will allow it to proceed. Pairing the unique dipolar reactivity of ylides with the ambiphilic nature of HVI reagents, several reaction types have been discovered. There are limited examples of reactions involving ylides with HVI reagents, but one well studied example of this, is the reactions of phosphonium ylides (Wittig reagents) with aryl- λ^3 -iodanes.

The α -carbon in phosphonium ylides is nucleophilic in nature and is therefore electrostatically attracted to the slightly positively charged hypervalent iodine atom in HVI reagents. The HVI reagent PhICl_2 has been reported to react with phosphonium ylides to give α -chlorophosphonium ylides.¹⁶⁴ The properties of PhICl_2 allow the reagent to function as a source of Cl^+ atoms and transfer a chlorine atom to phosphonium ylide **2.29a** to give α -chlorinated phosphonium salt **2.69** which can then lose a proton to yield α -chlorophosphonium ylide **2.70** as shown below in **Scheme 2.37**.



Scheme 2.37 Reaction of phosphonium ylides with aryl- λ^3 -iodanes

A similar, but slightly different method of accessing α -chlorophosphonium ylides from the reaction of phosphonium ylides with aryl- λ^3 -iodanes is shown below in **Scheme 2.38**.

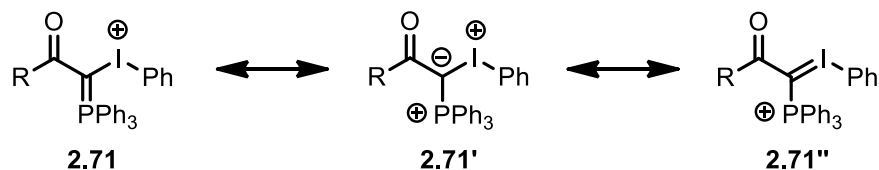


Scheme 2.38 Reaction of phosphonium ylides with aryl- λ^3 -iodanes

2.4 Mixed Phosphonium-Iodonium Ylides

Mixed phosphonium-iodonium ylides are generated by the ability of phosphonium ylides to react with HVI reagents and trap the hypervalent iodine group from leaving, forming the mixed phosphonium-iodonium ylide.

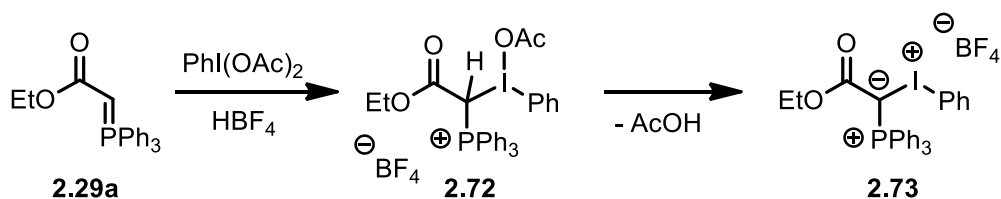
Mixed phosphonium-iodonium ylides (**2.71**) are described by the resonance structures as seen below in **Scheme 2.39** and represent a unique class of stable λ^3 -iodanes that combine a phosphonium ylide, and an iodonium salt. These compounds have attracted attention because of their potential to synthesize novel phosphorus-containing heterocycles that would be difficult to access via other methods.¹⁶⁵



Scheme 2.39 Mixed phosphonium-iodonium ylide resonance structures

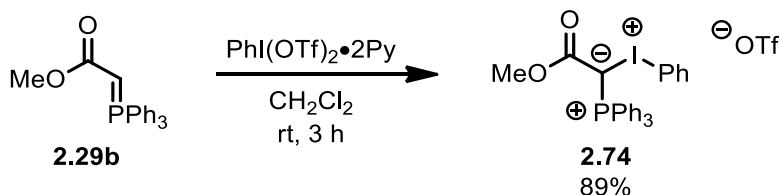
The synthesis of mixed phosphonium-iodonium ylides was first reported by Neilands and Vanags in 1964.¹⁶⁶ The chemistry of mixed phosphonium-iodonium ylides was then advanced by Moriarty in 1984 to include additional synthetic methods of accessing these unique ylides. The synthesis of mixed phosphonium-iodonium ylides was further developed using methods that were reported by groups such as Matveeva,¹⁶⁷ Moriarty,¹⁶⁸ and Zhdankin.¹⁶⁹

Phosphonium ylide **2.29a** can react with $\text{PhI}(\text{OAc})_2$ and HBF_4 to give mixed phosphonium-iodonium salt **2.72** with a BF_4 counterion. After loss of an acetate group and a proton, mixed phosphonium-iodonium ylide **2.73** is generated as shown below in **Scheme 2.40**.



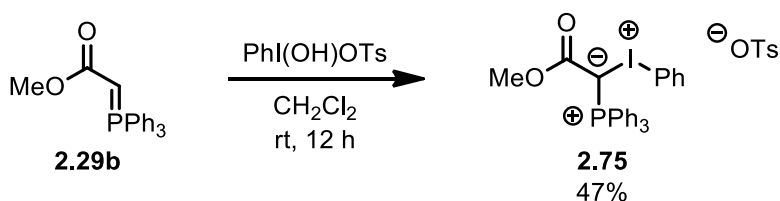
Scheme 2.40 Mixed phosphonium-iodonium ylide synthesis from phosphonium ylides

Mixed phosphonium-iodonium ylides with a TfO⁻ counterion (**2.74**) can be obtained by treating phosphonium ylide **2.29b** with PhI(OTf)₂•2Py as shown below in **Scheme 2.41**.



Scheme 2.41 Synthesis of mixed phosphonium-iodonium ylide

Another similar synthesis of mixed phosphonium-iodonium ylides which contain a TsO⁻ counterion (**2.75**) can be obtained by treating phosphonium ylide **2.29b** with PhI(OH)OTs as shown below in **Scheme 2.42**.



Scheme 2.42 Synthesis of mixed phosphonium-iodonium ylide

2.5 Iodosoarenes

Iodosoarenes are a class of HVI reagents that are known to participate in oxidation reactions, often with high efficiency and with minimal waste production, as benign iodobenzene

and water being the only by-products.¹⁷⁰ Because iodosoarenes play an important part in this chapter, a thorough understanding of this HVI reagent is essential for its effective use as an oxidant in the presented chemistry that follows.

Iodosobenzene (PhIO) is also referred to as iododibenzene and is a pale yellowish amorphous powder that is polymeric in nature and is insoluble in standard organic solvents, with exceptions such as dimethyl sulfoxide (DMSO) and methanol. Methanol has been used to dissolve iodosobenzene, which allows for depolymerization affording $\text{PhI}(\text{OMe})_2$ which alters the oxidative properties of iodosobenzene.

Storage should be under refrigerated conditions as extended periods of time at room temperature can result in disproportionation of PhIO to PhI and PhIO_2 . Disproportionation can also happen when samples of iodosoarenes are heated and should therefore be avoided as ArIO_2 compounds are known to be explosive.¹⁷¹ An incident was reported of an explosion occurring when a sample of iodosobenzene was being dried under vacuum at 110 °C.¹⁷²

Even though in literature the iodine-oxygen bond in iodosobenzene is often represented as a double bond (**2.76a**), there have been studies which determined the bond to actually be better represented as a single bond (**2.76a'**) but is often drawn as a double bond for simplicity (**Figure 2.6**). Structural information of iodosobenzene was determined using extended X-ray absorption fine structure (EXAFS) spectroscopy by Norman in 1994.¹⁷³ Using this method, it was deduced that the polymeric structure of iodosobenzene has a zigzag appearance. Despite iodosobenzene being reported in the literature as an amorphous powder, researchers were able to analyze structural properties with high precision using powder X-ray diffraction (PXRD) techniques on freshly synthesized samples of PhIO.¹⁷⁴ These methods were able to generate fairly accurate structural models to give the following data. In iodosobenzene, the iodine-oxygen bond distance is 2.04 Å (intramolecular covalent bonding), the iodine···oxygen bond distance is 2.38 Å (intermolecular secondary bonding), with an iodine-oxygen-iodine angle of 114° was determined. The carbon-iodine-oxygen angle was determined to be close to 90° by Mössbauer spectroscopy.¹⁷⁵

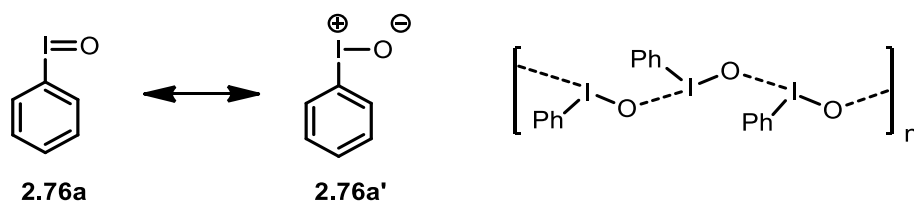


Figure 2.6 Resonance structures and zigzag polymeric network of iodosobenzene

Computational studies have allowed for finer details to be revealed into the unique bonding in iodosoarenes, which has led to a more accurate way of representing the key hypervalent bond within the molecule.¹⁷⁶ The following data was theoretically calculated using density functional theory (DFT) calculations, and shows the partial atomic charges and bond lengths to be consistent with an assignment of the iodine-oxygen bond in PhIO to be a single dative bond, represented as I→O. Within this bond, the electrons are distributed evenly between iodine and oxygen. The carbon-iodine-oxygen angle was calculated to be 106°, indicative of a sp^3 -type spatial arrangement of the orbitals on the iodine.¹⁷⁷ Computational studies suggest the iodine-oxygen bond to have a clean σ character, with a bond order of 1. It was reinforced computationally that the bonding in iodosobenzene be referred to as a single bond instead of being represented as an I=O double bond.¹⁷⁸

2.5.1 Synthesis of Iodosoarenes

The most common procedure for the synthesis of iodosoarenes is based on the alkaline hydrolysis of (diacetoxyiodo)arenes.¹⁷⁹ This methodology has been used for the preparation of a variety of *ortho*, *meta*, and *para*-substituted iodosoarenes, and is suitable for both EDG and EWG groups.

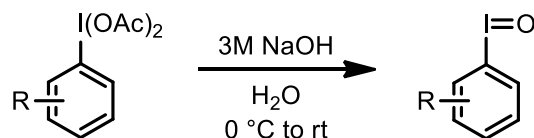
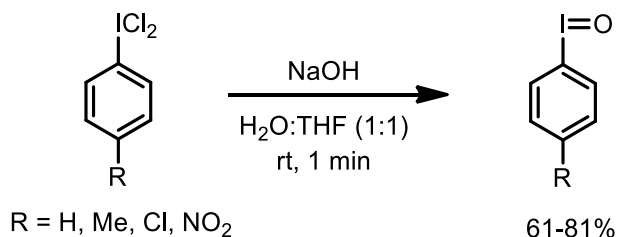


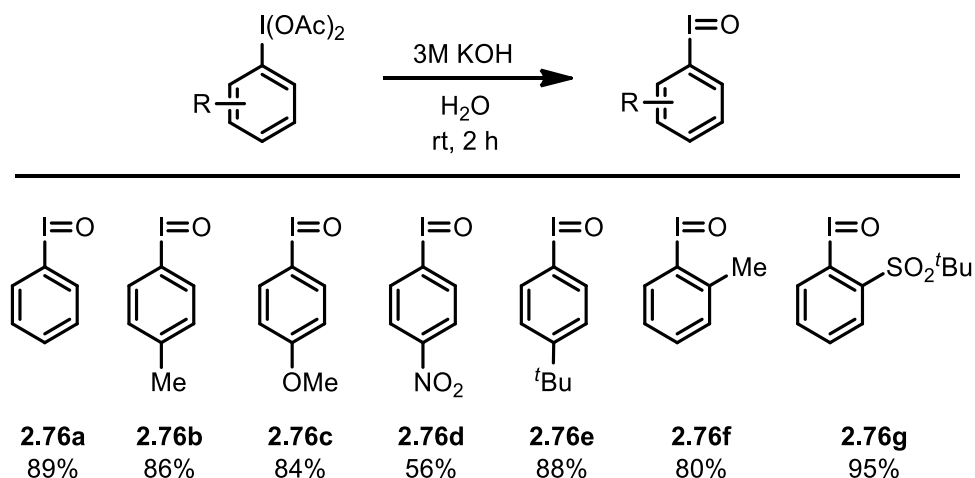
Figure 2.7 Synthesis of iodosoarenes from (diacetoxyiodo)arenes

A preparation of iodosoarenes from the hydrolysis of (dichloroiodo)arenes under basic conditions is similar to the alkaline hydrolysis of (diacetoxyiodo)arenes.¹⁸⁰ When dealing with starting materials that are poorly soluble or have solubility issues, a modified procedure can be used that includes tetrahydrofuran as a co-solvent to help with creating a more nearly homogeneous solution.¹⁸¹ This methodology has been utilized in the synthesis of *para*-substituted iodosoarenes as shown below in **Scheme 2.43**.



Scheme 2.43 Synthesis of iodosoarenes from (dichloroiodo)arenes

To investigate the Wittig-type reaction in greater detail with the intention of finding optimized conditions, there was a need to synthesize a variety of iodosoarenes. (Diacetoxyiodo)arene compounds are generally slightly more stable and easier to work with than (dichloroiodo)arenes, so the synthesis of a small library of iodosoarenes was carried out from the diacetates. To probe the electronic effects of the MCIY synthesis reaction, iodosoarenes with EDG and EWG were synthesized. EDG such as *ortho*-methyl, *para-tert*-butyl, *para*-methyl and *para*-methoxy and EWG such as *para*-nitro and *ortho-tert*-butyl sulfone were synthesized as shown below in **Scheme 2.44**.

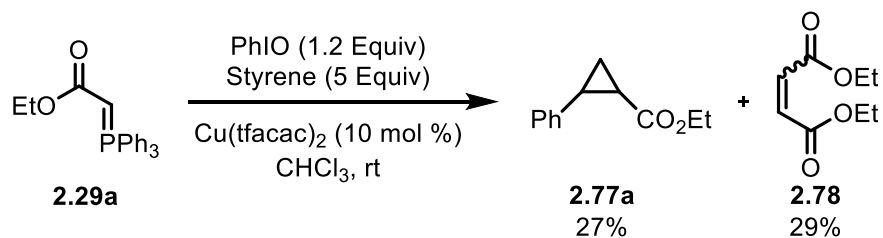


Scheme 2.44 Synthesis of iodosoarenes from (diacetoxyiodo)arenes

After synthesizing the small library of iodosoarenes shown above, they were then reacted with Wittig reagents and subjected to the optimized conditions in the Wittig-type reaction to see what type of functional groups on the iodosoarenes will be beneficial or detrimental to the reaction.

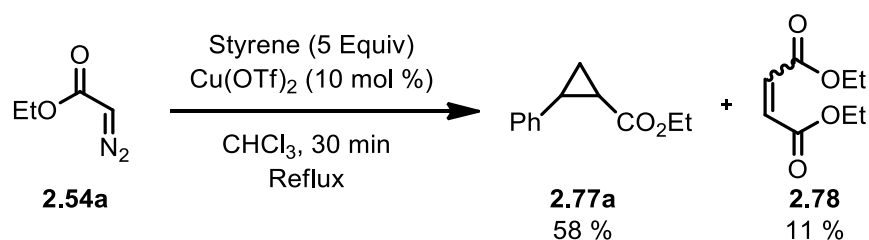
2.6 Cyclopropanation of MCIYs

A proof-of-concept study was performed by the Murphy group in 2013 which demonstrated the ability of MCIY to be generated in situ and trapped with alkenes in the presence of transition metal catalysts such as copper.¹⁴⁹ The cyclopropanation reaction, as seen below in **Scheme 2.45**, did yield produce the desired cyclopropane but was not fully optimized at the time of publishing. The yields were based on GC analysis and the cyclopropane formed as a mixture of diastereomers (~2:1) with *trans* being the major diastereomer.



Scheme 2.45 Murphy group cyclopropanation reaction of MCIY

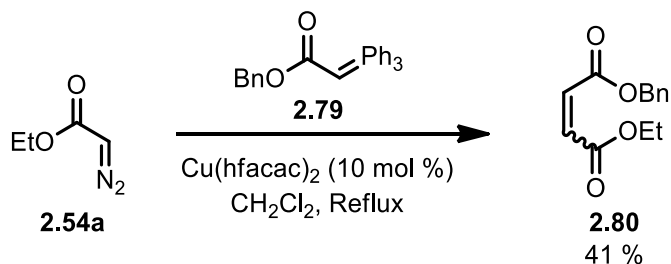
Initial studies were based on the ability of diazo-based compounds to react in an analogous manner to iodonium ylides. There is a lot of information in the literature which suggests that diazonium ylides are interchangeable with iodonium ylides in some reactions, and in fact the use of iodonium ylides often functions as a safer alternative. Preliminary results showed the ability of diazo-based compounds to engage with styrene in the presence of catalytic transition metals such as copper to form cyclopropanes and dimerization products as shown below in **Scheme 2.46**.



Scheme 2.46 Cyclopropanation of ethyl diazoacetate (EDA) with styrene

At the time of publishing this proof-of-concept paper by the Murphy group, the cross-coupling of carbenes and Wittig reagents was unknown. Hence, in order to establish this as a credible mode of reactivity, it was essential to show the cross-coupling of carbenes and Wittig reagents in order to support and make sense of the proposed Wittig-type reaction.

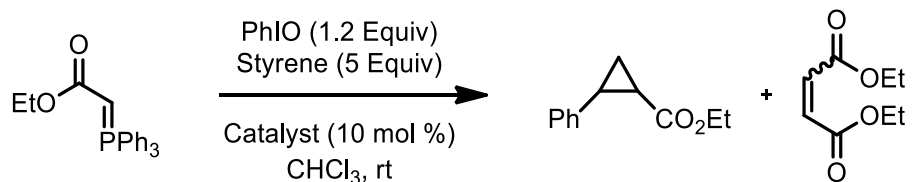
A series of experiments were conducted to support the proposed mode of reactivity, showing Wittig reagents capable of reacting with carbenes, which were generated from diazos in the presence of transition metals. The cross-coupling reaction between EDA (**2.54a**) and Wittig reagent **2.79** accomplished using the catalyst $\text{Cu}(\text{hfacac})_2$ which gave dimerization product **2.80** in 41% yield, as shown below in **Scheme 2.47**.



Scheme 2.47 Cross-coupling reactions between Wittig reagents and diazoesters

After observing the presence of carbenoid reactivity, the effect of catalysts on this transformation was investigated. A variety of catalysts that are commonly used in metallocarbene chemistry were tested and is shown below in **Table 2.1**.

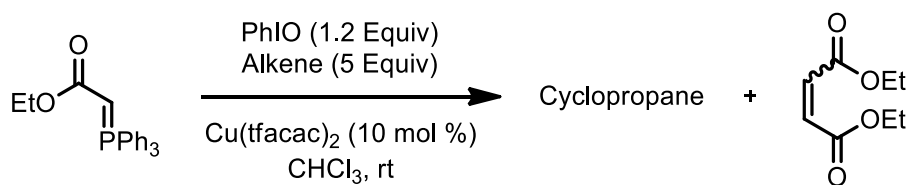
Table 2.1 Catalyst screening in cyclopropanation reaction of MCIY



Catalyst	Cyclopropane Yield (%) ^[a]	Dimer Yield (%) ^[a]
Rh ₂ (OAc) ₄	-	18
Cu(acac) ₂	-	11
Cu(tfacac) ₂	27	29
Cu(hfacac) ₂	14	15

^[a] Yields were determined by GC analysis of the crude reaction mixture.

After establishing the cyclopropanation reaction and testing various catalysts, the alkene scope was investigated, and cyclopropanation was successful for cyclohexene (**2.81**), norbornene (**2.82**), and *trans*-stilbene (**2.83**). Although the yields were moderate, this provided evidence that Wittig reagents can be used to generate MCIYs *in situ* and can be used for metallocarbene chemistry such as cyclopropanation and dimerization formation.



Alkene	Cyclopropane	Yield
 2.81	 CO_2Et	37 %
 2.82	 CO_2Et	46 %
 2.83	 EtO_2C and Ph	44 %

Scheme 2.48 Cyclopropanation of Wittig reagent with iodosobenzene and various alkenes

2.7 Optimization of Cyclopropanation Reaction of MCIYs with Alkenes

The highest yield of the cyclopropanation reaction of Wittig reagents with iodosobenzene and alkenes from our group's 2013 report was 27% of the cyclopropane and 29% of the dimerized Wittig reagent starting material. The objective of this chapter was to find optimal conditions for this cyclopropanation reaction either by decreasing the amount of starting material that is wasted through the dimerization process, or by directly increasing the amount of cyclopropane produced.

It was initially anticipated that the poor yields observed in the preliminary studies were partially responsible due to solubility issues encountered by iodosobenzene, which is a well-documented issue. Two options were proposed to address this issue of poor solubility of the iodosobenzene. One option is to use an iodosoarene derivative that is more soluble in organic solvents by preventing the formation of the polymeric structure. The second option is the use of additives which have been shown to successfully disrupt the polymeric network of iodosobenzene, providing higher concentrations of “free” monomeric iodosobenzene.

The first option, which addressed the ability of the iodosoarene to be chemically modified to increase solubility properties was based on research performed in the Protasiewicz group. Theoretically, if iodosobenzene was adjusted to become more soluble, then it may have a better chance of reacting with the Wittig reagent and giving a higher concentration of metalcarbene intermediates which could then go onto giving higher amounts of cyclopropanation.

Because of research performed by the Protasiewicz group which address the issue of reduced solubilities of iodosobenzene and had developed a HVI reagent that encompasses the iodoso functional group, but with better solubility, we directed our attention to seeing if improvements could be made with respect to the issue of solubility.

The Protasiewicz group discovered in 1999 that the incorporation of a *tert*-butylsulfonyl in the *ortho* position of iodosobenzene, which gives 1-(*tert*-butylsulfonyl)-2-iodosobenzene, an iodosoarene that has increased solubility properties in organic solvents.¹⁸² The *ortho*-substituted *tert*-butyl sulfone iodosoarene is soluble in organic solvents due to intramolecular secondary bonding interactions that exist between the hypervalent iodine atom and an oxygen atom in the sulfone group, as shown below in **Figure 2.8** Intramolecular secondary bonding in soluble iodosoarene. The soluble *ortho*-substituted iodosoarene **2.76g** has also already been proven to be an effective alternative to iodosobenzene for various transition metal-catalyzed oxidation reactions.

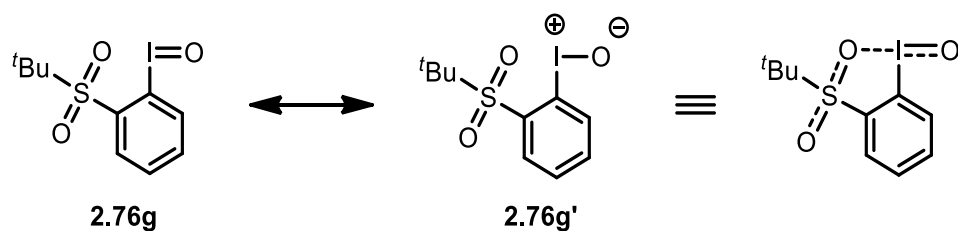
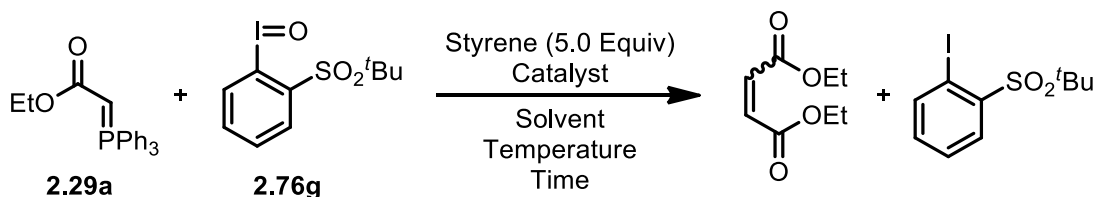


Figure 2.8 Intramolecular secondary bonding in soluble iodosoarene

After synthesizing soluble iodosoarene **2.76g**, it was subjected to the Wittig-type cyclopropanation reaction with styrene to observe the cyclopropanation efficiency. **Table 2.2** below shows a summary of different conditions that were tested in the cyclopropanation reaction with Wittig reagent **2.29a**. Copper catalysts were investigated in different organic solvents,

temperatures and equivalents of iodosoarene, but unfortunately no cyclopropane product was produced. The only products that were observed to form were the dimerization of Wittig reagent starting material, and the consumption of the iodosoarene into its respective iodoarene.

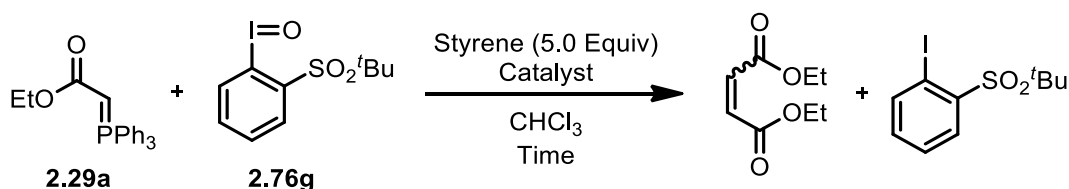
Table 2.2 Screening of conditions for cyclopropanation reaction



Entry	Solvent	Catalyst ^[a]	Equivalent (Iodosoarene)	Temperature (°C)	Time (h)	Cyclopropane Yield (%) ^[b]
1	CHCl ₃	Cu(tfacac) ₂	1.2	25	2	0
2	CHCl ₃	Cu(tfacac) ₂	1.2	-78	18	0
3	CHCl ₃	Cu(tfacac) ₂	2.0	25	15	0
4	CHCl ₃	Cu(tfacac) ₂	3.0	25	8	0
5	CHCl ₃	Cu(acac) ₂	5.0	25	14	0
6	CHCl ₃	-	1.0	25	7	0
7	Et ₂ O	-	1.0	-78	1	0
8	CH ₂ Cl ₂	-	1.0	0	6	0
9	CHCl ₃	Cu(acac) ₂	1.2	25	12	0

^[a] Catalyst loading was 10 mol %. ^[b] Yield based on ¹H NMR using HMDSO (10 μL) as an internal standard.

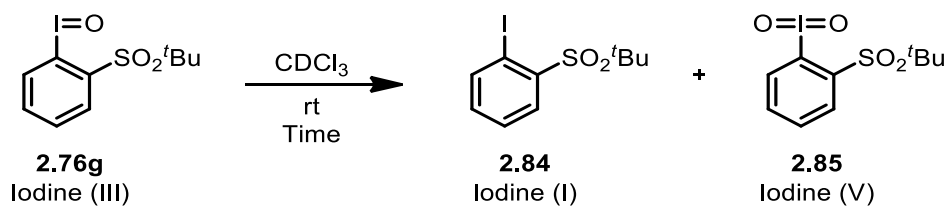
The screening of other metal catalysts for metallocarbene formation were also investigated as shown below in **Table 2.3**, but again, no cyclopropane products were observed to form.

Table 2.3 Screening of catalysts for cyclopropanation reaction

Entry	Catalyst ^[a]	Time (h)	Cyclopropane Yield (%) ^[b]
1	$\text{Rh}_2(\text{OAc})_4$	2	0
2	$\text{Rh}_2(\text{Opiv})_4$	5	0
3	$\text{Rh}_2(\text{tpa})_4$	5	0
4	$\text{Cu}(\text{acac})_2$	10	0
5	$\text{Cu}(\text{tfacac})_2$	10	0
6	$\text{Cu}(\text{hfacac})_2$	2	0

^[a] Catalyst loading was 10 mol %. ^[b] Yield based on ^1H NMR using HMDSO (10 μL) as an internal standard.

A possible reason why the soluble iodosoarene was not effective at producing any yield of the cyclopropanation product may possibly be due to disproportionation of **2.76g**, which is a documented process that occurs with some HVI reagents such as iodosoarenes.¹⁸³ The rate of disproportionation is also known to increase when greater amounts of the free iodosoarene are dissolved in solution. A scheme illustrating the disproportionation reaction of iodine (III) reagents to iodine (V) and iodine (I) is shown below in **Table 2.4**, which was investigated to gain mechanistic information into why the reaction was failing to give cyclopropane.

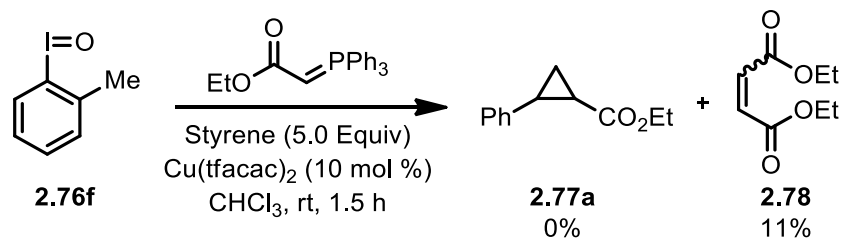
Table 2.4 Disproportionation rate of soluble iodosoarene

Time (h)	Iodine (III) (Relative amount) ^[a]	Iodine (I) + Iodine (V) (Relative amount) ^[a]
0	100	0
1	41	59
2	18	82
6.5	2	98

^[a] Rate of disproportionation determined by ^1H NMR using HMDSO (10 μL) as an internal standard.

As shown above in **Table 2.4**, after 6.5 h at room temp, 98% of the entire sample of iodosoarene **2.76g** was fully consumed by disproportionation. This indicates a narrow window of time required to perform the desired reaction, after which the iodosoarene would be consumed and therefore no longer available to engage in a reaction. Despite this window of time that is available for the iodosoarene to engage with the Wittig reagent and undergo oxygen transfer, these reactions failed, presumably due to the sterically crowded environment created by the *ortho* substituent.

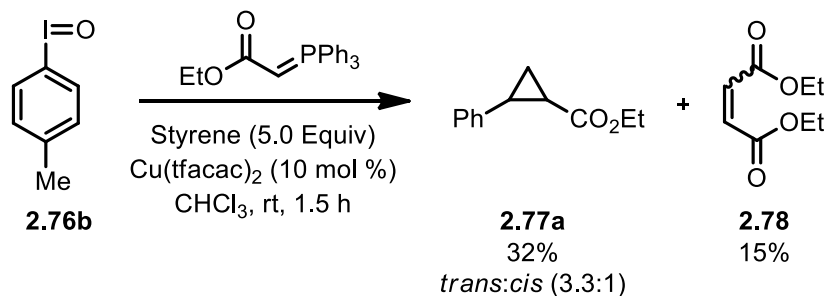
The presence of functional groups in the *ortho* position on the iodosoarene might be the reason why the cyclopropanation reaction was not occurring when using soluble iodosoarene **2.76g** perhaps due to a sterically crowded environment. To probe this idea, an iodosoarene containing an *ortho* methyl group (**2.76f**) was synthesized and reacted with Wittig reagent **2.29a** under the optimized reaction conditions, as shown below in **Scheme 2.49**.



Scheme 2.49 Reaction of *ortho*-substituted iodosoarene with Wittig reagent

The results from the reaction above suggest iodosoarenes which contain groups at the *ortho* position are not tolerated in the Wittig-type cyclopropanation reaction. This can most likely be explained by a situation in which the environment around the active part of the iodosoarene (HVI atom) is too sterically crowded by the presence of the *ortho* group, and this prevents the bulky Wittig reagent from getting close enough to react.

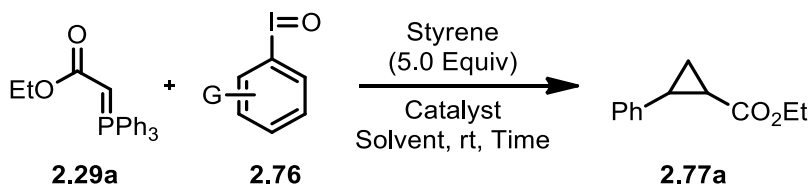
When Wittig reagents are reacted with an iodosoarene that is substituted at the *para* position, such as *para* methyl iodosobenzene (**2.76b**), an increase in the cyclopropane yield was observed as shown below in **Scheme 2.50**.



Scheme 2.50 Reaction of para-substituted iodosoarene with Wittig reagent

A summary of the different iodosoarenes that were synthesized and tested in the cyclopropanation reaction are shown below in **Table 2.5**. There was success in increasing the yield of the cyclopropane product when iodosoarenes substituted at the *para* position were tested, most likely due to a beneficial electronic interaction that allowed for a more efficient coupling of the Wittig reagent with the iodosoarene.

Table 2.5 Optimization of the cyclopropanation reaction

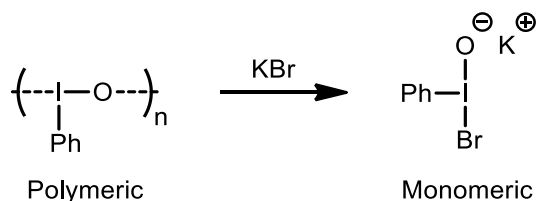


Entry ^[a]	Iodosoarene 2.76 (G =)	2.76 (Equiv)	Solvent	Time (h)	Catalyst (mol %)	Yield (%)
1	G = H (2.76a)	1.2	CHCl ₃	1.5	Cu(tfacac) ₂ (10)	17
2	G = <i>p</i> -Me (2.76b)	2	CHCl ₃	1.5	Cu(tfacac) ₂ (10)	53
3	G = <i>p</i> -OMe (2.76c)	2	CHCl ₃	1.5	Cu(tfacac) ₂ (10)	0
4	G = <i>p</i> -NO ₂ (2.76d)	2	CHCl ₃	1.5	Cu(tfacac) ₂ (10)	48
5	G = <i>p</i> - ^t Bu (2.76e)	2	CHCl ₃	1.5	Cu(tfacac) ₂ (10)	45
6	G = <i>o</i> -Me (2.76f)	2	CHCl ₃	1.5	Cu(tfacac) ₂ (10)	0
7	G = <i>o</i> -SO ₂ ^t Bu (2.76g)	1.2	CHCl ₃	24	Cu(tfacac) ₂ (10)	0
8	2.76b	1.2	CHCl ₃	1.5	Cu(tfacac) ₂ (10)	34
9	2.76b	3	CHCl ₃	1	Cu(tfacac) ₂ (10)	30
10	2.76b	4	CHCl ₃	1.5	Cu(tfacac) ₂ (10)	0
11	2.76b	2	CH ₂ Cl ₂	1.5	Cu(tfacac) ₂ (10)	43
12	2.76b	2	CH ₃ CN	1.5	Cu(tfacac) ₂ (10)	0
13	2.76b	2	CHCl ₃	1.5	Rh ₂ (OAc) ₄ (5)	0
14 ^[b]	2.76b	2	CHCl ₃	1.5	Cu(tfacac) ₂ (10)	0

^[a] Reaction conditions: **2.29a** is added dropwise via syringe pump over one hour to a solution of **2.76**, catalyst and styrene (5 Equiv) in solvent (0.1 M) at room temperature. The reaction is further stirred until the indicated length of time is reached. Isolated yields of 2.3:1 *trans:cis* mixtures. ^[b] The tri-*n*-butyl variant of **2.29a** was used.

The second option for increasing the cyclopropanation reaction efficiency by addressing the issue of the poorly soluble iodosobenzene, was based on the use of additives. This concept was investigated to see if improvements to the cyclopropane yield could be obtained as this is a well-known problematic issue that has hindered the use of iodosobenzene in chemical synthesis. Different attempts to get around this solubility issue have included the use of additives to disrupt the polymeric network of secondary bonding to give “free” monomers of iodosobenzene in solution.

The depolymerization of $(\text{PhIO})_n$ was reported by Viktor V. Zhdankin¹⁸⁴ and investigation into whether iodosobenzene could be depolymerized in solution was attempted by various researchers.¹⁸⁵ Some salts are known to disrupt the polymeric network in iodosobenzene which frees up monomeric units of iodosobenzene as shown below in **Scheme 2.51**. Producing monomeric iodosobenzene has been shown to increase the reactivity in some reactions. This increase in reactivity may be attributed to increased solubility, or by making the iodoso functional group more accessible to reaction partners.¹⁸⁶



Scheme 2.51 Depolymerization of iodosobenzene $(\text{PhIO})_n$ with the use of salt additives

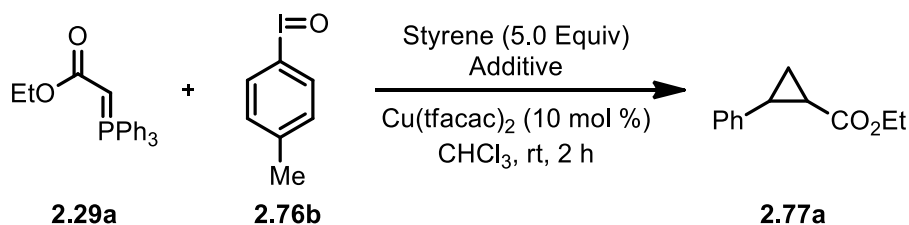
In addition to the use of salt additives, Lewis acids were also investigated such as zinc cations in $\text{Zn}(\text{ClO}_4)_2$ which are known to operate by depolymerizing, which in turn activates iodosobenzene, even when used in catalytic amounts.¹⁸⁷ Other developments include additives such as the homogeneous metal-based catalysts like $[\text{Fe}(\text{tpena})]^{2+}$ which work by breaking up the polymeric PhIO to extract monomeric PhIO.⁴¹

Preliminary studies performed by the Murphy group in the 2013 report tested Lewis acids such as $\text{BF}_3 \cdot \text{OEt}_2$, ZnCl_2 , and $\text{MgBr}_2 \cdot \text{OEt}_2$ with the intention of breaking down the polymeric network of iodosobenzene but failed to provide higher yields of the cyclopropane.

Because KBr is known to be an effective additive for the depolymerization of iodosobenzene, it was added to the reaction mixture in which *para* methyl iodosobenzene

(**2.76b**) was reacted with Wittig reagent **2.29a**, but this did not lead to an increased yield of cyclopropane. The use of Bu₄NI as an additive was also investigated using the same reaction conditions, but again, no increase in the yield of cyclopropane was witnessed. The yield of the cyclopropanation reaction run under identical conditions but without the use of additives was 53%, as shown below in **Table 2.6**, and it was therefore concluded that using additives was most likely not the appropriate option for optimizing this reaction.

Table 2.6 Effects of additives on the cyclopropanation reaction



Entry ^[a]	Additive	Cyclopropane Yield (%) ^[b]
1	KBr	47
2	Bu ₄ NI	51
3	-	53

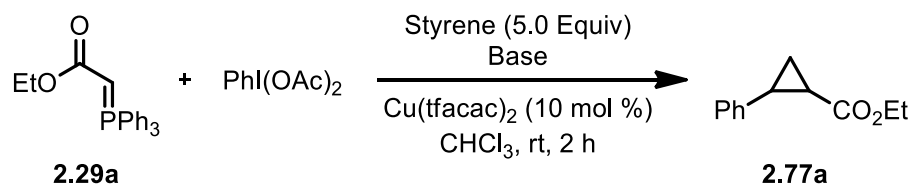
^[a] Reaction conditions: **2.29a** is added dropwise via syringe pump over one hour to a solution of **2.76b** (2 Equiv), catalyst and styrene (5 Equiv) in solvent (0.1 M) at room temperature. ^[b] Yield based on ¹H NMR using HMDSO (10 μL) as an internal standard.

Other attempts to optimizing the reaction conditions were directed towards running the reaction at different temperatures, with the hope of using colder conditions to enable greater amounts of the MCIY to form. Ochiai reported MCIYs to be unstable above -30 °C so it was anticipated that performing the cyclopropanation reaction at lower temperatures would give higher yields.¹⁴⁷ The proof-of-concept paper performed reactions at -60, -40, and 0 °C which all failed to provide the formation of cyclopropanation products. Analysis of their reaction mixtures revealed mostly Wittig reagent starting material, which suggest the reaction failed to initiate at lower temperatures.

The possibility of using different HVI reagents to replace the use of iodosobenzene in the cyclopropanation reaction was also investigated. In efforts to work with HVI reagents that have better solubility properties than iodosoarenes, (diacetoxyiodo)benzene (PIDA) or PhI(OAc)₂ was attempted to engage with Wittig reagents, to test for compatibility with the

cyclopropanation reaction. The reaction of Wittig reagent **2.29a** with PIDA was performed in the presence of styrene and Cu(tfacac)₂. The reaction using PIDA failed to initiate and form any reasonable amount of cyclopropane, as shown below in **Table 2.7**. Testing to see if this reaction could be initiated by using a base was also investigated, but the addition of a base to the reaction of Wittig reagents with PIDA did not yield any observable amount of cyclopropane.

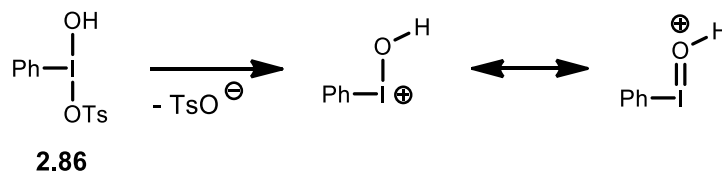
Table 2.7 The use of PIDA for the generation for cyclopropanation reaction



Entry ^[a]	Base	Cyclopropane
1	-	-
2	NaHCO ₃	-
3	K ₂ CO ₃	-

^[a]Reaction conditions: **2.29a** is added dropwise via syringe pump over one hour to a solution of PhI(OAc)₂ (1 Equivalent), catalyst and styrene (5 Equivalents) in solvent (0.1 M) at room temperature.

Hydroxy(phenyl)iido tosylate (HTIB, **2.86**) also known as Koser's reagent, is a useful oxidizing reagent for a myriad of organic transformations based on its ability to form a reactive electrophilic iodine centre.¹⁸⁸ The complete ionization of HTIB to give PhI⁺OH and a tosylate ion as fully solvated species in water or in organic solvents is shown below in **Scheme 2.52**. This is a known process which might lead to an increased ability to react with Wittig reagents, but was not tried in this thesis.



Scheme 2.52 Reactivity of Koser's reagent

Other HVI reagents that have the potential to engage with Wittig reagents in an oxygen transfer reaction are the iodine (V) class of compounds known as iodosylarenes. Iodosylbenzene

(**2.87**), which is shown below in **Figure 2.9**, is a known oxidizing reagent capable of transferring an oxygen atom when reacted with the appropriate reaction partner under specific conditions.

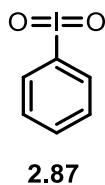
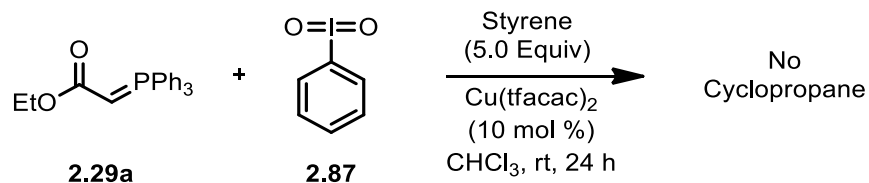


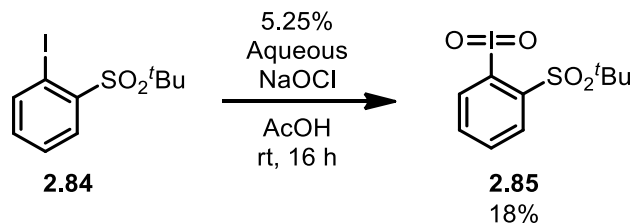
Figure 2.9 Structure of iodosylbenzene

The synthesis of iodosylbenzene was performed, followed by its introduction into the Wittig-type reaction with styrene under metal catalyzed conditions, but failed at producing any cyclopropane product, shown below in **Scheme 2.53**.



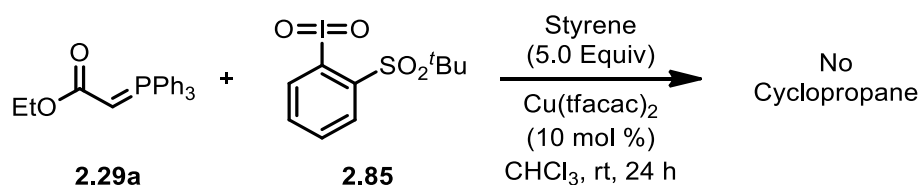
Scheme 2.53 Reaction of Wittig reagent with iodine (V) iodoxybenzene

The properties of iodoxyarenes are again known to be associated with poor solubility in organic solvents. It was therefore proposed that synthesizing iodoxyarenes with enhanced solubility may enable the cyclopropanation reaction to occur between Wittig reagents and iodine (V) compounds. To test this hypothesis, the *ortho-tert*-butyl sulfone derivative of iodoxybenzene was synthesized, as shown below in **Scheme 2.54**. Although the reaction gave a poor yield of only 18% of 1-(*tert*-butylsulfonyl)-2-iodylbenzene (**2.85**), this was still suitable for obtaining enough of a sample for running a trial reaction.



Scheme 2.54 Synthesis of soluble iodine (V) iodoxyarene

Subjecting iodoxyarene **2.85** to Wittig reagent **2.29a** under the optimized cyclopropanation reaction conditions failed to yield any cyclopropane as shown below in **Scheme 2.55**.



Scheme 2.55 Reaction of Wittig reagent with soluble iodine (V) iodoxyarene

Since absolutely no cyclopropane was produced from reacting Wittig reagents with iodoxyarenes, this idea was concluded to be a non suitable approach for increasing the yield of cyclopropane formation.

Investigations to find optimal yielding cyclopropanation conditions were then directed towards addressing the properties of the Wittig reagent starting material. A traditional Wittig reaction uses triaryl phosphoranes as the starting materials as they are more stable and are therefore more easily accessible when compared to their less stable trialkyl analogues. These properties make trialkyl phosphoranes more reactive than their triaryl counterparts, therefore it is possible to anticipate that reacting iodosoarenes with trialkyl phosphoranes might give higher yields of the *in situ* generated MCIY, which in turn might lead to a higher yielding cyclopropanation reaction.

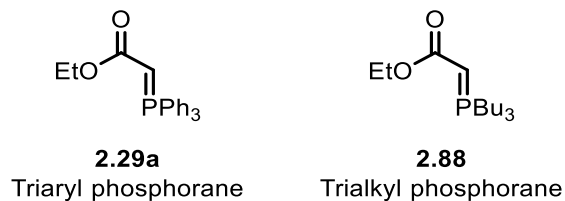
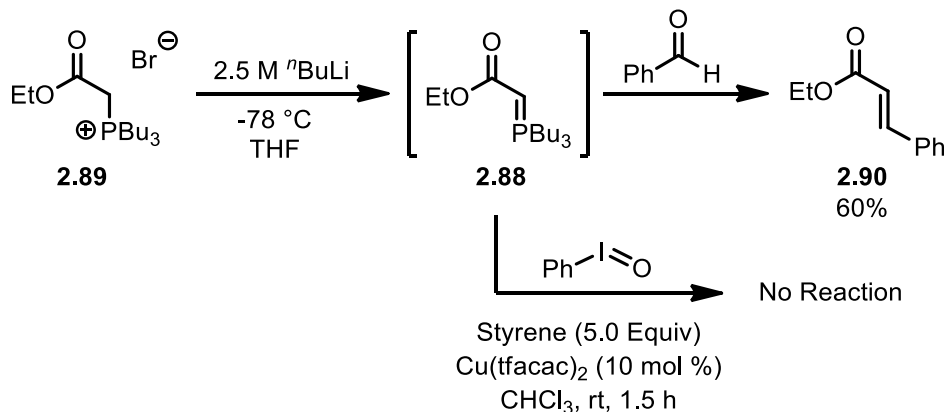


Figure 2.10 Examples of a triaryl and trialkyl phosphoranes (Wittig reagents)

Due to the instability and oxygen sensitivity of trialkyl phosphoranes, they were strategically generated *in situ* from their respective salt-based starting material (**2.89**) before reaction with the iodosoarene, as shown below in **Scheme 2.56**. To test the viability of this procedure and conditions, the trialkyl phosphorane (**2.88**) was trapped with an aldehyde to form an alkene (**2.90**), and the formation of this alkene was an indication that the reaction is effectively forming the trialkyl phosphorane *in situ*. Even though the alkene was observed to form under these specific conditions, the ability of the trialkyl phosphorane to react with iodosobenzene and form a cyclopropane was not successful as there was no observable cyclopropane produced.

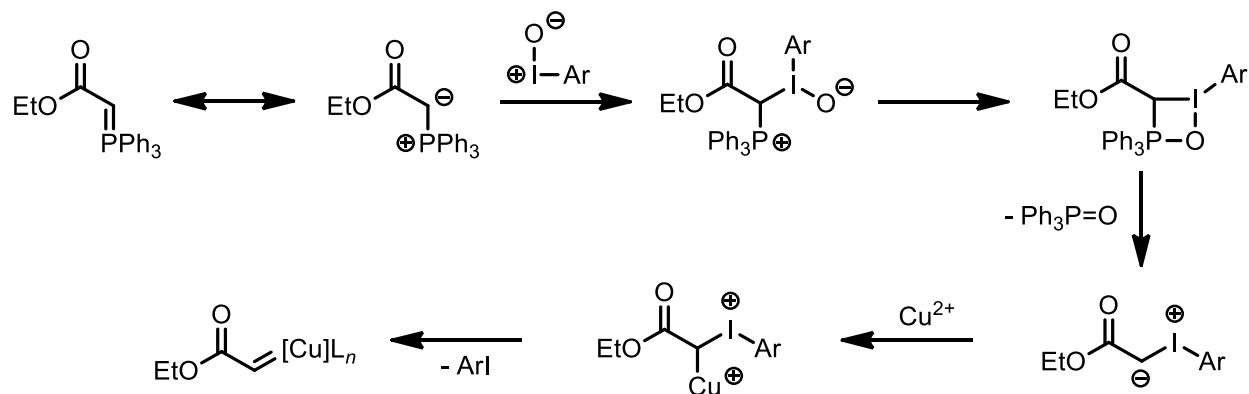


Scheme 2.56 Cyclopropane synthesis attempt using trialkyl phosphoranes

2.7.1 Proposed Reaction Mechanism

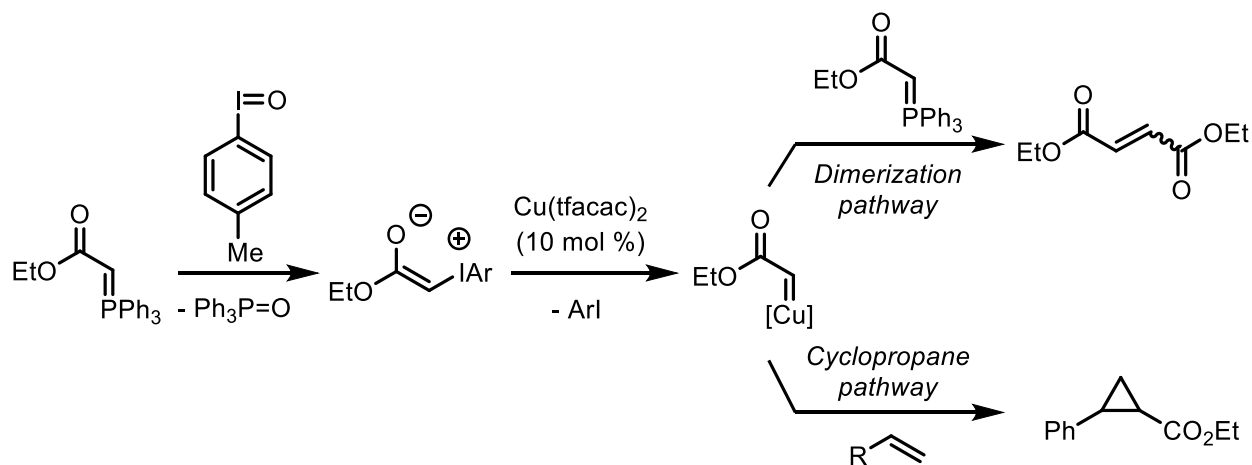
A mechanistic interpretation of the cyclopropanation reaction of Wittig reagents with iodosoarenes is shown below in **Scheme 2.57**, illustrating the formation of $\text{Ph}_3\text{P=O}$ which is believed to be the driving force of the reaction, and is observed to form in the reaction mixture

according to ^{31}P NMR. The energetically favourable process of displacing $\text{Ph}_3\text{P}=\text{O}$ theoretically allows for *in situ* production of the MCIY. The unstable MCIY can then be intercepted by the transition metal catalyst present, which eliminates the iodoarene by-product (confirmed by ^1H NMR), forming the metallocarbene intermediate.



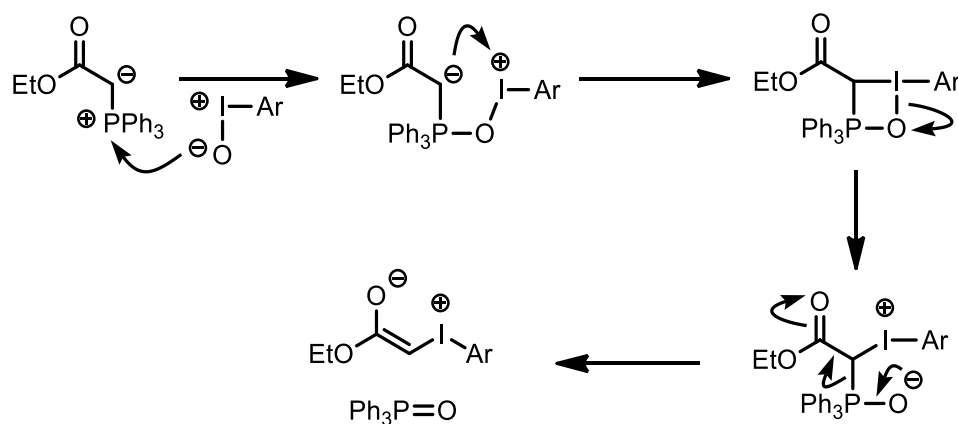
Scheme 2.57 Mechanism of metallocarbene formation using Wittig reagents

The metallocarbene intermediate can then proceed onwards to form two different products involving two different reaction pathways. **Scheme 2.58** below shows the two different divergent pathways which illustrate how the cyclopropanation and dimerization process occurs. The dimerization pathway may result from the metallocarbene intermediate reacting with the initial Wittig reagent, while the cyclopropanation results from the reaction of the metallocarbene with an alkene.



Scheme 2.58 Pathways for cyclopropanation and dimerization products

An alternative way to think about the mechanism is if the iodosoarene was to be more nucleophilic than the Wittig reagent. The oxygen of the iodosoarene may be sufficiently nucleophilic enough to engage with the positively charged phosphorus atom in the starting material ylide. The intermediate generated could then go on to form a four-membered ring (oxephosphetane) in a stepwise manner, which is necessary to allow for the Wittig-type reaction to proceed. This would allow for the formation of the phosphorus-oxygen double bond in an either stepwise or concerted process, followed by simultaneous formation of the MCIY, as shown below in **Scheme 2.59**.



Scheme 2.59 Alternative mechanism for Wittig-type reaction

There were no experiments performed to investigate the reaction mechanism, so the analysis of the transformation is purely theoretical, but is backed up by the confirmation of by-products observed to form in the process. The by-products which were observed to form include the aryl iodide and $\text{Ph}_3\text{P}=\text{O}$.

2.8 Scope of The Reaction

The optimal conditions for the cyclopropanation reaction were determined to be one equivalent of the Wittig reagent, 2 equivalents of iodosotoluene, and 5 equivalents of alkene in chloroform with 10 % catalytic loading of $\text{Cu}(\text{tfacac})_2$ as shown below in **Scheme 2.60**.

and the TMS-enol ether of cyclohexanone, which gave **2.77u** and **2.77v** in 60% and 63% yield, respectively. Therefore, it appears that moderate yields can be obtained with non-styrenyl, aliphatic alkenes and enol ethers, without observing products of competing C-H insertion, oxonium ylide formation or cycloaddition processes. It should be noted that the cyclopropane products are often produced as a mixture of diastereomers, and the yields shown in **Figure 2.11** represent the combined yield of both diastereomers, with the major diastereomer showing. The cyclopropanes were typically recovered as ~2:1 *trans:cis* mixture of diastereomers, except **2.77k**, **2.77m**, **2.77q**, and **2.77r** which were single diastereomers by ¹H NMR.

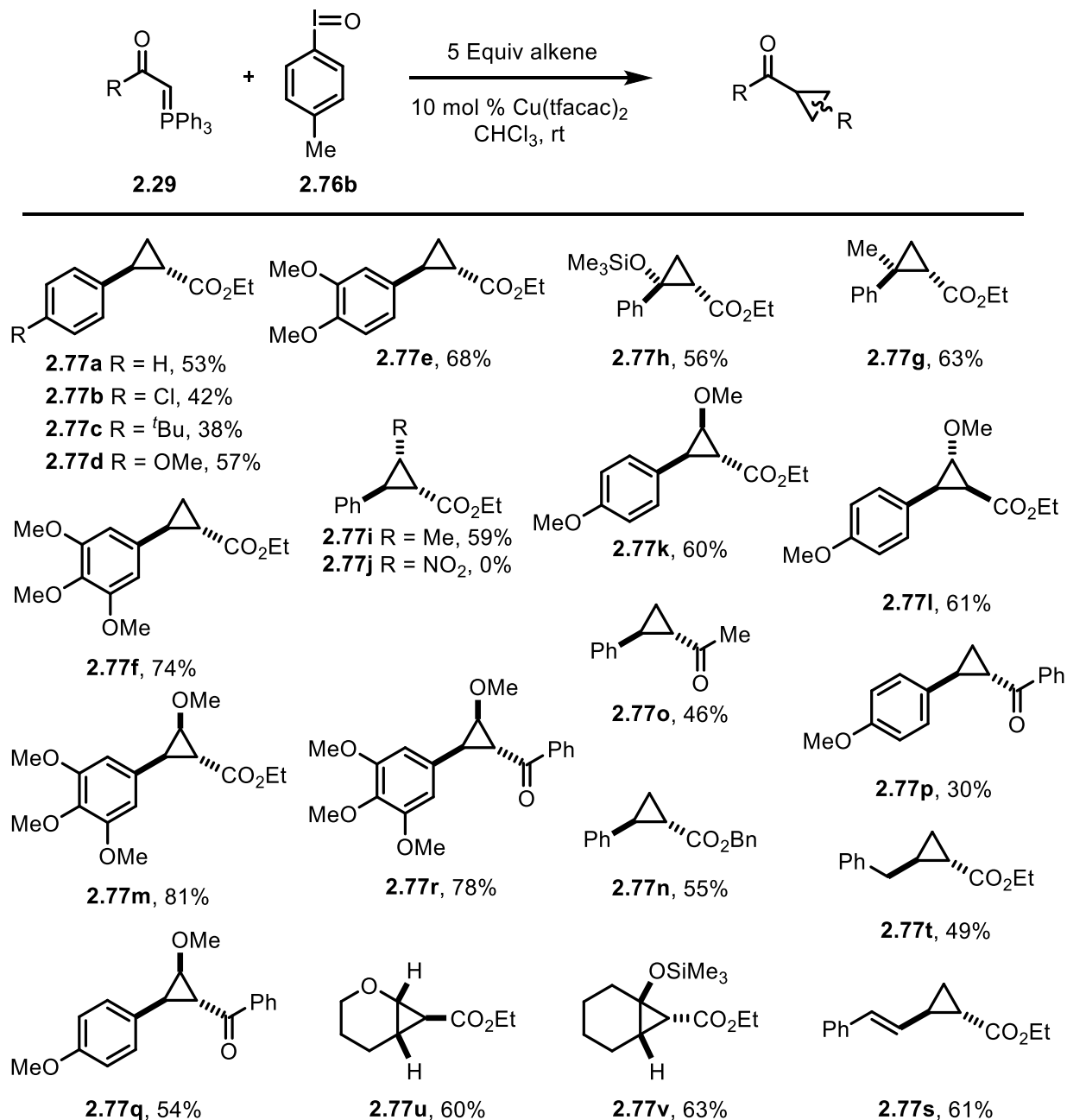


Figure 2.11 Cyclopropanation of MCIYs reaction scope

2.8.1 Intramolecular Cyclopropanation of MCIYs

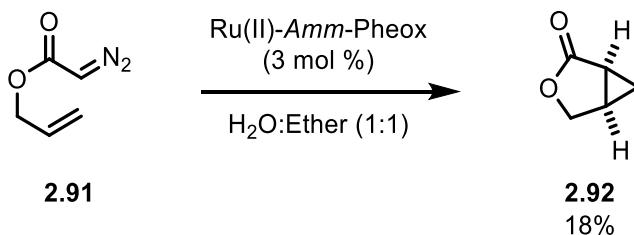
Given the vast number of molecules that can be accessed using intramolecular cyclopropanation reactions with the use of diazo-based starting material, and the similarities in

reactivity between diazos and iodonium ylides, it appears logical to try and perform intramolecular cyclopropanation reactions using MCIYs.¹⁸⁹

The synthesis of fused [3.1.0] cyclopropanes have been accessed using diazo compounds with alkenes tethered in an intramolecular fashion, but with poor yields (18%) when using terminal alkenes as shown in **Scheme 2.61**.¹⁹⁰ Perhaps the use of iodonium ylides might provide a way of increasing the yield due to slightly different reactivity properties. The use of terminal alkenes tethered to the ylide was chosen for preliminary investigations due to the ease of synthesis of the required starting materials.

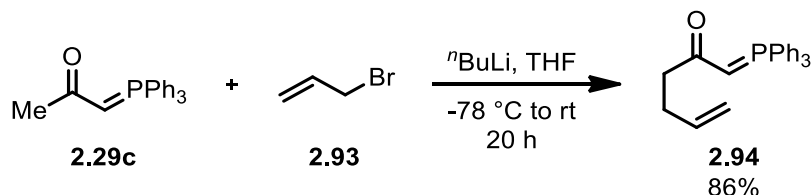
Bicyclo[3.1.0]hexane derivatives are attractive motifs which are pursued as synthetic targets because of their usefulness in containing both a cyclopentane and cyclopropane ring. The versatility of cyclopropanes, combined with their occurrence in natural and non-natural products, often containing biological activity, makes these fused bicyclo motifs valuable synthons. It is therefore of interest to have an efficient and simple method of synthesizing these systems.

Copper-catalyzed intramolecular cyclopropanation of unsaturated diazocarbonyl compounds are well known for providing access to bicyclo[3.1.0]hexane compounds, including enantioselective examples. The mechanisms of these transition metal-catalyzed carbene transfer reactions of diazo compounds to carbon-carbon double bonds has been thoroughly investigated.¹⁹¹ In contrast to this, little is known about the transition metal-catalyzed carbene transfer reactions of iodonium ylides for cyclopropanation, and very few studies have been performed from a mechanistic point of view.¹⁹² Because iodonium ylides are safer to use and could virtually replace diazonium ylides in transition metal-catalyzed cyclopropanation reactions, it would seem logical to pursue the advancement and understanding of this chemistry, and in this case, intramolecular cyclopropanation chemistry.



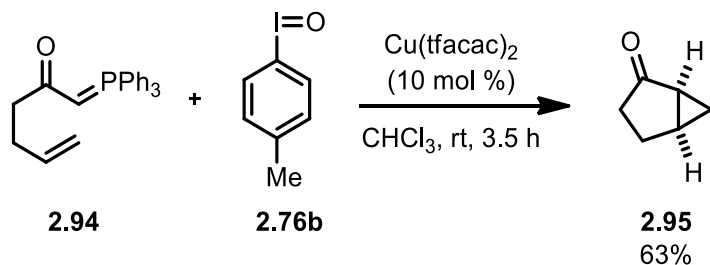
Scheme 2.61 Intramolecular cyclopropanation of diazo

To test the possibility of the MCIY cyclopropanation reaction occurring in an intramolecular fashion, it was envisioned that synthesis of Wittig reagent **2.94** would allow for answering this question. It was important to create a Wittig reagent in which an alkene would be tethered at the appropriate distance from the ylidic carbon to allow for an intramolecular cyclopropanation reaction to occur in which a five-membered or six-membered ring could form. Commercially available Wittig reagent **2.29c** was allylated with allyl bromide (**2.93**) to give **2.94** in 86% yield as shown in **Scheme 2.62**.



Scheme 2.62 Synthesis of Wittig reagent for intramolecular cyclopropanation

With Wittig reagent **2.94** synthesized, it was then subjected to the optimized cyclopropanation conditions using 2 equivalents of iodosoarene **2.76b** and $\text{Cu}(\text{tfacac})_2$ at 10 mol % in chloroform as shown in **Scheme 2.63**. The cyclopropanation reaction occurred successfully giving the fused [3.1.0] cyclopropane **2.95** in 63% yield with the expected five-membered ring orientation.



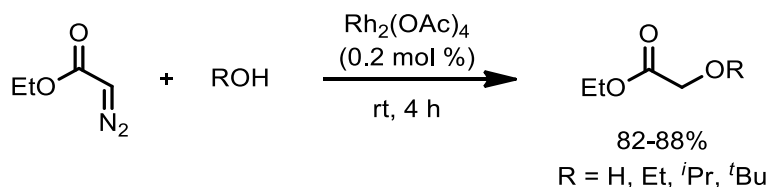
Scheme 2.63 Intramolecular cyclopropanation of in situ generated MCIY

It was observed that the intramolecular cyclopropanation reaction above produced small quantities of **2.94** dimerization, even when the Wittig reagent was added as a chloroform solution by syringe pump over one hour to the reaction mixture. Both *cis* and *trans* dimers of Wittig reagent starting material were isolated from the reaction mixture, with a combined yield of less than 10%. To account for the remainder of the mass balance, it is possible that intermolecular

cyclopropanation could be occurring, although this cyclopropane product was not observed or isolated from the reaction mixture. It is also possible that a series of intermolecular cyclopropanation reactions could produce a quantity of polymerization products that may be insoluble or poorly soluble in organic solvents and may account for the remainder of the mass balance, although this was not observed in the crude ^1H NMR spectrum or isolated.

2.9 Insertion Reactions of MCIYs

Diazo-based compounds are known to engage in insertion reactions such as C-H, O-H, N-H for example, when reacted with a transition metal such as copper or rhodium.¹⁹³ The reaction of ethyl diazoacetate with various alcohols in the presence of catalytic rhodium was reported by Teyssié in 1973 as shown in **Scheme 2.64**.¹⁹⁴

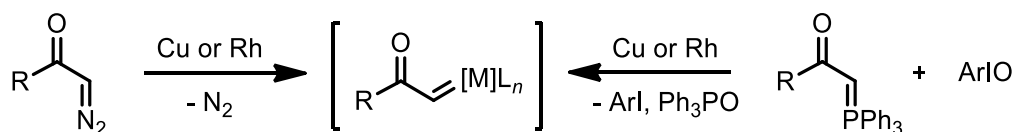


Scheme 2.64 O-H Insertion reactions of diazos with alcohols

These reports of metal-catalyzed insertion reactions of diazo compounds raised the question of whether an analogous reactivity pattern could be paralleled and accessed using MCIYs generated *in situ*, because of the similarity in reactivity patterns that exist between these two species. Based off the successful ability to capture MCIYs with a metal catalyst and use in cyclopropanation reactions with alkenes, it may be theoretically possible to swap out the alkene for a different reaction partner which may then be able to undergo an insertion reaction. Initial investigations were aimed as using alcohols as the reaction partner, which could possibly allow for an intermolecular O-H insertion reaction to occur. If this same type of reactivity could be accessed using iodonium ylides, then the possibility of discovering many more reactions in which the reactivity of diazo compounds is paralleled with their HVI analogous seems probable.

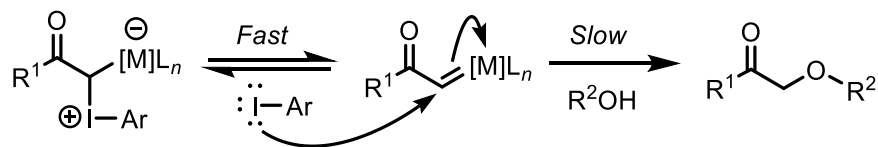
An important question that is still not fully understood, is the properties of the metallocarbene generated from diazo compounds, compared to the metallocarbene generated

from Wittig reagents in combination with iodosoarenes. In the presence of transition metals, both diazos and Wittig reagents, in combination with iodosoarenes, generate a metallocarbene which in theory should be able to engage with an appropriate reaction partner. The metallocarbene structure should be equivalent, but the presence of different species in the solution may give different properties in terms of overall reactivity. By-products from the reaction of Wittig reagents and iodosoarene include iodoarene and $\text{Ph}_3\text{P}=\text{O}$, as shown in **Scheme 2.65**, and these by-products may be able to act as ligands and dock to the metal in the metallocarbene. These potential ligands, which would not be present in the reaction of diazos, may alter the properties of the metallocarbene enough to prevent reactions from occurring, or alter the rates of reactions due to sterics or electronical differences.



Scheme 2.65 Metallocarbene generation from diazos or Wittig reagents

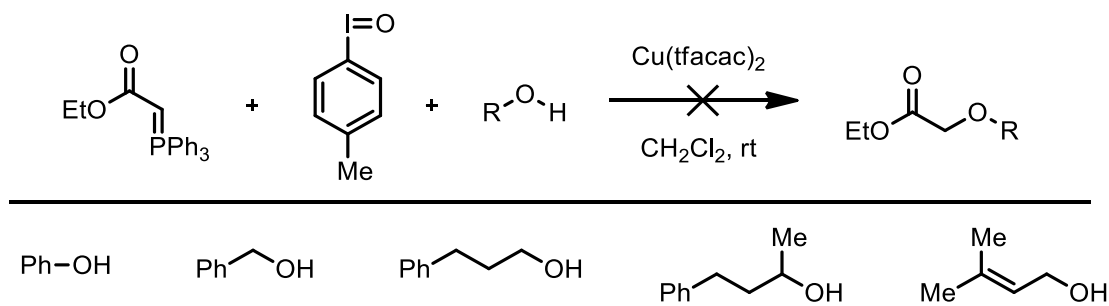
Metallocarbenes containing a single carbonyl acceptor group are electrophilic, and the iodine in aryl iodides has highly polarizable properties, making it slightly nucleophile. There could be an equilibrium that exist between the aryl iodide and the metallocarbene which may be a fast process, as shown in **Scheme 2.66**. This may prevent insertion reactions from ever occurring under these conditions, so observing no O-H insertion products may be the result of this undesired interaction. This concept was tested by reacting Wittig reagents with iodosoarenes and alcohols and checking to see if O-H insertion reactions were occurring.



Scheme 2.66 Reversible interaction of aryl iodide with metallocarbene

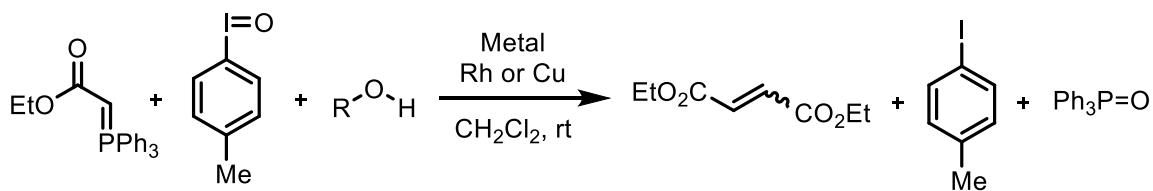
Using optimized reaction conditions from the Wittig-type cyclopropanation reaction, including Wittig reagent **2.29a** and iodosoarene **2.76b**, an analogous reaction was attempted

except the alkene was removed and an alcohol was instead inserted into the reaction mixture. $\text{Cu}(\text{tfacac})_2$ was used as the metal catalyst (10 mol %) and the reactions were run in dichloromethane at room temperature. **Scheme 2.67** summarizes the observed results, which tested aryl, primary, secondary, and allylic alcohols, but did not produce any substantial amounts of O-H insertion reaction products.



Scheme 2.67 Alcohols tested in O-H insertion reactions

The products obtained from the above conditions were dimerization of Wittig reagent starting material, iodoarene, triphenylphosphine oxide, and recovered alcohol, as shown in **Scheme 2.68**. The fact that oxidation of the Wittig reagent was occurring, presumably from the iodoarene, does indicate the potential for this reaction to be successful if specialized conditions were found, but there was no more time invested to search for these conditions.



Scheme 2.68 Reaction of Wittig reagent with iodoarene and alcohols

2.10 Experimental

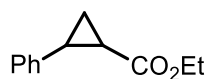
All reactions were carried out in flame-dried glassware under a dry nitrogen atmosphere, unless otherwise noted. All solvents were obtained pure and dry from a JC Meyer solvent purification system. All reagents were purchased from Sigma-Aldrich and used without further purification. ^1H NMR spectra were recorded on Bruker instruments at 300 MHz and were referenced to residual ^1H shift in CDCl_3 (7.24 ppm). All ^{13}C NMR were recorded at 75 MHz, and CDCl_3 (77.0 ppm) was used as the internal reference. ^{31}P NMR spectra were recorded at 121 MHz and referenced to the H_3PO_4 signal at 0 ppm. The following abbreviations were used to explain the multiplicities: s = singlet, d = doublet, t = triplet, q = quartet, br s = broad singlet. Reactions were monitored by thin-layer chromatography (TLC) on commercial silica pre-coated plates with a particle size of 60 Å and viewed by UV lamp (254 nm), by gas chromatography (HP5890A Series II) with a J&W Scientific 30 m x 0.53 mm DB624 column with 3 micron film thickness (run settings: 2.5 min at 75 °C, 7.5 °C/min to 250 °C), and by ^{31}P NMR. Flash chromatography was performed using 60Å (230-400 mesh) silica gel. Melting points were performed using a MeltTemp apparatus. InfraRed (IR) data was recorded using an ATR-FTIR (Attenuated Total Reflection Fourier Transform InfraRed) instrument. The following abbreviations were used to explain the IR peak intensities: (s) = strong, (m) = medium, (w) = weak. Positive ion electrospray ionization (ESI) was performed with a Thermo Scientific Q-Exactive hybrid mass spectrometer. Accurate mass determinations were performed at a mass resolution of 70,000. For ESI, samples were infused at 10 $\mu\text{L}/\text{min}$ in a 1:1 MeOH/ H_2O + 0.1% formic acid solution.

2.10.1 General Procedure 1 (GP1) - Synthesis of Cyclopropanes

In a dry 10 mL round bottom flask, iodosoarene (0.28 mmol, 2 equiv), $\text{Cu}(\text{tfacac})_2$ (0.014 mmol, 0.1 equiv), alkene (0.70 mmol, 5 equiv), then CHCl_3 (3 mL) was stirred at room temperature. Wittig reagent (0.14 mmol, 1 equiv) in CHCl_3 (1 mL) was then added to the solution by syringe pump addition over 1 hour, and the reaction stirred for an additional 0.5 hour (1.5 hours total time) at room temperature. The reaction was quenched with 10 % K_2CO_3 (2 mL) and transferred to a separatory funnel. Extraction of product using CH_2Cl_2 (3 x 10 mL), followed by washing the combined organic extracts with brine (2 x 10 mL). The organic extracts were

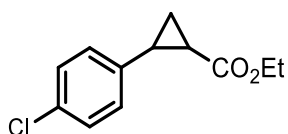
dried over MgSO₄, filtered, concentrated on a rotary evaporator, and then placed under high vacuum. The crude reaction mixture was loaded onto a column of silica gel using a minimal amount of CH₂Cl₂. Elution was accomplished using mixtures of EtOAc/hexanes.

Ethyl 2-phenylcyclopropanecarboxylate (2.77a)



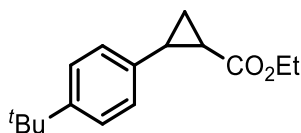
Synthesized according to **GP1** using iodosoarene **2.76b** (0.201 g, 0.86 mmol, 2 equiv), Cu(tfacac)₂ (0.016 g, 0.043 mmol, 0.1 equiv), styrene (0.247 mL, 2.15 mmol, 5 equiv), CHCl₃ (4.3 mL), and Wittig reagent **2.29a** (0.150 g, 0.43 mmol, 1 equiv). Purification by flash chromatography through a column of silica gel (hexanes:EtOAc 8:1) led to the title compound isolated as a pale yellow oil (0.042 g, 53% yield) with a 2.3:1 *trans:cis* ratio. R_f = 0.64 (hexanes:EtOAc 3:1). The characterization data matches what has been previously reported in the literature.¹⁹⁵

Ethyl 2-(4-chlorophenyl)cyclopropanecarboxylate (2.77b)



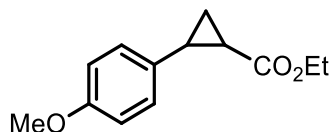
Synthesized according to **GP1** using iodosoarene **2.76b** (0.200 g, 0.86 mmol, 2 equiv), Cu(tfacac)₂ (0.016 g, 0.043 mmol, 0.1 equiv), 4-chlorostyrene (0.288 mL, 2.15 mmol, 5 equiv), CHCl₃ (4.3 mL), and Wittig reagent **2.29a** (0.150 g, 0.43 mmol, 1 equiv). Purification by flash chromatography through a column of silica gel (hexanes:EtOAc 10:1) led to the title compound isolated as a pale yellow oil (0.040 g, 42% yield) with a 2.3:1 *trans:cis* ratio. R_f = 0.30 (hexanes:Et₂O 10:1). The characterization data matches what has been previously reported in the literature.¹⁹⁶

Ethyl 2-(4-(tert-butyl)phenyl)cyclopropanecarboxylate (**2.77c**)



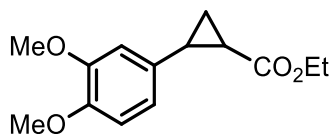
Synthesized according to **GP1** using iodosoarene **2.76b** (0.066 g, 0.28 mmol, 2 equiv), Cu(tfacac)₂ (0.005 g, 0.014 mmol, 0.1 equiv), 4-*tert*-butylstyrene (0.128 mL, 0.70 mmol, 5 equiv), CHCl₃ (1.9 mL), and Wittig reagent **2.29a** (0.050 g, 0.14 mmol, 1 equiv). Purification by flash chromatography through a column of silica gel (hexanes:EtOAc 10:1) led to the title compound isolated as a pale yellow oil (0.013 g, 38% yield) with a 2.4:1 *trans:cis* ratio. R_f = 0.63 (hexanes:EtOAc 3:1). The characterization data matches what has been previously reported in the literature.¹⁹⁷

Ethyl 2-(4-methoxyphenyl)cyclopropanecarboxylate (**2.77d**)



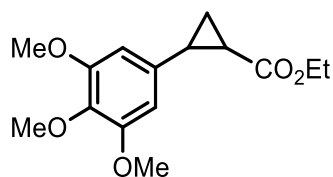
Synthesized according to **GP1** using iodosoarene **2.76b** (0.201 g, 0.86 mmol, 2 equiv), Cu(tfacac)₂ (0.016 g, 0.043 mmol, 0.1 equiv), 4-methoxystyrene (0.286 mL, 2.15 mmol, 5 equiv), CHCl₃ (4.3 mL), and Wittig reagent **2.29a** (0.150 g, 0.43 mmol, 1 equiv). Purification by flash chromatography through a column of silica gel (hexanes:EtOAc 9:1) led to the title compound isolated as a pale yellow oil (0.054 g, 57% yield) with a 2.3:1 *trans:cis* ratio. R_f = 0.59 (hexanes:EtOAc 3:1). The characterization data matches what has been previously reported in the literature.⁶⁷

Ethyl 2-(3,4-dimethoxyphenyl)cyclopropanecarboxylate (**2.77e**)



Synthesized according to **GP1** using iodosoarene **2.76b** (0.065 g, 0.28 mmol, 2 equiv), Cu(tfacac)₂ (0.005 g, 0.014 mmol, 0.1 equiv), 3,4-dimethoxystyrene (0.115 g, 0.70 mmol, 5 equiv), CHCl₃ (3.0 mL), and Wittig reagent **2.29a** (0.050 g, 0.14 mmol, 1 equiv). Purification by flash chromatography through a column of silica gel (hexanes:EtOAc 12:1) led to the title compound isolated as a pale yellow oil (0.024 g, 68% yield) with a 2.3:1 *trans:cis* ratio. R_f = 0.34 (hexanes:EtOAc 3:1). The characterization data matches what has been previously reported in the literature.¹⁹⁸

Ethyl 2-(3,4,5-trimethoxyphenyl)cyclopropanecarboxylate (**2.77f**)



Synthesized according to **GP1** using iodosoarene **2.76b** (0.065 g, 0.28 mmol, 2 equiv), Cu(tfacac)₂ (0.005 g, 0.014 mmol, 0.1 equiv), 3,4,5-trimethoxystyrene (0.136 g, 0.70 mmol, 5 equiv), CHCl₃ (3.0 mL), and Wittig reagent **2.29a** (0.050 g, 0.14 mmol, 1 equiv). Purification by flash chromatography through a column of silica gel (hexanes:EtOAc 12:1 to 8:1) led to the title compound isolated as a pale yellow oil (0.029 g, 74% yield) with a 1.9:1 *trans:cis* ratio. R_f = 0.28 (hexanes:EtOAc 3:1). The characterization data matches what has been previously reported in the literature.¹⁹⁹

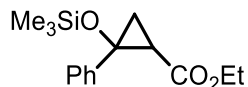
Ethyl 2-methyl-2-phenylcyclopropanecarboxylate (**2.77g**)



Synthesized according to **GP1** using iodosoarene **2.76b** (0.135 g, 0.58 mmol, 2 equiv), Cu(tfacac)₂ (0.010 g, 0.029 mmol, 0.1 equiv), α -methylstyrene (0.189 mL, 1.45 mmol, 5 equiv), CHCl₃ (4.0 mL), and Wittig reagent **2.29a** (0.100 g, 0.29 mmol, 1 equiv). Purification by flash chromatography through a column of silica gel (hexanes:EtOAc 12:1 to 10:1) led to the title compound isolated as a pale yellow oil (0.037 g, 63% yield) with a 1.4:1 *trans:cis* ratio. R_f =

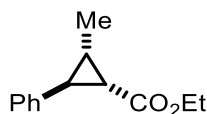
0.62 (hexanes:EtOAc 3:1). The characterization data matches what has been previously reported in the literature.²⁰⁰

Ethyl 2-phenyl-2-((trimethylsilyl)oxy)cyclopropanecarboxylate (**2.77h**)

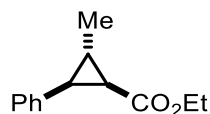


Synthesized according to **GP1** using iodosoarene **2.76b** (0.201 g, 0.86 mmol, 2 equiv), Cu(tfacac)₂ (0.016 g, 0.043 mmol, 0.1 equiv), α -(trimethylsilyloxy)styrene (0.410 g, 2.15 mmol, 5 equiv), CHCl₃ (5.0 mL), and Wittig reagent **2.29a** (0.150 g, 0.43 mmol, 1 equiv). Purification by flash chromatography through a column of silica gel (hexanes:EtOAc 9:1) led to the title compound isolated as a pale yellow oil (0.067 g, 56% yield) with a 1:1 *trans:cis* ratio. R_f = 0.36 (hexanes:EtOAc 9:1). The characterization data matches what has been previously reported in the literature.²⁰¹

Ethyl 2-methyl-3-phenylcyclopropanecarboxylate (**2.77i**)



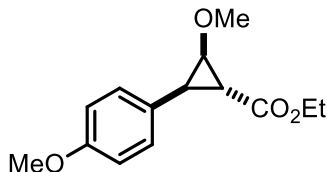
Major Diastereomer



Minor Diastereomer

Synthesized according to **GP1** using iodosoarene **2.76b** (0.065 g, 0.28 mmol, 2 equiv), Cu(tfacac)₂ (0.005 g, 0.014 mmol, 0.1 equiv), *trans*- β -methylstyrene (0.091 mL, 0.70 mmol, 5 equiv), CHCl₃ (4.0 mL), and Wittig reagent **2.29a** (0.050 g, 0.14 mmol, 1 equiv). Purification by flash chromatography through a column of silica gel (hexanes:EtOAc 6:1 to 5:1) led to the title compound isolated as a pale yellow oil (0.017 g, 59% yield) with a 2.5:1 *dr*. R_f = 0.51 (hexanes:EtOAc 3:1). The characterization data matches what has been previously reported in the literature.²⁰²

Ethyl 2-methoxy-3-(4-methoxyphenyl)cyclopropanecarboxylate (**2.77k**)



Synthesized according to **GP1** using iodosoarene **2.76b** (0.131 g, 0.56 mmol, 2 equiv), Cu(tfacac)₂ (0.010 g, 0.029 mmol, 0.1 equiv), (Z)-1-methoxy-4-(2-methoxyvinyl)benzene (0.230 g, 1.4 mmol, 5 equiv), CHCl₃ (4.0 mL), and Wittig reagent **2.29a** (0.100 g, 0.29 mmol, 1 equiv). Purification by flash chromatography through a column of silica gel (hexanes:EtOAc 10:1 to 8:1) led to the title compound isolated as a pale yellow oil (0.042 g, 60% yield). R_f = 0.53 (hexanes:EtOAc 3:1).

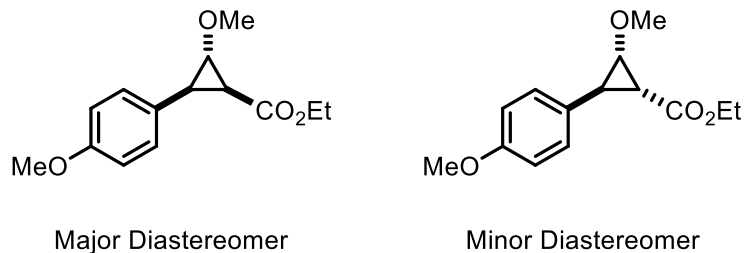
¹H NMR (300 MHz, CDCl₃): δ 7.18 (app d, *J* = 9.0 Hz, 2H), 6.83 (app d, *J* = 9.0 Hz, 2H), 4.15 (q, *J* = 7.2 Hz, 2H), 3.77-3.80 (m, 4H), 3.30 (s, 3H), 2.65 (t, *J* = 6.3 Hz, 1H), 2.11 (dd, *J* = 6.0, 2.7 Hz, 1H), 1.27 (t, *J* = 7.1 Hz, 3H).

¹³C NMR (75 MHz, CDCl₃): δ ¹³C NMR (100 MHz, CDCl₃) 175.1, 161.3, 132.2, 129.5, 116.5, 68.8, 63.6, 61.5, 58.1, 34.8, 30.9, 17.1.

HRMS (ESI⁺ [M+H]⁺): Calculated for C₁₄H₁₉O₄ 251.1278, found 251.1278.

IR (ATR): 2935 (w), 1717 (s), 1515 (s), 1287 (m), 830 (s) cm⁻¹.

Ethyl 2-methoxy-3-(4-methoxyphenyl)cyclopropanecarboxylate (**2.77l**)



Synthesized according to **GP1** using iodosoarene **2.76b** (0.140 g, 0.60 mmol, 2 equiv), Cu(tfacac)₂ (0.011 g, 0.030 mmol, 0.1 equiv), (E)-1-methoxy-4-(2-methoxyvinyl)benzene (0.246 g, 1.50 mmol, 5 equiv), CHCl₃ (4.0 mL), and Wittig reagent **2.29a** (0.104 g, 0.30 mmol, 1 equiv). Purification by flash chromatography through a column of silica gel (hexanes:EtOAc

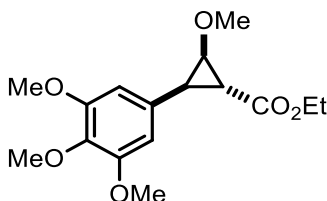
20:1 to 8:1) led to the title compound isolated as a pale yellow oil (0.046 g, 61% yield) with a 2.9:1 *dr*. $R_f = 0.40$ (hexanes:EtOAc 3:1).

$^1\text{H NMR}$ (300 MHz, CDCl_3): δ 7.32 (app d, $J = 8.6$ Hz, 2H), 6.82 (app d, $J = 8.6$ Hz, 2H), 4.04 (dq, $J = 7.1, 4.1$ Hz, 2H), 3.77-3.81 (m, 4H), 3.41 (s, 3H), 2.51 (dd, $J = 10.1, 7.1$ Hz, 1H), 1.97 (dd, $J = 10.1, 6.1$ Hz, 1H), 1.13 (t, $J = 7.1$ Hz, 3H).

$^{13}\text{C NMR}$ (75 MHz, CDCl_3): δ 171.1, 161.1, 134.2, 128.4, 116.3, 66.3, 62.9, 62.1, 58.1, 30.6, 26.8, 17.1.

HRMS (ESI⁺ [M+H]⁺): Calculated for $\text{C}_{14}\text{H}_{19}\text{O}_4$ 251.1278, found 251.1275.

Ethyl 2-methoxy-3-(3,4,5-trimethoxyphenyl)cyclopropanecarboxylate (**2.77m**)



Synthesized according to **GP1** using iodosoarene **2.76b** (0.065 g, 0.28 mmol, 2 equiv), $\text{Cu}(\text{tfacac})_2$ (0.005 g, 0.014 mmol, 0.1 equiv), (*Z*)-1,2,3-trimethoxy-5-(2-methoxyvinyl)benzene (0.157 g, 0.70 mmol, 5 equiv), CHCl_3 (4.0 mL), and Wittig reagent **2.29a** (0.050 g, 0.14 mmol, 1 equiv). Purification by flash chromatography through a column of silica gel (hexanes:EtOAc 12:1 to 8:1) led to the title compound isolated as a pale yellow oil (0.035 g, 81% yield). $R_f = 0.27$ (hexanes:EtOAc 3:1).

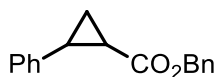
$^1\text{H NMR}$ (300 MHz, CDCl_3): δ 6.49 (s, 2H), 4.16 (q, $J = 7.2$ Hz, 2H), 3.78 - 3.85 (m, 10H), 3.34 (s, 3H), 2.62 (t, $J = 6.3$ Hz, 1H), 2.12 (dd, $J = 6.0, 2.7$ Hz, 1H), 1.28 (t, $J = 7.1$ Hz, 3H).

$^{13}\text{C NMR}$ (75 MHz, CDCl_3): δ 172.1, 153.1, 137.0, 130.7, 105.6, 66.2, 61.0, 59.0, 56.2, 32.8, 28.7, 14.4.

HRMS (ESI⁺ [M+H]⁺): calculated for $\text{C}_{16}\text{H}_{23}\text{O}_6$ 311.1489, found 311.1487.

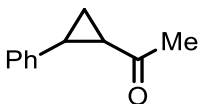
IR (ATR): 2936 (w), 1718 (s), 1587 (m), 1123 (s), 834 (w) cm^{-1} .

Benzyl 2-phenylcyclopropanecarboxylate (2.77n)



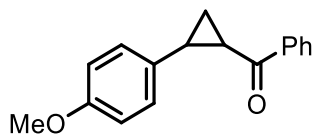
Synthesized according to **GP1** using iodosoarene **2.76b** (0.112 g, 0.48 mmol, 2 equiv), Cu(tfacac)₂ (0.009 g, 0.024 mmol, 0.1 equiv), styrene (0.137 mL, 1.20 mmol, 5 equiv), CHCl₃ (4.0 mL), and Wittig reagent **2.29d** (0.100 g, 0.24 mmol, 1 equiv). Purification by flash chromatography through a column of silica gel (hexanes:EtOAc 9:1 to 3:1) led to the title compound isolated as a pale yellow oil (0.033 g, 55% yield) with a 3:1 *trans:cis* ratio. R_f = 0.56 (hexanes:EtOAc 3:1). The characterization data matches what has been previously reported in the literature.²⁰³

1-(2-Phenylcyclopropyl)ethanone (2.77o)



Synthesized according to **GP1** using iodosoarene **2.76b** (0.112 g, 0.48 mmol, 2 equiv), Cu(tfacac)₂ (0.009 g, 0.024 mmol, 0.1 equiv), styrene (0.137 mL, 1.20 mmol, 5 equiv), CHCl₃ (2.5 mL), and Wittig reagent **2.29c** (0.075 g, 0.24 mmol, 1 equiv). Purification by flash chromatography through a column of silica gel (hexanes:EtOAc 10:1) led to the title compound isolated as a pale yellow oil (0.018 g, 46% yield) with a 2:1 *trans:cis* ratio. R_f = 0.73 (hexanes:EtOAc 2:1). The characterization data matches what has been previously reported in the literature.²⁰⁴

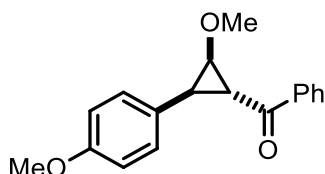
(2-(4-Methoxyphenyl)cyclopropyl)(phenyl)methanone (2.77p)



Synthesized according to **GP1** using iodosoarene **2.76b** (0.182 g, 0.78 mmol, 2 equiv), Cu(tfacac)₂ (0.014 g, 0.039 mmol, 0.1 equiv), 4-methoxystyrene (0.250 mL, 1.95 mmol, 5 equiv), CHCl₃ (3.5 mL), and Wittig reagent **2.29e** (0.150 g, 0.39 mmol, 1 equiv). Purification by flash chromatography through a column of silica gel (hexanes:EtOAc 10:1) led to the title

compound isolated as a pale yellow oil (0.029 g, 30% yield) with a 2:1 *trans:cis* ratio. $R_f = 0.58$ (hexanes:EtOAc 3:1). The characterization data matches what has been previously reported in the literature.²⁰⁵

2-Methoxy-3-(4-methoxyphenyl)cyclopropyl(phenyl)methanone (2.77q)



Synthesized according to **GP1** using iodosoarene **2.76b** (0.031 g, 0.13 mmol, 2 equiv), $\text{Cu}(\text{tfacac})_2$ (0.002 g, 0.007 mmol, 0.1 equiv), (*Z*)-1-methoxy-4-(2-methoxyvinyl)benzene (0.054 g, 0.33 mmol, 5 equiv), CHCl_3 (3.0 mL), and Wittig reagent **2.29e** (0.025 g, 0.07 mmol, 1 equiv). Purification by flash chromatography through a column of silica gel (hexanes:EtOAc 10:1 to 8:1) led to the title compound isolated as a pale yellow oil (0.010 g, 54% yield). $R_f = 0.51$ (hexanes:EtOAc 3:1).

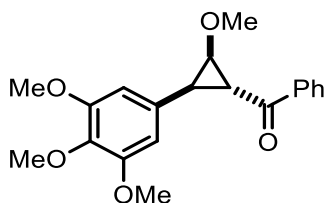
^1H NMR (300 MHz, CDCl_3): δ 8.02 (app d, $J = 7.5$ Hz, 2H), 7.58 (app t, $J = 7.2$ Hz, 1H), 7.48 (app t, $J = 7.5$ Hz, 2H), 7.28 (app d, $J = 8.4$ Hz, 2H), 6.86 (app d, $J = 8.1$ Hz, 2H), 3.98 (dd, $J = 6.6, 3.0$ Hz, 1H), 3.79 (s, 3H), 3.36 (s, 3H), 3.14 (dd, $J = 6.0, 2.4$ Hz, 1H), 2.98 (t, $J = 6.0$ Hz, 1H).

^{13}C NMR (75 MHz, CDCl_3): δ 200.4, 161.4, 140.4, 136.0, 132.4, 131.6, 131.0, 130.3, 116.7, 72.6, 61.8, 58.2, 38.1, 36.6.

HRMS (ESI^+ [$\text{M}+\text{H}$] $^+$): calculated for $\text{C}_{18}\text{H}_{19}\text{O}_3$ 283.1329, found 283.1332.

IR (ATR): 2934 (w), 1658 (m), 1245 (s), 1178 (m), 832 (m), 690 (s) cm^{-1} .

2-Methoxy-3-(3,4,5-trimethoxyphenyl)cyclopropyl(phenyl)methanone (2.77r)



Synthesized according to **GP1** using iodosoarene **2.76b** (0.164 g, 0.70 mmol, 2 equiv), Cu(tfacac)₂ (0.013 g, 0.035 mmol, 0.1 equiv), (Z)-1,2,3-trimethoxy-5-(2-methoxyvinyl)benzene (0.392 g, 1.75 mmol, 5 equiv), CHCl₃ (4.0 mL), and Wittig reagent **2.29e** (0.133 g, 0.35 mmol, 1 equiv). Purification by flash chromatography through a column of silica gel (hexanes:EtOAc 20:1 to 8:1) led to the title compound isolated as a pale yellow oil (0.093 g, 78% yield). R_f = 0.19 (hexanes:EtOAc 3:1).

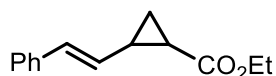
¹H NMR (300 MHz, CDCl₃): δ 8.09 (app d, *J* = 7.3 Hz, 2H), 7.56 (app t, *J* = 7.1 Hz, 1H), 7.48 (app t, *J* = 7.8 Hz, 2H), 6.38 (s, 2H), 3.97 (dd, *J* = 6.4, 4.4 Hz, 1H), 3.83 (s, 6H), 3.80 (s, 3H), 3.42 (dd, *J* = 5.0, 4.2 Hz, 1H), 3.28 (s, 3H), 3.04 (dd, *J* = 6.5, 6.5 Hz, 1H).

¹³C NMR (75 MHz, CDCl₃): δ 195.7, 156.2, 141.1, 139.9, 136.8, 135.8, 131.5, 131.0, 107.0, 72.4, 63.8, 62.0, 59.1, 38.4, 34.2.

HRMS (ESI⁺ [M+H]⁺): calculated for C₂₀H₂₃O₅ 343.1540, found 343.1538.

IR (ATR): 2932 (w), 1669 (m), 1587 (m), 1448(m), 1217 (m), 1124 (s), 1008 (s), 689 (m) cm⁻¹.

(E)-Ethyl 2-styrylcyclopropanecarboxylate (**2.77s**)



Synthesized according to **GP1** using iodosoarene **2.76b** (0.066 g, 0.28 mmol, 2 equiv), Cu(tfacac)₂ (0.005 g, 0.014 mmol, 0.1 equiv), (E)-1-phenyl-1,3-butadiene (0.091 g, 0.70 mmol, 5 equiv), CHCl₃ (3.0 mL), and Wittig reagent **2.29a** (0.050 g, 0.14 mmol, 1 equiv). Purification by flash chromatography through a column of silica gel (hexanes:EtOAc 8:1) led to the title compound isolated as a pale yellow oil (0.018 g, 61% yield) with a 1.6:1 *trans:cis* ratio. R_f = 0.45 (hexanes:EtOAc 3:1). The characterization data matches what has been previously reported in the literature.²⁰⁶

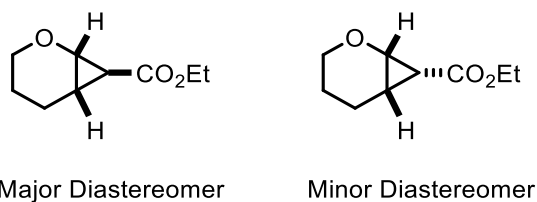
Ethyl 2-benzylcyclopropanecarboxylate (**2.77t**)



Synthesized according to **GP1** using iodosoarene **2.76b** (0.065 g, 0.28 mmol, 2 equiv), Cu(tfacac)₂ (0.005 g, 0.014 mmol, 0.1 equiv), allylbenzene (0.082 g, 0.70 mmol, 5 equiv), CHCl₃

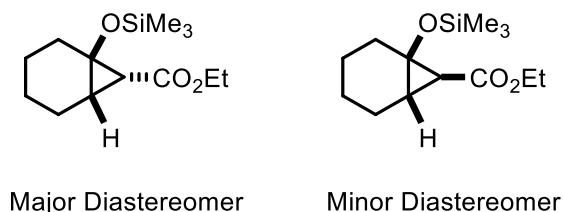
(3.0 mL), and Wittig reagent **2.29a** (0.050 g, 0.14 mmol, 1 equiv). Purification by flash chromatography through a column of silica gel (hexanes:EtOAc 20:1 to 10:1) led to the title compound isolated as a pale yellow oil (0.014 g, 49% yield) with a 1.9:1 *trans:cis* ratio. $R_f = 0.68$ (hexanes:EtOAc 3:1). The characterization data matches what has been previously reported in the literature.²⁰⁷

Ethyl 2-oxabicyclo[4.1.0]heptane-7-carboxylate (**2.77u**)



Synthesized according to **GP1** using iodosoarene **2.76b** (0.066 g, 0.28 mmol, 2 equiv), Cu(tfacac)₂ (0.005 g, 0.014 mmol, 0.1 equiv), dihydropyran (0.064 mL, 0.70 mmol, 5 equiv), CHCl₃ (2.5 mL), and Wittig reagent **2.29a** (0.050 g, 0.14 mmol, 1 equiv). Purification by flash chromatography through a column of silica gel (hexanes:EtOAc 8:1 to 3:1) led to the title compound isolated as a pale yellow oil (0.014 g, 60% yield) with a 3:1 *dr*. $R_f = 0.80$ (EtOAc:petroleum ether 1:4). The characterization data matches what has been previously reported in the literature.²⁰⁸

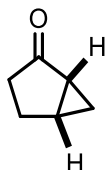
Ethyl 1-((trimethylsilyloxy)bicyclo[4.1.0]heptane-7-carboxylate (**2.77v**)



Synthesized according to **GP1** using iodosoarene **2.76b** (0.135 g, 0.58 mmol, 2 equiv), Cu(tfacac)₂ (0.010 g, 0.029 mmol, 0.1 equiv), 1-(trimethylsilyloxy)cyclohexene (0.286 mL, 1.45 mmol, 5 equiv), CHCl₃ (4.0 mL), and Wittig reagent **2.29a** (0.100 g, 0.29 mmol, 1 equiv). Purification by flash chromatography through a column of silica gel (hexanes:EtOAc 20:1 to 10:1) led to the title compound isolated as a pale yellow oil (0.047 g, 63% yield) with a 1.7:1 *dr*.

$R_f = 0.53$ (hexanes:EtOAc 9:1). The characterization data matches what has been previously reported in the literature.⁷¹

Bicyclo[3.1.0]hexan-2-one (**2.95**)



To a dry 10 mL round bottom flask was added iodosoarene **2.76b** (0.102 g, 0.44 mmol, 2 equiv), $\text{Cu}(\text{tfacac})_2$ (0.008 g, 0.022 mmol, 0.1 equiv), Wittig reagent **2.94** (0.080 g, 0.22 mmol, 1 equiv), then CHCl_3 (4 mL), and the resulting mixture stirred at room temperature for 3.5 hours. The reaction was quenched with 10 % K_2CO_3 (2 mL), transferred to a separatory funnel and extracted using CH_2Cl_2 (3 x 10 mL). The combined organic extracts were washed with brine (2 x 10 mL), dried over MgSO_4 , filtered, and concentrated by rotary evaporation (keeping the bath temperature below 30 °C). The crude reaction mixture was loaded onto a column of silica gel using a minimal amount of CH_2Cl_2 and elution was accomplished using (hexanes:EtOAc 10:1 to 5:1), which gave 0.013 g of **2.95** as a pale yellow oil in 63% yield. The characterization data matches what has been previously reported in the literature.²⁰⁹

2.11 NMR Spectra for Chapter 2

Figure 2.12 ^1H NMR (300 MHz, CDCl_3) spectrum of ethyl 2-methoxy-3-(4-methoxyphenyl)cyclopropanecarboxylate

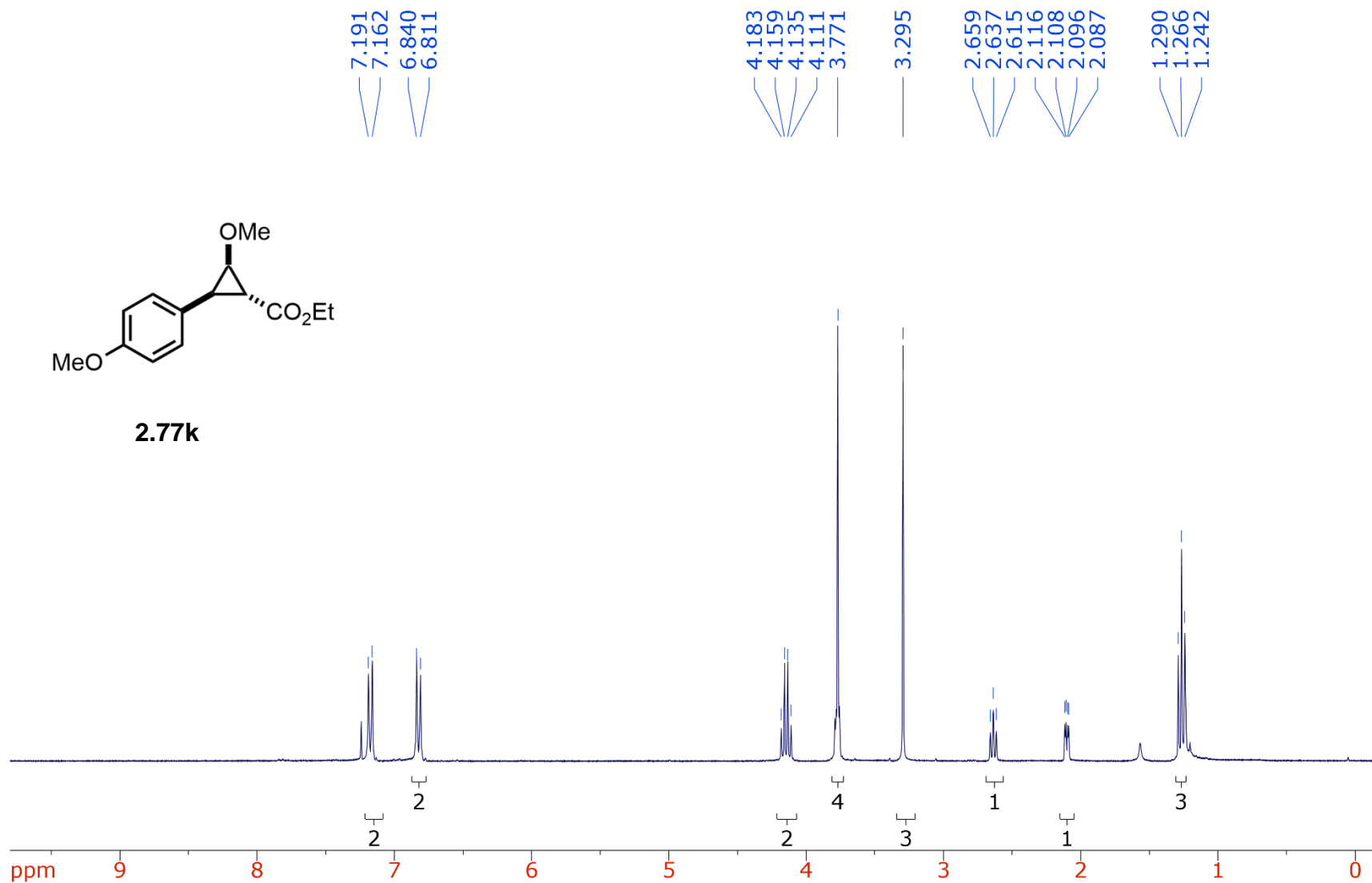


Figure 2.13 ^{13}C NMR (75 MHz, CDCl_3) spectrum of ethyl 2-methoxy-3-(4-methoxyphenyl)cyclopropanecarboxylate

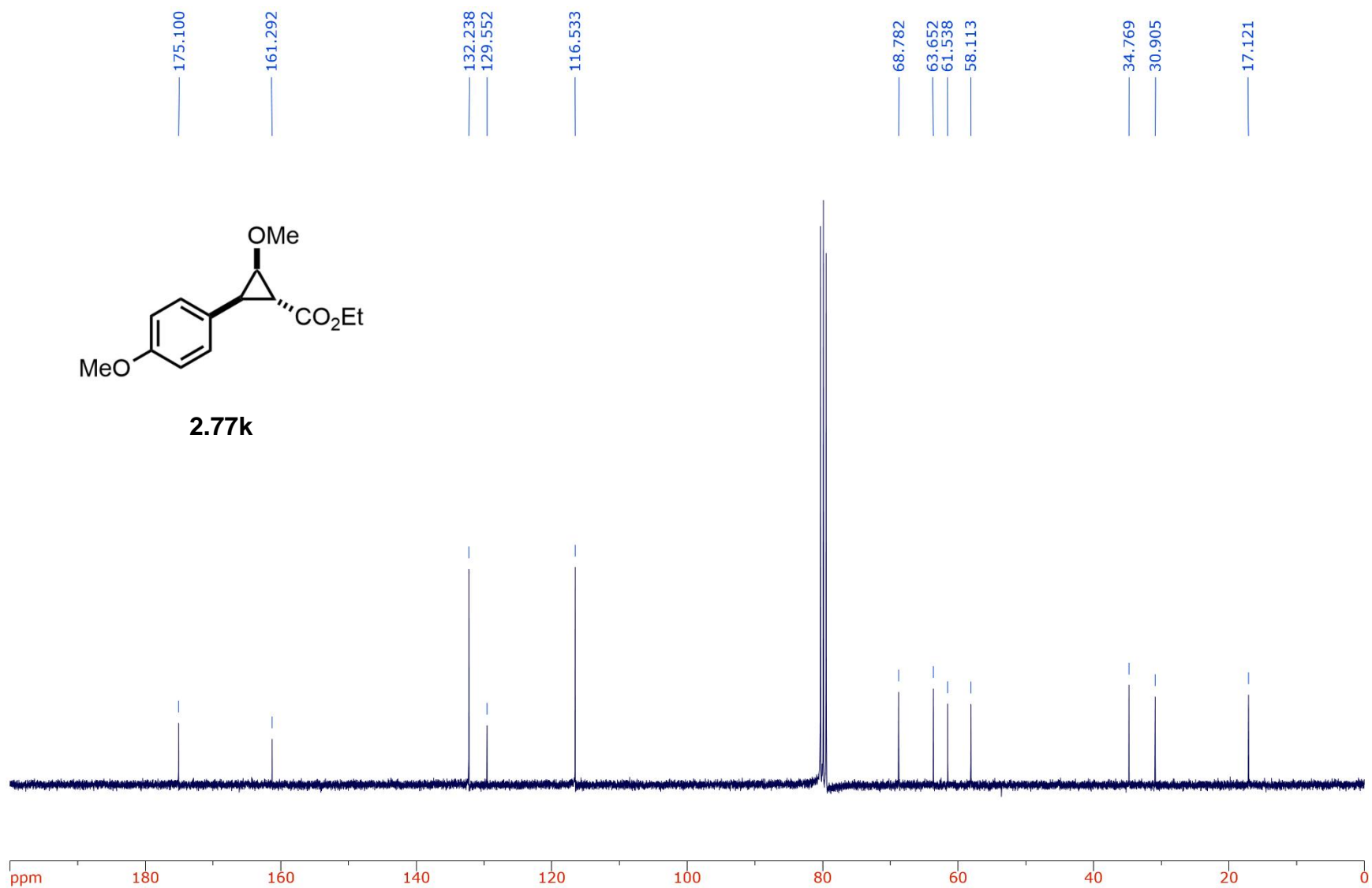


Figure 2.14 ^1H NMR (300 MHz, CDCl_3) spectrum of ethyl 2-methoxy-3-(4-methoxyphenyl)cyclopropanecarboxylate

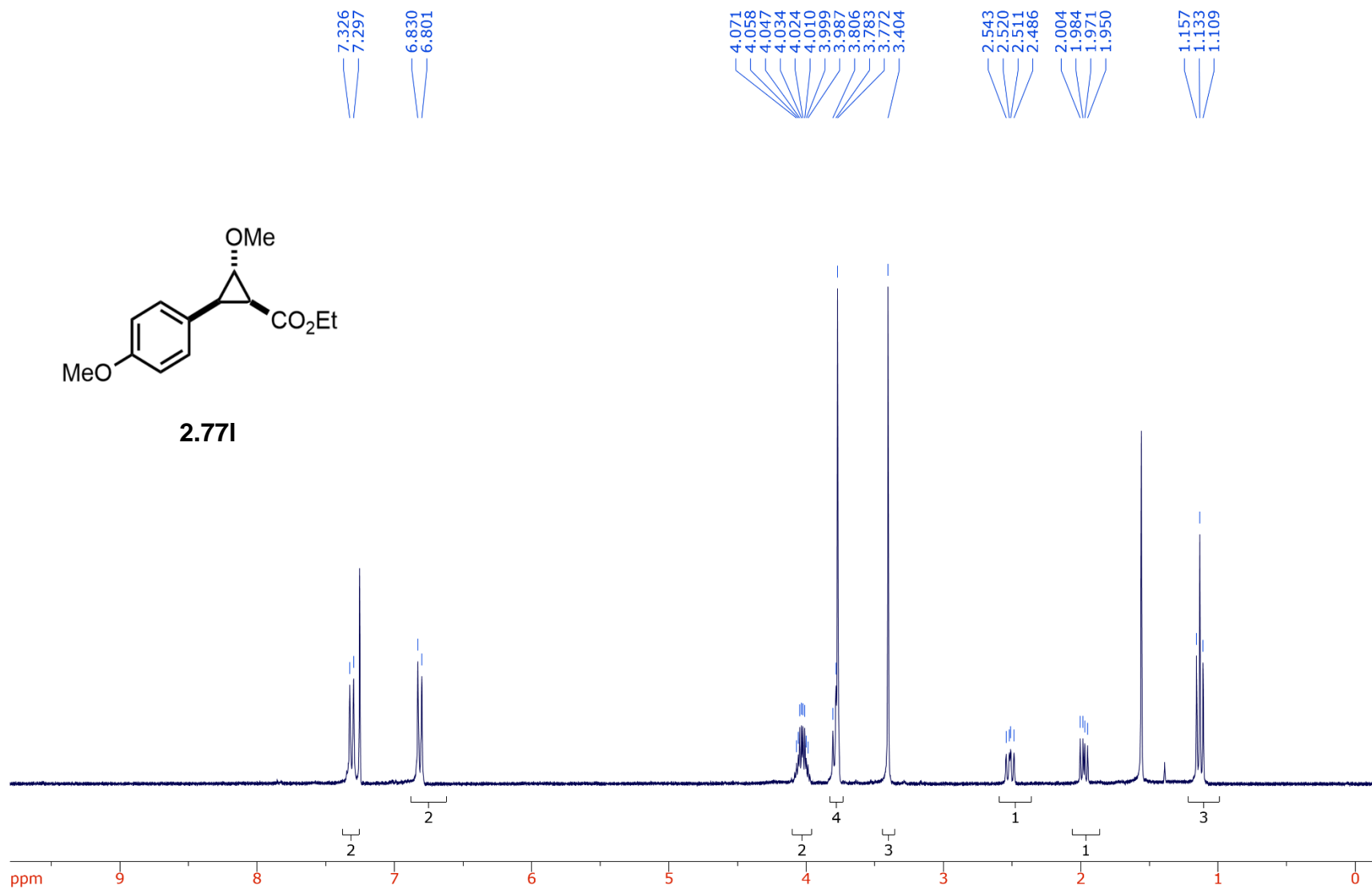


Figure 2.15 ^{13}C NMR (75 MHz, CDCl_3) spectrum of ethyl 2-methoxy-3-(4-methoxyphenyl)cyclopropanecarboxylate

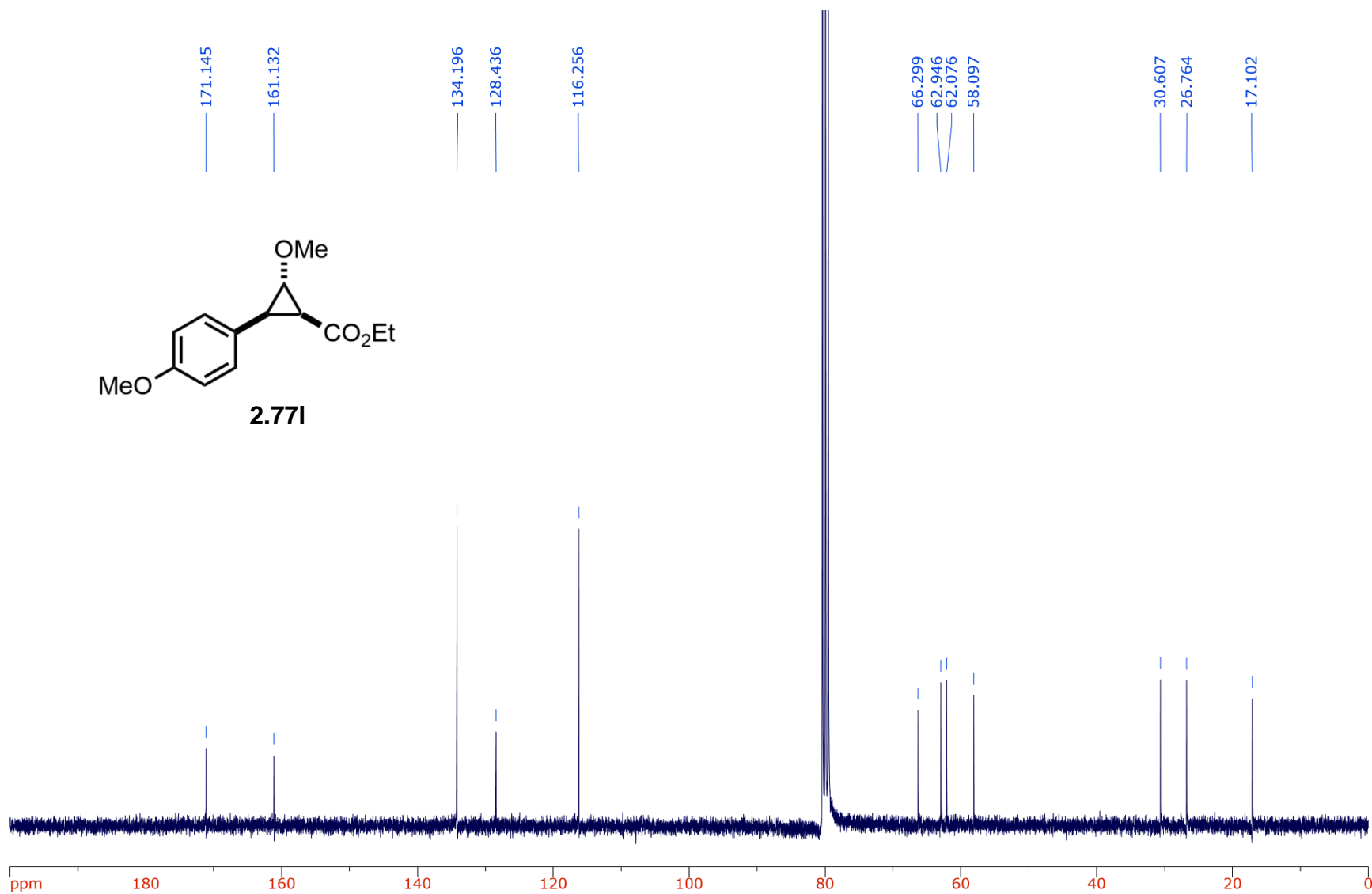


Figure 2.16 ^1H NMR (300 MHz, CDCl_3) spectrum of ethyl 2-methoxy-3-(3,4,5-trimethoxyphenyl)cyclopropanecarboxylate

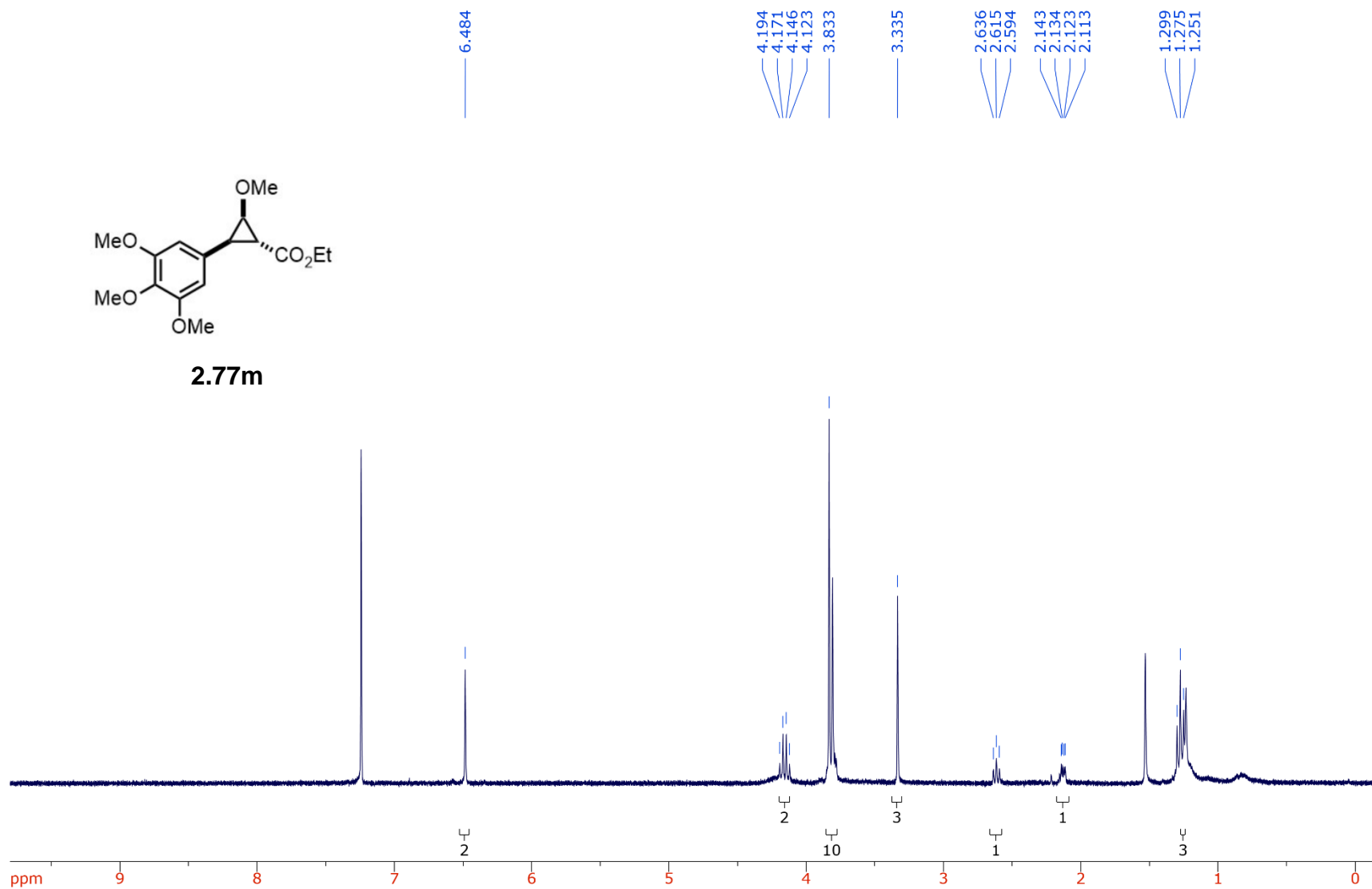


Figure 2.17 ^{13}C NMR (75 MHz, CDCl_3) spectrum of ethyl 2-methoxy-3-(3,4,5-trimethoxyphenyl)cyclopropanecarboxylate

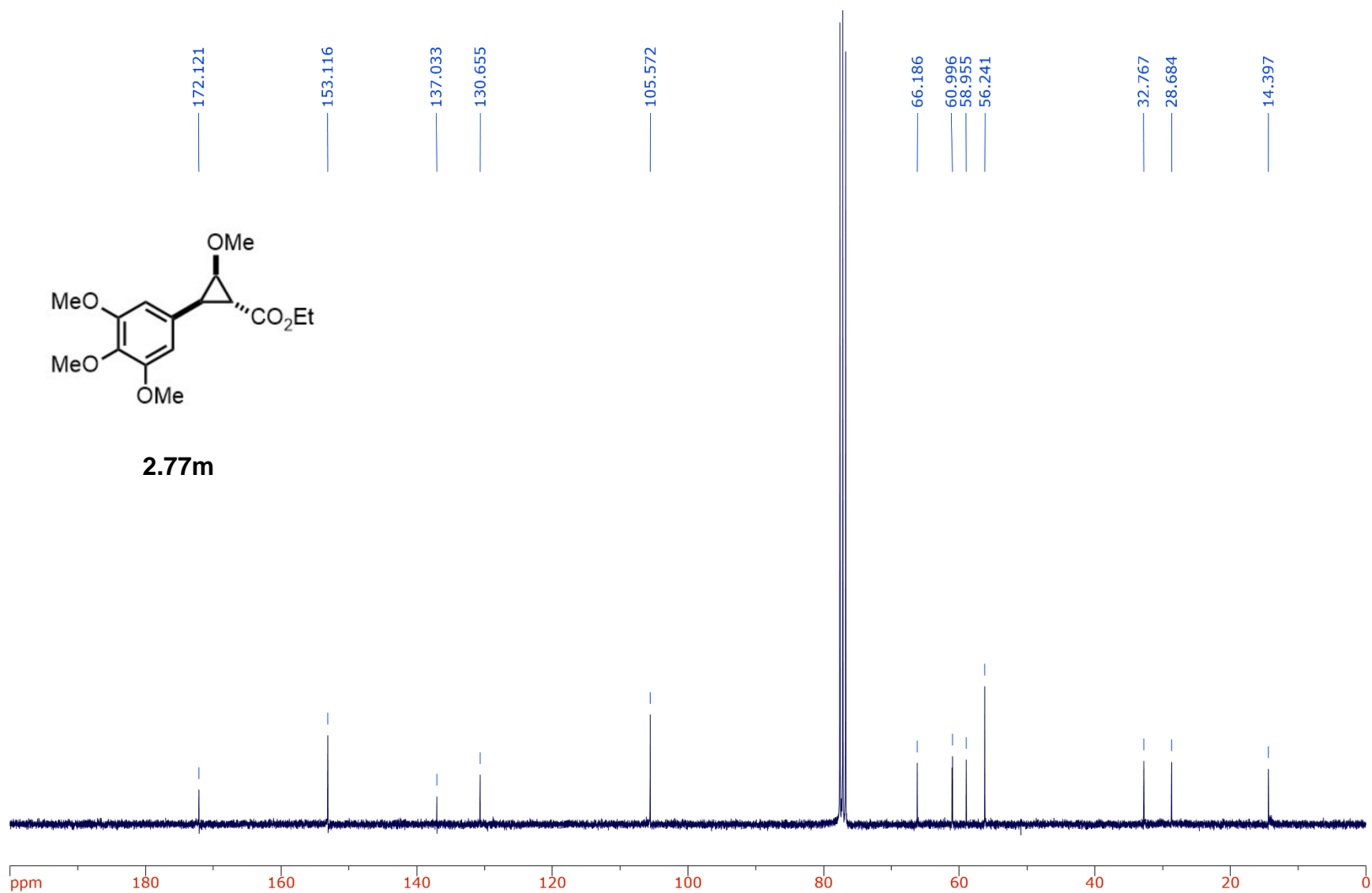


Figure 2.18 ^1H NMR (300 MHz, CDCl_3) spectrum of 2-methoxy-3-(4-methoxyphenyl)cyclopropyl(phenyl)methanone

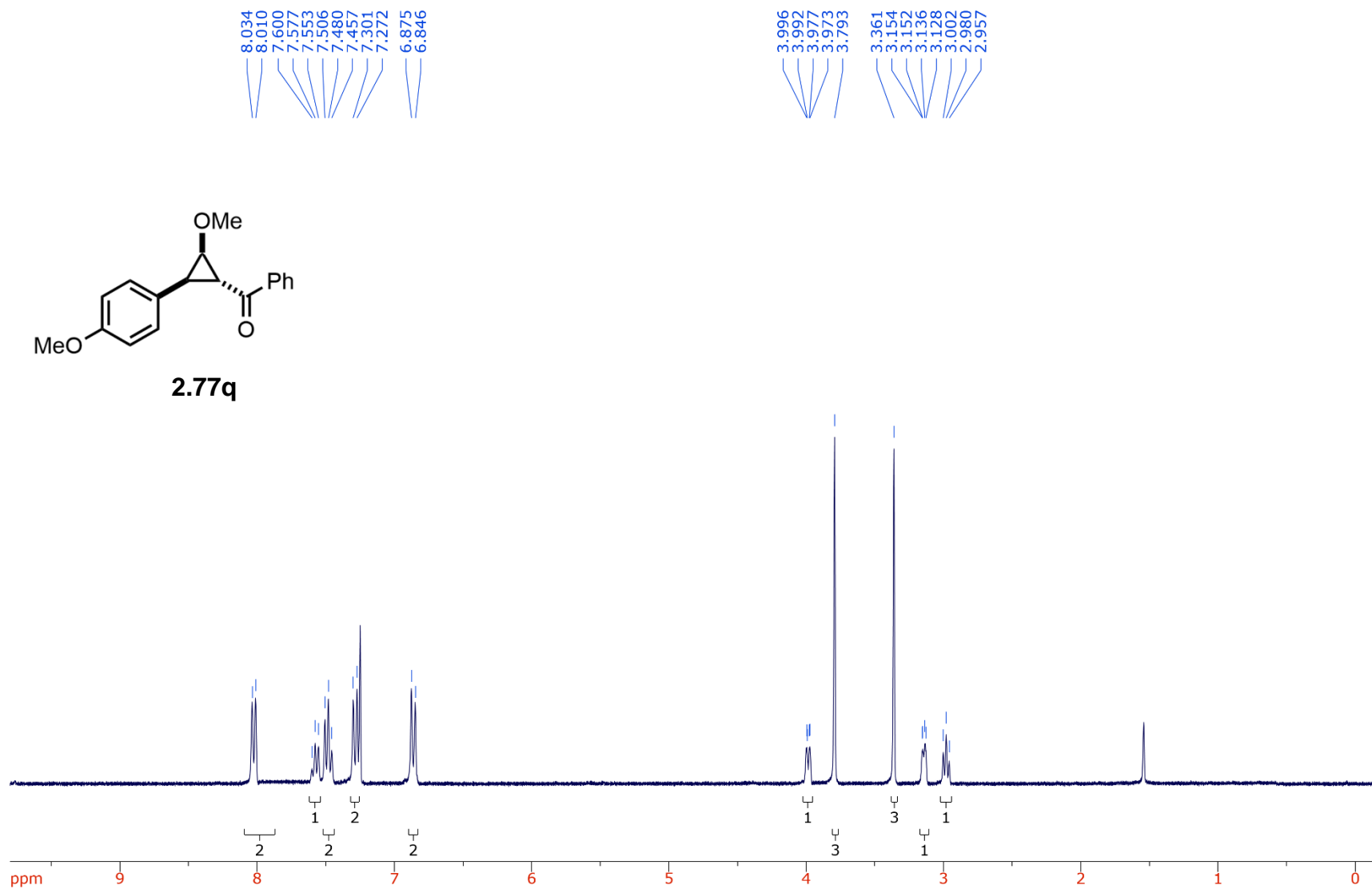


Figure 2.19 ^{13}C NMR (75 MHz, CDCl_3) spectrum of 2-methoxy-3-(4-methoxyphenyl)cyclopropyl)(phenyl)methanone

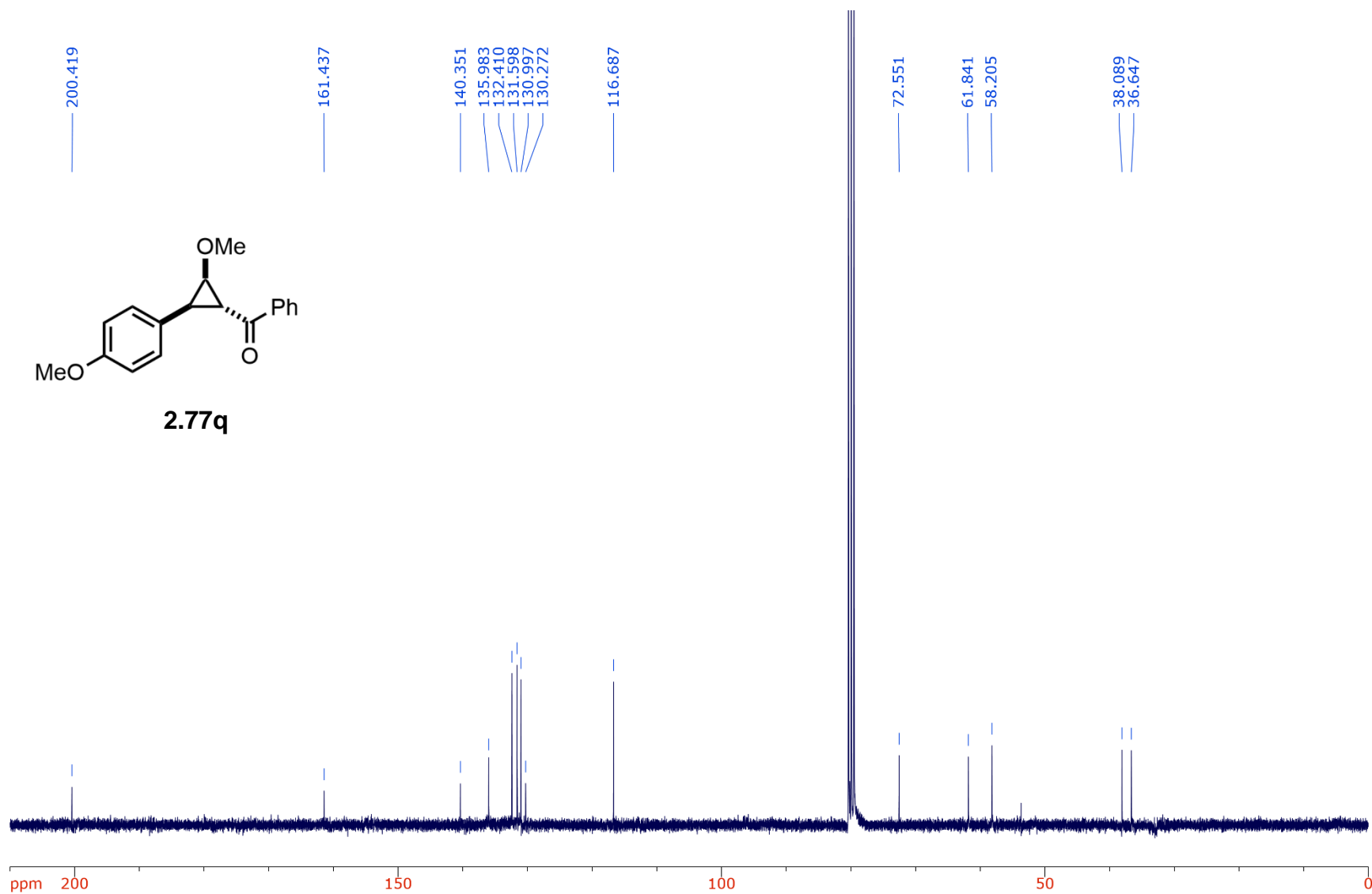


Figure 2.20 ^1H NMR (300 MHz, CDCl_3) spectrum of 2-methoxy-3-(3,4,5-trimethoxyphenyl)cyclopropyl(phenyl)methanone

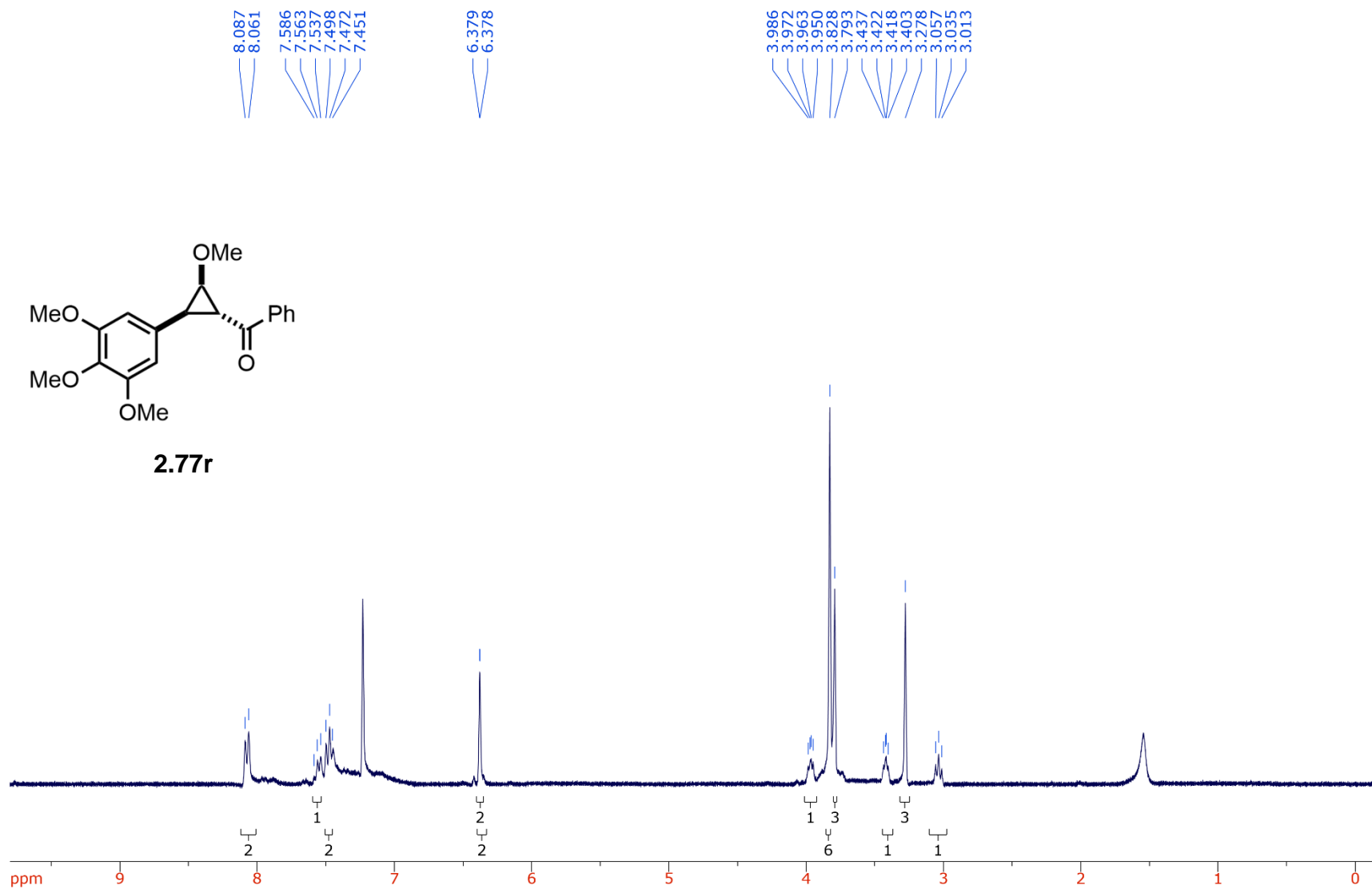
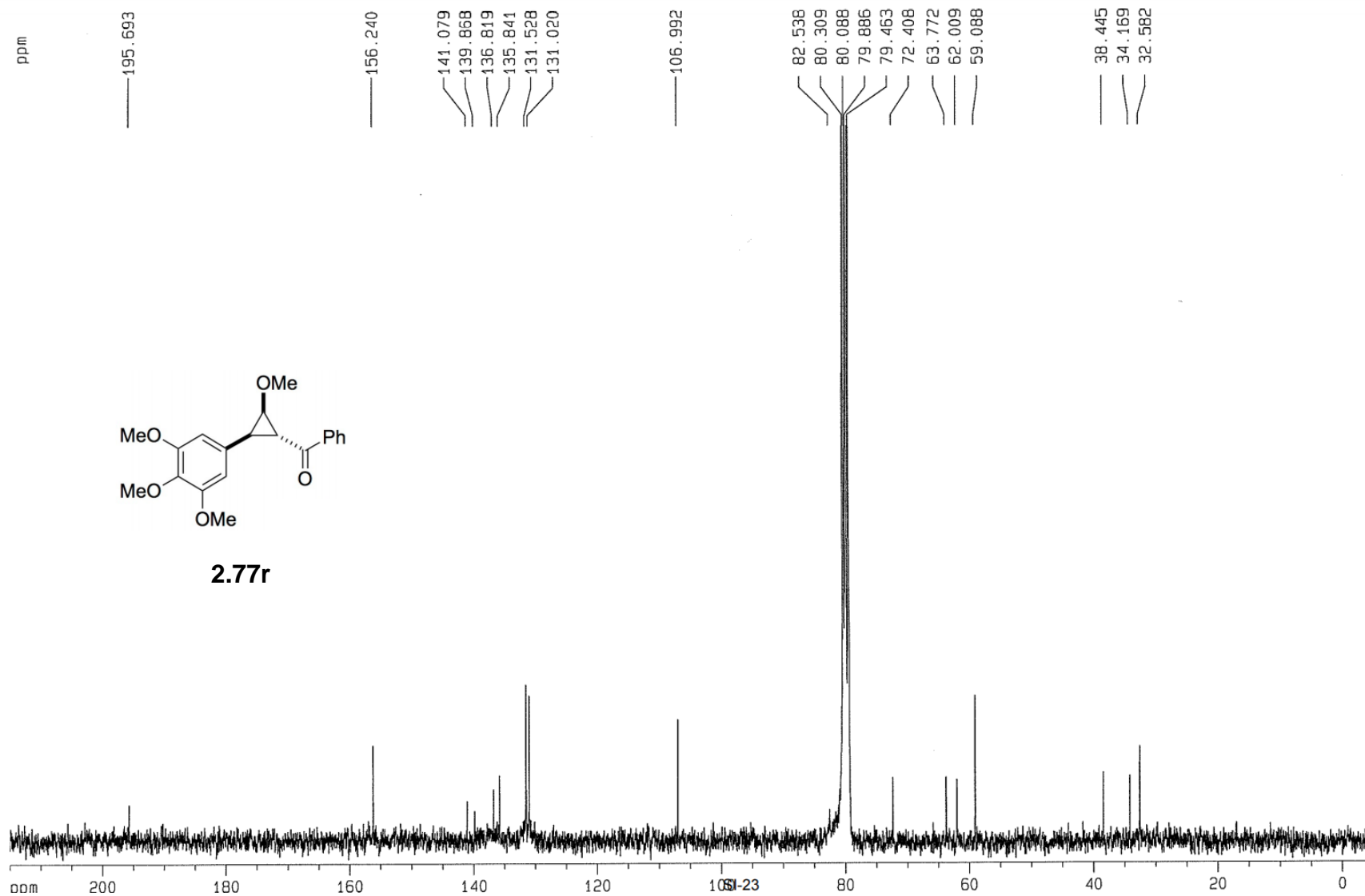


Figure 2.21 ^{13}C NMR (75 MHz, CDCl_3) spectrum of 2-methoxy-3-(3,4,5-trimethoxyphenyl)cyclopropyl(phenyl)methanone

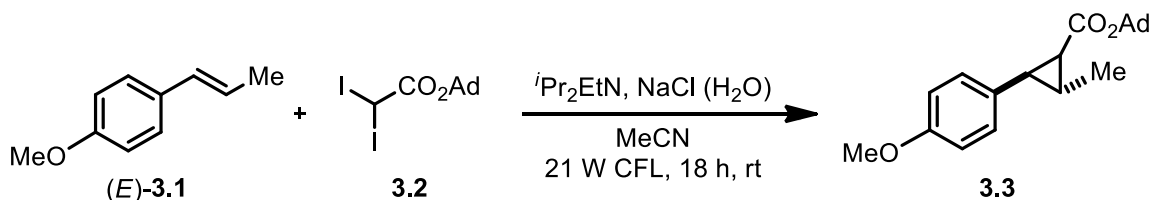


Chapter 3: Cyclopropanation of Iodonium Ylides & Alkenes Using Blue Light

3.1 Introduction

The use of light in organic chemistry can be considered a green and renewable method, which has encouraged its utilization as an attractive alternative to the sometimes more expensive reagents needed to perform the equivalent reactions.²¹⁰ A transition metal-free & diazo-free cyclopropanation between alkenes (**3.1**) and *gem*-diiodomethyl carbonyl reagents (**3.2**) was developed based on the concept of using visible light generated from cheap and simple compact fluorescence lamps (CFL).²¹¹ The visible light-induced generation of iodonium carbonyl radicals from **3.2** were shown to generate cyclopropanes effectively with a variety of diversely-substituted styrenes, demonstrating excellent chemoselectivity with just a simple CFL bulb as the visible light source.²¹¹ The optimization studies are shown in **Table 3.1**, which display a large difference in cyclopropane **3.3** yields when using light from a CFL bulb (entry 1, 91%) vs running the same reaction in the dark (entry 6, 0%), all without the use of transition-metals.

Table 3.1 Optimization studies of metal-free photocyclopropanation reaction



Entry	Deviation from the reaction conditions ^[a]	Yield (%) ^[b]
1	None	91 ^[c] 75 ^[d]
2	Without NaCl (H ₂ O)	17
3	Without NaCl	48
4	Under air	10
5	Without <i>i</i> Pr ₂ EtN	0
6	In the dark	0

^[a] Reaction conditions: (*E*)-**3.1** (0.10 mmol), **3.2** (0.10 mmol), *i*Pr₂EtN (0.20 mmol), MeCN (1 mL), NaCl (1.25 M in H₂O, 0.5 mL). Reactions were degassed prior to irradiation. ^[b] ¹H NMR yields calculated using 1,2-dimethoxyethane as the internal standard. ^[c] Yield of the isolated product adding additional **3.2** (0.10 mmol, 1 equiv) and *i*Pr₂EtN (0.20 mmol, 2 equiv) after 4 hours. ^[d] Yield of the isolated product using 1 gram of (*E*)-**3.1** and 1 equiv of **3.2**.

A distinctive feature of photochemical reactions is the ability of an organic molecule to absorb photons of light, which induce a change in the energy state of electrons contained within the molecule. An organic molecule, originally in the ground state, can be converted to an excited state upon absorption of a photon ($h\nu$) which promotes an electron from the highest occupied molecular orbital (HOMO) state to the lowest unoccupied molecular orbital (LUMO). This type of process can occur in molecules such as alkenes if photons are introduced to the system and contain a specific amount of energy which allows for the promotion of an electron to an excited state.²¹² When the newly promoted electron enters a higher energy excited state it results in two new singly-occupied molecular orbitals (SOMOs) with an overall energy that is higher than that the ground state molecule (**Figure 3.1**). The photo-excited state has a finite lifetime with physical and chemical properties that are different from the ground state and is the starting point for subsequent steps in most photochemical reactions.²¹²

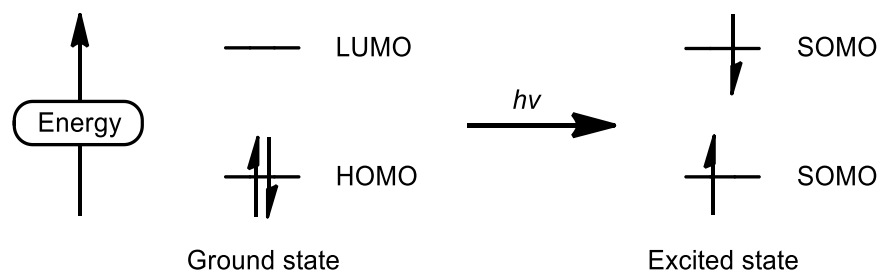


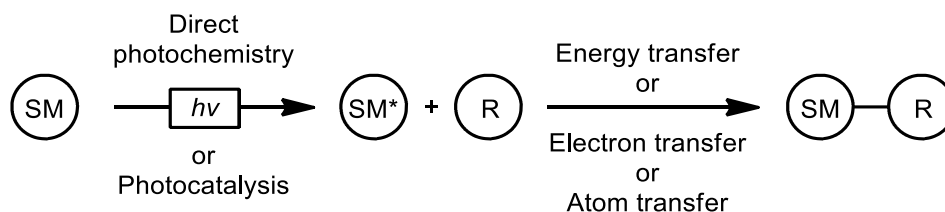
Figure 3.1 Electron energy levels in a molecule undergoing photochemical excitation

The properties of light can be analyzed using units such as hertz (Hz) for frequency of the photon, wavelength (nm), or energy (J). The frequencies, wavelengths, and energies of some commonly used light sources in organic chemistry are shown in **Table 3.2**.²¹²

Table 3.2 Frequency, wavelength, and energy units of common light sources

Light Source	Frequency (s^{-1})	Wavelength (nm)	Energy (kJ/mol)
Far Ultraviolet	3.00×10^{15}	100	1200
Ultraviolet	1.20×10^{15}	250	480
Ultraviolet	0.68×10^{15}	350	343
Blue-Green	0.60×10^{15}	500	240
Red	0.43×10^{15}	700	171
Near Infrared	0.30×10^{15}	1000	120

To effectively use light in a chemical reaction, it is important to know the wavelength of light used and the absorption properties of the reactants and products to understand if the chemical reaction in question will obey the Grotthuss-Draper law. This law states that “light must be absorbed by a chemical substance in order for a chemical reaction to take place.” Once the reaction is complete, the reaction product must not absorb the light used in the reaction to prevent side product formation, or the decomposition of the desired product.²¹³ The ability of a molecule in an electronically-excited state to trigger a chemical process can occur either by direct excitation of the starting material (direct photochemistry) or by the action of a catalyst capable of absorbing light (photocatalysis) which then activates the starting material.²¹⁴ Once the starting material (SM) has become photoexcited (SM*), it can then interact with other reactants (R) by either energy transfer, electron transfer, or atom transfer mechanisms, described in **Figure 3.2**.



Energy transfer	Electron transfer	Atom transfer
<ul style="list-style-type: none"> • Photosensitization (PS) • The photoexcited species transfers energy directly to an accepting reaction component 	<ul style="list-style-type: none"> • Photo-induced electron transfer (PET) • The photoexcited species transfers a single electron (oxidation) or accepts a single electron (reduction) 	<ul style="list-style-type: none"> • Hydrogen atom transfer (HAT) • The photoexcited species abstracts an atom from a reaction component

Figure 3.2 Interaction modes of photoexcited species

Since most small organic molecules that contain chromophore-based functional groups absorb ultraviolet (UV) light, the direct photoexcitation with UV light has been widely used.²¹⁵ Before the discovery of light-emitting diode (LED) technology, UV was the primary light source that was available and was often generated from mercury lamps. These systems produce high energy photons, but typically these light sources will also generate background heat which is

often undesired due to the detrimental effects caused by excess heat being present. Excess heat will sometimes cause molecular rearrangements to occur leading to product decomposition or the formation of side-products. As a consequence, UV-photoreactors have often been developed to contain fans as a cooling source.

As stated in **Table 3.2** the wavelength range of UV light spans from 100-350 nm which limits the versatility of the molecular design since many functional groups may react under such conditions.²¹⁶ Because of the negative attributes of using UV as the light source in photochemical reactions, the integration of shorter-range wavelength light sources such as LED and compact fluorescence lamps (CFL) have become the preferred choice for applications in organic synthesis. Organic chemistry has therefore seen the use of CFLs and LEDs become increasingly popular in synthesis to induce reactions by indirect photosensitization/photoredox catalysis.²¹⁷ Not only do LEDs and CFLs emit lower energy light in the visible region, they are also more efficient and last longer than traditional light sources. A comparison of energy efficiencies and lifetimes of standard light bulbs used in common households (incandescent) with light sources such as CFL and LED used in organic synthesis can be found in **Figure 3.3**.




		
<p><u>Incandescent</u></p> <ul style="list-style-type: none">• 90% of total energy wasted as heat• 1,000 h lifetime	<p><u>CFL</u></p> <ul style="list-style-type: none">• 75% more energy efficient than incandescent• 10,000 h lifetime	<p><u>LED</u></p> <ul style="list-style-type: none">• 80% more energy efficient than incandescent• 50,000 h lifetime

Figure 3.3 Comparison of incandescent, CFL, and LED light bulbs

LEDs have revolutionized the lighting industry, as they are much more efficient in terms of the luminous efficacy and lifetime of usage. Typical consumer LED light bulbs operate at 10-20% of the power needed to run an incandescent bulb of comparable brightness, and they also have a lifetime of over 25,000 hours, compared to only 1000 hours for incandescent bulbs.

Red, green, and yellow LEDs were developed in the 1950s and 1960s, but their full potential was not realized until much later. In the 1990s the invention of the blue LEDs enabled the creation of white light, by combining red, green, and blue light. Isamu Akasaki, Hiroshi Amano, and Shuji Nakamura are credited with the invention of blue LED technology, and for this, they were awarded the Nobel prize in physics in 2014.²¹⁸

Quickly after the discovery of LED technology, the chemical community adapted LEDs as an energy source into chemical reactions and a recent boom in the field of photochemistry has ignited. There has been an incredible amount of research being actively investigated into photochemistry based on LEDs. LEDs are a preferable light source for synthetic photochemistry due to the narrow emission band (± 20 nm) they provide which is optimal for achieving selective irradiation of a chromophore system.²¹⁹ This narrow band of emission wavelengths implies a specific amount of energy is being applied which is an important factor to control, as excess energy may cause unwanted side reactions to occur. LEDs are generally cheap and sold in a broad selection of wavelengths (250-800 nm) making their use as a light source ideal for reaction development.

The energy of light used in a chemical reaction can be calculated using Planck's equation $E = hv$ (**Equation 3.1**). As stated in the calculation, a single photon of blue light with a wavelength of 465 nm has an energy of 4.27×10^{-19} J. Using Avogadro's number (6.02×10^{23} mol⁻¹) and converting to kJ, gives an energy of 256 kJ/mol for blue light photons.

$$E = hv = h \frac{c}{\lambda} = (6.626 \times 10^{-34} \text{ J} \cdot \text{s}) \left[\frac{2.998 \times 10^8 \text{ m/s}}{465 \times 10^{-9} \text{ m}} \right] = 4.27 \times 10^{-19} \text{ J} = 256 \text{ kJ/mol} \quad (3.1)$$

This energy value can be compared to the properties of photons as stated in J. D. Coyle's chart of values (**Table 3.2**) to determine if the energy of bonds within a molecule may break or remain intact in the presence of the radiation applied. The energy of the different colours in the red-green-blue (RGB) LED light strips used in visible light-activated chemistry was calculated (**Table 3.3**). Photoreactors can be designed to contain either RGB LED light strips, or just a single colour, based on what specific type of reaction is to be targeted, or what research-related purpose the photoreactor is to be used for.

Table 3.3 Wavelengths and calculated energies of colours used in a RGB LED strip

LED Colour	Wavelength of λ_{max} (nm)	Energy (kJ/mol)
Red	630	190
Green	510	235
Blue	465	256

The beneficial features of LEDs have enabled their integration into a branch of photochemistry known as photoredox catalysis, which has undergone tremendous growth over the last few years. Standard photoredox systems are composed of a light source, such as blue light from an LED, a photoredox catalyst, and an oxidant. The photoredox catalyst, which is active only when exposed to light, is made of an organic framework with a transition-metal housed in the centre, such as iridium or ruthenium. An example of the components of a typical photoredox system are shown in **Figure 3.4**.

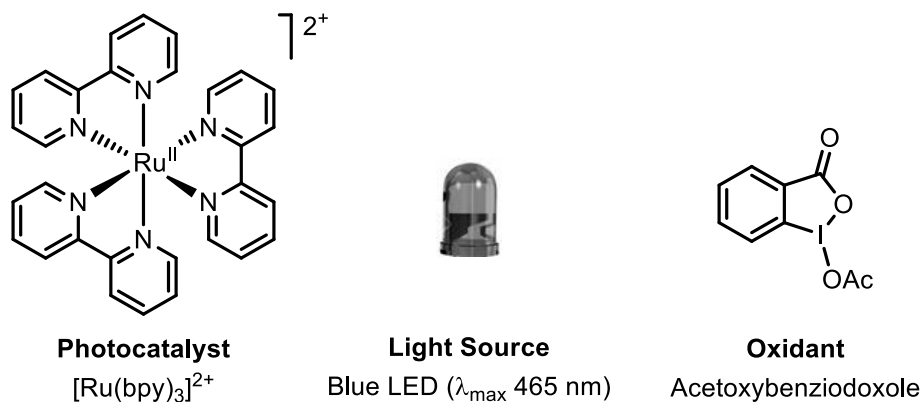


Figure 3.4 Examples of components of a photoredox system

This field of photoredox catalysis uses transition-metals, such as iridium or ruthenium in the catalyst, and therefore improvements may still be possible to eliminate the use of metals but retain the overall reactivity. Photo-sensitizers, possibly derived from HVI reagents, which are not metal-based, could be considered as a “greener” approach to photo-redox catalysis if the overall desired reactivity is still maintained. This idea of incorporating HVI reagents into photochemistry for new applications that enable a “greener” approach is a theme of this chapter.

3.2 Photochemical Activation of Ylides

The use of light to activate different types of ylides is a well-studied and documented area of organic chemistry. There are numerous examples in the literature of ylides such as diazonium, iodonium, phosphonium, and sulfonium ylides have shown the ability to be photochemically activated, which can then react with different reaction partners and form new products. Traditionally this branch of photochemistry relied on using UV light as the source of photons, and it has only been the last couple of decades where the light source has started shifting towards using LEDs. Therefore, there are many more examples in the literature showing photochemical applications of ylides with the use of UV light, but many of the more recent publications in photochemistry have shown how the beneficial properties of LEDs can be used for new reaction discovery. Because blue LEDs have only existed since the 1990's and there are fewer examples in the chemical literature, in this chapter, more attention was given to examples of photochemical activation of ylides using visible light, specifically from blue LEDs.

3.2.1 Activation of Diazonium Ylides with Light

The photochemical activation of diazonium ylides was initially investigated several decades ago and would have relied on older forms of technology being used as the light source, such as UV light.²²⁰ With the invention of LED-based technology, newer applications have emerged, which are the visible light-mediated reactions of diazo compounds. This area has recently become popular with many new reactions being actively reported. This new style of chemistry in which diazonium ylides are photochemically activated by visible light was introduced in 2018 independently by researchers such as Davies and Suero.²²¹

The reaction of acyclic aryl ester diazos with alkanes, alkenes, amines, arenes, and carboxylic acids in the presence of visible light (blue LED) was reported by Davies in 2018.²²² In this report the UV-Vis absorbance properties of two aryldiazoacetates **3.1a** and **3.1b**, ethyl 2-diazoacetate **3.2a**, and dimethyl 2-diazomalonate **3.2b** were tested to see if there was any excitation in the visible light region. The four diazonium ylides are shown in **Figure 3.5**.

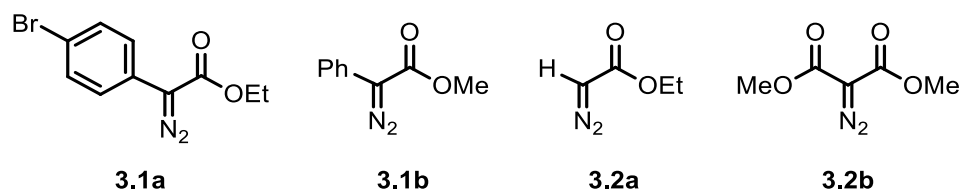


Figure 3.5 Diazo compounds tested for visible light activation

The donor/acceptor diazo compounds **3.1a** and **3.1b** show a very similar absorbance spectra with larger absorbance peaks in the 400-500 nm (violet/blue) region (

Figure 3.6). This absorbance is presumably attributed to a $n \rightarrow \pi^*$ transition of the diazo group.²²³ In contrast to this, the acceptor-only diazo compounds **3.2a** and **3.2b** do not show peaks in the visible light region and therefore do not undergo direct activation by visible light.

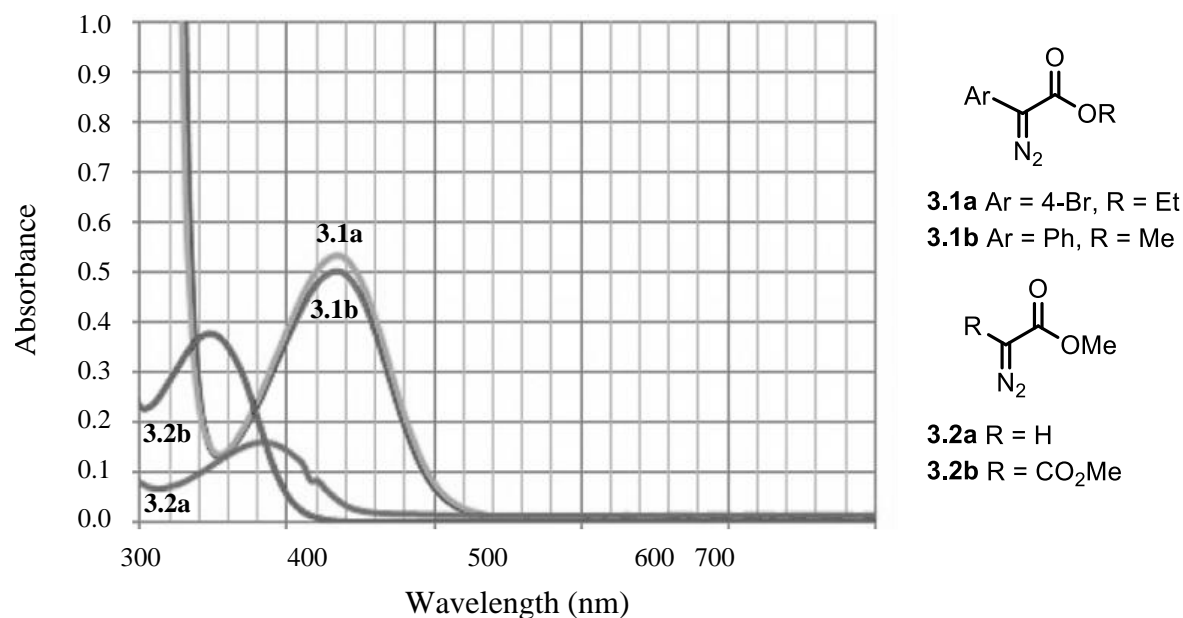
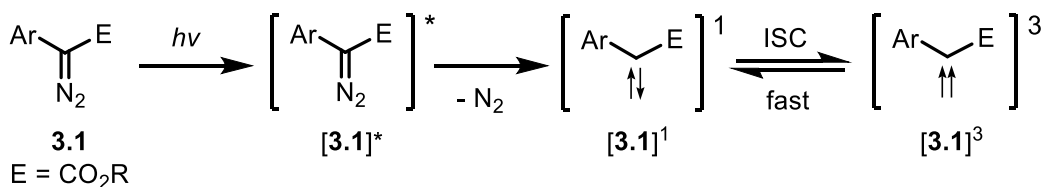


Figure 3.6 UV-Vis absorbances of diazos **3.1a**, **3.1b**, **3.2a**, **3.2b** (0.05 mM in CH₂Cl₂)

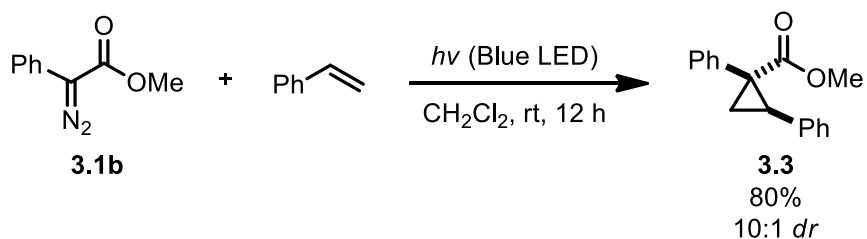
The photochemical reactivity observed is likely to involve the generation of carbenes (**Scheme 3.1**). Aryldiazoacetate **3.1** can undergo photoexcitation using blue LEDs to generate excited state [**3.1**]* followed by the extrusion of N₂ to give singlet carbene [**3.1**]¹. The singlet carbene or the excited state of the diazo can potentially both be trapped by a reacting partner to form a new product. Another possibility is inter-system crossing (ISC) which converts singlet

carbene $[3.1]^1$ to triplet carbene $[3.1]^3$ which is proposed to be a fast process and is backed by experimental evidence that suggests this to be a reversible event.²²⁴



Scheme 3.1 Photochemical activation of diazos with LED

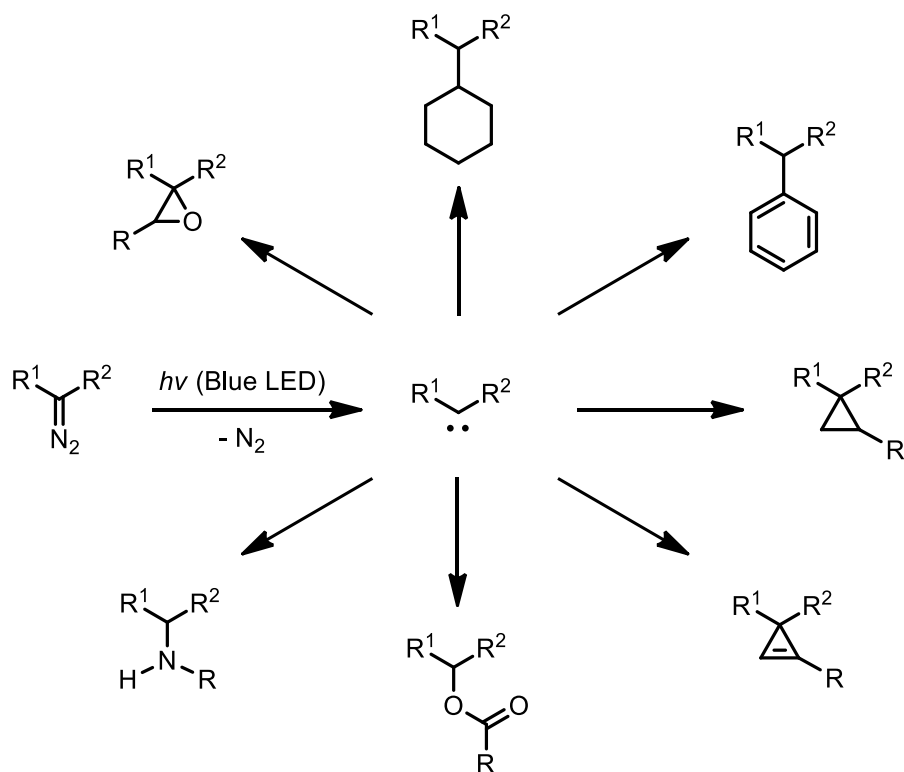
Trapping singlet carbenes, generated by the visible light activation of diazo compounds with styrenes, was explored by Davies in 2018. For example, in the presence of blue LED diazo **3.1b** can form a carbene which is trapped by styrene giving cyclopropane **3.3** (**Scheme 3.2**). This chemistry was limited to aryldiazoacetates and was only performed with styrene as the alkene but was able to successfully generate cyclopropanes in yields ranging from 37-94% and diastereoselectivities varying from 10:1 to >20:1.



Scheme 3.2 Photochemical cyclopropanation of aryldiazoacetate with styrene

A report by Koenigs in 2019 on the blue-light-induced carbene-transfer reactions of diazoalkanes showed alkynes are also able to intercept the singlet carbene and form cyclopropenes.²²⁵ The triplet carbene is not believed to react with alkenes or alkynes under these conditions, and a study by Platz also reinforces this theory.²²⁶

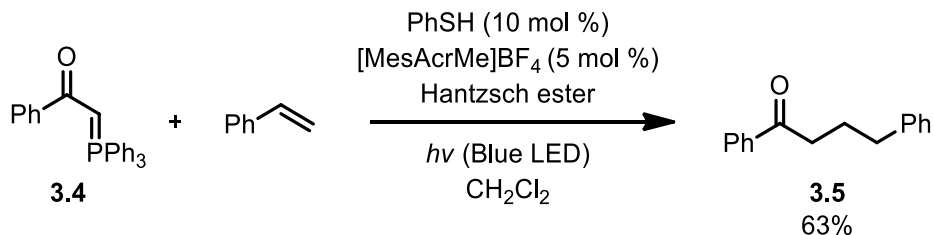
In addition to Davie's research on the blue light-promoted photolysis of aryldiazoacetates, many other applications of using LEDs to activate diazonium ylides have been reported, represented below in the multiple reactions shown in **Scheme 3.3**.



Scheme 3.3 Photochemically-induced reactions of diazos using LED

3.2.2 Activation of Phosphonium Ylides with Light

The first application of photoredox chemistry used on phosphonium ylides, also referred to as Wittig reagents, was reported by Xiao and co-workers in 2016 for a cyclization reaction forming 3-acyloxindoles.²²⁷ Several more reactions were developed including a novel light-induced umpolung reactivity of phosphonium ylides by Liu in 2019²²⁸ as well as a metal-free photoredox reaction of phosphonium ylides with alkenes, which was carried out by Liu in 2019.²²⁹ The metal-free photoredox methodology uses visible light to enable the generation of synthetic equivalents to carbynes using mono-stabilized phosphonium ylides. Phosphonium ylide **3.4** was coupled with alkenes to form carbon-carbon bonds in a highly regioselective hydrocarbonation reaction forming product **3.5** when using styrene (**Scheme 3.4**).



Scheme 3.4 Visible light photoredox reaction of phosphonium ylides with alkenes

This photoredox reaction uses blue light from LEDs which was proposed by the authors to activate the phosphonium ylide causing a photo-excited C-H activation event, forming an ylide radical intermediate. The ylide radical can then serve as a synthetic equivalent to a carbyne motif. The catalytic cycle completes itself with a final reduction to make the product using 1.2 equivalents of Hantzsch ester. This metal-free transformation was made possible by using the organophotocatalyst 9-mesityl-10-methylacridinium tetrafluoroborate $[\text{MesAcrMe}]\text{BF}_4$ which functions as a photosensitizer in this experiment (**Figure 3.7**).

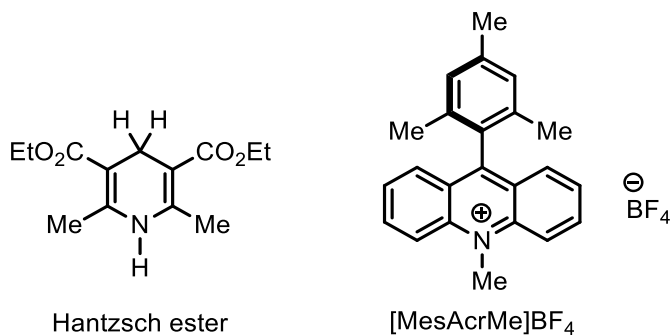
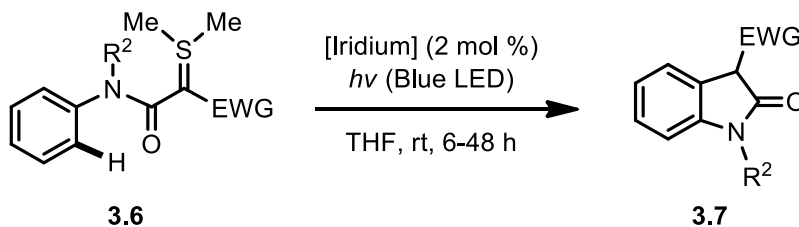


Figure 3.7 Structures of Hantzsch ester and $[\text{MesAcrMe}]\text{BF}_4$ organophotocatalyst

3.2.3 Activation of Sulfonium Ylides with Light

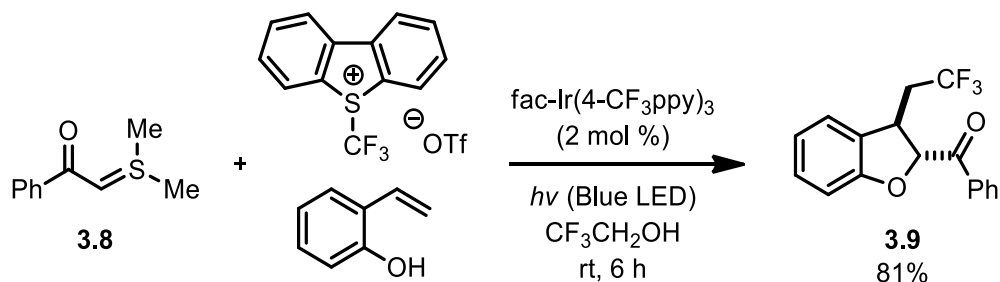
With the advancement of LED technology, in conjunction with visible light-driven photoredox catalysis reactions, new ways of activating sulfonium ylides have showed up in literature. The use of photocatalysis for the activation of sulfonium ylides is very rare, but there is an example by Xiao in 2016 who discovered the photocatalytic insertion of sulfonium ylides into C-H bonds for oxindole synthesis.²³⁰ It was discovered that activating iridium complexes with blue light from LEDs allows the excited state iridium complex to enter in a catalytic cycle

which can strip an electron away from a sulfonium ylide to generate a highly reactive radical cation. The radical cation can then induce a series of reactions leading to ring closure and formation of oxindole systems through a formal C-H insertion reaction (**Scheme 3.5**).



Scheme 3.5 Photocatalytic insertion of sulfonium ylides into C-H bonds

A visible light photoredox-catalyzed reaction of sulfonium ylides with 2-vinyl phenol and Umemoto's reagent for 2,3-dihydrobenzofuran synthesis was reported by Chen and Xiao in 2019.²³¹ This multicomponent cyclization reaction of 2-vinyl phenols, Umemoto's reagent, and sulfur ylides, providing access to trifluoromethylated 2,3-dihydrobenzofurans through the *in situ* formation of *ortho*-quinone methides. Blue light from LEDs are used to photochemically-activate the iridium-based photocatalyst, which can then in turn activate Umemoto's reagent and allow the production of CF_3 radicals. These radicals can engage with the alkene in 2-vinyl phenol, and after a SET event, the *ortho*-quinone methide can form which sets up a final [4+1] annulation reaction with the sulfur ylide to deliver the final product. The following **Scheme 3.6** shows the overall multicomponent cyclization reaction.



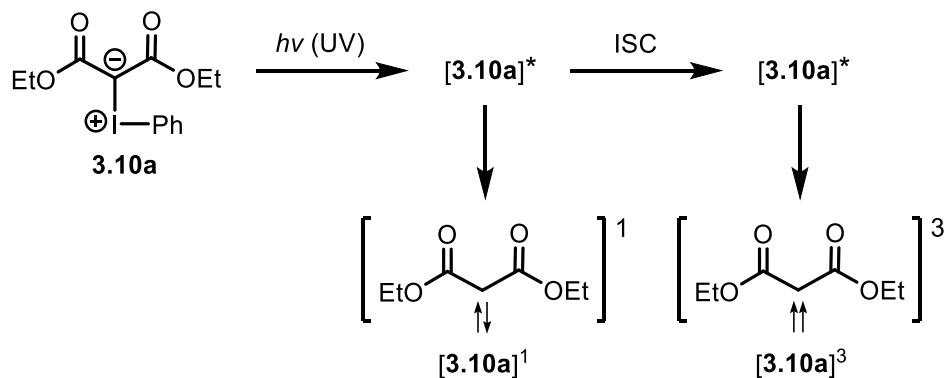
Scheme 3.6 Photoredox multicomponent cyclization reaction of sulfonium ylides

3.2.4 Activation of Iodonium Ylides with Light

A few different types of HVI reagents are capable of absorbing light such as aryl diacetates, diaryl iodonium salts, and iodonium ylides. These classes of compounds have already been successfully implemented in various photochemical reactions and application. Because iodonium ylides are the class of ylides that are focussed on in this thesis, their photochemical activation using both UV and LED light sources are analyzed and discussed in this Chapter. Initial discoveries were based on the use of UV light, but more current applications have been found that use LEDs.²³² The photochemical activation of iodonium ylides was first introduced by Hadjiarapoglou and Spyroudis around 1985. Both researchers used UV light as the source of energy as this was the common way of performing photochemical reactions in the 1980's before the discovery of LEDs.

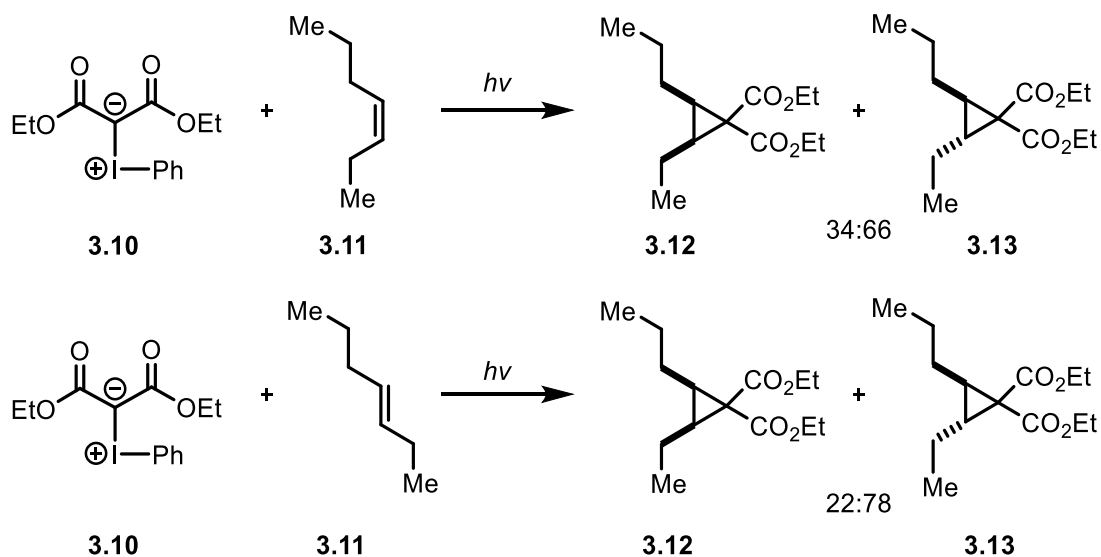
The notion of exciting iodonium ylides with the use of UV light was first introduced by Hadjiarpoglou, Spyroudis, and others in the 1980s.²³³ The relatively higher energy contained in UV light may possibly allow for extrusion of iodobenzene and formation of a free carbene, but direct convincing experimental evidence to support this theory remains questionable. If a free carbene is present as an intermediate in the reaction medium in the presence of alcohols or primary/secondary amines, there should be some observable amount of insertion products forming, but this is not the case, raising the question of whether free carbenes are generated or not with photo-induced reactions of iodonium ylides.

The irradiation of iodonium ylides with UV is believed to induce the formation of carbene intermediates. The diagram below (**Scheme 3.7**) shows the activation of acyclic iodonium ylide **3.10a** with UV light.



Scheme 3.7 Photochemical activation of acyclic iodonium ylides

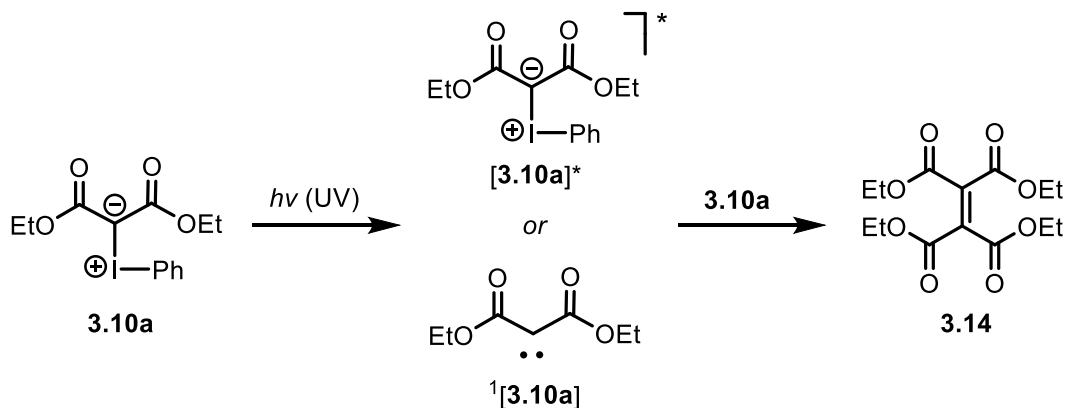
To examine the spin states of the “carbene” intermediates involved in the photolysis reaction of iodonium ylides, cyclopropanation reactions using *cis*-3-heptene and *trans*-3-heptene were performed to investigate the relative amounts of *cis*-cyclopropane and *trans*-cyclopropane formed. A mixture of **3.10a** and *cis*-3-heptene was subjected to photolysis, producing low yields of the cyclopropanes, but in a ratio 34:66 (*cis:trans*) (**Scheme 3.8**). A mixture of **3.10a** and *trans*-3-heptene was subjected to photolysis, producing a ratio of 22:78 (*cis:trans*). Therefore, the photoexcited ylide intermediate **[3.10]*** most likely undergoes ISC, giving an excited state triplet intermediate **[3.10]³** which then engages with the alkene to form a mixture of *cis* and *trans* cyclopropanes due to the non-stereospecific cyclopropanation reaction known to occur between triplet carbenes and alkenes. The large extent of non-stereospecific cyclopropane formation indicates an efficient ISC event, possibly caused by the iodine atom (heavy atom effect).²³⁴



Scheme 3.8 Photochemical cyclopropanation of acyclic iodonium ylides with alkenes

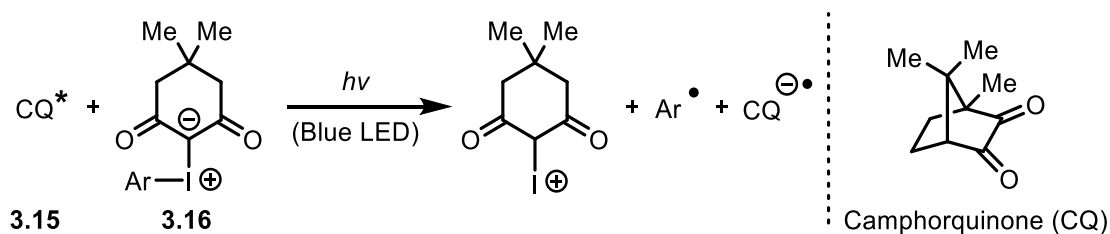
The studies above that examined the spin states of the intermediates involved in the photolysis reaction of iodonium ylides led to the understanding that the decomposition of iodonium ylides by a photochemical process is not stereospecific, and therefore a triplet carbene most accurately describes the “carbene-like” intermediate. This understanding is in contrast to the thermal decomposition process of iodonium ylides, which is believed to be a stereospecific reaction, involving a “carbene-like” intermediate that is most accurately described as a singlet carbene.

Photolysis of **3.10a** with UV light is known to give significant amounts of dimerization product **3.14** which has been explained by a high affinity of the photo-excited species [**3.10**]^{*} for the starting material iodonium ylide. It is also possible that dimerization product **3.14** can be explained by the photolysis of **3.10a** producing a free carbene intermediate [**3.10a**]¹. The free carbene intermediate could then engage with the starting material iodonium ylide in an analogous manner giving the dimer product (**Scheme 3.9**).



Scheme 3.9 Photo-dimerization intermediates of acyclic iodonium ylides

LEDs have recently emerged as a new method for photochemical activation, the only known report in literature that involves the activation of iodonium ylides with blue LEDs prior to this work is a polymerization process discovered by Lalevée in 2019.²³⁵ Iodonium ylides were studied as new reagents for radical chemistry by inducing polymerization of (meth)acrylates as a replacement over traditionally-used diaryliodonium salts. Diaryliodonium salts are already established as photo-initiators in radical-based reactions but are known to suffer drawbacks due to the presence of unavoidable counter ions. Iodonium ylides **3.16** were shown to undergo photochemical activation using blue LEDs, which enabled an electron transfer between an excited camphorquinone (CQ) **3.15** and iodonium ylide **3.16**, for the generation of aryl radicals Ar^{\bullet} (**Scheme 3.10**). The Ar^{\bullet} are then able to initiate free radical polymerization of (meth)acrylate monomers and form desired polymers of choice.



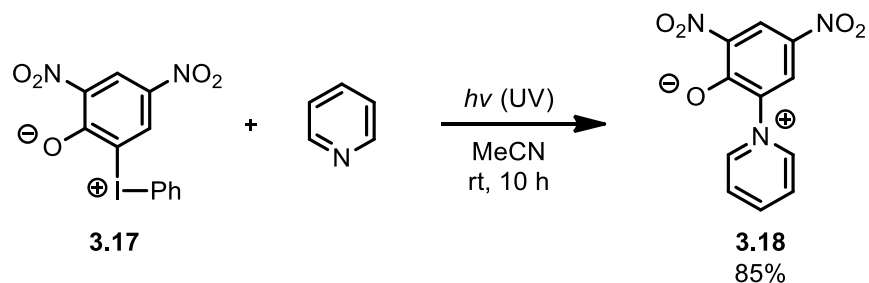
Scheme 3.10 Activation of iodonium ylides with blue light from LED

Lalevée reported the use of lower energy visible light enabled an electron transfer to occur between the iodonium ylide and a reaction partner,²³⁵ so perhaps the use of lower energy

visible light may allow for mechanistic probing into the reactivity of iodonium ylides, hopefully resulting in a new understanding of how iodonium ylides react under photolytic conditions.

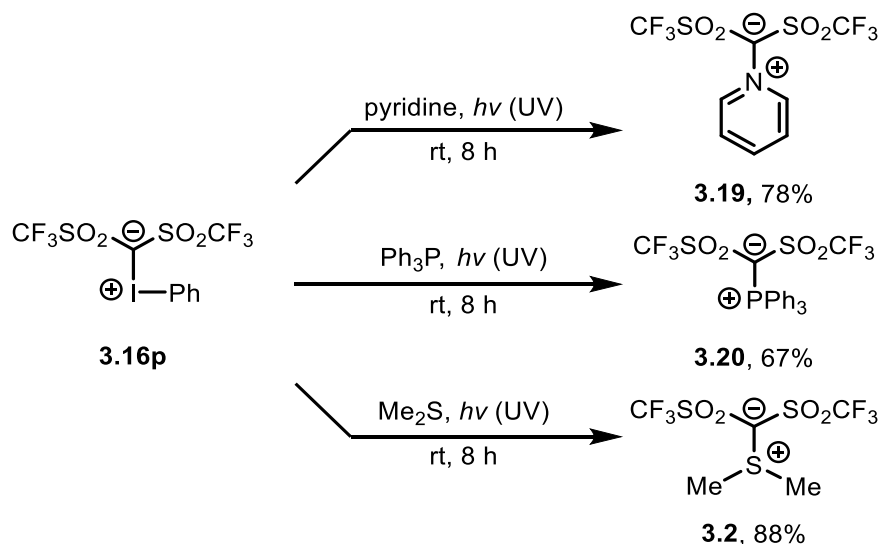
3.2.4.1 Photochemical Transylidation Reactions

The first photochemically induced transylidation reaction of iodonium ylides was reported in the literature by Spyroudis in 1986.²³⁶ The first photochemically-induced transylidation reaction between nitro-stabilized iodonium ylide **3.17** and pyridine was shown to give pyridinium ylide **3.18** as the major transylidation product with an 85% yield (**Scheme 3.11**).



Scheme 3.11 First photochemical transylidation reaction of iodonium ylides

The initial discovery of a photochemically induced transylidation reaction of an iodonium ylide was followed by more examples in which different types of ylides were generated from irradiating acyclic iodonium ylides with UV light. These transformations presumably operate by either going through a “free” carbene or a carbenoid-like intermediate. The synthesis of pyridinium ylide, triphenylphosphonium ylide, and sulfonium ylides was accomplished by the reaction between iodonium ylide **3.16p** and pyridine, triphenylphosphine, dimethyl sulfide, respectively, under UV irradiation (**Scheme 3.12**).²³⁷

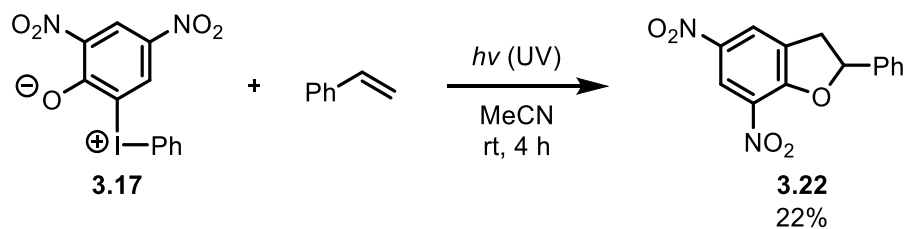


Scheme 3.12 Transylidation reactions under photochemical activation

The reasonably good yields of the above photochemically induced transylidation reactions suggest the possibility that free carbenes may not be involved in the process. Instead, a photo-activated species may be responsible for the efficiency of the observed product formation. If free carbenes were involved in the photo-transformation, there should be substantial amounts of starting material dimer formation, as both reactants were placed in a quartz flask and irradiated with UV light. It is also possible that free carbenes react reversibly with iodobenzene to reform the iodonium ylide which prevents dimerization to some extent.

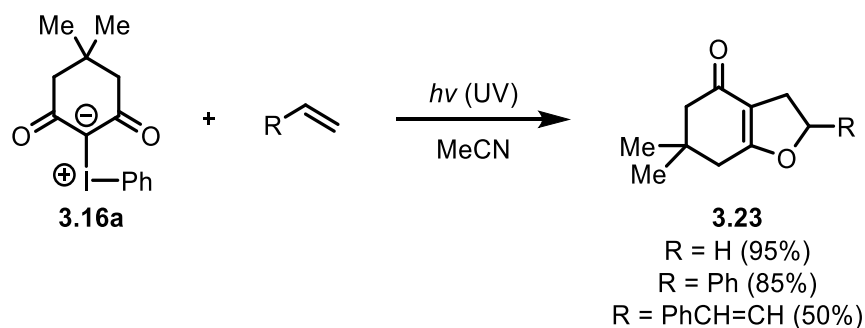
3.2.4.2 Photochemical Cycloaddition Reactions

The use of iodonium ylides in photochemically activated cycloaddition chemistry was first developed in 1985 by Spyroudis.²³⁸ An example of a photo-induced cycloaddition discovered by Spyroudis is shown in **Scheme 3.13** in the reaction of iodonium ylide **3.17** with styrene to give heterocyclic product **3.22**.²³⁹ It was reported that the involvement of carbenes or carbenoid species in the photochemical reaction seems unlikely because no Wolff rearrangement were isolated from the reaction mixture. It was also observed that irradiation of **3.17** in acetonitrile was left unchanged.



Scheme 3.13 Photochemical [3+2] cycloaddition of an iodonium ylide with styrene

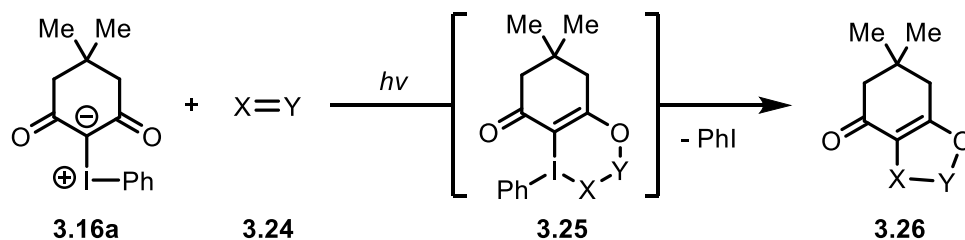
The chemistry of photolytically generated carbenes, or carbene equivalents, from iodonium ylides was explored by Hadjiarapoglou in 1987.²⁴⁰ The photolytic process was conducted using a 400 W low-pressure Hg lamp which allowed cyclic iodonium ylides derived from dimedone (**3.16a**) to engage with alkenes and undergo cyclization reactions to form dihydrofurans (**3.23**) as shown in **Scheme 3.14**.



Scheme 3.14 Photochemical [3+2] cycloaddition of iodonium ylides with alkenes

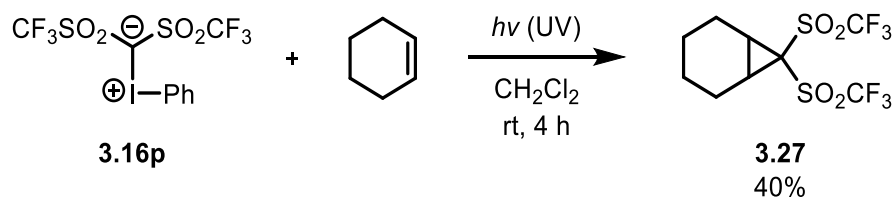
The reaction of iodonium ylides (**3.16a**) with dipolarophiles (**3.24**) under photochemical activation has been proposed to occur via the formation of a five-membered ring heterocycle in an overall formal [3+2] cycloaddition. The five-membered ring product (**3.26**) is believed to form from a six-membered ring intermediate (**3.25**) containing the hypervalent iodine atom as shown in **Scheme 3.15**. This six-membered ring iodo-cycle has been proposed by many different researchers to explain the observed product formation and is considered an energetically favourable process as the oxidized iodine (III) is reduced to iodine (I). Formation of **3.25** is shown below to occur in a concerted style, but this intermediate can also be explained to form via a step-wise approach, most likely depending on the properties and atomic composition of **3.24**. It should be noted here that production of **3.26** is not described as proceeding through the

involvement of a free carbene, even when using UV light, and is proposed to occur as shown below in almost all reports in literature.



Scheme 3.15 Photochemical induced cycloaddition reactivity of iodonium ylides

Photochemically induced cycloadditions of iodonium ylides most commonly operate through the formation of five-membered ring products in a formal [3+2] transformation, but there are a few, extremely rare examples of other cycloadditions such as [2+1] cycloadditions, capable of forming cyclopropane products. The photochemically induced [2+1] cycloaddition reaction of **3.16p** with cyclohexene giving cyclopropane **3.27** was reported by Zhu in 1994 (**Scheme 3.16**).²⁴¹

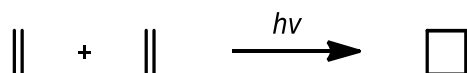


Scheme 3.16 Photochemical [2+1] cycloaddition of an iodonium ylide with cyclohexene

The use of light for initiating iodonium ylides to participate in cycloadditions to form heterocyclic and carbocyclic structures has been established as a viable synthetic option but has relied on using UV light. The development of alternative procedures using less detrimental light sources, such as LED, could be of value and interest to synthetic chemists.

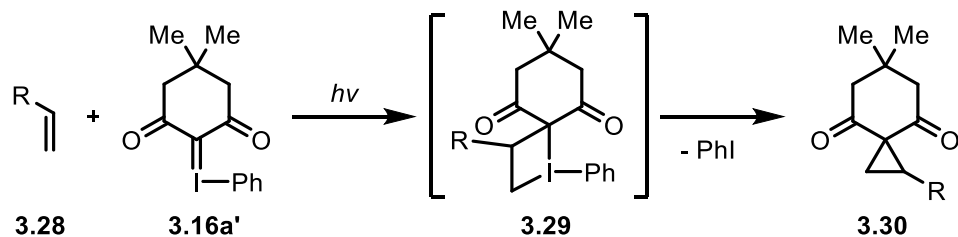
3.3 Proposed Photochemical Activation of Iodonium Ylides with Blue Light

The use of light to initiate cycloaddition reactions is a concept that dates back over 100 years to research performed by Ciamician and Silber, who were the first to report a [2+2] light-induced cycloaddition in 1908.²⁴² In these studies, it was discovered that exposure of carvone to sunlight for one year resulted in carvone camphor formation. The [2+2] cycloaddition is one example of many reactions that are initiated with light and has been a topic of significant interest over the years. Paul DeMayo also contributed largely to this area of photo-chemistry, with detailed attention given to reaction mechanism understandings.²⁴³ He was also the first to establish that intermolecular [2+2] cycloaddition reactions were possible. A general photo-induced [2+2] cycloaddition reaction is shown in **Scheme 3.17**.



Scheme 3.17 Photochemical [2+2] cycloaddition

It was theoretically proposed that because iodonium ylides exist as ylene and ylide resonance structural forms, and in the ylene form (**3.16a'**) there is a double bond between the ylidic carbon atom and the hypervalent iodine atom, that a photo-induced [2+2] cycloaddition reaction might occur in the presence of an alkene (**3.28**). The [2+2] cycloaddition could form four-membered ring iodo-cycle intermediate **3.29**, which has already been proposed as a possible intermediate in other HVI reactions in literature.²⁴⁴ After formation of this four-membered ring intermediate, iodobenzene can be extruded to form cyclopropane **3.30**, resulting in an overall formal [2+1] cycloaddition as shown in **Scheme 3.18**. The idea that iodobenzene can be reductively eliminated out of a cyclic intermediate, undergoing ring contraction, has also been proposed as a mechanistic explanation in the literature for other reactions involving iodonium ylides.²⁴⁵



Scheme 3.18 Proposed photochemical [2+2] cycloaddition of iodonium ylides

To test the proposed photo-induced [2+2] cycloaddition reaction of iodonium ylides with alkenes, cyclic iodonium ylides, which are more stable and therefore easier to work with than acyclic iodonium ylides, were selected for initial investigations. Dimedone-derived iodonium ylide was synthesized and dissolved in an organic solvent, starting with CH_2Cl_2 , to visually observe the colour of the solution, which was pale yellow in appearance. This yellow-coloured solution in theory absorbs blue light because blue light is the complementary colour to yellow.

To investigate why a yellow-coloured solution of an iodonium ylide should absorb visible light, understanding the MOs should help with the theory behind the photochemical activation. The geometry of iodonium ylides dictates a 90° angle between the 1,3-dicarbonyl system and the aromatic ring thereby creating two separate systems that are not in conjugation with each other (**Figure 3.8**). These two individual systems should therefore be examined separately with their own energy levels and electronic transitions.

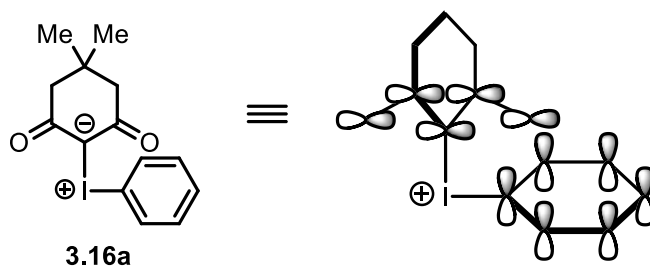


Figure 3.8 Geometry of orbital systems in iodonium ylides

The aromatic ring system can be examined by looking into the UV-Vis properties of benzene and iodobenzene, which do not exactly represent the environment found in an iodonium ylide but provide an approximation for analysis. The UV-Vis properties of benzene show λ_{max}

peaks at 180 and 255 nm²⁴⁶ and iodobenzene shows a λ_{max} peak at 229 nm.²⁴⁷ This implies blue light from LED (λ_{max} 465 nm) is highly unlikely to not induce electronic transitions within the aromatic system.

The 1,3-dicarbonyl system can be simplified by representing the positively charged iodobenzene group as a single EWG group (X) creating a conjugated 5-atom π system containing a total of 6 electrons because of the anion, as shown below in **Figure 3.9**.

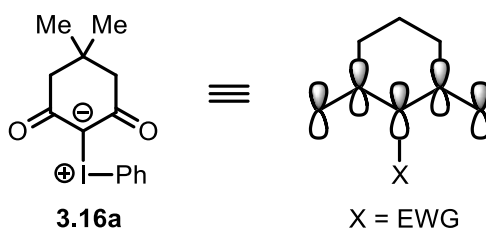


Figure 3.9 Representation of dimedone iodonium ylide as a MO diagram with 5 atoms

A HOMO to LUMO transition of a 5-atom π system, believed to occur in iodonium ylides upon photo excitation shown in **Figure 3.10**. Information that can be gained from analyzing the electronic excitation levels include understanding where electron density occurs, and where it doesn't occur (nodes) which may be helpful for discussing how the light activation process happens.

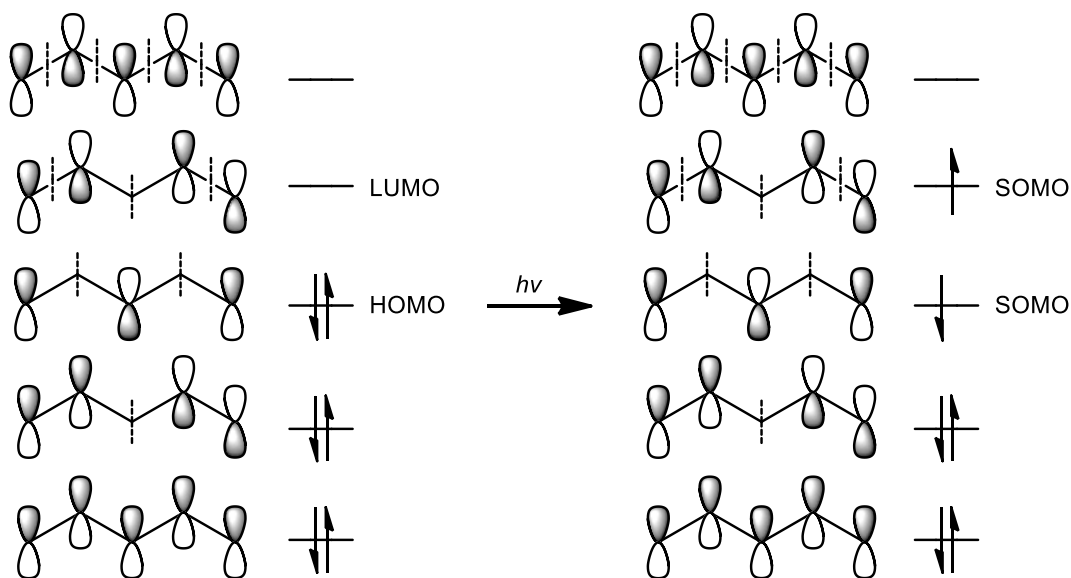


Figure 3.10 Electronic excitation levels of a 1,3-dicarbonyl anion system by light

The 1,3-dicarbonyl anion system is just an approximation of the iodonium ylide's chromophore, and to generate a more realistic model of the electronic environment, computational modeling was required.

3.4 Computational Modeling of Iodonium Ylides Under Blue Light Irradiation

Professor Scott Hopkins performed computational modeling on a series of six, structurally similar cyclic iodonium ylides as a way of comparing structural features to electron densities and excitation energies. Calculating the energy required for a HOMO to LUMO transition within the iodonium ylides, gives an approximate value which can be converted into a wavelength of light. Irradiating an iodonium ylide in solution with the calculated wavelength (colour) of light may enable an electronic transition to an excited state, which can then react with an appropriate molecular partner. Computational modeling will also be of benefit for knowing more precisely what the electron density looks like on the iodonium ylides for the ground and excited state. This will enable a better mechanistic understanding for predicting which compatible reaction partners can react.

Six iodonium ylides (**3.16a**, **3.16b**, **3.16g**, **3.16h**, **3.16i**, **3.16j**) were subjected to a computational study in which a search for the optimal molecular geometry was performed at the B3LYP/6-311+G(d,p) level of theory, and are shown in **Figure 3.11**.

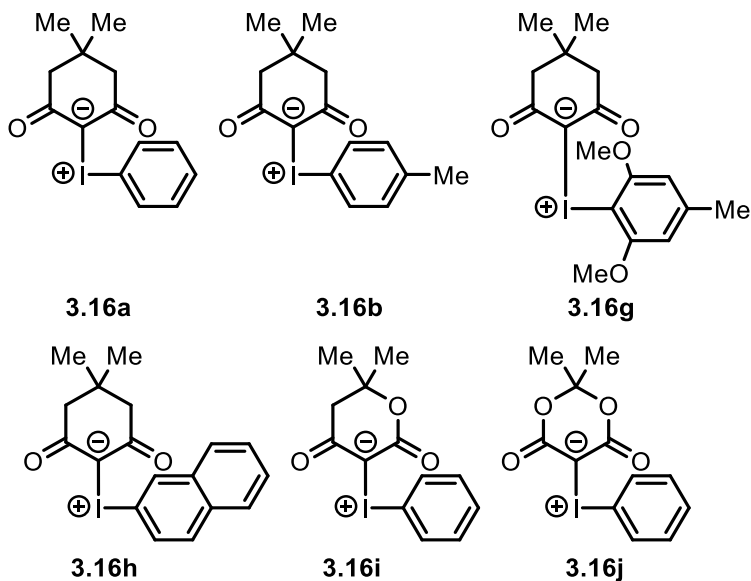
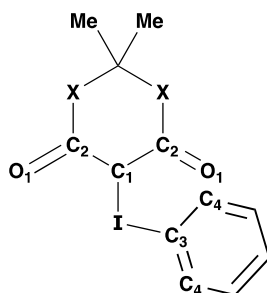


Figure 3.11 Cyclic iodonium ylides used in computational studies

The optimal ground state structure was employed for TD-DFT calculations of the ten lowest-energy excited electronic states. Natural population analysis was also conducted to calculate the partial charges on the atoms present in the iodonium ylides. The data generated on the calculated partial charges from the six iodonium ylides tested was conducted by Professor Scott Hopkins and is shown in **Table 3.4**.

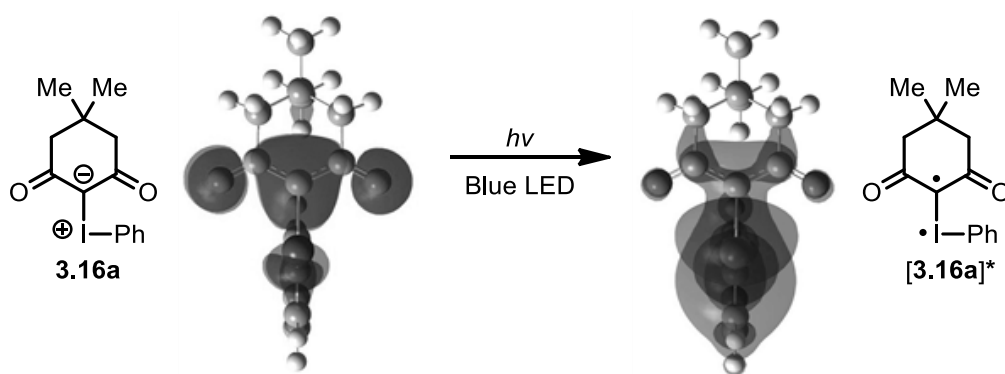
Table 3.4 Partial charges determined through computational analysis



Ylide	State	C2	O1	C1	I	C3	X	C4
3.16a	S0	0.49	-0.68	-0.54	1.01	-0.19	-0.45	-0.24
3.16b	S0	0.49	-0.69	-0.54	1.01	-0.20	-0.45	-0.23
3.16g	S0	0.48	-0.69	-0.52	1.02	-0.33	-0.45	0.34
3.16h	S0	0.49	-0.68	-0.55	1.00	-0.16	-0.45	-0.23/-0.09
3.16i	S0	0.48/0.75	-0.69	-0.59	1.03	-0.22	-0.48/-0.6	-0.22
3.16j	S0	0.74	-0.67	-0.65	1.06	-0.22	-0.60	-0.22
3.16a	S1	0.46	-0.69	-0.43	0.87	-0.09	-0.44	-0.25
3.16b	S1	0.48	-0.70	-0.57	0.61	0.25	-0.45	-0.30
3.16g	S1	0.48	-0.67	-0.47	0.76	-0.03	-0.45	0.28
3.16h	S1	0.47	-0.58	-0.45	0.70	0.13	-0.45	-0.29/-0.15
3.16i	S1	0.44/0.72	-0.69	-0.41	0.88	-0.13	-0.47/-0.59	-0.25
3.16j	S1	0.66	-0.68	-0.23	0.77	-0.22	-0.58	-0.22

Natural population analysis (averaged over 6 iodonium ylides) indicates that 0.26 e of electron density is transferred to iodine in the excited state (S1) upon irradiation of the iodonium ylides in the ground state (S0) with blue LED. To visualize the movement of electron density that occurs upon excitation of the iodonium ylide, computational modeling was used to construct HOMO and LUMO images from MO contributions. The HOMO and LUMO images generated computationally also contain nodes of zero electron density that are located in agreement with the 5 atom, 6 electron MO diagram of the 1,3-dicarbonyl anion system.

After obtaining the computationally generated models and examining the activation of iodonium ylide **3.16a** with blue light, the data reveals an activated species [**3.16a**]* that may react in a similar way to a 1,2-diradical intermediate due to the shifting of electron density towards iodine in the LUMO as shown in **Scheme 3.19**. This electronic excitation would be different than diazo compounds, as iodonium ylides may absorb blue light to generate 1,2-diradical intermediates while diazos undergo heterolytic cleavage to produce free carbenes. The HOMO and LUMO images for the other five iodonium ylides are similar in appearance and can be found in the experimental section at the end of this chapter.



Scheme 3.19 HOMO to LUMO photoexcitation of iodonium ylide **3.16a**

The energy required for HOMO to LUMO transitions of each of the six iodonium ylides were computationally calculated and converted into the equivalent energy of a wavelength of light. For example, iodonium ylide **3.16a** requires using light with a calculated wavelength of 332 nm to induce a HOMO to LUMO transition. These transitional energies are displayed as calculated electronic spectra with a Gaussian curve fitting added to account for vibrational transitions as shown in **Figure 3.12**.

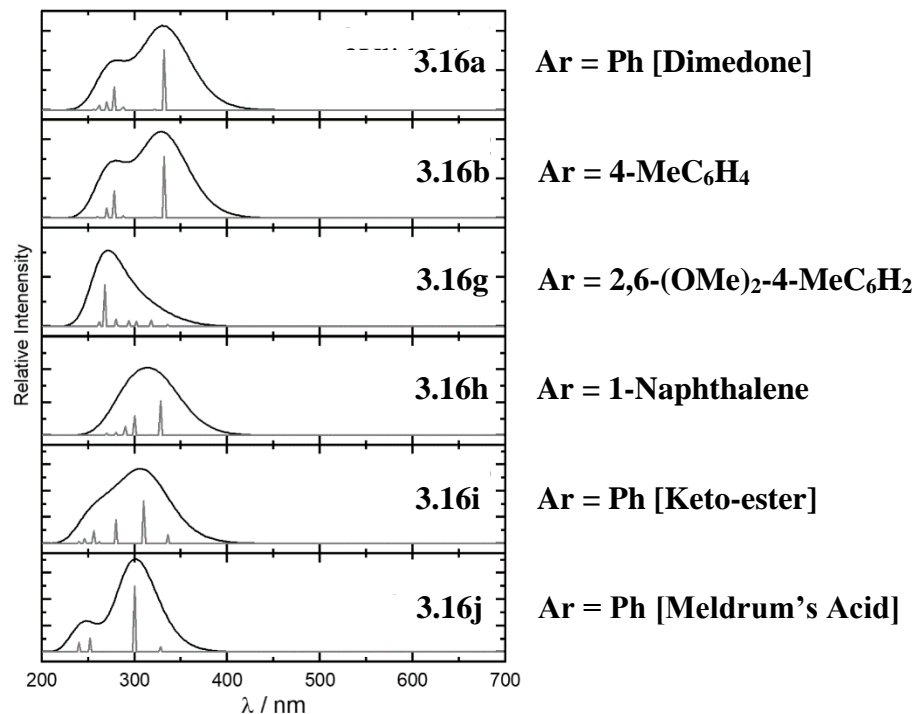


Figure 3.12 Calculated spectra, B3LYP/6-311++G(d,p) level of theoretical iodine

3.5 UV-Vis Absorbance of Iodonium Ylides

To begin photochemical activation studies of iodonium ylides, it was important to obtain absorbance properties of the iodonium ylides. The preparation of a 0.1 M solution of iodonium ylide **3.16a** in CH_2Cl_2 was performed and the absorbance properties were measured using a UV-Vis spectrophotometer. The UV-Vis absorbance of the iodonium ylide was overlaid with emission data collected from a RGB (red, green, blue) LED strip using a spectrometer (Ocean Optics, Model: USB 4000) as shown below in **Figure 3.13**.

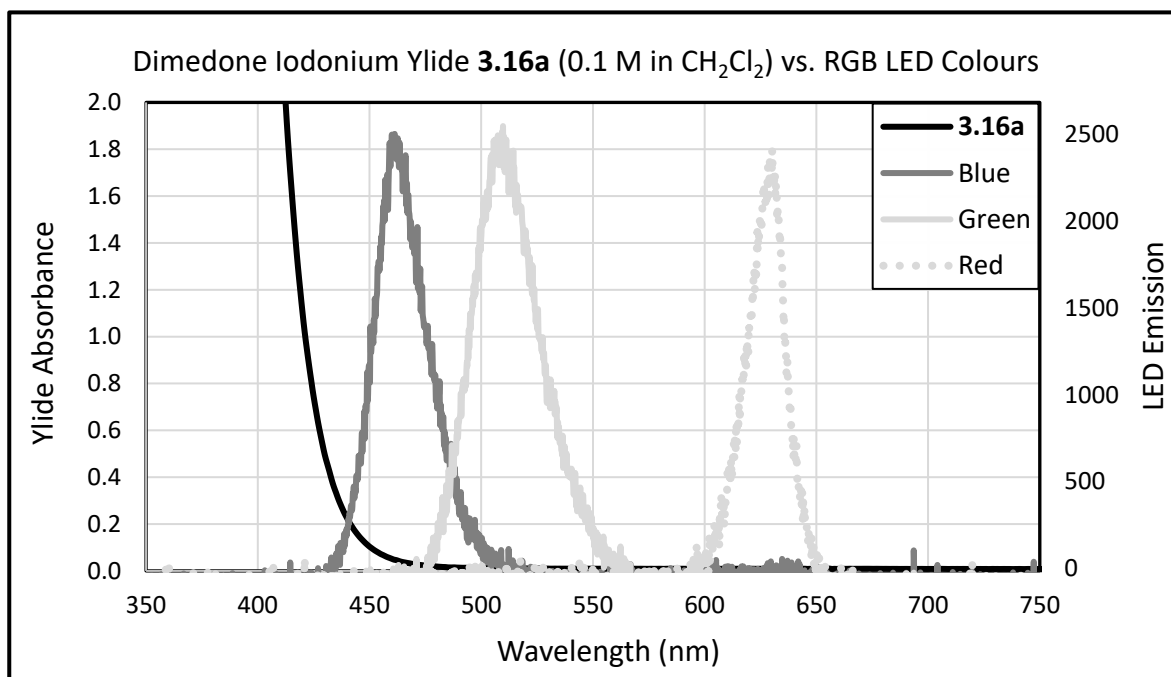


Figure 3.13 UV-Vis absorbance of ylide **3.16a** overlaid on RGB LED colours

The UV-Vis absorbance of dimedone iodonium ylide **3.16a** shows that at 0.1 M concentration, there is a significant absorbance in the blue light region. There is an observable overlapping region of the iodonium ylide's absorbance with the blue LED's emission, suggesting that blue light from a LED would theoretically be possible at exciting the iodonium ylide which may allow for a reaction to occur with an appropriate reaction partner. To supply the right amount of light from LEDs, a photoreactor had to be designed with the goal of irradiating a solution of iodonium ylide without applying excessive amounts of unwanted heat, which may possibly lead to undesirable background reactions.

To test the validity exciting an iodonium ylide with blue light and capturing the excited state intermediate with a reaction partner, a cyclopropanation reaction was envisioned. Preliminary investigations were focused on using dimedone iodonium ylide **3.16a** and styrene as the reaction partners to make dimedone-derived cyclopropanes. The visible light-mediated cyclopropanation reaction of iodonium ylides with alkenes relies on the photoexcitation of the iodonium ylide and not the alkene. Because this was a new process, obtaining the UV-Vis data for both starting materials was important to consider all possibilities of photoexcitation. Since

optimization experiments were conducted using styrene as the alkene, the properties of styrene were measured first to eliminate the possibility that photoexcitation of the alkene was responsible for yielding a cyclopropane.

The UV-Vis absorbance spectrum of styrene was measured in CH_2Cl_2 at a concentration of 0.1 M and is shown in **Figure 3.14**. The UV-Vis data for styrene has also been reported in the literature, showing λ_{max} peaks recorded at 247 and 281 nm.

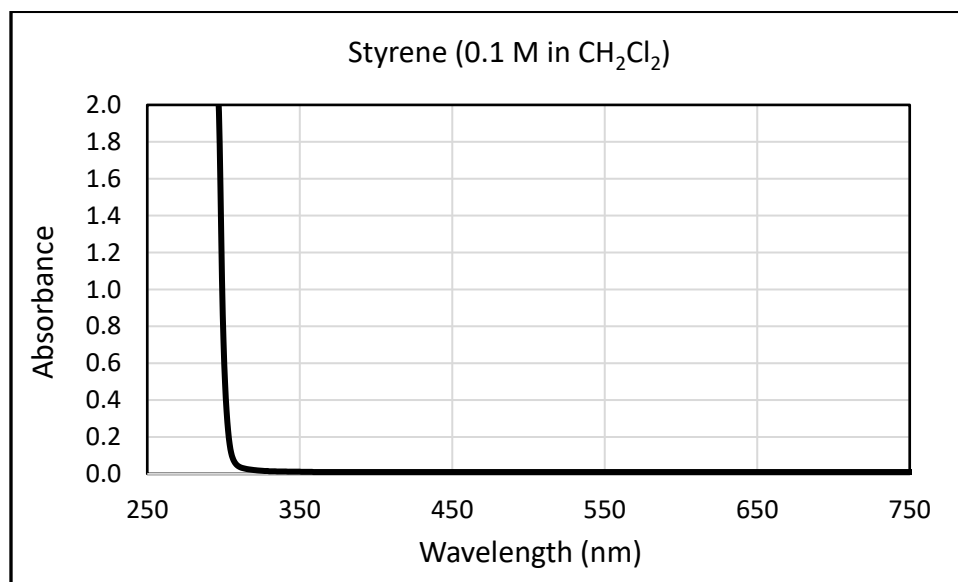


Figure 3.14 UV-Vis absorbance of styrene

As shown above in the UV-Vis spectrum of styrene, there would be little to zero overlap with the blue light from the LED. This implies that photoexcitation of blue light from the LED (λ_{max} 465 nm) does not involve the alkene, but most likely, the iodonium ylide is the species that undergoes photoexcitation.

This data is also qualitatively consistent with preparing individual solutions of styrene and iodonium ylide in solvents such as CH_2Cl_2 or MeCN. For example, a 0.1 M solution of styrene in CH_2Cl_2 is colourless, while a 0.1 M solution of dimesityl iodonium ylide in CH_2Cl_2 is pale yellow. A yellow-coloured solution is yellow because it absorbs blue light. While a colourless solution is colourless because it most likely does not absorb visible light.

3.6 Photoreactor Design

A strong foundation of the scientific method is the reproducibility of an experiment which applies to science in general and in this case photochemistry, creating a need for reliable and accurate equipment, such as photoreactors.²⁴⁸ Recently, advancements have been made to standardize the experimental set-ups required for photochemical processes to enhance reproducibility to meet the standards in both academic and industrial settings.²⁴⁹ In the designing of a photoreactor set-up, it is important to consider several factors to ensure consistent and reproducible results can be obtained. Parameters include the light source, distance from light source, temperature, and the geometry of the reactor set-up.

3.6.1 Photoreactor #1 Round-bottom Flask Design

Initial efforts to test the viability of a photo-induced reaction of iodonium ylides with alkenes involved simply wrapping a strip of blue LED lights (10) around a 25 mL round-bottom flask (**Figure 3.15**). There was a considerable amount of heat generated from the LED strips which warmed the flask up to ~40 °C as measured by a laser thermometer.

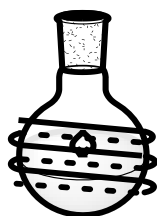
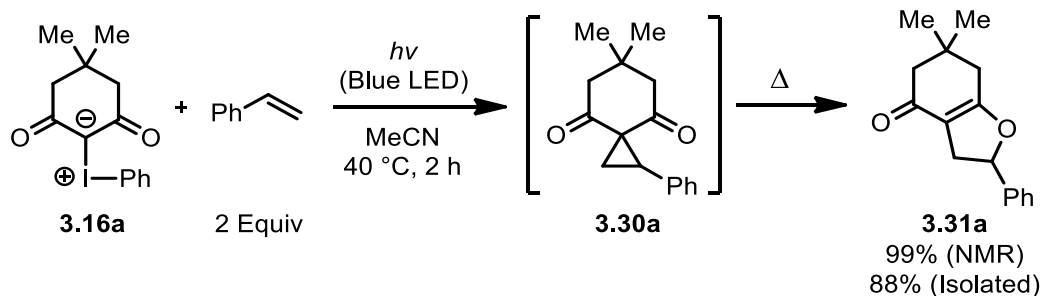


Figure 3.15 Photoreactor #1 round-bottom flask design

The formation of cyclopropane **3.30a** was not observed, instead nearly quantitative formation of dihydrofuran **3.31a** was formed, as shown below in **Scheme 3.20**.



Scheme 3.20 Reaction using photoreactor #1

Although forming the dihydrofuran was not the intention, the high yield indicated a promising result in the viability of this method for forming cyclopropanes in an efficient process because of the already known heat-induced isomerization of cyclopropanes to dihydrofurans reported in the literature. Inhibiting the unwanted heat-induced isomerization was tested by wrapping the entire photoreactor setup in a sealed plastic bag and submersing it into an ice bath. Running the same reaction again, but at 0 °C for 3.5 h gave the desired cyclopropane in 14% NMR yield with no observable formation of the dihydrofuran.

3.6.2 Photoreactor #2 Displacement Tube Design

A photoreactor was designed to give a thin layer of solution that could be evenly irradiated with light over an area specifically intended to increase the surface area for direct light exposure. This setup used a large glass solvent tube which was filled with a solution containing the iodonium ylide, alkene, and solvent. A stir bar was placed at the bottom for internal stirring when placed onto a magnetic stir plate. A smaller glass displacement tube was inserted into the larger tube to displace the solution along the walls with an average thickness of approximately 1 mm. A strip of blue LED lights (10) was then wrapped around the outside of the large solvent tube facing inwards to apply even irradiation over the entire solution as shown in **Figure 3.16**. A rubber septum was then used to cap the whole setup which enabled the use of a nitrogen filled balloon to create an inert environment when needed. The key idea behind this photoreactor design was intentionally displacing the solution of iodonium ylide and alkene over a large enough surface area to allow for the reaction to reach completion in a short time.

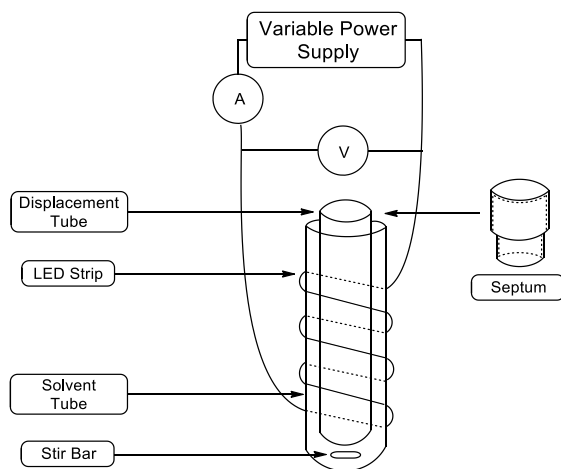
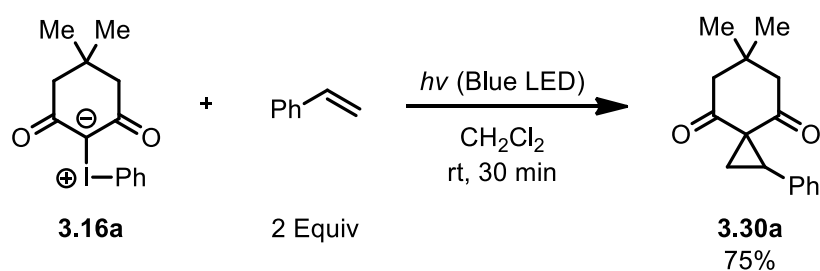


Figure 3.16 Photoreactor #2 displacement tube design

The displacement tube photoreactor enabled the cyclopropanation reaction to occur in a shorter reaction time when compared against the previously designed photoreactor setup. The cyclopropanation reaction (**Scheme 3.21**) was complete in only 30 minutes yielding 75% of the cyclopropane product **3.30a**, at which point the iodonium ylide starting material was fully consumed when checked by NMR. Some of the disadvantages of this photoreactor is the inconvenience of setting up one reaction at a time, the LED strip was directly in contact to the solvent tube, and the use of 10 LED lights for a single reaction.



Scheme 3.21 Cyclopropanation reaction using photoreactor #2

3.6.3 Photoreactor #3 Bowl Design

A limitation with photoreactor #2 was the inability to perform multiple reactions at once along with other issues stated above, therefore, a more convenient set-up was the inspiration

behind designing a new photoreactor. Photoreactor #3 was built from an aluminum bowl ~ 20 cm in diameter with a small test tube rack in the centre to hold 1 dram reaction vials, with an 18 vial capacity (**Figure 3.17**). The RGB LED strip was fixed to the inside wall of the bowl with all the lights (63) being directed towards the centre, and with a remote control capable of adjusting the colours of light to red, green, or blue, plus additional mixtures of the three. The photoreactor had eight light-intensity settings, and the entire system was open to the air for allowing residual heat to escape. In case of longer reactions when heat became an issue, a fan was used to flush out hot air.

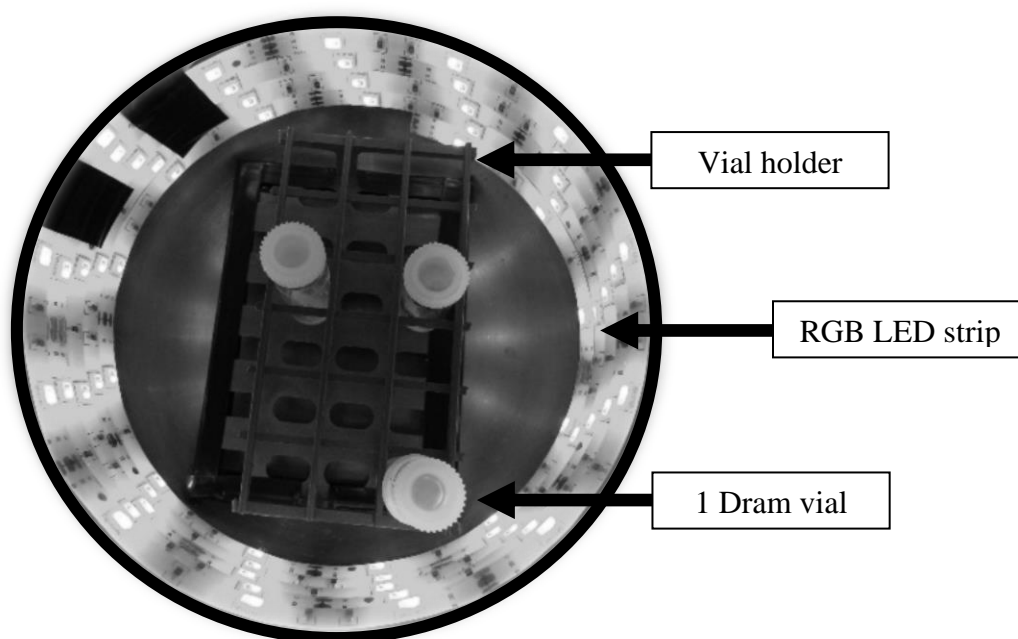


Figure 3.17 Photoreactor #3 bowl design

To calculate the current at each intensity setting, a 2.7 Ohm resistor was used, and with the resistor in series, the current and power was calculated for each intensity setting. Because 63 LEDs were used in total, the wattage per individual LED was calculated and is shown in **Table 3.5**.

Table 3.5 Light-intensity data for photoreactor #3

Intensity	Voltage (V)	Current (A)	Power (W)	Watts/LED
1	1.53	0.028	0.04	0.001
2	3.05	0.057	0.17	0.003
3	4.59	0.086	0.39	0.006
4	6.12	0.116	0.71	0.011
5	7.66	0.146	1.12	0.018
6	9.19	0.176	1.62	0.026
7	10.73	0.206	2.21	0.035
8	12.25	0.236	2.89	0.046

The efficiency of energy consumption displayed by LED lights is demonstrated in the data obtained from photoreactor #3 which showed that on the brightest intensity setting only 45 mW/LED was being used, and on the lowest intensity setting only 0.63 mW/LED was used.

The amount of light reaching vials in the centre of the photoreactor compared to vials directly beside the light source was tested to evaluate and understand the issue of consistency and reproducibility between reactions. It was hypothesized that vials placed directly beside a light source would possibly experience faster reaction times or higher yields of cyclopropanation, so a spectrophotometer was placed inside photoreactor #3 at different distances from the light source to collect light intensity data. A measurement of light intensity was taken at 1 cm from the LEDs to reveal that the relative emission was much higher than at 7 cm as shown in **Figure 3.18**.

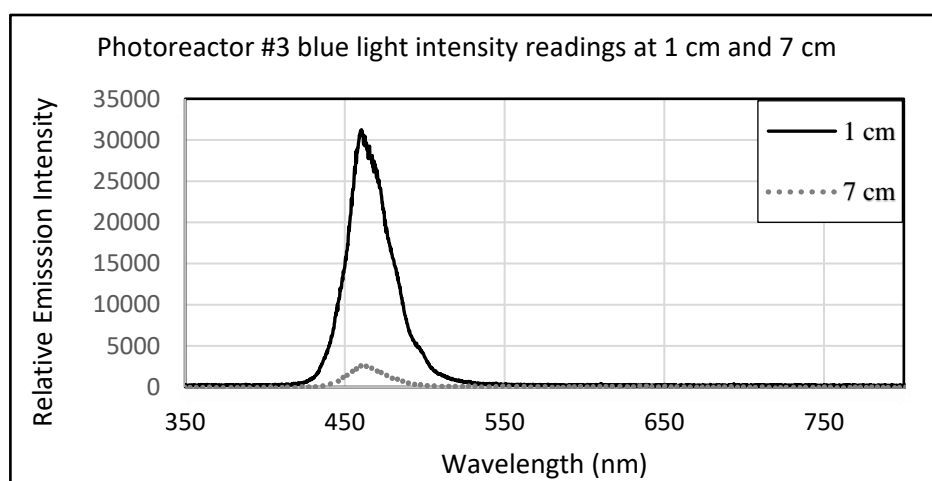


Figure 3.18 Photoreactor#3 light intensity readings

The correlation between light intensity and cyclopropane yield in photoreactor #3 was demonstrated in the following reaction of iodonium ylide **3.16a** with styrene. The reaction was run using CDCl_3 as the solvent so that incremental measurements of cyclopropane yield could be taken at specific time intervals. The internal standard HMDSO (10 μL) was added at the beginning to each reaction vial, enabling aliquots to be removed and checked using ^1H NMR, and from this, the yield of cyclopropane could be determined at each time interval.

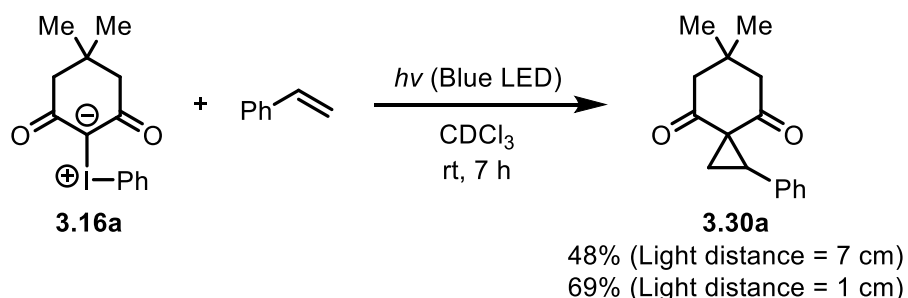


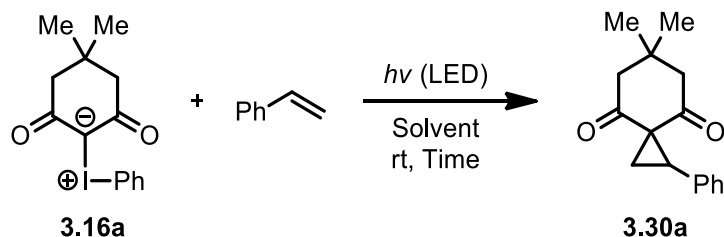
Figure 3.19 Photoreactor #3 cyclopropane yield at different distances from LED

As observed from the blue light-induced reaction of iodonium ylide with styrene using photoreactor #3, the overall yield of cyclopropane **3.30a** was 48% at 7 cm and 69% at 1 cm. These results imply there is a correlation between light intensity and cyclopropane yield, with a higher yield coming from placement of the reaction vial closer to the light source (1 cm). At a 1 cm distance from the LEDs, the yield of cyclopropane was higher than at the 7 cm distance, for each time interval checked. This implies that in addition to there being a correlation between light intensity and cyclopropane yield, there is also a correlation between light intensity and reaction rate. These discoveries for our iodonium ylide reaction with alkenes was incorporated into the next design of our photoreactor.

Because of the use of RGB LED strips in photoreactor #3, colours other than blue could be tested on the activation of iodonium ylides. A RGB LED light is composed of three individual LED chips each with a size of 3528 for red, green, and blue colours. The 3528 refers to the size in mm (3.5 mm x 2.8 mm) of the dimensions of the individual chip, with each colour having its own chip. Switching the lights on photoreactor #3 to red and placement of the iodonium ylide, alkene solution directly beside the LED at 1 cm resulted in no observable cyclopropane formation, even after irradiating for 72 h, as shown in **Table 3.6**. The same experiment was set

up, except turning the lights to green, and again resulted in no observable cyclopropane formation after 72 h.

Table 3.6 Photoreactor #3 cyclopropanation using different colours



Entry	LED Colour	Solvent	Time (h)	Distance (cm)	NMR Yield (%) ^[a]
1	Red	MeCN	72	1	0
2	Green	MeCN	72	1	0
3	Blue	CDCl ₃	7	1	69

The iodonium ylide was used on a 0.1 mmol scale with 2 equivalents of styrene and 1.0 mL of solvent (0.1 M). ^[a] Yields determined by ¹H NMR using HMDSO (10 μL) as an internal standard.

Observing that no cyclopropane was formed when using colours of light with lower energy than blue was in agreement with the UV-Vis absorbance data. UV-Vis absorbance of the iodonium ylide indicates that blue light is required to achieve activation, with red and green light not containing enough energy to induce activation. Because red and green light are not useful in the cyclopropanation reaction of iodonium ylides, the designing of an optimized photoreactor was focused on finding a source of intense blue light.

3.6.4 Photoreactor #4 Design

High-intensity blue LED lights were obtained, containing blue sapphire coloured 5050 LED chips. The blue 5050 LED chip type produces a greater amount of light intensity than the blue 3528 LED chip contained with RGB LED strips. With experimental evidence suggesting the reaction yield is increased when placed closer to the light source, design of the new photoreactor was also based upon getting the reaction vials as close to the LED as possible without transferring unwanted background heat. While testing the number of LEDs required per reaction

vial to give the highest yield of cyclopropane, it was discovered that only 1 single LED per vial was needed to give nearly quantitative formation of cyclopropane.

It was concluded that using a single LED placed directly below the reaction vial gave the best results in terms of yield and consistency if the bottom of the vial was placed 0.5 mm above the LED. The LED strip was placed below the plastic test tube rack to minimize heat transfer, giving a total capacity of 8 vials as shown in **Figure 3.20**. One dram vials were selected as they have a plastic cap containing a rubber septum insert which can be pierced with a needle allowing for an inert environment of nitrogen gas.

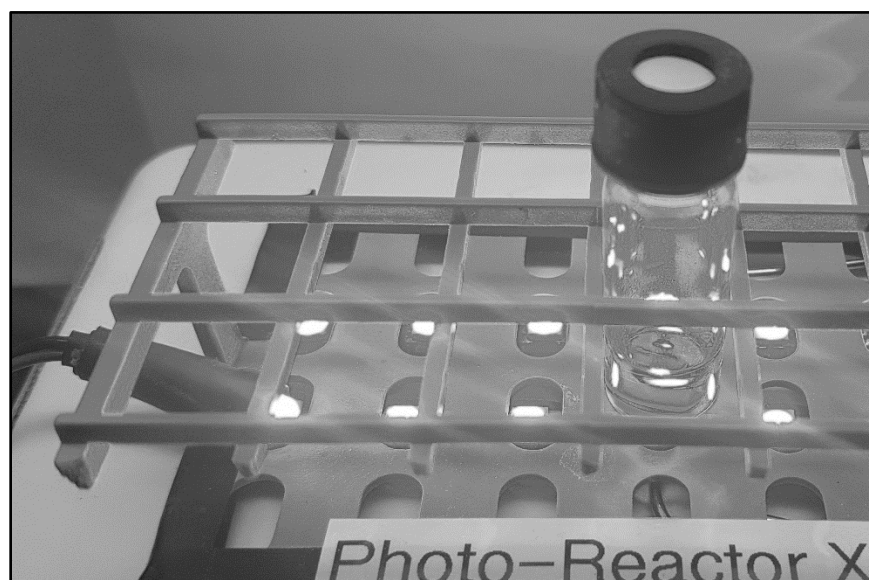
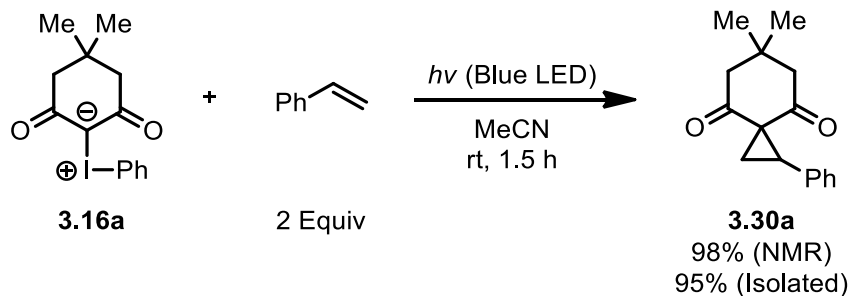


Figure 3.20 Photoreactor #4 design

Comparing the design of photoreactor #3 (contains 3528 LED chip) to photoreactor #4 (contains 5050 LED chip) it was discovered that the 5050 LED chip gave the cyclopropane in 96% NMR yield and 95% isolated yield after only 1.5 h as shown below in **Scheme 3.22**. The same reaction performed with photoreactor #3 gave only 69% of cyclopropane and required 7 h to reach completion.

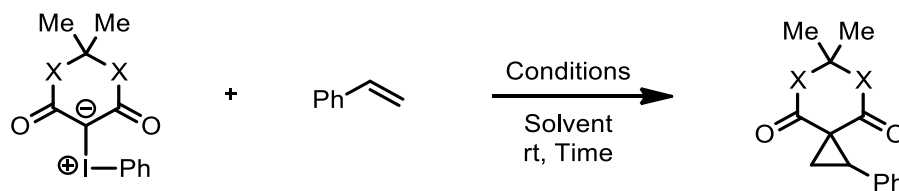


Scheme 3.22 Cyclopropanation reaction using photoreactor #4

After construction of a series of photoreactors, it was concluded that photoreactor #4 was the optimal reactor as it provided the highest yields in a short amount of time, produced little residual heat, and gave consistent, reproducible results. Photoreactor #4 was therefore used for the remainder of the thesis, including optimization of conditions, reaction scope development, mechanistic studies, etc.

3.7 Optimization of Photo-Induced Reaction of Iodonium Ylides with Alkenes

Before optimizing the cyclopropanation reaction of iodonium ylides with alkenes, control reactions were necessary to determine if the reaction was truly a photochemical process. Control reactions to check for activation of the iodonium ylide with light were performed by running the cyclopropanation reaction in the dark. When stirring either dimedone or Meldrum's acid iodonium ylide with styrene in the dark, no cyclopropanation occurred (**Table 3.7**, entries 1 & 3). When running the same reactions with the blue LED turned on, nearly quantitative formation of cyclopropanes was observed (**Table 3.7**, entries 2 & 4), indicating this chemistry to be truly a photochemical process. Even heating dimedone iodonium ylide and styrene to 45 °C (**Table 3.7**, entry 5) gave no observable formation of cyclopropane.

Table 3.7 Cyclopropanation control reactions

Entry	Iodonium Ylide	Conditions	Solvent	Time (h)	NMR Yield (%) ^[a]
1	3.16a X = CH ₂	Dark	MeCN	48	0
2	3.16a X = CH ₂	Blue LED	MeCN	24	98
3	3.16j X = O	Dark	MeCN	48	0
4	3.16j X = O	Blue LED	MeCN	24	95
5	3.16a X = CH ₂	45 °C	CH ₂ Cl ₂	3	0

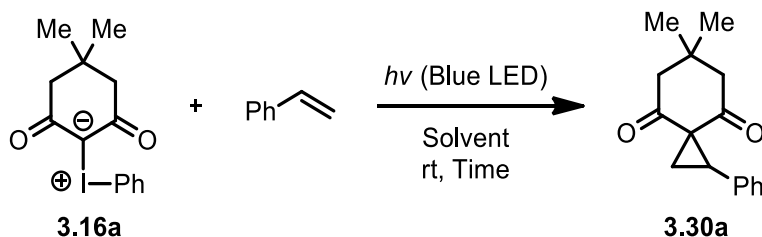
The iodonium ylide was used on a 0.1 mmol scale with 2 equivalents of styrene and 1.0 mL of solvent (0.1 M). ^[a] Yields determined by ¹H NMR using HMDSO (10 μL) as an internal standard.

To test the effects of alkene equivalents on cyclopropane yield, the reactions were performed in CDCl₃ so that quick NMR analysis could be used to follow the reaction with frequent monitoring to determine the exact point at which the reaction was complete. It was found that there was a clear observable trend that developed, which indicated the more styrene used, the higher the yield of cyclopropane. Considering that using 4 equivalents of alkene did not give a significantly higher yield of cyclopropane (**Table 3.8**, entry 5), it was decided that 2 equivalents of alkene (**Table 3.8**, entry 4) was the optimal amount.

During the screening of solvents to find optimal conditions for the cyclopropanation reaction, it was discovered that impurities in the solvent can have an impact on which product was obtained, either cyclopropane or dihydrofuran. Special care was carried out with purifying solvents by removing any particles by filtration, and acidic impurities by treatment with freshly dried K₂CO₃. A typical procedure used for obtaining dry MeCN was as follows. Stir MeCN (500 mL) over flame dried K₂CO₃ (20 g) for 24 h under nitrogen gas, filter into a dry round-bottom flask containing activated 3 Å molecular sieves. Sparge with nitrogen gas for 15 min and sealed. Both MeCN and CH₂Cl₂ were treated with the procedure above and only cyclopropanation would occur without ever observing dihydrofuran formation. If the solvent contained particles, such as those left from 3 Å molecular sieves without being removed by filtration, dihydrofuran was formed, contaminating the cyclopropane (**Table 3.8**, entry 12). Adding acid to the solvent

gave trace amounts of dihydrofuran to be present (**Table 3.8**, entry 13) indicating the importance of using a basic drying agent (K_2CO_3).

Table 3.8 Optimization of the cyclopropanation reaction using photoreactor #4



Entry	Styrene (Equiv)	Solvent	Time (h)	NMR Yield (%) ^[a]
1	1	$CDCl_3$	2.5	71
2	1.25	$CDCl_3$	2.5	75
3	1.5	$CDCl_3$	2.5	84
4	2	$CDCl_3$	1.5	96 (95) ^[b]
5	4	$CDCl_3$	1.5	98
6	2	MeCN	1.5	98 (95) ^[b]
7	2	$CHCl_3$	2	95
8	2	1,2-DCE	2	92
9	2	EtOAc	2	91
10	2	MeOH	8	0
11	2	H_2O	10	0
12 ^[c]	2	CH_2Cl_2	2	80 ^[d]
13 ^[e]	2	CH_2Cl_2	2	74 ^[d]
14 ^[f]	2	CH_2Cl_2	2	92

The iodonium ylide was used on a 0.1 mmol scale with 1.0 mL of solvent (0.1 M). ^[a] Yields determined by 1H NMR using HMDSO (10 μ L) as an internal standard. ^[b] Isolated yield after column chromatography. ^[c] CH_2Cl_2 was contaminated with particles from 3 Å molecular sieves. ^[d] Product contaminated with dihydrofuran. ^[e] 2 M HCl/Et₂O (0.5 mL) added to CH_2Cl_2 (0.5 mL). ^[f] CH_2Cl_2 pre-dried over K_2CO_3 .

After obtaining optimal reaction conditions and the optimal photoreactor setup, attention was then directed towards understanding the effects of the overlap that occurs between the iodonium ylide's absorbance, and the LED's emission. Some reactions, such as the cyclopropanation of Meldrum's acid iodonium ylide **3.16j** with styrene, take longer to reach completion (24 h) when compared to the cyclopropanation using dimedone iodonium ylide **3.16a** (1.5 h). This difference in reaction time was monitored closely by repeating the reaction and monitoring the appearance of cyclopropane and disappearance of iodonium ylide and the

cyclopropanation of **3.16j** with styrene is consistently slower. To explain these experimental observations, two different approaches were considered to gain insight into how the cyclopropanation reaction works, and if we can shorten the reaction time of ylides such as **3.16j** that react slower than others.

One approach is to use a different LED colour, with a different wavelength of light, with the intention of providing more overlap between the ylide's absorbance and the LED's emission. A violet-coloured LED (λ_{max} 397 nm) was obtained, and the emission was compared together with the standard blue LED (λ_{max} 465 nm) against the UV-Vis absorbance of **3.16j** as shown below in **Figure 3.21**.

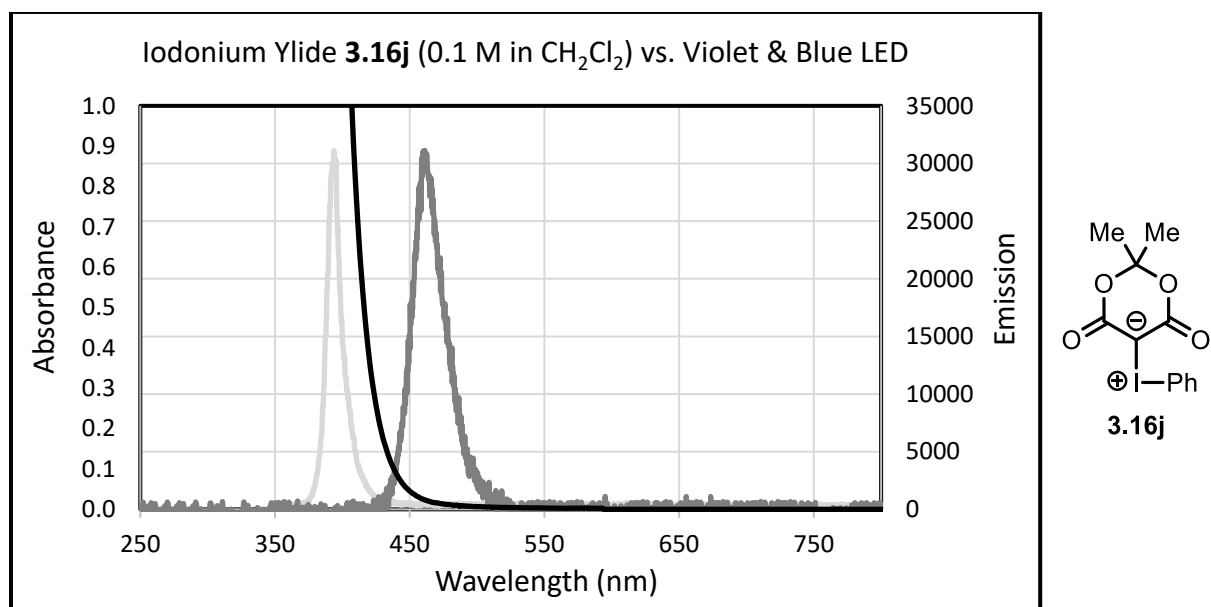
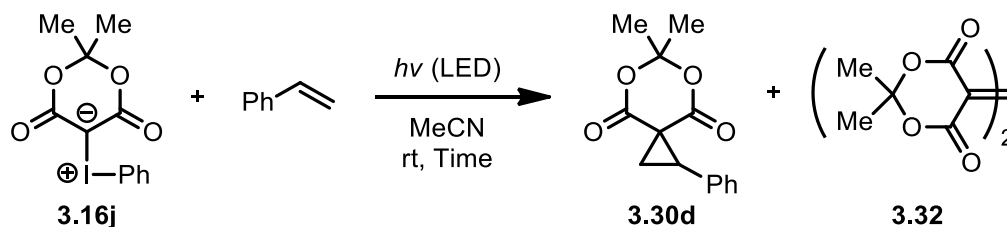


Figure 3.21 Overlay of violet and blue LED with iodonium ylide **3.16j**

Although there is more overlap between the UV-Vis absorbance of iodonium ylide **3.16j** and violet LED light compared to blue LED light, irradiating a mixture of **3.16j** and styrene under the optimized conditions using violet LEDs decreased the yield of cyclopropane to 67%. The rate of the reaction was increased as witnessed by the reaction time dropping from 24 h to 1 h, at which point **3.16j** was fully consumed, but the increased amount of overlap gave an unexpected dimerization side reaction (**Table 3.9**). Dimer **3.32** was detected at 33% and was confirmed by observation of an ESI-LRMS $(M+H)^+ = 285.05$ peak.

Table 3.9 Cyclopropanation of **3.16j** with styrene using violet and blue LED

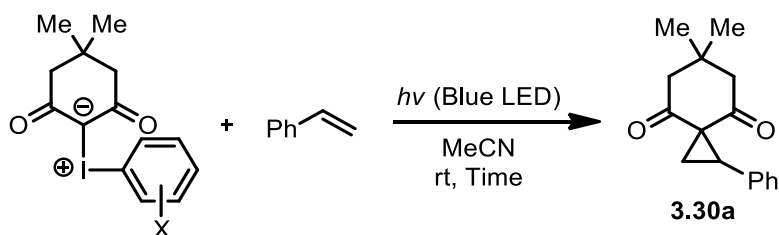


Entry	LED Colour	Wavelength (nm)	Time (h)	Yield (%) ^[a]	Dimer ^[a]
1	Violet	400	1	67	33
2	Blue	465	24	95	0

The iodonium ylide was used on a 0.1 mmol scale with 2 equivalents of styrene and 1.0 mL of solvent (0.1 M). ^[a] Yields determined by ¹H NMR using HMDSO (10 μL) as an internal standard.

A second approach that was considered to increase the rate of cyclopropanation for some of the slower reacting iodonium ylides was designed around the idea that the iodoarene portion of the iodonium ylide is basically a by-product of the reaction as it is not incorporated into the product. Therefore, an opportunity was investigated to see if fine tuning of the iodoarene to induce a bathochromic (red) or hypsochromic (blue) shift in the ylides absorbance could be possible.

Attention was diverted to evaluating the impact of the substitution pattern of the aromatic section of the ylide on the rate and efficiency of the cyclopropanation reaction. Dimedone-derived iodonium ylides containing EDG and EWG on the iodoarene were synthesized, then subjected to our cyclopropanation reaction. In each case, the ylide was consumed within 2.5 h, giving **3.30a** in yields ranging from 59 to 98% as shown below in **Table 3.10**.

Table 3.10 Cyclopropanation of iodonium ylides containing different aryl groups

Entry	Iodonium Ylide (X =)	Time (h)	Cyclopropane Yield (%) ^[a]
1	3.16a (H)	1.5	98
2	3.16b (4-Me)	2	70
3	3.16c (4-Cl)	2.5	70
4	3.16d (4-CN)	1.5	80
5	3.16e (4-CF ₃)	1.5	89
6	3.16f (4-OMe)	2.5	87
7	3.16g (2,6-dimethoxy-4-methyl)	2	59
8	3.16h (1-naphthalene)	1.5	85

The iodonium ylide was used on a 0.1 mmol scale with 2 equivalents of styrene and 1.0 mL of solvent (0.1 M). ^[a] Yields determined by ¹H NMR using HMDSO (10 μ L) as an internal standard.

The results above surprisingly show no correlation between reaction rates or yields and either the electron-poor or electron-rich character of the substrates. For example, **3.16e** which contains an EWG gave **3.30a** in 89% (entry 5) while **3.16f** which contains an EDG gave **3.30a** in 87% (entry 6). UV-Vis absorbances of the iodonium ylides from the table above (**3.16a-3.16h**) were obtained (found in experimental section) and show little deviations in their absorbances in the blue light region. These results agree with the theoretical model of breaking down an iodonium ylide into two isolated light absorbing systems (1,3-dicarbonyl and aromatic) with visible light effecting the 1,3-dicarbonyl system, as adjusting the aromatic system had little effect on the ylides reactivity in blue light.

The experimentally obtained UV-Vis absorbances (0.1 M in CH₂Cl₂) of iodonium ylides **3.16a**, **3.16b**, **3.16h** which contain differences in the aromatic portion of the ylide are shown below in **Figure 3.22**. It can be clearly seen that adjustments made to the aromatic systems cause little change in the UV-Vis absorbance properties of the ylides, which explains why there is essentially no change to the ylides reactivity in blue light. There rest of the UV-Vis absorbances

of iodonium ylides used in these studies can be found in the experimental section at the end of this chapter.

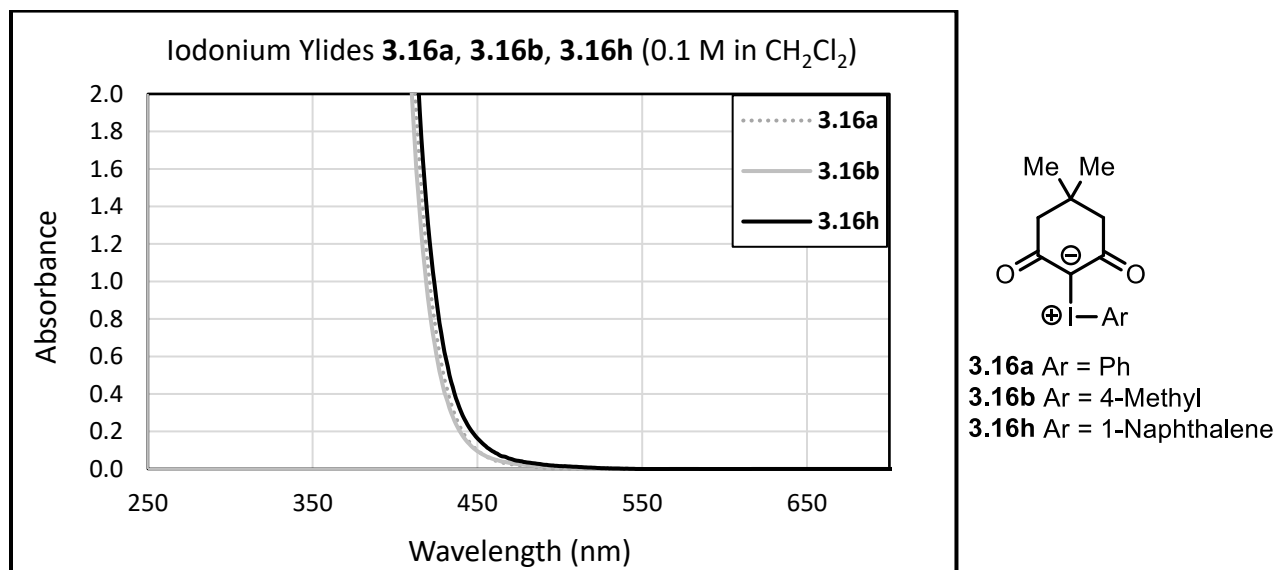


Figure 3.22 Overlap of UV-Vis absorbance of **3.16a**, **3.16b**, **3.16g**, **3.16h** with blue LED

The differences in adjustments made to the 1,3-dicarbonyl system such as switching from ketone-based ylide **3.16a** to keto-ester ylide **3.16i** to pure ester-based ylide **3.16j** showed a blue shift upon increasing ester function incorporation. The experimentally obtained UV-Vis absorbances (0.1 M in CH₂Cl₂) of these three iodonium ylides are shown below in **Figure 3.23**.

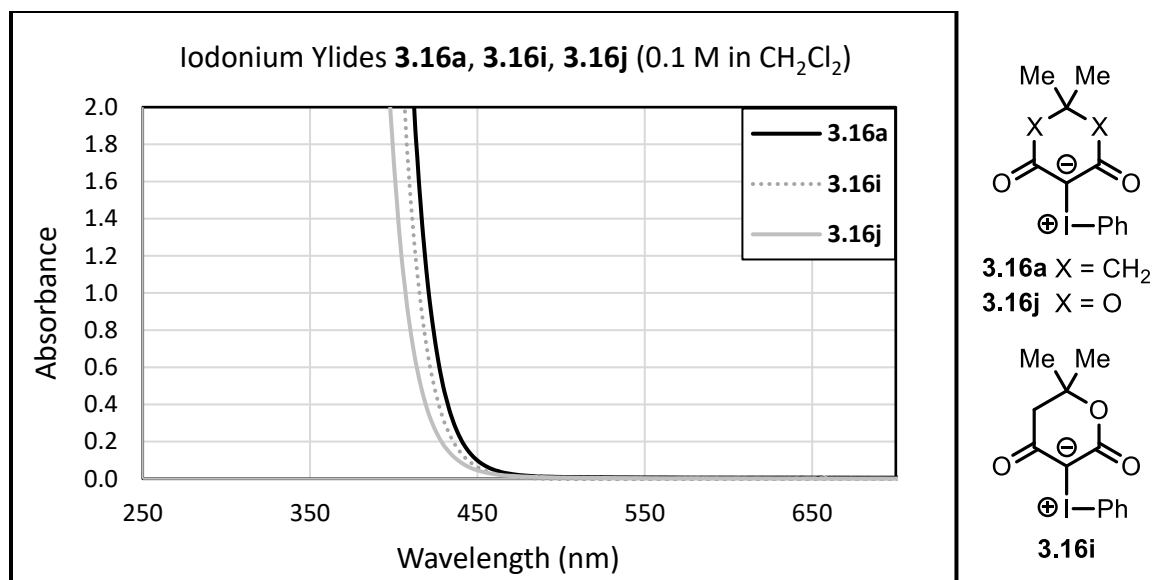
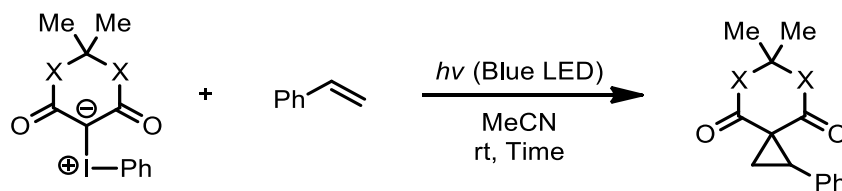


Figure 3.23 Overlap of UV-Vis absorbance of **3.16a**, **3.16i**, **3.16j** with blue LED

The blue shift trend observed upon increasing ester functionality of the iodonium ylide was also paralleled in the rate of cyclopropanation of the ylide with styrene. Ketone-based ylide **3.16a** was fully consumed into cyclopropane in 1.5 h, while keto-ester ylide **3.16i** was consumed after 4 h, and ester-based ylide **3.16j** was consumed after 24 h as shown below in **Table 3.11**.

Table 3.11 Cyclopropanation reaction with different carbonyl-based iodonium ylides



Entry	Iodonium Ylide (X =)	Time (h)	Yield (%) ^[a]
1	3.16a (CH ₂)	1.5	98
2	3.16i (O, CH ₂)	4	94
3	3.16j (O)	24	95

The iodonium ylide was used on a 0.1 mmol scale with 2 equivalents of styrene and 1.0 mL of solvent (0.1 M). ^[a] Yields determined by ¹H NMR using HMDSO (10 μL) as an internal standard.

The idea of improving the rate of cyclopropanation of slower reacting iodonium ylides such as **3.16j** was realized to be an issue and deserving of more time and investigations. The

results provide a deeper understanding of how the cyclopropanation reaction operates and supports the idea of breaking the iodonium ylide into two light absorbing systems with the 1,3-dicarbonyl section having a greater influence on absorbance properties than the aromatic section.

After optimization experiments were performed with the LED-induced cyclopropanation of cyclic iodonium ylides with alkenes, acyclic iodonium ylide systems were investigated. The theory behind this concept is based off the slightly different properties between acyclic and cyclic iodonium ylide systems. Some properties that exist in cyclic iodonium ylides include greater stability in both solution and solid phase storage. Also, acyclic iodonium ylides are less soluble in many organic solvents compared to cyclic iodonium ylides. These considerations developed into a study to investigate how the LED-induced cyclopropanation reaction would respond to acyclic iodonium ylides and alkenes in the presence of visible light, performed under the same optimized conditions already established to be successful for the cyclopropanation of cyclic iodonium ylides.

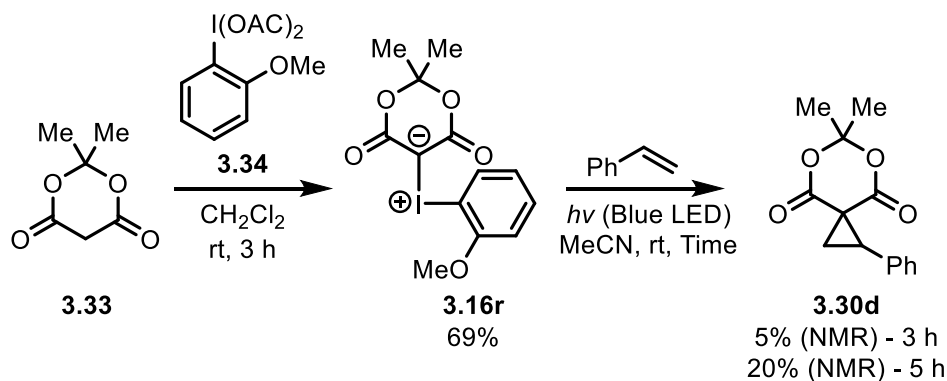
The visible light-induced cyclopropanation of acyclic iodonium ylides with alkenes was investigated, and on average, gave lower yields and longer reaction times when compared to cyclic iodonium ylides (**Table 3.12**). The lower yielding trend can be explained by a photo-induced dimerization of the acyclic iodonium ylide, which does not occur with cyclic iodonium ylides. Another issue that possibly contributed to lower yields was poor solubility, resulting in a suspension of acyclic iodonium ylide when prepared at a 0.1 M concentration in both CH_2Cl_2 and MeCN. Experiments were conducted to address the poor yielding situation such as increasing the equivalents of styrene and switching the acyclic iodonium ylide to a soluble analogue discovered by Zhdankin. The more soluble acyclic analogue containing an *ortho* methoxy group on the ylide's aromatic ring did not lead to a significant change in cyclopropane yield or reaction time as shown below (**Table 3.12**, entries 3-4). There was however a beneficial effect by increasing the equivalents of styrene to 10 equivalents which brought the reaction time down to two hours and resulted in a slightly higher yield of 74% (**Table 3.12**, entry 5) with the remaining mass going to dimerization. Iodonium ylide **3.160** is highly soluble and created a homogeneous solution at 0.1 M but did not bring down the reaction time suggesting the slower rate may be attributed to absorbance properties of the ylide and not dependant on solubility.

Finally, reacting **3.16n** with 20 equivalents of styrene (**Table 3.12**, entry 6) led to the highest yield of cyclopropane at 81%.

Additional attempts to raise the reaction yield and rate of cyclopropane formation from Meldrum's acid iodonium ylide derivatives were based on a concept developed by Zhdankin in 2012.²⁸ In Zhdankin's work, he elegantly and simply just installed an *ortho* alkoxy group (methoxy, propoxy, etc.) onto the iodoarene of the iodonium ylide leading to a more stable, highly soluble ylide via disruption of secondary bonding interactions which was a concept he applied to other systems, such as acyclic iodonium ylides, which consistently achieved higher yielding results and often faster reaction rates due to generally increased better solubility of the iodonium ylide.

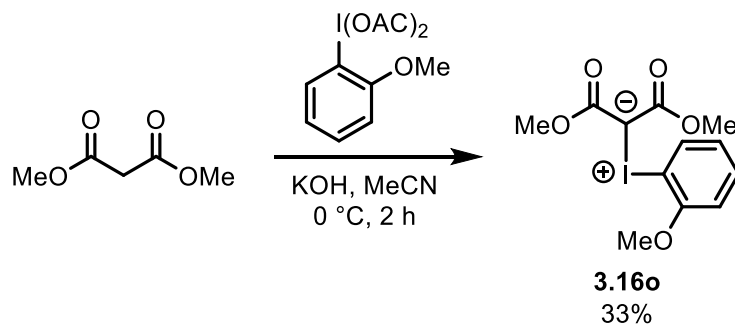
The concept of using an *ortho* alkoxy group on the iodoarene was first attempted with the slower reacting cyclic iodonium ylides such as Meldrum's acid iodonium ylide **3.16j**, then later with acyclic iodonium ylides which also were observed to react at a slow rate.

The use of an *ortho* methoxy group on the iodoarene was examined by preparing iodonium ylide **3.16r** using standard reaction conditions for analogous ylide synthesis reactions as shown below in **Scheme 3.23**. Iodonium ylide **3.16r** was reacted with styrene (2 equiv) under our optimized conditions but gave unsatisfactory results with very little formation of the desired cyclopropane. Obtaining cyclopropane **3.30d** in only 5% (NMR yield) after 3 h and 20% (NMR yield) after 5 h showed increasing the cyclopropanation reaction rate using this approach would not be optimizable with the desired enhancement anticipated. Due to the slow progression of the reaction when compared to similar reactions using dimedone-based iodonium ylide **3.16a** which finish quantitatively after 1.5 h, the approach of using a more soluble iodonium ylide appeared to indicate that solubility was not an issue when it comes to rate enhancement of the light-induced cyclopropanation reaction.



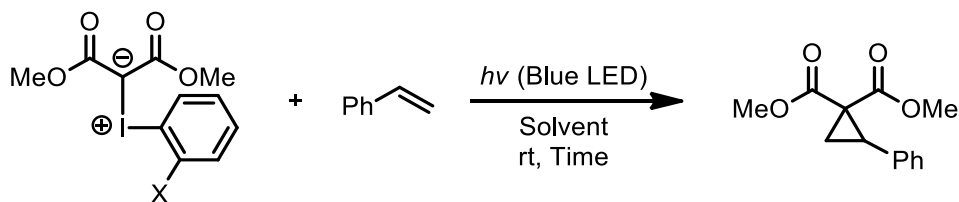
Scheme 3.23 Synthesis of soluble Meldrum's acid iodonium ylide derivative

Synthesis of soluble acyclic iodonium ylide **3.16o** was achieved using the standard iodonium ylide synthesis method as shown in **Scheme 3.24**. Placement of a methoxy group in the *ortho* position of the acyclic iodonium ylide was theorized to provide an ylide with increased solubility properties allowing for investigation into the dependency of the cyclopropane yield on the solubility properties of the ylide.



Scheme 3.24 Synthesis of soluble iodonium ylide derivative

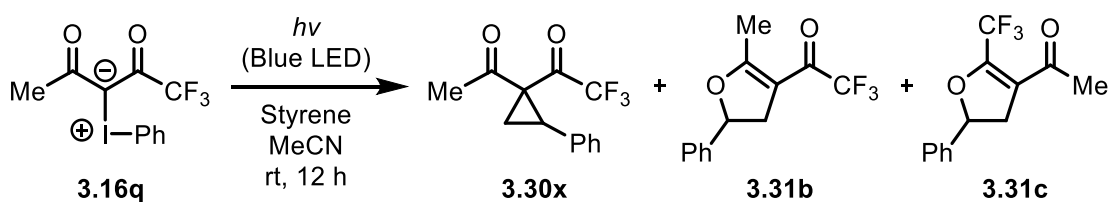
After synthesis of the soluble acyclic iodonium ylide, experiments were performed to evaluate whether enhancing the solubility of the iodonium ylide could yield more cyclopropane product.

Table 3.12 Cyclopropanation of acyclic iodonium ylides

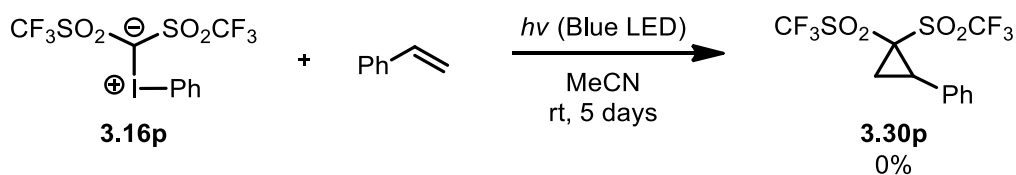
Entry	Iodonium Ylide (X =)	Solvent	Time (h)	Yield (%) ^[a]
1	3.16n (H)	MeCN	17	51
2	3.16n (H)	CH ₂ Cl ₂	29	56
3	3.16o (OMe)	MeCN	22	64
4	3.16o (OMe)	CH ₂ Cl ₂	15	58
5 ^[b]	3.16o (OMe)	MeCN	2	74
6 ^[c]	3.16n (H)	MeCN	3	81

The iodonium ylide was used on a 0.1 mmol scale with 2 equivalents of styrene and 1.0 mL of solvent (0.1 M). ^[a] Yields determined by ¹H NMR using HMDSO (10 μ L) as an internal standard. ^[b] 10 Equivalents of styrene used. ^[c] 20 Equivalents of styrene used.

Other acyclic iodonium ylides containing trifluoromethyl ketone and (trifluoromethyl)sulfonyl groups were subjected to the visible light induced cyclopropanation reaction but gave undesired results. The reaction of trifluoromethyl ketone-stabilized acyclic iodonium ylide **3.16q** with styrene resulted in a mixture of cyclopropane **3.30x** and dihydrofurans **3.31b** and **3.31c** after irradiation with blue LEDs for 12 h as shown below in **Scheme 3.25**.

**Scheme 3.25** Photochemical reaction of trifluoromethyl ketone-stabilized iodonium ylide

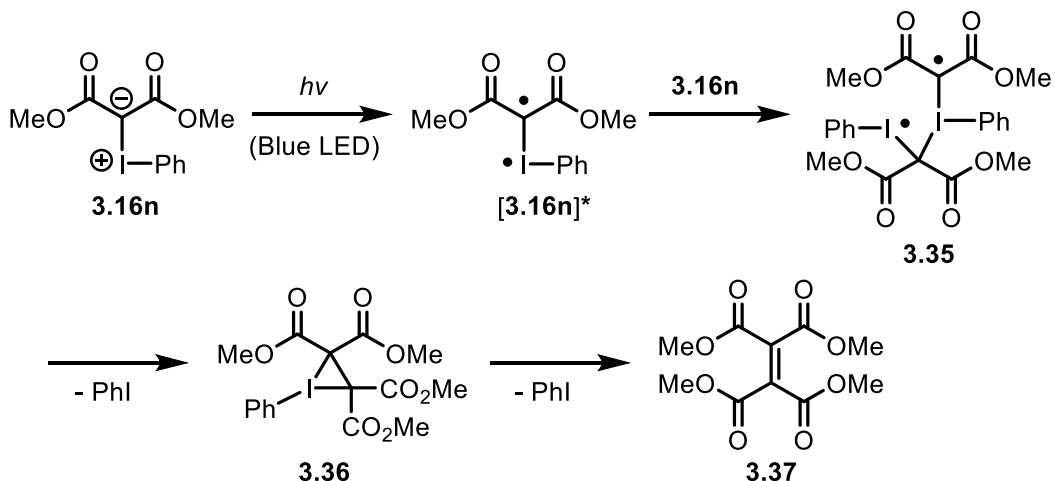
No reaction was observed in the attempted cyclopropanation of (trifluoromethyl)sulfonyl-stabilized acyclic iodonium ylide **3.16p** with styrene as shown below in **Scheme 3.26**. The acyclic SO₂CF₃-stabilized iodonium ylide **3.16p** was recovered quantitatively from the reaction mixture, even after 5 days of irradiation under blue LEDs.



Scheme 3.26 Failed cyclopropanation reaction with SO₂CF₃-stabilized iodonium ylide

When acyclic iodonium ylides are irradiated with blue LED in the presence of alkenes, substantial amounts of iodonium ylide dimerization occurred resulting in a wasteful reaction because the goal was to produce cyclopropanes in an efficient and reliable method. When acyclic iodonium ylides were irradiated with LED in the absence of alkene at 465 and 400 nm, almost quantitative dimerization occurred. The mechanism of the dimerization process is unknown, as no thorough studies have been investigated, and little effort was directed towards performing critical control reactions. The involvement of free carbenes in photochemical-induced reactions of iodonium ylides in literature have been suggested, but never proven with any significant amount of convincing certainty, which begs the question of whether these intermediates exist or not.

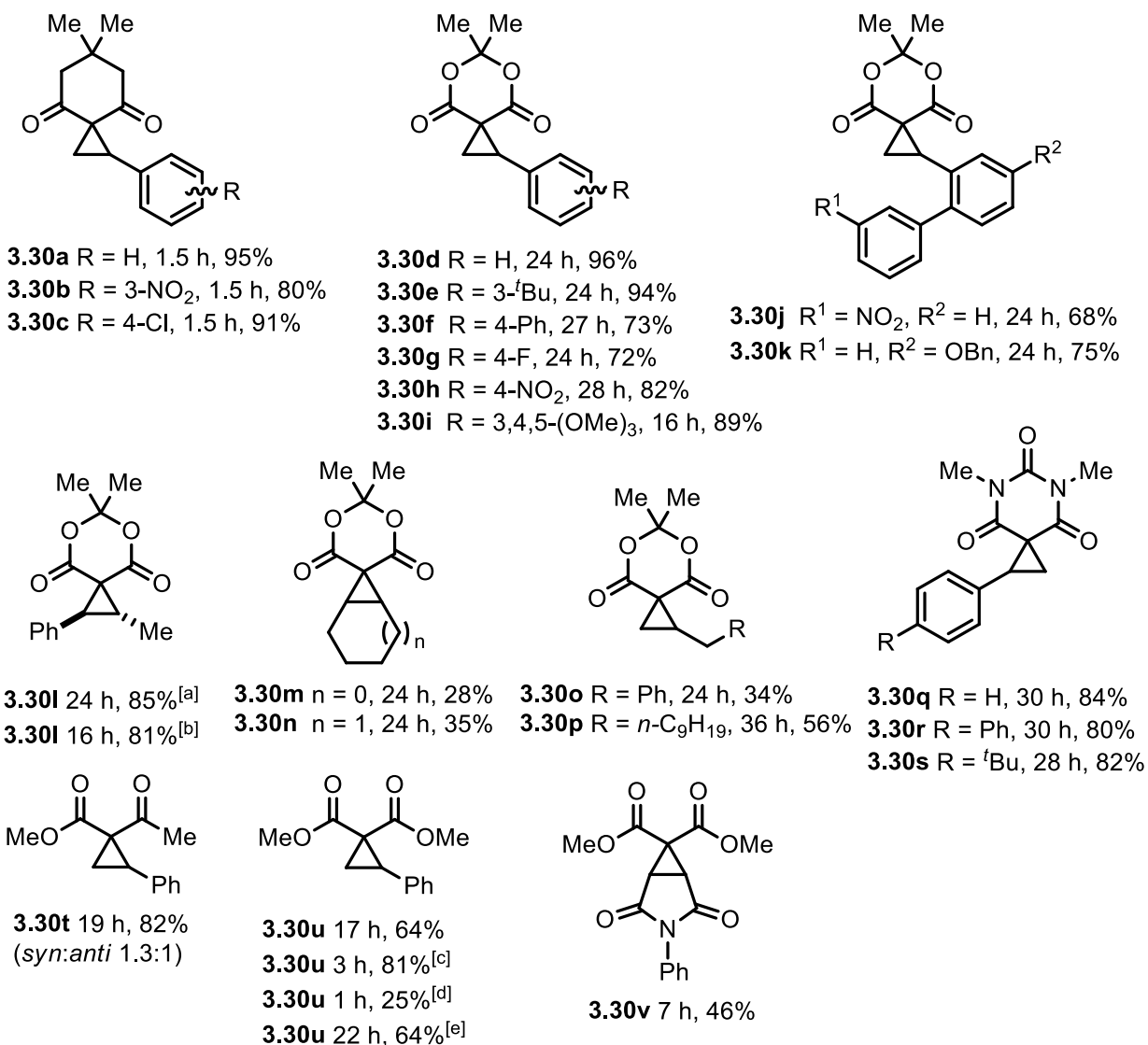
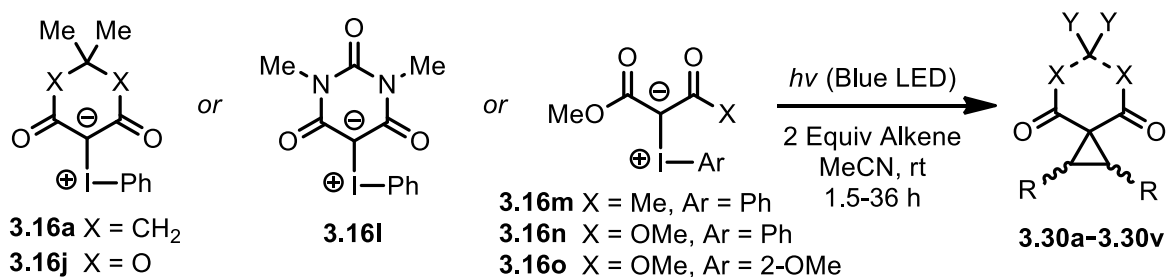
A mechanistic understanding explaining why substantial amounts of the acyclic iodonium ylide underwent dimerization would be of interest because the ability to minimize this side reaction would be beneficial for increasing the overall yield of the desired cyclopropane. For example, acyclic iodonium ylide **3.16n** undergoes LED-induced photoactivation giving intermediate **[3.16n]*** which could then interact with non-excited ground state starting material **3.16n** giving intermediate **3.35**. The statistics of **[3.16n]*** interacting with **[3.16n]*** can essentially be ruled out due to the short lifetimes of these intermediates. Biradical intermediate **3.35** could then fragment, losing iodobenzene and forming a three-membered ring iodo-cycle intermediate **3.36** which has previously been proposed as an intermediate in a thesis describing metal-free dimerization pathways of acyclic iodonium ylides.²⁵⁰ Intermediate **3.36** may undergo fragmentation losing iodobenzene, giving dimerization product **3.37** as shown below in **Scheme 3.27**, in a favourable ring-contraction process by which iodine (III) gets reduced to iodine (I).



Scheme 3.27 Possible photo-induced dimerization pathway of acyclic iodonium ylides

3.8 Cyclopropanation Reaction Scope

After establishing a more detailed understanding of how the visible light-induced cyclopropanation reaction works with different types of iodonium ylides, the attention was then focussed on establishing the scope of the cyclopropanation reaction. Different types of alkenes were investigated using optimized conditions with the intention of demonstrating the reaction viability, showing the successfully synthesized cyclopropanes summarized below in **Scheme 3.28**.



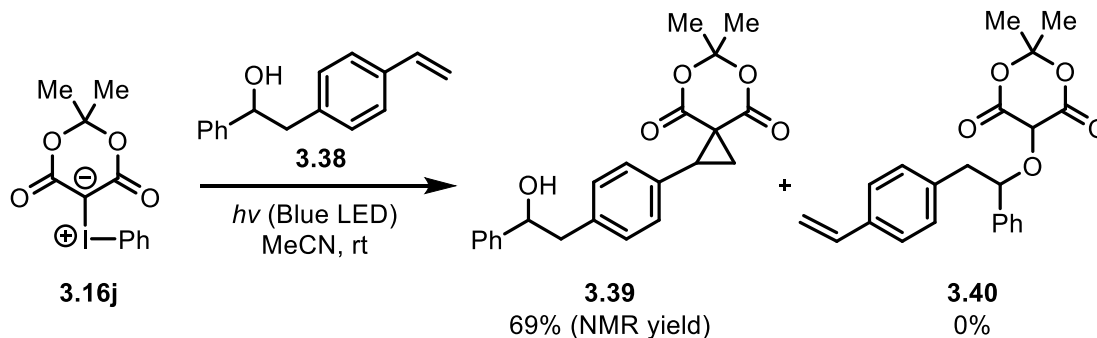
Scheme 3.28 Light-induced cyclopropanation reaction of iodonium ylides with alkenes

^[a] Using *trans*- β -methylstyrene. ^[b] Using *cis*- β -methylstyrene. ^[c] 20 Equivalents of styrene used.

^[d] Violet LED used, also gave 27% of malonate dimer. ^[e] Using soluble iodonium ylide **3.16o**.

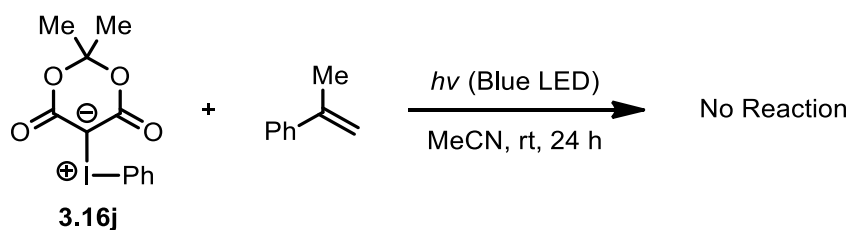
Dimedone-derived iodonium ylide **3.16a** was found to undergo cyclopropanation with *meta* and *para*-substituted styrene derivatives in reaction times of 1.5 h giving **3.30b** in 80% and **3.30c** in 91%. Meldrum's acid-derived iodonium ylide **3.16j** was coupled with styrene derivatives containing either EDGs or EWGs giving cyclopropanes **3.30d-3.30l** in yields ranging from 68-96%. Ylide **3.16j** was also reacted with a variety of non-styrenyl alkenes with limited success giving cyclopropanes **3.30m-3.30p** in yields ranging from 28-56%. Barbituric acid-derived iodonium ylide **3.16l** was effectively coupled with styrene derivatives giving cyclopropanes **3.30q-3.30s** in yields ranging from 80-84%. Acyclic iodonium ylides were then tested, methylacetoacetate-derived iodonium ylide **3.16m** gave cyclopropane **3.30t** in 82% yield, while dimethylmalonate-derived iodonium ylide **3.16n** gave cyclopropane **3.30u** in 64% yield after 17 h but was increased to 81% in 3 h when 20 equivalents of styrene were used. When acyclic soluble ylide **3.16o** was used, which contains an *ortho*-methoxy group known to increase solubility properties, cyclopropane **3.30u** was formed in 64% after 22 h indicating that solubility of the ylide was not relatable to the chemical yield of the cyclopropane. Acyclic ylide **3.16n** was also coupled with *N*-phenylmaleimide to give cyclopropane **3.30v** in 46% yield after 7 h.

An interesting observation was made when running the cyclopropanation reaction with alkenes containing unprotected O-H groups. The chemoselectivity nature of the light-induced cyclopropanation reaction to operate in the presence of unprotected alcohols. Only cyclopropanation was observed without any traces of O-H insertion reactions occurring. If a free carbene was forming in the reaction process, the O-H insertion event may occur, but according to NMR analysis, no O-H product was observed which indicates the chemoselectivity nature of this cyclopropanation reaction (**Scheme 3.29**). This could be beneficial under specific circumstances such as showing an advantage over visible-light induced diazo-based reactions where it has been established that a free carbene is generated after the photo-degradation of the N₂ group, giving a free carbene, capable of performing O-H insertions reactions, amongst many other uncontrollable side-reactions that can lead to undesirable products.



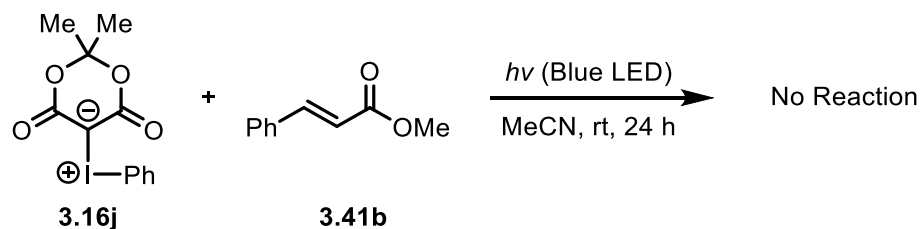
Scheme 3.29 Chemoselective cyclopropanation of **3.16j** with O-H containing alkene

Some alkenes were reacted with cyclic iodonium ylides **3.16a** and **3.16j** under the optimized conditions but did not have success in forming the desired cyclopropane products. Surprisingly ylide **3.16j** did not react with α -methyl styrene to afford cyclopropane (**Scheme 3.30**). This result may simply be attributed to a sterically crowded transition state but obtaining additional mechanistic information to help explain if the reaction failed due to electronic reasons, was not procured.



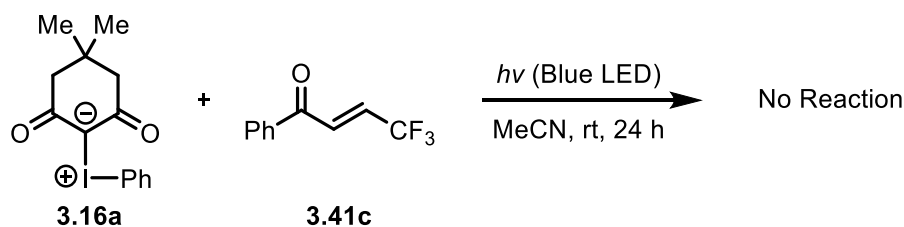
Scheme 3.30 Failed cyclopropanation of **3.16j** with α -methyl styrene

Other alkene substrates that did not react with iodonium ylides in the presence of blue LED include alkenes in conjugation with carbonyl groups (**Scheme 3.31**). Free radicals are atoms with unpaired electron and do not have a full octet, therefore, they are electron deficient. They can be stabilized by resonance, hyperconjugation, and an adjacent EDG. The presence of an EWG such as a carbonyl group lowers the stability of the radical intermediate which might have led to no cyclopropanation product observed (**Scheme 3.31**).



Scheme 3.31 Failed reactions of iodonium ylides with carbonyl-containing alkenes

Another example of a failed reaction that occurred between iodonium ylide **3.16a** and carbonyl-containing alkene **3.41c** is shown in **Scheme 3.32**. There was no observable amount of cyclopropane produced, indicating a limitation of the LED-induced cyclopropanation reaction towards alkenes containing carbonyls. It is not fully understood if conjugation of the alkene to the carbonyl is the source of the failed reaction, or if all carbonyl-containing alkenes will result in failure of the cyclopropanation reaction.



Scheme 3.32 Failed reactions of iodonium ylides with carbonyl-containing alkenes

A list of alkenes that did not undergo the cyclopropanation reaction to fail due to the inability to react with the iodonium ylides are shown below in **Figure 3.24**.

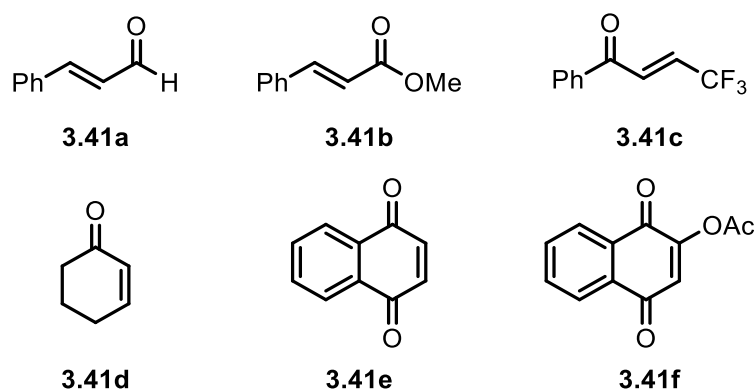


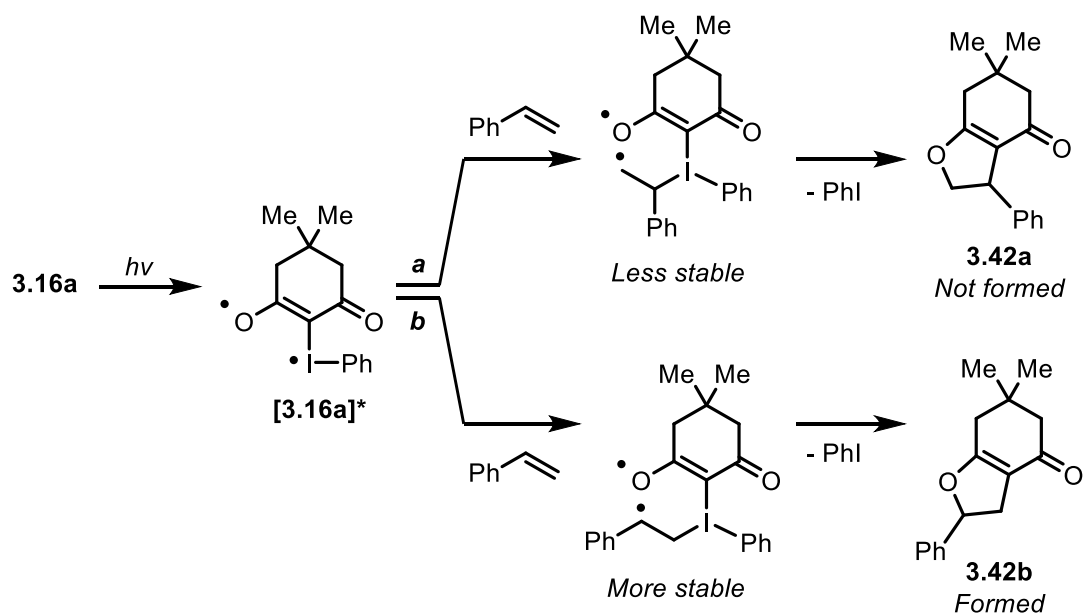
Figure 3.24 Alkenes that did not react with iodonium ylides

3.9 Mechanistic Analysis

In the reactions where dihydrofuran systems were formed and not cyclopropane, the formation of only one single regio-isomer was observed. Based off our working hypothesis on how the photochemical activation of iodonium ylides occurs with blue light, the diradical species that is first formed is in resonance in which a radical is placed on the iodine and the other radical is delocalized over the oxygen carbonyls and α -carbon. Because of the relative stability of this delocalized radical electron compared to the other radical electron on iodine, when styrene approaches this activated biradical system, the electron on iodine would be first to engage with the styrene. Dividing the two possible regio-isomer outcomes into two different pathways that are different in energy is shown in **Scheme 3.33**. The top pathway **a** represents an outcome that is higher in energy than the bottom pathway **b**, due to the placement of the newly formed radical on the terminal position on styrene. The location of this radical is in a primary position and would be less stable than the bottom pathway which places the newly formed radical on the internal position of styrene, which is secondary and benzylic, making this intermediate more stable. In terms of bond strengths, benzylic C-H bonds have bond strengths of approximately 90 kcal/mol and primary C-H bonds are approximately 100 kcal/mol which implies benzylic radicals are easier to form than alkyl radicals.²⁵¹

Studies on the radical-initiated polymerization of styrene using benzoyl peroxide has shown interesting results which help with explaining the observed regioselective preference by examining the reaction mixture. When using benzoyl peroxide as the radical initiator, both isomers were observed to form with the major product coming from the benzylic radical-based intermediate and the minor product coming from the alkyl radical-based intermediate in a 13:1 ratio. The presence of the minor product provides supporting evidence that kinetic factors dominate over thermodynamic factors in this reaction. The minor product would not be expected to form if thermodynamics were the controlling factor in the radical addition.²⁵²

The dihydrofuran isolated from the reaction mixture was characterized using ¹H NMR, and coupling constants, coupling patterns, and chemical shifts were all in agreement with the assignment of the single regio-isomer proposed to form. Analysis of the crude reaction mixture by ¹H NMR indicated that no other products were formed when irradiating iodonium ylides with blue light from LEDs.



Scheme 3.33 Regio-selective pathways for dihydrofuran formation

To study the cyclopropanation mechanism of the reaction, an experiment was designed to observe if the reaction operated through a carbene mechanism. To do this experiment, both *cis*- and *trans*- β -methylstyrenes were reacted with Meldrum's acid iodonium ylide **3.16j** and the cyclopropanes produced were compared and analyzed to probe mechanistic details.

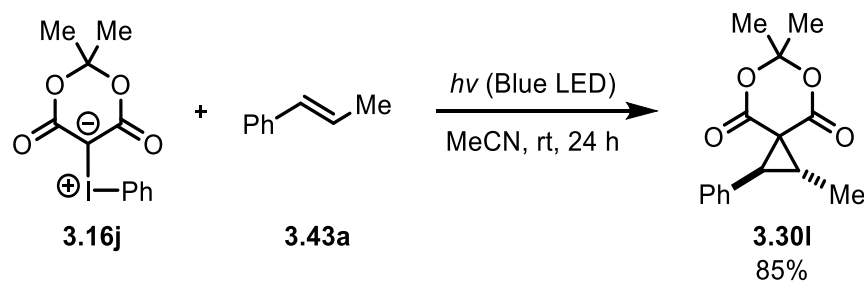
To investigate the mechanism of the visible light-mediated cyclopropanation reaction of iodonium ylides with alkenes, *vicinal* substituted alkenes were used. Both *cis* and *trans* substituted alkenes were used as starting material and monitoring the orientation of these groups in the cyclopropane product was a way of providing mechanistic information.

Mechanistic information was also attempted to be obtained by reacting iodonium ylides with alkenes substituted in a *geminal* relationship. There was the possibility of observing rearrangement that might occur as this would contribute to enhancing our understanding of how this transformation happens.

Results from the blue LED-induced cyclopropanation of Meldrum's acid iodonium ylide with *cis* and *trans*-substituted alkenes are shown below. *Cis* and *trans*- β -methylstyrene were selected as the alkenes of choice to probe this reaction mechanistically because of the similarities in structures. There should be very little difference between these two alkenes in terms of sterics or electronics. Using derivatives of styrene was also important as the best results of the

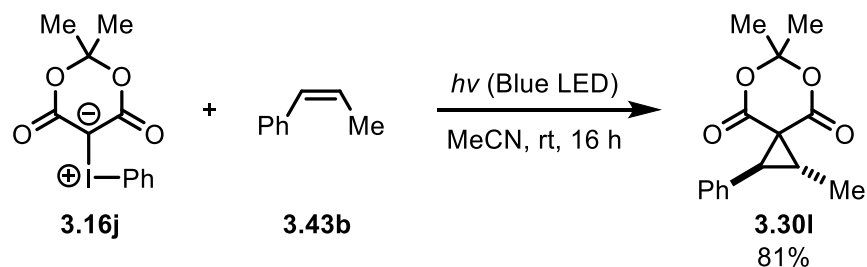
cyclopropanation reaction were obtained when the alkene used was derived from a styrene structure.

Using optimized reaction conditions and the optimized photoreactor, Meldrum's acid iodonium ylide (**3.16j**) was reacted with *trans*- β -methylstyrene (**3.43a**) under blue LED in acetonitrile as shown in **Scheme 3.34**. After 24 hours the reaction was completed, and the crude reaction mixture was checked by ^1H NMR which revealed only a single isomer of cyclopropane (**3.30l**) produced.



Scheme 3.34 Cyclopropanation of iodonium ylide with *trans*- β -methylstyrene

The same optimized reaction conditions were used in the analogous reaction of Meldrum's acid iodonium ylide (**3.16j**) with *cis*- β -methylstyrene (**3.43b**) as shown in **Scheme 3.35**. After 16 hours the reaction was completed, and the crude reaction mixture was checked by ^1H NMR which revealed again, only a single isomer of cyclopropane (**3.30l**). Interestingly, the ^1H NMR spectrum was identical to the spectrum produced from the experiment using *trans*- β -methylstyrene. Assigning the correct stereochemistry to the Meldrum's acid-derived cyclopropane (**3.30l**) was of importance and therefore analysis using ^1H NMR should also be accompanied by an additional method to verify the correct structure. In fact, in literature there are even conflicting reports on whether the characterization data recorded corresponds to the *cis* or *trans* **3.30l** cyclopropane. The exact same ^1H NMR spectra was obtained by two different research groups with one group assigning the spectra to the *cis* isomer²⁵³ and the other research group assigning the spectra the *trans* isomer.²⁵⁴ Due to this confusion, assigning the correct stereochemistry to **3.30l** was challenging and required careful analysis with more than just ^1H NMR data.



Scheme 3.35 Cyclopropanation of iodonium ylide with *cis*- β -methylstyrene

Because identical spectra were obtained from both *cis* and *trans* alkene experiments, assigning the correct relative configuration of the cyclopropane was extremely important and was accomplished by not just relying on ^1H NMR spectra, but obtaining a crystal structure was necessary to clearly identify the position of atoms in three-dimensional space. For this reason, the cyclopropanes were analyzed using X-ray crystallography. Since both experiments gave identical spectra, implying the same cyclopropane isomer formed, it was only necessary to solve the structure from one experiment. Working with the cyclopropane obtained from the *cis*- β -methylstyrene experiment, a crystal was grown by dissolving the cyclopropane in Et_2O creating a saturated solution and allowing slow evaporation to take place overnight. Submitting this single crystal to X-ray analysis revealed the *trans*-cyclopropane. The X-ray crystal of iodonium ylide **3.30I** indicates a *trans vicinal* relationship between the phenyl and methyl groups on the cyclopropane ring (**Figure 3.25**).

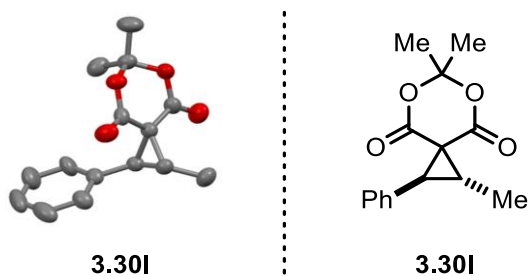


Figure 3.25 X-Ray crystal structure image & molecule of *trans*-cyclopropane **3.30I**

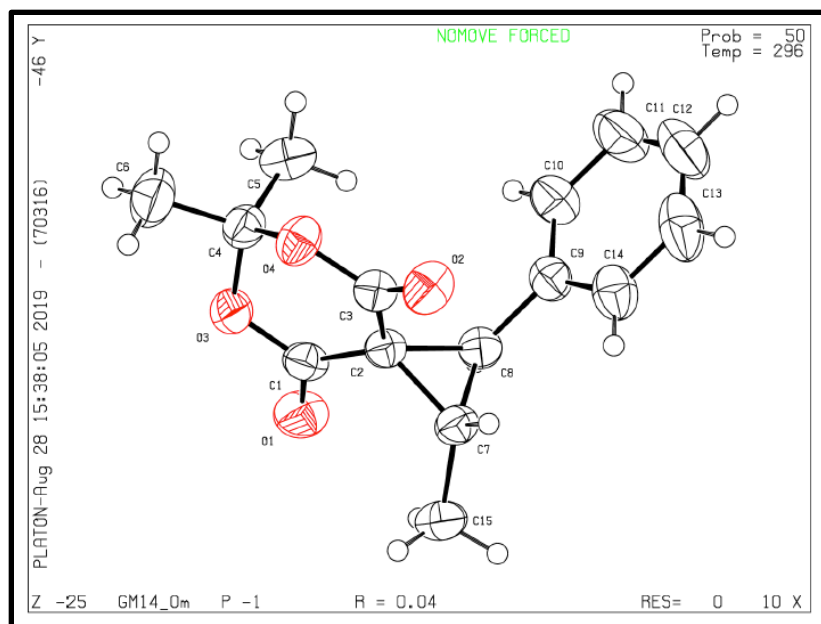


Figure 3.26 Crystal structure of *trans*-cyclopropane **3.301** at 50% probability

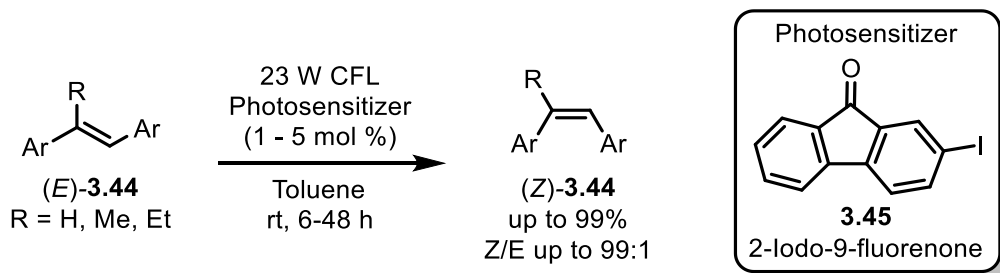
The crystal structure of *trans*-cyclopropane **3.301** has been deposited to the Cambridge Crystallographic Data Centre (CCDC), deposition Number 1949989, and the additional structural data information and parameters used to generate the structure can be found at the end of this chapter in the SI.

3.9.1 Control Reactions for Photo-Isomerization of β -Methylstyrenes

The single *trans* cyclopropane isomer may be interpreted as coming from isomerization of *cis*- β -methylstyrene to *trans*- β -methylstyrene under the photo-irradiation conditions caused by the blue LED light. Therefore, it was necessary to independently confirm if *cis* to *trans* isomerization was happening, or perhaps even *trans* to *cis* isomerization. This was only believed to be a conceivable event because of literature precedence²⁵⁵ that shows similar process happening, but the visible-light-promoted photocatalytic isomerization of (*E*) to (*Z*) alkenes usually happens in the presence of a metal, photosensitizer, or photocatalyst.

Visible-light-promoted photocatalytic isomerization of (*E*) to (*Z*) alkenes is believed to occur due to the presence of ketone-based triplet photosensitizers (**3.45**).²⁵⁵ This methodology

features metal-free reaction conditions and uses a household CFL light bulb (23 W) as the light source as shown in **Scheme 3.36**.



Scheme 3.36 Photocatalytic (*E*) to (*Z*) isomerization of alkenes by visible light

This allows for the synthesis of both electron-rich and electron-deficient *Z*-alkenes with different types of functional groups tolerated on the alkene. This could be a possible way of describing a photo-induced rearrangement of *cis* to *trans* β -methylstyrene which would ultimately yield a possible mixture of *cis* and *trans* cyclopropanes, or conversion of *cis* to *trans* cyclopropane, but was ruled out by performing the following control reactions.

Subjecting both *cis*- and *trans*- β -methylstyrenes to visible light (blue LED, λ_{max} 465 nm) resulted in no photo-induced isomerization of the alkene double bond. These results are consistent with the understanding that photo-induced isomerization of alkenes requires higher amounts of energy such as that supplied under UV irradiation.

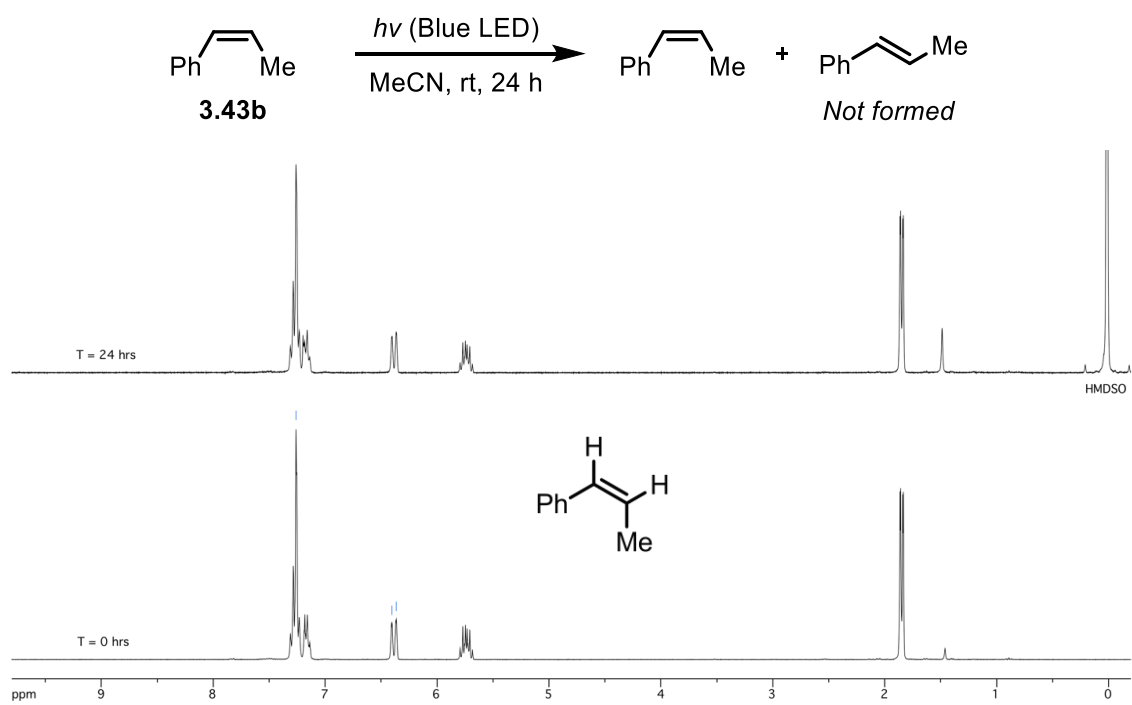


Figure 3.27 Photo-induced isomerization check of *cis*- β -methylstyrene

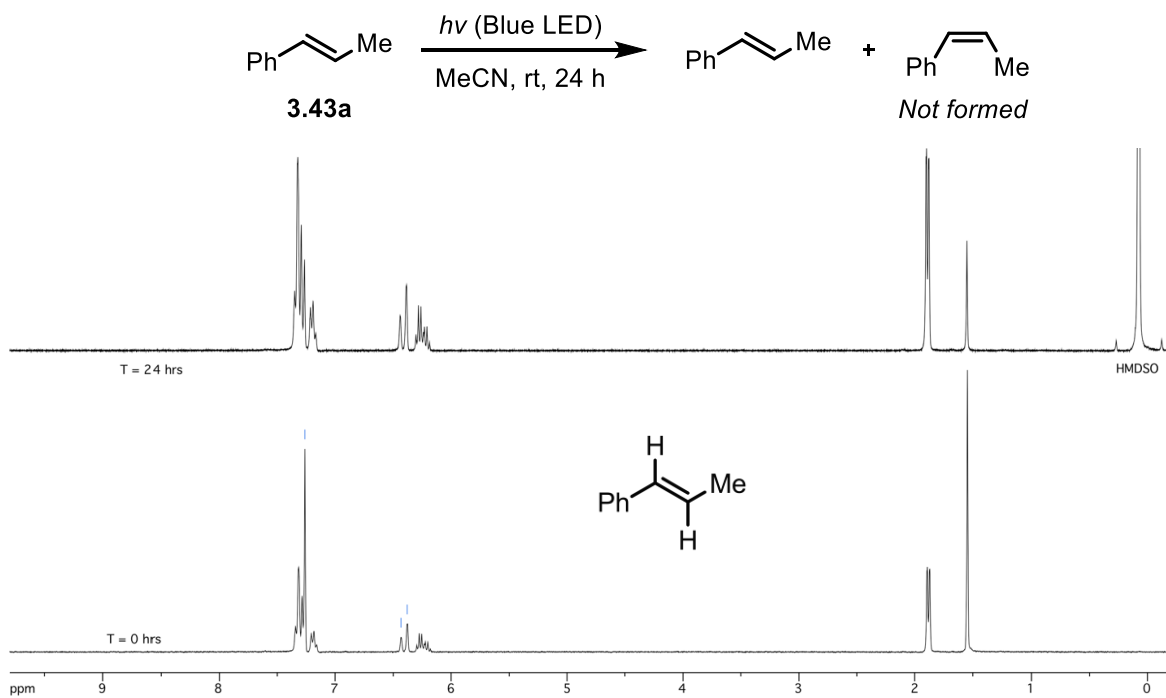
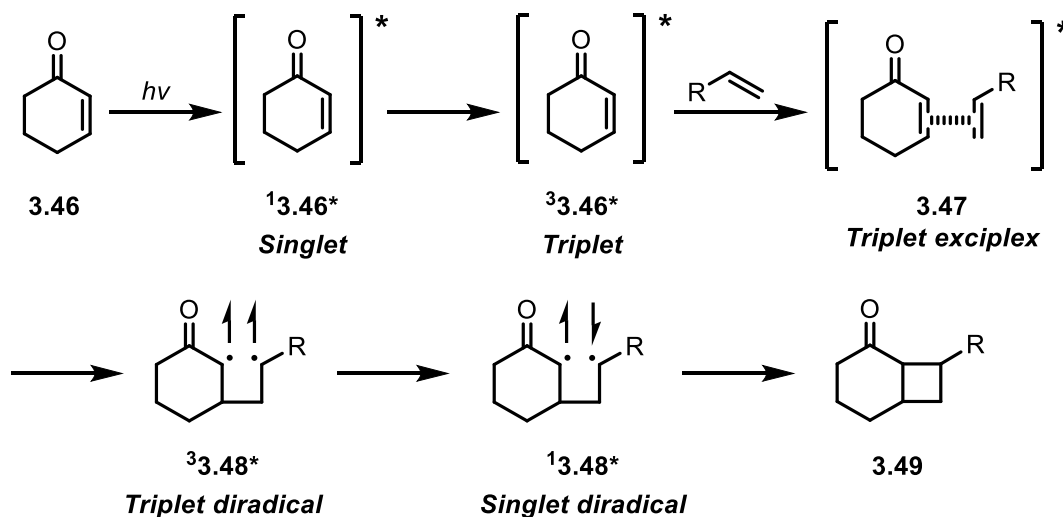


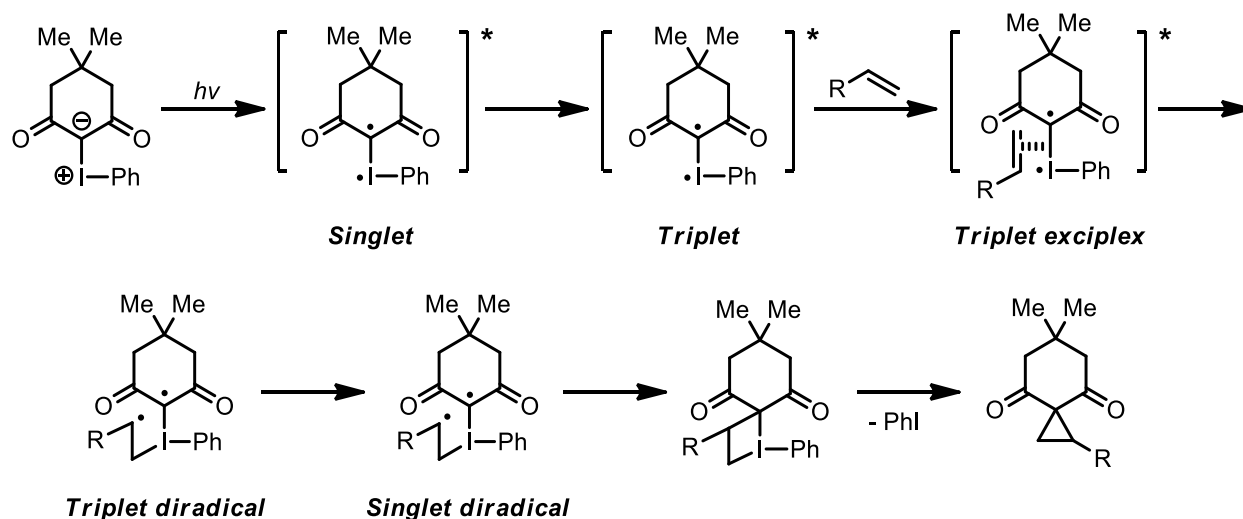
Figure 3.28 Photo-induced isomerization check of *trans*- β -methylstyrene

As observed in the literature in photo-initiated [2+2] cycloaddition reactions, such as the formation of cyclobutanes from α,β -unsaturated ketones and alkenes, there have been different mechanisms proposed. As more experimental evidence is gathered, the mechanism can be refined and gives a more accurate representation of what is occurring at the atomic level in this transformation. The mechanism of [2+2] photo-induced cyclization is believed to begin with photoexcitation of enone **3.46** to a singlet excited state ($^1\mathbf{3.46}^*$). The singlet state is typically very short lived, and intersystem crossing to the triplet state ($^3\mathbf{3.46}^*$) then occurs. At this point, the enone forms an excited complex (**3.47**, exciplex) with the ground-state alkene, eventually forming a triplet diradical intermediate ($^3\mathbf{3.48}^*$). For ring closure to take place and give cyclobutane product **3.49**, spin inversion to the singlet diradical ($^1\mathbf{3.48}^*$) must occur as shown in **Scheme 3.37**. Therefore, the overall prevailing mechanism of [2+2] cycloadditions under photo-excited conditions, has been shown to operate through a light-activated complex, formed between the alkene and activated enone.²⁴³



Scheme 3.37 Light-induced [2+2] cycloaddition between ketones and alkenes

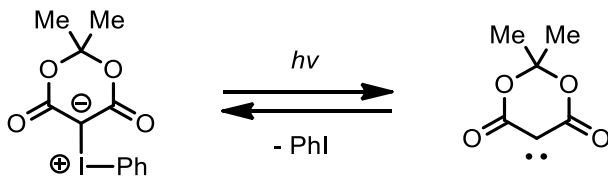
There are similarities between the above photo-induced [2+2] cycloaddition reaction and our cyclopropanation reaction between iodonium ylides and alkenes. The fact that both *cis*- β -methylstyrene and *trans*- β -methylstyrene produced the same cyclopropane isomer from independent reactions provides evidence into the mechanism shown below, which is entirely consistent with the initial proposed mechanism.



Scheme 3.38 Photo-induced formal [2+2] asynchronous cycloaddition reaction mechanism

The triplet diradical intermediate produced must undergo spin inversion to the singlet diradical before forming the four-membered iodo-butane ring. This gives a short window of time for carbon-carbon bond rotation to occur before the ring closes. It is during this time that both *cis*- β -methylstyrene and *trans*- β -methylstyrene can undergo rotation and give the same cyclopropane isomer. This could be rationalized by the more thermodynamically stable *trans* cyclopropane isomer, or an intermediate, such as the four-membered iodo-cycle, that is more thermodynamically stable.

The question of whether the iodonium ylide undergoes free carbene formation is a long-lived question that researchers have not fully answered. The formation of the high energy free carbene seems unlikely as no insertion (O-H, N-H) products are observed to form, and no dimerization of the starting material is ever present. The iodobenzene produced may reversibly bind to the free carbene, reforming the iodonium ylide in a relatively fast process compared to other side-reactions that may occur.



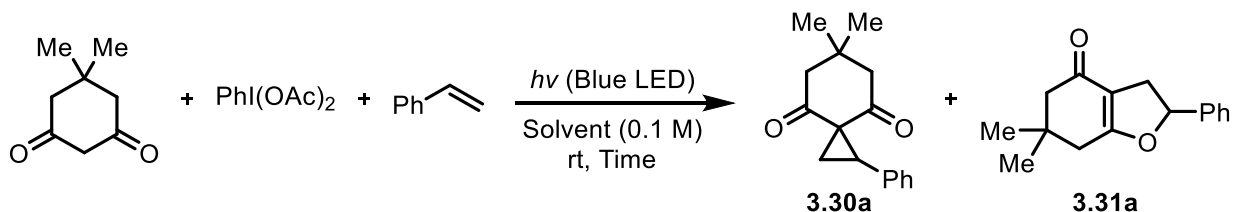
Scheme 3.39 Free carbene generation from iodonium ylides

Due to the limitations of today's technology, an accurate mechanism may be hard to fully describe, but so far, the diradical process occurring in a photo-induced formal [2+2] asynchronous cycloaddition reaction mechanism seems probable and is supported by experimental evidence observed in the merging isomerization process of the *cis* and *trans*- β -methylstyrenes converging into the single *trans* isomer cyclopropane.

3.10 One-Pot Cyclopropanation Reaction

Testing the tandem *in situ* iodonium ylide formation, followed by cyclopropanation reaction, with dimedone, $\text{PhI}(\text{OAc})_2$ and styrene all being conducted under blue LED showed promising results for eventually making this visible-light methodology into potentially a one-pot synthetic procedure if desired. The overall yield (determined using ^1H NMR) was a combined yield of both, the cyclopropane plus the dihydrofuran added up.

Table 3.13 One-pot cyclopropanation reaction with dimedone

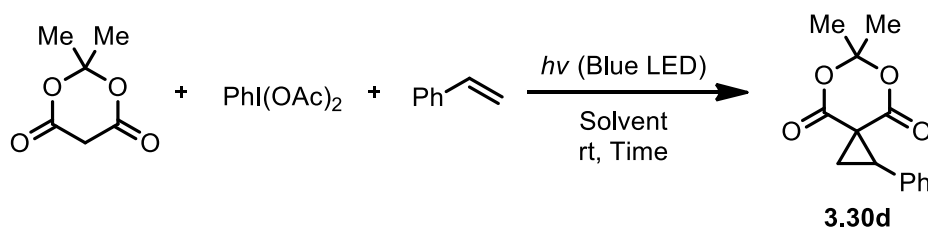


Entry	Solvent	Time (h)	(3.30a:3.31a) Ratio	Overall Yield (%) ^[a]
1	CDCl_3	2	1:1	80
2	CH_2Cl_2	4	10:1	84
3	MeCN	2	3.30a (Pure)	86

Dimedone was used on a 0.1 mmol scale with 1 equivalents of $\text{PhI}(\text{OAc})_2$ and 2 equivalents of styrene with 1.0 mL of solvent (0.1 M). ^[a] Yields determined by ^1H NMR using HMDSO (10 μL) as an internal standard.

The large differences in ratios between the cyclopropane and dihydrofuran, such as (Table 3.13, entry 2) could mainly be attributed to the solvent purity or water level content. Using solvents such as CH₂Cl₂ could have had a larger influence in the product distribution ratio but not much additional care was taken to ensure dry conditions were achieved. Such as, no distillation was taken place, and no previous attempts to filter out any impurities were performed, the solvent was just used directly out of the 4-litre bottle with no extra methods of drying or purifying to the best of our knowledge.

Table 3.14 One-pot cyclopropanation reaction with Meldrum's acid

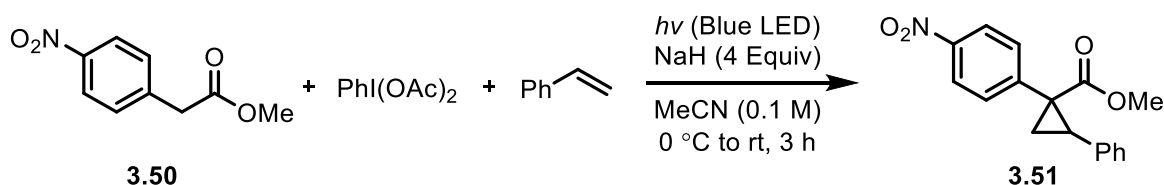


Entry	Solvent	Time (h)	Yield (%) ^[a]
1	CDCl ₃	24	32
2	MeCN	20	62
3	MeCN	24	60

^[a] NMR yield of cyclopropane using 10 μL HMDSO as the internal standard. 1 Equivalents of PhI(OAc)₂ and 2 equivalents of styrene used.

Acyclic iodonium ylides containing only a single carbonyl group were subjected to a one-pot cyclopropanation reaction. Optimized conditions that were successful for cyclic dicarbonyl iodonium ylides, unfortunately failed to produce any cyclopropane. Specific conditions were eventually realized for the formation of α-aryl ester systems. The reaction was sensitive to temperature and required using NaH as the base, while bases like NaOMe or K₂CO₃ were not useful for this reaction, even when previously dried under standard conditions found in the purification of laboratory chemicals handbook.²⁵⁶ The best conditions discovered for this one-pot cyclopropanation reaction are shown below in **Table 3.15**.

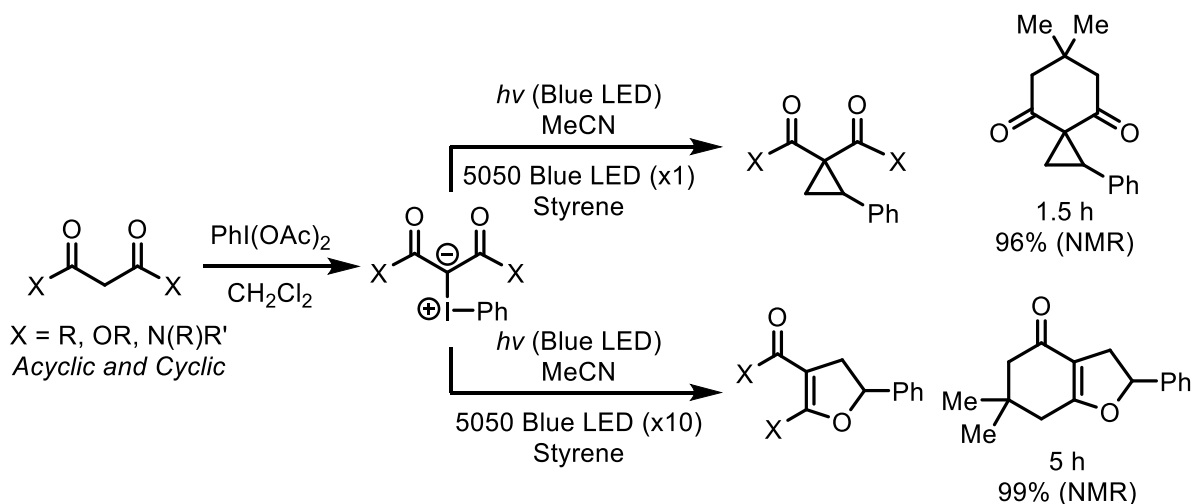
Table 3.15 One-pot cyclopropanation reaction of α -aryl ester with styrene



Entry	α -Aryl Ester	Yield (%) ^[a]
1	0.1 mmol	42
2	0.2 mmol	49

The α -aryl ester was used on a 0.1 mmol scale (unless otherwise noted, 0.2 mmol) with 1 equivalent of $\text{PhI}(\text{OAc})_2$ and 2 equivalents of styrene with 1.0 mL of solvent (0.1 M). ^[a] Isolated yield after column chromatography.

A more general approach that could involve both dihydrofuran (Condition 2) or cyclopropane (Condition 1) synthesis starting from the same alkene and dicarbonyl starting materials would be a nice addition to the methodology. A scheme which represents this dual pathway possibility is shown below in **Scheme 3.40**.



Scheme 3.40 One-pot cyclopropanation or dihydrofuran reaction

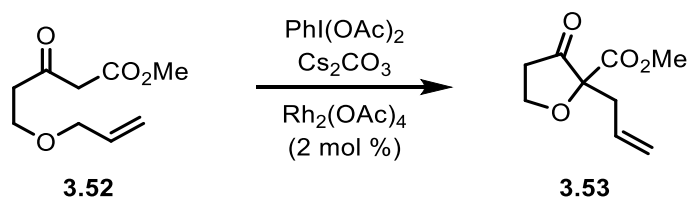
3.11 Applications of Blue Light Induced Reactivity of Iodonium Ylides

This section will discuss newly discovered applications of light induced reactions of iodonium ylides. After the discovery that blue light has the energy required to drive HOMO to LUMO excitation in iodonium ylides, generating a higher energy activated species that is

capable of engaging with reaction partners such as alkenes to form cyclopropanes, it is theoretically possible to engage the photo-induced activated intermediate with other reaction partners for the construction of new products. Investigations to see if visible-light induced activation of iodonium ylides to participate in rearrangement, oxidation, O-H insertion, cycloaddition, or transylidation reactions would be worth-while, and may have the possibility of working if the correct conditions can be found.

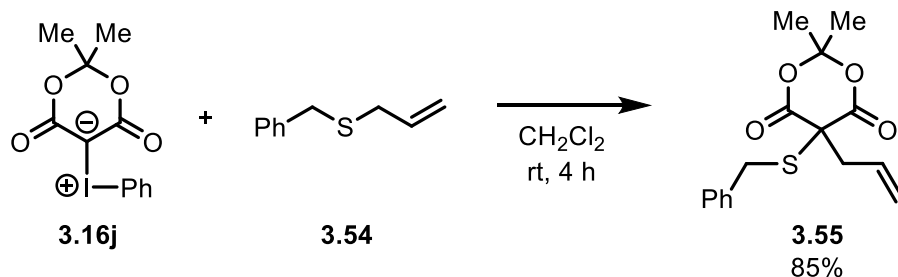
3.11.1 Blue Light Induced Rearrangements

The ability of diazonium and iodonium ylides to undergo metal-catalyzed [1,2] or [2,3]-rearrangement reactions is documented in the literature, such as work performed by Murphy and West in 2006.²⁵⁷ In West's report, starting material **3.52** was shown to react with metals, giving metallocarbenes that were capable of participating in a tandem transylidation reaction through the conversion to allyl- or benzyl-substituted oxonium ylides, which was followed by a sigmatropic rearrangement to give the corresponding heterocycle **3.53** as shown below in **Scheme 3.41**.



Scheme 3.41 Rearrangement reaction of iodonium ylides generated *in situ*

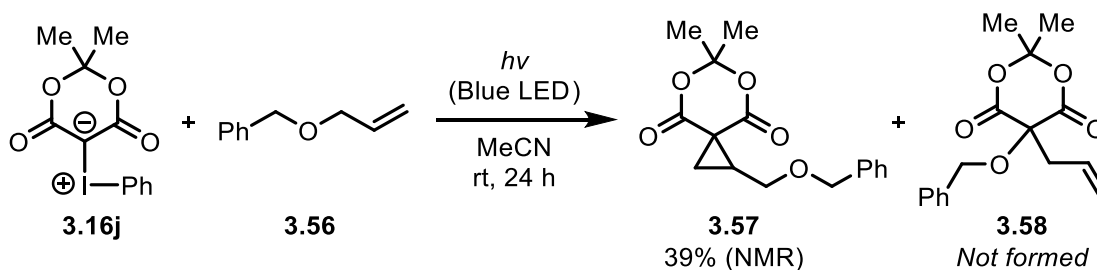
An additional example that shows iodonium ylides capable of engaging in rearrangement style reactions is shown below in **Scheme 3.42**. This tandem transylidation reaction followed by [2,3]-sigmatropic rearrangement was reported by Dai in 1992.²⁵⁸ In the overall process an allylic group, and a sulfide group from **3.54** are transferred to the α -carbon of the iodonium ylide in one efficient overall reaction giving **3.55** as the final product.



Scheme 3.42 Rearrangement reaction of iodonium ylide with allylic sulfide

The ability to make the transition metal catalyzed rearrangement reaction into an equivalent metal-free reaction would be of interest to the synthetic community, and therefore exploration into the possibility of eliminating metals from the reaction was examined.

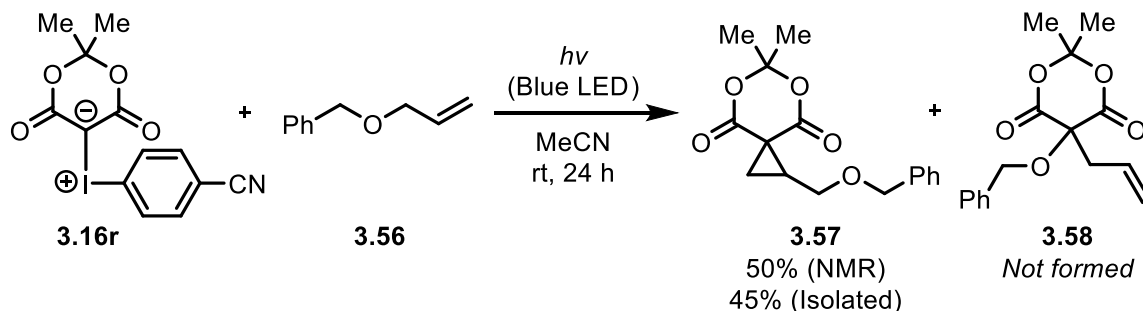
The question of whether iodonium ylides can participate in visible light-induced rearrangement reactions was tested to see if this transformation could be accessed. The following scheme shows how cyclic iodonium ylides were reacted with allylic ether **3.56** in the hopes of forming a rearranged product **3.58**, or if just a cyclopropanation reaction would occur to give cyclopropane **3.57**. The theory behind this attempted rearrangement is believed to originate from halogen bonding interactions between the oxygen and the iodine center of iodonium ylide. These interactions have been shown to exist with the iodine in the HVI system and heteroatoms such as nitrogen or oxygen. The combination of halogen bonding with photochemistry has not been explored or reported currently in literature.²⁵⁹



Scheme 3.43 Cyclopropanation vs. rearrangement reaction of iodonium ylides

Adjusting the aryl iodide to contain an EWG at the *para* position was next performed to check for any increase in reactivity. It can be theorized that the HVI atom is already electrophilic

in nature, but the presence of an EWG may increase the electrophilic iodide to a greater extent and create a stronger attraction to the oxygen of the ether.

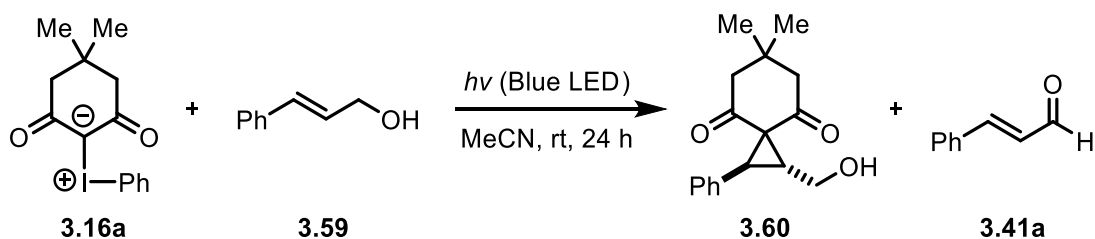


Scheme 3.44 Cyclopropanation vs. rearrangement reaction of iodonium ylides

Unfortunately, the use of blue light and the cyclic iodonium ylides tested did not undergo a rearrangement process with allylic ether **3.56**. The outcome was the formation of cyclopropane **3.57** which is still a useful reaction as a 45% isolated yield. This relatively higher yielding cyclopropanation reaction may be attributed to halogen bonding between the oxygen atom in the allylic ether with the HVI atom in the iodonium ylide, but this is still just theoretical speculation as no further experiments were conducted to test this hypothesis.

3.11.2 Blue Light-Induced Oxidation of Allylic Alcohols

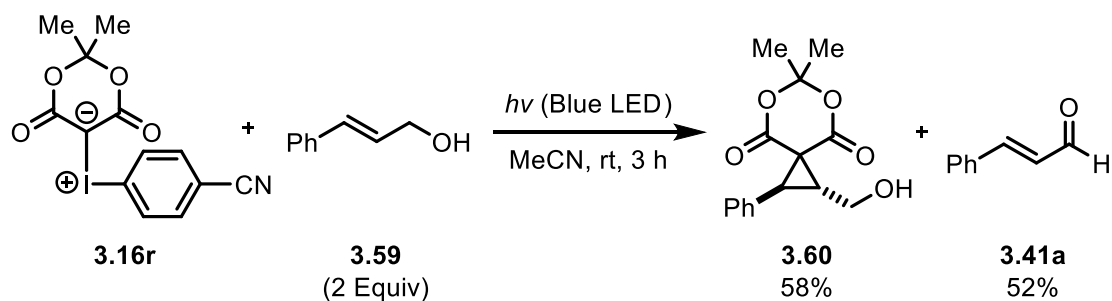
In attempts of exploring broader types of styrene derivatives for the light-activated cyclopropanation reaction with iodonium ylides, it was discovered that using allylic alcohols such as cinnamyl alcohol (**3.59**), oxidation of the alcohol to cinnamaldehyde (**3.41a**) was unexpectedly observed, in addition to formation of cyclopropane **3.60** as shown in **Table 3.16**. It also should be noted here that only the *trans*-cinnamaldehyde product was observed to form, based off ^1H NMR analysis.

Table 3.16 Light-activated oxidation of allylic alcohols with iodonium ylide

Entry	Ylide (Equiv)	Alcohol (Equiv)	Cyclopropane (%) ^[a]	Aldehyde (%) ^[a]
1	1	2	32	57
2	2	1	47	46

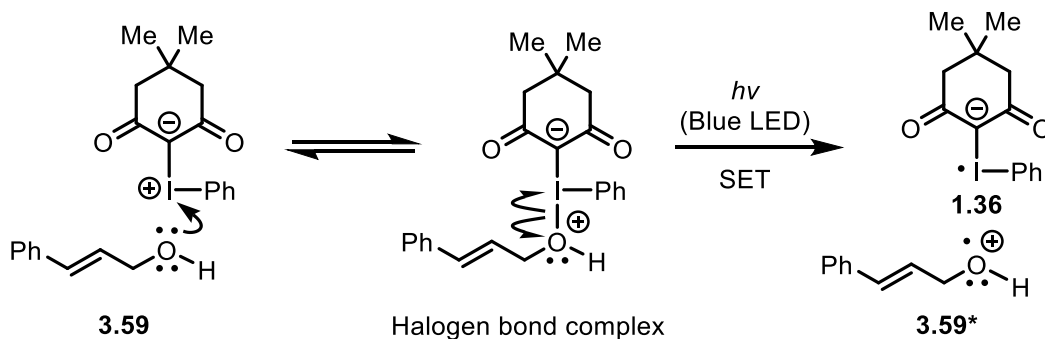
The iodonium ylide was used on a 0.1 mmol scale with 1.0 mL of solvent (0.1 M). ^[a] Yields determined by ¹H NMR using HMDSO (10 μ L) as an internal standard.

Using an EWG at the *para* position such as a nitrile group, was intended to increase the electrophilicity of the iodine in the iodonium ylide to encourage an initial complex to form with the oxygen present in the alcohol. Using two equivalents of cinnamyl alcohol (**3.59**) and reaction with Meldrum's acid-derived iodonium ylide (**3.16r**) gave approximately a 1:1 mixture of cyclopropane and aldehyde. Although there appeared to be no difference to product ratio proportions (cyclopropane:aldehyde still 1:1), the reaction time was increased down to 3 h, as checked by TLC as shown in **Scheme 3.45**.

**Scheme 3.45** Light-activated oxidation of allylic alcohols with iodonium ylides

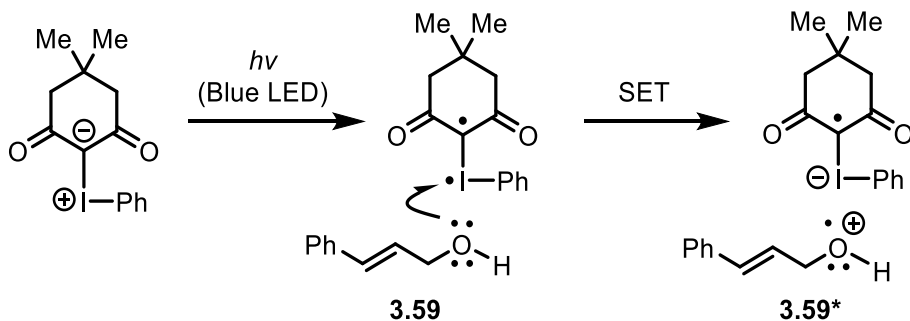
Lewis acids such as $\text{BF}_3 \cdot \text{OEt}_2$ are known to enhance the oxidizing ability of iodonium ylides by forming a complex, providing a stronger SET-oxidant.²⁶⁰ Adding $\text{BF}_3 \cdot \text{OEt}_2$ to the oxidation reaction of allylic alcohols with iodonium ylides might be a way of tuning the reactivity to selectively form more of the oxidized product and less of the cyclopropane product.

In terms of the mechanism, the reaction may possibly be occurring through a combination of halogen bonding and photo-activation. The concept of first forming a halogen bond complex followed by blue light activation of the complex is being proposed to mechanistically make sense of the observed oxidation of allylic alcohol **3.59** to aldehyde **3.41a**. The ability of iodonium ylides to induce a SET event under photo-chemical activation has been proposed in the literature, including a recent report from 2021.²⁶¹ It is not clear whether photo-chemical activation occurs before or after the alcohol is “docked” with the iodonium ylide. The proposed mechanism shown in **Scheme 3.46** illustrates a possibility in which halogen bonding occurs first, followed by an excitation event with irradiation from the blue LEDs to form intermediates **1.36** and **3.59***.



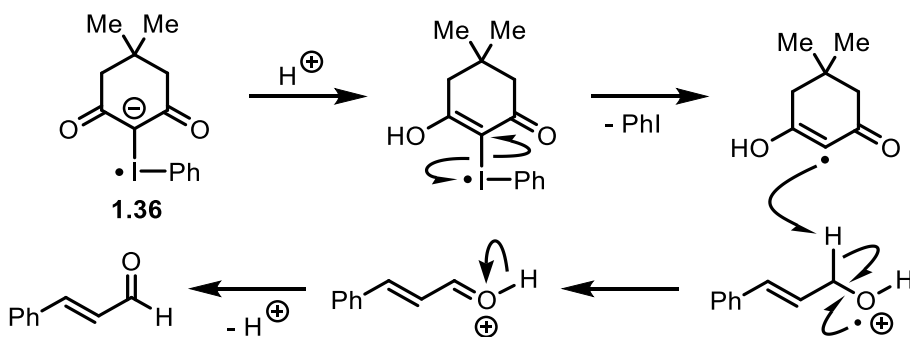
Scheme 3.46 Mechanism for oxidation of allylic alcohols with iodonium ylides

An alternative proposed mechanism shown below illustrates a possibility in which an excitation event with irradiation from the blue LEDs occurs first, generating a biradical intermediate. This biradical intermediate could then, in theory, initiate the transfer of a single electron (SET) from allylic alcohol **3.59** to give the same radical cation intermediate **3.59*** from the above scheme, as shown below in **Scheme 3.47**. The mechanism shown below is theoretically less likely to occur based on observations made when reacting iodonium ylides with SET reagents such as copper (I). In chapter 1 (**Figure 1.22**) where SET reactions of iodonium ylides are mentioned, intermediate **1.36** is shown to preferentially occur, which supports a mechanism represented by **Scheme 3.46** above. The reaction of copper (I) with iodonium ylides is also reported in the literature with intermediate **1.36** being proposed as seen in chapter 1 (**Scheme 1.37**).



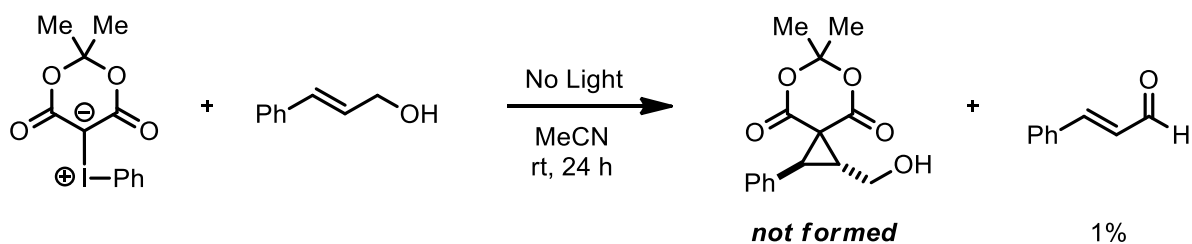
Scheme 3.47 Alternative mechanism for oxidation of allylic alcohols with iodonium ylides

After formation of radical-based intermediates **1.36** and **3.59***, the following mechanism could explain the formation of aldehyde **3.41a** as shown below in **Scheme 3.48**. There were no mechanistic studies performed on this oxidation reaction, so the mechanism presented is purely theoretical, but involves the more likely intermediate **1.36**.



Scheme 3.48 Mechanism for oxidation of allylic alcohols with iodonium ylides

A control reaction for the oxidation of the allylic alcohols with iodonium ylides was performed to understand if the process was light-dependent or not. The control reaction, which was run in complete darkness (no ambient light entered the system) did not produce any significant amount of cinnamaldehyde (**3.41a**) oxidation product as shown below in **Scheme 3.49**.

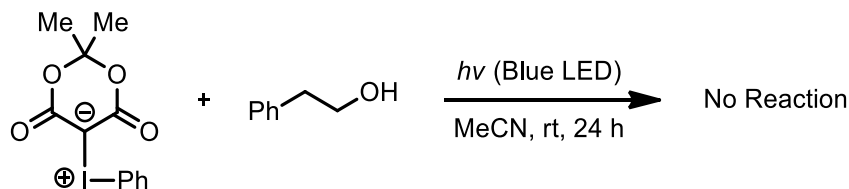


Scheme 3.49 Control reaction of Meldrum's acid iodonium ylide with cinnamyl alcohol

Results of the control reaction (no light) demonstrate a need for the blue light for oxidation to occur. Because the cyclopropanation reaction occurs at the same time as the oxidation process when using cinnamyl alcohol (**3.59**), the full potential of this oxidation chemistry was not realized. Competition between cyclopropanation and oxidation reactions gave mixtures of both products, and therefore the ability to have control over this process was severely impaired. Although chemoselectivity is an issue in this process, this new idea of a halogen bonding complex forming, followed by a SET event, might be an avenue for new reactions to be discovered in the future.

Further studies that were conducted to provide a better understanding of oxidation reactions of alcohols with iodonium ylides were performed to see if systems other than allylic alcohols could undergo oxidation, or if O-H insertion reactions could be made possible with the correct conditions.

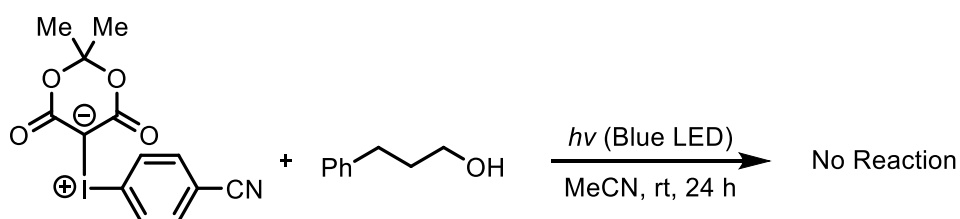
Oxidation was not observed between the reaction of iodonium ylides with non-allylic alcohols. The presence of an allylic group in the alcohol must be an important factor for the oxidation reaction to occur, presumably through stabilization of the intermediate(s) involved. The reaction, as shown in **Scheme 3.50**, resulted in no oxidation, just quantitative recovery of the primary alcohol was observed. This is another example where adding $\text{BF}_3 \cdot \text{OEt}_2$ to the reaction mixture might potentially allow for the iodonium ylide to engage in the oxidation of the alcohol.



Scheme 3.50 Non-oxidative reaction of iodonium ylides with primary alcohols

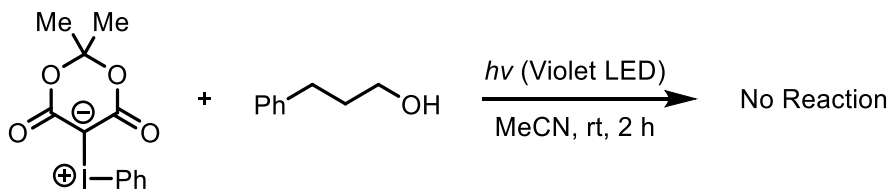
3.11.3 Blue Light Induced O-H Insertion of Iodonium Ylides

The question of whether iodonium ylides can undergo O-H insertion reactions when photochemically activated using blue light from an LED was answered based on the following reactions. The use of a nitrile group as an EWG at the *para* position of the iodonium ylide was intended to increase the electrophilicity of the iodine with the hope of encouraging a stronger tendency to form a complex between the oxygen in the alcohol and the iodine in the iodonium ylide.



Scheme 3.51 Failure of O-H insertion of iodonium ylides under blue light

The use of stronger wavelengths of light from LEDs was also attempted for inducing an O-H insertion reaction of the iodonium ylide. Using violet-coloured 365 nm LEDs failed to yield any O-H insertion product, as shown in **Scheme 3.52**.

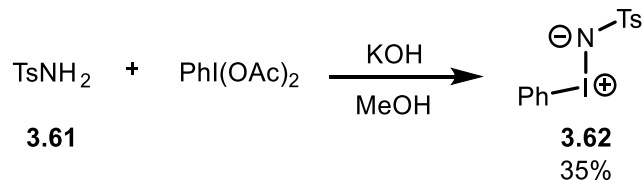


Scheme 3.52 Failure of O-H insertion of iodonium ylides at 365 nm

3.11.4 Blue Light Induced Aziridination Reaction

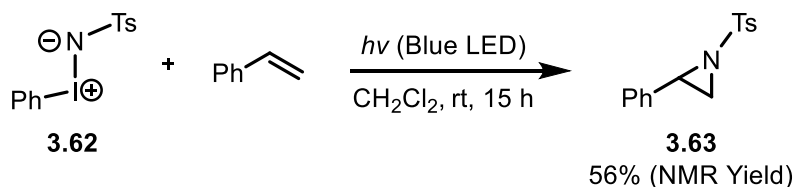
It was conceivable that our photoreactor could also be used for the synthesis of aziridines using *p*-toluenesulphonamide (PhI=NTs, **3.62**) HVI reagents and alkenes. To better understand this process a small amount of the iminoiodane was synthesized according to the reaction conditions, as shown in **Scheme 3.53**. In this reaction 4-methylbenzenesulfonamide (TsNH₂,

3.61) was mixed with $\text{PhI}(\text{OAc})_2$ in the presence of KOH in MeOH to give *p*-toluenesulphonamide ($\text{PhI}=\text{NTs}$, **3.62**) in a 35% isolated yield.



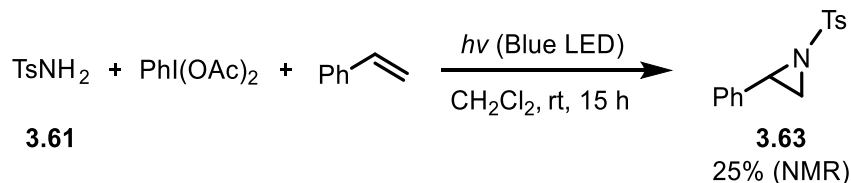
Scheme 3.53 Synthesis of $\text{PhI}=\text{NTs}$

An interesting result was observed to occur when iminoiodane **3.62** was irradiated with blue LED in the presence of styrene using our photoreactor #4 in CH_2Cl_2 for 15 h. Under these conditions aziridine **3.63** was formed, as shown in **Scheme 3.54**.



Scheme 3.54 Light-mediated aziridination reaction of iminoiodanes and styrene

The light-mediated aziridination reaction was extended to include a one-pot metal-free synthesis of aziridines by reacting TsNH_2 (**3.61**) with $\text{PhI}(\text{OAc})_2$ in the presence of styrene and blue LED as shown in **Scheme 3.55**.



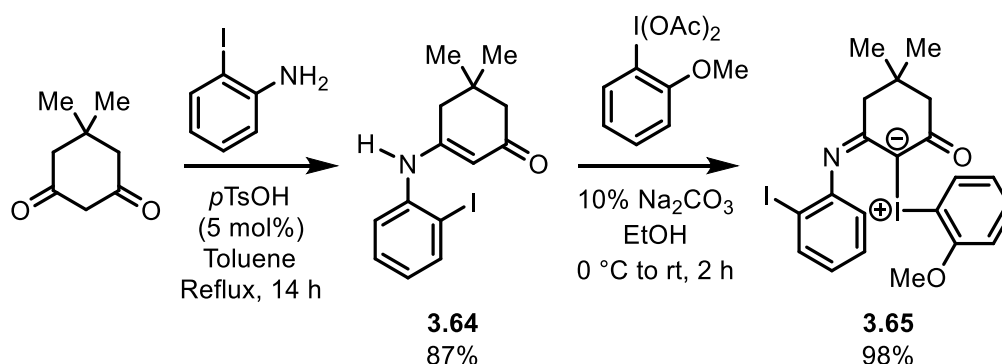
Scheme 3.55 One-pot light-mediated aziridination reaction

Although the reaction of iminoiodanes and styrene with blue light does not involve iodonium ylides, the concept of activating HVI reagents with light does fit within the theme of this chapter. It is also believed that the photo-chemical activation of iminoiodanes goes through a

biradical intermediate in an analogous process to the reactivity observed when iodonium ylides are irradiated with blue light.

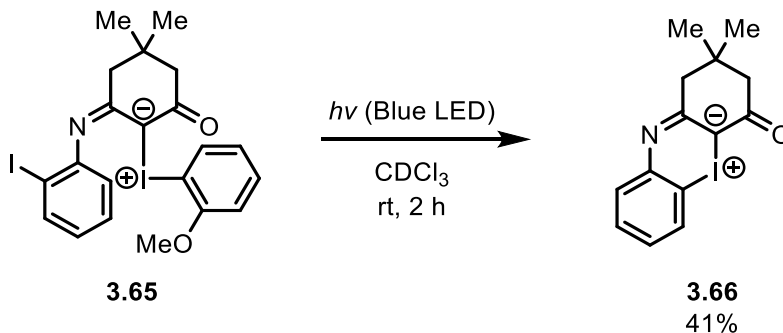
3.11.5 Blue Light Induced Transylation Reaction

Reacting dimedone with 2-iodoaniline under refluxing conditions in toluene using a Dean-Stark setup, gave precursor **3.64** which is known to rearrange from an imine into the more thermodynamically stable α,β -unsaturated carbonyl compound shown in **Scheme 3.56**. Care was taken to keep the next step under cold conditions, as Na_2CO_3 was first added, followed by the addition of the *ortho*-methoxy diacetate, to give the desired iodonium ylide **3.65** required for investigating transylation reactions.



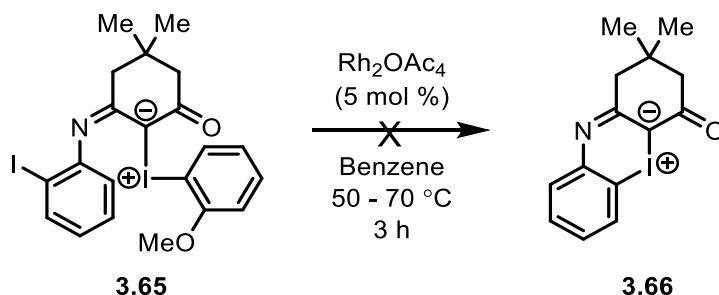
Scheme 3.56 Synthesis of iodonium ylide for transylation reaction

The transylation reaction shown in **Scheme 3.57**, was performed using photo-reactor #4 with a 0.5 cm distance from the LED light source. This reaction was only performed two times and is therefore not an optimized result. When the reaction was repeated using photo-reactor #4 with a 1.0 cm distance, there was no observable transylation product formed.



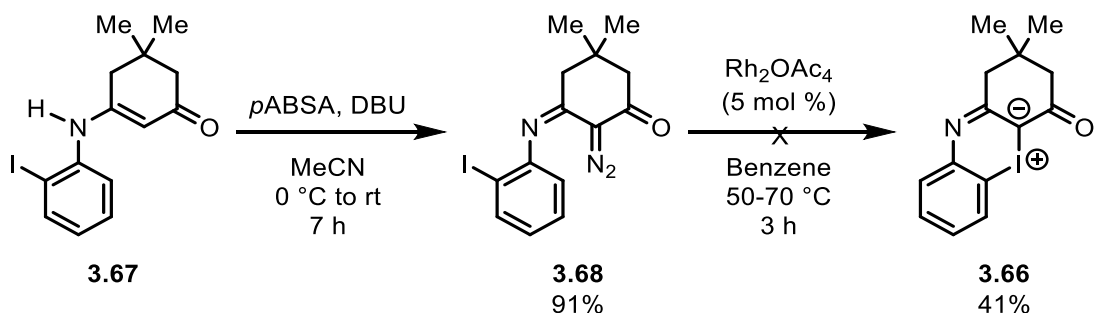
Scheme 3.57 Blue light-mediated transylation reaction

The transylation product **3.66** was confirmed by mass spectrometry with identification of the $[M+H]$ peak which was found to be 340.00. For this specific iodonium ylides system, using a transition metal catalyst was not suitable, and did not result in the transylation product to form. Refluxing in benzene using 5 mol % Rh_2OAc_4 did not give the desired product (**Scheme 3.58**).



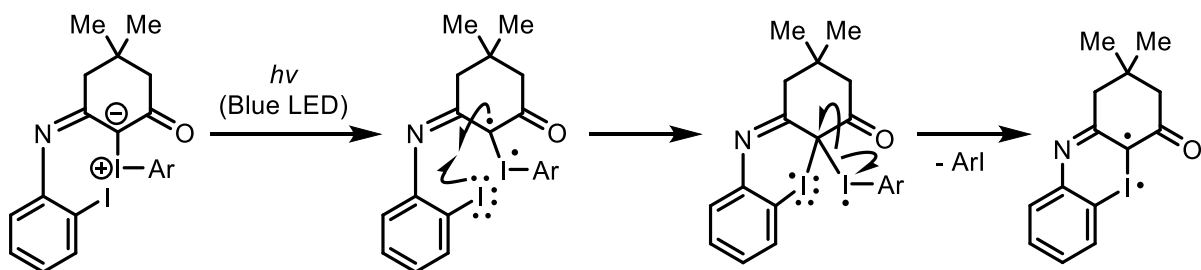
Scheme 3.58 Failure of metal-mediated transylation reaction using iodonium ylide

Attempts to use a diazo-based compound for the equivalent metal-mediated transylation reaction also failed, and only recovery of the diazo starting material was the outcome. Excessive heating and prolonged reaction time were attempted but were not successful at converting any of the diazo into the transylation product.



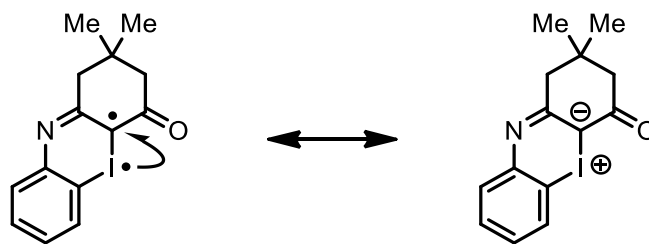
Scheme 3.59 Failure of metal-mediated transylidation reaction using diazo

A proposed mechanism is shown in **Scheme 3.60** which is based on our understanding of how iodonium ylides are activated with blue light to generate a diradical intermediate. The higher energy, diradical intermediate, is then able to interact with the iodine present on the aromatic ring in an intramolecular manner. This is followed by expulsion of iodobenzene to give a different iodonium ylide, temporarily existing in an excited state as a diradical, which may then undergo relaxation to give the iodonium ylide in the un-excited, ground state.



Scheme 3.60 Mechanism of visible light-mediated transylidation reaction

The understanding behind the mechanism is based off the assumption that the excited state configuration of the iodonium ylide is in some sort of an equilibrium process with the ground state. The relaxation of the diradical intermediate into the resting, ground state of the cyclic iodonium ylide is shown in **Scheme 3.61**.



Scheme 3.61 Conversion of excited state diradical species to ground state iodonium ylide

This unique transylidation reaction was only accessible using blue light from LEDs. Both metal-based or thermal-based activation both failed at producing the desired transylidation product.

3.12 Experimental

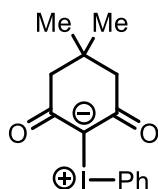
All reactions were carried out in flame-dried glassware under a dry nitrogen atmosphere, unless otherwise noted. All solvents were obtained pure and dry from a JC Meyer solvent purification system. All reagents were purchased from Sigma-Aldrich and used without further purification. ^1H NMR spectra were recorded on Bruker instruments at 300 MHz and were referenced to residual ^1H shift in CDCl_3 (7.24 ppm). All ^{13}C NMR were recorded at 75 MHz, and CDCl_3 (77.0 ppm) was used as the internal reference. ^{31}P NMR spectra were recorded at 121 MHz and referenced to the H_3PO_4 signal at 0 ppm. The following abbreviations were used to explain the multiplicities: s = singlet, d = doublet, t = triplet, q = quartet, br s = broad singlet. Reactions were monitored by thin-layer chromatography (TLC) on commercial silica pre-coated plates with a particle size of 60 Å and viewed by UV lamp (254 nm), by gas chromatography (HP5890A Series II) with a J&W Scientific 30 m x 0.53 mm DB624 column with 3 micron film thickness (run settings: 2.5 min at 75 °C, 7.5 °C/min to 250 °C), and by ^{31}P NMR. Flash chromatography was performed using 60Å (230-400 mesh) silica gel. Melting points were performed using a MeltTemp apparatus. InfraRed (IR) data was recorded using an ATR-FTIR (Attenuated Total Reflection Fourier Transform InfraRed) instrument. The following abbreviations were used to explain the IR peak intensities: (s) = strong, (m) = medium, (w) = weak. Positive ion electrospray ionization (ESI) was performed with a Thermo Scientific Q-Exactive hybrid mass spectrometer. Accurate mass determinations were performed at a mass resolution of 70,000. For ESI, samples were infused at 10 $\mu\text{L}/\text{min}$ in 1:1 MeOH/ H_2O + 0.1% formic acid.

3.12.1 General Procedure 1 (GP1) - Synthesis of Iodonium Ylides

Cyclic β -dicarbonyl iodonium ylides are known compounds and were prepared in one step from the corresponding β -dicarbonyl methylene compound (1 equiv), and (diacetoxyiodo)benzene (1 equiv) following procedures found in literature by Koser and Lick.²⁶² The iodonium ylides were purified as follows: the crude reaction mixture was dissolved in a minimal amount of CH_2Cl_2 (n mL), then this solution was added to Et_2O (10x n mL) in a flask

that was stirred and cooled in an ice bath. After stirring for 10 min, the suspension was filtered, and the solids were dried in air or under vacuum until a constant weight was obtained.

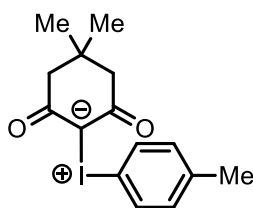
2-Phenylidonio-5,5-dimethyl-1,3-dioxacyclohexanemethylide (3.16a, dimedone iodonium ylide)



Iodonium ylide **3.16a** was prepared according to **GP1** from 5,5-dimethyl-1,3-cyclohexanedione (2.80 g, 20 mmol, 1 equiv) and (diacetoxyiodo)benzene (6.4 g, 20 mmol, 1 equiv) in CH₂Cl₂ (50 mL) for 3 h at room temperature. Purification by trituration (CH₂Cl₂:Et₂O 1:10) led to the title compound isolated as a white solid (5.14 g, 75% yield). The characterization data matches what has already been reported in the literature.²⁶³

¹H NMR (300 MHz, CDCl₃): δ 7.82 (d, *J* = 7.9 Hz, 2H), 7.51 (t, *J* = 7.8 Hz, 1H), 7.35 (t, *J* = 7.6 Hz, 2H), 2.50 (s, 4H), 1.05 (s, 6H).

(4-Methylphenyl)(4,4-dimethyl-2,6-dioxocyclohexyl)iodonium (3.16b)



Iodonium ylide **3.16b** was prepared according to **GP1** from 5,5-dimethyl-1,3-cyclohexanedione (0.280 g, 2.0 mmol, 1 equiv) and 4-methyl-(diacetoxyiodo)benzene (0.780 g, 2.0 mmol, 1 equiv) in CH₂Cl₂ (15 mL) for 1 h at room temperature. Purification by trituration (CH₂Cl₂:Et₂O 1:10) led to the title compound isolated as a white solid (0.610 g, 85% yield).

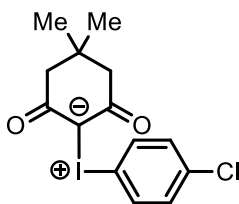
¹H NMR (300 MHz, CDCl₃): δ 7.70 (d, *J* = 8.2 Hz, 2H), 7.13 (d, *J* = 8.2 Hz, 2H), 2.46 (s, 4H), 2.34 (s, 3H), 1.02 (s, 6H).

¹³C NMR (75 MHz, CDCl₃): δ 191.2, 145.2, 137.1, 135.3, 111.1, 97.7, 53.7, 35.0, 31.1, 24.2.

HRMS (ESI): Calculated for C₁₅H₁₈ IO₂ (M+H)⁺ 357.0346, found 357.0340.

IR (ATR): 2947 (w), 1604 (m), 1521 (s), 1351 (m) cm⁻¹.

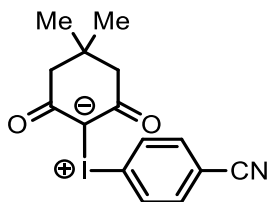
(4-Chlorophenyl)(4,4-dimethyl-2,6-dioxocyclohexyl)iodonium (3.16c)



Iodonium ylide **3.16c** was prepared according to **GP1** from 5,5-dimethyl-1,3-cyclohexanedione (0.280 g, 2.0 mmol, 1 equiv) and 4-chloro-(diacetoxyiodo)benzene (0.713 g, 2.0 mmol, 1 equiv) in CH₂Cl₂ (15 mL) for 2.5 h at room temperature. Purification by trituration (CH₂Cl₂:Et₂O 1:10) led to the title compound isolated as a white solid (0.545 g, 72% yield). The characterization data matches what has already been reported in the literature.¹⁴⁶

¹H NMR (300 MHz, CDCl₃): δ 7.78 (d, *J* = 8.6 Hz, 2H), 7.33 (d, *J* = 8.6 Hz, 2H), 2.49 (s, 4H), 1.05 (s, 6H).

(4-Cyanophenyl)(4,4-dimethyl-2,6-dioxocyclohexyl)iodonium (3.16d)



Iodonium ylide **3.16d** was prepared according to **GP1** from 5,5-dimethyl-1,3-cyclohexanedione (0.280 g, 2.0 mmol, 1 equiv) and 4-cyano-(diacetoxyiodo)benzene (0.694 g, 2.0 mmol, 1 equiv) in CH₂Cl₂ (20 mL) for 3.5 h at room temperature. Purification by trituration (CH₂Cl₂:Et₂O 1:10) led to the title compound isolated as a white solid (0.420 g, 57% yield).

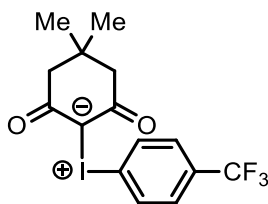
¹H NMR (300 MHz, CDCl₃): δ 7.92 (d, *J* = 8.4 Hz, 2H), 7.63 (d, *J* = 8.4 Hz, 2H), 2.53 (s, 4H), 1.08 (s, 6H).

¹³C NMR (75 MHz, CDCl₃): δ 191.4, 137.5, 137.1, 119.7, 118.8, 118.6, 97.6, 53.8, 35.0, 31.1.

HRMS (ESI): Calculated for C₁₅H₁₅INO₂ (M+H)⁺ 368.0142, found 368.0142.

IR (ATR): 2953 (w), 1603 (m), 1514 (s), 1351 (m), 1138 (m), 825 (m) cm⁻¹.

(4-Trifluoromethylphenyl)(4,4-dimethyl-2,6-dioxocyclohexyl)iodonium (3.16e)



Iodonium ylide **3.16e** was prepared according to **GP1** from 5,5-dimethyl-1,3-cyclohexanedione (0.100 g, 0.7 mmol, 1 equiv) and 1-iodo-4-(trifluoromethyl)benzene (0.273 g, 0.7 mmol, 1 equiv) in CH₂Cl₂ (10 mL) for 2 h at room temperature. Purification by trituration (CH₂Cl₂:Et₂O 1:10) led to the title compound isolated as a white solid (0.219 g, 76% yield).

¹H NMR (300 MHz, CDCl₃): δ 7.94 (d, *J* = 8.8 Hz, 2H), 7.61 (d, *J* = 8.8 Hz, 2H), 2.52 (s, 4H), 1.07 (s, 6H).

¹³C NMR (75 MHz, CDCl₃): δ 191.3, 137.0, 131.3 (q, *J* = 25 Hz), 97.3, 53.8, 35.0, 31.1.

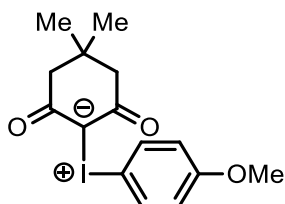
Note: The ylide decomposes before a complete spectrum can be acquired. Increasing sample concentration was not possible due to poor solubility in CDCl₃.

¹⁹F NMR (282 MHz, CDCl₃): δ -63.5.

HRMS (ESI): Calculated for C₁₅H₁₅F₃IO₂ (M+H)⁺ 411.0063, found 411.0058.

IR (ATR): 2962 (w), 1737 (m), 1610 (m), 1515 (s), 1325 (m), 1126 (m), 825 (m) cm⁻¹.

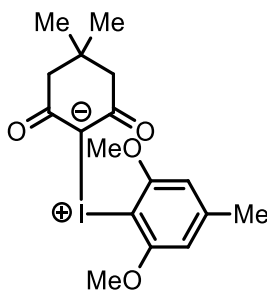
(4-Methoxyphenyl)(4,4-dimethyl-2,6-dioxocyclohexyl)iodonium (3.16f)



Iodonium ylide **3.16f** was prepared according to **GP1** from 5,5-dimethyl-1,3-cyclohexanedione (0.140 g, 1.0 mmol, 1 equiv) and 4-methoxy-(diacetoxyiodo)benzene (0.352 g, 1.0 mmol, 1 equiv) in CH₂Cl₂ (10 mL) for 2 h at room temperature. Purification by trituration (CH₂Cl₂:Et₂O 1:10) led to the title compound isolated as a white solid (0.364 g, 98% yield). The characterization data matches what has already been reported in the literature.²⁶⁰

¹H NMR (300 MHz, CDCl₃): δ 7.80 (d, *J* = 9.0 Hz, 2H), 6.84 (d, *J* = 9.0 Hz, 2H), 3.80 (s, 3H), 2.47 (s, 4H), 1.03 (s, 6H).

(2,6-Dimethoxy-4-methylphenyl)(4,4-dimethyl-2,6-dioxocyclohexyl)iodonium (3.16g)



Iodonium ylide **3.16g** was prepared according to **GP1** from 5,5-dimethyl-1,3-cyclohexanedione (0.210 g, 1.5 mmol, 1 equiv) and 2,6-dimethoxy-4-methyl-(diacetoxyiodo)benzene (0.594 g, 1.5 mmol, 1 equiv) in CH₂Cl₂ (15 mL) for 1.5 h at room temperature. Purification by trituration (CH₂Cl₂:Et₂O 1:10) led to the title compound isolated as a pale yellow-white solid (0.322 g, 52% yield).

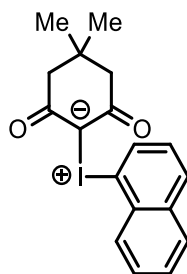
¹H NMR (300 MHz, CDCl₃): δ 6.36 (s, 2H), 3.87 (s, 6H), 2.40 (s, 4H), 2.36 (s, 3H), 1.00 (s, 6H).

¹³C NMR (75 MHz, CDCl₃): δ 190.9, 161.8, 148.4, 108.6, 93.8, 89.3, 59.6, 53.9, 35.0, 30.9, 25.2.

HRMS (ESI): Calculated for C₁₇H₂₂IO₄ (M+H)⁺ 417.0557, found 417.0554.

IR (ATR): 2925 (w), 1604 (m), 1561 (s), 1340 (m), 1235 (m), 1116 (s), 819 (m) cm⁻¹.

(4,4-Dimethyl-2,6-dioxocyclohexyl)(naphthalen-1-yl)iodonium (3.16h)



Iodonium ylide **3.16h** was prepared according to **GP1** from 5,5-dimethyl-1,3-cyclohexanedione (0.140 g, 1.0 mmol, 1 equiv) and 1-(diacetoxyiodo)naphthalene (0.372 g, 1.0 mmol, 1 equiv) in CH₂Cl₂ (10 mL) for 4 h at room temperature. Purification by trituration (CH₂Cl₂:Et₂O 1:10) led to the title compound isolated as a white solid (0.340 g, 87% yield).

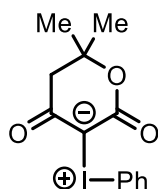
¹H NMR (300 MHz, CDCl₃): δ 8.27 (d, *J* = 7.5 Hz, 1H), 8.18 (d, *J* = 8.4 Hz, 1H), 8.01 (d, *J* = 8.1 Hz, 1H), 7.83 (d, *J* = 8.1 Hz, 1H), 7.71 (t, *J* = 7.2 Hz, 1H), 7.59 (t, *J* = 7.5 Hz, 1H), 7.38 (t, *J* = 7.9 Hz, 1H), 2.47 (s, 4H), 1.01 (s, 6H).

¹³C NMR (75 MHz, CDCl₃): δ 191.4, 139.2, 137.7, 135.7, 134.5, 132.4, 132.1, 131.8, 130.7, 129.9, 117.1, 96.3, 53.7, 35.0, 31.0.

HRMS (ESI): Calculated for C₁₈H₁₈IO₂ (M+H)⁺ 393.0346, found 393.0343.

IR (ATR): 2949 (w), 1738 (w), 1537 (s), 1345 (w), 1264 (w), 797 (m) cm⁻¹.

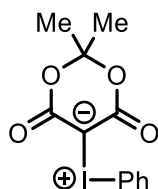
1-Oxa-2,2-dimethyl-4,6-dioxo-5-(phenyliodonio)-cyclohexan-5-ide (3.16i)



Iodonium ylide **3.16i** was prepared according to **GP1** from 6,6-dimethyldihydro-2H-pyran-2,4(3H)-dione (0.160 g, 1.1 mmol, 1 equiv) and (diacetoxyiodo)benzene (0.354 g, 1.1 mmol, 1 equiv) in CH₂Cl₂ (10 mL) for 2 h at room temperature. Purification by trituration (CH₂Cl₂:Et₂O 1:10) led to the title compound isolated as a white solid (0.247 g, 65% yield). The characterization data matches what has already been reported in the literature.¹⁸⁷

$^1\text{H NMR}$ (300 MHz, CDCl_3): δ 7.81 (d, $J = 7.6$ Hz, 2H), 7.51 (t, $J = 7.6$ Hz, 1H), 7.35 (t, $J = 7.6$ Hz, 2H), 2.64 (s, 2H), 1.42 (s, 6H).

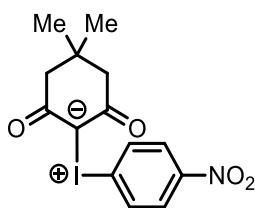
Meldrum's acid iodonium ylide (3.16j)



Iodonium ylide **3.16j** was prepared according to **GP1** from 2,2-dimethyl-1,3-dioxane-4,6-dione (0.288 g, 2.0 mmol, 1 equiv) and (diacetoxyiodo)benzene (0.644 g, 2.0 mmol, 1 equiv) in CH_2Cl_2 (15 mL) for 1.5 h at room temperature. Purification by trituration (CH_2Cl_2 : Et_2O 1:10) led to the title compound isolated as a white solid (0.540 g, 78% yield). The characterization data matches what has already been reported in the literature.²⁶⁴

$^1\text{H NMR}$ (300 MHz, CDCl_3): δ 7.88 (d, $J = 7.5$ Hz, 2H), 7.59 (t, $J = 7.4$ Hz, 1H), 7.43 (t, $J = 7.8$ Hz, 2H), 1.71 (s, 6H).

(4-Nitrophenyl)(4,4-dimethyl-2,6-dioxocyclohexyl)iodonium (3.16k)



Iodonium ylide **3.16k** was prepared according to **GP1** from 5,5-dimethyl-1,3-cyclohexanedione (0.280 g, 2.0 mmol, 1 equiv) and 4-nitro-(diacetoxyiodo)benzene (0.734 g, 2.0 mmol, 1 equiv) in CH_2Cl_2 (30 mL) for 2 h at room temperature. Purification by trituration (CH_2Cl_2 : Et_2O 1:10) led to the title compound isolated as a white solid (0.393 g, 51% yield).

¹H NMR (300 MHz, CDCl₃): δ 8.19 (d, *J* = 8.7 Hz, 2H), 7.99 (d, *J* = 8.7 Hz, 2H), 2.53 (s, 4H), 1.08 (s, 6H).

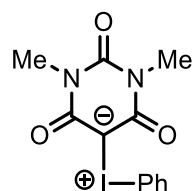
¹³C NMR (75 MHz, CDCl₃): δ 191.4, 152.6, 137.3, 129.1, 122.3, 53.8, 35.0, 31.1.

Note: The ylide decomposes before a complete spectrum can be acquired. Increasing sample concentration was not possible due to poor solubility in CDCl₃.

HRMS (ESI): Calculated for C₁₄H₁₅INO₄ (M+H)⁺ 388.0040, found 388.0037.

IR (ATR): 2956 (w), 1609 (m), 1510 (s), 1353 (m), 848 (m), 734 (s) cm⁻¹.

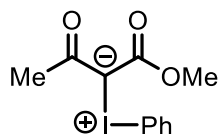
Phenyl(3,5-N,N-dimethyl-2,4,6-trioxocyclohexyl)iodonium (3.16l)



Iodonium ylide **3.16l** was prepared according to **GP1** from barbituric acid (0.156 g, 1.0 mmol, 1 equiv) and (diacetoxyiodo)benzene (0.322 g, 1.0 mmol, 1 equiv) in CH₂Cl₂ (10 mL) for 1 h at room temperature. Purification by trituration (CH₂Cl₂:Et₂O 1:10) led to the title compound isolated as a white solid (0.279 g, 78% yield). The characterization data matches what has already been reported in the literature.²⁶⁵

¹H NMR (300 MHz, CDCl₃): δ 7.87 (d, *J* = 7.6 Hz, 2H), 7.58 (t, *J* = 7.6 Hz, 1H), 7.42 (t, *J* = 7.6 Hz, 2H), 3.35 (s, 6H).

Methyl Acetoacetate iodonium ylide (3.16m)

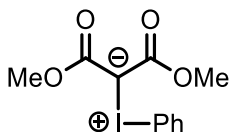


Iodonium ylide **3.16m** was prepared according to Charette's literature procedure from methyl acetoacetate (0.53 mL, 5.0 mmol, 1 equiv), KOH (1.68 g, 30 mmol, 6 equiv) and (diacetoxyiodo)benzene (1.60 g, 5.0 mmol, 1 equiv) in MeOH (15 mL) for 2 h at 0 °C. Purification by trituration (CH₂Cl₂:Et₂O 1:10) led to the title compound isolated as a white solid

(1.11 g, 70% yield). The characterization data matches what has already been reported in the literature.²⁶⁶

¹H NMR (300 MHz, CDCl₃): δ 7.76 (d, *J* = 8.1 Hz, 2H), 7.52 (t, *J* = 7.6 Hz, 1H), 7.37 (t, *J* = 7.8 Hz, 2H), 3.67 (s, 3H), 2.58 (s, 3H).

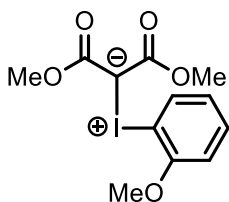
Bis(methoxycarbonyl)(phenyliodonium)methanide (3.16n)



Iodonium ylide **3.16n** was prepared according to Charette's literature procedure from dimethyl malonate (0.693 mL, 6.0 mmol, 1.0 equiv), KOH (2.0 g, 36 mmol, 6.0 equiv) and (diacetoxyiodo)benzene (2.13 g, 6.0 mmol, 1.0 equiv) in MeCN (20 mL) for 2 h at 0 °C. Purification by trituration (CH₂Cl₂:Et₂O 1:10) led to the title compound isolated as a white solid (1.51 g, 75% yield). The characterization data matches what has already been reported in the literature.²⁶⁴

¹H NMR (300 MHz, CDCl₃): δ 7.72 (d, *J* = 8.3 Hz, 2H), 7.52 (t, *J* = 7.5 Hz, 1H), 7.40 (t, *J* = 7.6 Hz, 2H), 3.73 (s, 6H).

Bis(methoxycarbonyl)(2-methoxyphenyliodonium)methanide (3.16o)

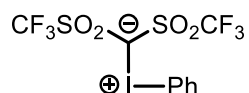


Iodonium ylide **3.16o** was prepared according to Charette's literature procedure from dimethyl malonate (0.693 mL, 6.0 mmol, 1.0 equiv), KOH (2.0 g, 36 mmol, 6.0 equiv) and 2-methoxy-(diacetoxyiodo)benzene (2.13 g, 6.0 mmol, 1.0 equiv) in MeCN (20 mL) for 2 h at 0 °C. Purification by trituration (CH₂Cl₂:Et₂O 1:10) led to the title compound isolated as a white solid

(1.51 g, 75% yield). The characterization data matches what has already been reported in the literature.²⁶⁴

¹H NMR (300 MHz, CDCl₃): δ 7.43 (t, *J* = 8.1 Hz, 1H), 7.34 (d, *J* = 8.1 Hz, 1H), 7.06 (t, *J* = 8.1 Hz, 1H), 6.92 (d, *J* = 8.1 Hz, 1H), 3.95 (s, 3H), 3.72 (s, 6H).

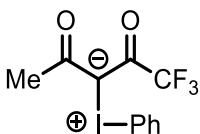
Phenyliodonium bis(perfluoromethanesulfonyl) methide (**3.16p**)



Iodonium ylide **3.16p** was prepared from bis((trifluoromethyl)sulfonyl)methane (0.730 g, 2.6 mmol, 1.0 equiv) and KOH (0.875 g, 15.6 mmol, 6.0 equiv) and (diacetoxyiodo)benzene (0.839 g, 2.6 mmol, 1.0 equiv) in MeCN (30 mL) for 2 h at room temperature. Purification by trituration (CH₂Cl₂:Et₂O 1:10) led to the title compound isolated as a white solid (0.912 g, 73% yield). The characterization data matches what has already been reported in the literature.²⁶⁷

¹H NMR (300 MHz, CDCl₃): δ 8.08 (d, *J* = 8.0 Hz, 2H), 7.76 (t, *J* = 7.8 Hz, 1H), 7.56 (t, *J* = 7.5 Hz, 2H).

(Trifluoromethyl carbonyl)acetoacetate(phenyliodonium)methanide (**3.16q**)



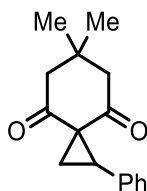
Iodonium ylide **3.16q** was prepared from 1,1,1-trifluoropentane-2,4-dione (0.59 mL, 5.0 mmol, 1.0 equiv), KOH (1.6 g, 30 mmol, 6.0 equiv) and (diacetoxyiodo)benzene (1.6 g, 5.0 mmol, 1.0 equiv) in MeOH (10 mL) for 1 h at 0 °C. Purification by trituration (CH₂Cl₂:Et₂O 1:10) led to the title compound isolated as a white solid (1.27 g, 72% yield).

¹H NMR (300 MHz, CDCl₃): δ 7.88 (d, *J* = 7.7 Hz, 2H), 7.59 (t, *J* = 7.4 Hz, 1H), 7.41 (t, *J* = 7.9 Hz, 2H), 2.61 (s, 3H).

3.12.2 General Procedure 2 (GP2) - Synthesis of Cyclopropanes

Into a dry 1 dram (4.0 mL) vial was added iodonium ylide (0.1 mmol, 1 equiv) and MeCN (1.0 ml, 0.1 M), and this loaded into photo-reactor #4 and stirred at room temperature for 2 min, giving either a clear solution or a slurry. Styrene (0.023 mL, 0.2 mmol, 2.0 equiv) was added in one portion and after stirring for 1 min, the blue LED was turned on. The reaction mixture was stirred at room temperature until the reaction was observed to be complete by TLC or NMR analysis. The mixture was then evaporated to dryness and purified by column chromatography, eluting with mixtures of ethyl acetate and hexanes.

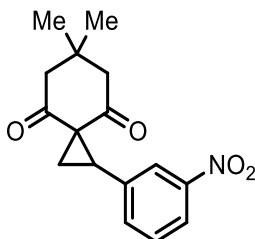
6,6-Dimethyl-1-phenylspiro[2.5]octane-4,8-dione (3.30a)



Synthesized according to **GP2** using iodonium ylide **3.16a** (0.034 g, 0.10 mmol, 1 equiv), styrene (0.023 mL, 0.20 mmol, 2.0 equiv), MeCN (1.0 mL). The reaction was stirred for 1.5 h at 25 °C until the ylide was consumed as indicated by NMR. Purification by flash chromatography through a column of silica gel (hexanes:EtOAc 8:1) led to the title compound isolated as a white solid (0.022 g, 95% yield). $R_f = 0.30$ (hexanes:EtOAc 3:1). The characterization data matches what has already been reported in the literature.²⁶⁵

¹H NMR (300 MHz, CDCl₃): δ 7.18-7.30 (m, 5H), 3.25 (t, $J = 9.0$ Hz, 1H), 2.49-2.66 (m, 3H), 2.18-2.37 (m, 3H), 1.12 (s, 3H), 1.03 (s, 3H)

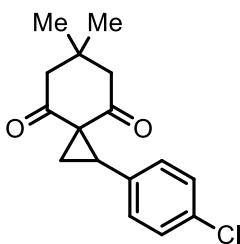
6,6-Dimethyl-1-(3-nitrophenyl)spiro[2.5]octane-4,8-dione (3.30b)



Synthesized according to **GP2** using iodonium ylide **3.16a** (0.034 g, 0.10 mmol, 1.0 equiv), 1-nitro-3-vinylbenzene (0.028 mL, 0.20 mmol, 2.0 equiv), MeCN (1.0 mL). The reaction was stirred for 1.5 h at 25 °C until the ylide was consumed as indicated by NMR. Purification by flash chromatography through a column of silica gel (hexanes:EtOAc 10:1 to 1:1) led to the title compound isolated as a pale-yellow solid (0.023 g, 80% yield). $R_f = 0.16$ (hexanes:EtOAc 3:1). The characterization data matches what has been previously reported in the literature.²⁶⁵

¹H NMR (300 MHz, CDCl₃): δ 8.08-8.12 (m, 2H), 7.54 (d, $J = 7.8$ Hz, 1H), 7.46 (t, $J = 7.8$ Hz, 1H), 3.33 (t, $J = 8.9$ Hz, 1H), 2.22-2.64 (m, 6H), 1.13 (s, 3H), 1.05 (s, 3H).

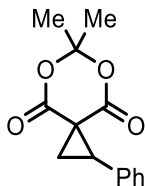
1-(4-chlorophenyl)-6,6-dimethylspiro[2.5]octane-4,8-dione (3.30c)



Synthesized according to **GP2** using iodonium ylide **3.16a** (0.034 g, 0.10 mmol, 1.0 equiv), 1-chloro-4-vinylbenzene (0.024 mL, 0.20 mmol, 2.0 equiv), MeCN (1.0 mL). The reaction was stirred for 1.5 h at 25 °C until the ylide was consumed as indicated by NMR. Purification by flash chromatography through a column of silica gel (hexanes:EtOAc 8:1) led to the title compound isolated as an off-white solid (0.025 g, 91% yield). $R_f = 0.36$ (hexanes:EtOAc 3:1). The characterization data matches what has been previously reported in the literature.²⁶⁵

¹H NMR (300 MHz, CDCl₃): δ 7.22-7.34 (m, 2H), 7.14 (d, $J = 8.3$ Hz, 2H), 3.21 (t, $J = 8.7$ Hz, 1H), 2.18-2.65 (m, 6H), 1.11 (s, 3H), 1.04 (s, 3H).

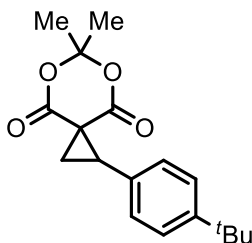
6,6-Dimethyl-1-phenyl-5,7-dioxaspiro[2.5]octane-4,8-dione (3.30d)



Synthesized according to **GP2** using iodonium ylide **3.16j** (0.035 g, 0.10 mmol, 1.0 equiv), styrene (0.023 mL, 0.20 mmol, 2.0 equiv), MeCN (1.0 mL). The reaction was stirred for 24 h at 25 °C until the ylide was consumed as indicated by NMR. Purification by flash chromatography through a column of silica gel (hexanes:EtOAc 8:1) led to the title compound isolated as a white solid (0.024 g, 96% yield). $R_f = 0.38$ (hexanes:EtOAc 3:1). The characterization data matches what has already been reported in the literature.²⁶⁸

¹H NMR (300 MHz, CDCl₃): δ 7.33 (broad s, 5H), 3.44 (dd, $J = 9.4, 9.4$ Hz, 1H), 2.68 (dd, $J = 9.4, 4.8$ Hz, 1H), 2.53 (dd, $J = 9.4, 4.8$ Hz, 1H), 1.72 (s, 6H).

1-(4-(tert-Butyl)phenyl)-6,6-dimethyl-5,7-dioxaspiro[2.5]octane-4,8-dione (3.30e)



Synthesized according to **GP2** using iodonium ylide **3.16j** (0.070 g, 0.20 mmol, 1.0 equiv), 1-(tert-butyl)-4-vinylbenzene (0.073 mL, 0.40 mmol, 2.0 equiv), MeCN (2.0 mL). The reaction was stirred for 24 h at 25 °C until the ylide was consumed as indicated by NMR. Purification by flash chromatography through a column of silica gel (hexanes:EtOAc 8:1) led to the title compound isolated as an off-white solid (0.057 g, 94% yield). $R_f = 0.40$ (hexanes:EtOAc 3:1).

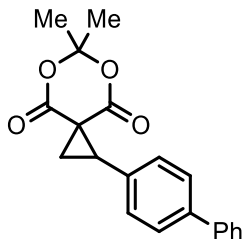
¹H NMR (300 MHz, CDCl₃): δ 7.33-7.38 (m, 2H), 7.23-7.29 (m, 2H), 3.40 (dd, $J = 9.5, 9.5$ Hz, 1H), 2.67 (dd, $J = 9.5, 4.8$ Hz, 1H), 2.52 (dd, $J = 9.5, 4.8$ Hz, 1H), 1.72 (s, 6H), 1.29 (s, 9H).

^{13}C NMR (75 MHz, CDCl_3): δ 170.7, 166.5, 154.7, 132.1, 130.9, 128.3, 107.8, 47.6, 37.5, 36.2, 34.1, 30.8, 30.6, 25.7.

HRMS (ESI): Calculated for $\text{C}_{18}\text{H}_{23}\text{O}_4$ ($\text{M}+\text{H}$) $^+$ 303.1591, found 303.1581.

IR (ATR): 2952 (w), 1738 (s), 1338 (m), 1182 (m), 968 (m) cm^{-1} .

1-([1,1'-Biphenyl]-4-yl)-6,6-dimethyl-5,7-dioxaspiro[2.5]octane-4,8-dione (3.30f)



Synthesized according to **GP2** using iodonium ylide **3.16j** (0.035 g, 0.10 mmol, 1.0 equiv), 4-vinyl-1,1'-biphenyl (0.036 mL, 0.20 mmol, 2.0 equiv), MeCN (1.0 mL). The reaction was stirred for 27 h at 25 °C until the ylide was consumed as indicated by NMR. Purification by flash chromatography through a column of silica gel (hexanes:EtOAc 20:1 to 5:1) led to the title compound isolated as a yellow solid (0.024 g, 73% yield). R_f = 0.29 (hexanes:EtOAc 3:1).

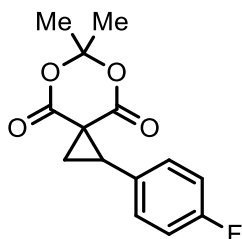
^1H NMR (300 MHz, CDCl_3): δ 7.55-7.58 (m, 4H), 7.32-7.45 (m, 5H), 3.48 (dd, J = 9.4, 9.4 Hz, 1H), 2.72 (dd, J = 9.2, 4.8 Hz, 1H), 2.58 (dd, J = 9.4, 4.6 Hz, 1H), 1.74 (s, 6H).

^{13}C NMR (75 MHz, CDCl_3): δ 167.7, 163.6, 141.6, 140.3, 130.1, 129.9, 128.8, 127.6, 127.1, 127.0, 105.0, 44.5, 33.3, 28.0, 27.7, 23.0.

HRMS (ESI): Calculated for $\text{C}_{20}\text{H}_{19}\text{O}_4$ ($\text{M}+\text{H}$) $^+$ 323.1278, found 323.1273.

IR (ATR): 2927 (m), 2856 (w), 1769 (m), 1740 (s), 1490 (w), 1340 (m), 1295 (m) cm^{-1} .

1-(4-Fluorophenyl)-6,6-dimethyl-5,7-dioxaspiro[2.5]octane-4,8-dione (3.30g)

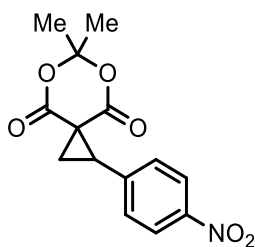


Synthesized according to **GP2** using iodonium ylide **3.16j** (0.035 g, 0.10 mmol, 1.0 equiv), 1-fluoro-4-vinylbenzene (0.024 mL, 0.20 mmol, 2.0 equiv), MeCN (1.0 mL). The reaction was stirred for 24 h at 25 °C until the ylide was consumed as indicated by NMR. Purification by flash chromatography through a column of silica gel (hexanes:EtOAc 8:1) led to the title compound isolated as a white solid (0.019 g, 72% yield). $R_f = 0.28$ (hexanes:EtOAc 3:1). The characterization data matches what has already been reported in the literature.²⁶⁹

¹H NMR (300 MHz, CDCl₃): δ 7.28-7.33 (m, 2H), 6.98-7.06 (m, 2H), 3.41 (dd, $J = 9.4, 9.4$ Hz, 1H), 2.62 (dd, $J = 9.4, 4.8$ Hz, 1H), 2.53 (dd, $J = 9.4, 4.8$ Hz, 1H), 1.72 (s, 3H), 1.70 (s, 3H).

¹⁹F NMR (282 MHz, CDCl₃): δ -112.7.

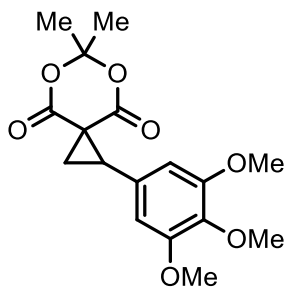
6,6-Dimethyl-1-(4-nitrophenyl)-5,7-dioxaspiro[2.5]octane-4,8-dione (**3.30h**)



Synthesized according to **GP2** using iodonium ylide **3.16j** (0.035 g, 0.10 mmol, 1.0 equiv), 1-nitro-4-vinylbenzene (0.30 g, 0.20 mmol, 2.0 equiv), MeCN (1.0 mL). The reaction was stirred for 28 h at 25 °C until the ylide was consumed as indicated by NMR. Purification by flash chromatography through a column of silica gel (hexanes:EtOAc 20:1 to 10:1) led to the title compound isolated as a pale-yellow solid (0.024 g, 82% yield). $R_f = 0.15$ (hexanes:EtOAc 3:1). The characterization data matches what has been previously reported in the literature.²⁶⁹

¹H NMR (300 MHz, CDCl₃): δ 8.20 (d, $J = 8.3$ Hz, 2H), 7.50 (d, $J = 8.3$ Hz, 2H), 3.51 (dd, $J = 9.2, 9.2$ Hz, 1H), 2.67 (dd, $J = 9.2, 4.9$ Hz, 1H), 2.59 (dd, $J = 9.2, 4.9$ Hz, 1H), 1.75 (s, 3H), 1.72 (s, 3H).

1-(3,4,5-Trimethoxyphenyl)-6,6-dimethyl-5,7-dioxaspiro[2.5]octane-4,8-dione (3.30i)



Synthesized according to **GP2** using iodonium ylide **3.16j** (0.035 g, 0.10 mmol, 1.0 equiv), 1,2,3-trimethoxy-5-vinylbenzene (0.039 g, 0.20 mmol, 2.0 equiv), MeCN (1.0 mL). The reaction was stirred for 16 h at 25 °C until the ylide was consumed as indicated by NMR. Purification by flash chromatography through a column of silica gel (hexanes:EtOAc 10:1 to 5:1) led to the title compound isolated as a clear oil (0.030 g, 89% yield). $R_f = 0.15$ (hexanes:EtOAc 3:1).

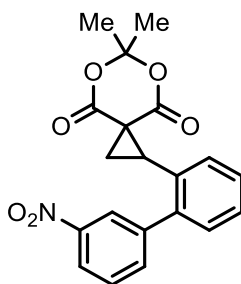
$^1\text{H NMR}$ (300 MHz, CDCl_3): δ 6.54 (s, 2H), 3.84 (s, 6H), 3.83 (s, 3H), 3.35 (dd, $J = 9.4, 9.4$ Hz, 1H), 2.63 (dd, $J = 9.4, 4.9$ Hz, 1H), 2.54 (dd, $J = 9.4, 4.9$ Hz, 1H), 1.74 (s, 3H), 1.73 (s, 3H).

$^{13}\text{C NMR}$ (75 MHz, CDCl_3): δ 170.5, 166.4, 155.9, 141.4, 129.5, 109.6, 107.8, 63.7, 59.1, 48.3, 36.3, 30.7, 30.6, 26.0.

HRMS (ESI): Calculated for $\text{C}_{17}\text{H}_{21}\text{O}_7$ ($\text{M}+\text{H}$) $^+$ 337.1281, found 337.1278.

IR (ATR): 2918 (m), 2853 (w), 1774 (m), 1735 (m), 1593 (w), 1511 (w), 1121 (s) cm^{-1} .

6,6-Dimethyl-1-(3'-nitro-[1,1'-biphenyl]-2-yl)-5,7-dioxaspiro[2.5]octane-4,8-dione (3.30j)



Synthesized according to **GP2** using iodonium ylide **3.16j** (0.035 g, 0.10 mmol, 1.0 equiv), 3'-nitro-2-vinyl-1,1'-biphenyl (0.045 g, 0.20 mmol, 2.0 equiv), MeCN (1.0 mL). The reaction was stirred for 24 h at 25 °C until the ylide was consumed as indicated by NMR. Purification by flash

chromatography through a column of silica gel (hexanes:EtOAc 20:1 to 5:1) led to the title compound isolated as a pale-yellow solid (0.025 g, 68% yield). $R_f = 0.14$ (hexanes:EtOAc 3:1).

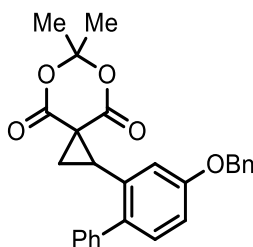
$^1\text{H NMR}$ (300 MHz, CDCl_3): δ 8.20-8.25 (m, 1H), 8.10 (s, 1H), 7.55-7.68 (m, 2H), 7.38-7.45 (m, 3H), 7.23-7.29 (m, 1H), 3.65 (dd, $J = 9.4, 9.4$ Hz, 1H), 2.27-2.36 (m, 2H), 1.62 (s, 3H), 1.51 (s, 3H).

$^{13}\text{C NMR}$ (75 MHz, CDCl_3): δ 167.5, 164.5, 148.3, 142.1, 140.9, 135.1, 130.8, 130.0, 129.6, 129.5, 128.7, 128.5, 124.2, 122.3, 104.6, 42.4, 30.9, 28.2, 27.3, 27.1.

HRMS (ESI): Calculated for $\text{C}_{20}\text{H}_{18}\text{NO}_6$ ($\text{M}+\text{H}$) $^+$ 368.1129, found 368.1126.

IR (ATR): 1733 (s), 1529 (s), 1349 (s), 1294 (s), 1201 (m), 772 (m) cm^{-1} .

1-(4-(Benzyloxy)-[1,1'-biphenyl]-2-yl)-6,6-dimethyl-5,7-dioxaspiro[2.5]octane-4,8-dione (3.30k)



Synthesized according to **GP2** using iodonium ylide **3.16j** (0.035 g, 0.10 mmol, 1.0 equiv), 4-(benzyloxy)-2-vinyl-1,1'-biphenyl (0.057 g, 0.20 mmol, 2.0 equiv), MeCN (1.0 mL). The reaction was stirred for 24 h at 25 °C until the ylide was consumed as indicated by NMR. Purification by flash chromatography through a column of silica gel (hexanes:EtOAc 20:1 to 15:1) led to the title compound isolated as a clear solid (0.032 g, 75% yield). $R_f = 0.32$ (hexanes:EtOAc 3:1).

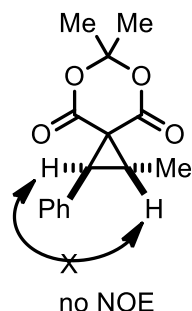
$^1\text{H NMR}$ (300 MHz, CDCl_3): δ 7.27-7.50 (m, 8H), 7.17-7.24 (m, 3H), 6.95-7.04 (m, 2H), 5.10 (s, 2H), 3.76 (dd, $J = 9.4, 9.4$ Hz, 1H), 2.26-2.35 (m, 2H), 1.60 (s, 3H), 1.45 (s, 3H).

$^{13}\text{C NMR}$ (75 MHz, CDCl_3): δ 167.8, 164.4, 158.1, 140.1, 136.9, 136.3, 132.0, 131.0, 129.4, 128.6, 128.5, 128.0, 127.6, 127.1, 116.5, 114.3, 104.5, 70.2, 42.9, 30.9, 28.2, 27.3, 27.2.

HRMS (ESI): Calculated for $\text{C}_{27}\text{H}_{25}\text{O}_5$ ($\text{M}+\text{H}$) $^+$ 429.1683, found 429.1684.

IR (ATR): 3030 (w), 1736 (s), 1562 (w), 1204 (s), 751 (m), 701 (s) cm^{-1} .

1,6,6-Trimethyl-2-phenyl-5,7-dioxaspiro[2.5]octane-4,8-dione (3.30l)

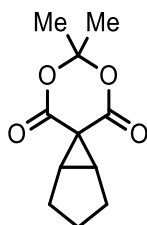


Synthesized according to **GP2** using iodonium ylide **3.16j** (0.035 g, 0.10 mmol, 1 equiv), *cis*- β -methylstyrene (0.026 mL, 0.20 mmol, 2 equiv), MeCN (1.0 mL). The reaction was stirred for 16 h at 25 °C until the ylide was consumed as indicated by NMR. Purification by flash chromatography through a column of silica gel (hexanes:EtOAc 20:1 to 10:1) led to the title compound isolated as a white solid (0.021 g, 81% yield). $R_f = 0.36$ (hexanes:EtOAc 3:1).

Synthesized according to **GP2** using iodonium ylide **3.16j** (0.035 g, 0.10 mmol, 1 equiv), *trans*- β -methylstyrene (0.026 mL, 0.20 mmol, 2 equiv), MeCN (1.0 mL). The reaction was stirred for 24 h at 25 °C until the ylide was consumed as indicated by NMR. Purification by flash chromatography through a column of silica gel (hexanes:EtOAc 20:1 to 8:1) led to the title compound isolated as a greyish-white solid (0.022 g, 85% yield). $R_f = 0.36$ (hexanes:EtOAc 3:1). The characterization data matches what has already been reported in the literature.²⁷⁰

^1H NMR (300 MHz, CDCl_3): δ 7.24-7.35 (m, 5H), 3.57 (d, $J = 9.8$ Hz, 1H), 3.13 (dq, $J = 9.8, 6.3$ Hz, 1H), 1.73 (s, 3H), 1.70 (s, 3H), 1.63 (d, $J = 6.3$ Hz, 3H).

2',2'-Dimethylspiro[bicyclo[3.1.0]hexane-6,5'-[1,3]dioxane]-4',6'-dione (3.30m)



Synthesized according to **GP2** using iodonium ylide **3.16j** (0.035 g, 0.10 mmol, 1 equiv), cyclopentene (0.018 mL, 0.20 mmol, 2 equiv), MeCN (1.0 mL). The reaction was stirred for 24 h at 25 °C until the ylide was consumed as indicated by NMR. Purification by flash chromatography through a column of silica gel (hexanes:EtOAc 20:1 to 5:1) led to the title compound isolated as a white solid (0.006 g, 28% yield). $R_f = 0.45$ (hexanes:EtOAc 3:1).

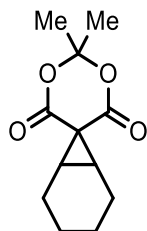
$^1\text{H NMR}$ (300 MHz, CDCl_3): δ 2.84-2.91 (m, 2H), 1.82-2.20 (m, 6H), 1.76 (s, 6H).

$^{13}\text{C NMR}$ (75 MHz, CDCl_3): δ 167.7, 164.6, 104.0, 46.1, 29.7, 27.4, 26.7, 26.3.

HRMS (ESI): Calculated for $\text{C}_{11}\text{H}_{15}\text{O}_4$ ($\text{M}+\text{H}$) $^+$ 211.0965, found 211.0958.

IR (ATR): 2921 (w), 2851 (w), 1733 (s), 1366 (m), 1275 (s), 1183 (s), 979 (m), 908 (m) cm^{-1} .

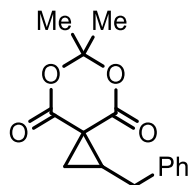
2',2'-Dimethylspiro[bicyclo[4.1.0]heptane-7,5'-[1,3]dioxane]-4',6'-dione (3.30n)



Synthesized according to **GP2** using iodonium ylide **3.16j** (0.035g, 0.10 mmol, 1 equiv), cyclohexene (0.020mL, 0.20 mmol, 2 equiv), MeCN (1.0 mL). The reaction was stirred for 24 h at 25 °C until the ylide was consumed as indicated by NMR. Purification by flash chromatography through a column of silica gel (hexanes:EtOAc 20:1to 3:1) led to the title compound isolated as a white solid (0.008 g, 35% yield). $R_f = 0.47$ (hexanes:EtOAc 3:1). The characterization data matches what has already been reported in the literature.²⁶³

¹H NMR (300 MHz, CDCl₃): δ 2.55-2.63 (m, 2H), 1.95-2.09 (m, 2H), 1.60-1.83 (m, 13H, overlap with H₂O peak), 1.22-1.40 (m, 2H).

1-Benzyl-6,6-dimethyl-5,7-dioxaspiro[2.5]octane-4,8-dione (3.30o)



Synthesized according to **GP2** using iodonium ylide **3.16j** (0.035 g, 0.10 mmol, 1 equiv), allyl benzene (0.026 mL, 0.20 mmol, 2 equiv), MeCN (1.0 mL). The reaction was stirred for 24 h at 25 °C until the ylide was consumed as indicated by NMR. Purification by flash chromatography through a column of silica gel (hexanes:EtOAc 10:1) led to the title compound isolated as a white solid (0.009 g, 34% yield). *R_f* = 0.39 (hexanes:EtOAc 3:1).

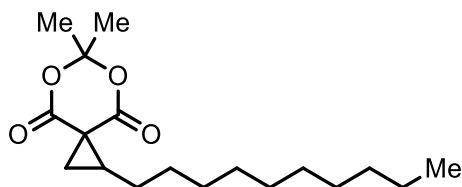
¹H NMR (300 MHz, CDCl₃): δ 7.08-7.37 (m, 5H), 3.21 (dd, *J* = 14.3, 6.0 Hz, 1H), 2.93 (dd, *J* = 14.3, 9.0 Hz, 1H), 2.55-2.64 (m, 1H), 2.28 (dd, *J* = 9.0, 3.8 Hz, 1H), 2.11 (dd, *J* = 8.7, 3.8 Hz, 1H), 1.67 (s, 3H), 1.16 (s, 3H).

¹³C NMR (75 MHz, CDCl₃): δ 171.3, 169.0, 141.4, 131.7, 129.8, 108.0, 53.6, 44.6, 35.8, 31.7, 31.1, 30.5, 29.3.

HRMS (ESI): Calculated for C₁₅H₁₆NaO₄ (M+Na)⁺ 283.0941, found 283.0927.

IR (ATR): 2927 (w), 2853 (w), 1739 (s), 1331 (m), 1199 (m), 968 (m), 703 (m) cm⁻¹.

1-Decyl-6,6-dimethyl-5,7-dioxaspiro[2.5]octane-4,8-dione (3.30p)



Synthesized according to **GP2** using iodonium ylide **3.16j** (0.070 g, 0.20 mmol, 1 equiv), 1-dodecene (0.089 mL, 0.40 mmol, 2 equiv), MeCN (2.0 mL). The reaction was stirred for 36 h at 25 °C until the ylide was consumed as indicated by NMR. Purification by flash chromatography

through a column of silica gel (hexanes:EtOAc 20:1 to 10:1) led to the title compound isolated as a clear oil (0.035 g, 56% yield). $R_f = 0.58$ (hexanes:EtOAc 3:1).

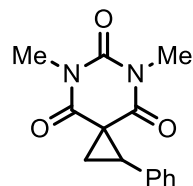
$^1\text{H NMR}$ (300 MHz, CDCl_3): δ 2.17-2.29 (m, 2H), 1.88-1.94 (m, 1H), 1.79 (s, 3H), 1.77 (s, 3H), 1.58-1.72 (m, 2H), 1.35-1.44 (m, 2H), 1.19-1.33 (m, 14H), 0.87 (t, $J = 6.8$ Hz, 3H).

$^{13}\text{C NMR}$ (75 MHz, CDCl_3): δ 171.5, 168.8, 107.6, 44.1, 34.8, 32.4, 32.3, 32.2, 32.1, 31.7, 30.6, 30.3(2C), 29.7, 25.6, 17.0.

HRMS (ESI): Calculated for $\text{C}_{18}\text{H}_{31}\text{O}_4$ ($\text{M}+\text{H}$) $^+$ 311.2217, found 311.2205.

IR (ATR): 2924 (m), 2854 (w), 1769 (w), 1741 (s), 1327 (m), 1198 (s), 968 (m) cm^{-1} .

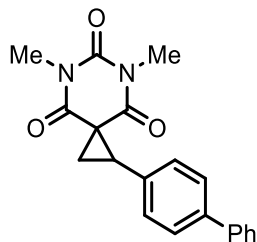
5,7-Dimethyl-1-phenyl-5,7-diazaspiro[2.5]octane-4,6,8-trione (3.30q)



Synthesized according to **GP2** using iodonium ylide **3.16l** (0.090 g, 0.25 mmol, 1 equiv), styrene (0.057 mL, 0.50 mmol, 2 equiv), MeCN (2.5 mL). The reaction was stirred for 30 h at 25 °C until the ylide was consumed as indicated by NMR. Purification by flash chromatography through a column of silica gel (hexanes:EtOAc 20:1 to 10:1) led to the title compound isolated as a clear solid (0.054 g, 84% yield). $R_f = 0.25$ (hexanes:EtOAc 3:1). The characterization data matches what has already been reported in the literature.²⁶⁵

$^1\text{H NMR}$ (300 MHz, CDCl_3): δ 7.23-7.35 (m, 5H), 3.52 (dd, $J = 9.3, 9.3$ Hz, 1H), 3.37 (s, 3H), 3.12 (s, 3H), 2.59 (dd, $J = 9.3, 4.0$ Hz, 1H), 2.45 (dd, $J = 9.3, 4.0$ Hz, 1H).

1-([1,1'-Biphenyl]-4-yl)-5,7-dimethyl-5,7-diazaspiro[2.5]octane-4,6,8-trione (3.30r)



Synthesized according to **GP2** using iodonium ylide **3.16l** (0.035 g, 0.10 mmol, 1 equiv), 4-vinyl-1,1'-biphenyl (0.036 g, 0.20 mmol, 2 equiv), MeCN (1.0 mL). The reaction was stirred for 30 h at 25 °C until the ylide was consumed as indicated by NMR. Purification by flash chromatography through a column of silica gel (hexanes:EtOAc 20:1 to 5:1) led to the title compound isolated as a white solid (0.027 g, 80% yield). $R_f = 0.23$ (hexanes:EtOAc 3:1).

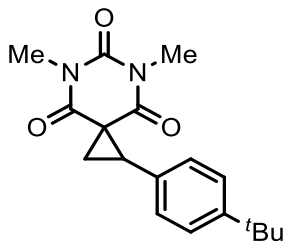
^1H NMR (300 MHz, CDCl_3): δ 7.42-7.60 (m, 4H), 7.39 (t, $J = 7.2$ Hz, 2H), 7.29-7.34 (m, 3H), 3.55 (dd, $J = 9.3, 9.3$ Hz 1H), 3.39 (s, 3H), 3.14 (s, 3H), 2.63 (dd, $J = 9.3, 3.9$ Hz, 1H), 2.49 (dd, $J = 9.3, 4.2$ Hz, 1H).

^{13}C NMR (75 MHz, CDCl_3): δ 168.3, 164.9, 152.0, 141.0, 140.4, 131.5, 130.2, 128.8, 127.5, 127.1, 126.8, 46.3, 36.2, 28.9, 28.7, 24.8.

HRMS (ESI): Calculated for $\text{C}_{20}\text{H}_{19}\text{N}_2\text{O}_3$ ($\text{M}+\text{H}$) $^+$ 335.1390, found 335.1382.

IR (ATR): 2922 (w), 1739 (w), 1686 (s), 1660 (s), 1425 (s), 1065 (m), 759 (m) cm^{-1} .

1-(4-(tert-Butyl)phenyl)-5,7-dimethyl-5,7-diazaspiro[2.5]octane-4,6,8-trione (3.30s)



Synthesized according to **GP2** using iodonium ylide **3.16l** (0.036 g, 0.10 mmol, 1.0 equiv), 1-(tert-butyl)-4-vinylbenzene (0.036 mL, 0.20 mmol, 2.0 equiv), MeCN (1.0 mL). The reaction was stirred for 28 h at 25 °C until the ylide was consumed as indicated by NMR. Purification by

flash chromatography through a column of silica gel (hexanes:EtOAc 20:1 to 10:1) led to the title compound isolated as a white solid (0.026 g, 82% yield). $R_f = 0.32$ (hexanes:EtOAc 3:1).

$^1\text{H NMR}$ (300 MHz, CDCl_3): δ 7.31 (d, $J = 8.3$ Hz, 2H), 7.19 (d, $J = 8.3$ Hz, 2H), 3.46 (dd, $J = 9.3, 9.3$ Hz, 1H), 3.36 (s, 3H), 3.12 (s, 3H), 2.59 (dd, $J = 9.3, 4.0$ Hz, 1H), 2.44 (dd, $J = 9.3, 4.0$ Hz, 1H), 1.29 (s, 9H).

$^{13}\text{C NMR}$ (75 MHz; CDCl_3): δ 168.4, 164.9, 152.0, 151.2, 129.5, 129.3, 125.0, 46.7, 36.3, 34.6, 31.3, 28.9, 28.6, 24.6.

HRMS (ESI): Calculated for $\text{C}_{18}\text{H}_{23}\text{N}_2\text{O}_3$ ($\text{M}+\text{H}$) $^+$ 315.1703, found 315.1695.

IR (ATR): 2956 (w), 2865 (w), 1742 (w), 1669 (s), 1382 (m), 757 (m) cm^{-1} .

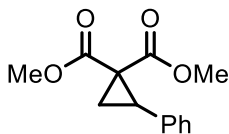
Methyl 1-acetyl-2-phenylcyclopropanecarboxylate (**3.30t**)



Synthesized according to **GP2** using iodonium ylide **3.16m** (0.032g, 0.10 mmol, 1.0 equiv), styrene (0.023 mL, 0.20 mmol, 2.0 equiv), MeCN (1.0 mL). The reaction was stirred for 19 h at 25 °C until the ylide was consumed as indicated by NMR. Purification by flash chromatography through a column of silica gel (hexanes:EtOAc 20:1 to 10:1) led to the title compound isolated as a cloudy white oil (0.018 g, 82% yield) with a 1.3:1 *dr*. $R_f = 0.47$ (hexanes:EtOAc 3:1). The characterization data matches what has already been reported in the literature.²⁶⁸

$^1\text{H NMR}$ (300 MHz, CDCl_3): δ 7.09-7.36 (m, 12H), 3.80 (s, 3H, major), 3.33 (s, 3H, minor), 3.23-3.30 (m, 2H, major and minor), 2.44 (s, 3H, minor), 2.21-2.32 (m, 2H, major and minor), 1.93 (s, 3H, major), 1.75-1.67 (m, 2H, major and minor).

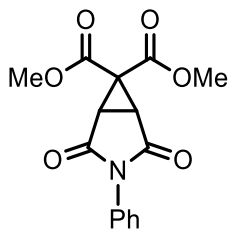
Dimethyl 2-phenylcyclopropane-1,1-dicarboxylate (3.30u)



Synthesized according to **GP2** using iodonium ylide **3.16n** (0.033g, 0.10 mmol, 1.0 equiv), styrene (0.023 mL, 0.20 mmol, 2.0 equiv), MeCN (1.0 mL). The reaction was stirred for 17 h at 25 °C until the ylide was consumed as indicated by NMR. Purification by flash chromatography through a column of silica gel (hexanes:EtOAc 20:1 to 10:1) led to the title compound isolated as a clear oil (0.015 g, 64% yield). $R_f = 0.45$ (hexanes:EtOAc 3:1). The characterization data matches what has already been reported in the literature.²⁷¹

¹H NMR (300 MHz, CDCl₃): δ 7.15-7.27 (m, 5H), 3.78 (s, 3H), 3.35 (s, 3H), 3.22 (dd, $J = 8.7, 8.7$ Hz, 1H), 2.19 (dd, $J = 7.8, 5.3$ Hz, 1H), 1.73 (dd, $J = 9.2, 5.2$ Hz, 1H).

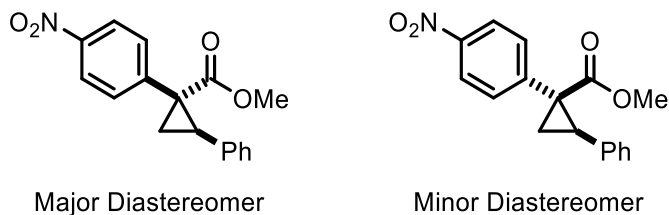
Dimethyl 2,4-dioxo-3-phenyl-3-azabicyclo[3.1.0]hexane-6,6-dicarboxylate (3.30v)



Synthesized according to **GP2** using iodonium ylide **3.16n** (0.033g, 0.10 mmol, 1.0 equiv), 1-phenyl-1H-pyrrole-2,5-dione (0.035 g, 0.20 mmol, 2.0 equiv), MeCN (1.0 mL). The reaction was stirred for 7 h at 25 °C until the ylide was consumed as indicated by NMR. Purification by flash chromatography through a column of silica gel (hexanes:EtOAc 20:1 to 1:1) led to the title compound isolated as a brownish-orange solid (0.014 g, 46% yield). $R_f = 0.08$ (hexanes:EtOAc 3:1). The characterization data matches what has already been reported in the literature.²⁶⁵

¹H NMR (300 MHz, CDCl₃): δ 7.33-7.47 (m, 3H), 7.16 (d, $J = 7.1$ Hz, 2H), 3.84 (s, 3H), 3.77 (s, 3H), 3.25 (s, 2H).

Methyl 1-(4-nitrophenyl)-2-phenylcyclopropanecarboxylate (3.30w)



Synthesized using methyl 2-(4-nitrophenyl)acetate (0.020 g, 0.1 mmol, 1.0 equiv) to which 60% dispersion NaH (pre-washed with pentane; 0.016 g, 0.4 mmol, 4.0 equiv) in MeCN (1.5 mL) at 0 °C, then raising to rt for 20 min. To this, was added (diacetoxyiodo)benzene (0.032 g, 0.1 mmol, 1.0 equiv) in MeCN (1.0 mL) at -10 °C for 10 min, then raising to 10 °C for 10 min. Styrene (0.023 mL, 0.2 mmol, 2.0 equiv) was then added at 10 °C and blue LED applied for 3 h. Purification by flash chromatography through a column of silica gel (hexanes:EtOAc 20:1 to 5:1) led to the title compound isolated as a yellowish solid (0.012 g, 42% yield) with a 1.7:1 *dr*. Major diastereomer: $R_f = 0.40$ (hexanes:EtOAc 3:1). Minor diastereomer: $R_f = 0.49$ (hexanes:EtOAc 3:1). The characterization data matches what has already been reported in the literature.²⁷²

Major diastereomer $R_f = 0.40$ (hexanes:EtOAc 3:1):

¹H NMR (300 MHz, CDCl₃): δ 7.97 (d, $J = 8.5$ Hz, 2H), 7.17 (d, $J = 8.5$ Hz, 2H), 7.06-7.08 (m, 3H), 6.77-6.79 (m, 2H), 3.67 (s, 3H), 3.20 (dd, $J = 8.8, 7.9$ Hz, 1H), 2.21 (dd, $J = 8.8, 5.4$ Hz, 1H), 1.94 (dd, $J = 7.9, 5.4$ Hz, 1H).

Minor diastereomer $R_f = 0.49$ (hexanes:EtOAc 3:1):

¹H NMR (300 MHz, CDCl₃): δ 8.22 (d, $J = 8.8$ Hz, 2H), 7.65 (d, $J = 8.8$ Hz, 2H), 7.25-7.35 (m, 5H), 3.31 (s, 3H), 2.88 (dd, $J = 8.0, 8.0$ Hz, 1H), 2.44 (dd, $J = 7.3, 5.4$ Hz, 1H), 1.67 (dd, $J = 9.3, 5.4$ Hz, 1H).

3.13 NMR Spectra for Chapter 3

Figure 3.29. ^1H NMR (300 MHz, CDCl_3) spectrum of (4-methylphenyl)(4,4-dimethyl-2,6-dioxocyclohexyl)iodonium

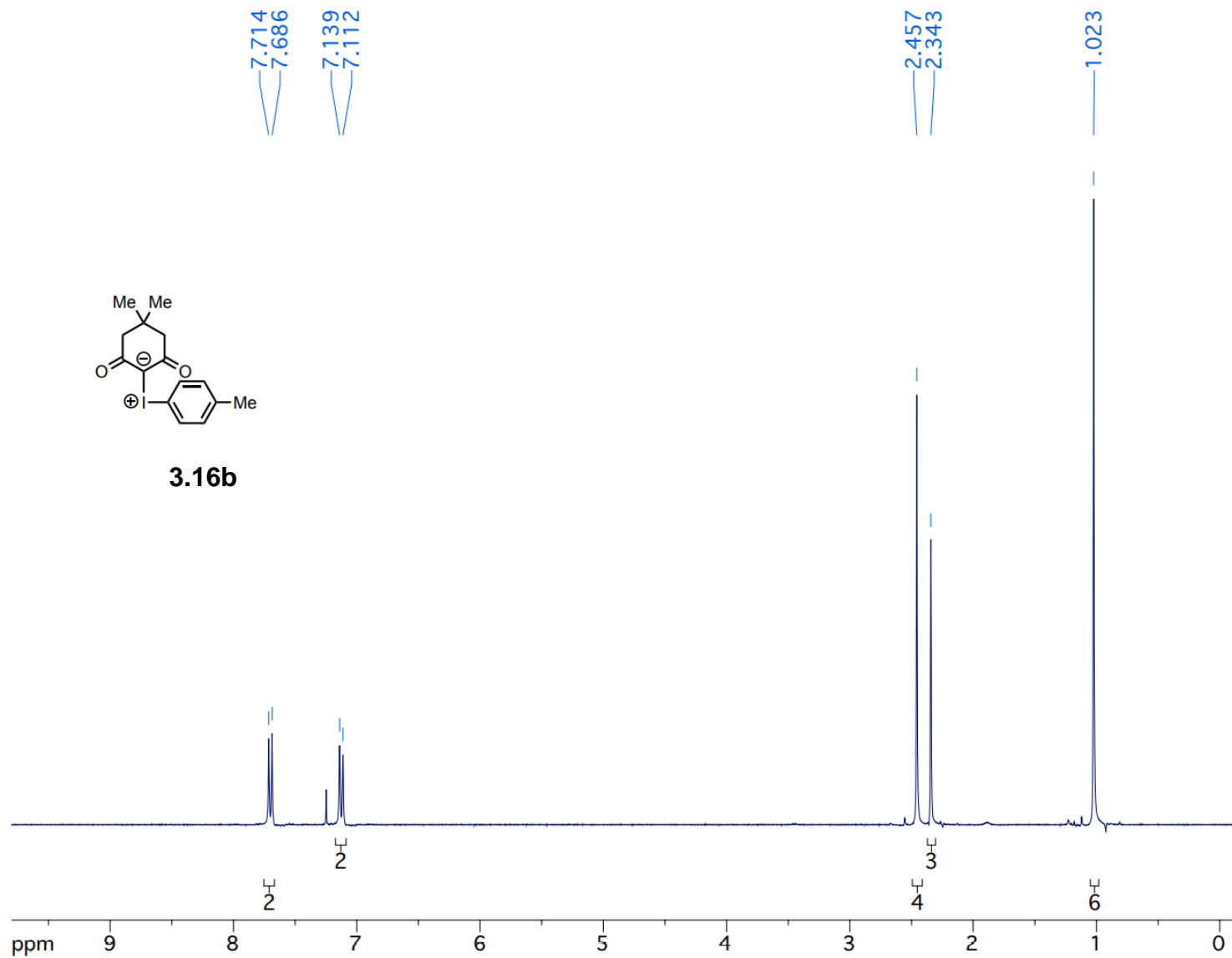


Figure 3.30 ^{13}C NMR (75 MHz, CDCl_3) spectrum of (4-methylphenyl)(4,4-dimethyl-2,6-dioxocyclohexyl)iodonium

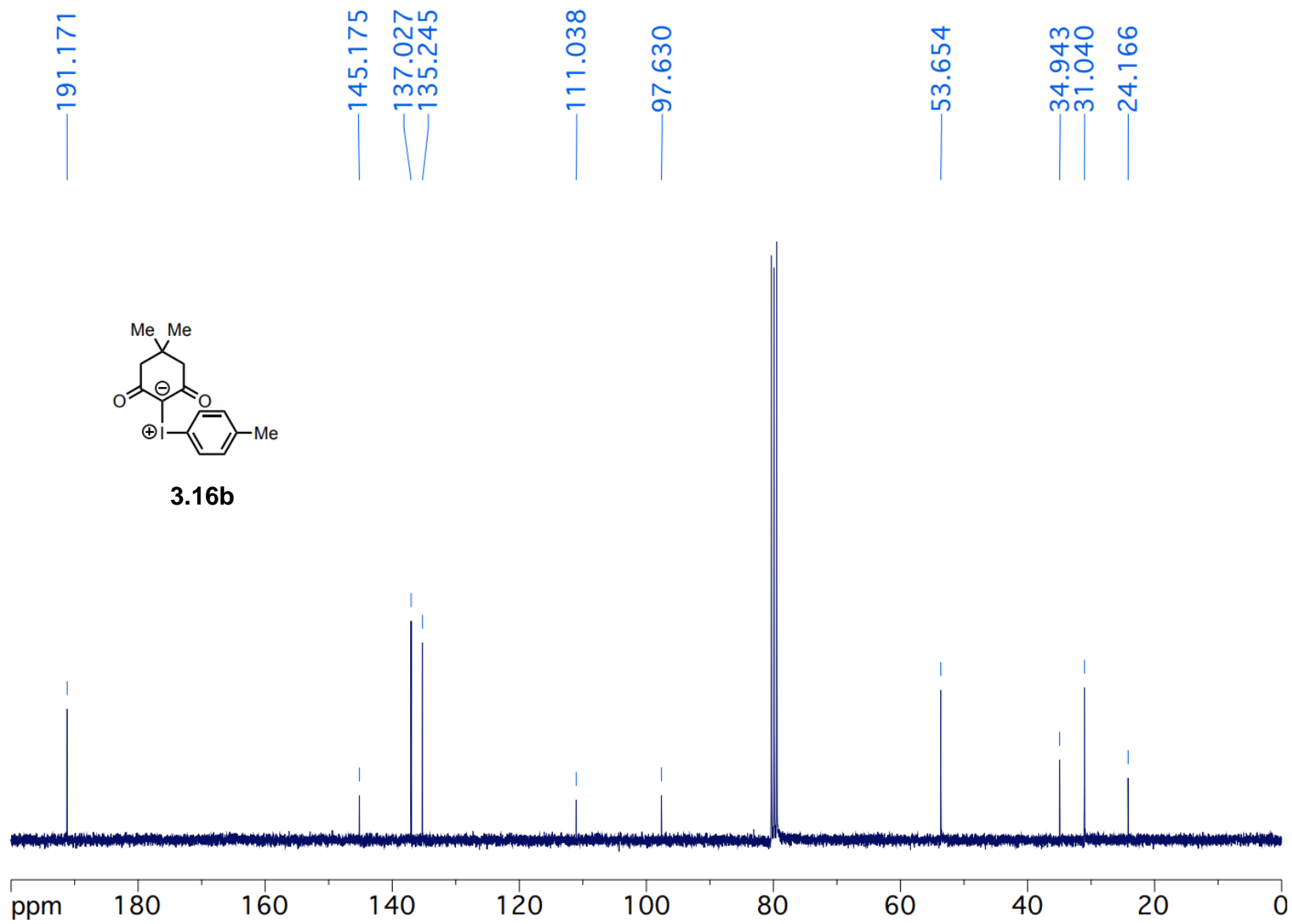


Figure 3.31 ^1H NMR (300 MHz, CDCl_3) spectrum of (4-cyanophenyl)(4,4-dimethyl-2,6-dioxocyclohexyl)iodonium

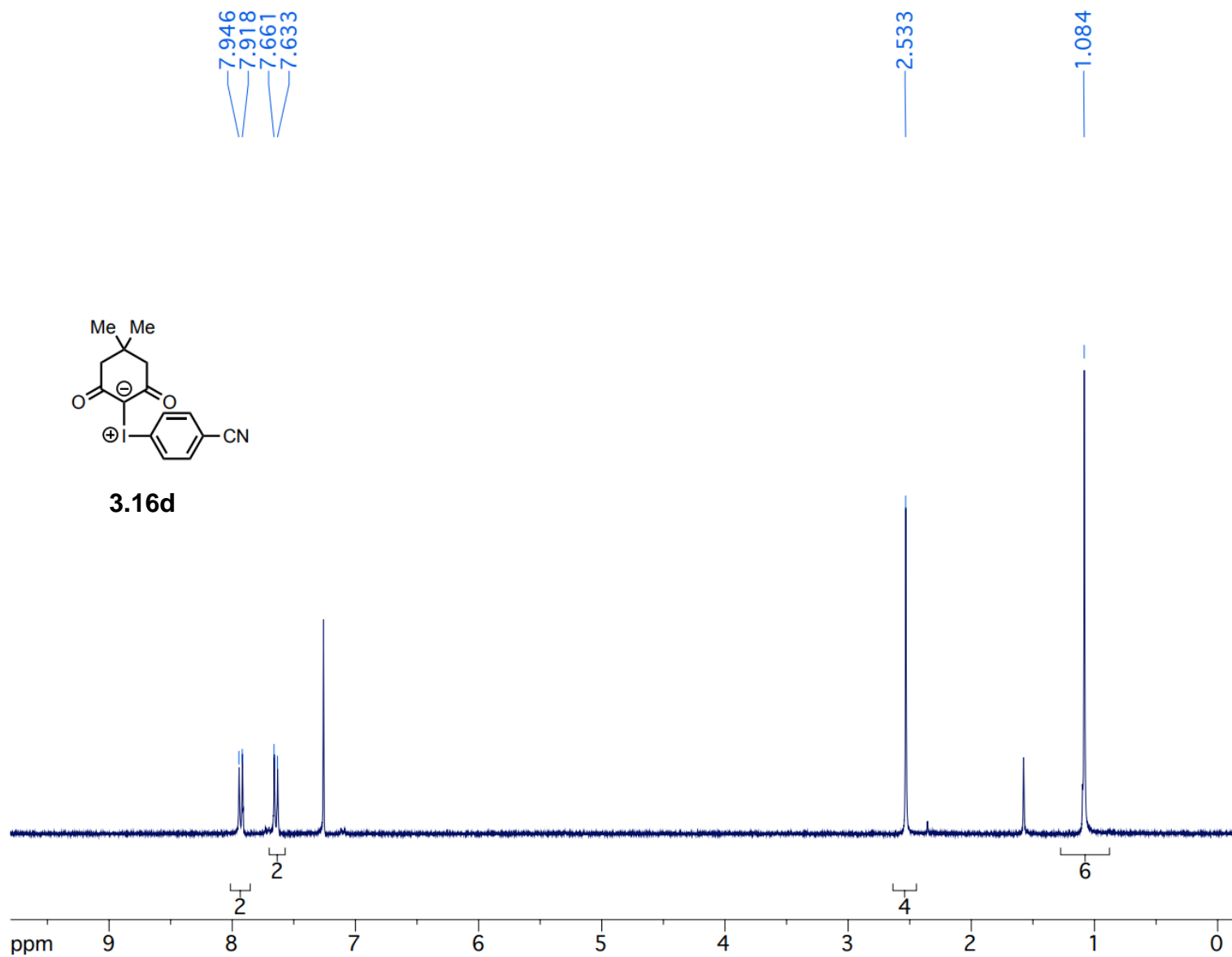


Figure 3.32 ^{13}C NMR (75 MHz, CDCl_3) spectrum of (4-cyanophenyl)(4,4-dimethyl-2,6-dioxocyclohexyl)iodonium

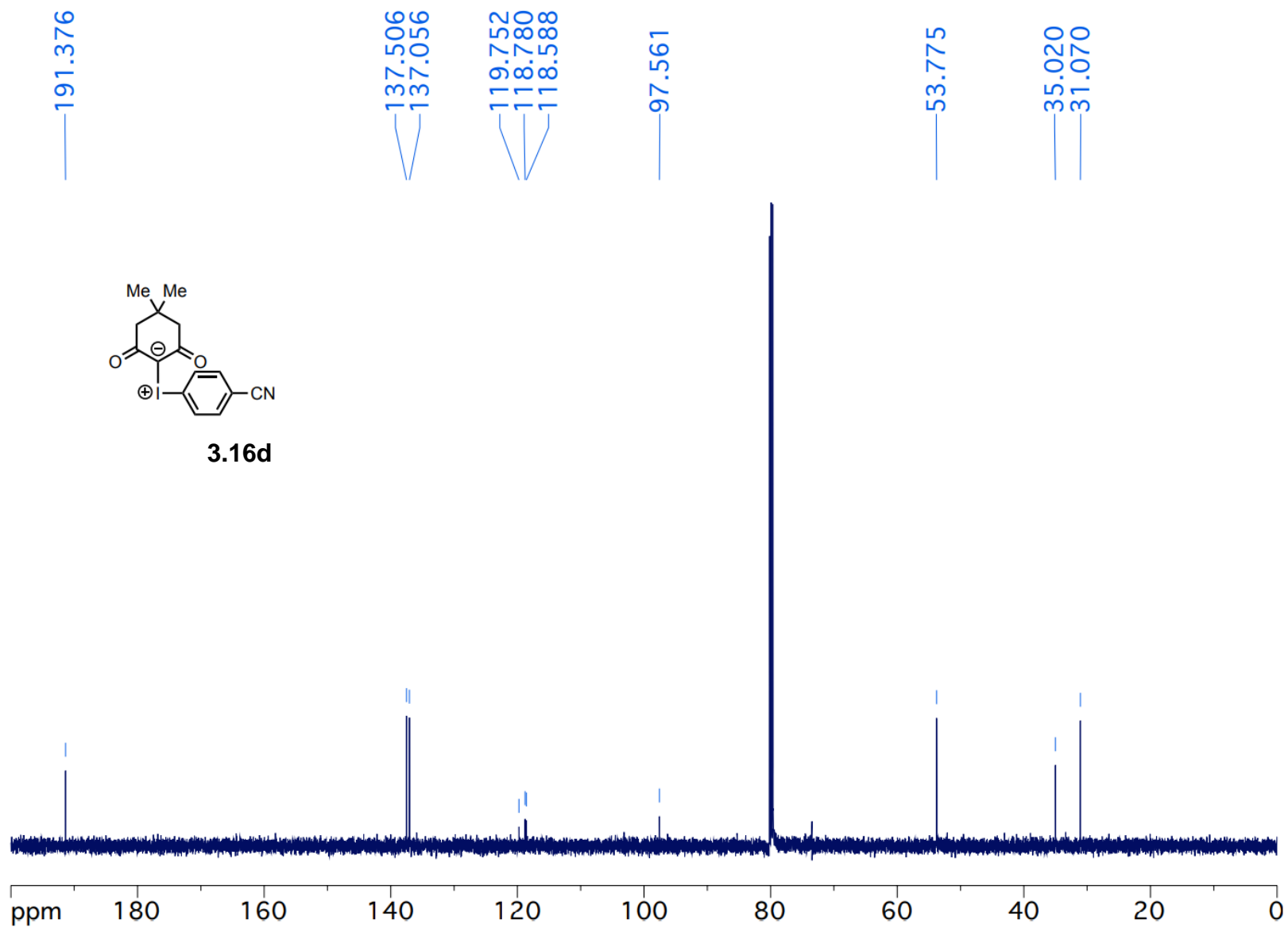


Figure 3.33 ^1H NMR (300 MHz, CDCl_3) spectrum of (4-trifluoromethylphenyl)(4,4-dimethyl-2,6-dioxocyclohexyl)iodonium

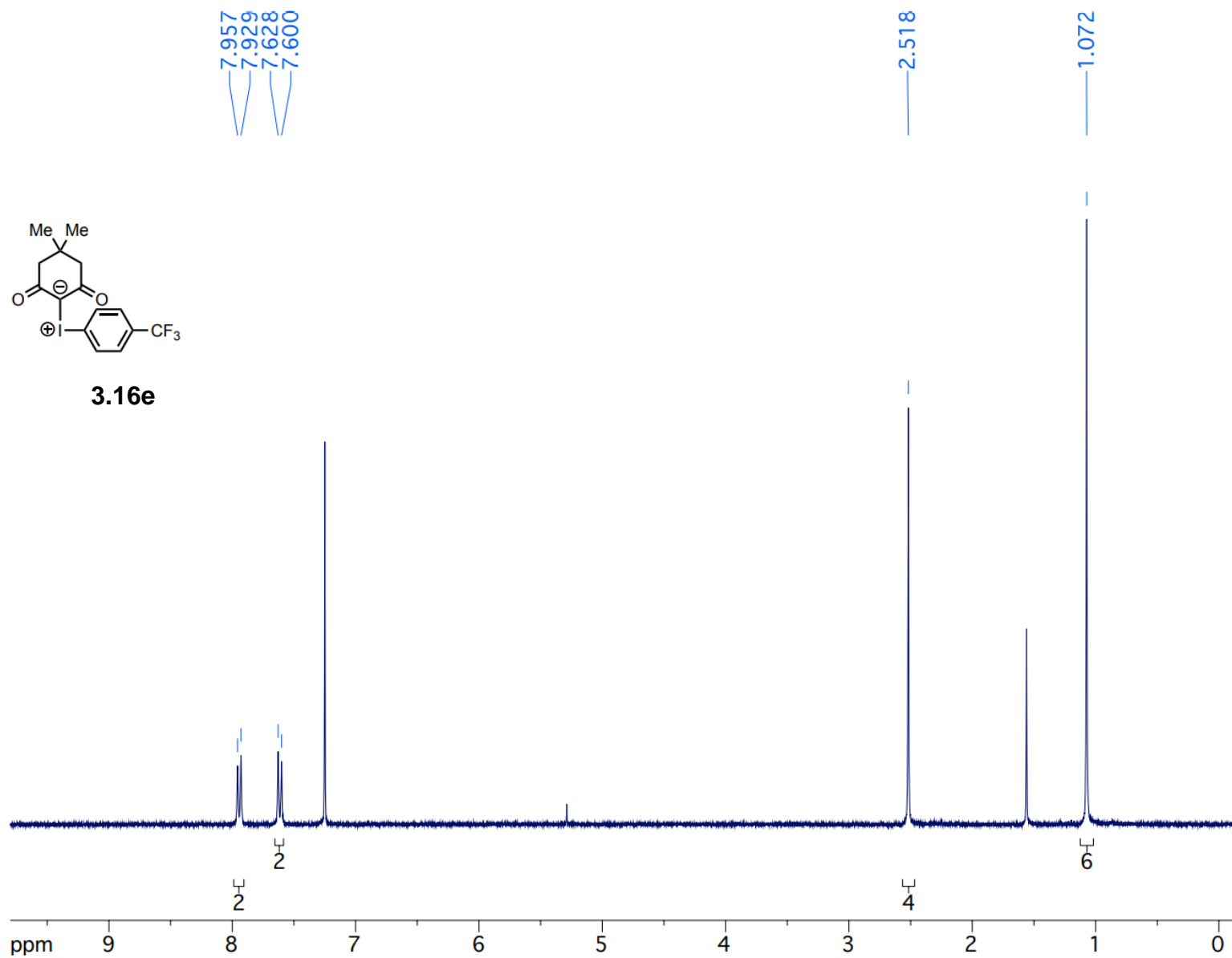


Figure 3.34 ^{13}C NMR (75 MHz, CDCl_3) spectrum of (4-trifluoromethylphenyl)(4,4-dimethyl-2,6-dioxocyclohexyl)iodonium

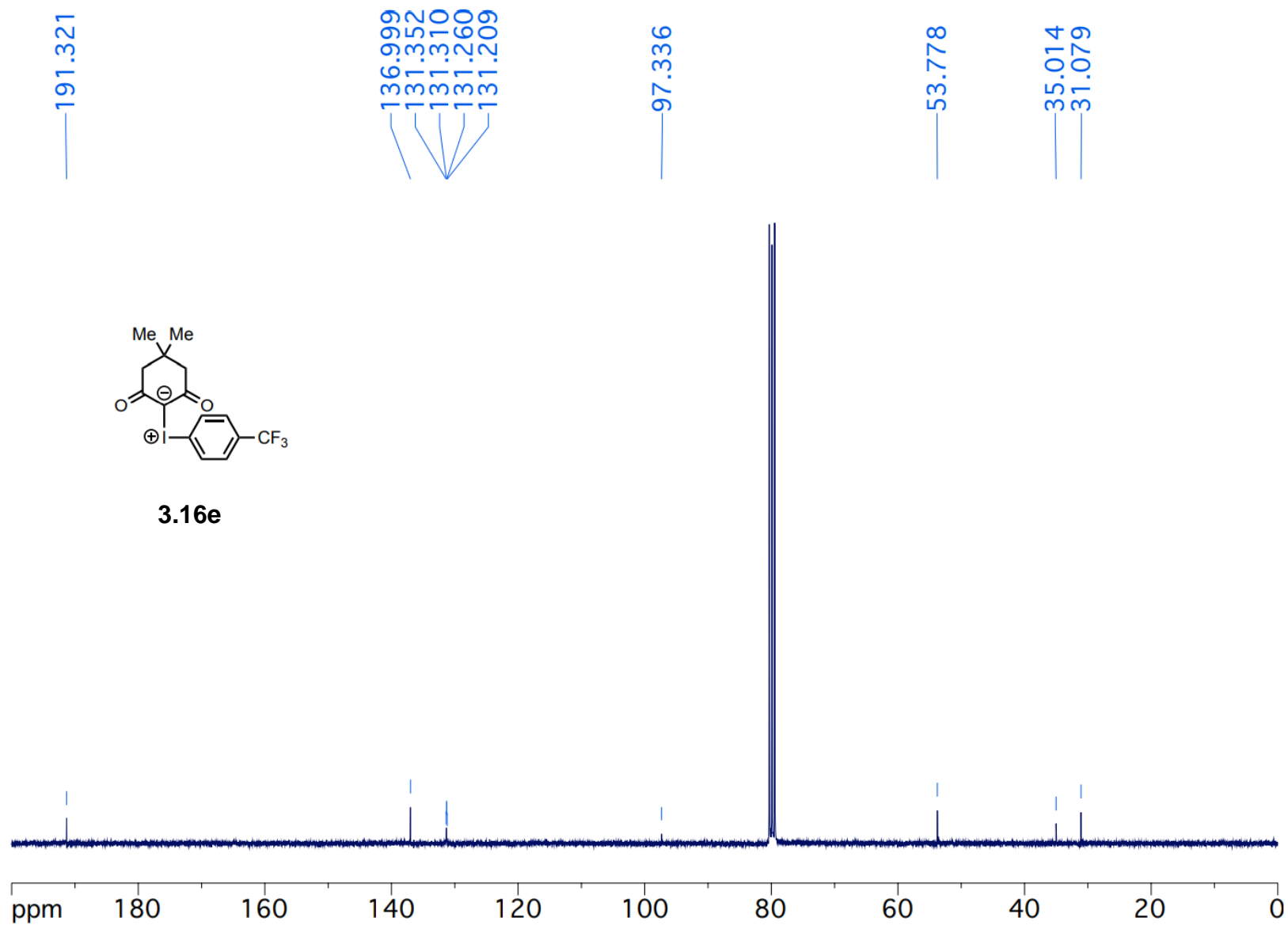


Figure 3.35 ^{19}F NMR (282 MHz, CDCl_3) spectrum of (4-trifluoromethylphenyl)(4,4-dimethyl-2,6-dioxocyclohexyl)iodonium

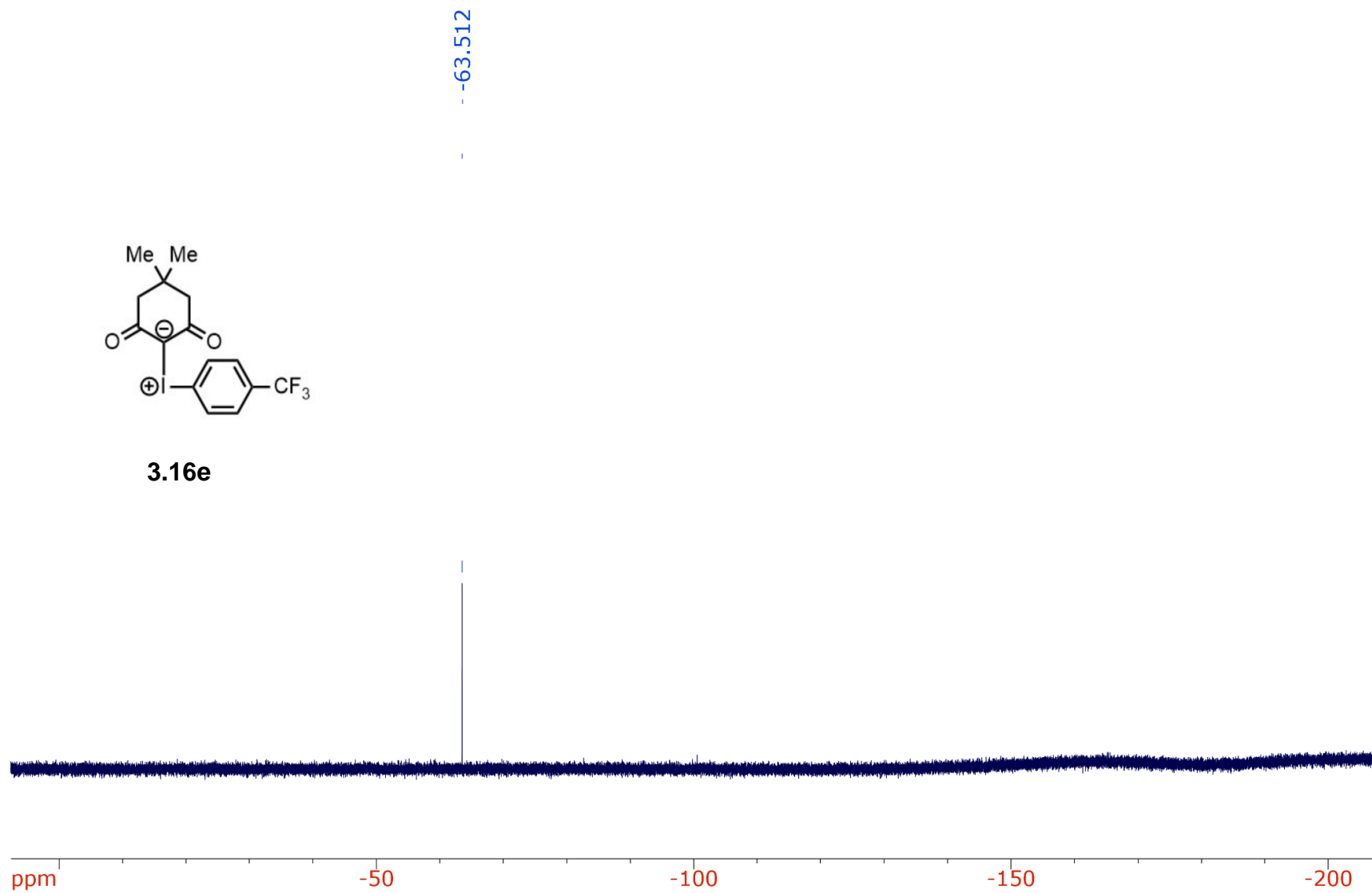


Figure 3.36 ^1H NMR (300 MHz, CDCl_3) spectrum of (2,6-dimethoxy-4-methylphenyl)(4,4-dimethyl-2,6-dioxocyclohexyl)iodonium

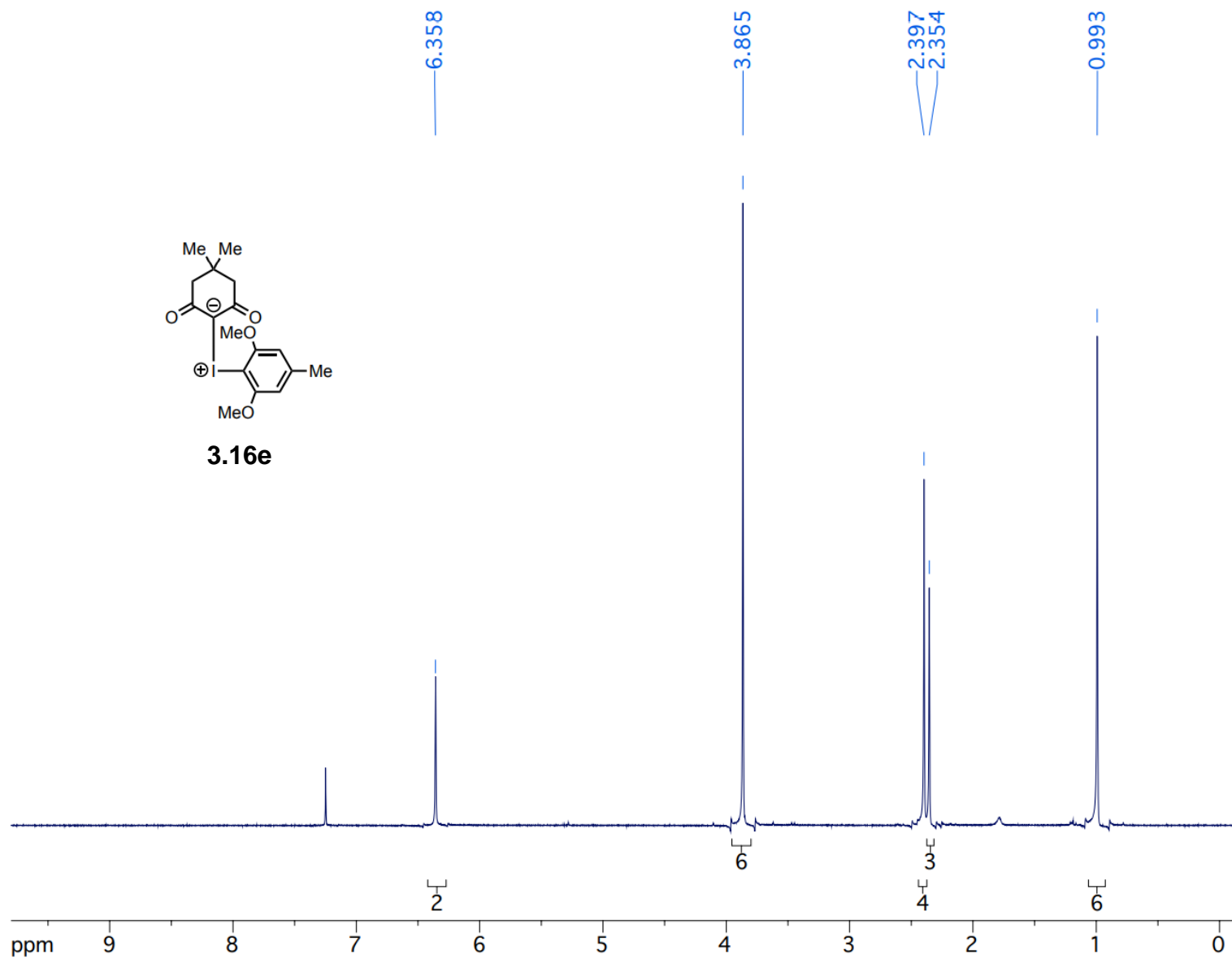


Figure 3.37 ^{13}C NMR (75 MHz, CDCl_3) spectrum of (2,6-dimethoxy-4-methylphenyl)(4,4-dimethyl-2,6-dioxocyclohexyl)iodonium

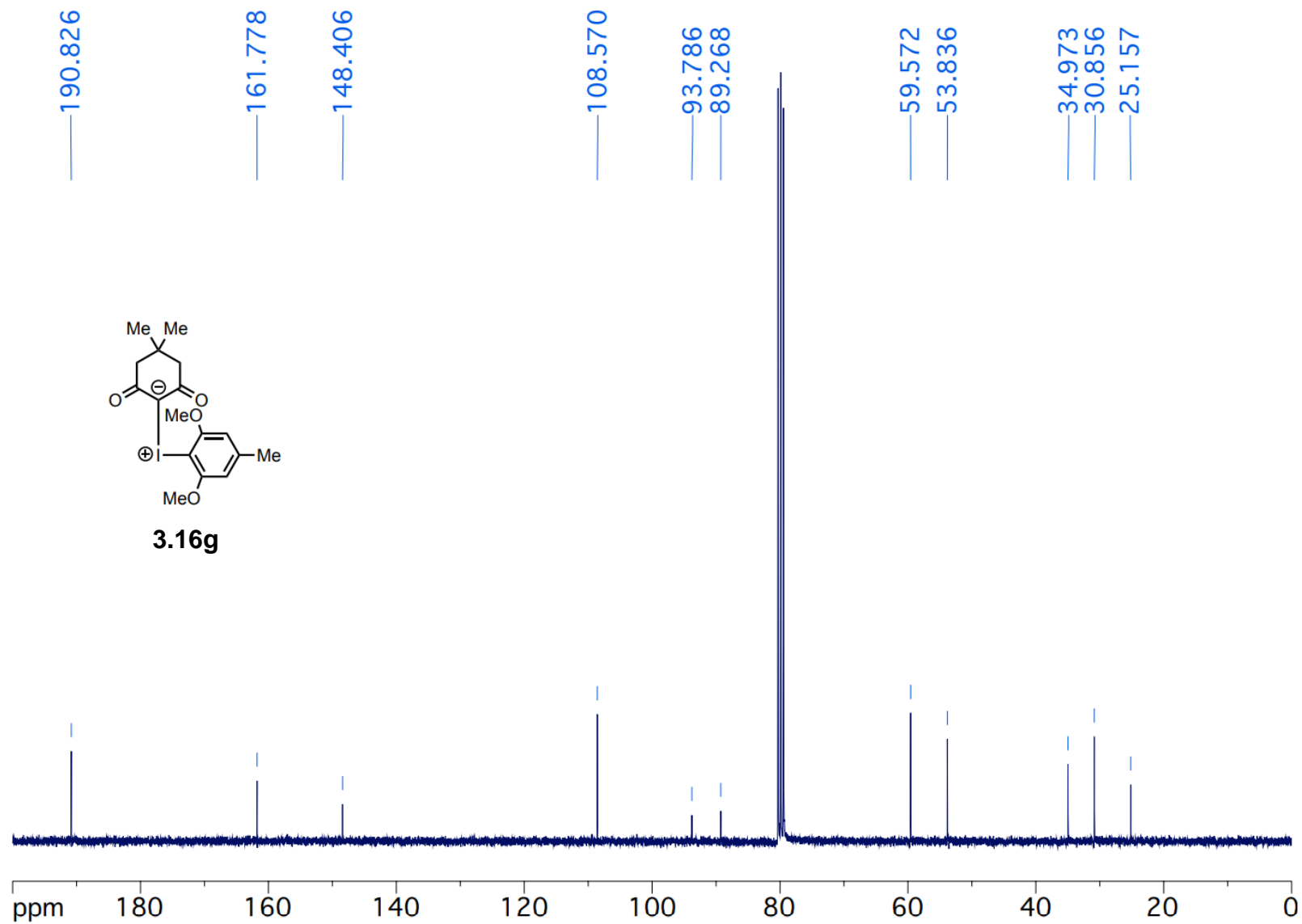


Figure 3.38 ^1H NMR (300 MHz, CDCl_3) spectrum of (4,4-dimethyl-2,6-dioxocyclohexyl)(naphthalen-1-yl)iodonium

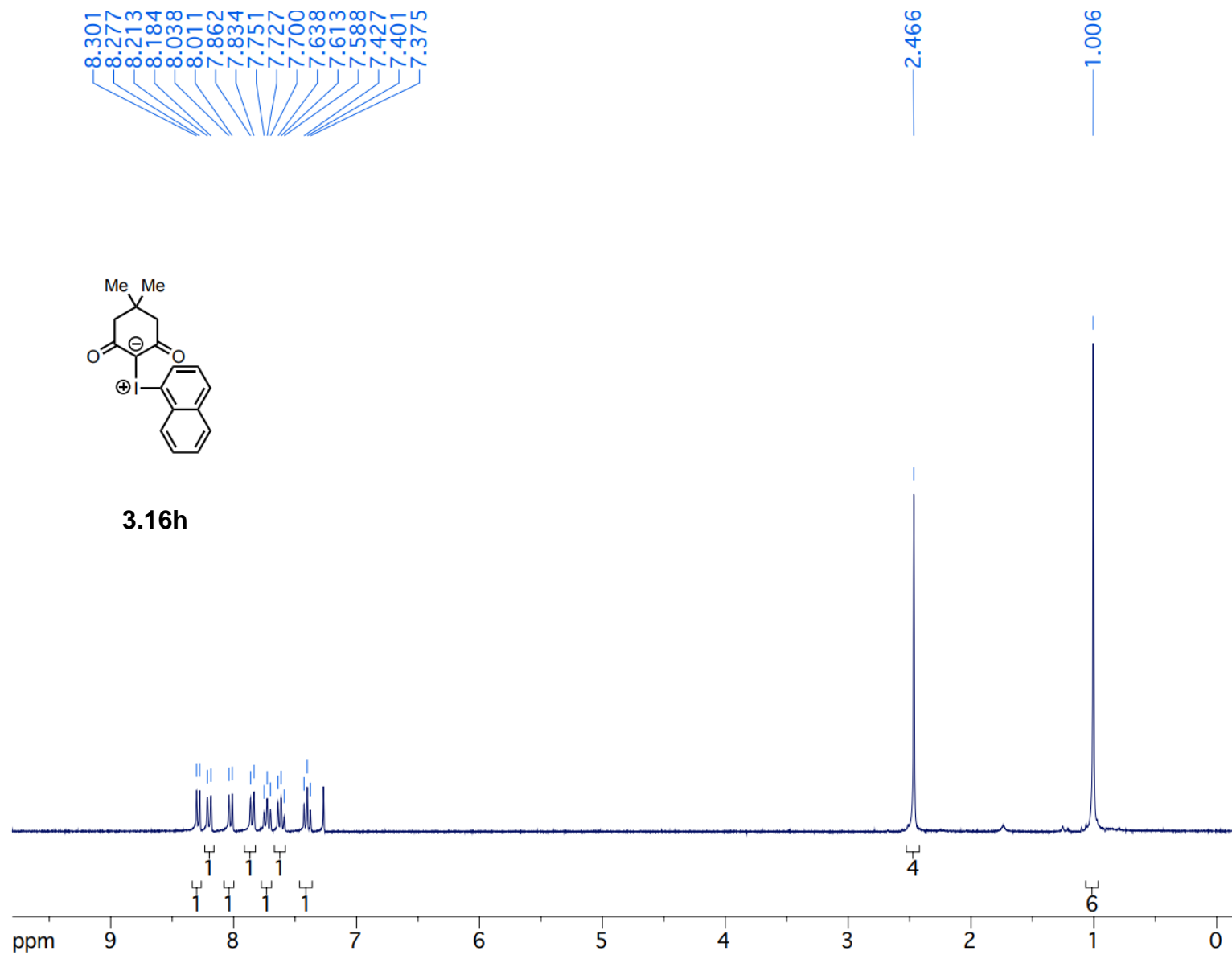


Figure 3.39 ^{13}C NMR (75 MHz, CDCl_3) spectrum of (4,4-dimethyl-2,6-dioxocyclohexyl)(naphthalen-1-yl)iodonium

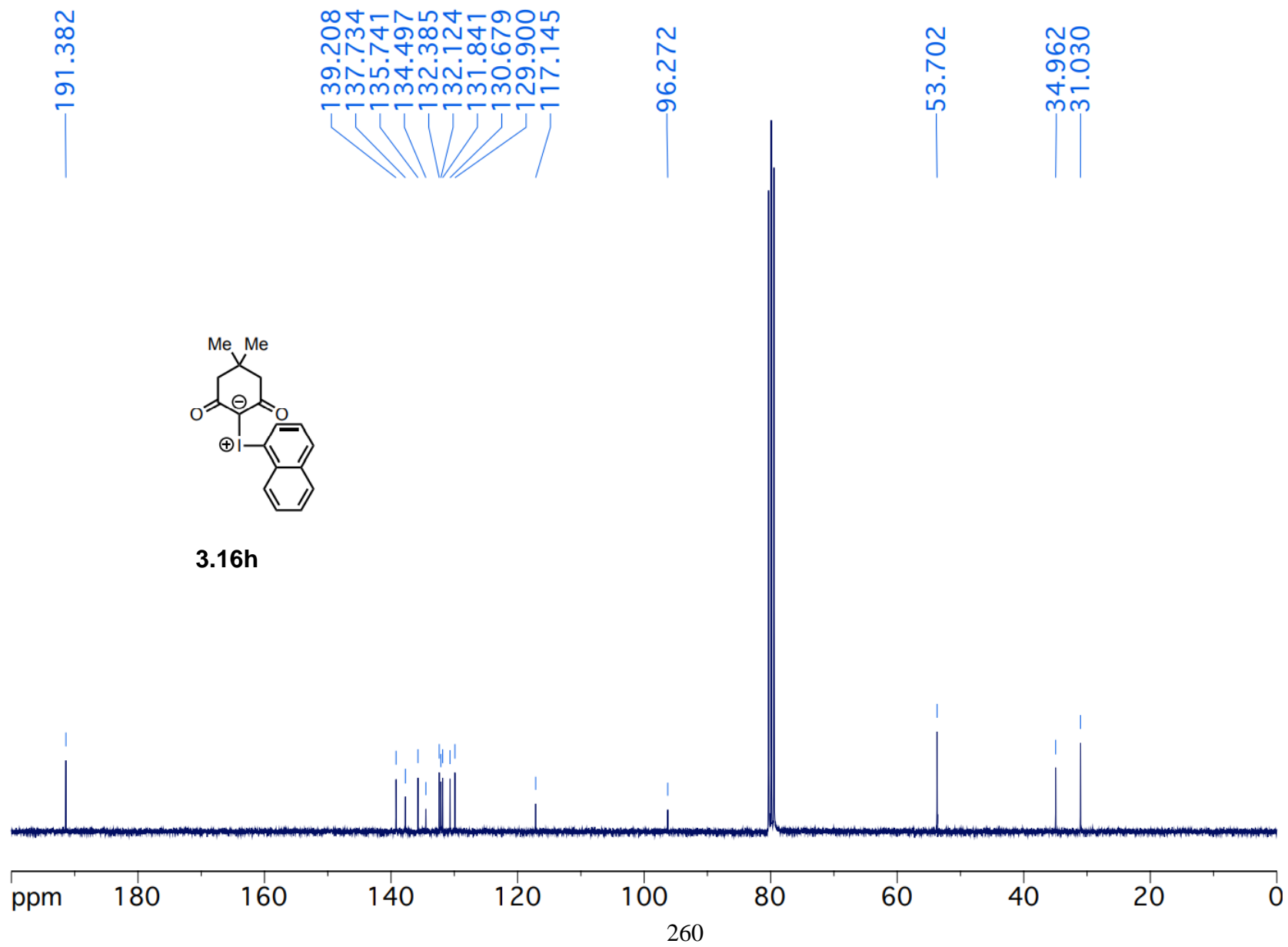


Figure 3.40 ^1H NMR (300 MHz, CDCl_3) spectrum of (4-nitrophenyl)(4,4-dimethyl-2,6-dioxocyclohexyl)iodonium

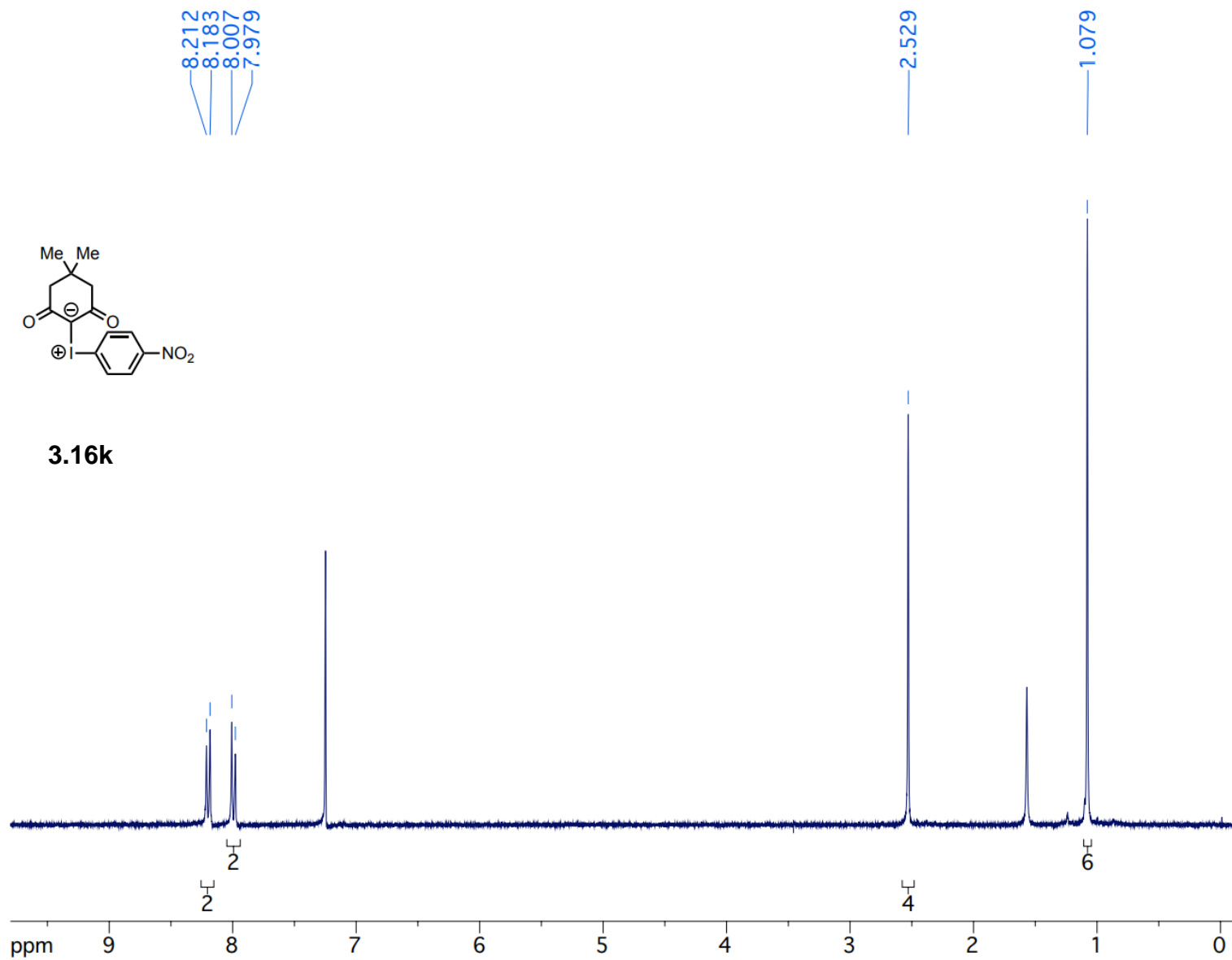


Figure 3.41 ^{13}C NMR (75 MHz, CDCl_3) spectrum of (4-nitrophenyl)(4,4-dimethyl-2,6-dioxocyclohexyl)iodonium

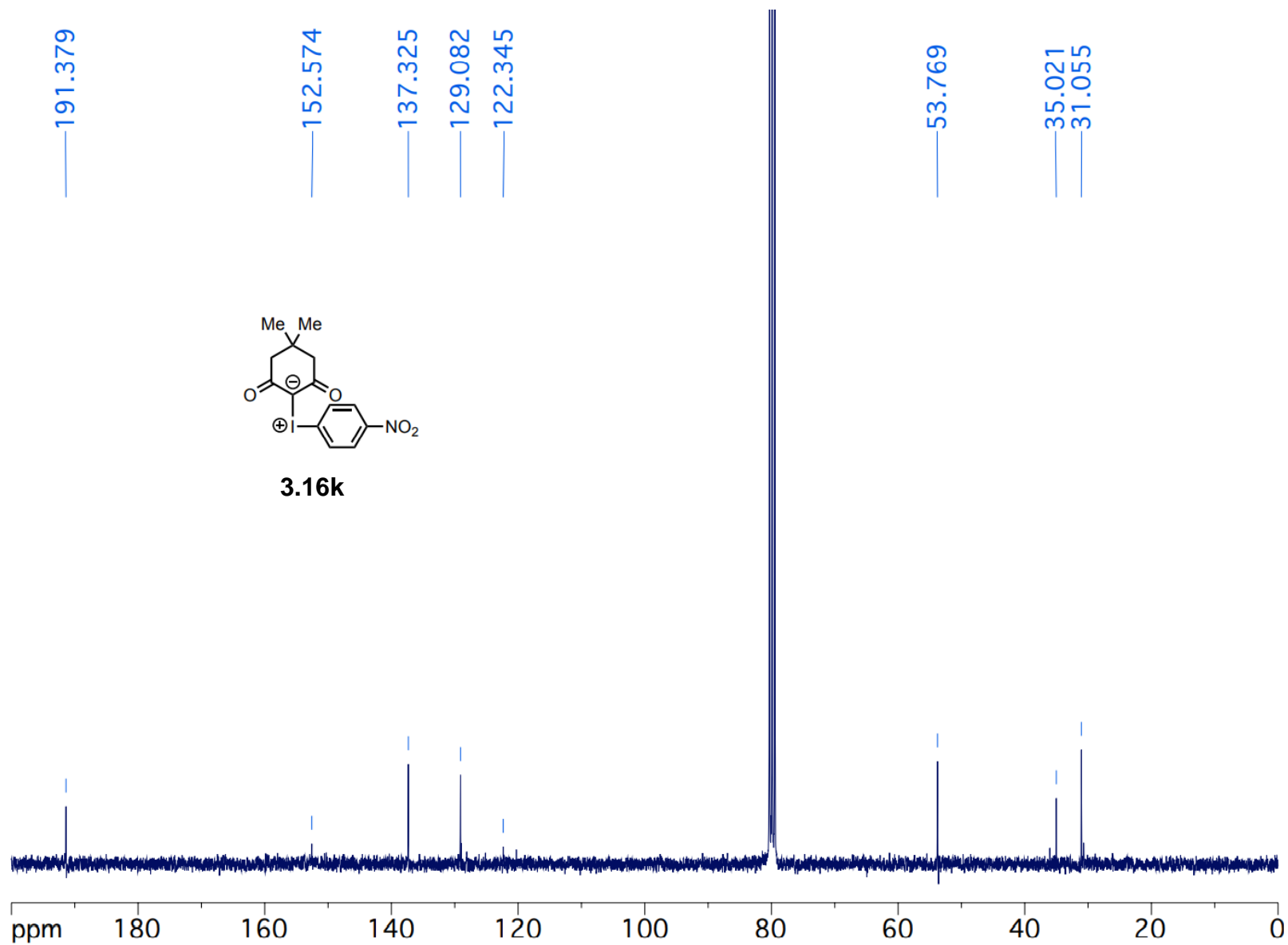


Figure 3.42 ^1H NMR (300 MHz, CDCl_3) spectrum of 1-(4-(tert-butyl)phenyl)-6,6-dimethyl-5,7-dioxaspiro[2.5]octane-4,8-dione

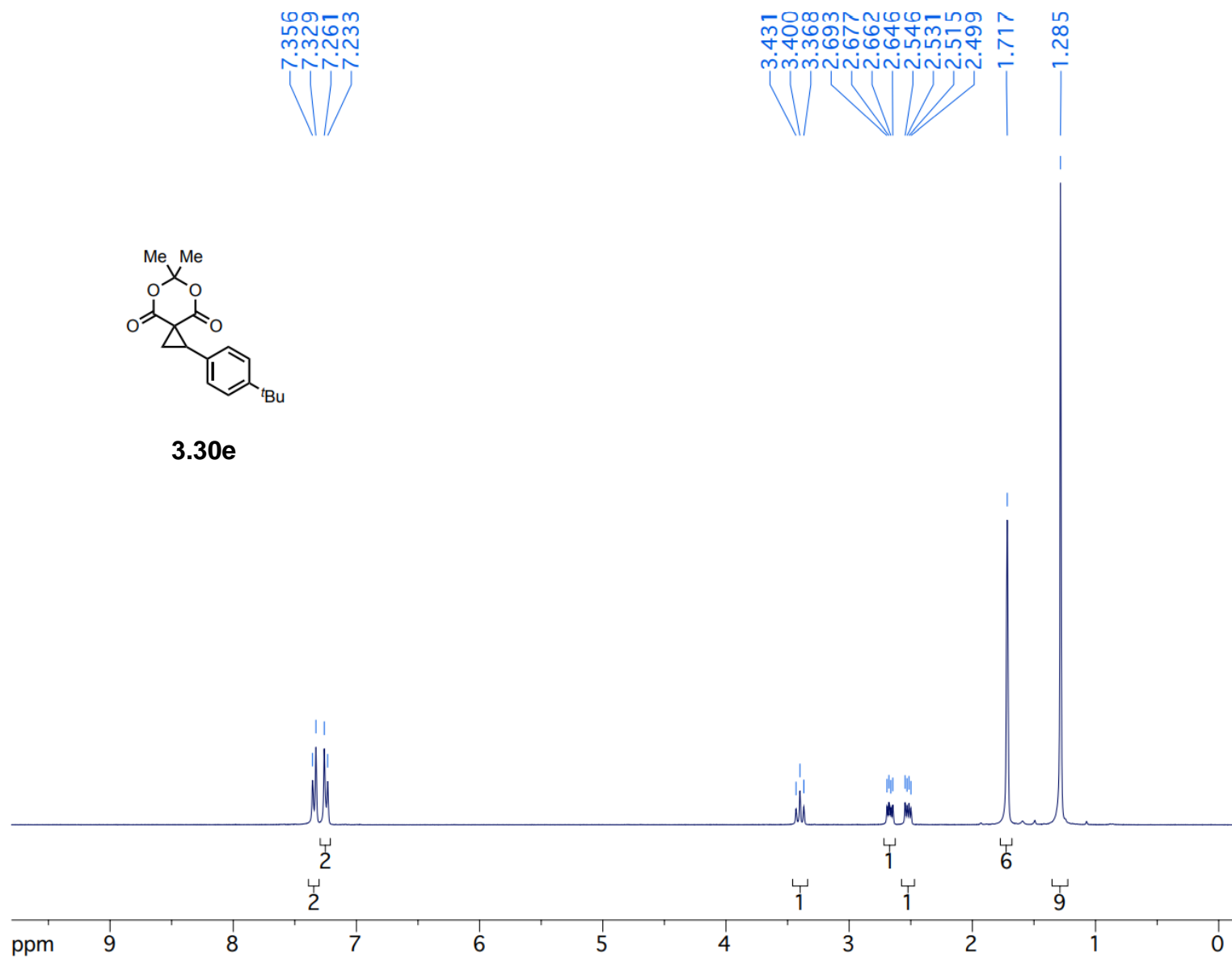


Figure 3.43 ^{13}C NMR (75 MHz, CDCl_3) spectrum of 1-(4-(tert-butyl)phenyl)-6,6-dimethyl-5,7-dioxaspiro[2.5]octane-4,8-dione

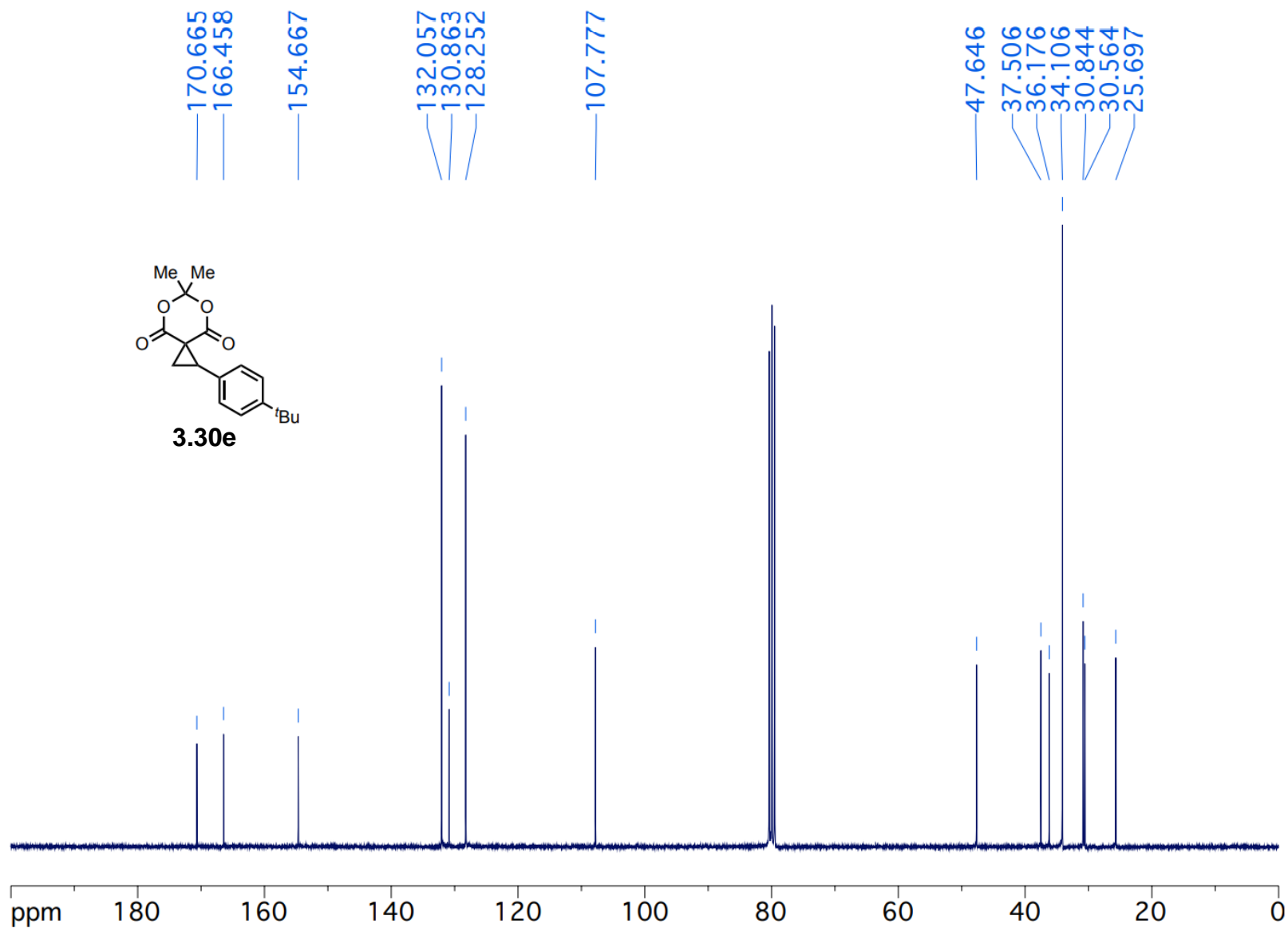


Figure 3.44 ^1H NMR (300 MHz, CDCl_3) spectrum of 1-([1,1'-biphenyl]-4-yl)-6,6-dimethyl-5,7-dioxaspiro[2.5]octane-4,8-dione

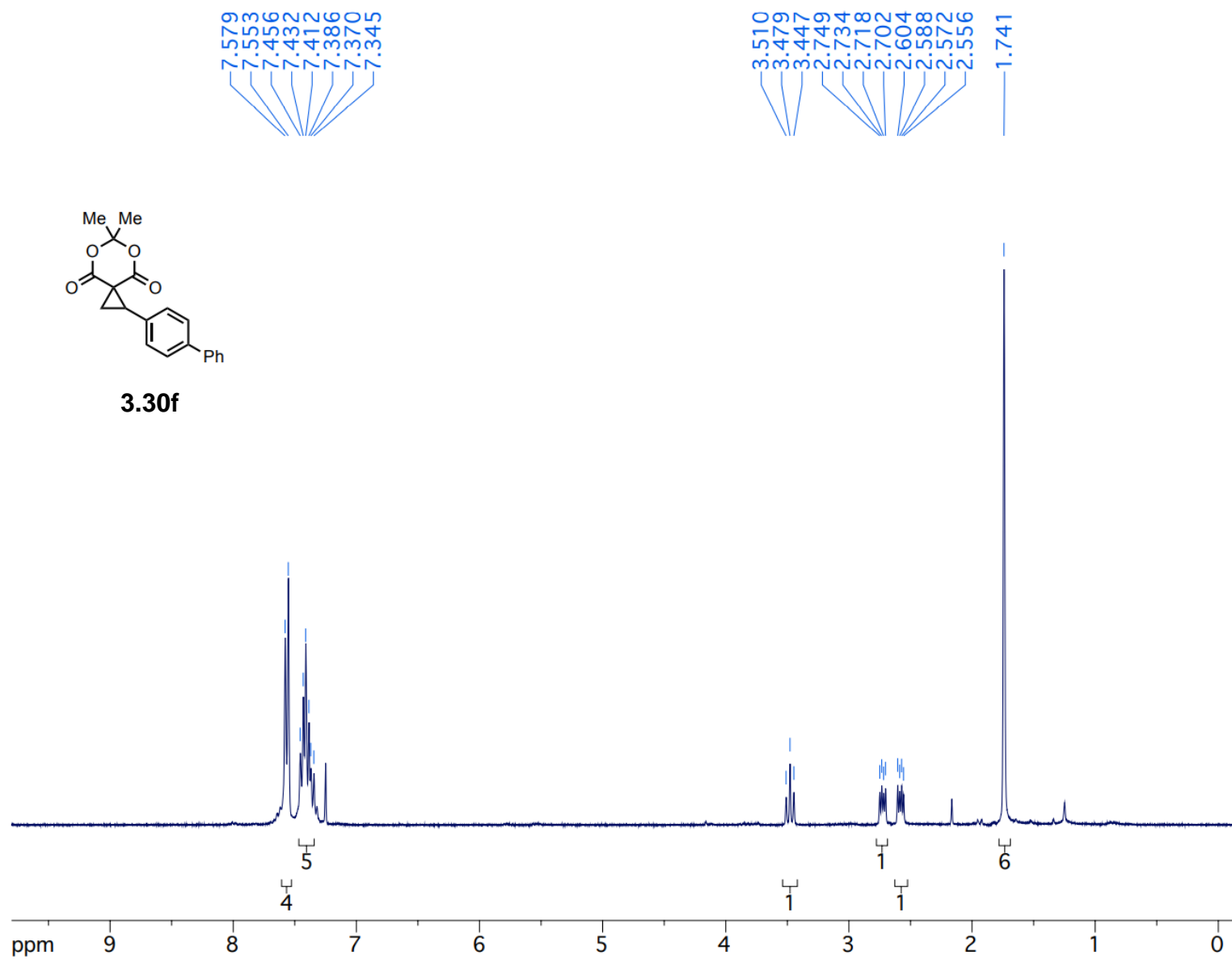
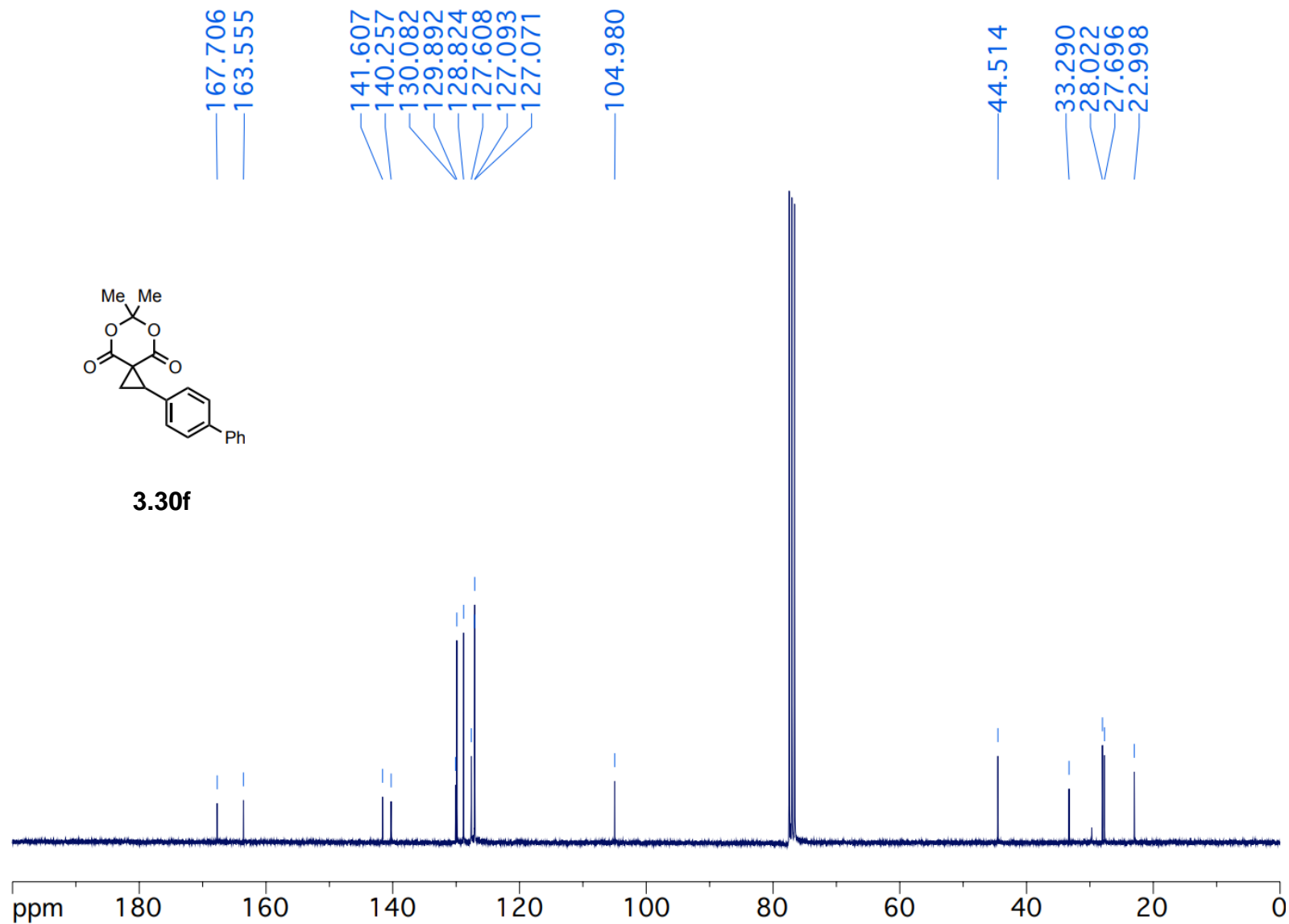


Figure 3.45 ^{13}C NMR (75 MHz, CDCl_3) spectrum of 1-([1,1'-biphenyl]-4-yl)-6,6-dimethyl-5,7-dioxaspiro[2.5]octane-4,8-dione



3.30f

Figure 3.46 ^1H NMR (300 MHz, CDCl_3) spectrum of 1-(3,4,5-trimethoxyphenyl)-6,6-dimethyl-5,7-dioxaspiro[2.5]octane-4,8-dione

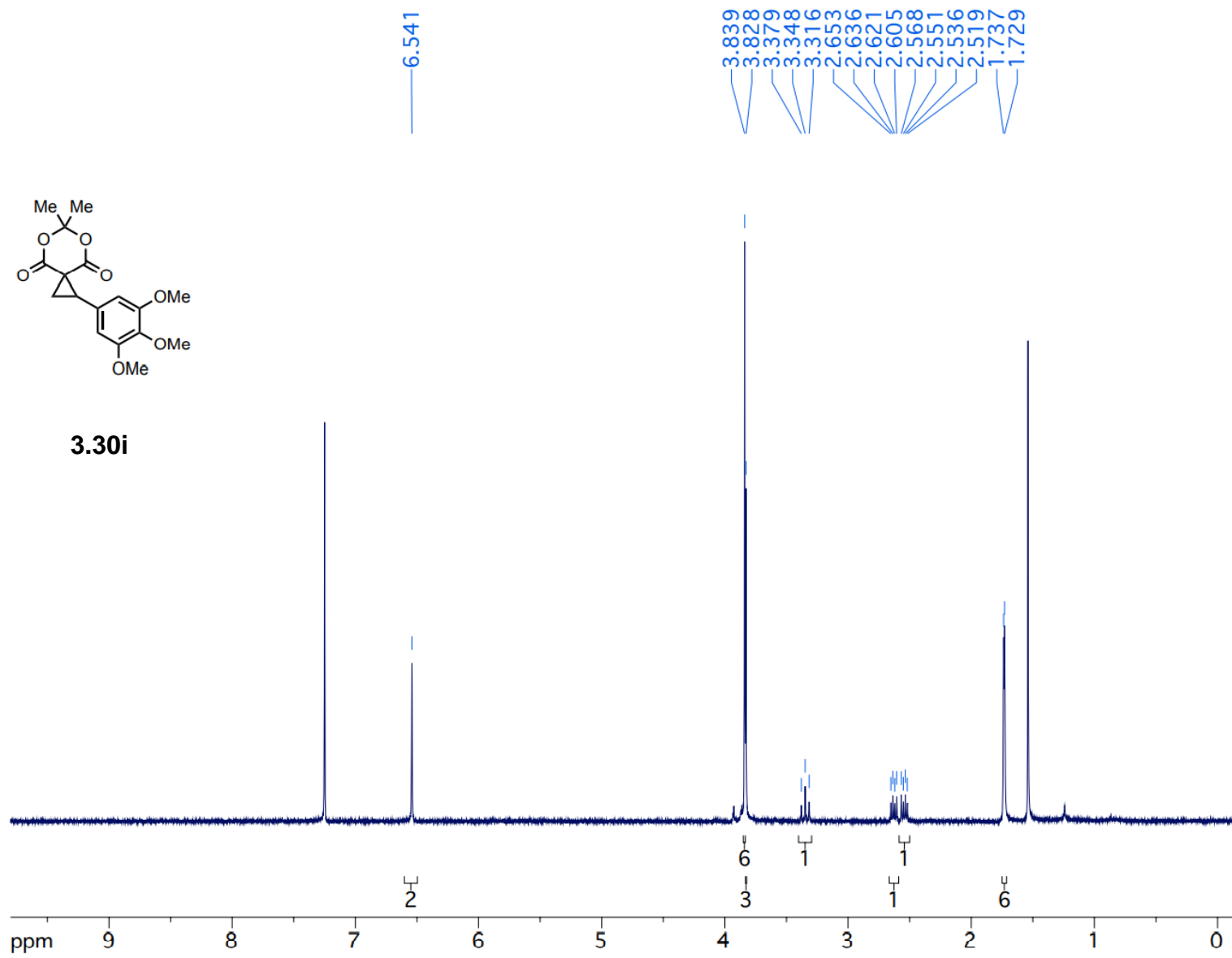


Figure 3.47 ^{13}C NMR (75 MHz, CDCl_3) spectrum of 1-(3,4,5-trimethoxyphenyl)-6,6-dimethyl-5,7-dioxaspiro[2.5]octane-4,8-dione

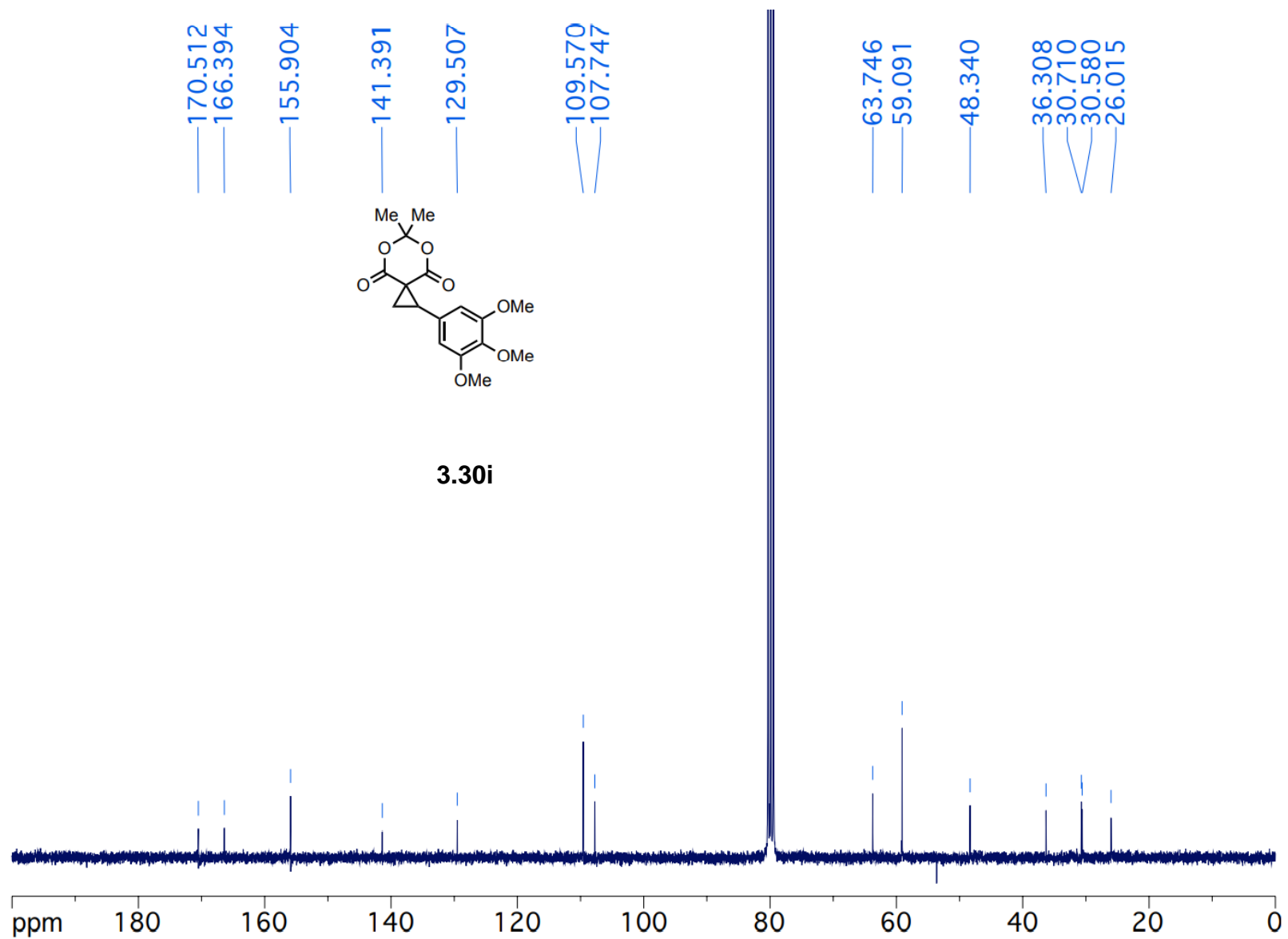


Figure 3.48 ^1H NMR (300 MHz, CDCl_3) spectrum of 6,6-dimethyl-1-(3'-nitro-[1,1'-biphenyl]-2-yl)-5,7-dioxaspiro[2.5]octane-4,8-dione

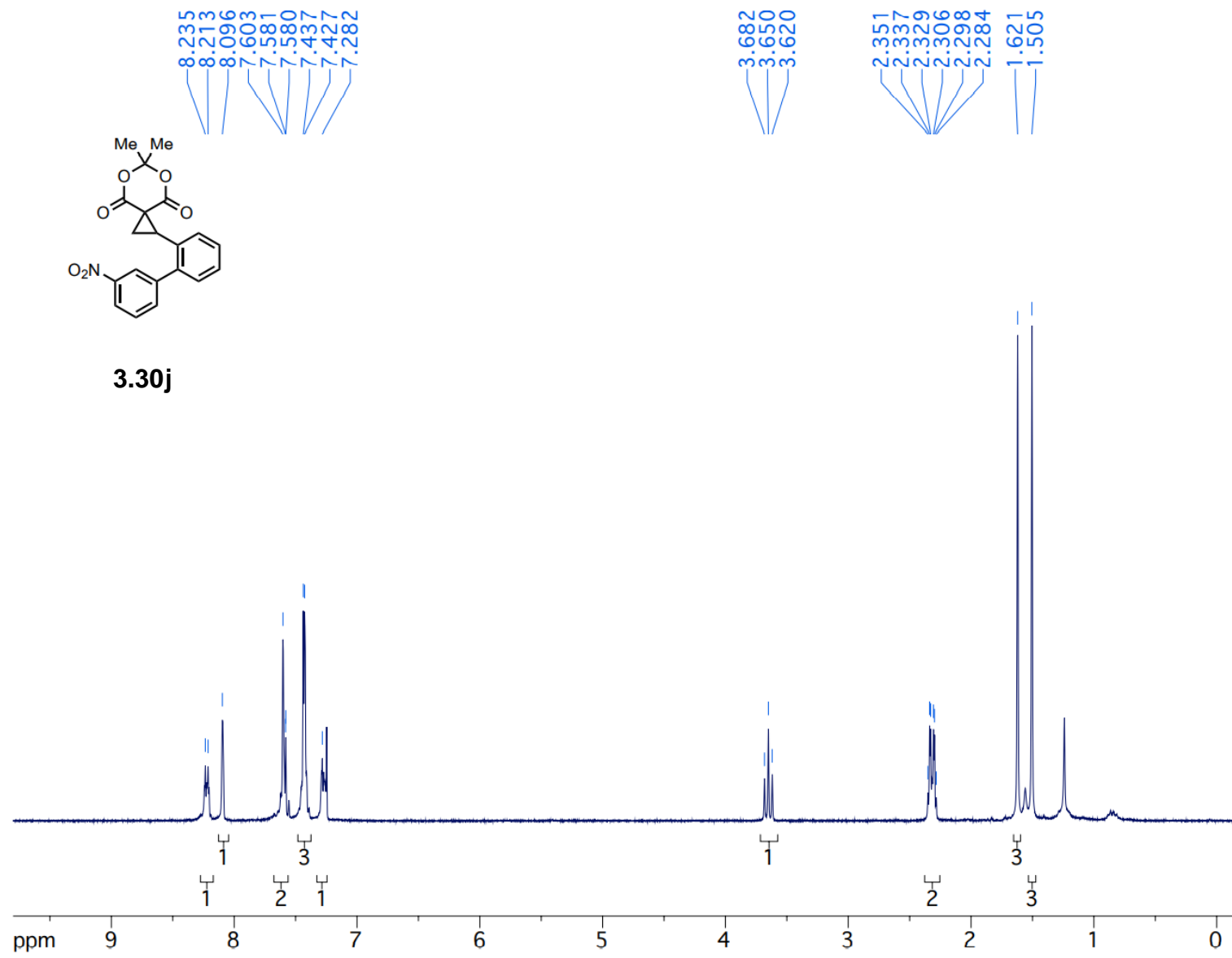


Figure 3.49 ^{13}C NMR (75 MHz, CDCl_3) spectrum of 6,6-dimethyl-1-(3'-nitro-[1,1'-biphenyl]-2-yl)-5,7-dioxaspiro[2.5]octane-4,8-dione

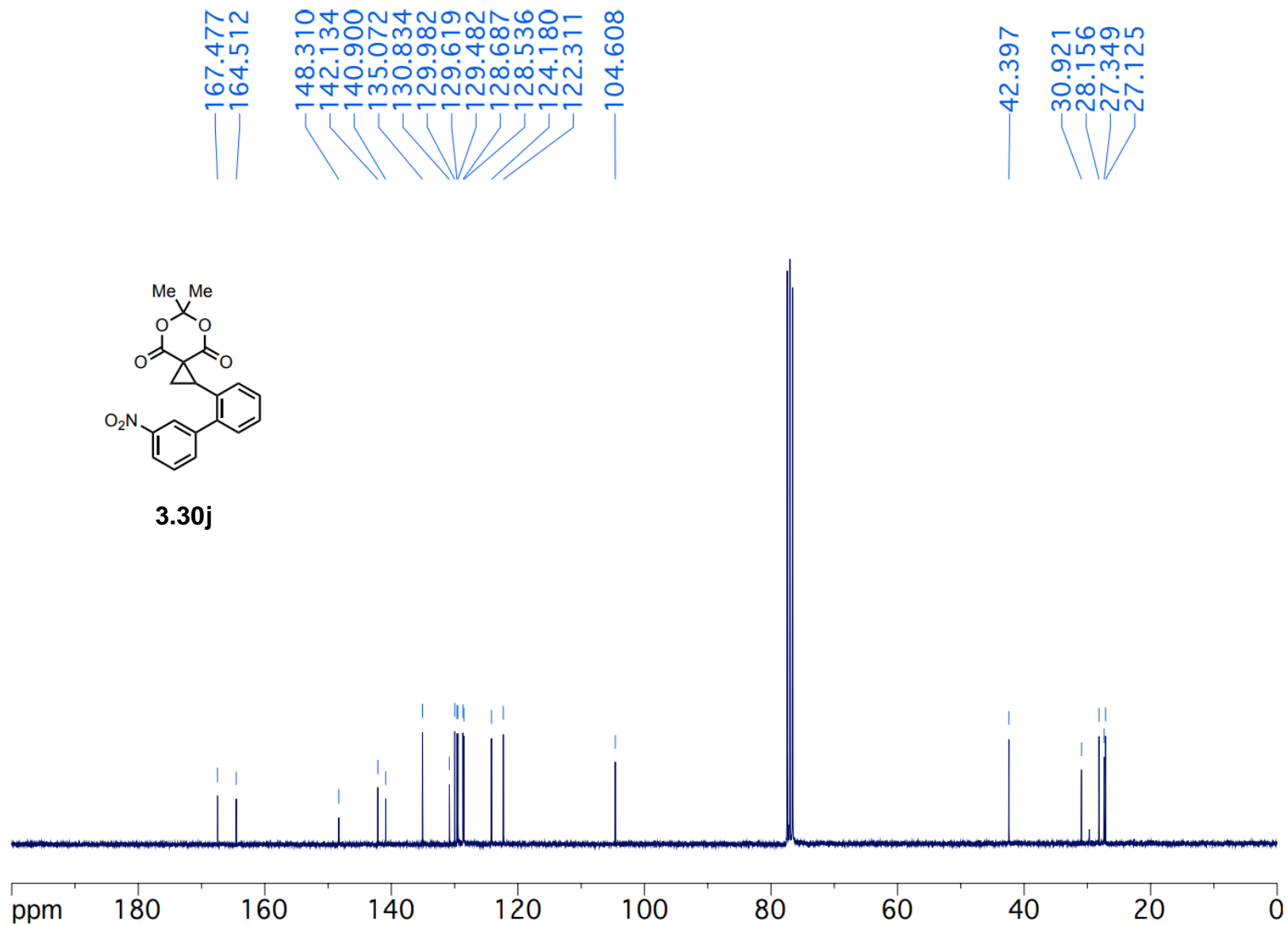


Figure 3.50 ^1H NMR (300 MHz, CDCl_3) spectrum of 1-(4-(benzyloxy)-[1,1'-biphenyl]-2-yl)-6,6-dimethyl-5,7-dioxaspiro[2.5]octane-4,8-dione

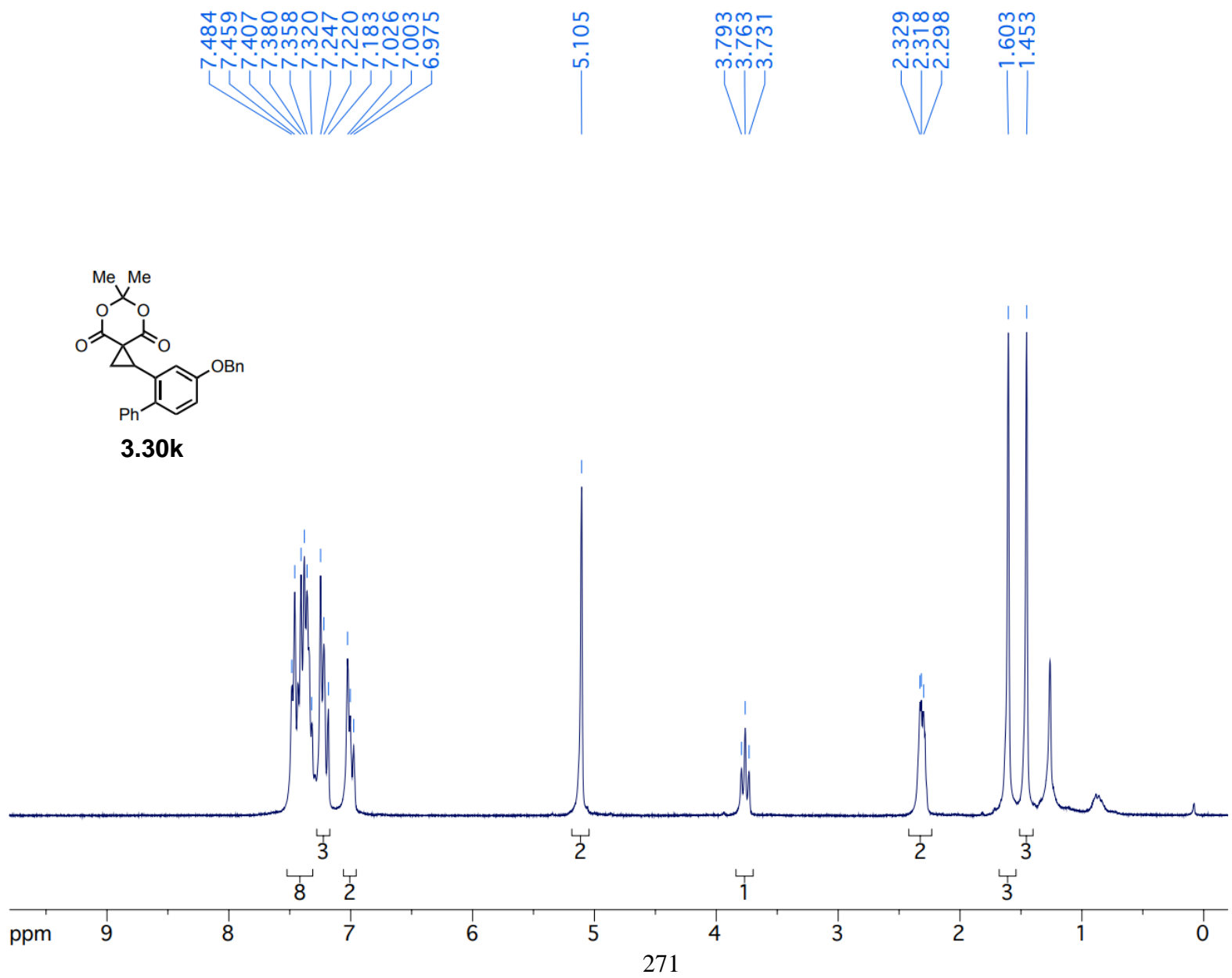


Figure 3.51 ^{13}C NMR (75 MHz, CDCl_3) spectrum of 1-(4-(benzyloxy)-[1,1'-biphenyl]-2-yl)-6,6-dimethyl-5,7-dioxaspiro[2.5]octane-4,8-dione

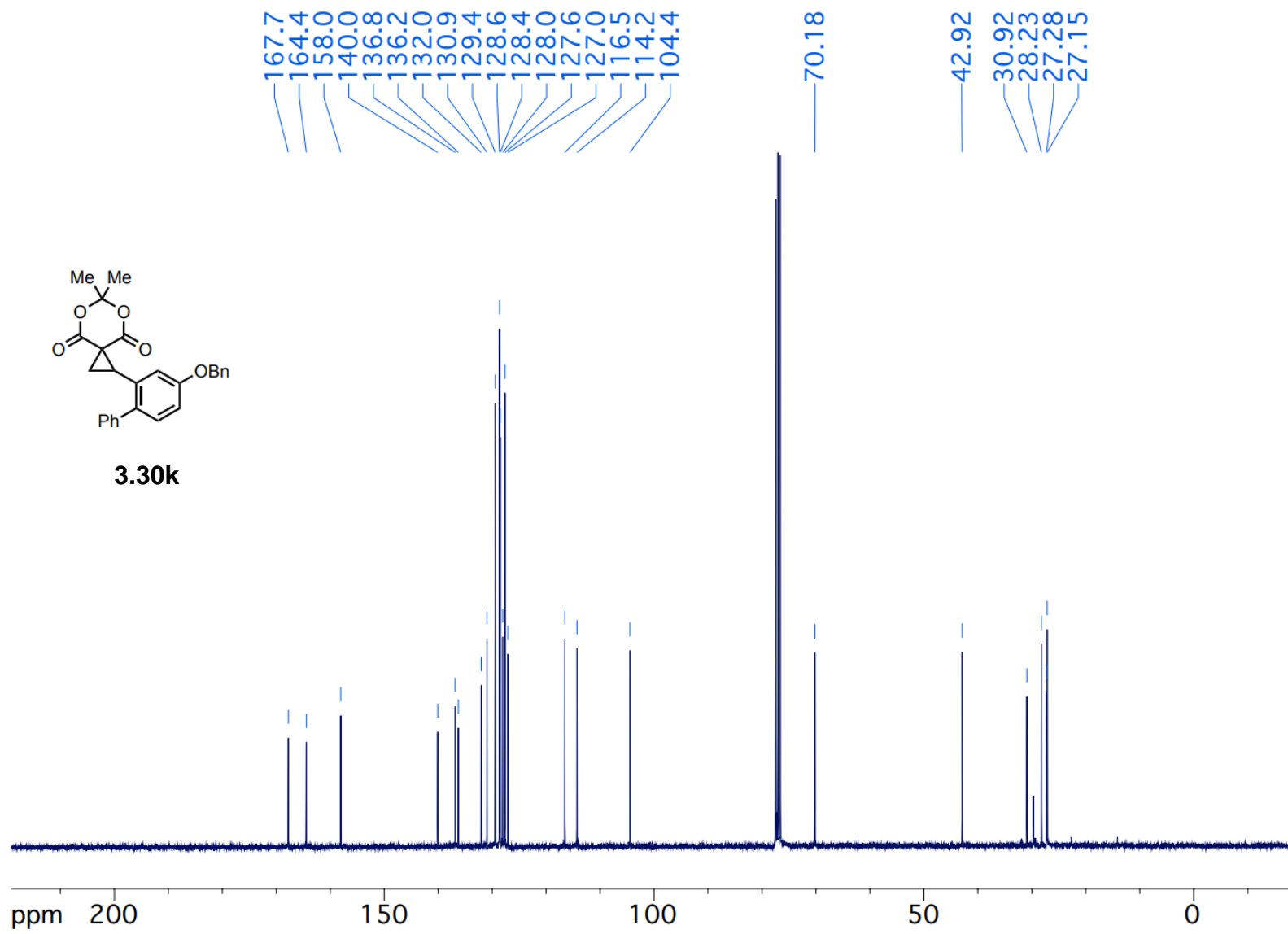


Figure 3.52 ^1H NMR (300 MHz, CDCl_3) spectrum of 2',2'-dimethylspiro[bicyclo[3.1.0]hexane-6,5'-[1,3]dioxane]-4',6'-dione

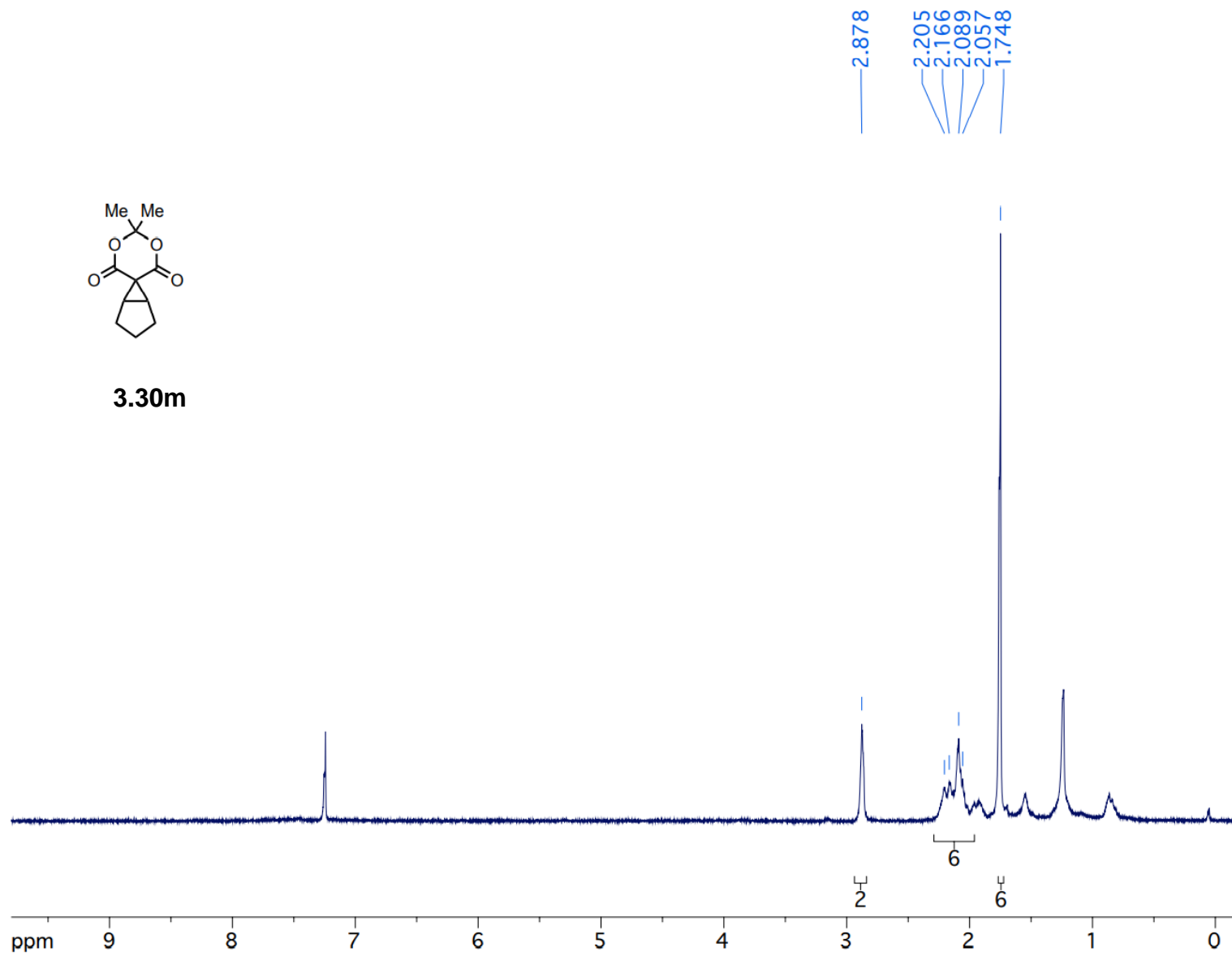


Figure 3.53 ^{13}C NMR (75 MHz, CDCl_3) spectrum of 2',2'-dimethylspiro[bicyclo[3.1.0]hexane-6,5'-[1,3]dioxane]-4',6'-dione

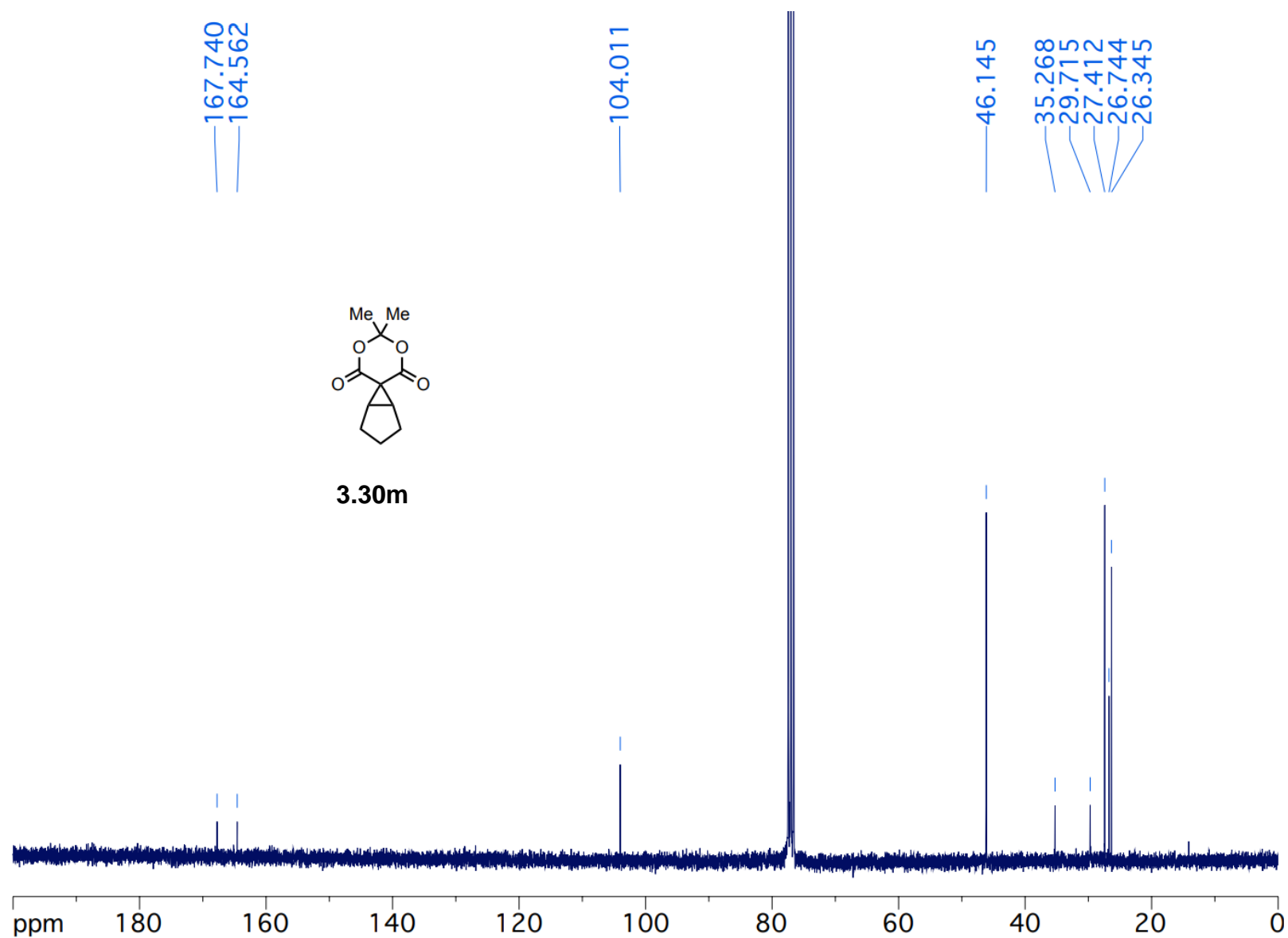


Figure 3.54 ^1H NMR (300 MHz, CDCl_3) spectrum of 1-benzyl-6,6-dimethyl-5,7-dioxaspiro[2.5]octane-4,8-dione

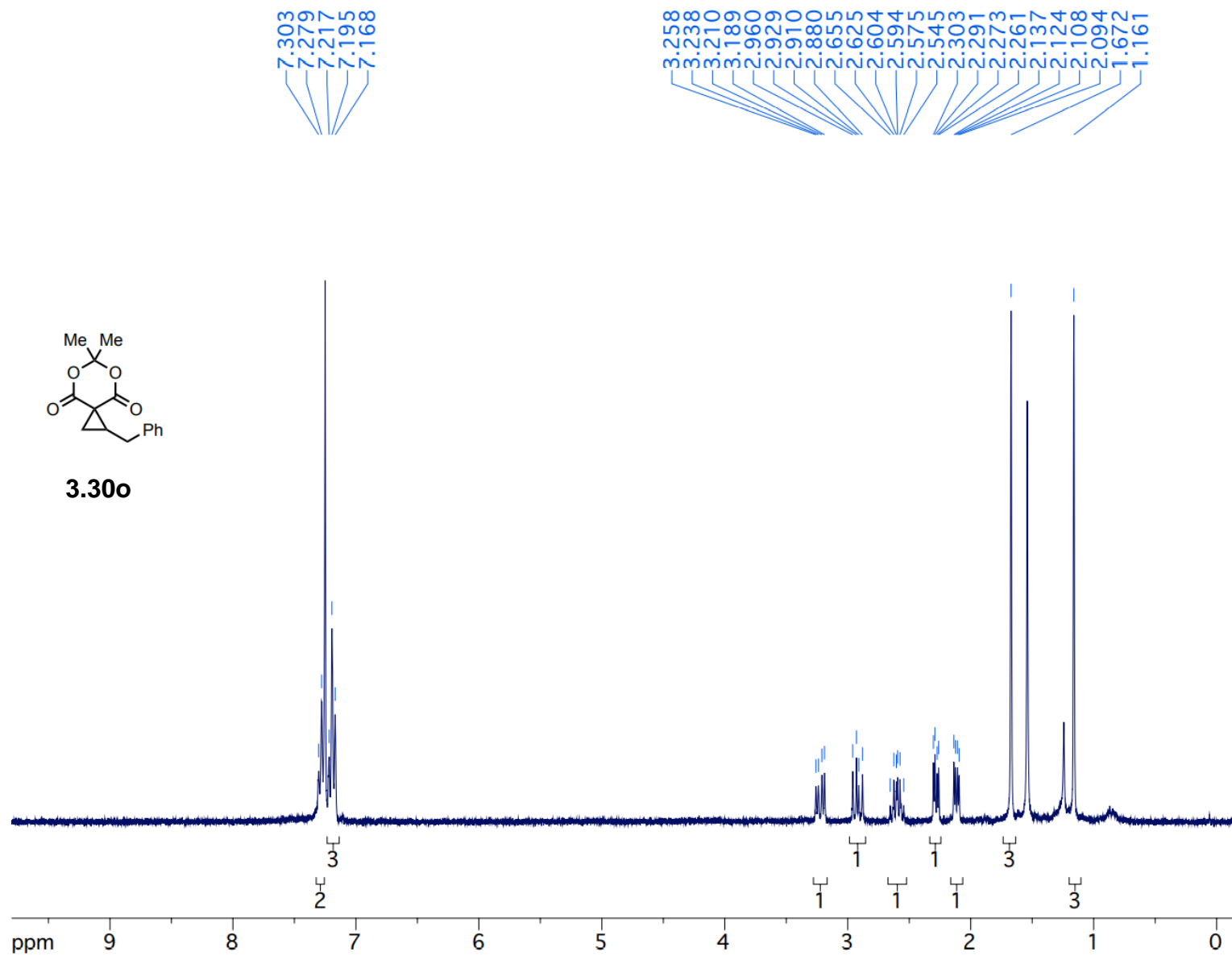


Figure 3.55 ^{13}C NMR (75 MHz, CDCl_3) spectrum of 1-benzyl-6,6-dimethyl-5,7-dioxaspiro[2.5]octane-4,8-dione

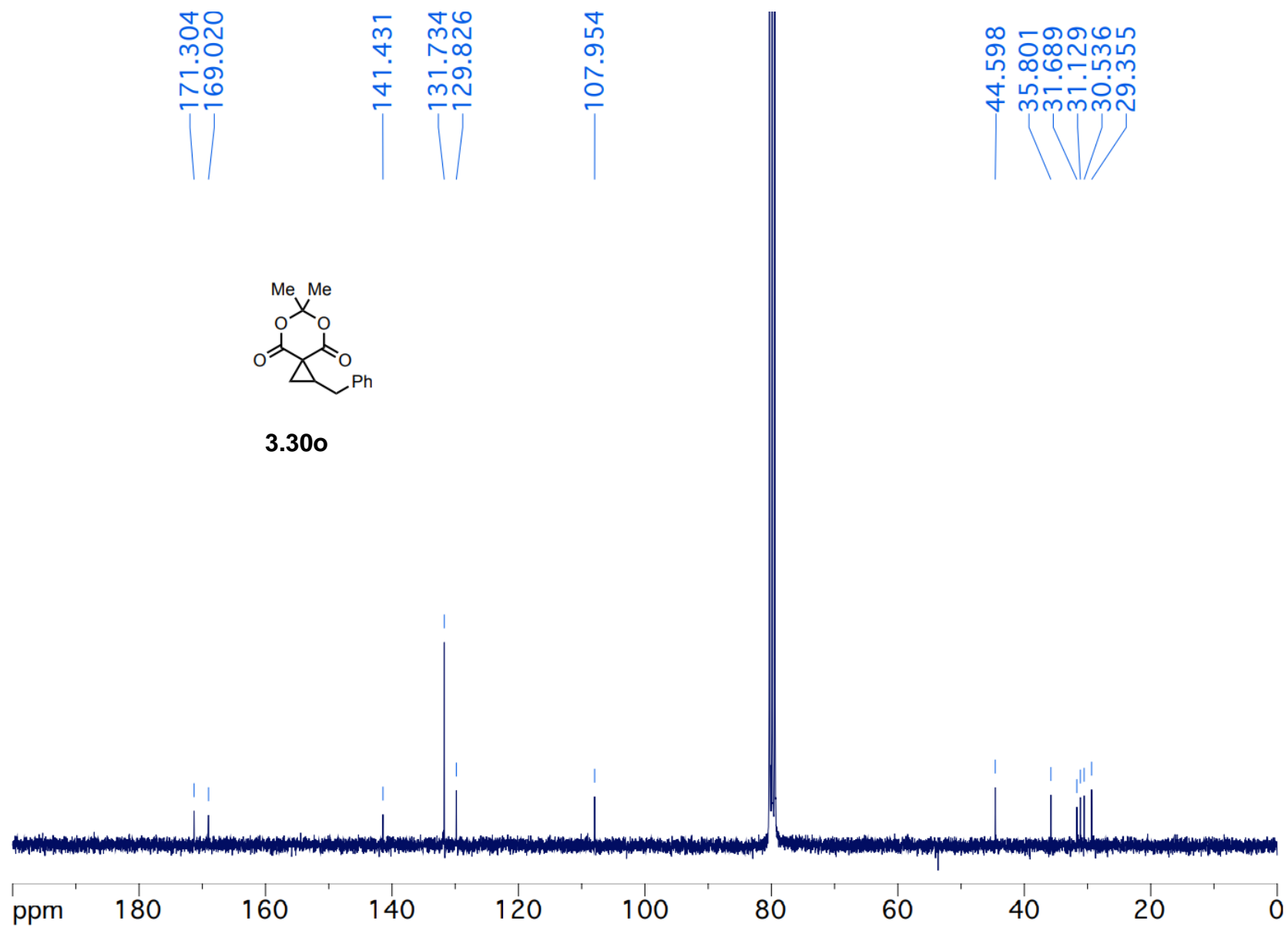


Figure 3.56 ^1H NMR (300 MHz, CDCl_3) spectrum of 1-decyl-6,6-dimethyl-5,7-dioxaspiro[2.5]octane-4,8-dione

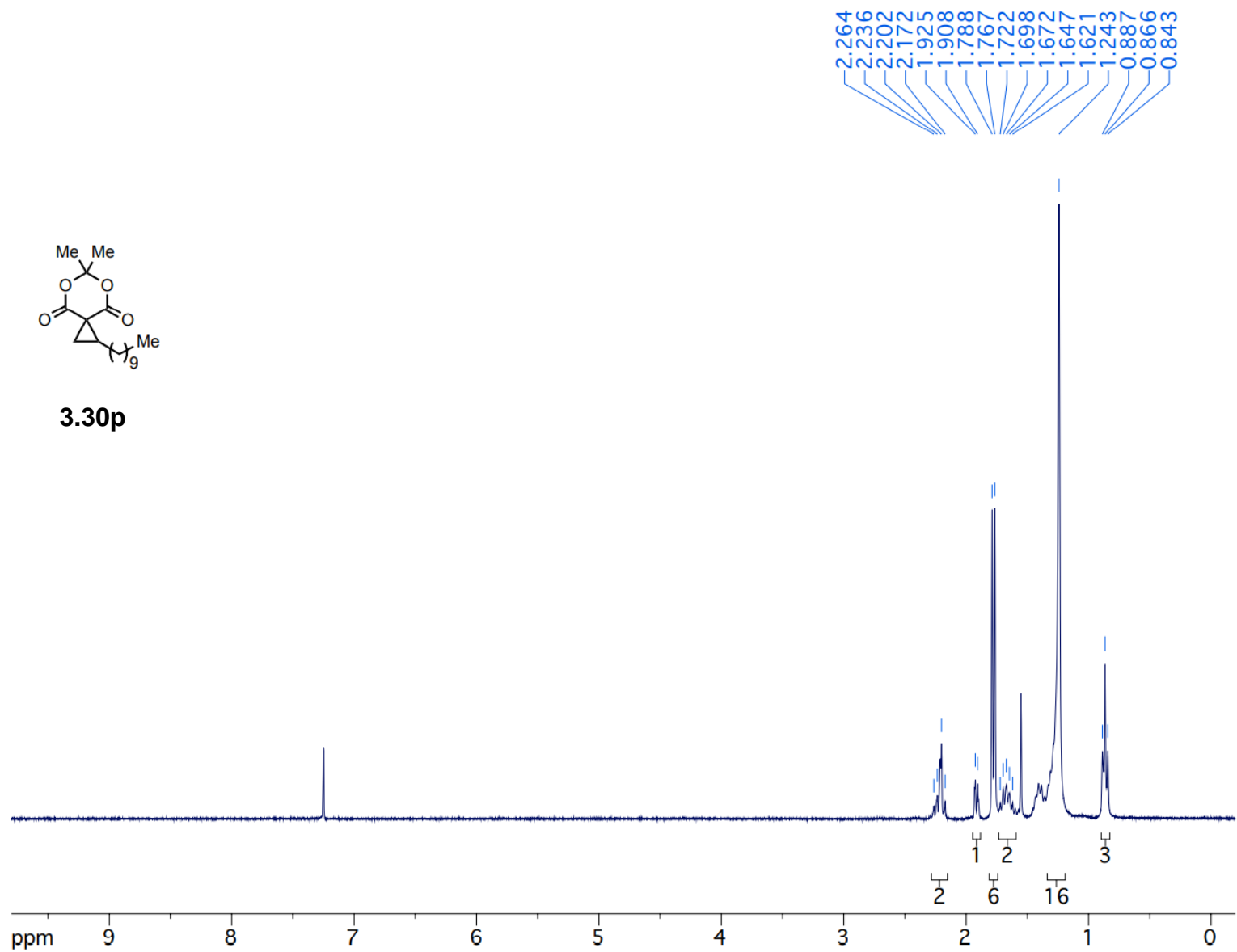


Figure 3.57 ^{13}C NMR (75 MHz, CDCl_3) spectrum of 1-decyl-6,6-dimethyl-5,7-dioxaspiro[2.5]octane-4,8-dione

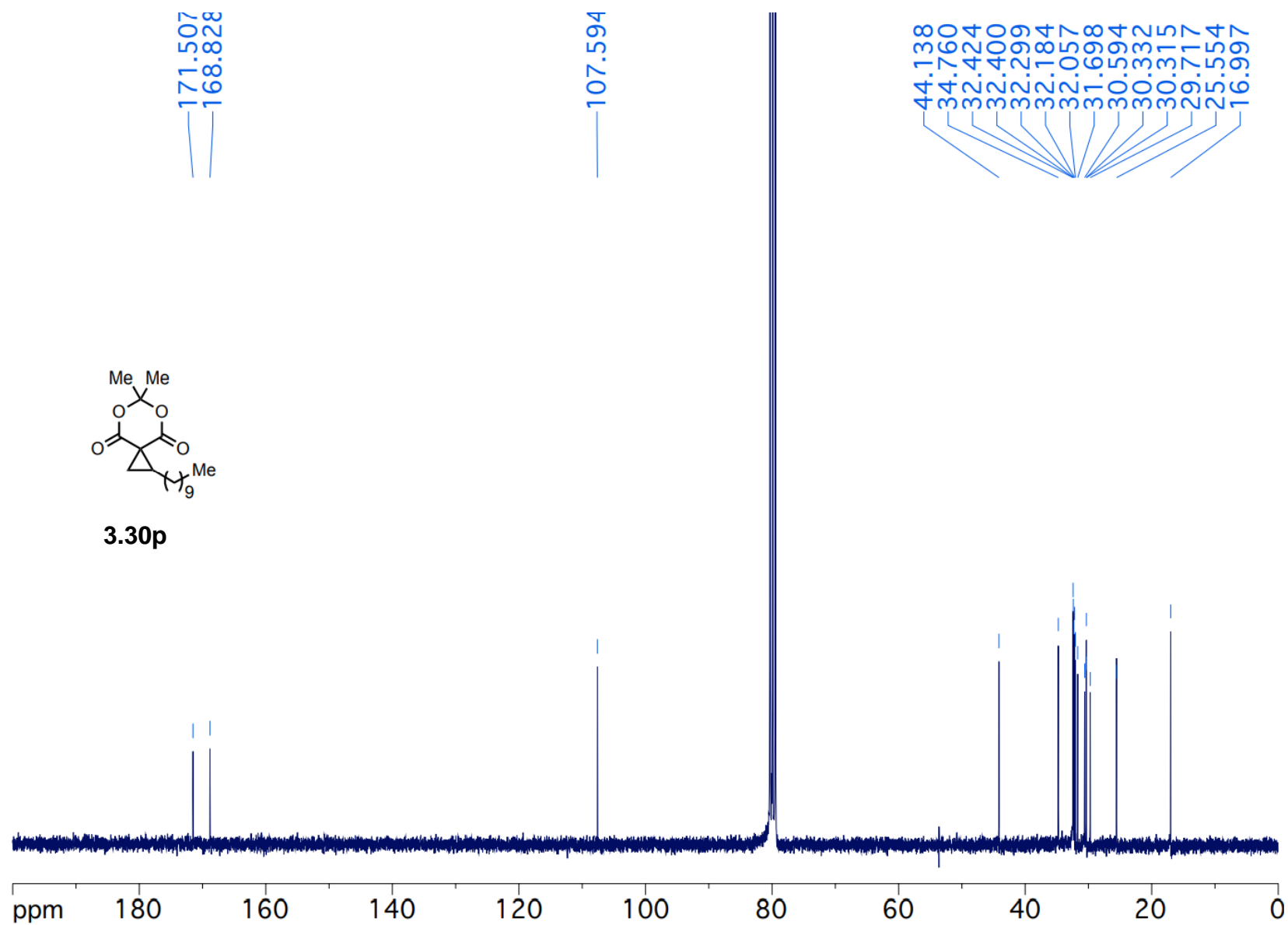


Figure 3.58 ^1H NMR (300 MHz, CDCl_3) spectrum of 1-([1,1'-biphenyl]-4-yl)-5,7-dimethyl-5,7-diazaspiro[2.5]octane-4,6,8-trione

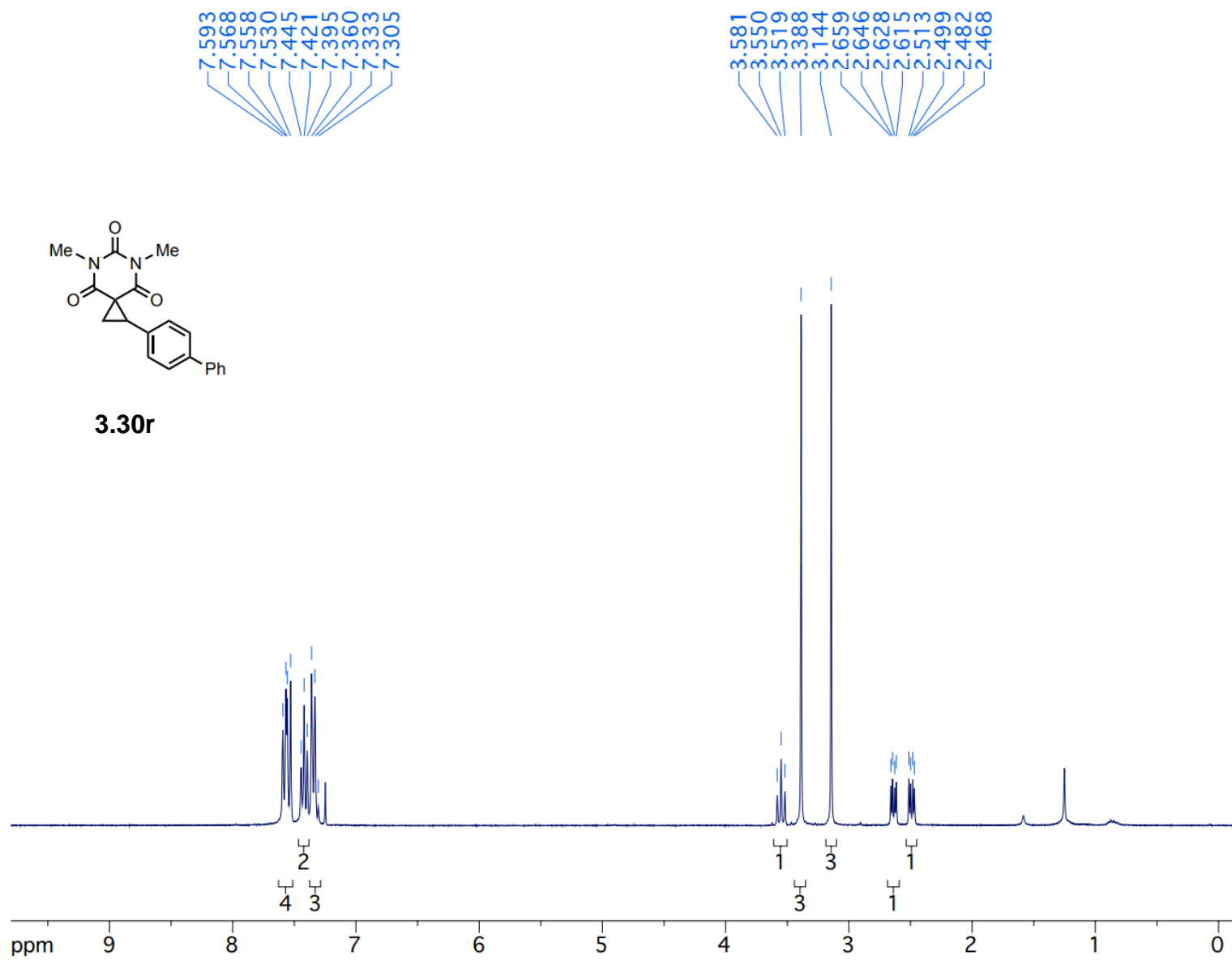


Figure 3.59 ^{13}C NMR (75 MHz, CDCl_3) spectrum of 1-([1,1'-biphenyl]-4-yl)-5,7-dimethyl-5,7-diazaspiro[2.5]octane-4,6,8-trione

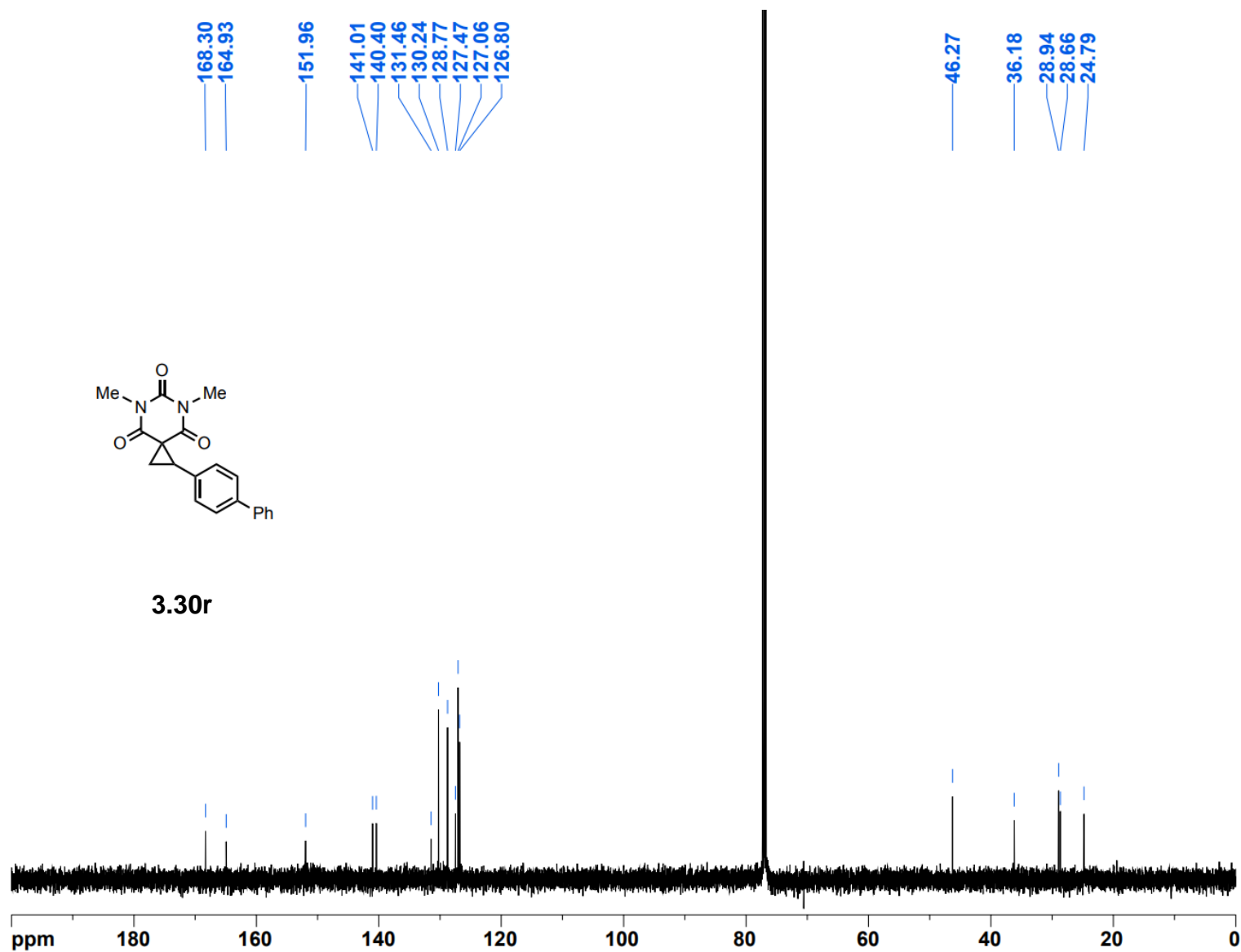


Figure 3.60 ^1H NMR (300 MHz, CDCl_3) spectrum of 1-(4-(tert-butyl)phenyl)-5,7-dimethyl-5,7-diazaspiro[2.5]octane-4,6,8-trione

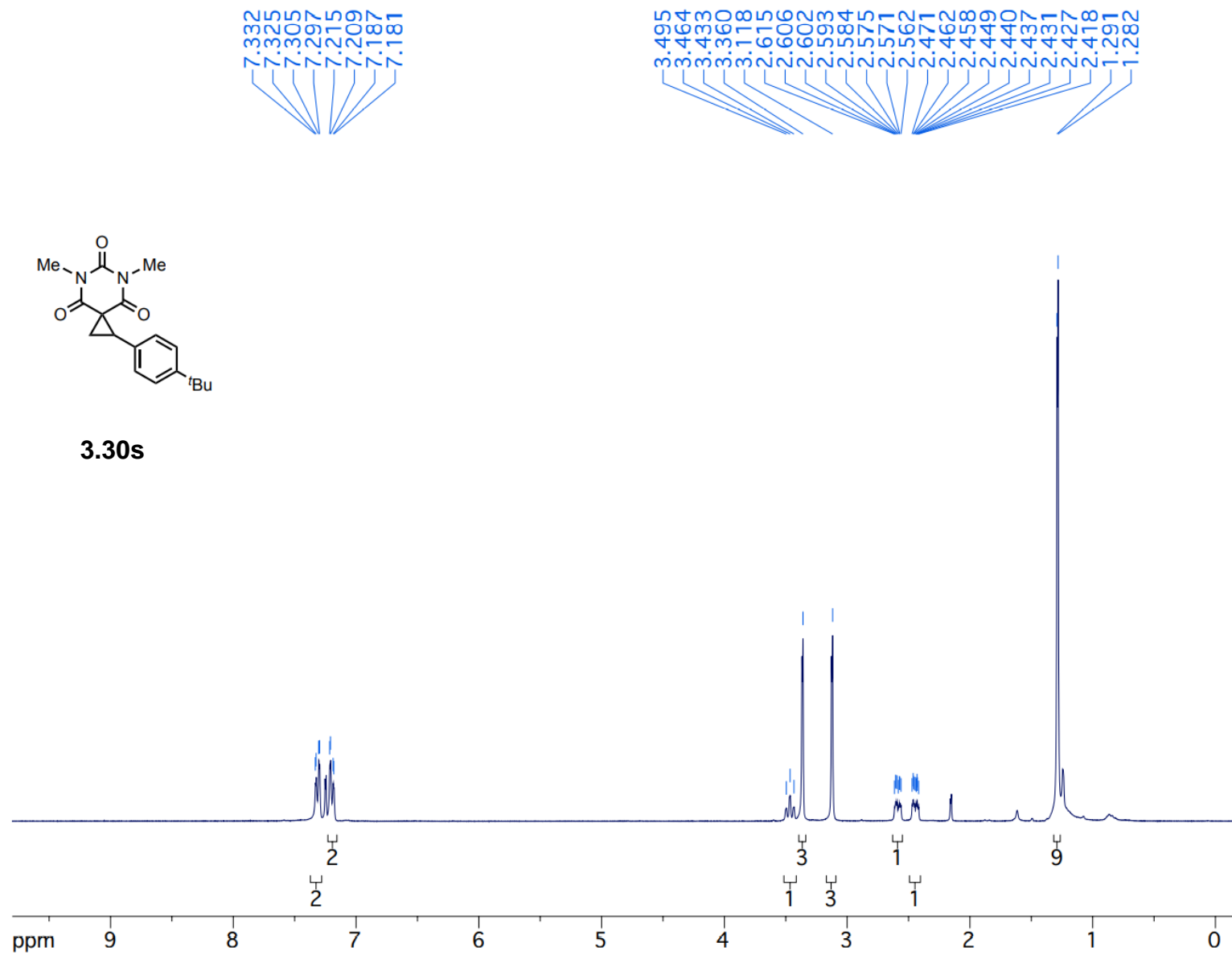
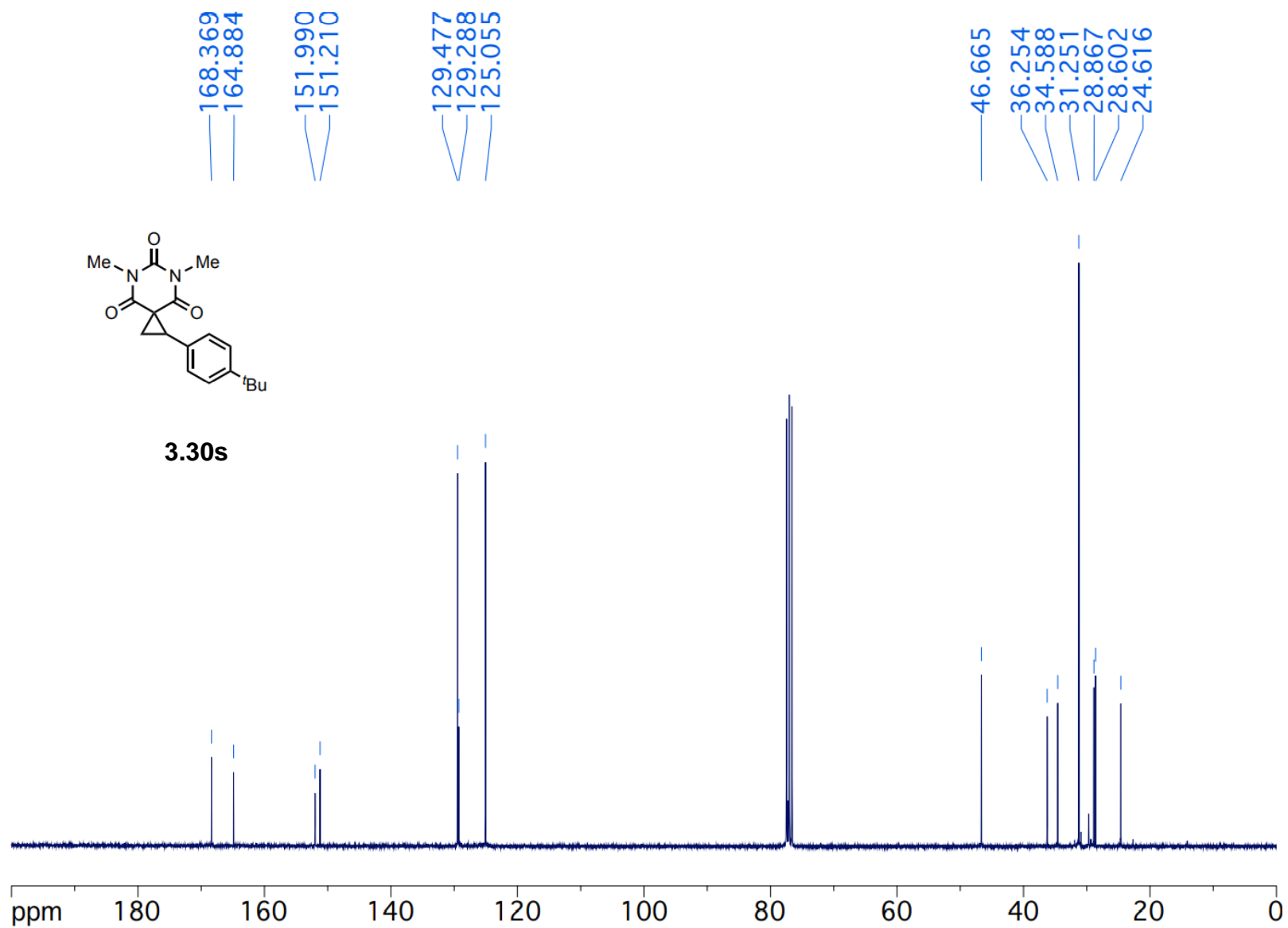


Figure 3.61 ^{13}C NMR (75 MHz, CDCl_3) spectrum of 1-(4-(tert-butyl)phenyl)-5,7-dimethyl-5,7-diazaspiro[2.5]octane-4,6,8-trione



Chapter 4: Synthesis of Asymmetric Iodonium Ylides and Their Use in Blue Light-Induced Asymmetric Cyclopropanation with Alkenes

4.1 Background of Asymmetric HVI Compounds

Achieving enantioselective reactions using hypervalent iodine compounds has emerged as a powerful method with the ability to adapt to many different types of organic reactions, and many recent reviews have been written on this topic in the last decade.²⁷³ The source of chirality can be built directly into the aryl iodide which is commonly found in essentially all organic hypervalent iodine structures. The aryl group is available to be derivatized with chiral functionality coming from sources such as amino acids or lactate derivatives to name a few of examples.

One of the first attempts of blending HVI reagents with asymmetric chemistry was by Pribam in 1907.²⁷⁴ Although the exact structures were not reported at the time of publishing, the compounds that resulted from mixing L-tartaric acid and iodosobenzene were believed to form structures **4.1** and **4.2** (Figure 4.1). Pribam's work was reinvestigated by Imamoto in 1986, who pioneered a synthetically-useful synthesis that could produce derivatives of the chiral seven-membered ring λ^3 -iodane **4.1** by a similar method utilizing iodosobenzene.²⁷⁵

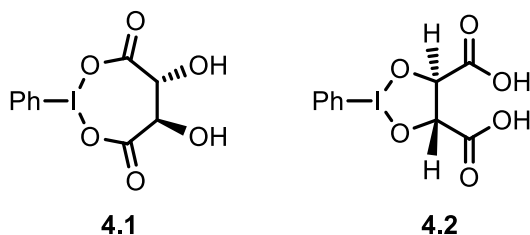


Figure 4.1 First reports of chiral HVI compounds

After the seminal work by Pribam, not much exploration into the field was performed until around 60 years later when Merkushev worked on combining HVI reagents with chiral amino acids in 1975.²⁷⁶ To prepare the chiral HVI derived compounds, the authors reacted PIDA with several chiral N-protected amino acids to give compounds **4.3** and **4.4** (Figure 4.2).

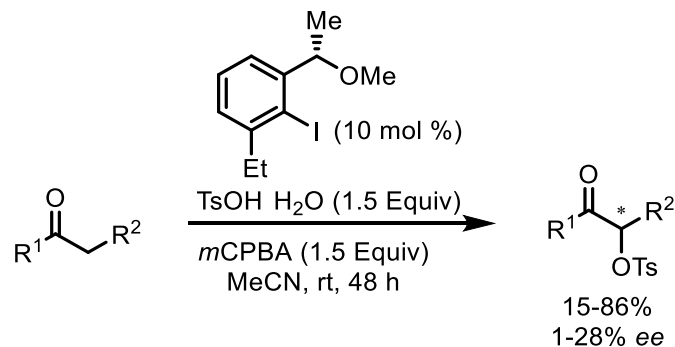


Figure 4.4 Asymmetric catalytic α -sulfonylation reaction

The ability to create carbon-fluorine bonds in a controllable stereoselective process, through chiral HVI reagents, has become an important synthetic method in recent organic chemistry due to the applications these fluorinated molecules have in the field of radiofluorination. An example of this is the asymmetric reactivity achieved by Rueping who reported on the nucleophilic fluorination of β -ketoesters using chiral aryl iodides.²⁷⁹ This newly discovered reaction was reported in 2018 and provides a way of adding fluorine into molecules containing β -ketoesters in an asymmetric manner (**Figure 4.5**).

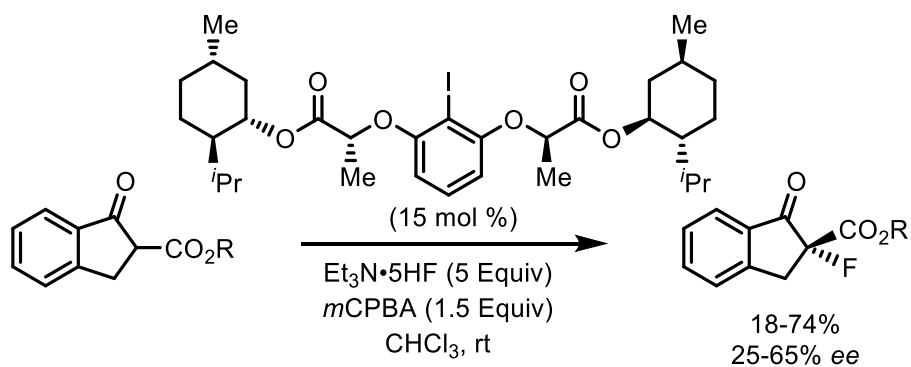


Figure 4.5 Asymmetric fluorination of β -ketoesters

4.1.1 Strategies for Controlling Stereoselectivity

The ability of synthetic chemists to form chiral environments on a molecular scale is perhaps the core at which enantioselective reactions operate. Inspiration for this is rooted in the observation and copying of nature, in which enzymes have been performing asymmetric

chemical reactions for millions of years. Because amino acids contain set stereogenic centers, the active site of the enzyme contains a chiral environment which enables highly selective asymmetric reactions to be carried out within the pocket of the active site of an enzyme. Building on this idea, chemists have been able to create chiral environments using the following strategies.

Many different chiral HVI systems have been developed over the years, and common strategies have emerged based on the use of chiral functional groups being built into the aryl iodide. These different strategies can be grouped into four main categories. These strategies are often based on arranging chiral groups around the aryl iodide, in different orientations, which have coordinative abilities to stabilize intramolecular interactions, and sometimes effectively form a chiral environment. The strategies that have been employed by various researchers over the years to control stereoselectivity is summarized in **Figure 4.6**.

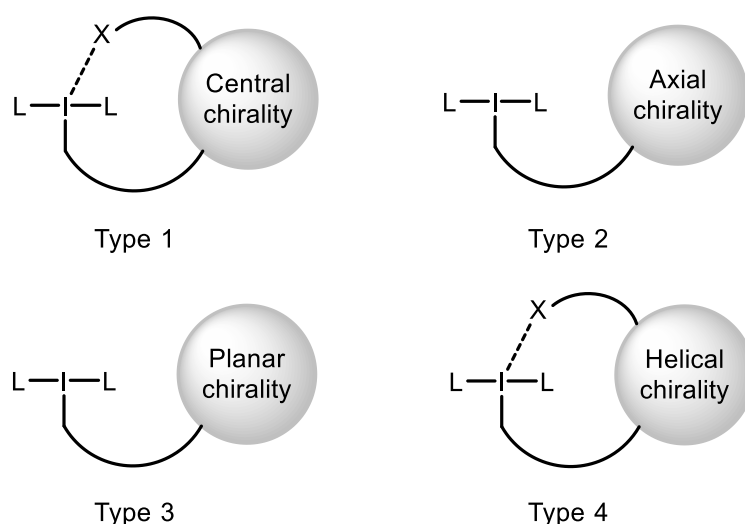


Figure 4.6 Examples of different strategies used to control stereochemistry

Type 1 (central chirality) makes use of central chirality and includes the use of chiral alcohols, amines, esters, or ethers. Type 2 (axial chirality) makes use of axial chirality and includes the use of chiral biphenyls, or binaphthyls. Type 3 (planar chirality) makes use of planar chirality and includes the use of chiral cyclophanes. Type 4 (helical chirality) makes use of helical chirality and includes the use of chiral resorcinol-lactate derived core, or helicenes.

Type 4 was concluded to be the most successful strategy and has the most promising future for carrying out asymmetric HVI promoted oxidations.²⁸⁰ In helical chirality-based

systems, the aryl iodide is derivatized at the 2- and 6- positions, both *ortho* to the iodine, allowing for the stereochemical environment to be positioned as close as possible in space to the hypervalent iodine centre. This appears to be critical for providing the desired chiral environment required for inducing high levels of *ee*. The credit for this strategy was given to Fujita²⁸¹ and Ishihara²⁸² for their research, which occurred around 2007 to 2010.

The ability to control stereochemistry in chemical reactions through Type 4 strategies has been explained by researchers through the following two intramolecular interactions. Hypervalent iodine reagents are able to participate in chiral n to σ^* interactions (**4.5**) which was first described by Ishihara. Another way for induction of chirality was described through H-bonding interactions (**4.6**), and these two modes of interactions are shown in **Figure 4.7**. Ishihara also observed a supramolecular helical scaffold by hydrogen bonding in some systems derived from resorcinol and amino alcohol systems.

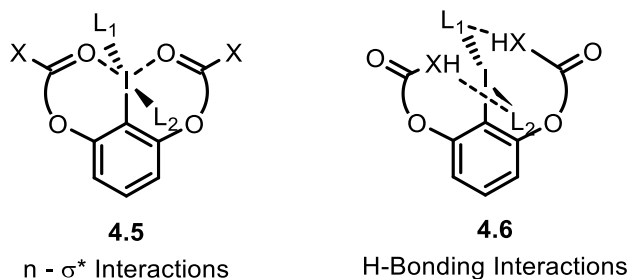
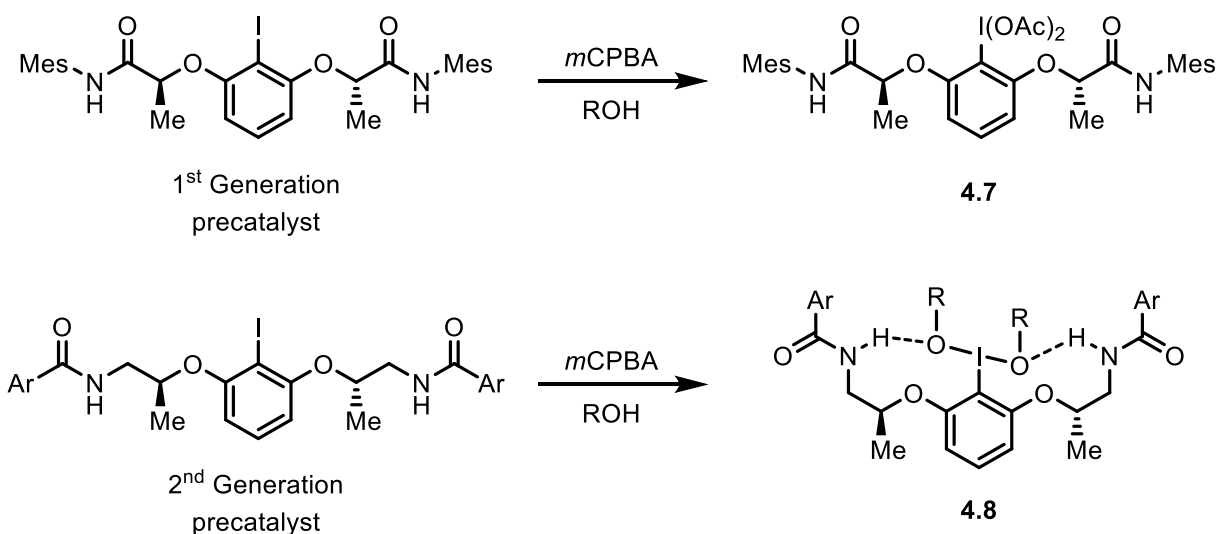


Figure 4.7 Structures representing helical chirality

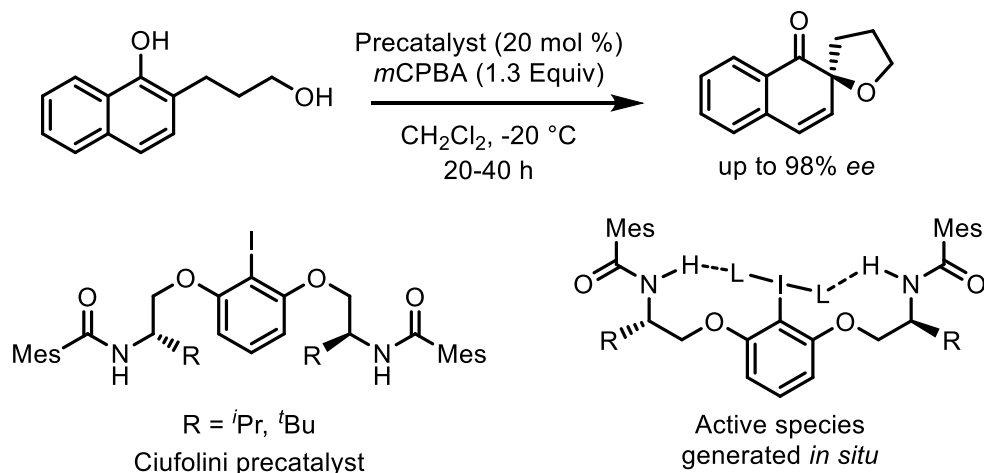
The design of chiral HVI catalysts that utilize H-bonding interactions was established by Ishihara, who is known for developing an entirely different catalytic system in 2013 which was termed as Ishihara's 2nd generation pre-catalyst system.²⁸³ H-bonding was proposed to construct chiral environments as shown in **Scheme 4.1**. For these systems to form active chiral reagents the 1st or 2nd generation precatalytic system must first undergo oxidation with an oxidant such as *m*CPBA to form a supramolecular scaffold which is believed to be helical. Ishihara's 1st generation precatalyst forms active species **4.7** *in situ* after oxidation while the 2nd generation precatalyst forms **4.8** after oxidation.



Scheme 4.1 Ishihara's 1st and 2nd generation precatalytic systems

Ishihara 1st and 2nd generation precatalytic systems which show conformationally-flexible chiral organoiodine catalysts, have successfully been applied to multiple enantioselective oxidative reactions. The flexible nature of the catalytic site in the 2nd generation systems are similar to enzymatic systems, and the presence of secondary bonding interactions have been observed by X-Ray and NOE analysis.²⁸⁴

Ciufolini also created a precatalytic system similar to Ishihara's 2nd generation system that involved a chiral centre next to an amide NH group to achieve high efficiency in the catalytic process.²⁸⁵ It was described as providing a better hydrogen-bonded conformation which imparted superior reactivity when compared to Ishihara's system without the need of alcohols as additives.²⁸⁶ Excellent enantioselectivities were achieved when using Ciufolini's precatalyst for the oxidative cyclization of phenolic derivatives to spirocyclic compounds as shown in **Scheme 4.2**.



Scheme 4.2 Ciufolini's precatalytic system

Other examples of Type 4 strategies in literature can be seen in reactions such as enantioselective vicinal damination, which has been shown to display facial selectivity towards alkenes.²⁸⁷ Chiral supramolecular helical environments are formed to provide facial selectivity with styrene, with chiral pockets being formed in these aggregated structures as shown in **Figure 4.8**. These chiral aggregates form a complex which favours a *re*-face attack in the examples shown below, enabling the formation of products with a preferred asymmetric outcome.

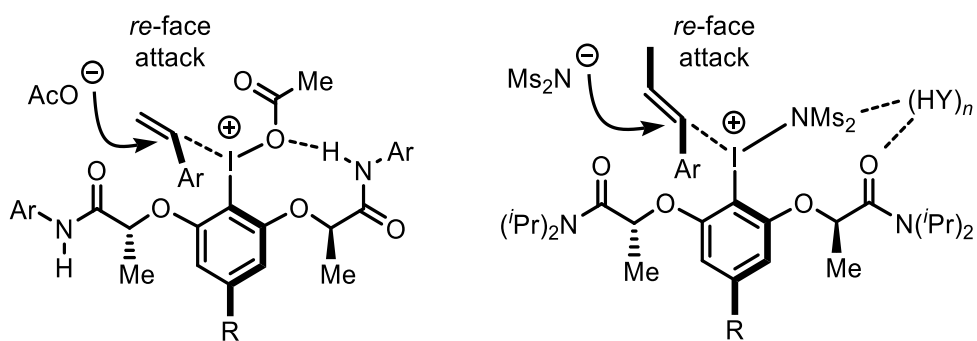
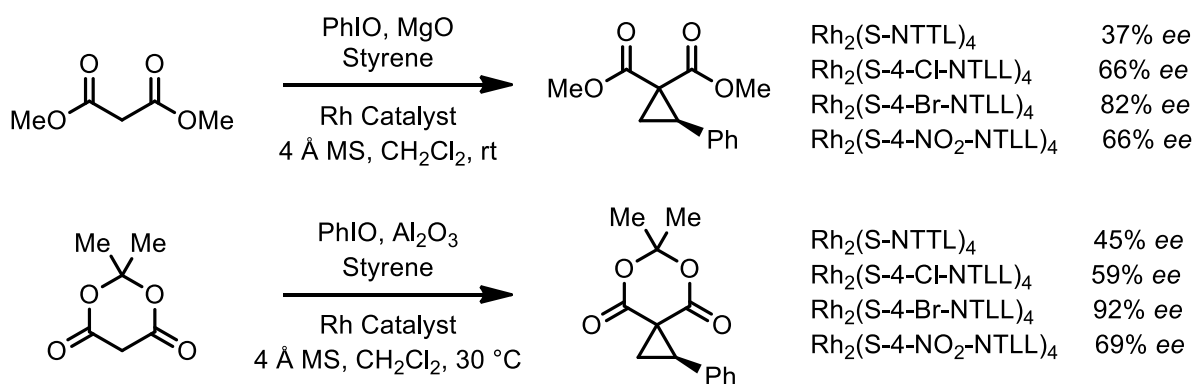


Figure 4.8 Chiral supramolecular scaffold environmental control for *re*-face attack

4.1.2 Asymmetric Cyclopropanation of Iodonium Ylides and Alkenes

The thought of using iodonium ylides for asymmetric cyclopropanation reactions was first described in the literature in 1998 by Müller, who noted that diazo compounds and

iodonium ylides gave identical enantioselectivities in intramolecular metal-catalyzed C-H insertion reactions.²⁸⁸ The actual history of asymmetric cyclopropanation reactions of iodonium ylides with alkenes was born in 2000 with the work of Müller showing how metals such as Cu(I) and Rh(II) were both capable of inducing cyclopropanation of iodonium ylides with alkenes. This started a movement away from the use of diazonium ylides for their use in cyclopropanation reactions, which was first reported back in 1966 by Nozaki, as iodonium ylides have been established as the safer alternative to diazo compounds.²⁸⁹ Phenyliodonium ylides have shown to be more active than their diazomalonate equivalent in carbene-transfer cyclopropanation reaction of olefins.²⁹⁰ Müller reported another example using Rh(II) to catalyze an asymmetric cyclopropanation of iodonium ylides with alkenes in 2003, which was another example of using iodonium ylides in replacement of diazo compounds in metal-catalyzed asymmetric cyclopropanation reactions.²⁹¹ Charette developed a Cu(I)-catalyzed asymmetric cyclopropanation of iodonium ylides with alkenes in 2005.²⁹² And examples of metal-catalyzed asymmetric cyclopropanation of iodonium ylides with alkenes was reported again by Müller in 2010.²⁹³ This chemistry was shown to be compatible with acyclic and cyclic iodonium ylides, and the alkenes that gave the highest yields were styrene-based compounds. Several different iterations of the rhodium-based metal catalyst system were used, which resulted in a range of *ee*'s being observed for cyclopropane formation, and the results are summarized in **Scheme 4.3**. Although the following scheme does not directly show iodonium ylides, the conditions stated imply that the iodonium ylide formed *in situ* prior to engagement with the metal-catalyst and the alkene.



Scheme 4.3 Metal-catalyzed asymmetric cyclopropanation of iodonium ylides with alkenes

As shown in the above scheme, changing the position of functional groups on the rhodium-based metal catalyst system can lead to drastic changes to the *ee* of the reaction. The rhodium-based catalyst with different iterations used in the asymmetric cyclopropanation methodology is shown in **Figure 4.9**.

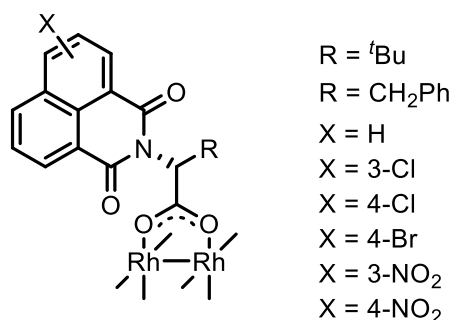
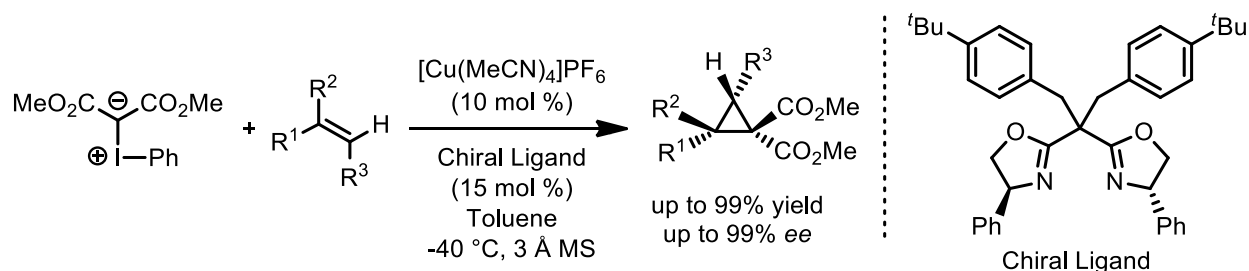


Figure 4.9 Rhodium-based metal catalyst system

A different strategy for the metal-catalyzed asymmetric cyclopropanation of iodonium ylides with alkenes was discovered using a chiral cage-like copper(I) catalyst which was reported by Tang in 2012.²⁹⁴ This cage-like bisoxazoline-derived Cu(I) catalyst was found to promote the asymmetric cyclopropanation of malonate-derived metallocarbenes with both terminal and multi-substituted olefins with high selectivity. The *in situ*-prepared bisoxazoline [Cu(Ligand)(MeCN)₄]PF₆ system catalyzes the cyclopropanation of alkenes with acyclic iodonium ylides to afford cyclopropanes. An example of this cyclopropanation methodology using malonate-derived phenyliodonium ylide and styrene is shown in **Scheme 4.4**. Several bisoxazoline-derived Cu(I) catalyst systems were used in the optimization of the cyclopropanation reaction, and the chiral ligand that gave the highest yield and *ee* is shown in the following reaction.



Scheme 4.4 Metal-catalyzed asymmetric cyclopropanation of iodonium ylides with alkenes

In order to understand the asymmetric induction in the cyclopropanation reaction, a single crystal of the $[\text{Cu}(\text{MeCN})_4]\text{PF}_6/\text{Ligand}$ complex was analyzed by X-ray crystallography (Hydrogen atoms and PF_6 are omitted for clarity) as shown in **Figure 4.10**. Obtaining the spatial orientation of the atoms in the chiral ligand is critical for building a model which can be used to assign and understand the correct configuration of the chiral centres formed in this reaction. The copper center is shown to adopt a distorted square-planar geometry in which copper binds to the two nitrogens in the oxazoline rings of the ligand, as well as binding to a molecule of acetonitrile. The two phenyl groups attached to the oxazoline rings with fixed chirality orientate towards the copper center, shielding both the upper and lower faces of the copper coordination plane, forming an overall structure with C_2 -symmetry. In this C_2 -symmetric orientation, approach of an alkene will be directed into thereby giving an enantioselective preference for which cyclopropane isomer can form, if the malonate-derived metallocarbene the less sterically crowded environments, is also anchored to the copper in a fixed orientation.

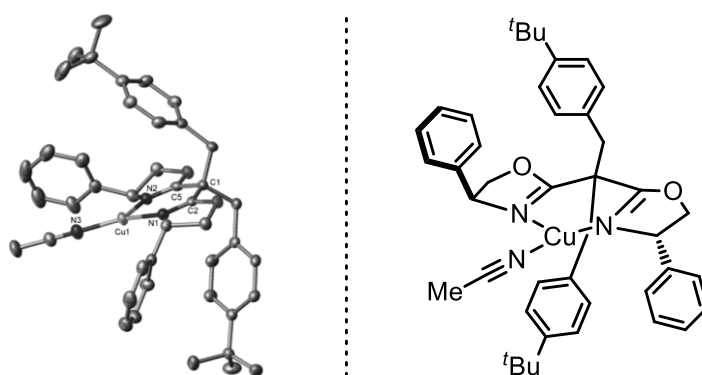
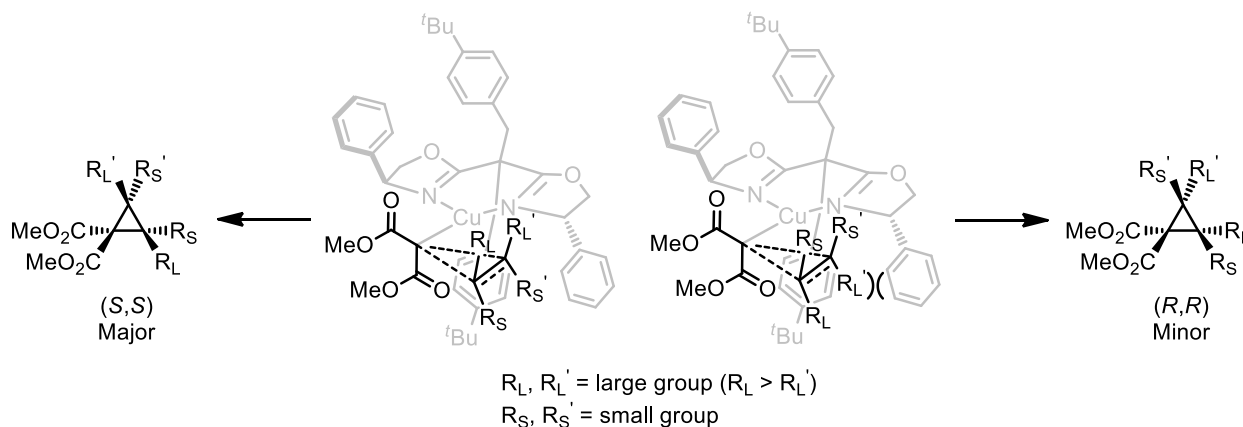


Figure 4.10 X-ray structure of $[\text{Cu}(\text{Ligand})(\text{MeCN})]^+$

Previous studies by the research groups of Doyle and Charette showed that malonate-derived metallocarbenes can adopt three different conformations (out-out, in-out, and in-in).²⁹⁵ In the bisoxazoline-copper catalyst system, the in-out conformation is the most probable orientation of the metallocarbene because of the beneficial increase in reactivity that occurs when one of the ester groups adopts an out-of plane conformation which stabilizes a partial positive charge formed on the β carbon of the alkene.²⁹⁶ A stereocontrol model was proposed to explain the stereochemistry of the reaction, by combining the molecular structure of $[\text{Cu}(\text{MeCN})/\text{Ligand}]^+$ with the model developed by Pfaltz and co-workers.²⁹⁷

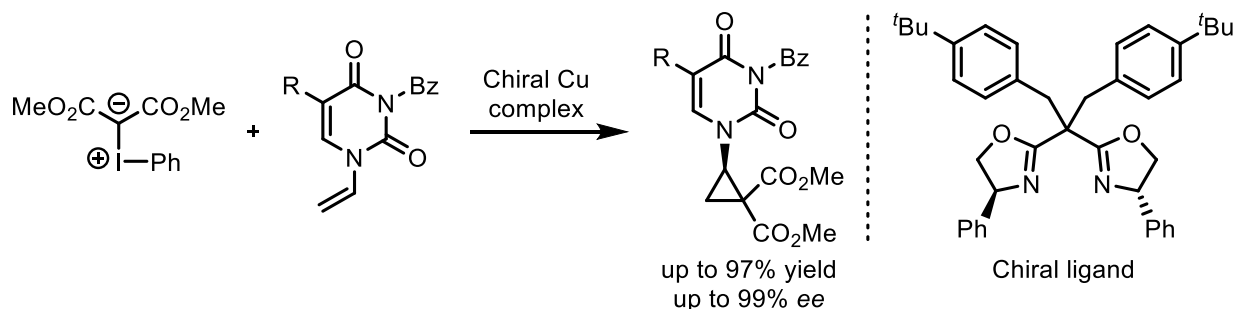
Approach of the multi-substituted alkene into the chiral environment created by the cage-like bisoxazoline-copper catalyst in which the malonate-derived metallocarbene is also attached and will produce major and minor cyclopropane isomers. The minor cyclopropane isomer (*R,R*) is the result of undesirable steric crowding between the larger groups on the alkene and the phenyl ring on the oxazoline. When the smaller groups on the alkene are favourably orientated towards the phenyl ring on the oxazoline, steric interactions are minimal, resulting in formation of the major cyclopropane isomer (*S,S*) as shown in **Scheme 4.5**.



Scheme 4.5 Stereochemical model for Cu-catalyzed cyclopropanation of substituted alkenes

Another example of an asymmetric cyclopropanation reaction using iodonium ylides and alkenes making use of the same chiral oxazoline ligand with copper was reported some years later, with again, high levels of enantioselectivity. The synthesis of chiral pyrimidine-substituted diester DA cyclopropanes via asymmetric cyclopropanation of phenyliodonium ylides was

reported by Guo in 2020, and the origin of enantioselectivity comes from the use of a chiral ligand in conjunction with a copper metal catalyst (**Scheme 4.6**).²⁹⁸



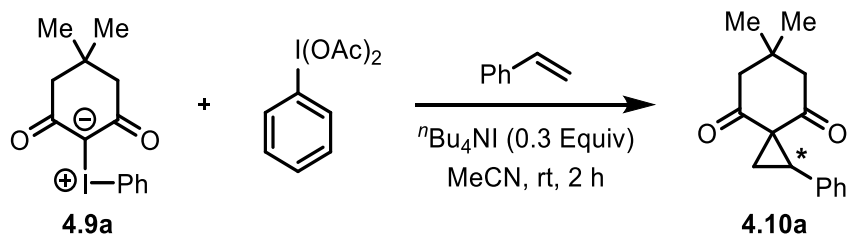
Scheme 4.6 Metal-catalyzed asymmetric cyclopropanation of iodonium ylides with alkenes

The best conditions were found when using a chiral Cu complex containing $\text{Cu}(\text{OTf})_2$ (10 mol %) and a chiral ligand (12 mol %). The chiral ligand was derived from two oxazoline rings, containing two pendant substituted benzyl groups, and using this as the optimal chiral Cu complex, gave 99% *ee* (**Scheme 4.6**).

Based off the success of others, merging of HVI reagents with chiral environments to induced asymmetric reactivity, it was our goal to observe if our cyclopropanation reaction of iodonium ylides could potentially merge with this type of chiral methodology. Because other researchers have pursued asymmetric cyclopropanation reactions using iodonium ylides with catalytic transition-metals, it was our intention to incorporate our metal-free LED technology for this similar cyclopropanation reactivity. The following results towards solving this idea and discovering if this is a viable option for asymmetric synthesis.

4.2 Preliminary Results

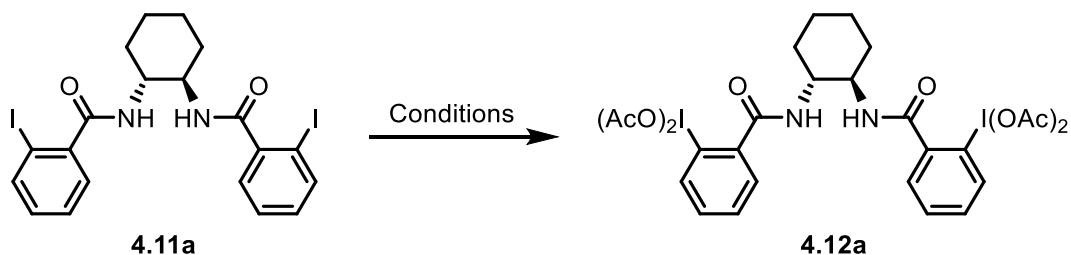
Initially, this project was started as a collaboration between the Murphy group at University of Waterloo and the Quideau group at the University of Bordeaux. In early stages we had not discovered that light can activate iodonium ylides (**4.9a**) to react with alkenes and form cyclopropanes (**4.10a**), so we started off by trying to incorporate Quideau's catalytic systems with a metal-free reaction of iodonium ylides discovered recently in our group in 2017.²⁶⁵



Scheme 4.7 Racemic metal-free cyclopropanation reaction

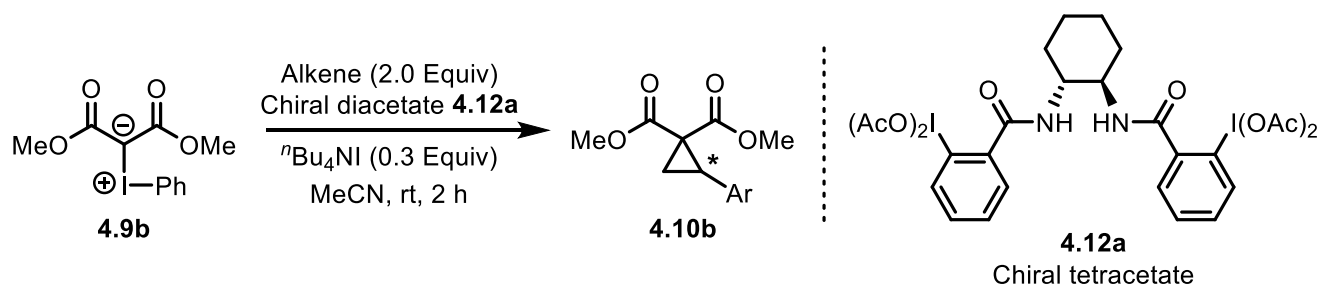
Working with Quideau's systems it was soon realized that working with two iodines in the same molecule would be problematic due to both being able to undergo oxidation and produce unnecessarily complex reaction mixtures. Working with salen-derived aryl iodide **4.11a**, a complex and hard to interpret NMR was produced making it difficult to understand if one or both iodine atoms were undergoing oxidation as shown in the following attempted reactions using both SelectfluorTM and NaBO₃ • 4H₂O to form chiral diacetate **4.12a**.

Table 4.1 Oxidation of chiral aryl iodide



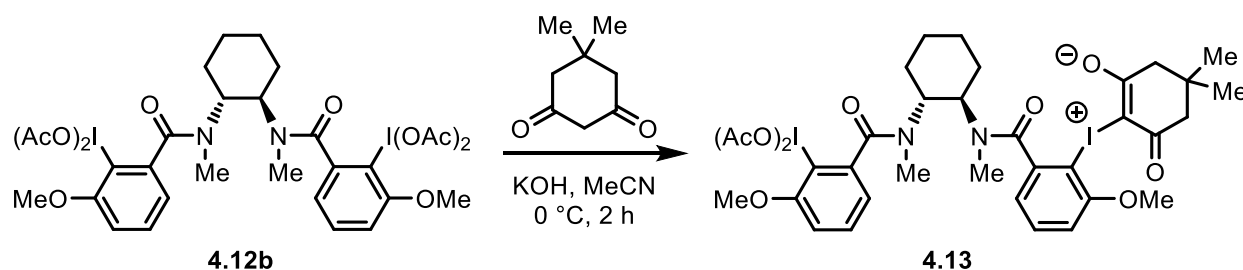
Entry	Oxidant	Solvent	Time (h)	Temp (°C)	Yield (%)
1	Selectfluor TM	MeCN:AcOH (3:1)	12	25	-
2	NaBO ₃ • 4H ₂ O	AcOH	17	40	-

After we thought we had obtained chiral tetracetate **4.12a** it was then subjected to the racemic metal-free cyclopropanation reaction as shown below in **Scheme 4.8**. This strategy for metal-free asymmetric cyclopropanation of iodonium ylides with alkenes was not ideal, due to the multiple iodines present and limited Quideaux systems made available to work with.



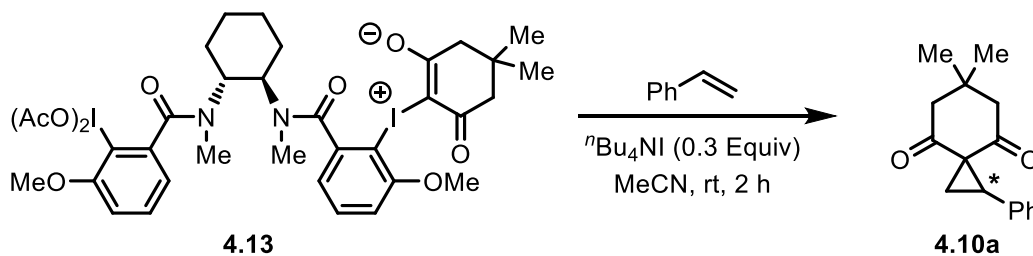
Scheme 4.8 Asymmetric cyclopropanation of acyclic iodonium ylides with alkenes

An alternative strategy for metal-free asymmetric cyclopropanation of iodonium ylides with alkenes was then conceived of by first pre-making a chiral iodonium ylide **4.13** from dimedone and chiral tetracetate **4.12b** as shown in **Scheme 4.9**.



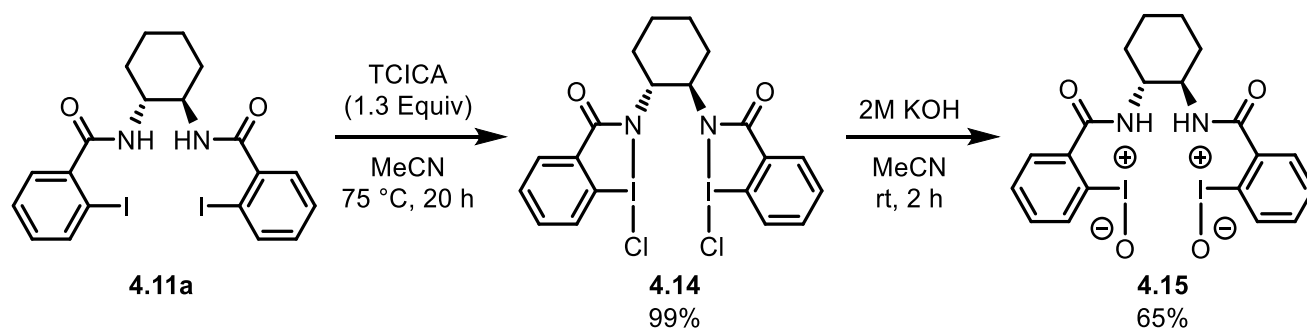
Scheme 4.9 Synthesis of chiral cyclic iodonium ylide

After obtaining chiral iodonium ylide **4.13** it was then subjected to the reaction conditions as shown in **Scheme 4.10** to give cyclopropane **4.10a** in a hopefully non-racemic manner. This reaction unfortunately failed at yielding any cyclopropane, which was attributed to the multiple iodines present in the starting iodonium ylide which were unnecessary giving a complex reaction mixture without the desired product forming.



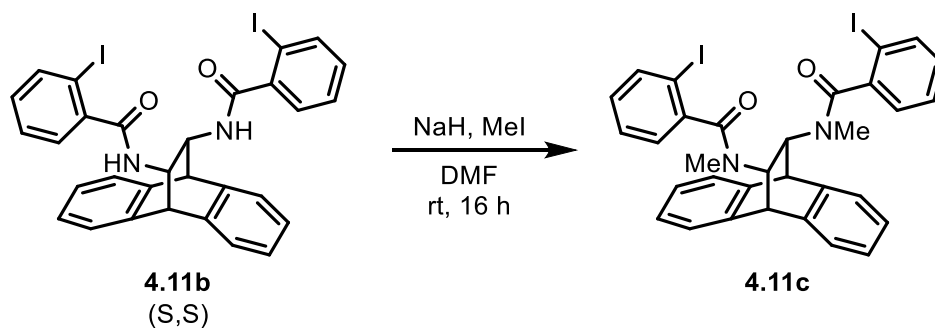
Scheme 4.10 Asymmetric cyclopropanation of cyclic iodonium ylides with alkenes

More chiral HVI systems were created using the examples that Quideau contributed to this collaboration, as shown in the following schemes. A chiral iodosoarene was created as it was important for attempting iodonium ylide reactions that require the HVI atom to be in the form of an iodosoarene and not a diacetate, such as the monocarbonyl iodonium ylide reactions talked about in Chapter 2 of this thesis. In the end, these reactions failed at giving us any answers to the question of whether this chemistry would work in an asymmetric protocol.



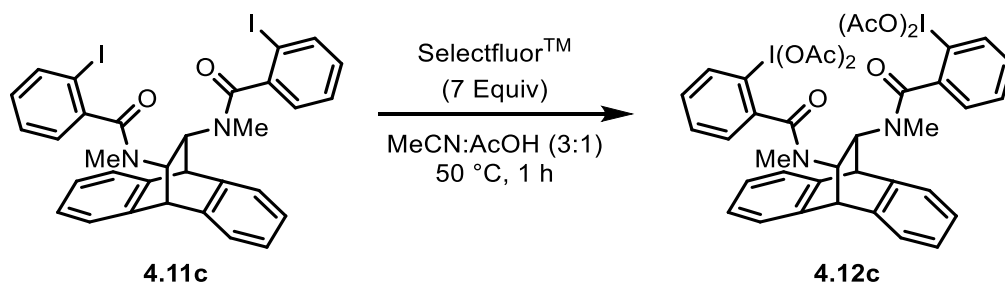
Scheme 4.11 Synthesis of chiral iodosoarene

Another example of a Quideau catalyst systems was prepared by an enantioselective Diels-Alder reaction to give **4.11b**. This compound was methylated on the nitrogens as a way to protect the nitrogens from undergoing unwanted oxidation with HVI reagents which may occur in subsequent steps. The starting material **4.11b** (S,S) was provided to the Murphy group in enantiomerically pure form as part of our collaboration, and after performing a nitrogen-methylation step in the Murphy lab, chiral aryl iodide **4.11c** was produced (**Scheme 4.12**).



Scheme 4.12 N-Methylation of chiral system

The N-methylated product **4.11c** was then subjected to oxidation conditions of the iodine (I) with SelectfluorTM (**Scheme 4.13**) with the intention of creating the HVI structure **4.12c**. The presence of two iodines in the starting material made the oxidation step problematic, giving a complex reaction mixture that was hard to analyze and confirm if the desired tetracetate product was produced.



Scheme 4.13 Synthesis of chiral tetracetate

Unfortunately, the presence of two iodine atoms within the single system was not compatible with Murphy groups iodonium ylide chemistry, and this became problematic in the cyclopropanation reaction. It is hypothesized that disproportionation maybe occurring between the two HVI centres within the aryl iodide system. It was around this time of failure that an exciting new reaction was discovered. After realizing that this strategy was not going to work, as part of the shared collaboration, we discovered that blue light could be used to activate iodonium ylides and allow them to react with alkenes to give cyclopropane products. We then turned our attention to analyze if this process could be turned into an asymmetric variant which should have a higher chance of working because the cyclopropanation reaction no longer would require additives and now other systems could be attempted limiting the iodines to just one per molecule. The next section will look at this strategy which started off by creating our own chiral systems with the intention of forming the chiral iodonium ylide first, and then subjecting the chiral ylide to the alkene under blue light activation.

4.3 Synthesis of Chiral Aryl Iodides

After our groups newly discovered light-induced cyclopropanation reaction of iodonium ylides with alkenes, the question began of whether an asymmetric variant could be applied here

with the correct conditions. To start off with, our initial attempts were directed towards synthesizing catalytic aryl iodide systems that had worked for other groups (for other reactions) obviously. The leaders of the asymmetric hypervalent iodine field being Quideau, Ishihara and Fujita provided inspiring systems to go after with the intention of attaching an iodonium ylide to the iodine in the chiral aryl iodide. To simplify this concept, aryl iodides that were accessible to our group by synthetic means were targeted, and in addition, systems containing a single iodine were at the top of the trial list.

Systems derived from lactate has shown to be amendable to many different reactions such as work done by Ishihara throughout 2010.²⁹⁹ Lactate which is the deprotonated anion that results from deprotonating lactic acid and can exist in both (*R*) and (*S*) enantiomeric forms, is shown in **Figure 4.11**.

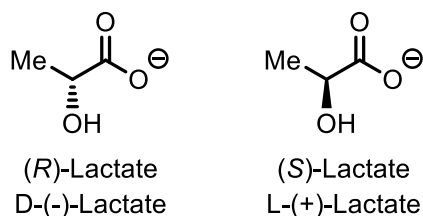


Figure 4.11 Structures of D-(-)-lactate and L-(+)-lactate

Insight by Ishihara³⁰⁰ and Fujita³⁰¹ identified lactic acid as a suitable chiral pool-derived auxiliary in the design of iodine catalysts, which went on to have a large impact in the development of many more chiral systems. The variability of R_1 and R_2 and X in the boxes, as shown in **Figure 4.12**, demonstrate a toolbox approach where modification of various combinations of groups can be used to create a library of chiral catalysts that can be used to determine optimal conditions for a given reaction.

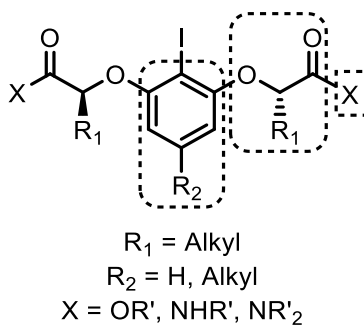
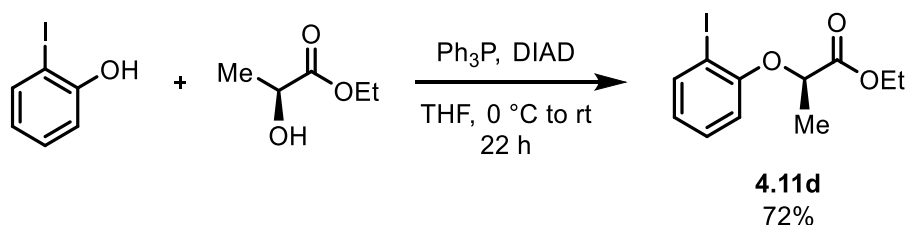


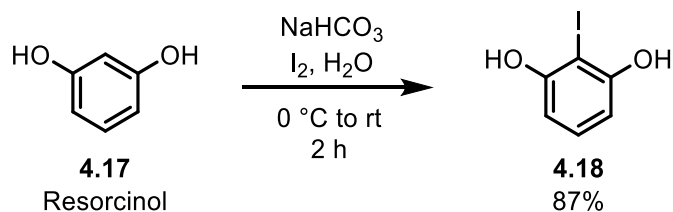
Figure 4.12 Lactic acid-based C_2 -symmetric aryl iodide systems

Even though C_2 -symmetric aryl iodide systems have shown to be highly successful, the use of lactate-derived aryl- λ^3 -iodanes containing a single group in some cases, have shown to give even higher yields in enantioselective dioxytosylation reactions than their C_2 -symmetric counterpart.³⁰² This observation was taken in consideration because there is very little known in the synthesis of chiral iodonium ylides, which are extremely rare, so assuming a C_2 -symmetric system should work better has no backing in the literature. Therefore, we began our studies with the synthesis of the following lactate-derived mono-substituted aryl iodide **4.11d**, which was accomplished using a Mitsunobu reaction. Commercially available L-(+)-ethyl lactate was used to react with 2-iodophenol, also commercially available, for the construction of chiral aryl iodide **4.11d** in an isolated yield of 72% as shown in **Scheme 4.14**.



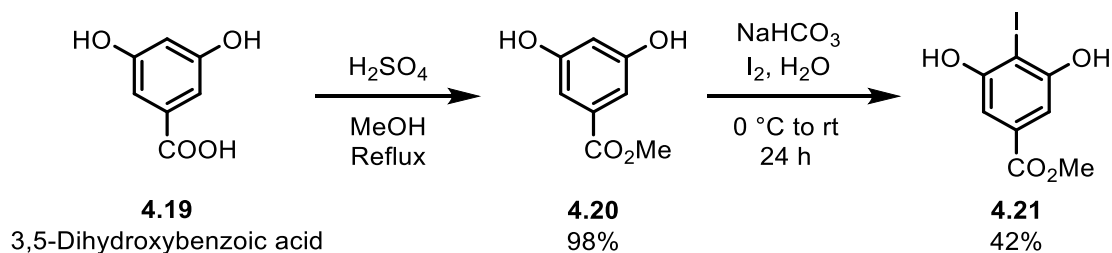
Scheme 4.14 Synthesis of chiral aryl iodide

There is an enhanced reactivity that is provided by a prominent catalyst system designed on combining two lactic acid derivatives bearing ester or amide groups to a resorcinol core.³⁰³ Due to the success of C_2 -symmetric aryl iodide systems for the use in multiple types of asymmetric reactions in organic synthesis, it seemed logical to try and synthesize a small library of these compounds to test with the conditions of the light-induced cyclopropanation reaction. To synthesize the required C_2 -symmetric aryl iodide systems, the appropriate aryl iodide (**4.18**) was needed. The synthesis was carried out starting from commercially available resorcinol (**4.17**) as shown in **Scheme 4.15**.



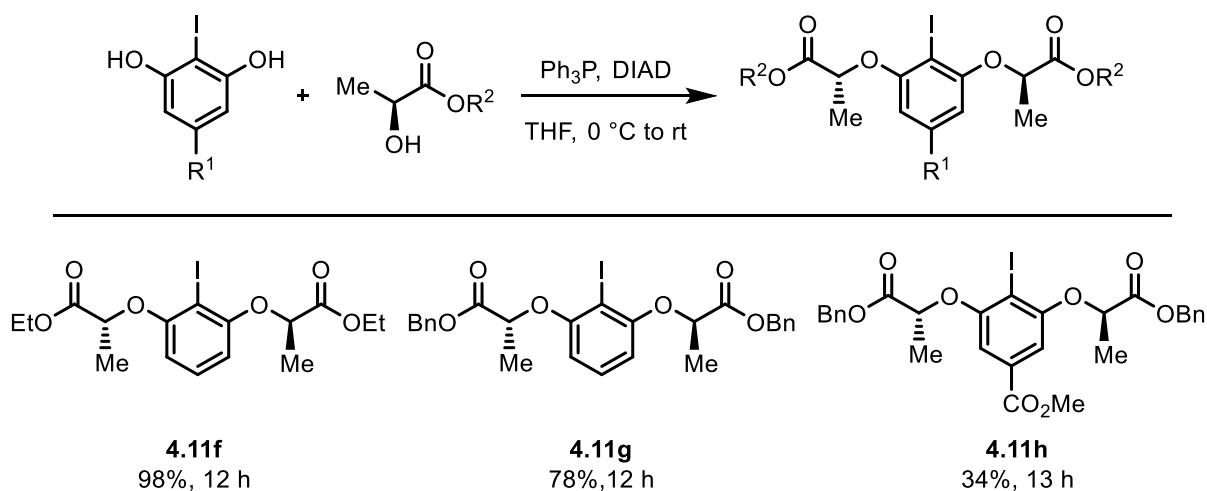
Scheme 4.15 Synthesis of 2-iodobenzene-1,3-diol from resorcinol

Another system that was to be investigated required the simple aryl iodide, methyl 3,5-dihydroxy-4-iodobenzoate (**4.21**), which was synthesized from methyl 3,5-dihydroxybenzoate (**4.20**), which came from commercially available 3,5-dihydroxybenzoic acid (**4.19**) as shown in **Scheme 4.16**.



Scheme 4.16 Synthesis of methyl 3,5-dihydroxy-4-iodobenzoate

The synthesis of the chiral aryl iodides **4.11f**, **4.11g**, and **4.11h** were accomplished using standard Mitsunobu reaction conditions as shown in **Scheme 4.17**.



Scheme 4.17 Synthesis of chiral aryl iodides

4.3.1 Synthesis of L-Proline Derived Aryl Iodides

Because of the chirality embedded within amino acids, this can also be a source of chirality if embedded within an aryl iodide system. Because of the success and involvement of proline in many asymmetric reactions, it was selected as a core for the construction of an aryl iodide system. The natural version of the amino acid, L-proline, was used in the synthesis to obtain a fixed chiral centre in which to hopefully induce chirality to the cyclopropane product.

Zhdankin showed how L-proline can induce asymmetry in the design of chiral aryl iodide (V) systems. In 2000 Zhdankin developed a novel benziodazole oxide system which was prepared by oxidation of the readily available 2-iodobenzamides derived from natural amino acids.³⁰⁴ In 2006 Zhdankin developed another chiral aryl iodide (V) system (**4.22**) prepared by chiral pseudo-benziodoxazine derivatives based off the inexpensive and readily available (S)-proline amino acid shown in **Figure 4.13**.³⁰⁵

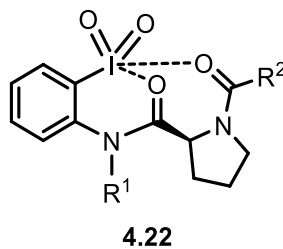


Figure 4.13 L-Proline derived chiral aryl iodides developed by Zhdankin

Inspired by Zhdankin's work in 2006, which showed that L-proline could form a higher-ordered chiral environment, with the highly ordered asymmetric structure being controlled by the chiral centre embedded in L-proline. A chiral environment could be formed even from remote regions in space as the electron-rich amide and esters would provide negatively charged atoms that would be electrostatically attracted to the positively charged HVI atom located 5 or 6 atoms away. Iodonium ylide **4.9c** shown in **Figure 4.14** is just one of many theoretical ways in which a chiral environment could be formed in the iodonium ylide derived from L-proline.

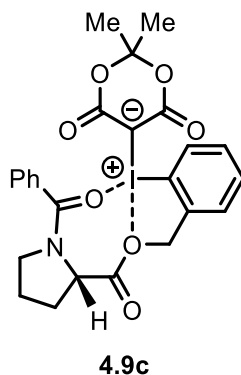
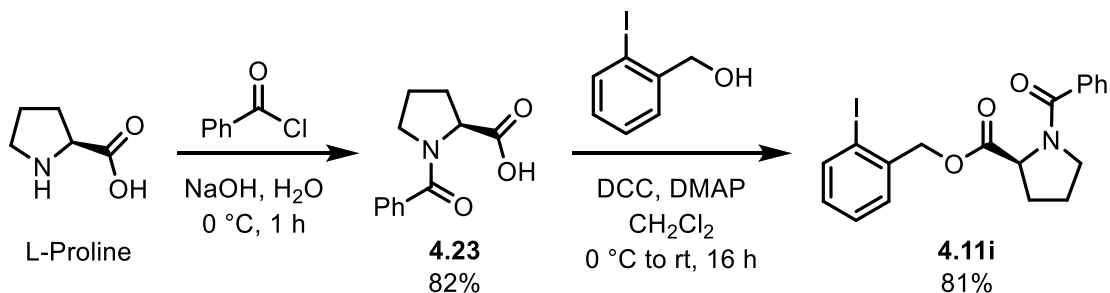


Figure 4.14 L-Proline derived chiral iodonium ylide environment

The ability of L-proline to form higher-ordered chiral environments through electrostatic interactions was the inspiration behind the design of chiral iodonium ylides that could be used in our visible light-induced cyclopropanation reaction. Initial attempts were aimed at finding a way to attaching L-proline onto an aryl iodide system. The free N-H in the L-proline was first protected by the attachment of a benzoyl group to avoid any side oxidation reactions, which can occur between HVI atoms and free N-H groups. The synthesis of **4.23** was achieved in 82% which was followed by DCC-coupling to form ester bonds with alcohols (2-iodophenyl)methanol and the carboxylic acid group in L-proline to give **4.11i** in 81% yield (**Scheme 4.18**).

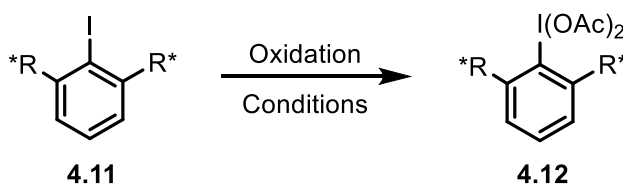


Scheme 4.18 Synthesis of L-proline derived aryl iodide

After construction of the chiral aryl iodide derived from L-proline, where the nitrogen is protected in the form of an amide (**4.11i**) the appropriate oxidation conditions were then applied, allowing for the construction of chiral diacetates.

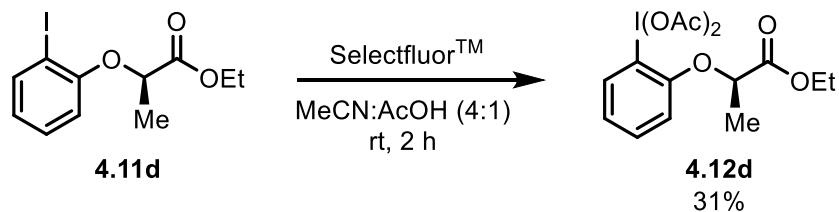
4.4 Synthesis of Chiral Diacetates

The strategy used to synthesize chiral aryl iodide diacetates was based off the regular oxidative synthetic methods used to synthesize racemic diacetates. Oxidants such as SelectfluorTM and $\text{NaBO}_3 \cdot 4\text{H}_2\text{O}$ both worked under conditions that mimic racemic literature examples. Starting from a chiral aryl iodide in the presence of SelectfluorTM using MeCN:AcOH (4:1) at room temperature was the ideal conditions for the majority of examples tried.



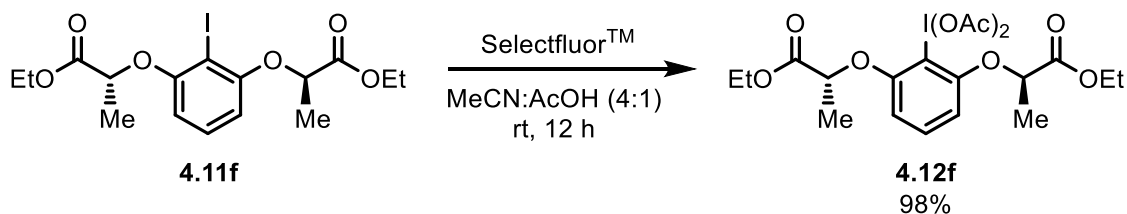
Scheme 4.19 Synthesis of general chiral aryl iodide diacetates

Using SelectfluorTM as the oxidant for turning chiral aryl iodide **4.11d** into diacetate **4.12d** worked, but in only a 31% yield (**Scheme 4.20**). This relatively low yield encouraged the use of other reaction conditions, such as longer reaction times, to see if the low yield could be increased in the synthesis of other chiral diacetate systems.



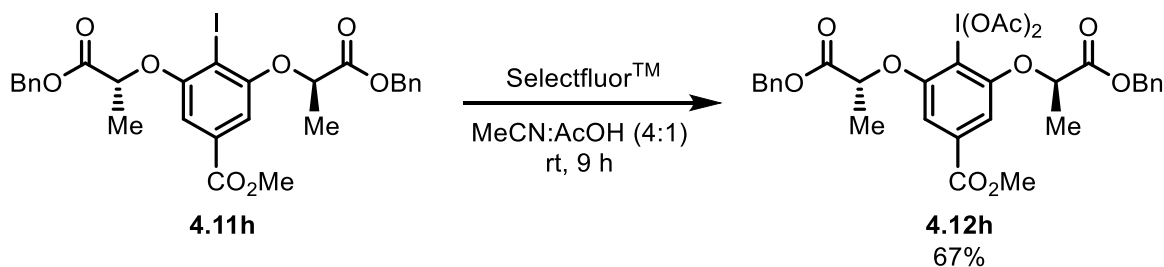
Scheme 4.20 Synthesis of chiral aryl iodide diacetate

Running an oxidation reaction with C_2 -symmetric aryl iodide systems such as **4.11f** for a total of 12 hours proved to be adequate for the reaction time, as a nearly quantitative yield of 98% was achieved for diacetate **4.12f** (**Scheme 4.21**).



Scheme 4.21 Synthesis of chiral aryl iodide diacetate

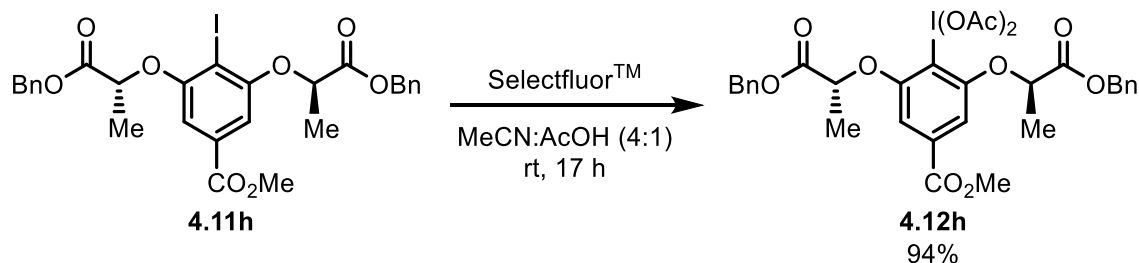
Application of SelectfluorTM oxidation on chiral aryl iodide **4.11h** gave diacetate product **4.12h** but in a yield that was lower than expected (**Scheme 4.22**). The low yield was assumed to be caused by the reaction time not being long enough at only 9 h.



Scheme 4.22 Synthesis of chiral aryl iodide diacetate

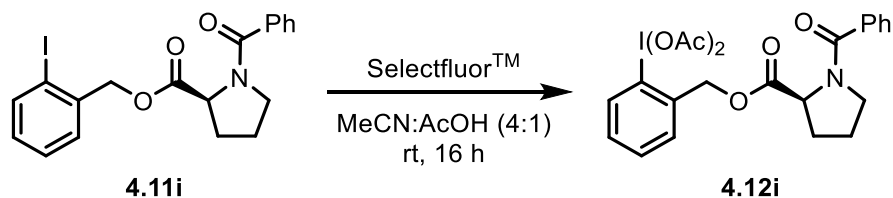
The same reaction was repeated with the only exception being allowing the SelectfluorTM to react with the chiral aryl iodide for a longer time. When the reaction was left for

17 h, more product was produced than at the 9 h mark, giving a relatively clean reaction mixture yielding chiral diacetate **4.12h** in an isolated yield of 94% (**Scheme 4.23**).



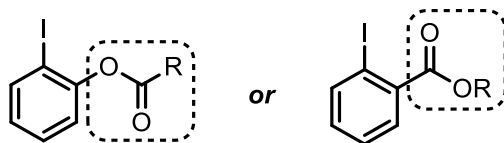
Scheme 4.23 Synthesis of chiral aryl iodide diacetate

In addition to forming the C_2 -symmetric chiral diacetates, chiral diacetates derived from L-proline were also produced using Selectfluor™ as the oxidant (**Scheme 4.24**).



Scheme 4.24 Synthesis of L-proline derived chiral aryl iodide diacetate

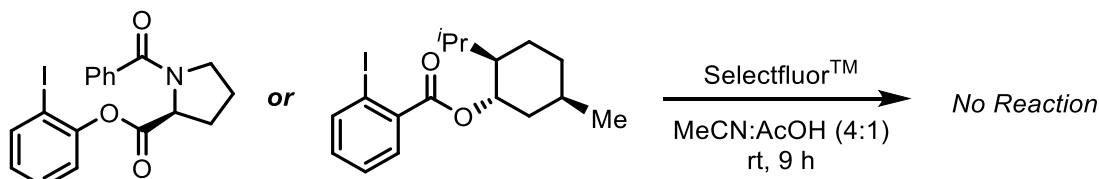
It is known that *ortho*-esters on aryl iodides are problematic when performing oxidation reactions that turn iodine (I) to iodine (III). Usually, these reactions either fail or require harsh conditions that often end up over-oxidating to iodine (V).³⁰⁶ It was found that both *ortho*-ester isomers failed to undergo oxidation to iodine (III) under standard conditions.



Both types of *ortho*-esters
prevent oxidation to iodine (III)

Figure 4.15 Problems with *ortho*-ester oxidation

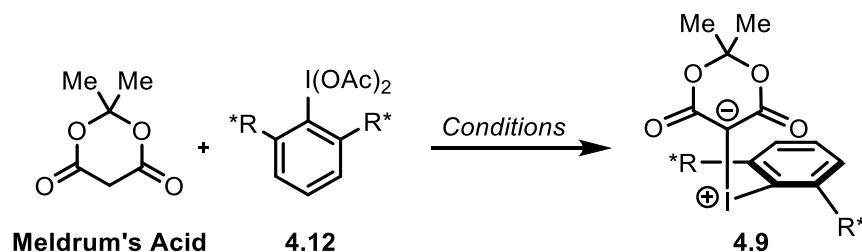
When attempting to oxidize chiral aryl iodides containing *ortho*-ester groups, it was quickly realized that Selectfluor™ conditions would not work (**Scheme 4.25**).



Scheme 4.25 Problems with *ortho*-ester oxidation

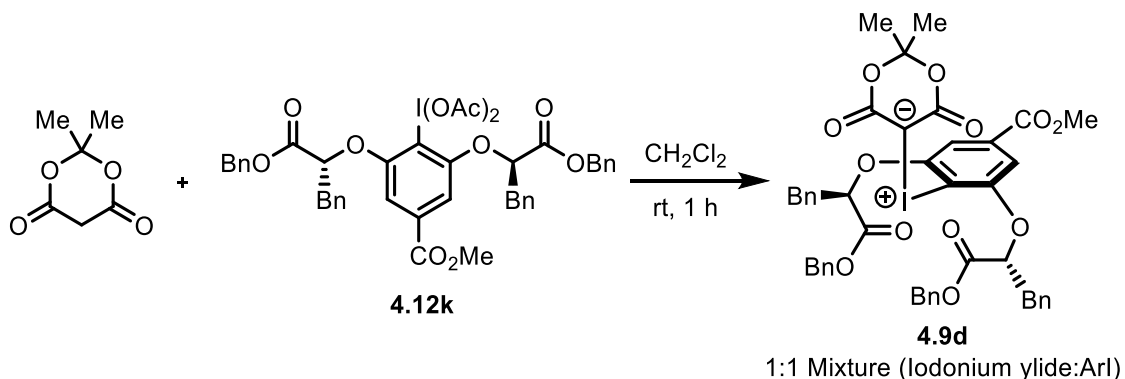
4.5 Synthesis of Chiral Iodonium Ylides

The synthesis of chiral iodonium ylides was accomplished using the regular synthetic method for synthesizing racemic iodonium ylides, using a 1,3-dicarbonyl motif and an aryl iodide diacetate. Under standard conditions using just solvent (CH_2Cl_2) the chiral iodonium ylide will form, but in lower yields. Slight adjustments can be made to improve the yield, and after a few attempts, optimized conditions were eventually found for the chiral iodonium ylides used in this chapter. A general reaction scheme illustrating the starting materials used in the synthesis of a typical chiral iodonium ylide is shown below in **Scheme 4.26**. Meldrum's acid was often selected as the desired β -dicarbonyl motif due to the nature of the iodonium ylide and cyclopropane being relatively more stable when compared to other β -dicarbonyl motifs such as dimedone-based systems. Cyclopropanes derived from dimedone as the dicarbonyl motif demonstrated a tendency for isomerization of the cyclopropane into the dihydrofuran. To prevent isomerization of cyclopropane to dihydrofuran Meldrum's acid was used as the dicarbonyl motif.



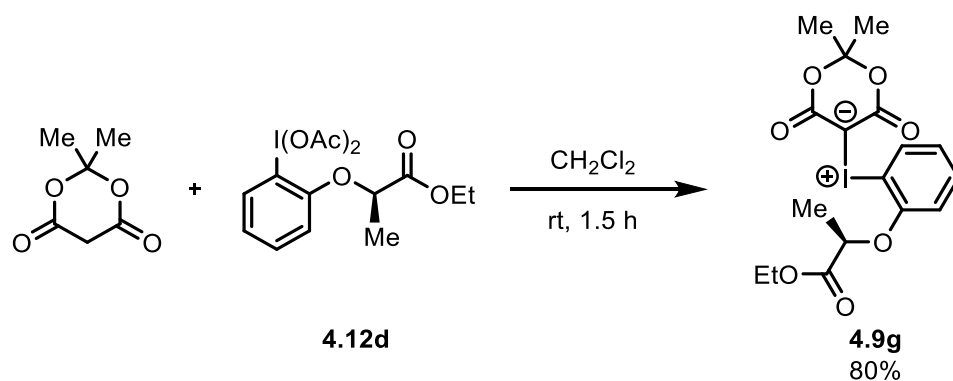
Scheme 4.26 General synthesis of chiral cyclic iodonium ylides

First attempts at synthesizing chiral iodonium ylides focused on using Meldrum's acid in conjunction with a relatively bulky C_2 -symmetric chiral diacetate using just CH_2Cl_2 as the solvent. This reaction did not give the iodonium ylide in pure form, instead the product was contaminated as a 1:1 mixture of starting material aryl iodide and iodonium ylide (**Scheme 4.27**). Because of the mixture, purification was made extremely hard, and using the standard method of purification, performed by trituration, a sample of pure chiral iodonium ylide was not obtained, and because of this, the following cyclopropanation reaction with an alkene was not attempted. The failed approach was believed to be the result of either using a chiral diacetate that was too bulky, or the reaction conditions were not appropriate for this type of chemistry. Adjustments were required to improve the reaction conditions such as using a different solvent or the use of additives was hypothesized as a possible alternative.



Scheme 4.27 Synthesis of chiral cyclic iodonium ylide

Initially it was hypothesized that perhaps a bulky C_2 -symmetric chiral diacetate might be giving an iodonium ylide that is sterically crowded, and this is why the ylide was not being formed. To limit the amount of over-crowding in the iodonium ylide, a non- C_2 -symmetric chiral diacetate (**4.12d**) was used and was successful at providing chiral iodonium ylide **4.9g** as shown below in **Scheme 4.28**



Scheme 4.28 Synthesis of chiral cyclic iodonium ylide

Finding better conditions for the synthesis of bulkier chiral iodonium ylides was then directed towards exploring the use of additives in the reaction mixture. The synthesis of some HVI compounds have been performed using hexafluoroisopropanol (HFIP) as an additive and has been shown to enhance the reactivity in some examples leading to increased yields and shorter reaction times.³⁰⁷ The nature of this activation is not yet fully understood, but there are studies into mechanistic interpretations of what may possibly account for subtle changes to reactivity when additives are used.

Solvent-based activation of HVI compounds is known, including the activation of PIDA using HFIP. Fluorinated alcohols such as HFIP and trifluoroethanol (TFE) are reported to be highly effective solvents for increasing the activity of HVI-mediated reactions. The origin of this beneficial enhancement is attributed to the ability of these solvents to stabilize reactive intermediates, and possibly transition states as well. Intermediates that are more polar than starting materials could benefit from being better stabilized, or better solvated when highly polar solvents such as alcohols are used. A unique feature of fluorinated alcohols, that makes them ideally suited for this scenario, is the property of having increased acidic oxygen-hydrogen bonds. The pKa of HFIP is 9.3 compared to the non-fluorinated analogue *t*PrOH, which has a pKa of 17.1. This feature may enable the fluorinated alcohol to participate in hydrogen bonding to a higher degree than standard alcohols.

A property of fluorinated alcohols such as HFIP or TFE is that they are highly polar but have low nucleophilicity.³⁰⁸ An example of this effect is the stabilization of aromatic radical cations involved in the HVI-mediated reaction of single electron-transfer oxidations of aromatic compounds.³⁰⁹ Investigation into the role of HFIP in a PIDA-catalysed [2+2] cycloaddition

reaction of styrenes was carried out by Donohoe and Compton in 2016 who monitored the reaction by electrochemical and spectroscopic analysis.³¹⁰ This reaction required the use of initiators while being performed, except when HFIP was used as a solvent, resulting in the reaction readily proceeding. PIDA also exhibited different volumetric reduction curves in HFIP and MeCN, suggesting that HFIP influences the reactivity of PIDA.

A large shift in the ¹H NMR spectra of the HFIP-PIDA adduct occurred, with the HFIP-OH signal changing from 2.88 to 5.88 ppm. This shift in the signal indicates the formation of a hydrogen bond interaction between the HFIP and PIDA. This PIDA-HFIP interaction is shown below as a dotted line in **Figure 4.16**.

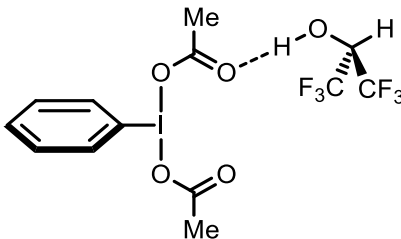
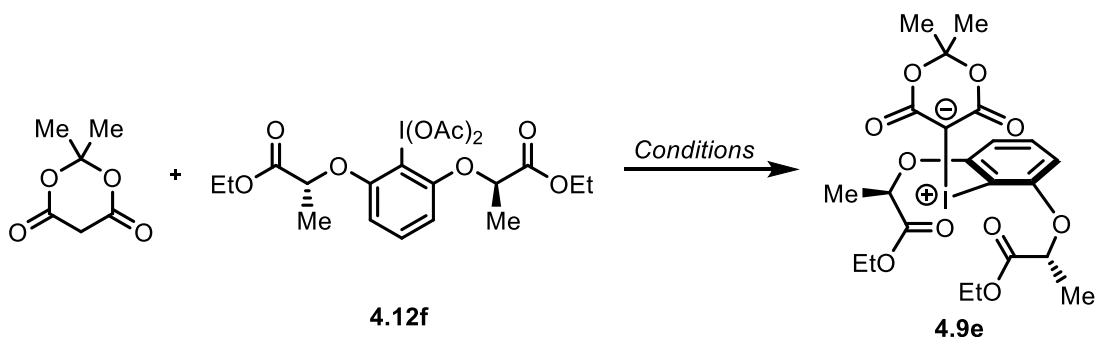


Figure 4.16 HFIP interaction with PIDA

In the reaction of chiral diacetates with dimedone or Meldrum's acid, without the use of HFIP, there was a lot of white insoluble particles in the reaction mixture. These insoluble particles were more abundant when conducting the reaction in an ice bath. A benefit of adding HFIP as a co-solvent was the ability to solubilize the particles to create a fully homogeneous mixture. This ensures proper mixing of starting materials, giving all the molecules a chance to fully react and give the highest yield possible.

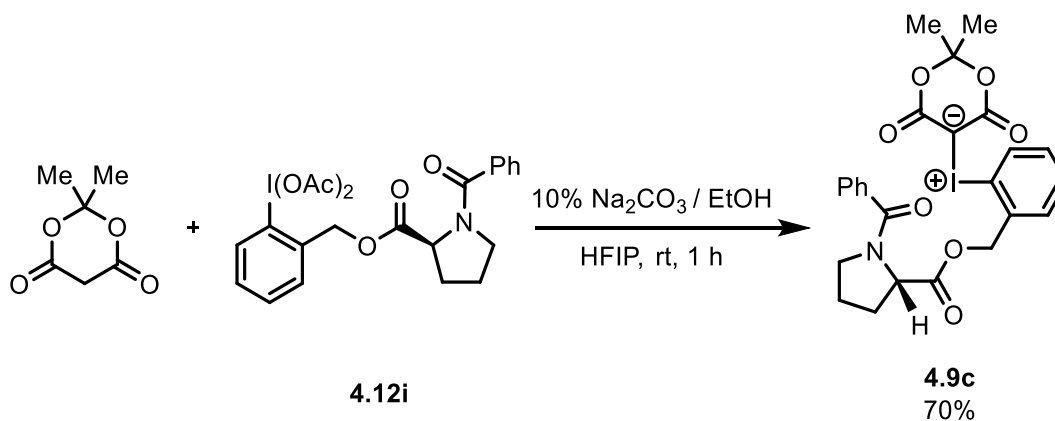
The use of an ice bath was important as these newly synthesized molecules have properties that are unknown and could be thermally unstable. It was therefore important to perform the ylide synthesis reactions at cooler temperatures to avoid decomposition. Using HFIP, in addition to the standard solvent a homogeneous reaction mixture while being cooled in an ice bath.

Another benefit of adding HFIP as a co-solvent, was the reduction in reaction time. Using HFIP as an additive, the reaction was cut back from 4 hours to 1.5 hours, as monitored by ¹H NMR at 0.5 h intervals.

Table 4.2 Synthesis of C_2 -symmetric chiral iodonium ylides

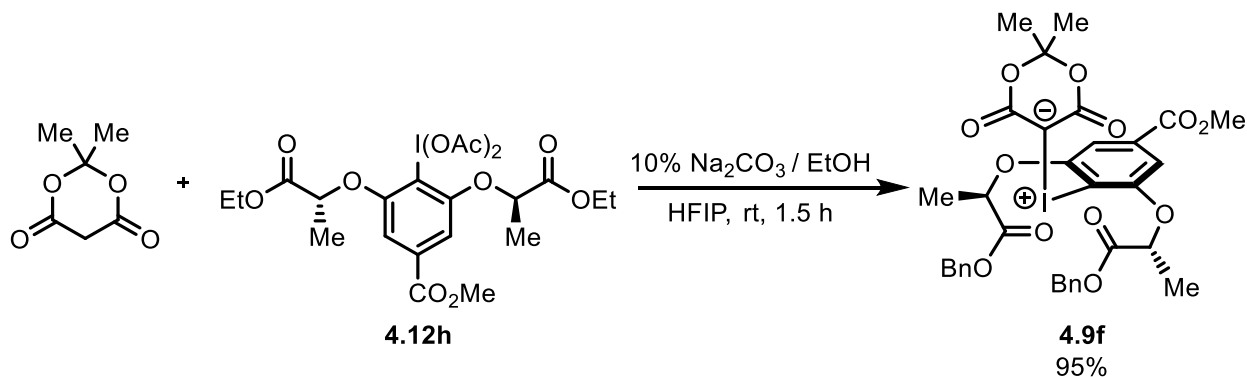
Procedure	Solvent	Additive	Temp (°C)	Time (h)	Yield (%)
1	10% Na ₂ CO ₃ / EtOH	-	25	4	56
2	10% Na ₂ CO ₃ / EtOH	HFIP (0.5 mL)	0	1.5	98

Based off the successful use of HFIP as an additive to the C_2 -symmetric chiral iodonium ylide synthesis, it was also added to the synthesis of other chiral iodonium ylides, such as the L-proline derived example shown below. The reaction of Meldrum's acid with L-proline derived chiral diacetate **4.12i** yielded chiral iodonium ylide **4.9c** in 70% in only 1 h reaction time with the short reaction time presumably being attributed to the use of HFIP (0.5 mL) as an additive.

**Scheme 4.29** Synthesis of chiral iodonium ylide

Using HFIP as an additive to the C_2 -symmetric chiral iodonium ylide synthesis proved to have effects that not only reduced reaction times but also gave chiral iodonium ylide **4.9f** in nearly quantitative yield when using 5 equivalents of SelectfluorTM as the oxidant (**Scheme 4.30**). The reaction of Meldrum's acid with C_2 -symmetric chiral diacetate **4.12h** provided chiral

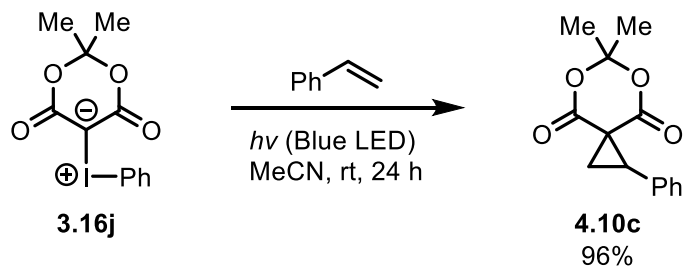
iodonium ylide **4.9f** in a short reaction time of only 1.5 h presumably being attributed to the use of HFIP (0.5 mL) as an additive which gave the desired chiral iodonium ylide product in a 95% isolated yield.



Scheme 4.30 Synthesis of chiral iodonium ylide

4.6 Synthesis of Chiral Cyclopropanes

To answer questions about the stereoselectivity of the cyclopropanation reaction that results when an iodonium ylide reacts with an alkene, it was necessary to synthesize a racemic sample of the cyclopropane to act as standards (**Scheme 4.31**).



Scheme 4.31 Synthesis of racemic cyclopropane standards

Once the cyclopropanation reaction was run, the product was subjected to chiral HPLC analysis using a Chiralcel OD-H column. Using the racemic sample there should clearly be two peaks of similar area which correspond to the (*R*) and (*S*) stereocenters in the cyclopropane (**Table 4.3**). These two peaks were observed and have retention times of 13.07 and 18.22

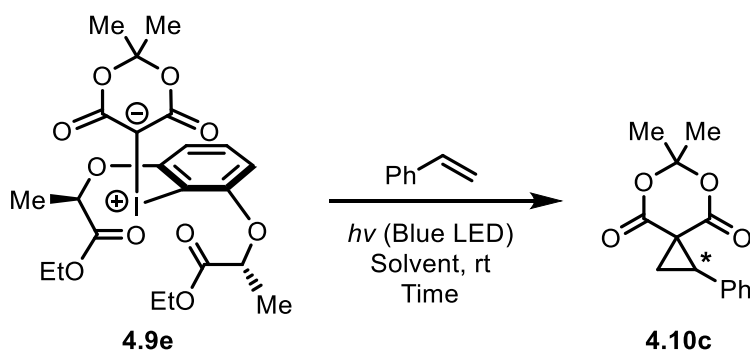
minutes. The two peaks could be clearly resolved using the optimal solvent system, which was found to be hexane:*i*PrOH (90:10) with a flow rate of 0.75 mL/min. These conditions were selected as the optimal conditions for collecting chiral HPLC data for the remainder of the cyclopropanes tested in this thesis.

Table 4.3 Chiral HPLC data from racemic standards

Retention Time (min)	Area (mAU•s)	Area (%)
13.07	407.36	44.4
18.22	411.81	44.9

It was not clear if working with chiral iodonium ylides would be a major difference in terms of reactivity when compared to the non-chiral iodonium ylides used in Chapter 3. Initial attempts at producing chiral cyclopropanes were based on using chiral iodonium ylides which were then irradiated with blue LEDs in the presence of styrene as this alkene typically gave the highest yields. A quick optimization of conditions was run to determine how long the cyclopropanation reaction would take and how many equivalents of styrene would be needed to give the highest yield of cyclopropane possible.

Table 4.4 Cyclopropanation of chiral iodonium ylide using blue LEDs



Entry	Solvent	Styrene (Equiv)	Time (h)	Yield (%) ^[a]
1	CDCl ₃	10	27	40
2	CDCl ₃	10	36	56
3	MeCN	2	6.5	30
4	MeCN	2	9	38
5	MeCN	2	22	55

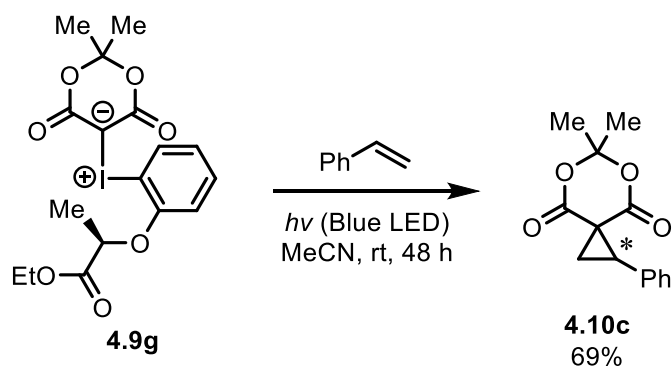
The iodonium ylide was used on a 0.1 mmol scale with 1.0 mL of solvent (0.1 M). ^[a] Yields determined by ¹H NMR using HMDSO (10 μL) as an internal standard.

As the results indicate from **Table 4.4** using even more equivalents of styrene (10 equiv) resulted in yields that are not much higher, only 1%, that using styrene at the optimized conditions of 2 equiv. It was therefore concluded that 2 equiv of styrene would be used as the optimized conditions for the remaining cyclopropanation reactions. Monitoring the blue light induced cyclopropanation reaction with ^1H NMR showed that the reaction time is an important factor, and iodonium ylide **4.9e** took approximately 36 hours to be fully consumed and turned into the cyclopropane. Over the course of the cyclopropanation reaction, the amount of iodonium ylide was observed to slowly react until fully consumed, at which point the reaction was determined to be complete, and on average required approximately 36 hours for most of the Meldrum's acid derived chiral iodonium ylides used in this chapter. After establishing that a chiral iodonium ylide can successfully combine with an alkene (styrene) and form a cyclopropane using blue LEDs, the next step was to determine if the reaction was occurring in a stereoselective manner.

Cyclopropane **4.10c** was successfully produced in an overall isolated yield of 69% using the chiral iodonium ylide **4.9g** as shown below in **Scheme 4.32**. To determine if the cyclopropane was being produced with any enantiomeric excess or if the sample was just racemic, chiral HPLC analysis was conducted. The HPLC analysis was performed using a chiral HPLC column (Chiralcel OD-H) with the optimal solvent system which was found to be hexane:*i*PrOH (90:10) with a flow rate of 0.75 mL/min. These conditions were discovered when working with the racemic sample of cyclopropane **4.10c** produced from the reaction of styrene with a non-chiral iodonium ylide. The cyclopropane produced was subjected to chiral HPLC analysis using the optimal conditions and it clearly showed the two peaks corresponding to the (*R*) and (*S*) stereocenters in the cyclopropane. These two peaks were observed and have retention times of 13.06 and 18.27 minutes and areas of 125.47 and 117.41 mAU•s respectively (**Table 4.5**). Unfortunately, the peaks are relatively the same in terms of area indicating the reaction is occurring, but the cyclopropane is being produced in a racemic form.

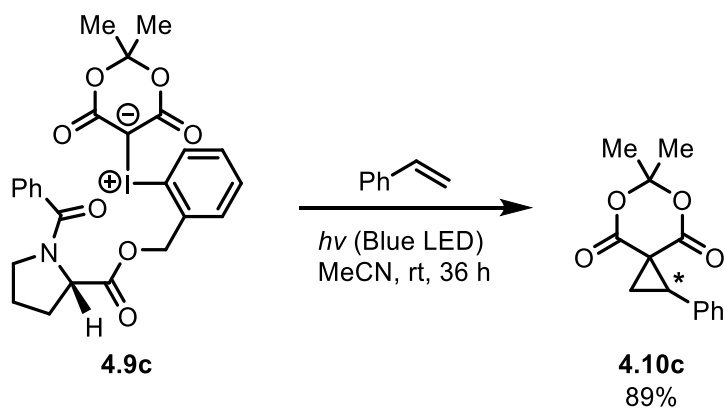
Table 4.5 Chiral HPLC data from cyclopropanation reaction

Retention Time (min)	Area (mAU•s)	Area (%)
13.06	125.47	51.7
18.27	117.41	48.3



Scheme 4.32 Cyclopropanation of chiral iodonium ylide using blue LEDs

Another system that was checked to see if the cyclopropanation reaction could occur in a stereoselective process can be seen in the following reaction of chiral iodonium ylide **4.9c** with styrene in the presence of blue LED (**Scheme 4.33**). The cyclopropane was produced in an overall yield of 89% after 36 hours and after performing this reaction the product could then be subjected to chiral HPLC analysis.



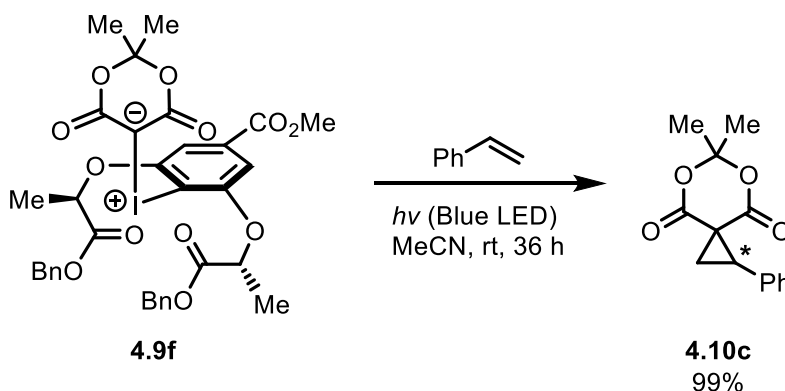
Scheme 4.33 Cyclopropanation of chiral iodonium ylide using blue LEDs

It was found that the chiral HPLC analysis gave two peaks with retention times of 13.06 and 18.27 minutes and areas of 192.44 and 185.95 mAU•s respectively (**Table 4.6**). This would again indicate that within experimental error of calculating the area under the curve of the HPLC graph, the two peaks have approximately the same area, indicating a racemic sample.

Table 4.6 Chiral HPLC data from cyclopropanation reaction

Retention Time (min)	Area (mAU•s)	Area (%)
13.06	192.44	50.9
18.27	185.95	49.1

The use of chiral iodonium ylide **4.9f** proved to be a successful system for an efficient cyclopropanation reaction which provided Meldrum's acid derived cyclopropane **4.10c** in an isolated yield of 99%. Because optimal conditions were achieved for this reaction, based on the quantitative yield of cyclopropane, the question of chiral aryl iodide recovery was investigated. It was found that upon purification of the reaction mixture using column chromatography, the chiral aryl iodide used to synthesize iodonium ylide **4.9f** was found to be recovered at an isolated yield of 97% providing experimental proof that the reaction is efficient in terms of recovery of the chiral auxiliary.



Scheme 4.34 Efficient cyclopropanation of chiral iodonium ylide using blue LEDs

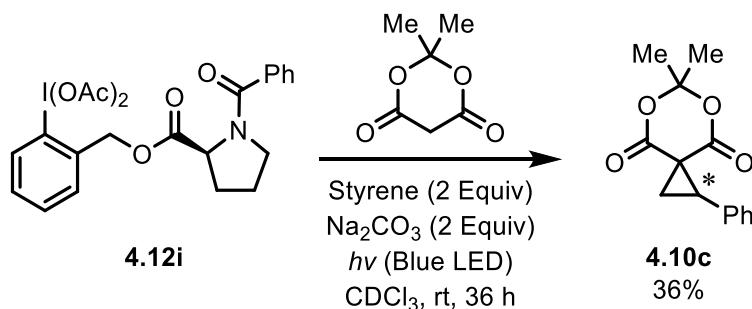
The stereochemistry of the above cyclopropanation reaction was analyzed using chiral HPLC techniques which indicated the product contains two major peaks at 13.25 and 18.58

minutes and areas of 534.26 and 556.30 mAU•s respectively (**Table 4.7**). These results again indicate that, within error, this sample of cyclopropane is racemic.

Table 4.7 Chiral HPLC data from cyclopropanation reaction

Retention Time (min)	Area (mAU•s)	Area (%)
13.25	534.26	43.9
18.58	556.30	45.7

Another extension of this methodology was to react a chiral diacetate with a dicarbonyl motif and an alkene in a one-pot protocol to see if the reaction could be performed using this simplified approach. The use of L-proline derived chiral diacetate **4.12i** were employed in the one-pot cyclopropanation procedure, but only gave Meldrum's acid derived cyclopropane **4.10c** in a 36% yield (**Scheme 4.35**). The low yielding reaction may have been caused by not providing enough time of pre-mixing of the Meldrum's acid with the diacetate. Pre-mixing only occurred for 30 mins prior to applying the blue LED and styrene, and the short time of only 30 mins may not have been long enough to allow for the iodonium ylide to completely form. This demonstrates a limitation to the one-pot procedure in that using a pre-made iodonium ylide ensures complete formation has already taken place and generally leads to higher yields when adding the pure iodonium ylide as a solid.



Scheme 4.35 One-pot procedure for chiral cyclopropane synthesis

Because the cyclopropane yield was relatively low using the one-pot procedure, it was concluded that using the standard procedure of obtaining the chiral iodonium ylide in its purified form first and then adding styrene in the presence of the blue LEDs was the better approach towards a more efficient cyclopropanation reaction.

4.7 Conclusions and Final Discussions

An obvious limitation to the light-induced cyclopropanation reactions were that most of the chemistry was optimized using styrene as the control alkene. This represents problems when it comes to developing enantioselective reactions. The double bond in styrene is relatively simple, as it just contains one phenyl ring which may not provide a big enough preferential for steric attack. As seen in literature examples, disubstituted alkenes were necessary for providing facial selectivity in a chiral environment which was created using chiral environments.²⁹⁷ Perhaps the same could hold true for the systems that were created and tested in the thesis with something along the lines of β -methylstyrene, perhaps both *cis* or *trans* could have been tested if more time was available in addition to other, more bulkier alkenes which may have shown a preference that could have resulted in the observations of non-racemic *ee* values. This may have indicated that this transformation has the potential to be optimized and eventually be useful as a stereoselective reaction. Unfortunately, because of the timing of the world-wide pandemic virus “COVID-19” research in the laboratory was brought to a minimum with restricted access, and therefore only the bare essential final results were obtained with the majority of laboratory research being put on pause until vaccinations have been developed and distributed to the general public.

Chapter 4 provided a new method of producing chiral iodonium ylides that has not been reported in the literature before. The chiral iodonium ylides may be used in the future for reactions other than cyclopropanation. Perhaps these iodonium ylides can be used for reactions such as O-H insertions. Using chiral iodonium ylides may also provide mechanistic interpretations and give insight into insertion reactions. Therefore, to better understand how these chiral iodonium ylides react, having a method to usefully synthesize the iodonium ylides is important and is provided in Chapter 4. Perhaps with the application of visible light from LEDs and the use of chiral iodonium ylides, new reactions will be discovered that were not discussed in this thesis.

4.8 Experimental

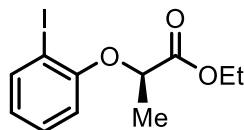
All reactions were carried out in flame-dried glassware under a dry nitrogen atmosphere, unless otherwise noted. All solvents were obtained pure and dry from a JC Meyer solvent purification system. All reagents were purchased from Sigma-Aldrich and used without further purification. ^1H NMR spectra were recorded on Bruker instruments at 300 MHz and were referenced to residual ^1H shift in CDCl_3 (7.24 ppm). All ^{13}C NMR were recorded at 75 MHz and CDCl_3 (77.0 ppm) was used as the internal reference. The following abbreviations were used to explain the multiplicities: s = singlet, d = doublet, t = triplet, q = quartet, br s = broad singlet. Reactions were monitored by thin-layer chromatography (TLC) on commercial silica pre-coated plates with a particle size of 60 Å and viewed by UV lamp (254 nm), by gas chromatography (HP5890A Series II) with a J&W Scientific 30 m x 0.53 mm DB624 column with 3 micron film thickness (run settings: 2.5 min at 75 °C, 7.5 °C/min to 250 °C), and by ^{31}P NMR. Flash chromatography was performed using 60Å (230-400 mesh) silica gel. Melting points were performed using a MeltTemp apparatus. InfraRed (IR) data was recorded using an ATR-FTIR (Attenuated Total Reflection Fourier Transform InfraRed) instrument. The following abbreviations were used to explain the IR peak intensities: (s) = strong, (m) = medium, (w) = weak. Positive ion electrospray ionization (ESI) was performed with a Thermo Scientific Q-Exactive hybrid mass spectrometer. Accurate mass determinations were performed at a mass resolution of 70,000. For ESI, samples were infused at 10 $\mu\text{L}/\text{min}$ in 1:1 MeOH/ H_2O + 0.1% formic acid.

4.8.1 General Procedure 1 (GP1) - Synthesis of Chiral Aryl Iodides

In a dry round-bottom flask, aryl iodide (3.4 mmol, 1 equiv), L-(+)-benzyl lactate (7.5 mmol, 2.2 equiv) and Ph_3P (8.5 mmol, 2.5 equiv) was dissolved in THF (25 ml, 0.14 M) and stirred at room temperature until fully dissolved (~5 min). The mixture was then cooled to 0 °C using an ice bath and DIAD (8.5 mmol, 2.5 equiv) was added dropwise over the course of 20 min. The ice bath was removed, and the mixture was allowed to reach room temp while stirring under an atmosphere of nitrogen until the reaction was observed to be complete by TLC or NMR

analysis. The mixture was then evaporated to dryness and purified by column chromatography, eluting with mixtures of ethyl acetate and hexanes.

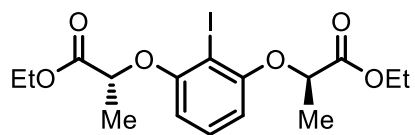
(S)-Ethyl 2-(2-iodophenoxy)propanoate (4.11d)



Aryl iodide **4.11d** was prepared according to **GP1** from 2-iodophenol (2.20 g, 10 mmol, 1 equiv), (S)-ethyl lactate (1.72 mL, 15 mmol, 1.5 equiv), Ph₃P (3.93 g, 15 mmol, 1.5 equiv), DIAD (2.94 mL, 15 mmol, 1.5 equiv), THF (10 mL). The reaction was stirred for 22 h at 25 °C until the SM aryl iodide was consumed as indicated by TLC. Purification by flash chromatography through a column of silica gel (hexanes:EtOAc 20:1 to 10:1) led to the title compound isolated as a colourless oil (2.30 g, 72% yield). R_f = 0.50 (hexanes:EtOAc 3:1). The characterization data matches what has already been reported in the literature.³¹¹

¹H NMR (300 MHz, CDCl₃): δ 7.78 (dd, *J* = 7.7 Hz, 1.5 Hz, 1H), 7.24 (ddd, *J* = 8.2 Hz, 6.5 Hz, 1.6 Hz, 1H), 6.75-6.69 (m, 2H), 4.74 (q, *J* = 6.8 Hz, 1H), 4.27 (q, *J* = 7.1 Hz, 2H), 1.69 (d, *J* = 6.8 Hz, 3H), 1.24 (t, *J* = 7.1 Hz, 3H).

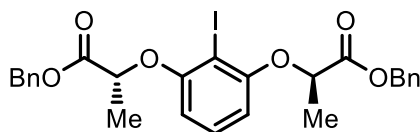
(2R,2'R)-Diethyl 2,2'-((2-iodo-1,3-phenylene)bis(oxy))dipropanoate (4.11f)



Aryl iodide **4.11f** was prepared according to **GP1** from 2-iodobenzene-1,3-diol (1.18 g, 5 mmol, 1 equiv), (S)-ethyl lactate (1.30 mL, 11 mmol, 2.2 equiv), Ph₃P (2.9 g, 11 mmol, 2.2 equiv), DIAD (2.15 mL, 11 mmol, 2.2 equiv), THF (35 mL). The reaction was stirred for 12 h at 25 °C until the SM aryl iodide was consumed as indicated by TLC. Purification by flash chromatography through a column of silica gel (hexanes:EtOAc 20:1 to 10:1) led to the title compound isolated as a colourless oil (2.13 g, 98% yield). R_f = 0.49 (hexanes:EtOAc 3:1). The characterization data matches what has already been reported in the literature.³⁰⁰

$^1\text{H NMR}$ (300 MHz, CDCl_3): δ 7.11 (app t, $J = 8.2$ Hz, 1H), 6.35 (app d, $J = 8.3$ Hz, 2H), 4.72 (q, $J = 6.8$ Hz, 2H), 4.15-4.22 (m, 4H), 1.67 (d, $J = 6.8$ Hz, 6H), 1.22 (t, $J = 7.2$ Hz, 6H).

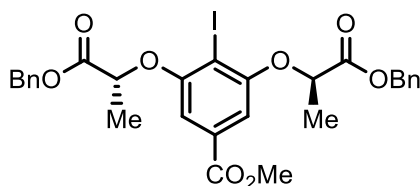
Dibenzyl 2,2'-((2-iodo-1,3-phenylene)bis(oxy))(2R,2'R)-dipropionate (4.11g)



Aryl iodide **4.11g** was prepared according to **GP1** from 2-iodobenzene-1,3-diol (1.18 g, 5 mmol, 1 equiv), benzyl (S)-2-hydroxy-3-phenylpropanoate (1.98 g, 11 mmol, 2.2 equiv), Ph_3P (2.9 g, 11 mmol, 2.2 equiv), DIAD (2.15 mL, 11 mmol, 2.2 equiv), THF (35 mL). The reaction was stirred for 12 h at 25 °C until the SM aryl iodide was consumed as indicated by TLC. Purification by flash chromatography through a column of silica gel (hexanes:EtOAc 20:1 to 10:1) led to the title compound isolated as a colourless oil (2.18 g, 78% yield). $R_f = 0.46$ (hexanes:EtOAc 3:1). The characterization data matches what has already been reported in the literature.³¹²

$^1\text{H NMR}$ (300 MHz, CDCl_3): δ 7.37-7.29 (m, 10H), 7.03 (t, $J = 8.5$ Hz, 1H), 6.34 (d, $J = 8.5$ Hz, 2H), 5.24 (d, $J = 12.5$ Hz, 2H), 5.18 (d, $J = 12.5$ Hz, 2H), 4.82 (q, $J = 6.5$ Hz, 2H), 1.73 (d, $J = 6.5$ Hz, 6H).

(2R,2'R)-Dibenzyl 2,2'-((2-iodo-5-(methoxycarbonyl)-1,3-phenylene)bis(oxy))dipropionate (4.11h)



Aryl iodide **4.11h** was prepared according to **GP1** from methyl 3,5-dihydroxy-4-iodobenzoate (1.00 g, 3.4 mmol, 1 equiv), L-(+)-benzyl lactate (1.35 g, 7.5 mmol, 2.2 equiv), Ph_3P (2.20 g, 8.5 mmol, 2.5 equiv), DIAD (1.67 mL, 8.5 mmol, 2.5 equiv), THF (25 mL). The reaction was stirred for 13 h at 25 °C until the SM aryl iodide was consumed as indicated by TLC. Purification by

flash chromatography through a column of silica gel (hexanes:EtOAc 20:1 to 10:1) led to the title compound isolated as a colourless oil (0.724 g, 34% yield). $R_f = 0.35$ (hexanes:EtOAc 3:1).

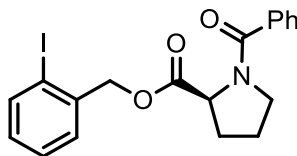
$^1\text{H NMR}$ (300 MHz, CDCl_3): δ 7.24-7.30 (m, 10H), 6.98 (s, 2H), 5.21 (d, $J = 12.4$ Hz, 2H), 5.15 (d, $J = 12.4$ Hz, 2H), 4.91 (q, $J = 6.7$ Hz, 2H), 3.81 (s, 3H), 1.72 (d, $J = 6.7$ Hz, 6H).

$^{13}\text{C NMR}$ (75 MHz, CDCl_3): δ 173.9, 168.8, 161.0, 138.1, 134.5, 131.4, 131.3, 131.1, 110.0, 90.0, 76.9, 69.9, 55.3, 21.3.

HRMS (ESI): Calculated for $\text{C}_{28}\text{H}_{28}\text{IO}_8$ ($\text{M}+\text{H}$) $^+$ 619.0829, found 619.0827.

IR (ATR): 2983 (w), 1726 (s), 1235 (s), 1091 (s) cm^{-1} .

(S)-2-Iodobenzyl 1-benzoylpyrrolidine-2-carboxylate (**4.11i**)



Aryl iodide **4.11i** was prepared according to **GP1** from (2-iodophenyl)methanol (1.00 g, 4.3 mmol, 1 equiv), (S)-1-benzoylpyrrolidine-2-carboxylic acid (0.94 g, 4.3 mmol, 1.0 equiv), Ph_3P (1.70 g, 6.5 mmol, 1.5 equiv), DIAD (1.30 mL, 6.5 mmol, 1.5 equiv), THF (25 mL). The reaction was stirred for 16 h at 25 °C until the SM aryl iodide was consumed as indicated by TLC. Purification by flash chromatography through a column of silica gel (hexanes:EtOAc 20:1 to 2:1) led to the title compound isolated as a colourless oil (1.239 g, 81% yield). $R_f = 0.15$ (hexanes:EtOAc 3:1).

Title compound isolated as a mixture of rotomers, with major rotomer being reported below.

$^1\text{H NMR}$ (300 MHz, CDCl_3): δ 7.84 (app d, $J = 7.9$ Hz, 1H), 7.52-7.55 (m, 2H), 7.30-7.46 (m, 5H), 6.99-7.04 (m, 1H), 5.25 (d, $J = 13.0$ Hz, 1H), 5.19 (d, $J = 13.0$ Hz, 1H), 4.74-4.78 (m, 1H), 3.61-3.69 (m, 1H), 3.49-3.56 (m, 1H), 1.84-2.16 (m, 4H).

$^{13}\text{C NMR}$ (75 MHz, CDCl_3): δ 171.7, 169.7, 139.4, 138.1, 136.2, 130.2, 129.9, 129.9, 129.6, 128.5, 128.2, 127.2, 98.2, 70.6, 59.2, 49.9, 29.4, 25.4.

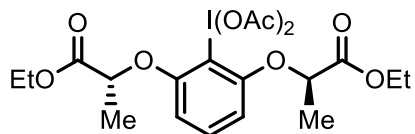
HRMS (ESI): Calculated for $\text{C}_{19}\text{H}_{19}\text{INO}_3$ ($\text{M}+\text{H}$) $^+$ 436.0409, found 436.0404.

IR (ATR): 2978 (w), 1745 (s), 1631 (s), 1411 (s), 1169 (s) cm^{-1} .

4.8.2 General Procedure 2 (GP2) - Synthesis of Chiral Diacetates

In a dry round-bottom flask, aryl iodide (0.1 mmol, 1 equiv), was dissolved in MeCN (4 mL) and AcOH (1 ml) and stirred at room temperature until fully dissolved (1 min). To this mixture was then added SelectfluorTM (0.5 mmol, 5 equiv) in three portions over 2 min. This mixture was stirred at room temp under an atmosphere of nitrogen until the reaction was observed to be complete, by consumption of aryl iodide according to TLC analysis, typically 8 - 12 hours. The mixture was then evaporated to half the original volume and water (50 mL) and CH₂Cl₂ (50 mL) added. The mixture was transferred to a separatory funnel and the two layers were separated. The aqueous layer was extracted with CH₂Cl₂ (2 x 50 mL). The combined organic layers were washed with brine (2 x 25 mL) then dried over MgSO₄, filtered, and evaporated to dryness with a rotary evaporator. More CH₂Cl₂ (10 mL) was added and again evaporated to dryness with a rotary evaporator to fully dry the product. The residue (often yellow) was suspended in CH₂Cl₂ (5 mL) and added to stirred Et₂O (25 mL) followed by cooling in a refrigerator for 15 min. Filtration gave a white powder which was air dried until a constant weight was observed.

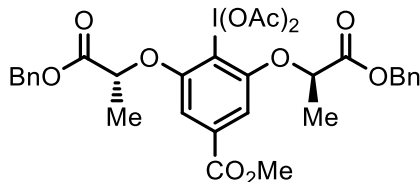
(2R,2'R)-Diethyl 2,2'-((2-iodo-1,3-phenylene)bis(oxy))dipropanoate Diacetate (4.12f)



Diacetate **4.12f** was prepared according to **GP2** from chiral aryl iodide **4.11f** (0.436 g, 1.0 mmol, 1 equiv), SelectfluorTM (1.70 g, 5.0 mmol, 5.0 equiv) in MeCN:AcOH (4:1) 42 mL. The reaction was stirred for 12 h at 25 °C until the SM aryl iodide was consumed as indicated by TLC. Purification by dissolving in CH₂Cl₂ followed by aqueous washing and filtering until a white powder was observed after concentration, which led to the title compound (0.544 g, 98% yield). The characterization data matches what has already been reported in the literature.³¹³

¹H NMR (300 MHz, CDCl₃): δ 7.38 (app t, *J* = 8.4 Hz, 1H), 6.56 (app d, *J* = 8.4 Hz, 2H), 4.83 (q, *J* = 6.8 Hz, 2H), 4.20 (q, *J* = 7.2 Hz, 4H), 1.96 (s, 6H), 1.66 (d, *J* = 6.8 Hz, 6H), 1.27 (t, *J* = 7.2 Hz, 6H).

**Dibenzyl 2,2'-((2-(diacetoxy-1,3-iodaneryl)-5-(methoxycarbonyl)-1,3-phenylene)bis(oxy))
(2R,2'R)-dipropionate (4.12h)**



Diacetate **4.12h** was prepared according to **GP2** from chiral aryl iodide **4.11h** (0.620 g, 1.0 mmol, 1 equiv), SelectfluorTM (1.77 g, 5.0 mmol, 5.0 equiv) in MeCN:AcOH (4:1) 50 mL. The reaction was stirred for 17 h at 25 °C until the SM aryl iodide was consumed as indicated by TLC. Purification by dissolving in CH₂Cl₂ followed by aqueous washing and filtering until a white powder was observed after concentration, which led to the title compound (0.692 g, 94% yield).

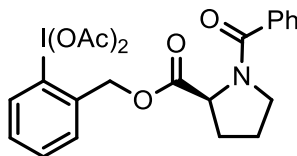
¹H NMR (300 MHz, CDCl₃): δ 7.29-7.30 (m, 10H), 7.16 (s, 2H), 5.18-5.19 (m, 4H), 4.97 (q, *J* = 6.8 Hz, 2H), 3.83 (s, 3H), 1.91 (s, 6H), 1.70 (d, *J* = 6.8 Hz, 6H).

¹³C NMR (75 MHz, CDCl₃): δ 176.5, 171.0, 158.1, 135.2, 133.8, 131.6, 130.2, 128.5, 128.4, 128.2, 107.1, 74.0, 67.1, 52.4, 20.6, 18.4.

HRMS (ESI): Calculated for C₃₂H₃₄IO₁₂ (M+H)⁺ 737.1095, found 737.1098.

IR (ATR): 2988 (w), 1750 (m), 1725 (s), 1422 (m), 1243 (s), 1129 (s), 667 (m) cm⁻¹.

(2-(((benzoyl-L-prolyl)oxy)methyl)phenyl)-λ³-iodanediyl diacetate (4.12i)



Diacetate **4.12i** was prepared according to **GP2** from chiral aryl iodide **4.11i** (0.880 g, 2.0 mmol, 1 equiv), SelectfluorTM (3.60 g, 10.0 mmol, 5 equiv), in MeCN:AcOH (4:1) 12.5 mL. The reaction was stirred for 16 h at 25 °C until the SM aryl iodide was consumed as indicated by TLC. Purification by dissolving in CH₂Cl₂ followed by aqueous washing and filtering until a white powder was observed after concentration, which led to the title compound (1.039 g, 94% yield).

Title compound isolated as a mixture of rotomers, with major rotomer being reported below.

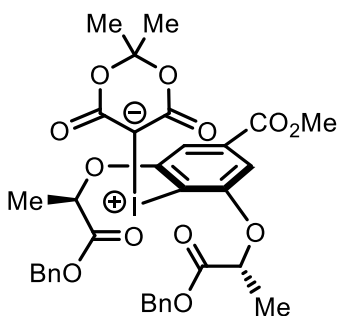
¹H NMR (300 MHz, CDCl₃): δ 7.94 (d, *J* = 8.4 Hz, 1H), 7.36-7.50 (m, 8H), 5.45 (d, *J* = 12.6 Hz, 1H), 5.39 (d, *J* = 12.6 Hz, 1H), 4.56-4.60 (m, 1H), 3.45-3.65 (m, 2H), 1.87-2.34 (m, 4H), 1.69 (s, 6H).

¹³C NMR (75 MHz, CDCl₃): δ 174.8, 172.7, 166.8, 138.8, 138.1, 136.8, 135.1, 134.8, 134.6, 133.5, 131.3, 130.2, 121.5, 107.3, 76.5, 71.5, 62.3, 53.9, 32.1, 28.8, 28.5.

HRMS (ESI): Calculated for C₂₅H₂₅INO₇ (M+H)⁺ 578.0676, found 578.0675.

IR (ATR): 2988 (w), 1745 (w), 1627 (s), 1282 (s), 752 (m) cm⁻¹.

Dibenzyl 2,2'-((2-((2,2-dimethyl-4,6-dioxo-1,3-dioxan-5-ylidene)-λ³-iodaneyl)-5-(methoxycarbonyl)-1,3-phenylene)bis(oxy))(2R,2'R)-dipropionate (4.9f)



Iodonium ylide **4.9f** was prepared according to **GP3** from 2,2-dimethyl-1,3-dioxane-4,6-dione (0.020 g, 0.14 mmol, 1 equiv) and chiral diacetate **4.12h** (0.100 g, 0.14 mmol, 1 equiv) in 10% Na₂CO₃/EtOH (4 mL) and HFIP (0.5 mL) for 1.5 h at room temperature. Purification by trituration (CH₂Cl₂:Et₂O 1:10) led to the title compound isolated as a white solid (0.101 g, 95% yield).

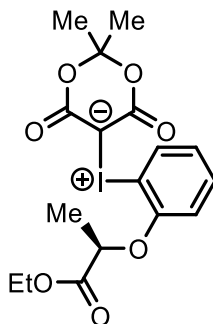
¹H NMR (300 MHz, CDCl₃): δ 7.24-7.26 (m, 10H), 6.98 (s, 2H), 5.20 (d, *J* = 12.0 Hz, 2H), 5.06 (d, *J* = 12.0 Hz, 2H), 4.94 (q, *J* = 6.8 Hz, 2H), 3.80 (s, 3H), 1.78 (d, *J* = 6.8 Hz, 6H), 1.63 (s, 6H).

¹³C NMR (75 MHz, CDCl₃): δ 173.3, 166.2, 160.4, 138.8, 137.8, 131.4, 111.1, 107.0, 102.5, 77.9, 70.3, 55.7, 28.9, 21.1.

HRMS (ESI): Calculated for C₃₄H₃₄IO₁₂ (M+H)⁺ 761.1095, found 761.1098.

IR (ATR): 2971 (w), 1742 (s), 1630 (m), 1217 (m), 768 (w) cm⁻¹.

Ethyl (R)-2-(2-((2,2-dimethyl-4,6-dioxo-1,3-dioxan-5-ylidene)- λ^3 -iodaneyl)phenoxy)propanoate (4.9g)



Iodonium ylide **4.9g** was prepared according to **GP3** from 2,2-dimethyl-1,3-dioxane-4,6-dione (0.069 g, 0.48 mmol, 1 equiv) and chiral diacetate **4.12d** (0.210 g, 0.48 mmol, 1 equiv) in CH_2Cl_2 (10 mL) for 1.5 h at room temperature. Purification by trituration (CH_2Cl_2 : Et_2O 1:10) led to the title compound isolated as a white solid (0.177 g, 80% yield).

^1H NMR (300 MHz, CDCl_3): δ 7.40-7.43 (m, 2H), 7.09-7.14 (m, 1H), 6.87-6.90 (m, 1H), 4.86 (q, $J = 6.6$ Hz, 1H), 4.21 (q, $J = 7.2$, 2H), 1.78 (s, 6H), 1.70 (d, $J = 6.0$ Hz, 3H), 1.24 (d, $J = 7.2$ Hz, 3H).

^{13}C NMR (75 MHz, CDCl_3): δ 173.5, 166.7, 156.6, 135.5, 132.4, 128.6, 117.9, 107.5, 104.8, 78.2, 65.0, 51.2, 28.9, 21.3, 17.0.

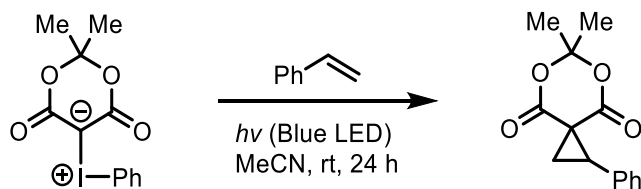
HRMS (ESI): Calculated for $\text{C}_{17}\text{H}_{20}\text{IO}_7$ ($\text{M}+\text{H}$) $^+$ 463.0254, found 463.0256.

IR (ATR): 2981 (w), 1732 (s), 1233 (m), 745 (m) cm^{-1} .

4.8.4 General Procedure 4 (GP4) - Synthesis of a Standard Racemic Cyclopropane

In a dry 1 dram (4 mL) vial, iodonium ylide (0.1 mmol, 1 equiv) was dissolved in MeCN (1.0 mL, 0.1 M) and stirred at room temperature until fully dissolved (~2 min). Styrene (0.023 mL, 0.2 mmol, 2 equiv) was added in one portion and stirred for an additional 1 min. The mixture was then subjected to blue LED light using photoreactor #4 and stirred at room temperature (25 °C) until the reaction was observed to be complete by TLC or NMR analysis. The mixture was then evaporated to dryness and purified by column chromatography, eluting with mixtures of ethyl acetate and hexanes.

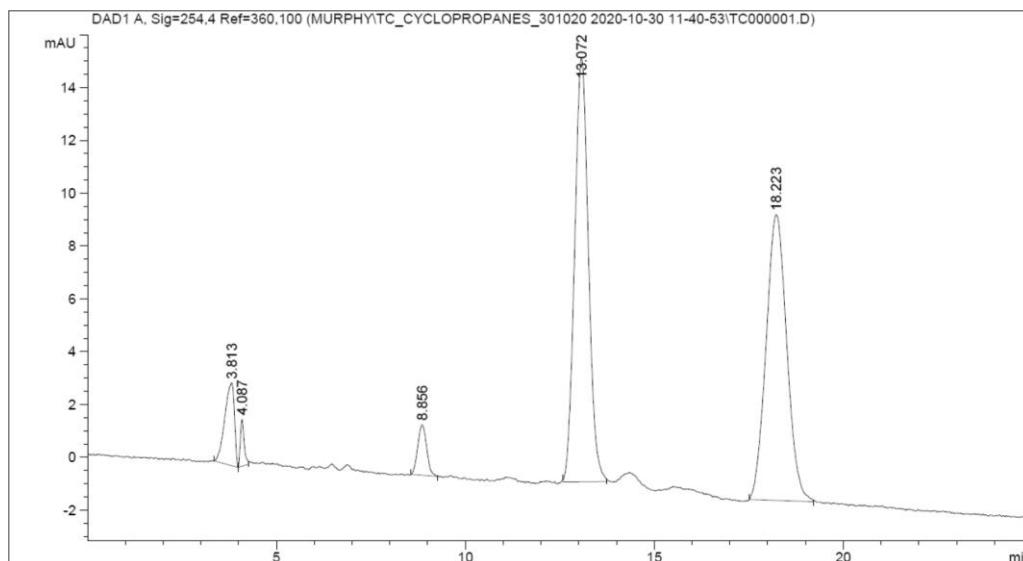
6,6-Dimethyl-1-phenyl-5,7-dioxaspiro[2.5]octane-4,8-dione (4.10c)



Synthesized according to **GP4** using iodonium ylide **3.16j** (0.035 g, 0.10 mmol, 1.0 equiv), styrene (0.023 mL, 0.20 mmol, 2.0 equiv), MeCN (1.0 mL). The reaction was stirred for 24 h at room temperature until the ylide was consumed as indicated by NMR. Purification by flash chromatography through a column of silica gel (hexanes:EtOAc 8:1) led to the title compound isolated as a white solid (0.024 g, 96% yield). $R_f = 0.38$ (hexanes:EtOAc 3:1). The characterization data matches what has already been reported in the literature.²⁶⁸

¹H NMR (300 MHz, CDCl₃): δ 7.33 (broad s, 5H), 3.44 (dd, $J = 9.4, 9.4$ Hz, 1H), 2.68 (dd, $J = 9.4, 4.8$ Hz, 1H), 2.53 (dd, $J = 9.4, 4.8$ Hz, 1H), 1.72 (s, 6H).

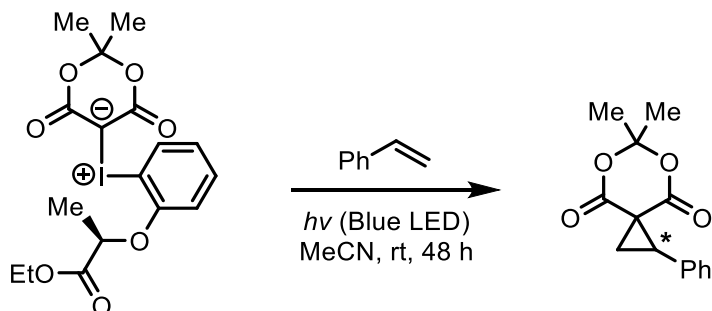
HPLC (Chiralcel OD-H): Hexane:*i*PrOH (90:10), flow rate: 0.75 mL/min.



Retention Time (min)	Area (mAU·s)	Area (%)
13.07	407.36	44.4
18.22	411.81	44.9

4.8.5 Synthesis of Chiral Cyclopropanes

6,6-Dimethyl-1-phenyl-5,7-dioxaspiro[2.5]octane-4,8-dione (4.10c)

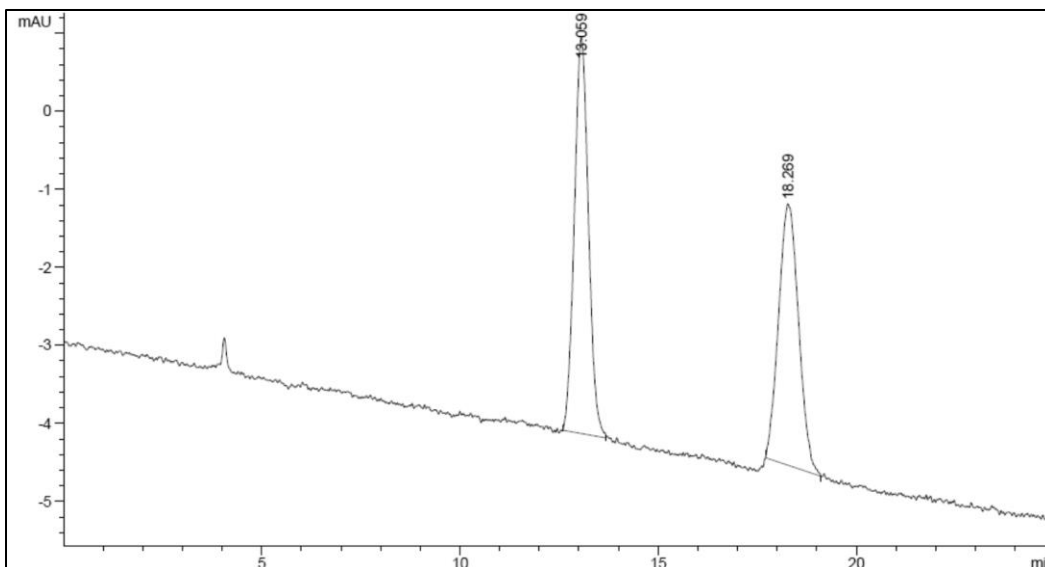


Synthesized according to **GP4** using iodonium ylide **4.9g** (0.046 g, 0.10 mmol, 1 equiv), styrene (0.023 mL, 0.20 mmol, 2 equiv), MeCN (1.0 mL). The reaction was stirred for 48 h at room temperature until the ylide was consumed as indicated by TLC or NMR. Purification by flash chromatography through a column of silica gel (hexanes:EtOAc 20:1 to 15:1) led to the title compound isolated as a white solid (0.017 g, 69% yield). $R_f = 0.38$ (hexanes:EtOAc 3:1). The characterization data matches what has already been reported in the literature.²⁶⁸

¹H NMR (300 MHz, CDCl₃): δ 7.33 (broad s, 5H), 3.44 (dd, $J = 9.4, 9.4$ Hz, 1H), 2.68 (dd, $J = 9.4, 4.8$ Hz, 1H), 2.53 (dd, $J = 9.4, 4.8$ Hz, 1H), 1.72 (s, 6H).

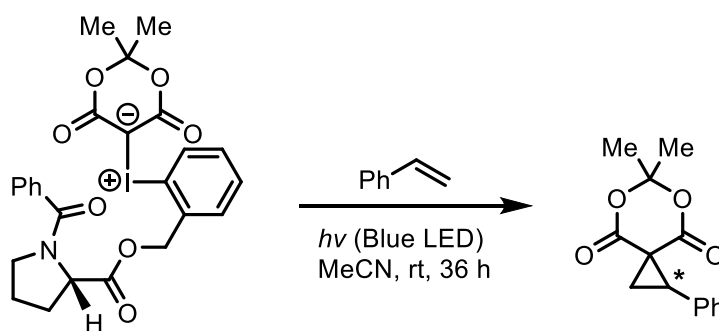
Polarimeter: $[\alpha]_D^{22} = -1.17$ (c 0.0006, CHCl₃)

HPLC (Chiralcel OD-H): Hexane:*i*PrOH (90:10), flow rate: 0.75 mL/min.



Retention Time (min)	Area (mAU•s)	Area (%)
13.06	125.47	51.7
18.27	117.41	48.3

6,6-Dimethyl-1-phenyl-5,7-dioxaspiro[2.5]octane-4,8-dione (4.10c)

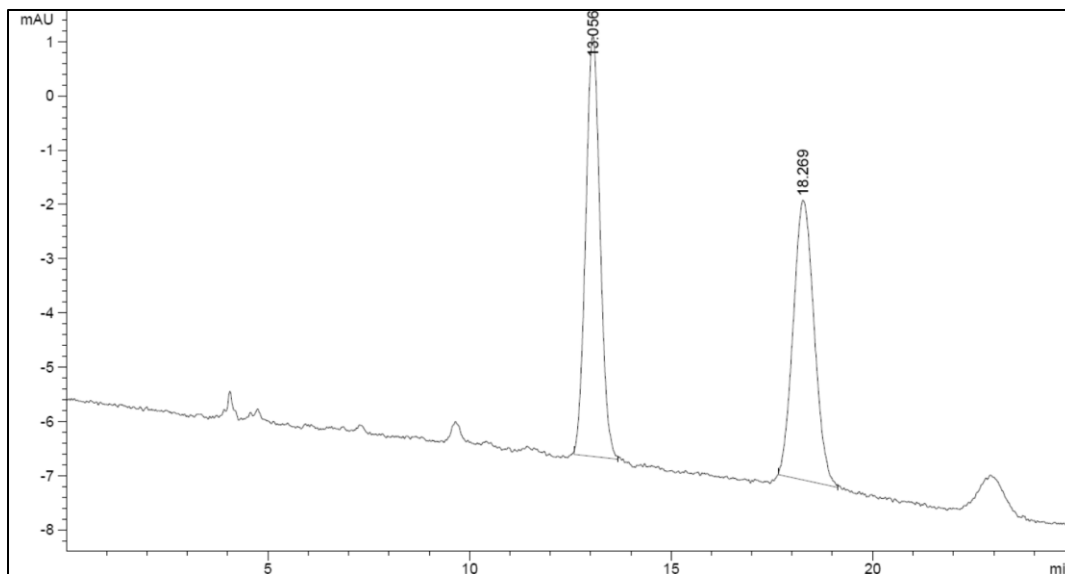


Synthesized according to **GP4** using iodonium ylide **4.9c** (0.029 g, 0.05 mmol, 1 equiv), styrene (0.011 mL, 0.10 mmol, 2 equiv), MeCN (0.5 mL). The reaction was stirred for 36 h at room temperature until the ylide was consumed as indicated by TLC or NMR. Purification by flash chromatography through a column of silica gel (hexanes:EtOAc 20:1 to 15:1) led to the title compound isolated as a white solid (0.011 g, 89% yield). $R_f = 0.38$ (hexanes:EtOAc 3:1). The characterization data matches what has already been reported in the literature.²⁶⁸

$^1\text{H NMR}$ (300 MHz, CDCl_3): δ 7.33 (broad s, 5H), 3.44 (dd, $J = 9.4, 9.4$ Hz, 1H), 2.68 (dd, $J = 9.4, 4.8$ Hz, 1H), 2.53 (dd, $J = 9.4, 4.8$ Hz, 1H), 1.72 (s, 6H).

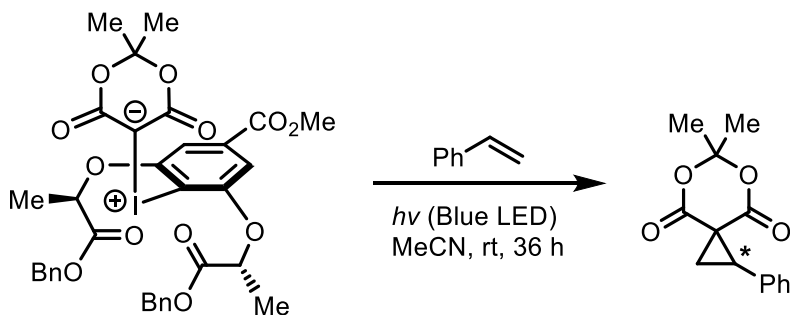
Polarimeter: $[\alpha]_{\text{D}}^{22} = -1.37$ (c 0.0006, CHCl_3)

HPLC (Chiralcel OD-H): Hexane:*i*PrOH (90:10), flow rate: 0.75 mL/min.



Retention Time (min)	Area (mAU*s)	Area (%)
13.06	192.44	50.9
18.27	185.95	49.1

6,6-Dimethyl-1-phenyl-5,7-dioxaspiro[2.5]octane-4,8-dione (4.10c)



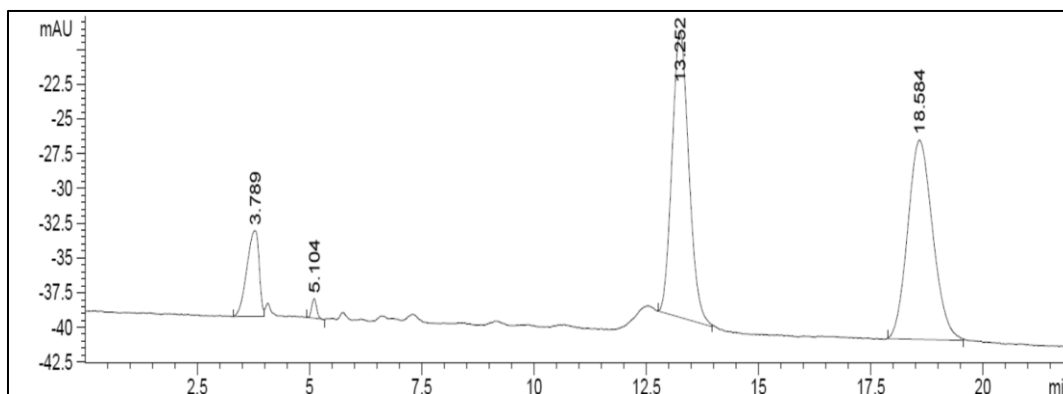
Synthesized according to **GP4** using iodonium ylide **4.9f** (0.034g, 0.045 mmol, 1 equiv), styrene (0.010 mL, 0.09 mmol, 2 equiv), MeCN (1.0 mL). The reaction was stirred for 36 h at room

temperature until the ylide was consumed as indicated by TLC or NMR. Purification by flash chromatography through a column of silica gel (hexanes:EtOAc 20:1 to 15:1) led to the title compound isolated as a white solid (0.011 g, 99% yield). $R_f = 0.38$ (hexanes:EtOAc 3:1). The characterization data matches what has already been reported in the literature.²⁶⁸

^1H NMR (300 MHz, CDCl_3): δ 7.33 (broad s, 5H), 3.44 (dd, $J = 9.4, 9.4$ Hz, 1H), 2.68 (dd, $J = 9.4, 4.8$ Hz, 1H), 2.53 (dd, $J = 9.4, 4.8$ Hz, 1H), 1.72 (s, 6H).

Polarimeter: $[\alpha]_D^{22} = 2.20$ (c 0.0006, CHCl_3)

HPLC (Chiralcel OD-H): Hexane: i PrOH (90:10), flow rate: 0.75 mL/min.



Retention Time (min)	Area (mAU*s)	Area (%)
13.25	534.26	43.9
18.58	556.30	45.7

4.9 NMR Spectra for Chapter 4

Figure 4.17 ^1H NMR (300 MHz, CDCl_3) spectrum of (2R,2'R)-dibenzyl 2,2'-((2-iodo-5-(methoxycarbonyl)-1,3-phenylene)bis(oxy))dipropanoate

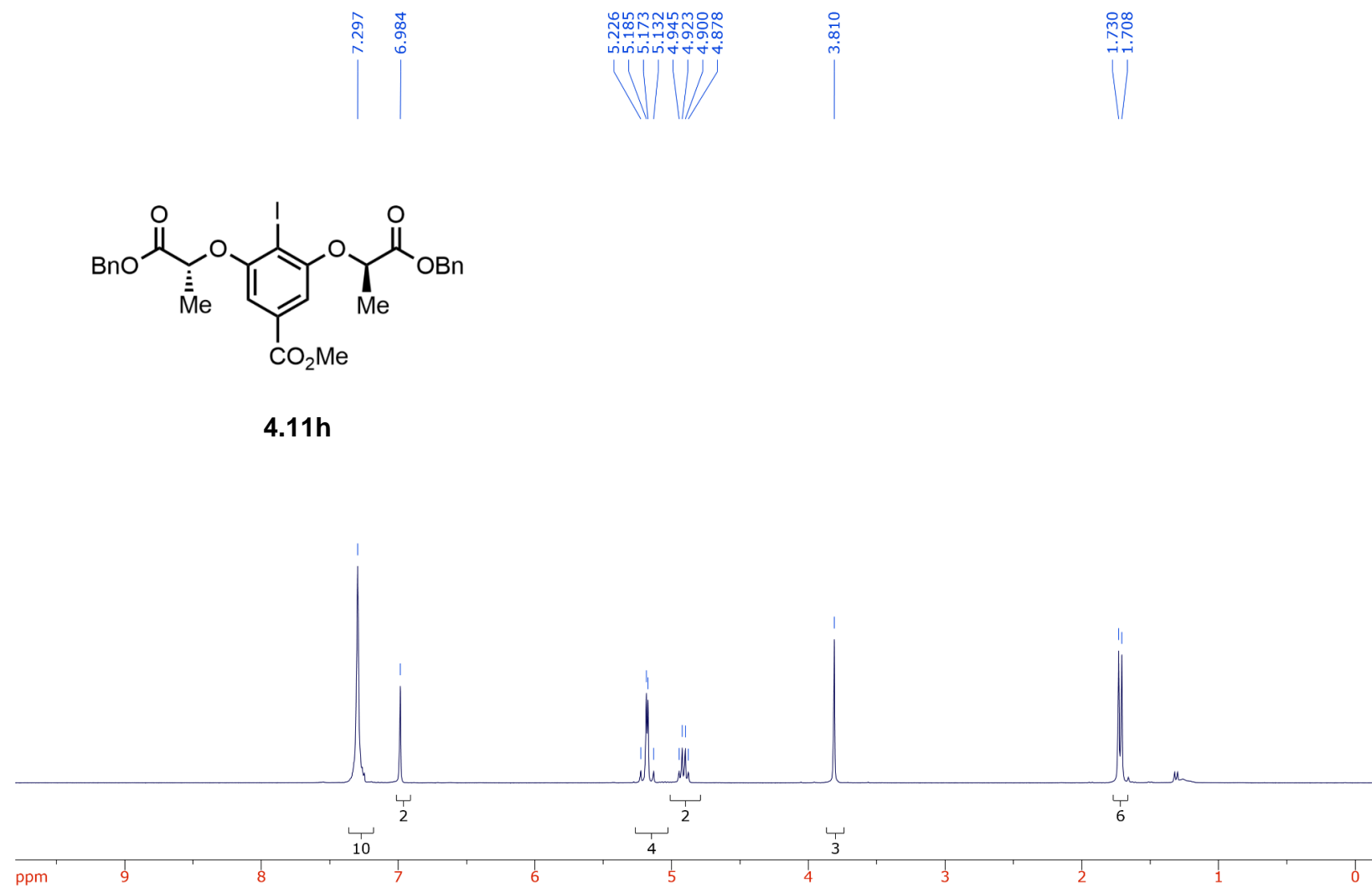


Figure 4.18 ^{13}C NMR (75 MHz, CDCl_3) spectrum of (2R,2'R)-dibenzyl 2,2'-((2-iodo-5-(methoxycarbonyl)-1,3-phenylene)bis(oxy))dipropanoate

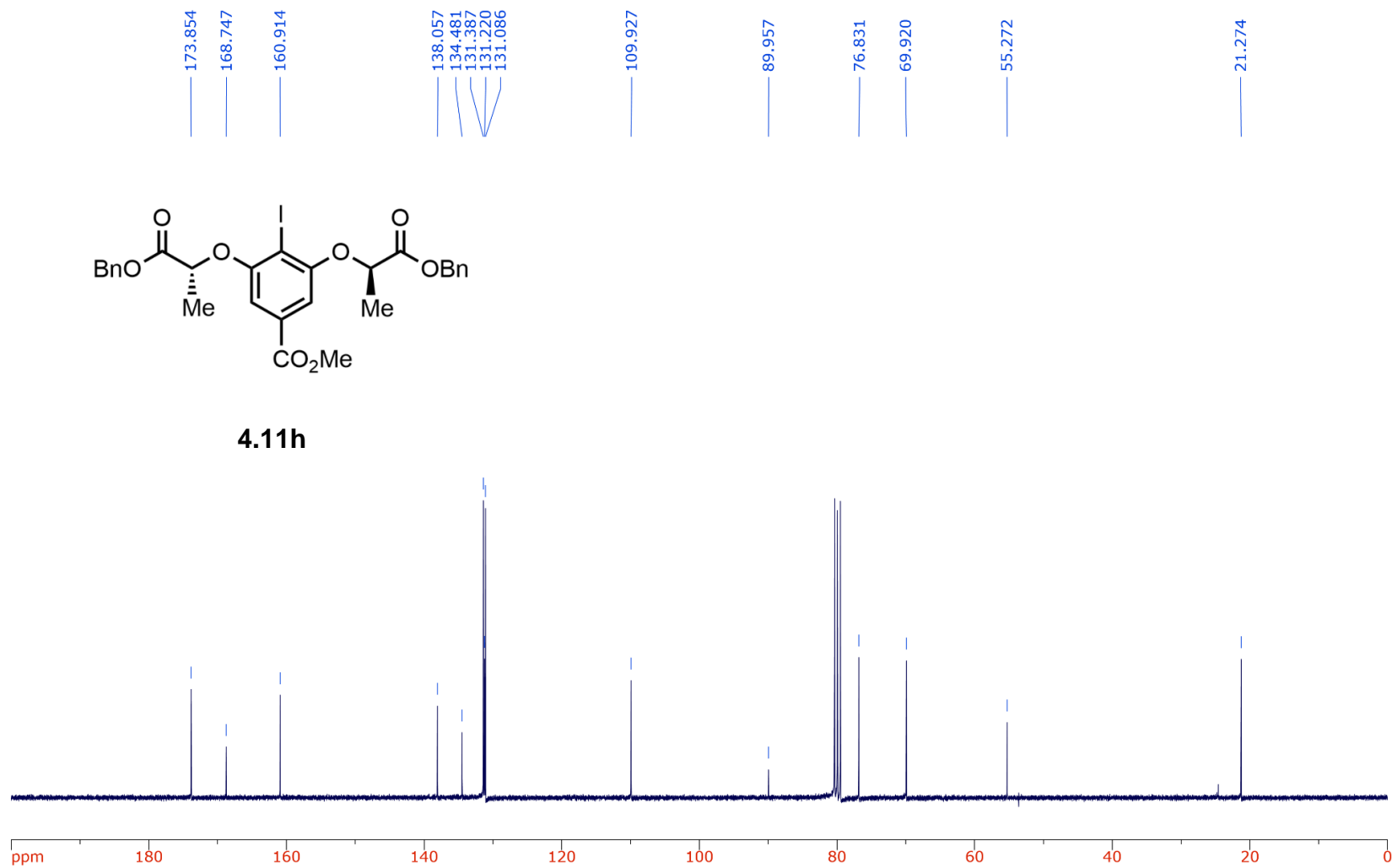


Figure 4.19 ^1H NMR (300 MHz, CDCl_3) spectrum of (S)-2-iodobenzyl 1-benzoylpyrrolidine-2-carboxylate

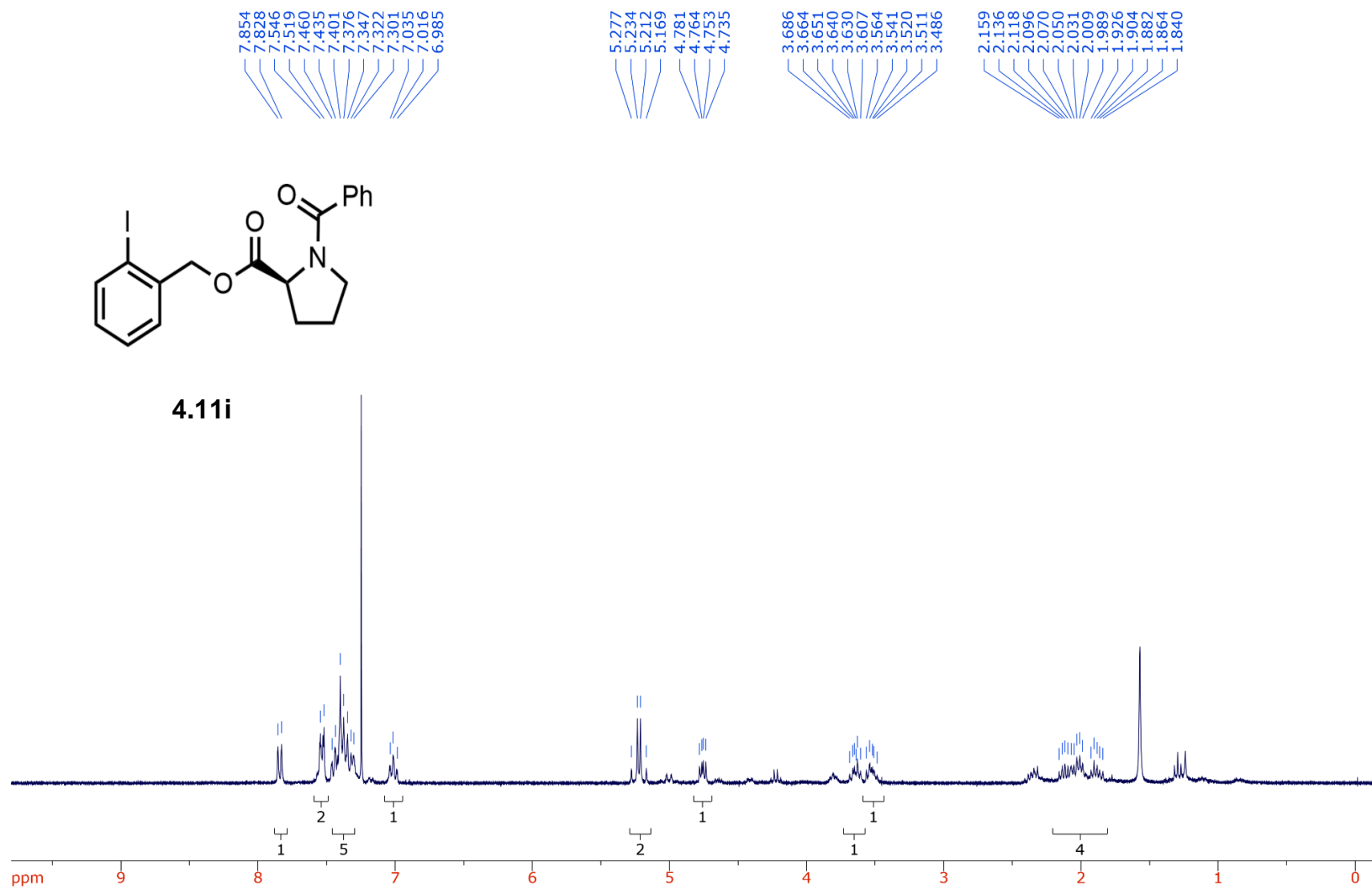


Figure 4.20 ^{13}C NMR (75 MHz, CDCl_3) spectrum of (S)-2-iodobenzyl 1-benzoylpyrrolidine-2-carboxylate

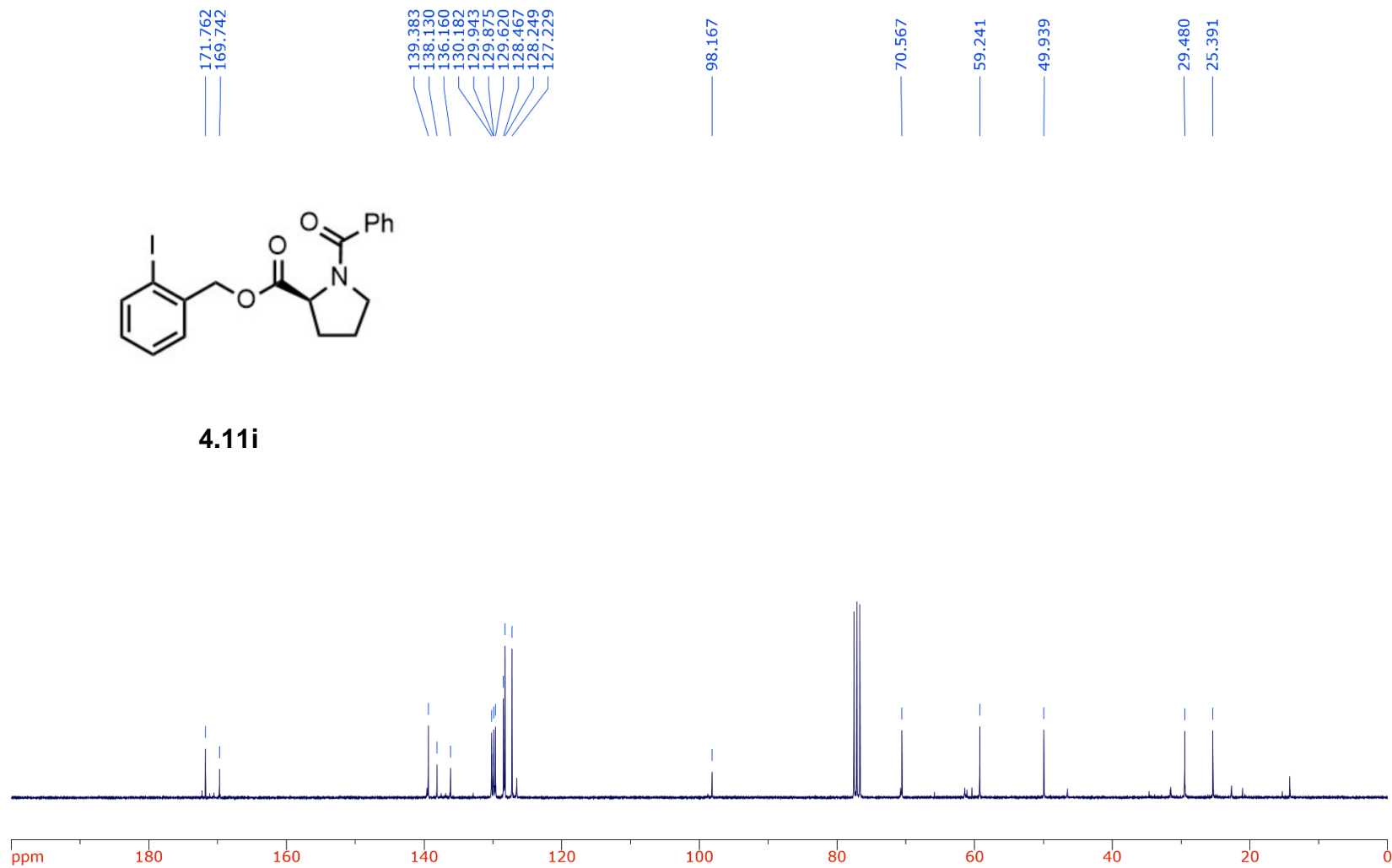


Figure 4.21 ^1H NMR (300 MHz, CDCl_3) spectrum of dibenzyl 2,2'-((2-(diacetoxy-13-iodaneryl)-5-(methoxycarbonyl)-1,3-phenylene)bis(oxy)) (2R,2'R)-dipropionate

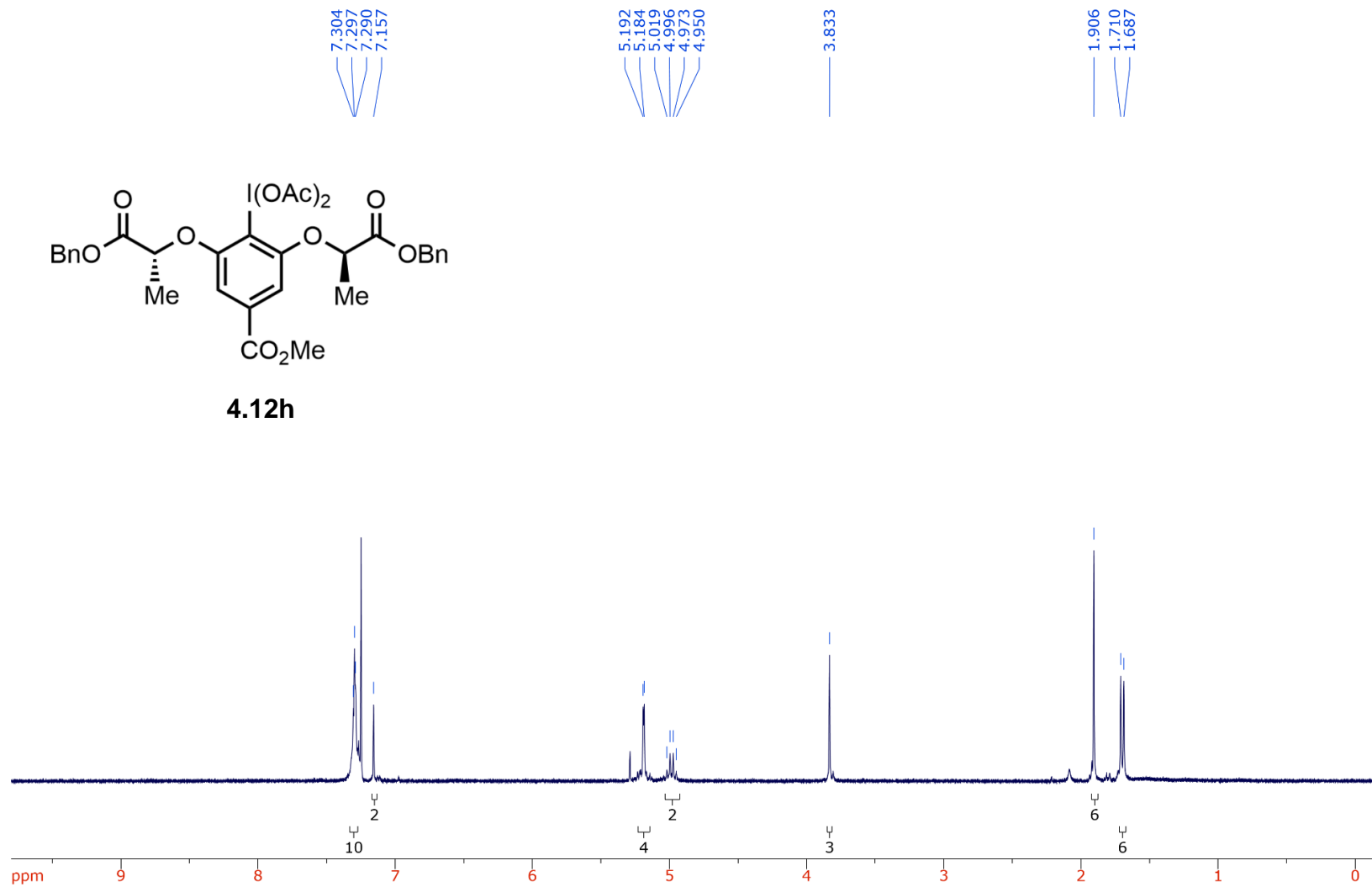


Figure 4.22 ^{13}C NMR (75 MHz, CDCl_3) spectrum of dibenzyl 2,2'-((2-(diacetoxy-13-iodaneryl)-5-(methoxycarbonyl)-1,3-phenylene)bis(oxy)) (2R,2'R)-dipropionate

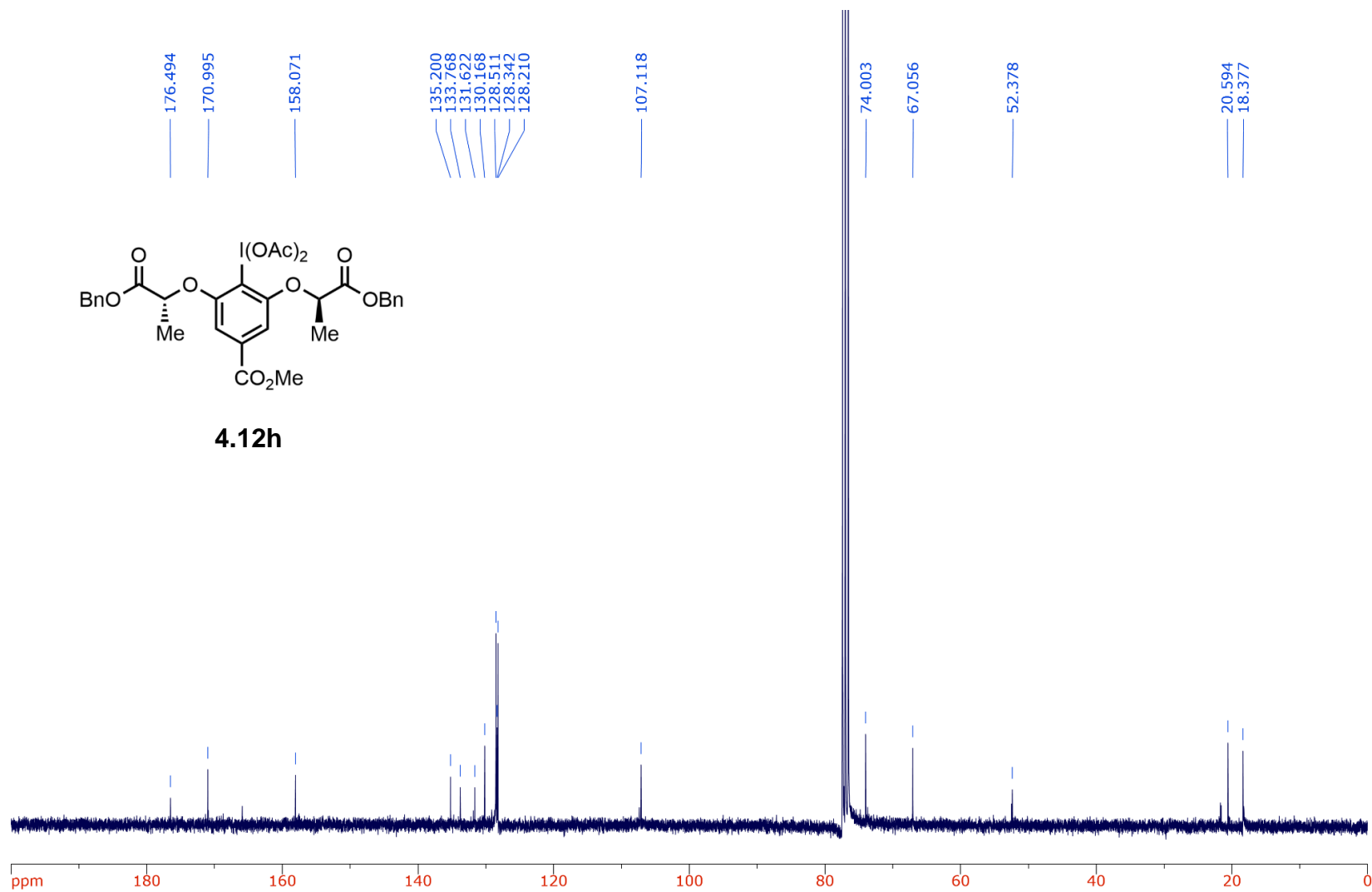


Figure 4.23 ^1H NMR (300 MHz, CDCl_3) spectrum of (2-(((benzoyl-L-prolyl)oxy)methyl)phenyl)- λ^3 -iodanediyl diacetate

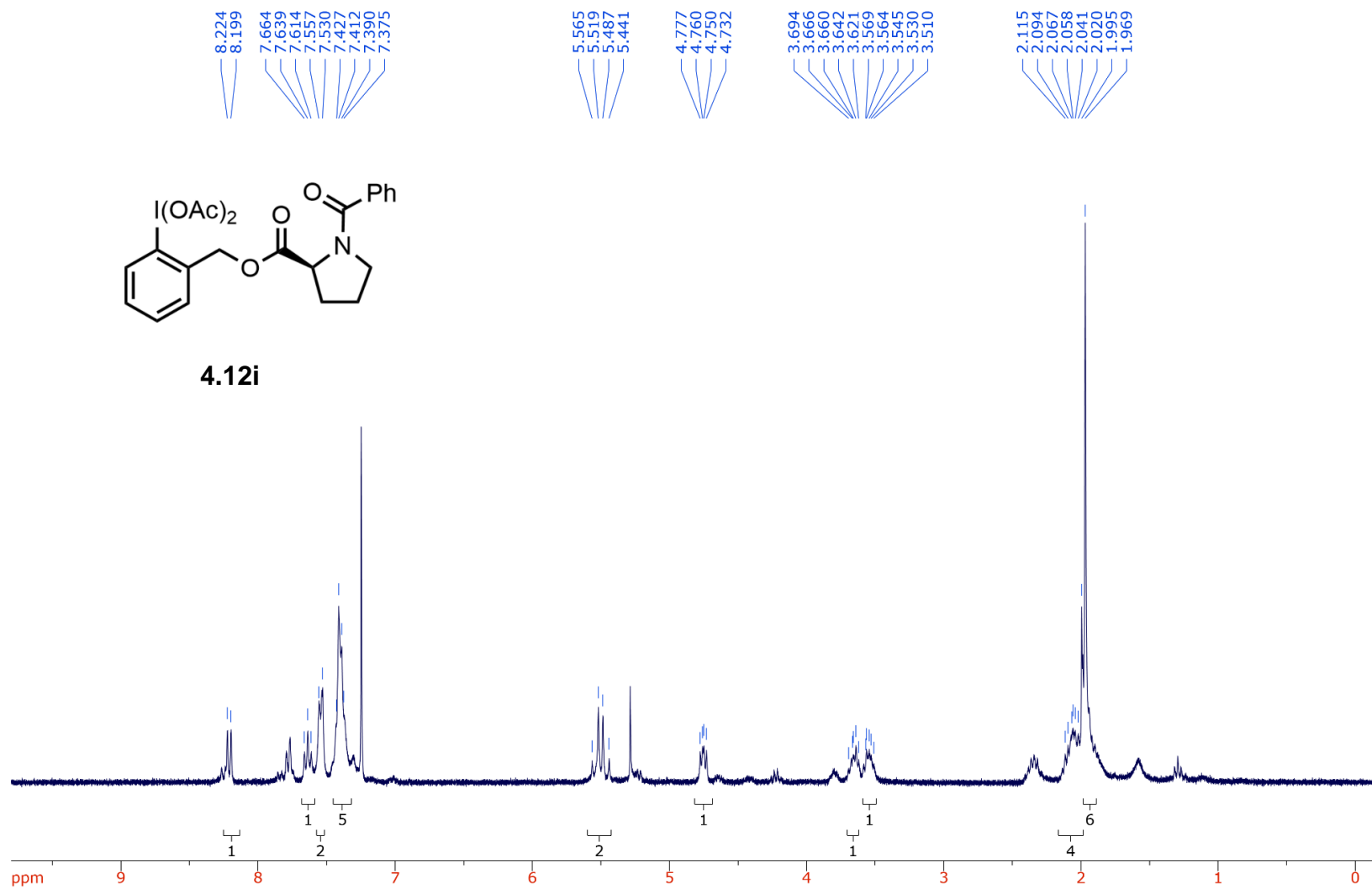


Figure 4.24 ^{13}C NMR (75 MHz, CDCl_3) spectrum of (2-(((benzoyl-L-prolyl)oxy)methyl)phenyl)- λ^3 -iodanediyl diacetate

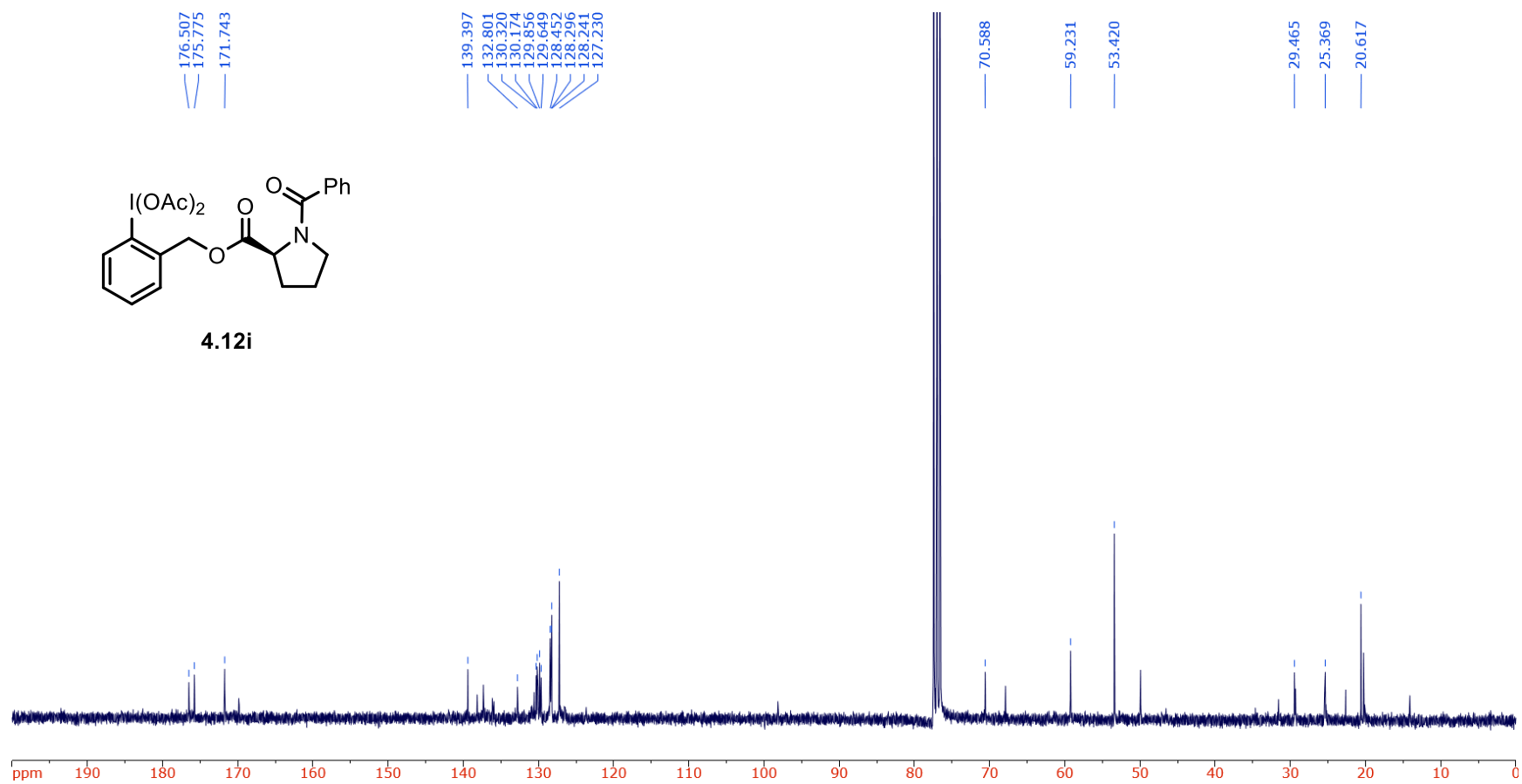


Figure 4.25 ^1H NMR (300 MHz, CDCl_3) spectrum of ethyl (R)-2-(2-((2,2-dimethyl-4,6-dioxo-1,3-dioxan-5-ylidene)- λ^3 -iodaneyl)phenoxy)propanoate

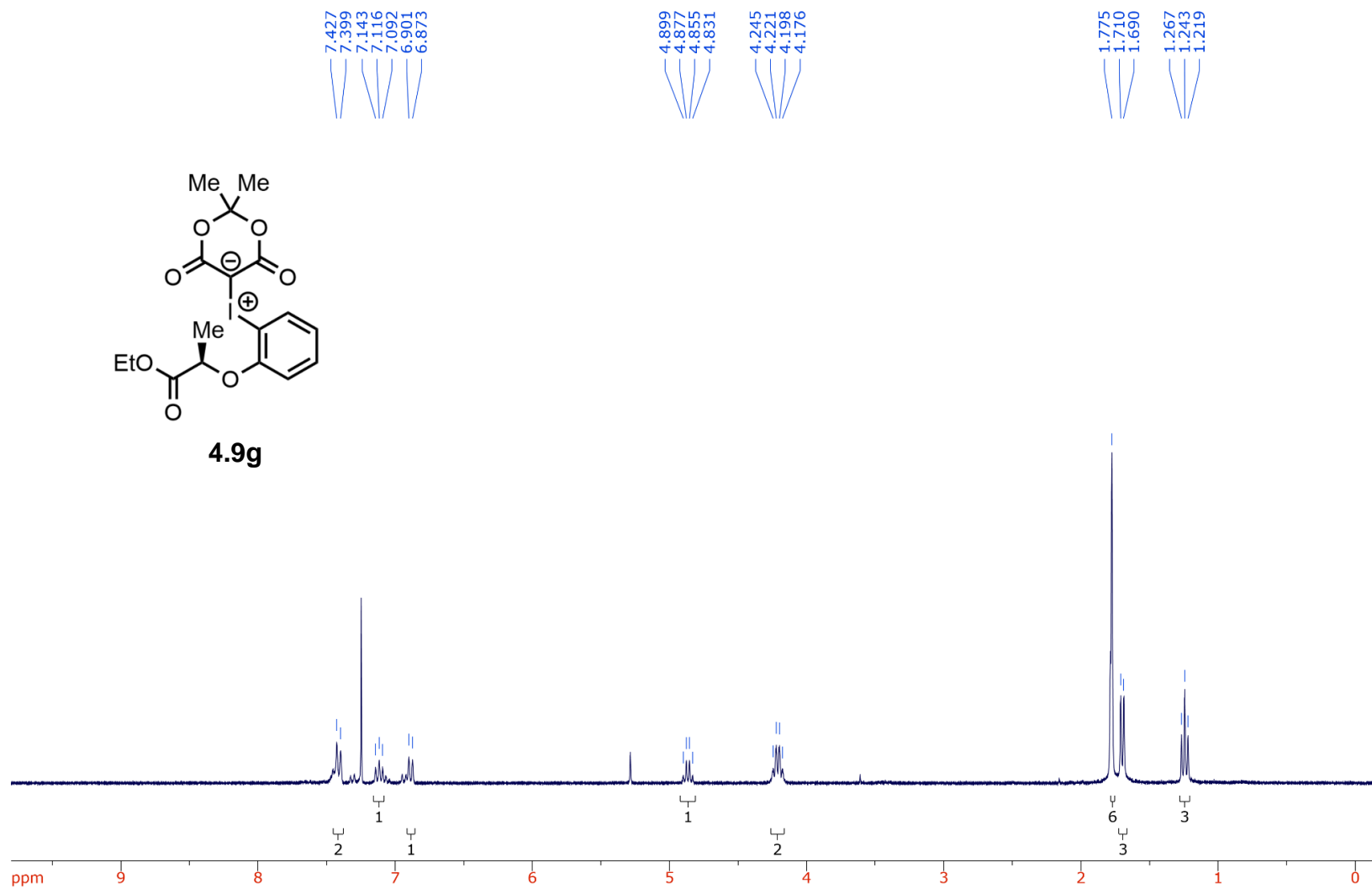


Figure 4.26 ^{13}C NMR (75 MHz, CDCl_3) spectrum of ethyl (R)-2-(2-((2,2-dimethyl-4,6-dioxo-1,3-dioxan-5-ylidene)- λ^3 -iodaneyl)phenoxy)propanoate

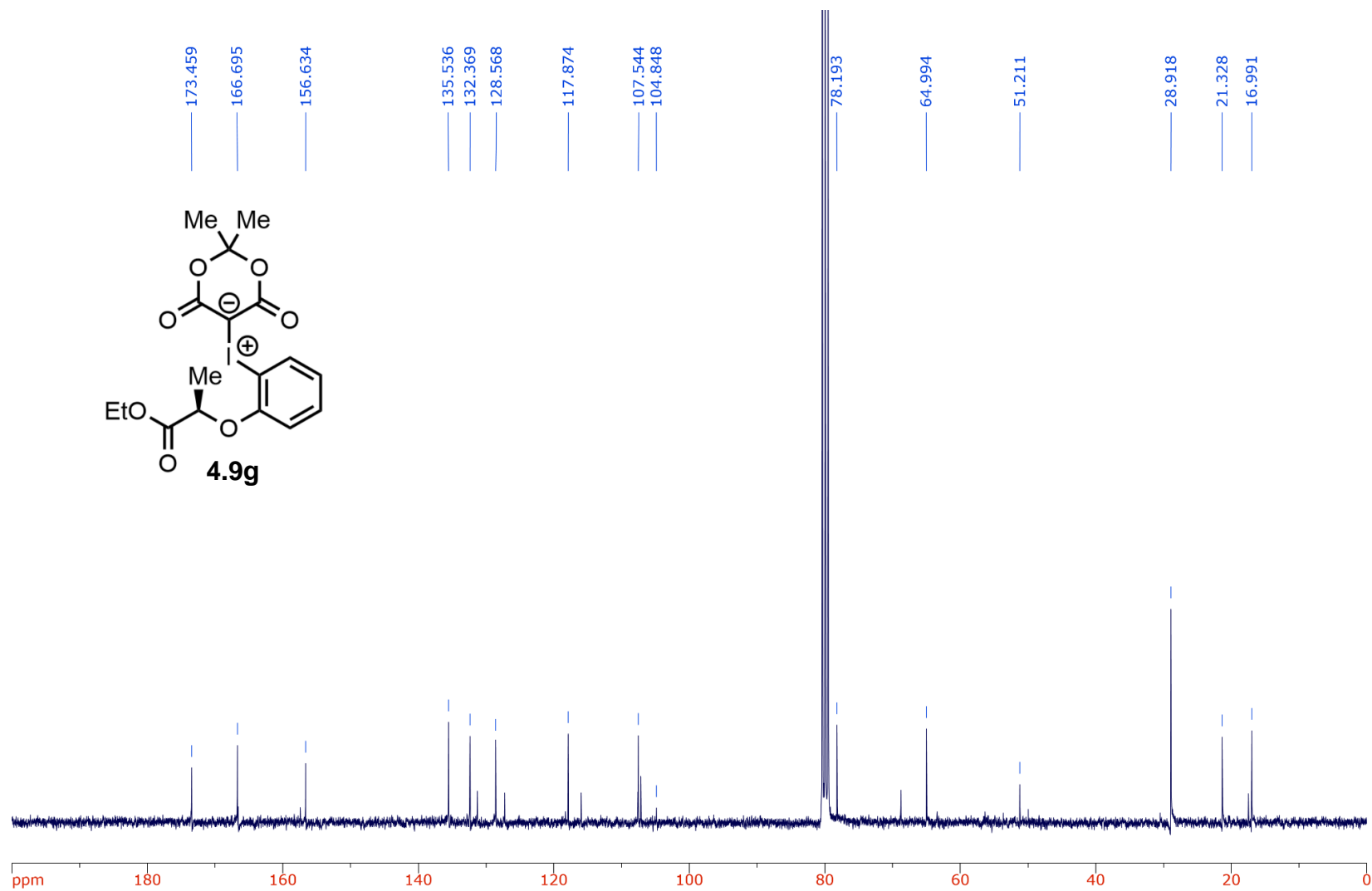


Figure 4.27 ^1H NMR (300 MHz, CDCl_3) spectrum of (2-(((benzoyl-L-prolyl)oxy)methyl)phenyl)- λ^3 -iodonium ylide

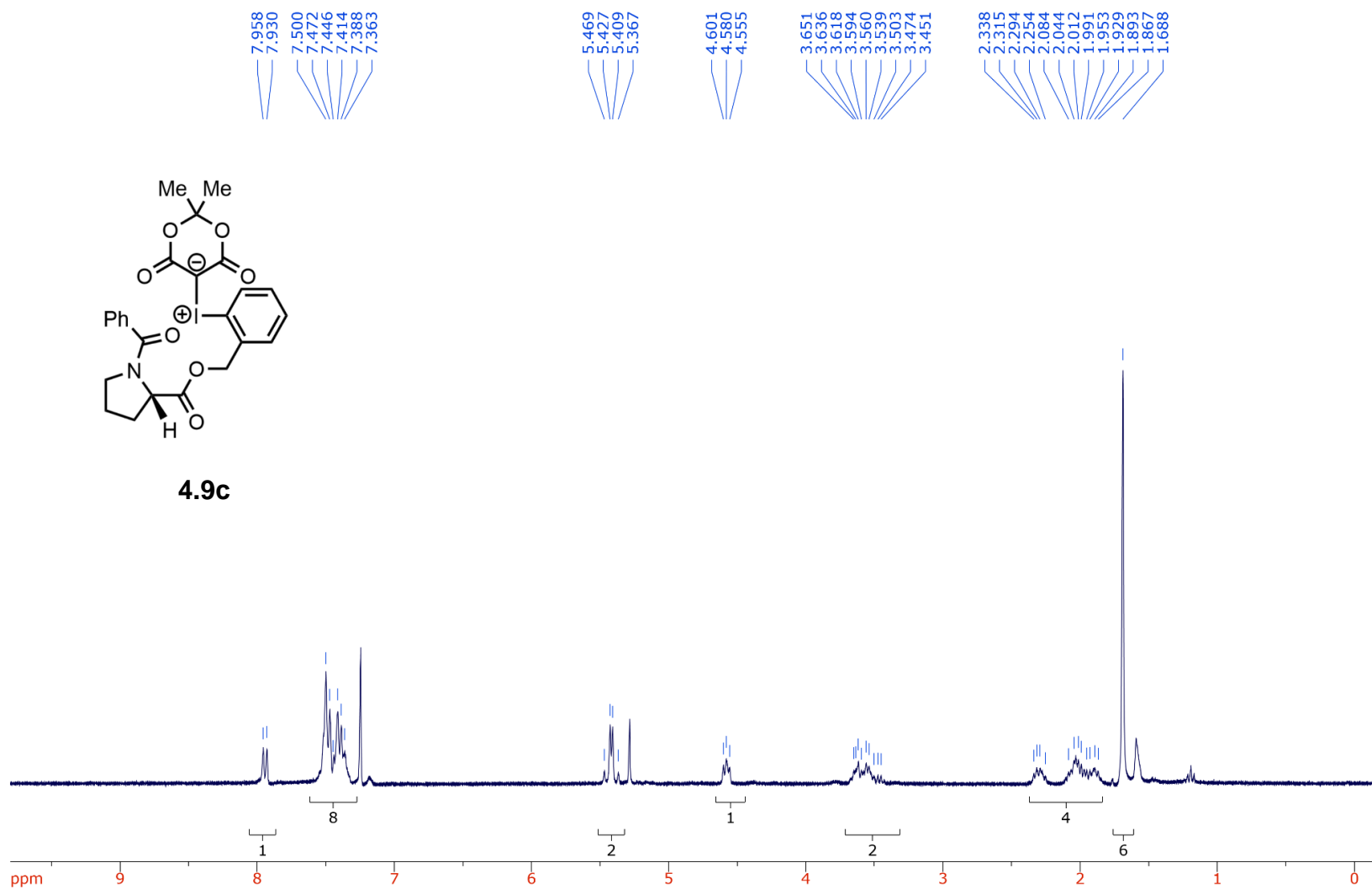


Figure 4.28 ^{13}C NMR (75 MHz, CDCl_3) spectrum of (2-(((benzoyl-L-prolyl)oxy)methyl)phenyl)- λ^3 -iodonium ylide

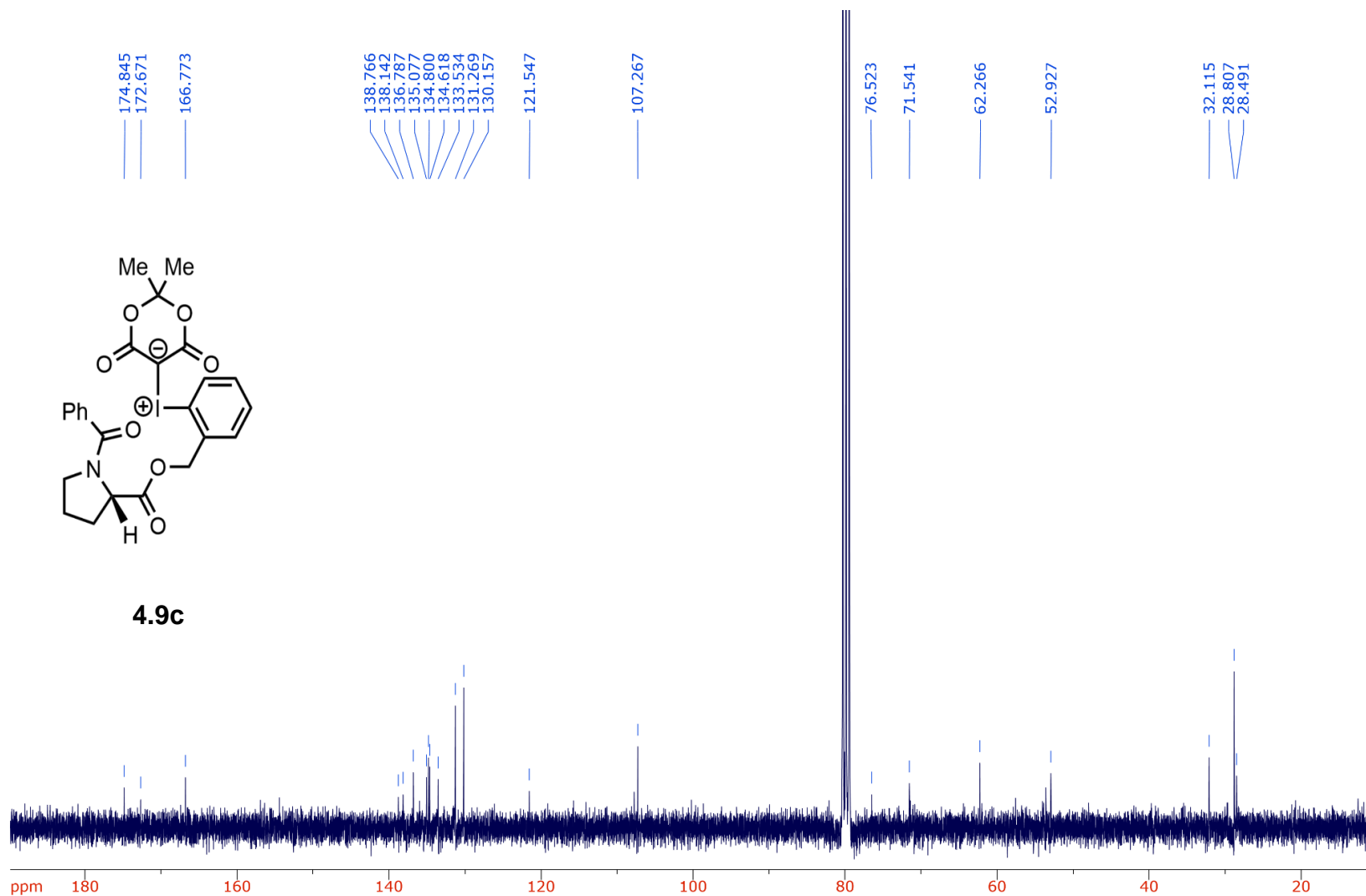


Figure 4.29 ^1H NMR (300 MHz, CDCl_3) spectrum of diethyl 2,2'-((2-((2,2-dimethyl-4,6-dioxo-1,3-dioxan-5-ylidene)- λ^3 -iodaneyl)-1,3-phenylene)bis(oxy))(2R,2'R)-dipropionate

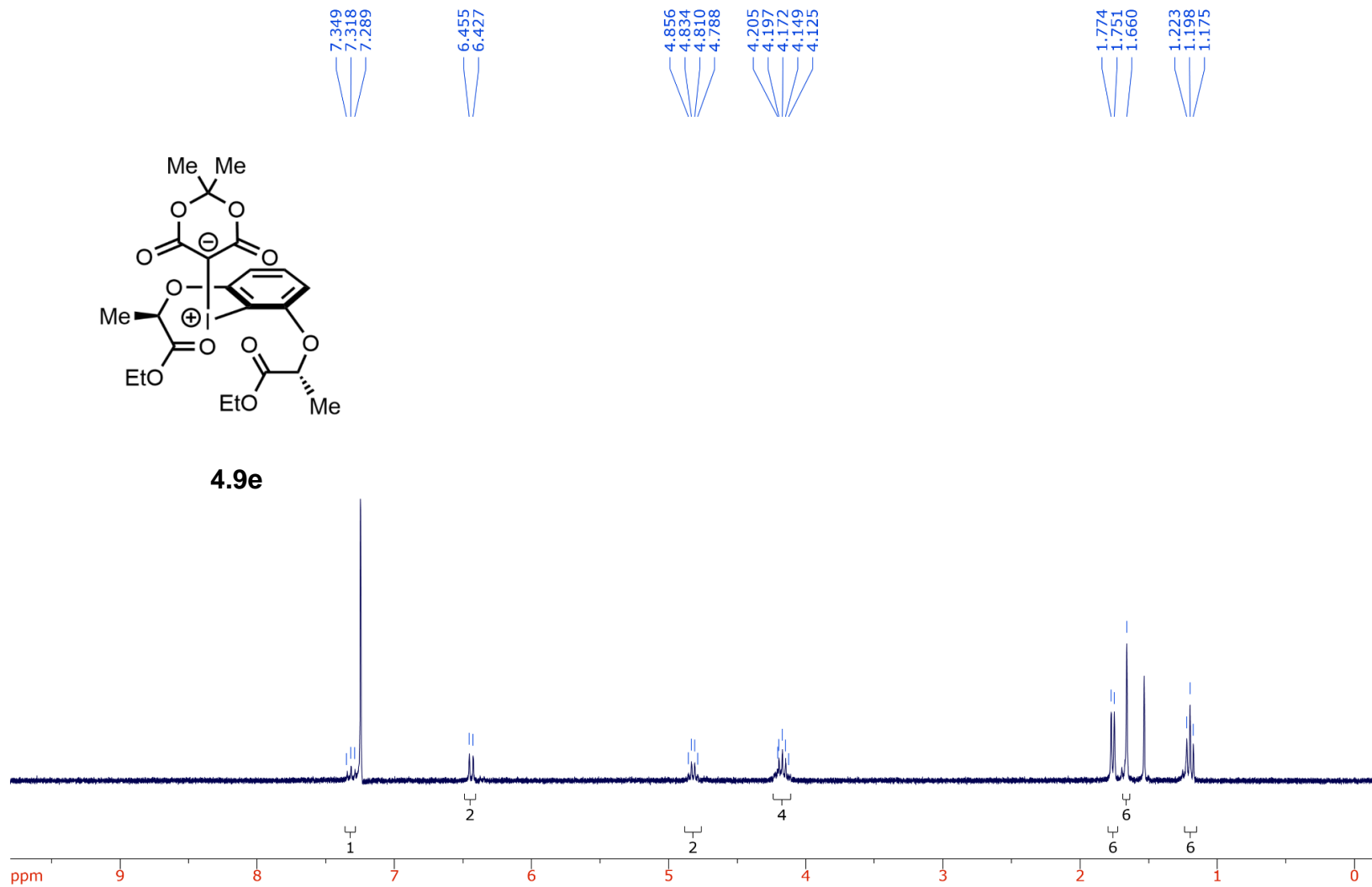


Figure 4.30 ^{13}C NMR (75 MHz, CDCl_3) spectrum of diethyl 2,2'-((2-((2,2-dimethyl-4,6-dioxo-1,3-dioxan-5-ylidene)- λ^3 -iodaneyl)-1,3-phenylene)bis(oxy))(2R,2'R)-dipropionate

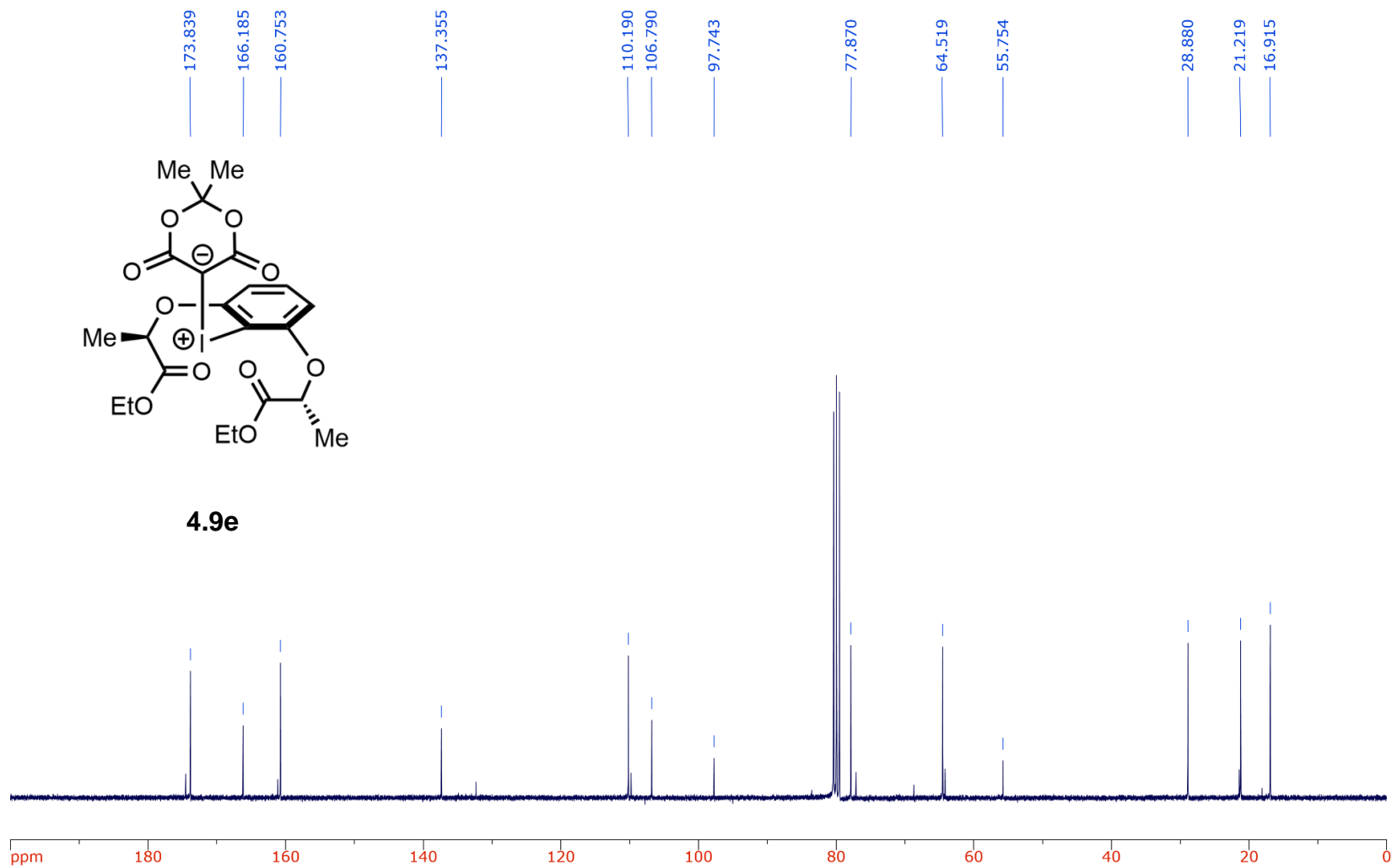


Figure 4.31 ^1H NMR (300 MHz, CDCl_3) spectrum of dibenzyl 2,2'-((2-((2,2-dimethyl-4,6-dioxo-1,3-dioxan-5-ylidene)- λ^3 -iodaneyl)-5-(methoxycarbonyl)-1,3-phenylene)bis(oxy))(2R,2'R)-dipropionate

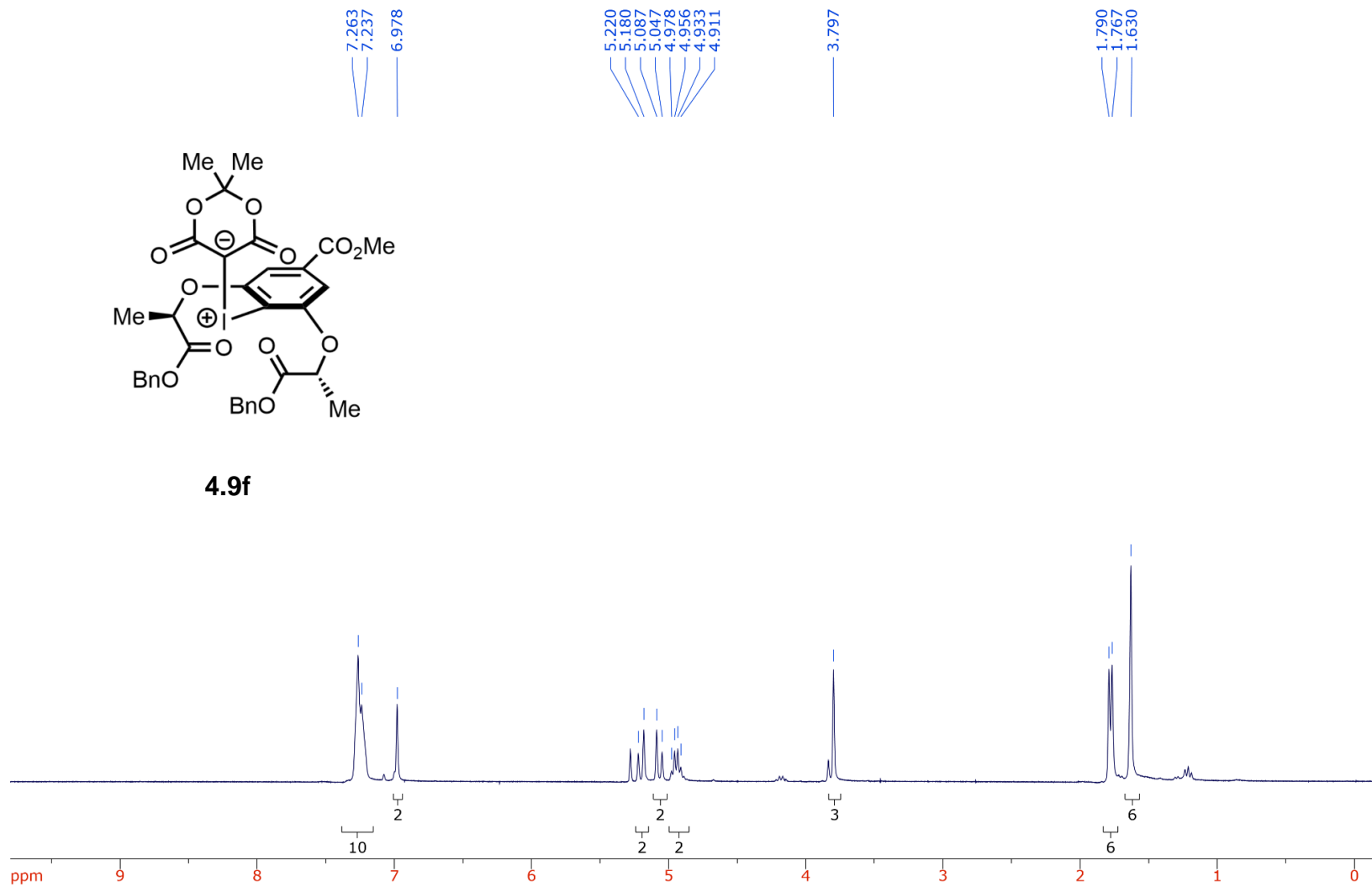
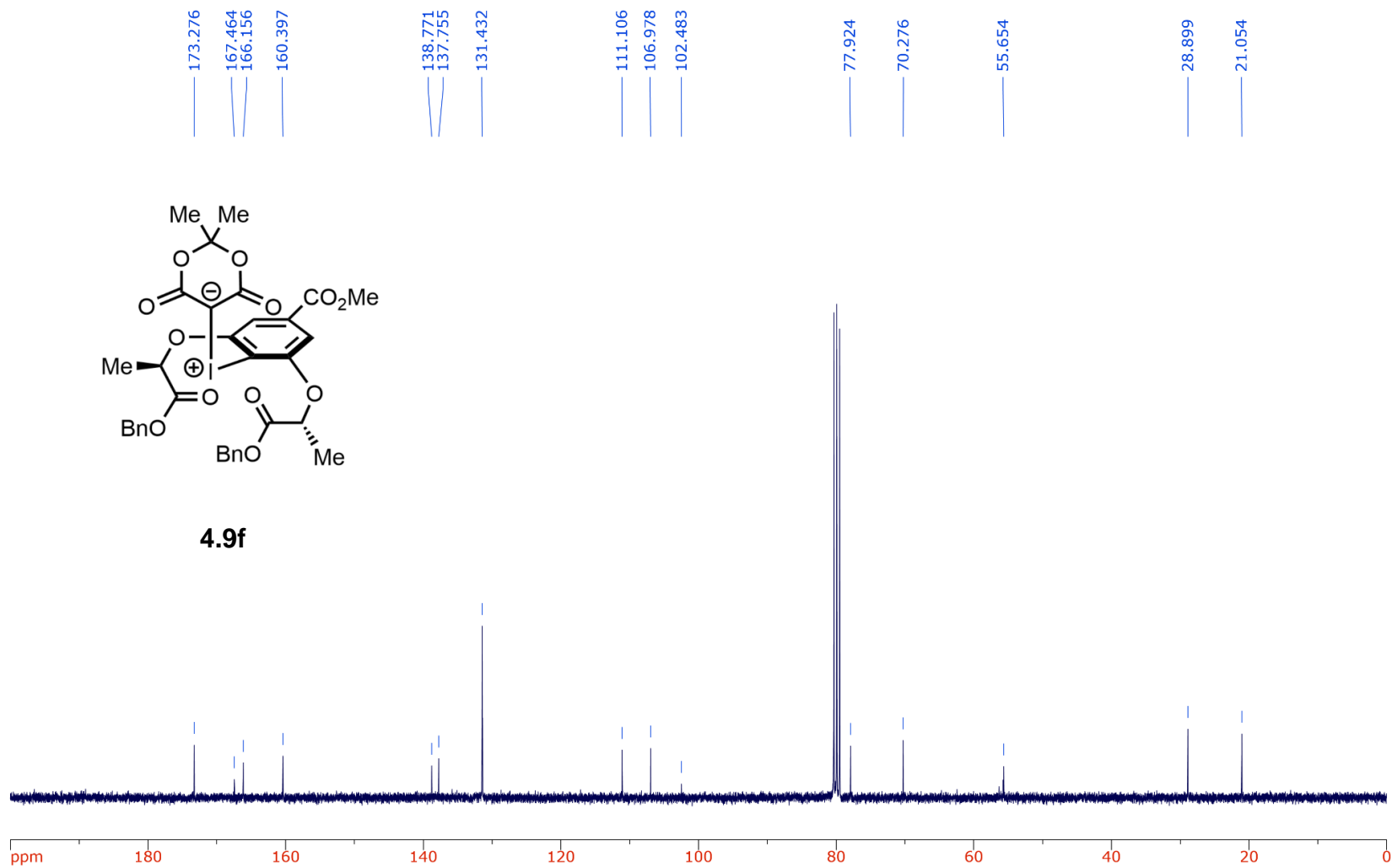


Figure 4.32 ^{13}C NMR (75 MHz, CDCl_3) spectrum of dibenzyl 2,2'-((2-((2,2-dimethyl-4,6-dioxo-1,3-dioxan-5-ylidene)- λ^3 -iodaneyl)-5-(methoxycarbonyl)-1,3-phenylene)bis(oxy))(2R,2'R)-dipropionate



References

- ¹ Courtois, B. *Ann. Chim.* **1813**, 88, 304.
- ² Salay, D. L. *PMHB.* **1975**, 99, 435-439.
- ³ Lauer, K. *J. Clin. Epidemiol.* **1991**, 44, 261-264.
- ⁴ Institute of Medicine, Food and Nutrition Board. Dietary Reference Intakes for Vitamin A, Vitamin K, Arsenic, Boron, Chromium, Copper, Iodine, Iron, Manganese, Molybdenum, Nickel, Silicon, Vanadium, and Zinc. Washington, DC: National Academy Press, 2001.
- ⁵ He, P.; Hou, X.; Aldahan, A.; Possnert, G.; Yi, P. *Sci. Rep.* **2013**, 3, 2685.
- ⁶ Walsh, J. P. *Med. J. Aust.* **2016**, 205, 179-184.
- ⁷ Kaczor, T. *J. Nat. Med.* **2014**, 6, 6.
- ⁸ Duarte, D. J. R.; Sosa, G. L.; Peruchena, N. M.; Alkorta, I. *Phys. Chem. Chem. Phys.* **2016**, 18, 7300-7309.
- ⁹ Musher, J. I. *Angew. Chem. Int. Ed. Engl.* **1969**, 8, 54-68.
- ¹⁰ Minkin, V. I. *Pure Appl. Chem.* **1999**, 71, 1919-1981.
- ¹¹ (a) Hach, R. J.; Rundle, R. E. *J. Am. Chem. Soc.* **1951**, 73, 4321-4324. (b) Pimentel, G. C. *J. Chem. Phys.* **1951**, 19, 446-448.
- ¹² Ochiai, M. *Coord. Chem. Rev.* **2006**, 250, 2771-2781.
- ¹³ Luliński, P.; Sosnowski, M.; Skulski, L.; Luliński, P.; Sosnowski, M.; Skulski, L. *Molecules.* **2005**, 10, 516-520.
- ¹⁴ Willgerodt, C. *J. Für Prakt. Chem.* **1886**, 33, 154-160.
- ¹⁵ Zhang, C.; Zhao, X. -F. *Sci. Synth.* **2007**, 4, 551-557.
- ¹⁶ McKillop, A.; Kemp, D. *Tetrahedron Lett.* **1989**, 45, 3299-3306.
- ¹⁷ Uyanik, M.; Yasui, T.; Ishihara, K. *Angew. Chem.* **2010**, 122, 2221-2223.
- ¹⁸ Hossain, M. D.; Kitamura, T. *Tetrahedron Lett.* **2006**, 47, 7889-7891.
- ¹⁹ Ye, C.; Twamley, B.; Shreeve, J. M. *Org. Lett.* **2005**, 7, 3961-3964.
- ²⁰ Moriarty, R. M.; Prakash, O. *Acc. Chem. Res.* **1986**, 19, 244-250.
- ²¹ Pimentel, G. C. *J. Chem. Phys.* **1951**, 19, 446-448.
- ²² Koser, G. F. *The Chemistry of Functional Groups*, John Wiley & Sons, Ltd, **1983**.
- ²³ Zhdankin, V. V.; Kuposov, A. E.; Smart, J. T. *J. Am. Chem. Soc.* **2001**, 123, 4095-4096.
- ²⁴ Nemykin, V. N.; Kuposov, A. Y.; Netzel, B. C. *Inorg. Chem.* **2009**, 48, 4908-4917.
- ²⁵ Alcock, N. W.; Countryman, R. M.; Esperas, S.; Sawyer, J. F. *J. Chem. Soc. Dalton Trans.* **1979**, 854-860.
- ²⁶ Sreenithya, A.; Sunoj, R. B. *Dalton Trans.* **2019**, 48, 4086-4093.
- ²⁷ Alcock, N. W.; Bozopoulos, A. P.; Hatzigrigoriou, E.; Varvoglis, A. *Acta. Cryst.* **1990**, 46, 1300-1303.
- ²⁸ Zhu, C.; Yoshimura, A.; Ji, L.; Wei, Y.; Nemykin, V. N.; Zhdankin, V. V. *Org. Lett.* **2012**, 14, 3170-3173.
- ²⁹ (a) Stang, P. J. *Chem. Rev.* **1996**, 96, 1123-1178. (b) Zhdankin, V. V.; Stang, P. J. *Chem. Rev.* **2008**, 108, 5299-5358. (c) Yoshimura, A.; Zhdankin, V. V. *Chem. Rev.* **2016**, 116, 3328-3435.
- ³⁰ Bugaut, X.; Glorius, F. *Angew. Chem. Int. Ed.* **2011**, 50, 7479-7481.
- ³¹ Dohi, T.; Ito, M.; Morimoto, K.; Iwata, M.; Kita, Y. *Angew. Chem. Int. Ed.* **2008**, 47, 1301-1304.
- ³² Okuyama, T.; Takino, T.; Sueda, T.; Ochiai, M. *J. Am. Chem. Soc.* **1995**, 117, 3360-3367.

- ³³ Ochiai, M. (1999) Organic Synthesis Using Hypervalent Organoiodanes. Chemistry of Hypervalent Compounds. Wiley-VCH, New York, Chapter 12, Page 359.
- ³⁴ Kajigaeshi, S.; Kakinami, T.; Moriwaki, M.; Tanaka, T.; Fujisaki, S. *Tetrahedron Lett.* **1988**, *29*, 5783-5786.
- ³⁵ Koleda, O.; Broese, T.; Noetzel, J.; Roemelt, M.; Suna, E.; Francke, R. *J. Org. Chem.* **2017**, *82*, 11669-11681.
- ³⁶ Wang, X.; Studer, A. *Acc. Chem. Res.* **2017**, *50*, 1712-1724.
- ³⁷ Togo, H.; Taguchi, R.; Yamaguchi, K.; Yokoyama, M. *J. Chem. Soc. Perkin Trans. 1* **1995**, 2135-2139.
- ³⁸ Sakamoto, R.; Kashiwagi, H.; Maruoka, K. *Org. Lett.* **2017**, *19*, 5126-5129.
- ³⁹ Dohi, T.; Ito, M.; Yamaoka, N.; Morimoto, K.; Fujioka, H.; Kita, Y. *Tetrahedron Lett.* **2009**, *65*, 10797-10815.
- ⁴⁰ Kita, Y.; Takada, T.; Tohma, H. *Pure. Appl. Chem.* **1996**, *68*, 627-630.
- ⁴¹ *IUPAC Compendium of Chemical Terminology*. Nič, M.; Jirát, J.; Košata, B.; Jenkins, A.; McNaught, A. IUPAC: Research Triangle Park, NC, **2009**.
- ⁴² Staudinger, H.; Meyer, J. *Helv. Chim. Acta.* **1919**, *2*, 635-646.
- ⁴³ Wittig, G.; Schöllkopf, U. *Chem. Ber.* **1954**, *87*, 1318-1330.
- ⁴⁴ Scharf, L. T.; Gessner, V. H. *Inorg. Chem.* **2017**, *56*, 8599-8607.
- ⁴⁵ Lischka, H. *J. Am. Chem. Soc.* **1977**, *99*, 353-360.
- ⁴⁶ Jerabek, P.; Schwerdtfeger, P.; Frenking, G. *J. Comput. Chem.* **2019**, *40*, 247-264.
- ⁴⁷ Tonner, R.; Öxler, F.; Neumüller, B.; Petz, W.; Frenking, G. *Angew. Chem. Int. Ed.* **2006**, *45*, 8038-8042.
- ⁴⁸ Alcarazo, M.; Lehmann, C. W.; Anoop, A.; Thiel, W.; Fürstner, A. *Nat. Chem.* **2009**, *1*, 295-301.
- ⁴⁹ Himmel, D.; Krossing, I.; Schnepf, A. *Angew. Chem. Int. Ed.* **2014**, *53*, 370-374.
- ⁵⁰ Ford, A.; Miel, H.; Ring, A.; Slattery, C. N.; Maguire, A. R.; McKervey, M. A. *Chem. Rev.* **2015**, *115*, 9981-10080.
- ⁵¹ von Pechmann, H. *Ber. Dtsch. Chem. Ges.* **1894**, *27*, 1888-1891.
- ⁵² Lewinn, E. B. *Am. J. Med. Sci.* **1949**, *218*, 556-562.
- ⁵³ Schoental, R. *Nature.* **1960**, *188*, 420-421.
- ⁵⁴ de Boer, T. J.; Backer, H. J. *Org. Syn.* **1956**, *36*, 16-18.
- ⁵⁵ Camacho, M. B.; Clark, A. E.; Liebrecht, T. A.; DeLuca, J. P. *J. Am. Chem. Soc.* **2000**, *122*, 5210-5211.
- ⁵⁶ Goudreau, S. R.; Marcoux, D.; Charette, A. B. *J. Org. Chem.* **2009**, *74*, 470-473.
- ⁵⁷ Goudreau, S. R.; Marcoux, D.; Charette, A. B.; Hughes, D. *Org. Synth.* **2010**, *87*, 115-125.
- ⁵⁸ Yusubov, M. S.; Yoshimura, A.; Zhdankin, V. V. *Arkivoc* **2016**, (i), 342-374.
- ⁵⁹ Neilands, O.; Vanags, G. *Proc. Acad. Sci. USSR (Engl. Transl.), Chem. Sect.*, **1960**, *131*, 425.
- ⁶⁰ Koser, G. F.; Yu, S. -M. *J. Org. Chem.* **1975**, *40*, 1166-1168.
- ⁶¹ Schank, K.; Lick, C. *Synthesis.* **1983**, 392-395.
- ⁶² Cardinale, J.; Ermert, J. *Tetrahedron Lett.* **2013**, *54*, 2067-2069.
- ⁶³ Komami, N.; Matsuoka, K.; Nakano, A.; Kojima, M.; Yoshino, T.; Matsunaga, S. *Chem. Eur. J.* **2019**, *25*, 1217-1220.
- ⁶⁴ Nishimura, T.; Iwasaki, H.; Takahashi, M.; Takeda, M. *J. Radioanal. Nucl. Chem.* **2003**, *255*, 499-502.

- ⁶⁵ Ivanov, A. S.; Popov, I. A.; Boldyrev, A. I.; Zhdankin, V. V. *Angew. Chem.* **2014**, *126*, 9771-9775.
- ⁶⁶ Zhu, S. -Z. *Heteroatom Chem.* **1994**, *5*, 9-18.
- ⁶⁷ Zhang, L.; Wang, Y. *Synlett* **2018**, *29*, 2337-2341.
- ⁶⁸ Müller, P.; Fernandez, D. *Helv. Chim. Acta.* **1995**, *78*, 947-958.
- ⁶⁹ Fairfax, D. J.; Austin, D. J.; Xu, S. L.; Padwa, A. *J. Chem. Soc., Perkin Trans. I* **1992**, 2837-2844.
- ⁷⁰ Koulouri, S.; Malamidou-Xenikaki, E.; Spyroudis, S.; Tsanakopoulou, M. *J. Org. Chem.* **2005**, *70*, 8780-8784.
- ⁷¹ Malamidou-Xenikaki, E.; Spyroudis, S.; *Synlett* **2008**, *18*, 2725-2740.
- ⁷² Zhang, L.; Kong, X.; Liu, S.; Zhao, Z.; Yu, Q.; Wang, W.; Wang, Y. *Org. Lett.* **2019**, *21*, 2923-2926.
- ⁷³ Telu, S.; Durmus, S.; Koser, G. F. *Tetrahedron Lett.* **2007**, *48*, 1863-1866.
- ⁷⁴ Pongratz, E.; Kappe, T. *Monatshefte Für Chem. Chem. Mon.* **1984**, *115*, 231-242.
- ⁷⁵ Li, W.-G.; Cai, B.; Xiao, H.-B.; Pi, S.-F.; Sun, H.-Z. *Synlett* **2016**, *27*, 794-798.
- ⁷⁶ Gondo, K.; Kitamura, T. *Molecules* **2012**, *17*, 6625-6632.
- ⁷⁷ Geary, G. C.; Hope, E. G.; Singh, K.; Stuart, A. M. *RSC Adv.* **2015**, *5*, 16501-16506.
- ⁷⁸ Gudrinietse, E.; Neilands, O.; Vanag, G. *J. Gen. Chem. USSR (Engl. Tranl.)* **1957**, *27*, 2777.
- ⁷⁹ Kefalidis, C. E.; Kanakis, A. A.; Gallos, J. K.; Tsipis, C. A. *J. Organomet. Chem.* **2010**, *695*, 2030-2038.
- ⁸⁰ Hartmann, M.; Li, Y.; Mück-Lichtenfeld, C.; Studer, A. *Chem. Eur. J.* **2016**, *22*, 3485-3490.
- ⁸¹ Papadopoulou, M.; Spyroudis, S.; Varvoglis, A. *J. Org. Chem.* **1985**, *50*, 1509-1511.
- ⁸² Buchner, E.; Feldmann, L. *Ber. Dtsch. Chem. Ges.* **1903**, *36*, 3509-3517.
- ⁸³ Frémont, P.; Marion, N.; Nolan, S. P. *Coord. Chem. Rev.* **2009**, *253*, 862-892.
- ⁸⁴ Staudinger, H.; Kupfer, O. *Ber. Dtsch. Chem. Ges.* **1912**, *45*, 501-509.
- ⁸⁵ Candeias, N. R.; Afonso, C. A. M. *Curr. Org. Chem.* **2009**, *13*, 763-787.
- ⁸⁶ Closs, G. L.; Moss, R. A. *J. Am. Chem. Soc.* **1964**, *86*, 4042-4053.
- ⁸⁷ Gessner, V. H. *Chem. Commun.* **2016**, *52*, 12011-12023.
- ⁸⁸ Knorr, R. *Chem. Rev.* **2004**, *104*, 3795-3849.
- ⁸⁹ Gómez-Gallego, M.; Sierra, M. A. *Chem. Rev.* **2011**, *111*, 4857-4963.
- ⁹⁰ Fischer, E. O.; Maasböl, A. *Angew. Chem. Int. Ed.* **1964**, *3*, 580-581.
- ⁹¹ Schrock, R. R. *J. Am. Chem. Soc.* **1974**, *96*, 6796-6797.
- ⁹² Schrock, R. R.; Meakin, P. *J. Am. Chem. Soc.* **1974**, *96*, 5288-5290.
- ⁹³ Schrock, R. R. *J. Am. Chem. Soc.* **1975**, *97*, 6577-6578.
- ⁹⁴ Wanzlick, H. W. *Angew. Chem. Int. Ed.* **1962**, *1*, 75-80.
- ⁹⁵ Wanzlick, H. W.; Schoenherr, H. J. *Angew. Chem. Int. Ed.* **1968**, *7*, 141-142.
- ⁹⁶ Arduengo, A. J.; Harlow, R. L.; Kline, M. *J. Am. Chem. Soc.* **1991**, *113*, 361-363.
- ⁹⁷ Freund, A. *J. Prakt. Chem.* **1881**, *26*, 367-377.
- ⁹⁸ Freund, A. *Monatsh. Chem.* **1882**, *3*, 625-635.
- ⁹⁹ Gustavson, G. *J. Prakt. Chem.* **1887**, *36*, 300-305.
- ¹⁰⁰ Lucas, G. H. W.; Henderson, V. E. *Can. Med. Assoc. J.* **1929**, *21*, 173-175.
- ¹⁰¹ de Meijere, A. *Small Ring Compounds in Organic Synthesis VI*; Springer: Berlin, **2000**, 207.
- ¹⁰² Faust, R. *Angew. Chem. Int. Ed.* **2001**, *40*, 2251-2253.
- ¹⁰³ Salaün, J.; Baird, M. S. *Curr. Med. Chem.* **1995**, *2*, 511-542.
- ¹⁰⁴ Meanwell, N. A. *J. Med. Chem.* **2016**, *59*, 7311-7351.

- 105 (a) Taylor, R. D.; MacCoss, M.; Lawson, A. D. G. *J. Med. Chem.* **2014**, *57*, 5845-5859. (b) Talele, T. T. *J. Med. Chem.* **2016**, *59*, 8712-8756.
- 106 Ebner, C.; Carreira, E. M. *Chem. Rev.* **2017**, *117*, 11651-11679.
- 107 Bruffaerts, J.; Pierrot, D.; Marek, I. *Nat. Chem.* **2018**, *10*, 1164-1170.
- 108 Schneider, T. F.; Kaschel, J.; Werz, D. B. *Angew. Chem. Int. Ed.* **2014**, *53*, 5504-5523.
- 109 Yu, M.; Pagenkopf, B. L. *Tetrahedron Lett.* **2005**, *61*, 321-347.
- 110 Garve, L. K. B.; Barkawitz, P.; Jones, P. G.; Werz, D. B. *Org. Lett.* **2014**, *16*, 5804-5807.
- 111 Richmond, E.; Yi, J.; Vukovic, V. D.; Sajadi, F.; Rowley, C. N. Moran, J. *Chem. Sci.* **2018**, *9*, 6411-6416.
- 112 Yadav, V. K.; Sriramurthy, V. *Org. Lett.* **2004**, *6*, 4495-4498.
- 113 Conrad, M.; Guthzeit, M. *Ber. Dtsch. Chem. Ges.* **1884**, *17*, 1185-1188.
- 114 (a) Perkin, W. H. *Ber. Dtsch. Chem. Ges.* **1884**, *17*, 54-59. (b) Perkin, W. H. *Ber. Dtsch. Chem. Ges.* **1884**, *17*, 323-373. (c) Perkin, W. H. *J. Chem. Soc.* **1885**, *47*, 801-855.
- 115 Michael, A. *J. Prak. Chem.* **1887**, *35*, 349-356.
- 116 Doering, W. V.; Hoffmann, A. K. *J. Am. Chem. Soc.* **1954**, *76*, 6162-6165.
- 117 Simmons, H. E.; Smith, R. D. *J. Am. Chem. Soc.* **1958**, *80*, 5323-5324.
- 118 Corey, E. J.; Chaykovsky, M. *J. Am. Chem. Soc.* **1962**, *84*, 867-868.
- 119 Corey, E. J.; Chaykovsky, M. *J. Am. Chem. Soc.* **1965**, *87*, 1353-1364.
- 120 Kulinkovich, O. G.; Sviridov, S. V.; Vasilevskii, D. A.; Pritytskaya, T. S. *Zh. Org. Khim.* **1989**, *25*, 2244-2245.
- 121 (a) Bertrand, G.; Reed, R. *Coord. Chem. Rev.* **1994**, *137*, 323-355. (b) Marcoux, D.; Charette, A. B. *Angew. Chem. Int. Ed.* **2008**, *47*, 10155-10158. (c) Frémont, P.; Marion, N.; Nolan, S. P. *Coord. Chem. Rev.* **2009**, *253*, 862-892. (d) Ebner, C.; Carreira, E. M. *Chem. Rev.* **2017**, *117*, 11651-11679.
- 122 Manna, S.; Antonchick, A. P. *Angew. Chem. Int. Ed.* **2016**, *55*, 5290-5293.
- 123 Hoyo, A. M.; Herraiz, A. G.; Suero, M. G. *Angew. Chem. Int. Ed.* **2017**, *56*, 1610-1613.
- 124 Nozaki, H.; Moriuti, S.; Takaya, H.; Noyori, R. *Tetrahedron Lett.* **1966**, *7*, 5239-5244.
- 125 Hood, J. N. C.; Lloyd, D.; MacDonald, W. A.; Shepherd, T. M. *Tetrahedron Lett.* **1982**, *38*, 3355-3358.
- 126 Müller, P.; Fernandez, D.; Nury, P.; Rossier, J. *Helv. Chim. Acta.* **1999**, *82*, 935-945.
- 127 Pauling, L. *J. Am. Chem. Soc.* **1931**, *53*, 1367-1400.
- 128 Wiberg, K. B. *Acc. Chem. Res.* **1996**, *29*, 229-234.
- 129 Boese, R.; Miebach, T.; De Meijere, A. *J. Am. Chem. Soc.* **1991**, *113*, 1743-1748.
- 130 Walsh, A. D. *Nature.* **1947**, *159*, 712-713.
- 131 Skinner, H. *Nature.* **1947**, *160*, 902-903.
- 132 Walsh, A. D. *Trans. Faraday Soc.* **1949**, *45*, 179-190.
- 133 Dewar, M. J. S. *J. Am. Chem. Soc.* **1984**, *106*, 669-682.
- 134 Kleinpeter, E.; Kruger, S.; Koch, A. *J. Phys. Chem.* **2015**, *119*, 4268-4276.
- 135 Bennett, W. A. *J. Chem. Educ.* **1967**, *44*, 17-24.
- 136 Seebach, D. *Angew. Chem. Int. Ed.* **1979**, *18*, 239-258.
- 137 Gudriniece, E.; Neiland, O.; Vanags, G. *Zh. Obshch. Khim.* **1957**, *27*, 2737-2740.
- 138 Fox, A. R.; Pausacker, K. H. *J. Chem. Soc.* **1957**, 295-301.
- 139 Kokil, P. B.; Nair, P. M. *Tetrahedron Lett.* **1977**, *47*, 4113-4116.
- 140 Page, S. W.; Mazzola, E. P.; Mighell, A. D.; Himes, V. L.; Hubbard, C. R. *J. Am. Chem. Soc.* **1979**, *101*, 5858-5860.

-
- ¹⁴¹ (a) Prakash, O.; Kumar, D.; Saini, R. K.; Singh, S. P. *Tetrahedron Lett.* **1994**, *35*, 4211-4214.
(b) Spyroudis, S. P. *Justus Liebigs Ann. Chem.* **1986**, *5*, 947-951.
- ¹⁴² Bakalbassis, E. G.; Spyroudis, S.; Tsiotra, E. *J. Org. Chem.* **2006**, *71*, 7060-7062.
- ¹⁴³ Takaku, M.; Hayasi, Y.; Nozaki, H. *Tetrahedron Lett.* **1970**, *26*, 1243-1247.
- ¹⁴⁴ Bonge, H. T.; Hansen, T. *Synlett* **2007**, *1*, 55-58.
- ¹⁴⁵ Wurz, R. P.; Charette, A. B. *Org. Lett.* **2003**, *5*, 2327-2329.
- ¹⁴⁶ Moriarty, R. M.; Bailey, B. R.; Prakash, O.; Prakash, I. *J. Am. Chem. Soc.* **1985**, *107*, 1375-1378.
- ¹⁴⁷ Ochiai, M.; Kitagawa, Y.; Yamamoto, S. *J. Am. Chem. Soc.* **1997**, *119*, 11598-11604.
- ¹⁴⁸ Ochiai, M. *J. Org. Chem.* **1989**, *54*, 4038-4041.
- ¹⁴⁹ Ho, P. E.; Tao, J.; Murphy, G. K. *Eur. J. Org. Chem.* **2013**, *29*, 6540-6544.
- ¹⁵⁰ Pecile, C.; Foffani, F.; Cherseti, S. *Tetrahedron Lett.* **1964**, *20*, 823-829.
- ¹⁵¹ Casanova, J.; Rutolo, D. A. *J. Chem. Soc. Chem. Commun.* **1967**, 1224-1225.
- ¹⁵² Ochiai, M.; Kitagawa, Y. *J. Org. Chem.* **1999**, *64*, 3181-3189.
- ¹⁵³ Zhu, S. -Z.; Chen, Q. -Y.; Kuang, W. *J. Fluor. Chem* **1993**, *60*, 39-42.
- ¹⁵⁴ Bonge, H. T.; Hansen, T. *Tetrahedron Lett.* **2008**, *49*, 57-61.
- ¹⁵⁵ Moreau, B.; Alberico, D.; Lindsay, V. N. G.; Charette, A. B. *Tetrahedron Lett.* **2012**, *68*, 3487-3496.
- ¹⁵⁶ Miyamoto, K.; Suzuki, M.; Suefuji, T.; Ochiai, M. *Eur. J. Org. Chem.* **2013**, 3662-3666.
- ¹⁵⁷ Ochiai, M.; Kitagawa, Y. *Tetrahedron Lett.* **1998**, *39*, 5569-5570.
- ¹⁵⁸ He, Z.; Zajdlik, A.; Yudin, A. K. *Dalton Trans.* **2014**, *43*, 11434-11451.
- ¹⁵⁹ (a) Xu, B.; Tambar, U. K. *J. Am. Chem. Soc.* **2016**, *138*, 12073-12076. (b) Xu, B.; Tambar, U. K. *Angew. Chem. Int. Ed.* **2017**, *56*, 9868-9871. (c) Xu, B.; Gartman, J. A.; Tambar, U. K. *Tetrahedron Lett.* **2017**, *73*, 4150-4159.
- ¹⁶⁰ Doyle, M. P.; Forbes, D. C.; Vasbinder, M. M.; Peterson, C. S. *J. Am. Chem. Soc.* **1998**, *120*, 7653-7654.
- ¹⁶¹ Maryanoff, B. E.; Reitz, A. B. *Chem. Rev.* **1989**, *89*, 863-927.
- ¹⁶² Vedejs, E.; Marth, C. F. *Ibhd.* **1988**, *110*, 3948-3958.
- ¹⁶³ Clayden, J.; Greeves, N.; Warren, S. G. (2012). *Organic Chemistry*. Oxford: Oxford University Press.
- ¹⁶⁴ Zbiral, E.; Rasberger, M. *Tetrahedron Lett.* **1969**, *25*, 1871-1874.
- ¹⁶⁵ Matveeva, E. D.; Podrugina, T. A.; Pavlova, A. S.; Mironov, A. V.; Borisenko, A. A.; Gleiter, R.; Zefirov, N. S. *J. Org. Chem.* **2009**, *74*, 9428-9432.
- ¹⁶⁶ Neilands, O.; Vanags, G. *Dokl. Akad. Nauk SSSR.* **1964**, *159*, 373-376.
- ¹⁶⁷ Matveeva, E. D.; Vinogradov, D. S.; Podrugina, T. A.; Nekipelova, T. D.; Mironov, A. V.; Gleiter, R.; Zefirov, N. S. *Eur. J. Org. Chem.* **2015**, 7324-7333.
- ¹⁶⁸ Moriarty, R. M.; Prakash, I.; Prakash, O.; Freeman, W. A. *J. Am. Chem. Soc.* **1984**, *106*, 6082-6084.
- ¹⁶⁹ Zhdankin, V. V.; Maydanovych, O.; Herschbach, J.; Bruno, J.; Matveeva, E. D.; Zefirov, N. S. *Tetrahedron Lett.* **2002**, *43*, 2359-2361.
- ¹⁷⁰ Allouche, E. M. D.; Charette, A. B. *Chem. Sci.* **2019**, *10*, 3802-3806.
- ¹⁷¹ Willgerodt, C. *Ber.* **1892**, *25*, 3494-3502.
- ¹⁷² McQuaid, K. M.; Pettus, T. R. R. *Synlett* **2004**, 2403-2405.
- ¹⁷³ Carmalt, C. J.; Crossley, J. G.; Knight, J. G.; Lightfoot, P.; Martin, A.; Muldowney, M. P.; Norman, N. C.; Orpen, A. G. *J. Chem. Soc. Chem. Commun.* **1994**, 2367-2368.

- 174 Wegeberg, C.; Frankær, C. G.; McKenzie, C. J. *Dalton Trans.* **2016**, 45, 17714-17722.
- 175 Ehrlich, B. S.; Kaplan, M. J. *J. Chem. Phys.* **1971**, 54, 612-620.
- 176 Silaghi-Dumitrescu, R. *J. Biol. Inorg. Chem.* **2004**, 9, 471-476.
- 177 Silaghi-Dumitrescu, R.; Cooper, C. E. *Dalton Trans.* **2005**, 3477-3482.
- 178 Leman, L.; Sanière, L.; Dauban, P.; Dodd, R. H. *Arkivoc.* **2003**, 6, 126-134.
- 179 Saltzman, H.; Sharefkin, J. G. *Org. Synth. Coll.* **1973**, 5, 658.
- 180 Lucas, H. J.; Kennedy, E. R.; Formo, M. W. *Org. Synth. Coll.* **1955**, 3, 483.
- 181 Sawaguchi, M.; Ayuba, S.; Hara, S. *Synthesis.* **2002**, 13, 1802-1803.
- 182 Macikenas, D.; Skrzypczak-Jankun, E.; Protasiewicz, J. D. *J. Am. Chem. Soc.* **1999**, 121, 7164-7165.
- 183 Meprathu, B. V.; Protasiewicz, J. D. *Arkivoc.* **2003**, 83-90.
- 184 Zhdankin, V. V.; Stang, P. J. *Chem. Rev.* **2002**, 102, 2523-2584.
- 185 Moriarty, R. M.; Kosmeder, J. W.; Zhdankin, V. V.; Courillon, C.; Lacôte, E.; Malacria, M.; Darses, B.; Dauban, P. Iodosylbenzene, *e-EROS*, **2012**.
- 186 Tohma, H.; Takizawa, S.; Maegawa, T.; Kita, Y. *Angew. Chem. Int. Ed.* **2000**, 39, 1306.
- 187 Yu, J.; Liu, S.-S.; Cui, J.; Hou, X.-S.; Zhang, C. *Org. Lett.* **2012**, 14, 832-835.
- 188 Richter, H. W.; Cherry, B. R.; Zook, T.D.; Koser, G. F. *J. Am. Chem. Soc.* **1997**, 119, 9614-9623.
- 189 Cavitt, M. A.; Phun, L. H.; France, S. *Chem. Soc. Rev.* **2014**, 43, 804-818.
- 190 Mandour, H. S. A.; Nakagawa, Y.; Tone, M.; Inoue, H.; Otog, N.; Fujisawa, I.; Chanthamath, S.; Iwasa, S. *Beilstein J. Org. Chem.* **2019**, 15, 357-363.
- 191 Doyle, M. P. *Acc. Chem. Res.* **1986**, 19, 348-356.
- 192 (a) Gallos, J. K.; Massen, Z. S.; Koftis, T. V.; Dellios, C. C. *Tetrahedron Lett.* **2001**, 42, 7489-7491. (b) Gallos, J. K.; Koftis, T. V.; Massen, Z. S.; Dellios, C. C.; Mourtzinis, I. T.; Coutouli-Argyropoulou, E.; Koumbis, A. E. *Tetrahedron Lett.* **2002**, 58, 8043-8053.
- 193 Yuan, W.; Eriksson, L.; Szabo, K. *Angew. Chem. Int. Ed.* **2016**, 55, 8410-8415.
- 194 Paulissen, R.; Reimlinger, H.; Hayez, E.; Hubert, A. J.; Teyssié, P. *Tetrahedron Lett.* **1973**, 14, 2233-2236.
- 195 Rosenberg, M. L.; Vlasana, K.; Sen Gupta, N.; Wragg, D.; Tilset, M. *J. Org. Chem.* **2011**, 76, 2465-27470.
- 196 Rosenberg, M. L.; Krivokapic, A.; Tilset, M. *Org. Lett.* **2009**, 11, 547-550.
- 197 Chen, Y.; Zhang, X. P. *J. Org. Chem.* **2007**, 72, 5931-5934.
- 198 Dey, R.; Kumar, P.; Banerjee, P. *J. Org. Chem.* **2018**, 83, 5438-5449.
- 199 Ty, N.; Kaffy, J.; Arrault, A.; Thoret, S.; Pontikis, R.; Dubois, J.; Morin-Allory, L.; Florent, J. C. *Biorg. Med. Chem. Lett.* **2009**, 19, 1318-1322.
- 200 Xu, X.; Lu, H. J.; Ruppel, J. V.; Cui, X.; de Mesa, S. L.; Wojtas, L.; Zhang, X. P. *J. Am. Chem. Soc.* **2011**, 133, 15292-15295.
- 201 Ebinger, A.; Heinz, T.; Umbricht, G.; Pfaltz, A. *Tetrahedron Lett.* **1998**, 54, 10469-10480.
- 202 Pezet, F.; Sasaki, I.; Daran, J. C.; Hydrio, J.; Ait-Haddou, H.; Balavoine, G. *Eur. J. Inorg. Chem.* **2001**, 2669-2674.
- 203 Lyle, M. P. A.; Wilson, P. D. *Org. Lett.* **2004**, 6, 855-857.
- 204 Velegaki, G.; Stratakis, M. *J. Org. Chem.* **2013**, 78, 8880-8884.
- 205 Ciaccio, J. A.; Aman, C. E. *Synth. Commun.* **2006**, 36, 1333-1341.
- 206 Suematsu, H.; Kanchiku, S.; Uchida, T.; Katsuki, T. *J. Am. Chem. Soc.* **2008**, 130, 10327-10337.

- ²⁰⁷ Barrett, A. G. M.; Braddock, D. C.; Lenoir, I.; Tone, H. *J. Org. Chem.* **2001**, *66*, 8260-8263.
- ²⁰⁸ Someswarao, B.; Khan, P. R.; Reddy, B. J. M.; Sridhar, B.; Reddy, B. V. S. *Org. Chem. Front.* **2018**, *5*, 1320-1324.
- ²⁰⁹ Barberis, M.; Perez-Prieto, J.; Stiriba, S. E.; Lahuerta, P. *Org. Lett.* **2001**, *3*, 3317-3319.
- ²¹⁰ (a) Burkhard, K. *Chemical Photocatalysis*, Walter de Gruyter, Berlin, 2013. (b) Mohammad, P. *Handbook of Photosynthesis*, 2nd ed., CRC Press, Boca Raton, 2005. (c) Mohammad, P. *Handbook of Photosynthesis*, 3rd ed., CRC Press, Boca Raton, 2016.
- ²¹¹ Herraiz, A. G.; Suero, M. G. *Chem. Sci.* **2019**, *10*, 9374-9379.
- ²¹² Coyle, J. D. *Introduction to Organic Photochemistry*, John Wiley & Sons: United Kingdom, **1986**.
- ²¹³ Daintith, J. A *Dictionary of Chemistry*, 5th ed. Oxford University Press: London, England, **2004**.
- ²¹⁴ Yoon, T. P.; Ischay, M. A.; Du, J. *Nat. Chem.* **2010**, *2*, 527-532.
- ²¹⁵ (a) Giese, B. *Angew. Chem. Int. Ed.* **1985**, *24*, 553-565. (b) Curran, D. P. *Synthesis.* **1988**, *7*, 489-513. (c) Togo, H.; Katohgi, M. *Synlett.* **2001**, 565-581.
- ²¹⁶ Poplata, S.; Tręster, A.; Zou, Y. -Q.; Bach, T. *Chem. Rev.* **2016**, *116*, 9748-9815.
- ²¹⁷ (a) Prier, C. K.; Rankic, D. A.; MacMillan, D. W. C. *Chem. Rev.* **2013**, *113*, 5322-5363. (b) Schultz, D. M.; Yoon, T. P. *Science.* **2014**, *343*, 985-994.
- ²¹⁸ Heber, J. *Nature Phys.* **2014**, *10*, 791.
- ²¹⁹ Buzzetti, L.; Crisenza, G. E. M.; Melchiorre, P. *Angew. Chem. Int. Ed.* **2019**, *58*, 3730-3747.
- ²²⁰ (a) Candeias, N. R.; Afonso, C. A. M. *Curr. Org. Chem.* **2009**, *13*, 763-787. (b) Galkina, O. S.; Rodina, L. L. *Russ. Chem. Rev.* **2016**, *85*, 537-555.
- ²²¹ Wang, Z.; Herraiz, A. G.; del Hoyo, A. M.; Suero, M. G. *Nature.* **2018**, *554*, 86-91.
- ²²² Jurberg, I. D.; Davies, H. M. L. *Chem. Sci.* **2018**, *9*, 5112-5118.
- ²²³ Li, Y. -Z.; Schuster, G. B. *J. Org. Chem.* **1987**, *52*, 4460-4464.
- ²²⁴ Zhu, Z.; Bally, T.; Stracener, L. L.; McMahon, R. J. *J. Am. Chem. Soc.* **1999**, *121*, 2863-2874.
- ²²⁵ Hommelsheim, R.; Guo, Y.; Yang, Z.; Empel, C.; Koenigs, R. M. *Angew. Chem. Int. Ed.* **2019**, *58*, 1203-1207.
- ²²⁶ Zhang, Y.; Kubicki, J.; Platz, M. S. *J. Am. Chem. Soc.* **2009**, *131*, 13602-13603.
- ²²⁷ Xia, X.-D.; Lu, L.-Q.; Liu, W.-Q.; Chen, D.-Z.; Zheng, Y.-H.; Wu, L.-Z.; Xiao, W.-J. *Chem. Eur. J.* **2016**, *22*, 8432-8437.
- ²²⁸ Vu, M. D.; Leng, W. -L.; Hsu, H. -C.; Liu, X. -W. *Asian J. Org. Chem.* **2019**, *8*, 93-96.
- ²²⁹ Das, M.; Vu, M. D.; Zhang, Q.; Liu, X. -W. *Chem. Sci.* **2019**, *10*, 1687-1691.
- ²³⁰ Xia, X. -D.; Lu, L. -Q.; Liu, W. -Q.; Chen, D. -Z.; Zheng, Y. -H.; Wu, L. -Z.; Xiao, W. -J. *Chem. Eur. J.* **2016**, *22*, 8432-8437.
- ²³¹ Zhou, F.; Cheng, Y.; Liu, X. -P.; Chen, J. -R.; Xiao, W. -J. *Chem. Commun.* **2019**, *55*, 3117-3120.
- ²³² (a) Huang, H.; Jia, K.; Chen, Y. *Angew. Chem. Int. Ed.* **2015**, *54*, 1881-1884. (b) Huang, H.; Zhang, G.; Chen, Y. *Angew. Chem. Int. Ed.* **2015**, *54*, 7872-7876. (c) Vaillant, F. L.; Courant, T.; Waser, J. *Angew. Chem., Int. Ed.* **2015**, *54*, 11200-11204. (d) Zhou, Q. -Q.; Guo, W.; Ding, W.; Wu, X.; Chen, X.; Lu, L. -Q.; Xiao, W. -J. *Angew. Chem. Int. Ed.* **2015**, *54*, 11196-11199.
- ²³³ (a) Papadopoulou, M.; Spyroudis, S.; Varvoglis, A. *J. Org. Chem.* **1985**, *50*, 1509-1511. (b) Hadjiarpoglou, L.; Spyroudis, S.; Varvoglis, A. *J. Am. Chem. Soc.* **1985**, *107*, 7178.
- ²³⁴ Michl, J.; Bonacic-Koutecky, V. *Electronic Aspects of Organic Photochemistry*. Wiley: New York, 1990, 77.

- 235 Kirschner, J.; Paillard, J.; Bouzrati-Zerelli, M.; Becht, J. M.; Klee, J. E.; Chelli, S.; Lakhdar, S.; Lalevée, J. *Molecules*. **2019**, *24*, 2913-2924.
- 236 Spyroudis, S. *Liebigs Ann. Chem.* **1986**, 947-951.
- 237 Zhu, S.; Li, A. *J Fluor Chem.* **1993**, *60*, 175-178.
- 238 Papadopoulou, M.; Spyroudis, S.; Varvoglis, A. *J. Org. Chem.* **1985**, *50*, 1509-1520.
- 239 Spyroudis, S. *J. Org. Chem.* **1986**, *51*, 3453-3456.
- 240 Hadjiarapoglou, L. P. *Tetrahedron Lett.* **1987**, *28*, 4449-4450.
- 241 Zhu, S. *Heteroat. Chem.* **1994**, *5*, 9-18.
- 242 Ciamician, G.; Silber, P. *Ber. Dtsch. Chem. Ges.* **1908**, *41*, 1928-1931.
- 243 Loutfy, R. O.; DeMayo, P. *Can. J. Chem.* **1972**, *50*, 3465-3471.
- 244 Kawashima, T.; Hoshihara, K.; Kano, N. *J. Am. Chem. Soc.* **2001**, *123*, 1507-1508.
- 245 Moriarty, R. M.; Tyagi, S.; Kinch, M. *Tetrahedron Lett.* **2010**, *66*, 5801-5810.
- 246 Quina, F. H.; Carroll, F. A. *J. Am. Chem. Soc.* **1976**, *98*, 6-9.
- 247 Taniguchi, M.; Lindsey, J. S. *J. Photochem. Photobiol.* **2018**, *94*, 290-327.
- 248 Baker, M.; Penny, D. *Nature*. **2016**, *533*, 452-454.
- 249 Le, C.; Wismer, M. K.; Shi, Z. -C.; Zhang, R.; Conway, D. V.; Li, G.; Vachal, P.; Davies, I. W.; MacMillan, D. W. C. *ACS Cent. Sci.* **2017**, *3*, 647-653.
- 250 Iodonium Ylides In Organic Synthesis. Thesis. Bhushan C. Surve. University of Illinois at Chicago, 2007.
- 251 Davico, G. E.; Bierbaum, V. M.; DePuy, C. H.; Ellison, G. B.; Squires, R. R. *J. Am. Chem. Soc.* **1995**, *117*, 2590-2599.
- 252 Solomon, D. H. *J. Polymer Sci.* **2005**, *43*, 5748-5764.
- 253 Lee, Y. -R.; Choi, J. -H. *Bull. Korean Chem. Soc.* **2006**, *27*, 503-507.
- 254 Müller, P.; Allenbach, Y.; Robert, E.; *Tetrahedron: Asymmetry* **2003**, *14*, 779-785.
- 255 Cai, W.; Fan, H.; Ding, D.; Zhang, Y.; Wang, W. *Chem. Commun.* **2017**, *53*, 12918-12921.
- 256 Purification of Laboratory Chemicals Textbook 5th edition, **2009**, ISBN 978-1-85617-567-8.
- 257 Murphy, G. K.; West, F. G. *Org. Lett.* **2006**, *8*, 4359-4361.
- 258 Yang, R.-Y.; Dai, L.-X.; Ma, R.-J. *Heteroat. Chem.* **1992**, *3*, 585-588.
- 259 Zhao, Z.; Luo, Y.; Liu, S.; Zhang, L.; Feng, L.; Wang, Y. *Angew. Chem., Int. Ed.* **2018**, *57*, 3792-3796.
- 260 Zefirov, N. S.; Zhdankin, V. V.; Koz'min, A. S.; Semerikov, V. N.; Agaev, A. T.; Magerramov, A. M. *Izv. Akad. Nauk, Ser. Khim.* **1987**, 2873.
- 261 Jalali, M.; Ho, C. C.; Fuller, R. O.; Lucas, N. T.; Ariafard, A.; Bissember, A. C. *J. Org. Chem.* **2021**, *86*, 1758-1768.
- 262 Schank, K.; Lick, C. *Synthesis* **1983**, *5*, 392-395.
- 263 Zhu, C. J.; Yoshimura, A.; Solntsev, P.; Ji, L.; Wei, Y. Y.; Nemykin, V. N.; Zhdankin, V. V. *Chem. Commun.* **2012**, *48*, 10108-10110.
- 264 Goudreau, S. R.; Marcoux, D.; Charette, A. B. *J. Org. Chem.* **2009**, *74*, 470-473.
- 265 Tao, J.; Estrada, C. D.; Murphy, G. K. *Chem. Commun.* **2017**, *53*, 9004-9007.
- 266 Batsila, C.; Kostakis, G.; Hadjiarapoglou, L. P. *Tetrahedron Lett.* **2002**, *43*, 5997-6000.
- 267 Zhu, S. -Z. *Heteroat. Chem* **1994**, *5*, 9-18.
- 268 Müller, P.; Ghanem, A. *Org. Lett.* **2004**, *6*, 4347-4350.
- 269 Izquierdo, M. L.; Arenal, I.; Bernabé, M.; Fernández Alvarez, E. *Tetrahedron* **1985**, *41*, 215-220.
- 270 Müller, P.; Allenbach, Y.; Robert, E. *Tetrahedron: Asymmetry* **2003**, *14*, 779-785.

- ²⁷¹ Ghorai, M. K.; Talukdar, R.; Tiwari, D. P. *Org. Lett.* **2014**, *16*, 2204-2207.
- ²⁷² Ovalles, S. R.; Hansen, J. H.; Davies, H. M. L. *Org. Lett.* **2011**, *13*, 4284-4287.
- ²⁷³ (a) Berthiol, F. *Synthesis* **2015**, *47*, 5872. (b) Dong, D. Q.; Hao, S. H.; Wang, Z. L.; Chen, C. *Org. Biomol. Chem.* **2014**, *12*, 42783. (c) Singh, F. V.; Wirth, T. *Chem. Asian. J.* **2014**, *9*, 9505. (d) Harned, A. M.; *Tetrahedron Lett.* **2014**, *55*, 4681. (e) Parra, A.; Reboredo, S. *Chem. Eur. J.* **2013**, *19*, 17244. (f) Singh, F. V.; Wirth, T. *Synthesis* **2013**, *45*, 2499.
- ²⁷⁴ Pribram, R. *Justus Liebigs Ann. Chem.* **1907**, *351*, 481-485.
- ²⁷⁵ Imamoto, T.; Koto, H. *Chem. Lett.* **1986**, 967-968.
- ²⁷⁶ Merkushev, E. B.; Novikov, A. N.; Makarchenko, S. S.; Moskal'chuk, A. S.; Glushkova, V. V.; Kogai, T. I.; Polyakova, L. G. *J. Org. Chem. USSR (Engl. Trans.)* **1975**, *11*, 1246-1249.
- ²⁷⁷ Kolb, H. C.; VanNieuwenhze, M. S.; Sharpless, K. B. *Chem. Rev.* **1994**, *94*, 2483-2547.
- ²⁷⁸ Richardson, R. D.; Page, T. K.; Altermann, S.; Paradine, S. M.; French, A. N.; Wirth, T. *Synlett* **2007**, 538-542.
- ²⁷⁹ Pluta, R.; Krach, P. E.; Cavallo, L.; Falivene, L.; Rueping, M. *ACS Catal.* **2018**, *8*, 2582-2588.
- ²⁸⁰ Narcis, M. J.; Takenaka, N. *Eur. J. Org. Chem.* **2014**, 21-34.
- ²⁸¹ Fujita, M.; Okuno, S.; Lee, H. J.; Sugimura, T.; Okuyama, T. *Tetrahedron Lett.* **2007**, *48*, 8691-8694.
- ²⁸² Uyanik, M.; Yasui, T.; Ishihara, K. *Tetrahedron* **2010**, *66*, 5841-5851.
- ²⁸³ Uyanik, M.; Yasui, T.; Ishihara, K. *Angew. Chem. Int. Ed.* **2013**, *52*, 9215-9218.
- ²⁸⁴ Uyanik, M.; Yasui, T.; Ishihara, K. *J. Org. Chem.* **2017**, *82*, 11946-11953.
- ²⁸⁵ Jain, N.; Xu, S.; Ciufolini, M. A. *Chem. Eur. J.* **2017**, *23*, 4542-4546.
- ²⁸⁶ Ghosh, S.; Pradhan, S.; Chatterjee, I. *Beilstein J. Org. Chem.* **2018**, *14*, 1244-1262.
- ²⁸⁷ Ruben, C.; Souto, J. A.; Gonzalez, Y.; Lishchynskiy, A.; Muciz, K. *Angew. Chem.* **2011**, *123*, 9478-9482; *Angew. Chem. Int. Ed.* **2011**, *50*, 9478-9482.
- ²⁸⁸ Müller, P.; Fernandez, D.; Nury, P.; Rossier, J.-C. *J. Phys. Org. Chem.* **1998**, *11*, 321-333.
- ²⁸⁹ Nozaki, H.; Moriuti, S.; Takaya, H.; Noyori, R. *Tetrahedron Lett.* **1966**, 5239.
- ²⁹⁰ Li, A. -H.; Dai, L. -X.; Aggarwal, V. K. *Chem Rev.* **1997**, *97*, 2341.
- ²⁹¹ Müller, P.; Allenbach, Y.; Robert, E. *Tetrahedron: Asymmetry* **2003**, *14*, 779.
- ²⁹² Moreau, B.; Charette, A. B. *J. Am. Chem. Soc.* **2005**, *127*, 18014-18015.
- ²⁹³ Ghanem, A.; Gardiner, M. G.; Williamson, R. M.; Müller, P. *Chem. Eur. J.* **2010**, *16*, 3291-3295.
- ²⁹⁴ Deng, C.; Wang, L. -J.; Zhu, J.; Tang, Y. *Angew. Chem. Int. Ed.* **2012**, *51*, 11620-11623.
- ²⁹⁵ Doyle, M. P.; Griffin, J. H.; Bagheri, V.; Dorow, R. L. *Organometallics* **1984**, *3*, 53-61.
- ²⁹⁶ Huang, Z. Z.; Kang, Y. B.; Zhou, J.; Ye, M. C.; Tang, Y. *Org. Lett.* **2004**, *6*, 1677-1679.
- ²⁹⁷ Fritschi, H.; Leutenegger, U.; Pfaltz, A. *Helv. Chim. Acta* **1988**, *71*, 1553-1565.
- ²⁹⁸ Guo, H.; Wang, H.; Li, W.; Zhang, M.; Xie, M.; Qu, G. *Chem. Commun.* **2020**, *56*, 11649-11652.
- ²⁹⁹ (a) Uyanik, M.; Yasui, T.; Ishihara, K. *Angew. Chem.* **2010**, *122*, 2221-2223. (b) Uyanik, M.; Yasui, T.; Ishihara, K. *Tetrahedron* **2010**, *66*, 5841-5851.
- ³⁰⁰ Uyanik, M.; Yasui, T.; Ishihara, K. *Angew. Chem. Int. Ed.* **2010**, *49*, 2175-2177.
- ³⁰¹ Fujita, M.; Ookubo, Y.; Sugimura, T. *Tetrahedron Lett.* **2009**, *50*, 1298-1300.
- ³⁰² Fujita, M.; Miura, K.; Sugimura, T. *Beilstein J. Org. Chem.* **2018**, *14*, 659-663.
- ³⁰³ Flores, A.; Cots, E.; Bergès, J.; Muñoz, K. *Adv. Synth. Catal.* **2019**, *361*, 2-25.
- ³⁰⁴ Zhdankin, V. V.; Smart, J. T.; Zhao, P.; Kiprof, P. *Tetrahedron Letters* **2000**, *41*, 5299-5302.

-
- ³⁰⁵ Ladziata, U.; Carlson, J.; Zhdankin, V. V. *Tetrahedron Letters* **2006**, *47*, 6301-6304.
- ³⁰⁶ Zhdankin, V. V. *Hypervalent iodine chemistry: preparation, structure and synthetic applications of polyvalent iodine compounds*. John Wiley & Sons Ltd: United Kingdom, **2014**.
- ³⁰⁷ Sreenithya, A.; Sunoj, R. B. *Dalton Trans.* **2019**, *48*, DOI: 10.1039/C9DT00472F.
- ³⁰⁸ Kita, Y.; Tohma, H.; Inagaki, M.; Hatanaka, K.; Yakura, T. *Tetrahedron Lett.* **1991**, *32*, 4321.
- ³⁰⁹ Dohi, T.; Yamaoka, N.; Kita, Y. *Tetrahedron* **2010**, *66*, 5775-5785.
- ³¹⁰ Colomer, I.; Batchelor-McAuley, C.; Odell, B.; Donohoe, T. J.; Compton, R. G. *J. Am. Chem. Soc.* **2016**, *138*, 8855-8861.
- ³¹¹ Lu, G.; Portscher, J. L.; Malinakova, H. C. *Organometallics* **2005**, *24*, 945-961.
- ³¹² Woerly, E. M.; Banik, S. M.; Jacobsen, E. N. *J. Am. Chem. Soc.* **2016**, *138*, 13858-13861.
- ³¹³ Farid, U.; Wirth, T. *Angew. Chem. Int. Ed.* **2012**, *51*, 3462-3465.

Appendix I: Crystal Structure Data of Cyclopropane

Cambridge Crystallographic Data Centre (CCDC), deposition Number 1949989

Oak Ridge Thermal Ellipsoid Plot (ORTEP) of *trans*-cyclopropane **3.301** at 50% probability

Formula weight	260.28
Temperature	296(2) K
Wavelength	0.71073 Å
Crystal system	Triclinic
Space group	<i>P</i> -1
Unit cell dimensions	$a = 8.2575(3) \text{ \AA}$ $\alpha = 65.1207(9)^\circ$ $b = 9.7660(4) \text{ \AA}$ $\beta = 68.4012(9)^\circ$ $c = 10.2196(4) \text{ \AA}$ $\gamma = 89.1757(10)^\circ$
Volume	685.45(5) Å ³
Z	2
Density (calculated)	1.261 g/cm ³
Absorption coefficient	0.091 mm ⁻¹
F(000)	276
Crystal size	0.220 x 0.210 x 0.070 mm ³
Theta range for data collection	2.331 to 30.077°
Index ranges	-10 ≤ h ≤ 11, -13 ≤ k ≤ 13, -14 ≤ l ≤ 14
Reflections collected	13502
Independent reflections	4014 [R(int) = 0.0200]
Completeness to theta = 25.242°	100.0 %
Absorption correction	Semi-empirical from equivalents
Max. and min. transmission	0.7460 and 0.7100
Refinement method	Full-matrix least-squares on F ²
Data / restraints / parameters	4014 / 0 / 177
Goodness-of-fit on F ²	1.189
Final R indices [I > 2σ(I)]	R1 = 0.0445, wR2 = 0.0820
R indices (all data)	R1 = 0.0655, wR2 = 0.0884
Extinction coefficient	0.019(2)
Largest diff. peak and hole	0.221 and -0.183 e.Å ⁻³

Appendix II: Permission for Figure 1.18 and Figure 1.19

This Agreement between University of Waterloo -- Tristan Chidley and John Wiley and Sons ("John Wiley and Sons") consists of your license details and the terms and conditions provided by John Wiley and Sons and Copyright Clearance Center.

License Number	5171371244264
License date	Oct 17, 2021
Licensed Content Publisher	John Wiley and Sons
Licensed Content Publication	Angewandte Chemie International Edition
Licensed Content Title	The I-X (X=O, N, C) Double Bond in Hypervalent Iodine Compounds: Is it Real?
Licensed Content Author	Viktor V. Zhdankin, Alexander I. Boldyrev, Ivan A. Popov, et al
Licensed Content Date	Jul 9, 2014
Licensed Content Volume	53
Licensed Content Issue	36
Licensed Content Pages	5
Type of use	Dissertation/Thesis
Requestor type	University/Academic
Format	Print and electronic
Portion	Figure/table
Number of figures/tables	1
Will you be translating?	No
Title	Applications of Iodonium Ylides for Donor-Acceptor Cyclopropane Synthesis
Institution name	University of Waterloo
Expected presentation date	Oct 2021
Portions	Figure 5
Requestor Location	University of Waterloo 510 Molinari St. Sarnia, ON N7W 0B1 Canada Attn: University of Waterloo
Publisher Tax ID	EU826007151
Total	0.00 USD